Enterotoxigenic Escherichia coli (ETEC) physiopathology and probiotic modulation in human gastrointestinal systems : Biotechnologie, Microbiologie et Santé

Charlène Roussel

Enterotoxigenic *Escherichia coli* (ETEC) pathophysiology and probiotic modulation in human gastrointestinal systems

Charlène Roussel

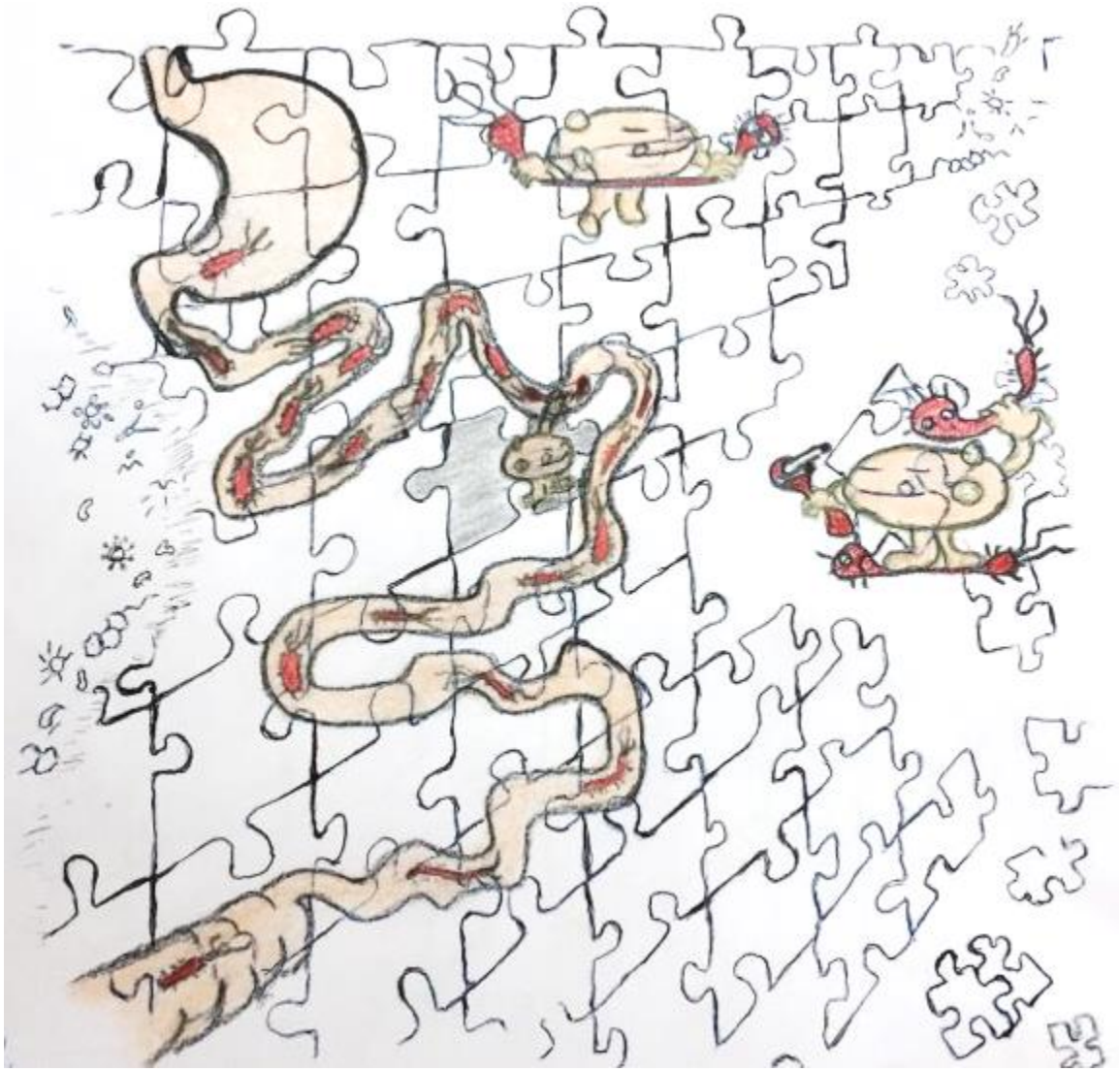

GHENT UNIVERSITY
UNIVERSITÉ Clermont Auvergne
FACULTY OF BIOSCIENCE ENGINEERING

Promotors:

Prof. dr. ir. Stéphanie Blanquet-Diot
UMR Laboratory of Microbiology, Digestive environment and Health (UMR 454 MEDIS)
Clermont-Auvergne University, Faculty of Pharmacy, Clermont-Ferrand, FRANCE

Prof. dr. ir. Tom Van de Wiele
Department of Biotechnology
Faculty of Bioscience Engineering, Ghent University, Ghent, BELGIUM

Members of the examination committee:

Prof. dr. ir. Mieke Uyttendaele (Chairman)
Department of Food Technology, Safety and Health
Faculty of Bioscience Engineering, Ghent University, Ghent, BELGIUM

Prof. dr. Nicolas Barnich (Secretary)
UMR Microbes Intestin Inflammation et Susceptibilité de l'hôte (UMR S1071 M2iSH)
Clermont-Auvergne University, Faculty of Pharmacy, Clermont-Ferrand, FRANCE

Prof. dr. Sarah Lebeer
Department of Bioscience Engineering
Faculty of Life Sciences, University of Antwerp, Antwerp, BELGIUM

Prof. dr. Marc Heyndrickx
Department of Food Safety,
ILVO, Melle, BELGIUM

Prof. dr. Marion Leclerc
UMR MICALIS
INRA, Jouy-en-Josas, FRANCE

Dean Faculty of Bioscience Engineering:
Prof. dr. ir. Marc Van Meirvenne

Rector of Ghent University:
Prof. dr. ir. Rik Van de Walle

Enterotoxigenic *Escherichia coli* (ETEC) pathophysiology and probiotic modulation in human gastrointestinal systems

Charlène Roussel

Thesis submitted in fulfillment of the requirements for the degree of Doctor (PhD) in Apllied Biological Sciences at Ghent University (Belgium) and Biotechnology, Microbiology and Health at Clermont-Auvergne University (France)

Cover illustration

Bernard Bartolo

Please refer to this work as:

Roussel, C. (2019). Enterotoxigenic *Escherichia coli* (ETEC) pathophysiology and probiotic modulation in human gastrointestinal systems. PhD thesis, Ghent University and Clermont-Auvergne University.

ISBN **978-9-4635718-1-4**

This work was supported by Lesaffre company (Marcq-en-Baroeul, France).

CONTENTS

ABSTRACT

The food and water-borne pathogen enterotoxigenic *Escherichia coli* (ETEC) is considered one of the leading cause of traveler's diarrhea and severe diarrhea in children living in resource-limited settings. 45% of the traveler's diarrhea worldwide are associated with ETEC infection. Such ETEC infection is mediated by a number of crucial virulence traits. In a first stage, ETEC is capable of attaching to the human intestinal epithelial cells in the distal part of the small intestine through a large set of colonization factors and adhesins. The subsequent release of the heat-labile (LT) and/or heat-stable (ST) enterotoxins leads to the onset of profuse watery diarrhea and dehydration. Beyond diarrheal symptoms, ETEC can have long-term implications, resulting in post-infectious chronic sequelae ranging from functional gastrointestinal (GI) disorder to irritable bowel syndrome. The understanding of ETEC behavior in the human GI tract through the survival of the pathogen and its virulence features is currently missing, which is reflected in a lack of prophylactic and/or curative treatments specific to ETEC infections.

In this context, this joint doctoral research aimed to (i) unravel the dynamics of survival and virulence of the reference strain ETEC H10407 in the human GI tract, with the use of well-controlled and validated multi-compartmented systems of the human digestion and fermentation, respectively the TNO gastrointestinal model (TIM-1) and the Mucosal Simulator of the Human Intestinal Microbial Ecosystem (M-SHIME); and (ii) examine the antimicrobial properties of the probiotic *Saccharomyces cerevisiae* CNCM I-3856 against ETEC H10407 using the TIM-1 and M-SHIME *in vitro* models, and evaluate this probiotic as a prophylactic approach for traveler's diarrhea.

In the TIM-1 system, the physicochemical parameters of the human digestion were reproduced. Although, according to plate counting, the survival of ETEC was low in the gastric environment, the pathogen was able to modulate its membrane physiology and enter in an intermediate viability state to withstand the stringent acid conditions. In the small intestine, a growth renewal of ETEC was observed at the end of the jejunal and ileal digestion, confirmed by a restoration of ETEC membrane integrity. The microbial bulk encountered in the M-SHIME ileum and ascending colon did not impede successful ETEC colonization of these gut regions. ETEC, particularly, efficiently attached to the mucosal microenvironment. Interactions of the pathogen with the gut microbiota were also examined. Following ETEC infection, although the microbial diversity was not altered, a bloom of opportunistic pathogens occurred in the ileum, while in the ascending colon a decrease of species with potential health promoting functions was observed. With respect to the virulence features of ETEC, most of the virulence genes under study, encoding for the enterotoxins and adhesins were switched on in the stomach and switched off in the ileum and ascending colon. At protein level, ETEC did not produce the LT enterotoxin under gastric conditions while the toxin was produced in the ileum, the prime site of action of the bacterium, and in the ascending colon.

Our study also contributed to the identification of the anti-microbial properties of the probiotic *Saccharomyces cerevisiae* CNCM I-3856 against ETEC. The pre-treatment with the probiotic inhibited ETEC adhesion to mucin-agar and to the human intestinal Caco-2/TC7 cells in a dose dependent manner. It, moreover suppressed ETEC-induced inflammation through the inhibition of the Interleukin-8 production in Caco-2/TC7 cells. In the *in vitro* digestive models, we have gathered evidence that the probiotic acts by impairing ETEC functionality in terms of virulence genes expression and LT toxin production, although it did not affect the survival of the pathogen. The probiotic tended to counteract the blooming of opportunistic bacteria members of *Klebsiella*, *Achromobacter* and *Mycobacterium* genera induced upon ETEC infection, while an increase of genera with potential health promoting functions was observed such as *Bifidobacterium*, *Faecalibacterium*, *Lactobacillus* or *Fusicatenibacter* genera. Finally the probiotic yeast led to a significant increase of the metabolic activity through acetate and propionate production.

To fill the knowledge gap concerning ETEC pathogenesis in the human GI tract, considered as a “black box” so far, this PhD research provided significant insights into the temporal and spatial modulation of ETEC survival and virulence in the adult gut, as well as in the interaction of ETEC with the gut microbes, simulated by the TIM-1 and M-SHIME. Further investigations by coupling the digestive systems with human intestinal cell cultures could serve to better unravel the scheme of the bacterial infection. The promising ETEC H10407-inhibitory properties displayed by the probiotic yeast *S. cerevisiae* CNCM I-3856 merit further attention as well. The assessment of other ETEC strains would be interesting to better conceptualize the probiotic efficacy.

SAMENVATTING

De door voedsel en water overdraagbare pathogeen, Enterotoxigene *Escherichia coli* (ETEC), wordt beschouwd als de hoofdoorzaak van reizigersdiarree en ernstige diarree bij kinderen in ontwikkelingslanden met beperkte basisvoorzieningen. Reizigersdiarree wordt in 45% van de geregistreerde gevallen gerelateerd aan ETEC infectie. Dergelijke ETEC infectie wordt gemedieerd door enkele cruciale ETEC virulentiefactoren. In eerste instantie hecht ETEC zich met behulp van tal van kolonisatiefactoren en ahesines vast aan de menselijke darmepitheel cellen in het distale gedeelte van de dunne darm. Vervolgens worden hitte-labiele (LT) en hitte-stabiele (ST) toxines vrijgesteld die aanleiding geven tot een extreme waterige diarree met dehydratatie tot gevolg. Naast de acute diarree symptomen, kan ETEC infectie ook op lange termijn de gezondheid schaden en resulteren in chronische ziektes zoals functionele maag en darm aandoeningen en prikkelbare darm syndroom. Een gebrek aan inzicht in de ETEC overleving en de regulatie en expressie van de ETEC virulentiefactoren in het menselijk spijsverteringskanaal bemoeilijk de ontwikkeling van effectieve profylactische en curatieve behandelingen voor ETEC infectie.

Daarom werden binnen de context van dit doctoraat, gebruik makend van de referentiestam ETEC H10407, volgende onderzoeksdoelen gesteld: i) het onderzoeken van de dynamiek van ETEC overleving en virulentie in gastro-intestinale omstandigheden aan de hand van het *TNO gastrointestinal model* (TIM-1) en *The Mucosal Simulator of the Human Intestinal Microbial Ecosystem* (M-SHIME). Dit zijn beide volledige gecontroleerde en gevalideerde *in vitro* systemen ter simulatie van de menselijke maag en dunne darm vertering en de microbiële fermentatie in het colon, respectievelijk. ii) het onderzoeken van de antimicrobiële activiteit van de probiotische stam *Saccharomyces cerevisiae* CNCM I-3856 ten opzichte van ETEC H10407 in de TIM-1 en M-SHIME *in vitro* modellen met als einddoel het evalueren van een profylactische strategie voor de behandeling van reizigersdiarree.

In het TIM-1 systeem worden de fysiologische parameters van de menselijke vertering nagebootst. Ondanks het feit dat de ETEC overleving volgens resultaten van uitplatingen werd aangetast in de zeer zure omstandigheden in de maag, bleek deze pathogeen in staat om dankzij wijzigingen in de membraan fysiologie een intermediaire viabiliteit status aan te nemen. Zodoende werd in de dunne darm een herstel van de membraan integriteit en een corresponderende hernieuwde ETEC uitgroei vastgesteld aan het eind van de jejunum en ileum passage. Ook in het ileum en colon ascendens in de M-SHIME werd een succesvolle kolonisatie, met name vooral van de mucosale micro-omgeving, geobserveerd. Dit ondanks de immense en diverse populatie darmbacteriën die reeds aanwezig waren voor aanvang van ETEC infectie. De effecten van ETEC op deze reeds aanwezige darm microbiota werden eveneens onderzocht. In het ileum bleef de microbiële diversiteit gehandhaafd, hoewel een proliferatie van opportunistische pathogenen werd waargenomen. In het colon ascendens, daarentegen werd een daling geconstateerd van enkele bacteriële soorten met potentiële gezondheidsbevorderende eigenschappen. Met betrekking tot de ETEC virulentie factoren, werd vastgesteld dat virulentie genen die instaan voor de productie van enterotoxines en adhesines doorgaans opregeruleerd werden in de

maag fase om vervolgens terug af te nemen in het ileum en colon ascendens. Het LT enterotoxine eiwit, echter, werd niet in de maag en enkel in het colon en ileum, de voornaamste ETEC infectie regio ,gedetecteerd.

In het tweede deel van onze studie, werden de anti-microbiële eigenschappen van *Saccharomyces cerevisiae* CNCM I-3856 ten opzichte van ETEC bestudeerd. Een profylactische toediening van deze probiotische stam, inhibeerde de ETEC adhesie aan mucine-agar en aan menselijk darmepitheel Caco-2/TC7 cellen in een dosis-afhankelijke manier. Bovendien, werd ETEC-geïnduceerde inflammatie in de Caco-2/TC7 cellijn tegengegaan door middel van Interleukine 8 inhibitie. Aan de hand van de voornoemde *in vitro* spijsvertering modellen, werd eveneens aangetoond dat de ETEC functionaliteit (virulentie gen expressie en LT toxine productie) ondermijnd werd. Dit in tegenstelling tot de ongewijzigde ETEC overleving. De proliferatie van opportunistische pathogenen (*Klebsiella, Achromobacter, Mycobacterium*) als gevolg van ETEC infectie, daarentegen, werd wel succesvol onderdrukt en enkele bacteriesoorten met potentieel gezondheid bevorderende eigenschappen leken toe te nemen (*Bifidobacterium, Faecalibacterium, Lactobacillus, Fusicatenibacter*). Tot slot, stimuleerde de probtioische gist de metabolische activiteit, met een significante stijging van zowel acetaat als propionaat productie.

Ter conclusie, dit doctotoraatsonderzoek heeft belangrijke inzichten opgeleverd omtrent de modulatie van ETEC overleving en virulentie, alsook, ETEC interactie met de darmmicrobiota in het menselijk spijsverteringsstelsel, gesimuleerd in de TIM-1 en M-SHIME *in vitro* modellen. Aldus, is dit onderzoek de eerste aanzet om de ETEC pathogenese in het spijsverteringsstelsel, wat vaak als een black box beschouw wordt, op te helderen. Het koppelen van menselijke darmepitheel cellijnen met de geavanceerde *in vitro* modellen is een noodzakelijke volgende stap om het volledige infectieproces te doorgronden. Ook de veelbelovende resultaten met de probiotische gist *S. cerevisiae* CNCM I-3856 vormen een interessante onderzoekspiste. In de toekomst zou de evaluatie van andere ETEC stammen interessant zijn om het probiotische effect beter te conceptualiseren.

RÉSUMÉ

Contexte scientifique de la thèse et objectifs principaux

Parmi les 13 agents étiologiques responsables de maladies diarrhéiques chez l'Homme (les bactéries *Clostridium difficile*, *Shigella spp.*, *Campylobacter*, *Vibrio cholerae*, ***Escherichia coli* enterotoxinogène (ETEC)**, *Escherichia coli* enteropathogène, *Salmonella* et *Aeromonas* ; les parasites *Entamoeba histolytica* et *Cryptosporidium spp.* ; et les virus adenovirus, rotavirus et norovirus), 6% de l'ensemble des cas retrouvés en 2015 étaient associés au pathogène ETEC, représentant annuellement près de 113 000 décès et 44 millions de cas de diarrhées.

Le **« fléau » ETEC** présente de considérables disparités en fonction de la tranche d'âge concernée mais aussi du niveau socio-économique des populations touchées. Le pathogène est principalement retrouvé dans les pays au climat tropical et à faible revenu tels que l'Afrique Subsaharienne, l'Asie du Sud et l'Amérique Latine. En effet, l'environnement insalubre et le manque de mesures d'assainissement des eaux rencontrés dans ces pays constituent des facteurs de risque à la propagation des ETEC dans **l'eau** de boisson.

Deux types de populations à risque sont distinguées, (i) les enfants vivants dans les pays en voie de développement, et (ii) les adultes voyageant dans ces régions endémiques, population cible de ce travail de thèse. La **diarrhée du voyageur**, communément appelée turista touche annuellement environ 22 millions de touristes, hommes / femmes d'affaires et militaires, soit 1 personne voyageant sur 6. Près de la moitié des cas recensés (10 millions d'individus) serait associée au pathogène ETEC. Les militaires résidant temporairement dans ces zones endémiques sont les plus exposés à ce risque d'infection et près de 70% des troupes déployées développeraient un épisode diarrhéique associé à ETEC. Enfin, ces dernières années des cas d'infections sporadiques ont été recensés dans les pays industrialisés suite à l'importation de produits frais contaminés par le pathogène et originaires de zones endémiques.

Chez l'adulte, une fois ingéré à une dose comprise entre 8 et 10 $\log_{10}$ bactéries, ETEC poursuit une stratégie des plus sophistiquée pour résister aux conditions drastiques de l'environnement digestif (acidité gastrique, sels biliaires, peptides antimicrobiens et microbiote intestinal). La bactérie exerce son pouvoir pathogène principalement au niveau de l'iléon distal, grâce à un ensemble de facteurs de virulence. Dans un premier temps, le pathogène dégrade la couche protectrice de mucus intestinal à l'aide de mucinases (EatA et YghJ), pour mieux accéder et coloniser la muqueuse intestinale par l'intermédiaire de **facteurs de colonisation** fimbriaux (CFA/I, FimH) et de protéines de la membrane externe (Tia, TibA, EtpA). L'adhésion d'ETEC va ensuite faciliter la production et le relargage d'une ou plusieurs **entérotoxines** thermolabiles (LT) et/ou thermostables (ST), en fonction du sérotype bactérien incriminé. La toxine LT, partageant 80% d'homologie avec la toxine cholérique (*Vibrio cholerae*), est sécrétée par le système de sécrétion de type 2 impliquant notamment la protéine LeoA, tandis que la

toxine ST est sécrétée par le système de pompes à efflux TolC. La production et le relargage de ces toxines au niveau de l'épithélium intestinal permettent l'activation d'une cascade de signalisation. Cette dernière provoque la fuite d'eau et d'électrolytes dans la lumière intestinale, à l'origine de diarrhées aqueuses abondantes de type cholériforme et d'une déshydratation.

Comme indiqué par les données épidémiologiques, la mortalité associée à ces infections reste faible, particulièrement chez le voyageur adulte comparativement au fort taux de morbidité chez les enfants dans les pays en voie de développement. De récentes études ont montré néanmoins que 10 à 14% des cas de diarrhées du voyageur associées à ETEC conduiraient à des complications chroniques assimilées à un **syndrome de l'intestin irritable post-infectieux**, se manifestant à long terme par des troubles du transit digestif et des douleurs abdominales. Au-delà de l'impact sanitaire, la prise en charge de ces infections génère d'importantes pertes économiques au niveau mondial.

A ce jour, aucun traitement reconnu et spécifique contre ETEC n'est commercialisé dans le monde La prise en charge de ces infections reste essentiellement symptomatique et suit les recommandations générales attribuées à tout épisode diarrhéique classique, incluant une réhydratation orale, l'usage d'anti-diarrhéiques ou de ralentisseurs de transit. Le recours à l'usage d'antibiotiques a également été fréquemment reporté, contribuant à l'augmentation croissante du phénomène d'**antibiorésistance** au niveau mondial et à son impact négatif sur la santé de l'Homme. Il est devenu alors nécessaire et urgent de développer de nouvelles stratégies visant à prévenir l'apparition des infections à ETEC.

L'ensemble de ces données épidémiologiques, cliniques et physiopathologiques soulèvent deux questions majeures: (i) **la nécessité d'une meilleure compréhension de la physiopathologie des ETEC dans l'environnement digestif humain**, en termes de survie et de virulence du pathogène et (ii) **le besoin de nouvelles stratégies préventives et/ou curatives** pour spécifiquement prendre en charge ces infections.

Jusqu'à présent dans le respect évident des contraintes éthiques chez l'Homme, les études cliniques visant à mieux comprendre la physiopathologie des ETEC ont été réalisées avec des dose infra-physiologiques du pathogène et/ou avec des souches génétiquement modifiées (atténuées) non virulentes. Alternativement, la majorité des études ont donc été conduites (i) chez l'animal tel que le porcelet largement concerné par les infections à ETEC, (ii) sur des modèles cellulaires de l'épithélium intestinal humain ou animal, et (iii) en modèles de digestion *in vitro* statiques et simples. Cependant, ces approches restent très éloignées de la physiologie digestive humaine et ne sont pas représentatives des environnements gastro-intestinaux (GI) successifs rencontrés par le pathogène.

Afin de pallier les limites de ces approches, des modèles *in vitro* dynamiques et multi-compartimentés de l'environnement digestif humain peuvent être utilisés, modèles reproduisant notamment le dynamisme du transit GI, l'arrivée séquentielle des sécrétions digestives, et la complexité des microenvironnements luminaux et associés à la muqueuse intestinale. Parmi ces modèles, le TNO gastro-intestinal model (**TIM-1**), reproduisant les principaux paramètres physico-chimiques du tractus GI haut (l'estomac et les trois parties de l'intestin grêle), ainsi que des modèles de fermentation colique

tels que le Mucosal Simulator of the Human Intestinal Microbial Ecosystem (**M-SHIME**) incorporant le microbiote intestinal luminal et mucosal (iléon et colon ascendant), représentent des systèmes innovants, pertinents et validés scientifiquement. Ces derniers permettent d'étudier de façon plus complète la pathogénicité des ETEC tout en appréhendant la complexité de la physiologie digestive humaine.

Comme mentionné ci-dessus, les mesures prophylactiques et/ou curatives des diarrhées associées à ETEC restent limitées. Les principales stratégies alternatives en cours de développement sont les vaccins, les stratégies nutritionnelles basées sur l'utilisation de micronutriments comme le zinc, les bactériophages, les prébiotiques, ou encore les **probiotiques**. Cependant, à ce jour, la plupart des études ayant évalué l'effet de probiotiques vis-à-vis des ETEC ont été conduites chez le porcelet, avec des sérotypes d'ETEC spécifiquement associés aux infections chez l'animal mais très rarement à celles chez l'Homme. De plus, la majorité des souches probiotiques étudiées étaient d'origine bactérienne, au détriment de souches levuriennes qui ont l'avantage d'être résistantes aux antibiotiques et n'échangent pas de matériel génétique avec les bactéries. Par ailleurs, de rares études ont montré un effet bénéfique de la levure *Saccharomyces boulardii* dans la réduction du risque des diarrhées du voyageur. Cependant, dans ces travaux, l'implication des ETEC dans les diarrhées du voyageur n'a pas été clairement identifiée. Enfin, un panel d'expert de l'International Society of Travel Medicine a récemment souligné l'insuffisance du niveau de preuves scientifiques permettant de recommander l'utilisation des souches probiotiques dans la prévention des diarrhées du voyageur. L'ensemble de ces données justifie pleinement l'intérêt de poursuivre les recherches sur les interactions entre probiotiques et ETEC.

Parmi les levures commercialisées comme probiotiques, ***Saccharomyces cerevisiae* CNCM I-3856** (brevetée par l'industriel Lesaffre, partenaire de ce travail de thèse), a déjà été reconnue scientifiquement pour ses propriétés inhibitrices intéressantes vis-à-vis d'autres *Escherichia coli* pathogènes, tels que les *E. coli* entérohémorragiques (EHEC) ou les *E. coli* adhérents et invasifs (AIEC) associés à la maladie de Crohn. Cette levure est notamment capable de limiter la reprise de croissance des EHEC dans les parties distales de l'intestin grêle du modèle *in vitro* TIM-1 et de réprimer l'expression du gène codant pour les toxines produites par ces bactéries dans un modèle colique *in vitro*. L'administration de la levure probiotique chez des souris colonisées par la bactérie AIEC a également permis d'améliorer la fonction de barrière intestinale et de réduire l'inflammation. Enfin, cette même levure a permis lors d'une étude clinique chez l'Homme, une amélioration significative des douleurs et/ou de l'inconfort abdominal chez des sujets souffrant du syndrome de l'intestin irritable. L'ensemble de ces propriétés nous a conduit à évaluer les effets antagonistes de la levure *S. cerevisiae* CNCM I-3856 vis-à-vis des ETEC.

Dans ce contexte, trois années de **cotutelles Européenne de thèse** entre deux laboratoires universitaires, l'unité mixte de recherche Microbiologie, Environnement Dlgestif et Santé (**UMR MEDIS**, Université Clermont-Auvergne, Clermont-Ferrand, France) et le Center for Microbial Ecology and Technology (**CMET**, Université de Gand, Gand, Belgique) ont permis de répondre à deux objectifs principaux : (i) **mieux comprendre les dynamiques de survie et de virulence de la souche de**

référence ETEC H10407 dans le tractus digestif humain, grâce à l'utilisation des systèmes de digestion et de fermentation *in vitro* TIM-1 et M-SHIME ; et (ii) **évaluer les propriétés antimicrobiennes de la levure probiotique *S. cerevisiae* CNCM I-3856 vis-à-vis de la souche ETEC H10407 grâce à l'utilisation de modèles *in vitro* simples et complexes**. La finalité de ce travail était d'envisager l'utilisation de cette levure comme approche préventive dans la lutte contre les infections à ETEC. En particulier, l'ensemble de cette étude s'est centré sur la population adulte et donc la prévention des diarrhées du voyageur.

Contexte organisationnel de la cotutelle de thèse

Pour la première fois, dans le cadre de cette thèse, un partenariat entre l'UMR MEDIS et le CMET a été mis en place. Ces deux laboratoires bénéficient de plus de 20 ans d'expertise et de savoir-faire internationalement reconnus dans les domaines de la digestion et fermentation artificielles. Ils ont tous deux développé un plateau technologique autour de l'environnement digestif associant des outils *in vitro* de digestion et de fermentation, des modèles cellulaires de l'épithélium intestinal humain, et des outils moléculaires de génomique et post-génomique. L'expertise en digestion artificielle représente ainsi le cœur biotechnologique de cette cotutelle de thèse. L'intérêt majeur de cette collaboration était d'associer de façon complémentaire le TIM-1 reproduisant l'estomac et l'intestin grêle (UMR MEDIS, France) et le M-SHIME reproduisant les parties distales de l'intestin grêle et le côlon (CMET, Belgique), afin de suivre pour la première fois le devenir d'ETEC tout le long du tractus digestif humain simulé, de l'estomac jusqu'au colon ascendant. Les interactions d'ETEC et/ou du probiotique avec le microbiote intestinal ont également été étudiées en détails grâce à l'expertise en écologie microbienne du CMET.

Le travail de thèse a été réparti de la manière suivante : les 18 premiers mois se sont déroulés en France, au sein de l'UMR MEDIS, où les expériences dans le TIM-1 ont été réalisées, tandis que les 18 derniers mois ont été effectués en Belgique, au sein du centre de recherche CMET, avec les expériences dans le M-SHIME.

Au-delà de ce partenariat académique, ce travail de thèse a fait l'objet d'un **partenariat avec l'industriel Lesaffre**, dont l'une des activités principales du groupe est le développement de levures probiotiques et de leurs produits dérivés dans le but de préserver la santé humaine. L'industriel Lesaffre s'est engagé à fournir la souche probiotique d'intérêt, la levure *S. cerevisiae* CNCM I-3856 et a également financé l'ensemble des expériences réalisées au cours de ces trois années de recherche.

Descriptif du contenu du manuscrit de thèse

Le manuscrit consiste tout d'abord en une revue de la littérature (section I) répartie en deux grands chapitres. Dans le chapitre 1, une première partie a compilé l'ensemble des données épidémiologiques récentes pour chacune des populations à risque (enfants et adultes), des données cliniques, ainsi que des éléments sur la physiopathologie générale d'ETEC. Les principaux facteurs de virulence connus pour la souche de référence ETEC H10407, isolée chez un adulte au Bangladesh en 1977, et utilisée dans ce travail de thèse ont été décrits.

La seconde partie de ce chapitre est dédiée à la présentation de la physiologie digestive humaine et des principaux **paramètres digestifs biotiques et abiotiques**. Ce travail de synthèse a été réalisé dans le but de mieux appréhender les données déjà connues sur la capacité d'ETEC à utiliser les **signaux GI** pour moduler à la fois sa survie et sa virulence tout au long du tractus digestif. Ce travail a fait l'objet d'un chapitre scientifique d'ouvrage, édité dans le livre *Escherichia coli (édition IntechOpen, 2017)*. Nous avons pu à l'issu de ce travail de revue de la littérature, identifier qu'un grand nombre de pièces du « puzzle » était absent et qu'il manquait des éléments permettant la compréhension de la pathogénicité d'ETEC dans l'environnement digestif humain. Au-delà de la rareté des travaux et du manque de modèles appropriés (comme précédemment évoqué), beaucoup d'études ont été réalisées en modèles *in vitro* statique où seul l'effet d'un paramètre digestif a été étudié, et d'autres limites ont été identifiées. Par exemple, la majeure partie de ces études n'ont évalué que l'effet d'une exposition des ETEC à un pH acide ou à une concentration élevée en sels biliaires, connus pour leurs propriétés lytiques des membranes bactériennes. Bien que ces deux facteurs représentent des stress dominants de l'environnement digestif, d'autres paramètres tout aussi importants dans la pathogénicité tels que l'effet des enzymes digestives, du niveau d'oxygène, et surtout les interactions du pathogène avec le microbiote intestinal, ont été en revanche majoritairement ignorés. Un autre constat était l'absence de justification dans le choix de certaines concentrations (e.g. les concentrations en sels biliaires), parfois anormalement élevées par rapport aux données de la physiologie humaine, et l'incohérence des concentrations choisies entre plusieurs études.

Cette étude de la littérature a pleinement confirmé l'intérêt d'utiliser des modèles *in vitro* plus complexes et compartimentés, comme le TIM-1 et le M-SHIME qui reproduisent au mieux la physiologie digestive humaine. Les potentialités de ces modèles ont également été comparées à celles d'autres modèles *in vitro* existant mono, bi et/ou multi-compartimentés au niveau mondial. Incontestablement, le TIM-1 et M-SHIME restent les modèles de digestion et de fermentation les plus complets, performants et validés scientifiquement.

Dans le chapitre 2, l'ensemble des stratégies thérapeutiques de lutte contre les infections à ETEC, actuellement en cours de développement, ont été décrites et dans le cadre de l'objectif de cette thèse, la stratégie probiotique a été particulièrement ciblée. A ce titre, une revue de la littérature compilant de manière exhaustive les données disponibles sur ETEC et probiotiques a été publiée dans le journal *Future Microbiology (2017)*. L'ensemble des travaux répertoriés ont été classés selon les trois

principaux modes d'action des probiotiques connus vis-à-vis des pathogènes entériques : (i) **l'antagonisme direct** où le probiotique agit directement en inhibant la croissance d'ETEC et/ou en diminuant la virulence du pathogène, par exemple via la sécrétion de composés antimicrobiens; (ii) **l'exclusion compétitive** où le probiotique diminue l'adhésion du pathogène aux cellules épithéliales intestinales, augmente l'intégrité de la barrière intestinale, module la composition et l'activité du microbiote intestinal ou encore acidifie le milieu luminal pour limiter la survie du pathogène et enfin, (iii) **l'immunomodulation** ou modulation du système immunitaire de l'hôte par le probiotique permettant notamment de limiter la capacité du pathogène à induire une réponse inflammatoire (e.g. diminution de la sécrétion de cytokines pro-inflammatoires). Cette revue de la littérature a également permis de mettre en avant les limites actuelles de la stratégie probiotique, principalement étudiée chez le porcelet et rarement en conditions digestives humaines. De plus, les travaux réalisés jusqu'à présent sont essentiellement descriptifs, les mécanismes d'action des probiotiques sont peu connus et restent pour la plupart à élucider, ce qui réaffirme l'intérêt de ce travail de thèse. Pour terminer le chapitre 2, les principales propriétés déjà connues des levures probiotiques en général et de la souche utilisée *S. cerevisiae* CNCM I-3856 ont été reportées.

Ensuite, la partie expérimentale de ce travail de thèse (section II) s'articule autour de cinq grands chapitres. Les principaux objectifs et méthodes sont détaillés par la suite pour chaque chapitre.

Le chapitre 1 présente d'un point de vue méthodologique les expériences menées dans le TIM-1 qui permettent de comparer différentes méthodes d'évaluation de la viabilité des ETEC dans les compartiments gastriques et intestinaux. Les méthodes classiques de dénombrement sur milieu gélosé, les méthodes moléculaires de qPCR utilisant le marquage au propidium monoazide (PMA) et les techniques de cytométrie en flux utilisant le marquage Live/Dead ont ainsi été comparées. Cette étude a démontré la pertinence de l'utilisation des techniques moléculaires PMA-qPCR et de la cytométrie en flux pour caractériser efficacement les bactéries viables et mortes. Pour une analyse plus fine des états physiologiques du pathogène, la cytométrie en flux s'est révélée être la méthode de choix. En effet, quatre sous-populations d'ETEC ont pu être discriminées dans l'environnement digestif simulé en fonction de l'intégrité membranaire du pathogène (viable, viable/altéré, altéré/mort, mort). Etre capable d'identifier qualitativement et quantitativement ces sous-populations, initialement non identifiables sur gélose, est d'un grand intérêt pour mieux comprendre les dynamiques de survie et de virulence d'ETEC dans l'environnement digestif.

Le chapitre 2 évalue l'effet des paramètres physicochimiques de la digestion sur les dynamiques de survie et de virulence d'ETEC de l'estomac au colon ascendant, reproduit par les modèles TIM-1 (de l'estomac à l'iléon) et M-SHIME (de l'iléon au colon ascendant). Plus précisément, ces systèmes ont été utilisés pour reproduire les conditions de **digestion et/ou de fermentation d'un adulte sain** observées suite à l'ingestion d'un verre d'eau contaminé par ETEC à une quantité finale de 10 $\log_{10}$ UFC (unité formant colonie). Pour le TIM-1, intégrant les principaux **paramètres physicochimiques** de la digestion humaine mais dépourvu du microbiote intestinal, deux types d'expériences ont été

réalisées : des **digestions gastriques** où seul l'estomac du système a été utilisé (digestions de 60 min), et des **digestions GI** utilisant le modèle au complet, de l'estomac à l'iléon (digestions de 300 min). Le modèle M-SHIME, quant à lui, dans la configuration utilisée au cours de ce travail de thèse, intègre les principaux paramètres abiotiques de l'iléon et du colon ascendant ainsi que le **microbiote intestinal de l'Homme** grâce à l'inoculation dans les bioréacteurs de microbiotes fécaux issus de six donneurs sains différents (trois hommes et trois femmes adultes). Les **environnements microbiens ont été reproduits à la fois longitudinalement et transversalement** : (i) pour la première fois, le microbiote intestinal spécifique de **l'iléon** du M-SHIME a été reproduit grâce à une inoculation répétée et rétrograde à faible dose du contenu microbien issu du **colon ascendant** du système ; (ii) les **microenvironnements luminaux et mucosaux** ont été distingués par l'incorporation de microcosmes tapissés de mucine porcine de type III introduits dans chacun des bioréacteurs de l'iléon et du colon ascendant. Les fermentations en M-SHIME ont été conduites sur 20 jours consécutifs avec une période de pré-infection de jour 0 à 12 pendant laquelle les environnements microbiens ont été stabilisés, l'infection d'ETEC à jour 13, et une période de post-infection de jour 14 à 20. La survie d'ETEC a été déterminée par les méthodes mises en place dans le chapitre 1. L'état physiologique du pathogène a aussi été mieux appréhendé en mesurant le potentiel de membrane et le pH intracellulaire d'ETEC par des techniques de cytométrie en flux. Enfin la virulence d'ETEC a été évaluée par transcription inverse quantitative en temps réelle (RT-qPCR) avec un total de sept gènes de virulence suivis et codant pour : les entérotoxines LT et ST (*eltB* et *estAB*), les systèmes de relargage de la toxine LT et ST (*leoA* et *tolC*), les adhésines CFA/I, Tia et FimH (*cfa/Ib*, *tia*, *fimH*) et le facteur de réponse au stress RpoS (*rpoS*). Au niveau protéique, la production de l'entérotoxine LT a été mesurée par ELISA.

En continuité avec les expériences dans le M-SHIME décrites dans le chapitre 2, le chapitre 3 tente d'élucider grâce au séquençage nouvelle génération de l'ADN bactérien, l'effet de l'infection à ETEC sur la modulation du microbiote de l'iléon / colon ascendant et de son activité métabolique (production des acides gras à chaines courtes -AGCC-). La variabilité interindividuelle des six donneurs fécaux a été étudiée. Ce chapitre décrit également brièvement la signature microbienne et métabolique du compartiment iléal, nouvellement mis au point dans le M-SHIME et intégrant désormais, comme la partie colique, les microenvironnements luminaux et mucosaux.

Le chapitre 4 évalue en modèles *in vitro* simplifiés et *in vivo* (en modèle murin) les propriétés antimicrobiennes de la levure *S. cerevisiae* CNCM I-3856 vis-à-vis de la souche de référence ETEC H10407. Une série de tests complémentaires utilisant des milieux de culture simples, des tests d'adhésion à la mucine, des modèles cellulaires de l'épithélium intestinal humain (cellules Caco-2) et des tests *in vivo* chez la souris ont été conduits.

Enfin, suite aux propriétés encourageantes démontrées en systèmes plus simples dans le chapitre 4, le chapitre 5 étudie de façon plus complète et dans des conditions *in vitro* les plus proches possibles de la physiologie digestive humaine les propriétés antimicrobiennes de la levure *S. cerevisiae* CNCM I-3856 sur les dynamiques de survie et de virulence d'ETEC dans les deux modèles TIM-1 et M-SHIME. De plus, ce chapitre étudie la capacité de la levure à moduler l'environnement microbien luminal et

mucosal de l'iéon et du côlon ascendant, ainsi que l'activité métabolique microbienne. Toutes les techniques décrites dans les chapitres 2 et 3 ont également été utilisées dans ce chapitre. Le probiotique a été co-administré avec le pathogène à une dose unique de 10 $\log_{10}$ UFC lors des expériences dans le TIM-1. En revanche, le probiotique a été pré-, co- et post-administré à une dose répétée de 10 $\log_{10}$ UFC deux fois par jours dans le M-SHIME de jour 2 à 20. Ces doses ont été choisies pour simuler une posologie classique qui pourrait être recommandée aux adultes voyageant dans des zones à risque d'infections à ETEC.

Les principaux résultats expérimentaux et éléments de discussion décrits dans les différents chapitres sont scindés en deux principales parties pour répondre aux deux questions de la thèse qui sont pour mémoire : (i) mieux comprendre la physiopathologie d'ETEC H10407 dans l'environnement digestif humain simulé et, (ii) évaluer les propriétés antagonistes de la levure probiotique *S. cerevisiae* CNCM I-3856 vis-à-vis d'ETEC H10407 en modèles *in vitro* simples et complexes.

(i) Mieux comprendre la physiopathologie d'ETEC H10407 dans l'environnement digestif humain simulé (chapitres 1, 2 et 3)

De façon originale, la modulation de la survie et de la virulence d'ETEC dans l'environnement digestif humain simulé a été décrite de manière spatio-temporelle. Les résultats ont montré qu'une mortalité d'ETEC survenait au cours de la digestion gastrique (TIM-1, chapitre 2). En effet, dans l'estomac, le pathogène est rapidement exposé à un pH acide se situant à pH 3.2 dès 10 min de digestion et atteignant 1.8 après 60 min de digestion. En accord avec ces données de survie, une augmentation du nombre de bactéries possédant des membranes endommagées (état intermédiaire et potentiellement réversible) ainsi qu'un pH cytoplasmique très bas (proche de 3) a été observé.

Dans le duodénum, la concentration élevée en sels biliaires spécifiquement retrouvée lors de la 1ère heure de digestion (en accord avec les données de la physiologie digestive humaine) est probablement à l'origine d'une importante mortalité d'ETEC jusqu'à 120 min de digestion. Dans les compartiments inférieurs de l'intestin grêle (jéjunum et iléon), les conditions digestives plus favorables à la survie du pathogène, notamment la ré-augmentation progressive du pH, la réabsorption passive des sels biliaires (système de dialyse présent dans le TIM-1) et la dilution des sécrétions digestives (jus pancréatique), ont permis une reprise de croissance du pathogène en fin de digestion dans le jéjunum et l'iléon. La restauration de l'intégrité membranaire d'ETEC, et le retour à un pH cytoplasmique proche de l'alcalinité ont aussi confirmé un meilleur état physiologique des bactéries dans les parties distales de l'intestin grêle. Des travaux antérieurs à ce travail de thèse dans l'UMR MEDIS avaient également démontré la capacité d'un autre pathotype d'*E. coli*, EHEC à reprendre sa croissance en fin de digestion intestinale.

Dans le M-SHIME, la présence du microbiote intestinal n'a pas empêché le pathogène de persister à une concentration élevée dans tous les environnements luminaux et mucosaux de l'iléon et du colon ascendant, et ce jusqu'à 5 jours post-infection. La remarquable capacité du pathogène à adhérer à la mucine en présence (chapitre 2) et en absence (chapitre 4) du microbiote intestinal a été mise en

évidence pour la première fois dans cette étude. En effet, nous avons montré que la souche d'ETEC étudiée était capable d'adhérer à un taux très élevé à la mucine (près de 50% lors de tests *in vitro* simples). Dans le M-SHIME, grâce à ce mécanisme d'attachement mucosal, la partie luminale a été continuellement ensemencée par le pathogène, ce qui a limité ainsi son élimination naturelle lors de la vidange intestinale.

L'ensemble de ces résultats obtenus dans le TIM-1 et M-SHIME révèlent ainsi l'adaptation remarquable d'ETEC aux environnements GI rencontrés (modification réversible de sa physiologie membranaire), mais aussi la possibilité qu'a le pathogène d'utiliser des niches écologiques telle que le mucus intestinal pour se maintenir dans l'environnement digestif, tout particulièrement au niveau de son site d'action dominant, l'iléon.

Pour la première fois, la signature microbienne de l'iléon a été reproduite dans le M-SHIME (chapitre 3). En accord avec les données de la littérature sur l'écologie digestive microbienne humaine, cette signature iléale se caractérise par une remarquable diminution de la diversité microbienne et de son activité métabolique associée (concentration en AGCC), comparativement aux régions coliques d'une diversité supérieure associée à une concentration élevée en AGCC. En effet, le microbiote de l'iléon est spécialisé dans l'utilisation et la conversion rapide des sucres simples, et est dominé par des genres bactériens à croissance rapide et anaérobies facultatifs tels que *Enterobacteriaceae*, *Veillonella*, *Clostridium* et *Klebsiella*. Au contraire, le microbiote colique se montre plus efficace dans la dégradation et la fermentation de sucres complexes par des anaérobies strictes tels que *Bacteroides*, *Faecalibacterium* et *Bifidobacterium*.

Le changement des populations microbiennes intestinales humaines à la suite de l'infection à ETEC, très peu étudié jusqu'à présent, a été exploré dans ce travail. L'unique administration d'ETEC n'a pas eu d'impact sur l'indice de diversité microbienne, mais a en revanche déséquilibré certaines communautés microbiennes, potentiellement associées à un état de dysbiose intestinale, même si il faut rester prudent quant à l'usage de cette terminologie. Malgré la variabilité interindividuelle dans la composition phylogénétique microbienne, l'infection à ETEC semble induire le développement de pathogènes opportunistes dans l'iléon tels que *Klebsiella*, *Achromobacter* et *Mycobacterium* ainsi que dans le colon ascendant tels que *Paraprevotella*. A contrario, certaines espèces ayant de potentiels effets bénéfiques sur la santé (tels que reporté dans de précédentes études) ont été significativement diminuées dans le colon ascendant, comme par exemple, *Bifidobacterium angulatum*, *Gemmiger formicilis* ou *Fusicatenibacter saccharivorans*. A la suite de l'infection à ETEC, l'activité métabolique n'a pas subi de changement majeur, à l'exception de l'augmentation de la concentration en propionate notée chez trois des six individus. Comme précédemment évoqué, à la suite d'une diarrhée du voyageur, des complications chroniques peuvent survenir telles qu'un syndrome de l'intestin irritable post-infectieux. Nous avons montré que l'infection à ETEC était associée à une diminution significative de l'abondance de l'actinobactérie *Collinsella aerofaciens* et de membres bactériens appartenant au genre *Bifidobacterium*, modifications considérées comme des « marqueurs » présumés du syndrome de l'intestin irritable post-infectieux, mises en évidence dans de précédentes études. Bien que cette

bactérie ne soit bien sûr pas une preuve suffisante à la définition de ce syndrome, ce résultat offre des perspectives intéressantes à ce travail de thèse dans la définition de marqueurs microbiologiques associés à cette pathologie.

Un autre aspect évalué lors de cette recherche était l'étude de la virulence d'ETEC en systèmes digestifs *in vitro*. De façon non surprenante, les profils d'expression des gènes de virulence d'ETEC ont fortement différé entre le TIM-1 et le M-SHIME, puisque ces deux modèles ne reproduisent pas les mêmes paramètres. Dans le M-SHIME, les gènes ont été suivis uniquement dans la partie luminale. Une importante variabilité interindividuelle a été observée parmi les six donneurs représentés. Dans l'ensemble (chapitre 2), les gènes suivis (codant pour les adhésines et les toxines) tendaient à être surexprimés dans l'estomac, à l'exception du gène *eltB* codant pour la toxine LT, et étaient sous exprimés dans les effluents iléaux du TIM-1 et M-SHIME, ainsi qu'en phase tardive de post-infection dans le colon ascendant du M-SHIME. Le gène *eltB* était surtout surexprimé dans le colon ascendant, tandis que le gène *estAB*, codant pour la toxine ST, était plutôt surexprimé dans l'estomac et le colon ascendant. L'expression des gènes codant pour les deux entérotoxines n'a ainsi pas été corrélée dans le tractus digestif *in vitro*, confirmant le fait que *eltB* et *estAB* ne sont pas régulés de la même façon, comme déjà suggéré dans d'autres études en systèmes *in vitro* plus simples. Au niveau protéique, aucune production de la toxine LT n'a été observée dans l'estomac en accord avec les données de la littérature montrant que la production de cette toxine est pH-dépendante et induite uniquement à pH alcalin. De façon intéressante, de plus hautes concentrations en toxines ont été retrouvées dans le colon ascendant pour certains donneurs en comparaison à l'iléon, site d'action principal du pathogène. De manière générale, l'expression du gène *eltB* n'était pas corrélée à la production la toxine LT, signe de l'existence de régulations post-transcriptionnelles et/ou post-traductionnelles importantes.

Enfin, pour mieux comprendre la susceptibilité individuelle aux infections à ETEC, une régression linéaire entre la composition du microbiote intestinal et les profils de virulences a été effectuée (chapitre 3). Bien que le model soit limité aux échantillons recueillis dans le colon ascendant 5 h post-infection, nous avons observé une co-occurrence du gène *eltB* avec les genres bactériens *Coprococcus* et *Allisonella*. Et une co-occurrence entre *Enterobacteriaceae* (ETEC) et la production de la toxine LT, ainsi que l'expression du gène *estAB*, a également été observée. Enfin, la production de la toxine LT et l'expression du gène *estAB* étaient négativement corrélées à la production d'acétate et de propionate, tandis que la production de butyrate était positivement corrélée à la production de la toxine LT. Ces résultats renforcent le fait que les deux gènes codant pour les toxines ne sont pas régulés de la même manière. Ces résultats sont totalement originaux et aucune donnée portant sur l'influence du microbiote et/ou des métabolites AGCC sur la pathogénicité d'ETEC n'est à ce jour disponible pour discuter les données obtenues.

Ce travail de thèse a ainsi permis de compléter quelques pièces du puzzle, parmi les nombreuses pièces toujours manquantes à la compréhension de la physiopathologie d'ETEC dans l'environnement digestif humain. Les modèles TIM-1 et M-SHIME se sont révélés être très pertinents dans cette étude

de par l'intégration du dynamisme des phénomènes de digestion et la reproduction des environnements digestifs successifs. Les expériences doivent être poursuivies afin d'étayer ces résultats et d'apporter de nouveaux aspects mécanistiques permettant de mieux expliquer les interactions observées entre paramètres physicochimiques de la digestion, microbiote intestinal, production en AGCC et facteurs de virulence d'ETEC. Tester chaque paramètre de la digestion de façon individualisée dans des valeurs physiologiques pourrait par exemple aider à dé-complexifier les résultats obtenus en rapport avec l'expression des facteurs de virulence. Dans des perspectives plus lointaines, la composante « hôte » qui manque aux approches *in vitro* utilisées dans ce travail, pourrait être ajoutée grâce au couplage des modèles avec des cellules intestinales en culture (cellules Caco-2 et HT-29MTX). Ainsi, l'ensemble des données nouvelles obtenues en terme de physiopathologie sont essentielles pour développer de nouvelles stratégies préventives et/ou thérapeutiques de lutte contre les infections à ETEC.

(ii) Evaluer les propriétés antagonistes de la levure probiotique S. cerevisiae CNCM I-3856 vis-à-vis d'ETEC H10407 en modèles in vitro simples et complexes (chapitres 4 et 5)

A la suite d'une phase de screening (six premiers mois de la thèse) où six souches probiotiques (3 levures et 3 bactéries) fournies par l'industriel Lesaffre ont été testées afin d'évaluer leurs propriétés antagonistes vis-à-vis de la souche de référence ETEC H10407, la souche *S. cerevisiae* CNCM I-3856 a été retenue. **Ce travail de thèse a permis d'obtenir des preuves encourageantes quant au potentiel inhibiteur de cette souche de levure probiotique vis-à-vis d'ETEC**. Les résultats obtenus sont résumés selon les trois grands mécanismes d'action du probiotique, définis précédemment : antagonisme direct, exclusion compétitive et immunomodulation. Avant de détailler ces mécanismes d'action, il est important de souligner que la survie de la levure probiotique n'a pas été impactée par l'acidité gastrique et/ou la présence de sels biliaires, et a ainsi été remarquablement maintenue dans le tractus digestif haut simulé par le TIM-1. Dans la tractus digestif bas, intégrant le microbiote intestinal et simulé par le M-SHIME, l'administration répétée du probiotique a été nécessaire pour le maintien de concentrations élevées en probiotique pendant les 20 jours de fermentation.

En termes d'antagonisme direct, nous avons montré que le probiotique agit préférentiellement en altérant la fonctionnalité d'ETEC. En effet, bien qu'en milieu de culture une diminution de la croissance d'ETEC a été observée en présence de la souche de levure, globalement dans les compartiments GI du TIM-1 et du M-SHIME, le probiotique n'a pas eu d'effet direct significatif sur la survie du pathogène. Néanmoins, le probiotique semble perturber l'état membranaire d'ETEC dans le TIM-1 avec une augmentation du nombre de cellules présentant des membranes endommagées (entrant dans un état physiologique intermédiaire), ainsi que le nombre de cellules mortes, comme déterminé par cytométrie en flux. Nous avons émis l'hypothèse que la forte production en éthanol, mesurée en présence du probiotique pourrait être l'un des mécanismes à l'origine de cette perturbation membranaire. En effet, ce solvant organique a déjà été reconnu pour ses propriétés antibactériennes.

La modulation de la virulence d'ETEC par le probiotique est l'un des effets les plus remarquables observés dans cette étude. Au niveau transcriptionnel, les gènes *eltB* et *estAB* codant pour les entérotoxines sont généralement sous-exprimés en présence du probiotique dans le TIM-1 et dans le M-SHIME, bien que ces conclusions soient moins nettes dans le M-SHIME en raison de l'importante variabilité interindividuelle. De façon très intéressante, une surexpression du gène *fimH* codant pour une des sous-unités protéiques du pili de type 1 a été notée tout au long des effluents iléaux du TIM-1 en présence du probiotique, alors que le gène n'est pas exprimé en condition contrôle. D'un point de vue mécanistique, la surexpression du gène *fimH* pourrait être associée aux interactions physiques entre la levure et ETEC, ou agglutination, comme observées dans le chapitre 4. Ce mécanisme, appartenant à l'exclusion compétitive, est expliqué de façon plus précise dans la section correspondante.

Au niveau protéique, les travaux initiés dans le chapitre 4 avaient démontré que la co-administration de la levure avec le pathogène en milieu de culture, permettait une diminution de la production de la toxine LT. Cette même propriété du probiotique a été observée dans les deux systèmes digestifs TIM-1 et M-SHIME confortant les premiers résultats obtenus. Quant au mécanisme d'action sous-jacent, plusieurs hypothèses ont été émises. Même si la levure est généralement peu reconnue pour produire des composés antimicrobiens (autre que l'éthanol), de précédents travaux ont montré la capacité d'une souche *S. boulardii* d'hydrolyser grâce à la production d'une protéase la toxine produite par *Clostridium difficile*. Une autre possibilité serait la « capture » de la toxine par la levure, la toxine se fixant sur des récepteurs portées par la levure, l'empêchant ainsi de se lier au récepteur des cellules intestinales de l'hôte. Des études complémentaires sont nécessaire pour confirmer ou non ces hypothèses.

L'exclusion compétitive a été démontrée à plusieurs niveaux, au travers de différentes expériences conduites tout au long de cette thèse. Notamment, l'administration préventive du probiotique a permis d'inhiber l'adhésion d'ETEC à la mucine et aux cellules épithéliales intestinales humaines Caco-2/TC7 de façon dose-dépendante, comparativement à la condition contrôle où le pathogène était fortement adhérent. En modèle murin, l'administration répétée du probiotique a également conduit à une réduction significative de la colonisation d'ETEC dans l'iléon, site d'action principal du pathogène.

Comme évoqué un peu plus haut, un phénomène d'agglutination entre la levure probiotique et ETEC a été observé lors de cultures simples. Le mécanisme sous-jacent pourrait être associé au mannose. En effet, nous avons montré une surexpression du gène codant pour une sous unité du pili de type 1 dans le TIM-1. Dans de précédentes études, il a été démontré que la sous-unité FimH du pili de type 1 était capable de se lier aux mannanes présentes à la surface de la levure *S. cerevisiae*. Ce mécanisme permettrait la « capture » d'ETEC, et pourrait expliquer l'inhibition de l'interaction du pathogène avec la muqueuse intestinale en présence du probiotque. D'autres mécanismes explicatifs ne sont pas à exclure, comme l'encombrement stérique. De façon pragmatique, la levure présente en moyenne une taille dix fois supérieure à celle de la bactérie, pouvant ainsi « gêner » l'accès direct d'ETEC à l'hôte. Enfin, un autre mécanisme possible (déjà montré avec d'autres souches de probiotiques) mais non

étudié ici serait la stimulation de la production de la mucine intestinale par la levure probiotique, limitant là encore le phénomène d'adhésion.

Dans le système M-SHIME, l'administration du probiotique a contribué à l'augmentation d'espèces ayant des effets potentiellement bénéfiques sur la santé humaine (d'après des données issues de la littérature) appartenant aux genres bactériens *Bifidobacterium*, *Faecalibacterium*, *Lactobacillus* ou *Fusicatenibacter*. De plus, une diminution qualitative et quantitative de certaines espèces considérées comme pathogènes opportunistes (initialement induites par l'infection à ETEC) a été observée en présence du traitement au probiotique comme les genres *Achromobacter*, *Mycobacterium* et *Klebsiella*. Le traitement a également induit une nette augmentation de la concentration en AGCC dans le colon ascendant, à la fois des AGCC majoritaires tels que acetate, propionate ou butyrate, mais aussi d'autres plus mineurs comme le caproate. Une telle augmentation de ces concentrations en AGCC pourrait conduire à une diminution du pH luminal *in vivo*. Cependant, les conditions expérimentales du M-SHIME n'ont pas permis d'étudier cet effet puisque le pH est contrôlé tout au long de la période de fermentation. Enfin, la contribution relative de chacun de ces métabolites dans la modulation de la virulence d'ETEC n'a pu être déterminée pour l'instant.

L'immunomodulation a été le mécanisme d'action le plus étudié dans les travaux réalisés par d'autres équipes en modèle porcelet. Bien que l'étude de ce mécanisme d'action est limitée dans ce projet de thèse, nous avons montré que l'induction de la production de la cytokine pro-inflammatoire IL-8 en cellules Caco-2/TC7, suite de l'infection à ETEC, était significativement inhibée par le prétraitement au probiotique, et ce, de façon dose-dépendante (chapitre 4). D'autres cytokines ou voies de signalisation pro-inflammatoires doivent être étudiées pour renforcer les conclusions sur le potentiel effet immunomodulateur de la levure probiotique.

Pour conclure, les propriétés antimicrobiennes de la levure probiotique *S. cerevisiae* CNCM I-3856 vis-à-vis de la souche ETEC H10407 ont été démontrées dans ces travaux grâce à un large panel de techniques utilisées allant de systèmes *in vitro* simples à des outils complexes de digestion et fermentation artificielles, et à un modèle *in vivo* murin. Ces résultats très encourageants méritent néanmoins d'être complétés par de nouvelles investigations. En effet, pour apporter encore plus de puissance scientifique à ces résultats, il serait nécessaire de tester l'effet antimicrobien du probiotique vis-à-vis de différents sérotypes d'ETEC ou d'étendre l'étude à d'autres populations à risque comme l'enfant. Ainsi, de nouvelles séries d'expériences de digestion/fermentation TIM-1 et M-SHIME pourraient être conduites en utilisant des protocoles permettant la simulation des conditions digestives de l'enfant. Si les résultats très encourageants obtenus lors de ce travail de thèse sont confirmés, l'efficacité du probiotique pourrait à son tour être confirmée lors d'une étude clinique chez l'Homme.

REMERCIEMENTS-ACKNOWLEDGMENTS

Mes premiers mots vont à mes directeurs de thèse Stéphanie Blanquet-Diot et Tom Van de Wiele.

Stéphanie, je me dois de reconnaitre que ton accompagnement dans ce long travail de thèse est inestimable ! En plus de ton appui scientifique, j'ai été touchée par tes gentilles attentions, ton écoute, ton importante disponibilité et ce, malgré mon expatriation en Terres Belges. Un grand merci pour tes encouragements, ta confiance dans mon travail de recherche et la mise en valeur de celui-ci. Tes grandes exigences m'ont également poussé vers le haut et le souci du détail. De plus, je te suis très reconnaissante de m'avoir rapidement intégré dans de nombreuses collaborations et publications scientifiques. Merci pour tes brillants conseils et méticuleuses corrections que ce soit lors de la rédaction de mon manuscrit de thèse ou de présentations power point. Enfin je te remercie de m'avoir permis de participer à de nombreux congrès en France comme à l'étranger et d'avoir partagé en ta compagnie quelques moments rigolo et atypiques lors de nos visites en Terres Etrangères.

Tom, I am very much appreciative to your guidance and tremendous support during my PhD despite your impressive busy schedules ! Your genuine serenity was essential for me to offset my doubts, my stress, to tone down some situations and feel more confident. Thanks to you, I also learned a lot from your research expertise, I gained greater independence and better recognized the value of my work. Thank you for helping me to summarize my idea, your insightful advice and corrections. Thank you for your generosity, you and Stéphanie gave me so many wonderful opportunities to travel in the frame of my research. Thank you for all your suggestions in general and career advice. You figured out my wish and help me to found my future postdoc in Canada with Yves Desjardins's group. I am so grateful for that ! It was finally pleasant to discover our common interest for cloud types and astronomy.

Kim, thank you for being my mentor with so much dedication in this last PhD year, it means a lot to me. This research on the SHIME experiments could not have been completed without your help in post-processing the data and solving problems. I am so grateful for that! Thank you for sharing with me all your skills and in-depth knowledge in Microbial ecology so willingly. I would also like to thank you for your thorough advice and corrections of my PhD manuscript. You are a kind and talented person. I wish you lots of success in your future projects and good luck in Vienna !

I would also like to thank my jury members for reading this PhD dissertation : ***Prof. Marion Leclerc***, ***Prof. Sarah Lebeer***, ***Prof. Marc Heyndrickx*** and ***Prof. Nicolas Barnich***, I enjoyed the fruitful discussions during the internal defence. I am grateful to your valuable input that improved the quality of my manuscript. ***Prof. Mike Uyttendaele***, thank you for taking up the task of chairman in Belgium.

Je remercie l'ensemble des personnes de L'UMR MEDIS et tout particulièrement : ***Sandrine***, un grand merci pour ton soutien et ton aide depuis mes débuts dans le laboratoire. Ton savoir-faire expérimental mais aussi ton dynamisme, ta bonne humeur ainsi que ton petit grain de folie m'ont été très appréciable et indispensable pour surmonter les quelques déconvenues de notre capricieux TIM. Merci également pour avoir spontanément aménagé ton rythme de travail à mes besoins lors de nos manip' TIM à VetagroSup. ***Sylvain***, merci pour ta sympathie, ton soutien tout au long de mon parcours, ton aide ainsi que tes précieux conseils nécessaire à la bonne réalisation de mes expériences. Je remercie également ***Monique***, ***Emmanuelle***, ***Suenia***, ***Gislain*** et ***Eric***, pour avoir participé de près ou de loin à mon projet de thèse, pour leur enthousiasme ainsi que nos échanges conviviaux lors de nos repas au RDC. Merci à mes anciens camarades secrétaires, stagiaires, doctorants et post doctorants qui ont permis chacun à leur manière de rendre ce travail de thèse plus agréable : ***Charlotte***, ***Clémence***, ***Hassana***, ***Raphaële Manon***, ***Caroline***, ***Alice***, ***Florelle***, ***Nicolas G***, ***Mickaël***, ***Ali***, ***Nicolas T***, ***Kevin***. ***Manon***, j'ai apprécié mes moments accoudés à ton « comptoir » et je te remercie aussi pour ton aide dans la réalisation des tâches administratives. J'envoie toutes mes bonnes ondes à ***Raphaële*** et ***Ali*** qui vont goûter dans les prochains mois aux joies de la rédaction de la thèse. ***Florelle***, merci pour ton investissement, ta gentillesse et ta jovialité. Je souhaite bon courage à ***Thomas***, successeur de la thématique ETEC.

Lucie, merci pour ta grande sympathie, tes encouragements à distance, avec quelques regrets de ne pas t'avoir connu avant.

Merci aux équipes externes avec qui j'ai eu la joie de collaborer, notamment à VetagroSup avec **Wessam**, **Françoise**, **Sylvie** et **Karine**, merci pour votre accueil et votre sympathie. **Wessam**, j'ai été ravie de notre collaboration et d'apprendre à tes côtés. Je te remercie aussi pour ta grande disponibilité et pour avoir toujours répondu à mes nombreux appels lors de ces derniers mois de thèse. J'ai été très touchée par tes encouragements et te souhaite une très belle réussite à Lyon. L'UMR M2iSH et plus particulièrement, **Adeline**, merci pour ton énergie, ton implication dans mon projet de thèse ainsi que tes précieux conseils. Je remercie également le groupe Lesaffre et en particulier **Nathalie Ballet** et **Pascal Vandeckerckove** pour le suivi attentif de mes expériences. Je remercie **Laetitia Delort** et **Florence Caldefie-Chezet** pour m'avoir accordé deux années de poste en tant que monitrice en Botanique et Sciences du Végétal à la Faculté de Médecine et de Pharmacie de Clermont-Ferrand. Merci pour votre sympathie, votre confiance et de m'avoir permis d'enrichir mes connaissances dans un domaine qui m'était peu familier mais pour lequel j'ai pris plaisir à enseigner.

I thank everyone at CMET for the nice environment, the support and help during my PhD. All the ATP, **Jana**, **Tim**, **Renée**, **Siska**, **Greet** and **Mike**, a huge thanks for your experimental support as well as your sympathy. Some special thanks goes to : **Jana,** for your joyful spirit and for sharing your knowledge and solving problems during my SHIME run. I wish you lots of happiness with your future baby ! **Tim**, thank you for your energy and assistance in the molecular techniques. **Regine**, **Christine** and **Sarah**, thank you for all the administrative help as well as your encouragement and good care. **Regine**, I am very grateful to your help in all the processing of my PhD dissertation and your efficient remote assistance. **Peter** and **Massimo** from Prodigest, thank you for sharing your knowledge and expertise in the SHIME experiments. I also would like to thank my office-mates for the great time I had with them as well as their support: **Eline**, **Marlies**, **Annelore**, **Jolien**, **Jo**, **Pieter**, **Jose**, **Jan** and **Ramon**, I enjoyed the nice and quiet atmosphere, the lunch breaks and office activities in your company. A special thanks to **Marlies**, for your simplicity, kindness and encouragement. I am so glad that we developed such complicity in a friendship. I wish you lots of success in your future ! All HAM (Host And Microbes)-Cluster members, **Charlotte**, **Annelore**, **Emma**, **Racha**, **Lisa**, **Marta**, **Kim**, **Laetitia**, **Floor**, **Joanna**, **Stanley**, **FM**. What an efficient group ! It was motivational to work with you. Thank you for your sympathy, the fruitful discussions, the interesting input and your commitment. I wish to everyone lots of success in your future projects!

Mes derniers mots vont naturellement à ma famille ainsi qu'à mes plus proches amis. Un immense merci n'est rien en comparaison de tout le soutien, bonheur, humour et amour que vous me procurez au quotidien. Merci de m'avoir supporté^^, ce ne fût et ne sera certainement jamais une mince affaire ! Sans toute cette cohésion et ces encouragements, je ne serais arrivée jusque-là aujourd'hui. Merci d'avoir compris et respecté les sacrifices qu'impliquaient ces 3 années de thèse partagées entre la France et la Belgique. Pour ces écrits je resterai sérieuse et m'abstient donc de mentionner vos petits surnoms que j'affectionne tant^^ J'espère que vous arriverai malgré tout à vous reconnaitre ;) Je dédie ainsi cette thèse à : Ma maman d'amour **Gisèle**, ma sœur **Rachel,** mon neveu **Noah**, et neveu bis^^, mon père **Claude,** mon beau-frère **Florian** et sa fille **Lana**, American Papa **Kevin**, American Maman **Kathleen**, **Yann, Vilma, Elsa, Billy**, ma meilleure amie **Ophélie** (et son Papa **Bernard** pour ce merveilleux dessin), mon amie d'enfance **Tiphaine,** mes chères camarades de fac qui sont bien plus que de simples 'camarades'^^ **Charlène F**, **Adrien**, **Hanadi**, **Saliha**, **Alex**, **Guillaume**, **Lucile, Tom**, **Benjamin.** Et enfin à toutes les personnes et animaux qui me sont chers et restent gravés à jamais dans mon **cœur**.

Charlène, le 22.02.2018

NOTATION INDEX

A	**A**	Adenylate Cyclase
	A/E	Attaching/Effacing
	AI	Anti-Inflammatory
	AIEC	Adherent Invasive *E. coli*
	AR	Acid Resistance
	ARCOL	ARtificial COLon
	ASC	Ascending Colon
	ATCC	American Type Culture Collection
B	**BIF**	Binding Inhibitory Factor
	BLAST	Basic Local Alignment Search Tool
C	**cAMP**	cyclic AMP
	CCCP	Carbonyl Cyanide m-ChloroPhenyl hydrazone
	CDC	Center for Disease Control
	CFA/I	Colonization Factor Antigen I
	CFs	Colonization Factors
	CFTR	Cystic Fibrosis Transmembrane Regulator
	CFU	Colony Forming Units
	cGMP	cyclic GMP
	CHERG	Child Health Epidemiology Reference Group
	CMET	Center for Microbial Ecosystem and Technology
	CNCM	National Collection of Microorganism Cultures
	CoMiniGut	Copenhagen MiniGut
	CRP	c-AMP Receptor Protein
	CS	Coli Surface antigen
D	**DAEC**	Diffusely Adherent E. coli
	db-RDA	Distance-based redundancy analysis
	DEC	Diarrheagenic *E. coli*
	DGM	Dynamic Gastric Model
	DMEM	Dulbecco's Modified Eagle's medium
E	**EAEC**	Enteroaggregative *E. coli*
	EAST1	EnteroAggregative heat-Stable enteroToxin 1
	ECSIM	Environmental Control System for Intestinal Microbiota
	EFSA	Food Safety Authority

	EHEC	Enterohemorrhagic *E. coli*
	EIEC	Enteroinvasive *E. coli*
	EPEC	Enteropathogenic *E. coli*
	ER	Endoplasmic Reticulum
	ESIN	Engineered Stomach and Small Intestine
	ETEC	Enterotoxigenic *E. coli*
	ETpA	ETEC two partner protein A
	ExPEC	Extraintestinal pathogenic *E. coli*
F	**FAO**	Food and Agriculture Organization
	FI	Fluorescence Intensity
	FNR	Fumarate and Nitrate Reduction
	FSC	Forward-angle light SCatter
G	**GAPDH**	Glyceraldehyde 3-Phosphate Dehydrogenase
	GBD	Global Burden of Disease
	GC-C	Guanylyl Cyclase
	GE $T_{1/2}$	Gastric Emptying half time
	GI	Gastro-Intestinal
	GM1	MonosialoGanglioside
H	**HCl**	Hydrochloridric acid
	HCO_3^-	Bicarbonate
	HGS	Human Gastric Simulator
	H-NS	Heat-stable Nucleoid Structural protein
I	**IBS**	Irritable Bowel Syndrome
	ICR	Institute Cancer Research
	IECs	Intestinal Epithelial Cells
	IL	Interleukin
	ILE	Ileum
	iTOL	Interactive Tree of Life
	iViDiS	*In Vitro* Digestive System
L	**LB**	Luria Bertani
	LeoA	Labile enterotoxin output
	LPF	Long Polar Fimbriae
	LPS	Lipopolysaccharide
	LT	Heat-labile toxin
M	**MAPK**	Mitogen Activated Protein Kinase

	M cells	Microfold cells
	MEDIS	Microbiology Digestive Environment and Health
	MOI	Multiplicity Of Infection
	M-SHIME	Mucosal-Simulator of the Human Intestinal Microbial Ecosystem
	MUC	Mucin
N	**NaCl**	Sodium Chloride
	NCBI	National Center for Biotechnology Information
	NCIMB	National Collection of Industrial and Marine Bacteria
	NFκβ	Nuclear Factor Kappa β
O	**OM**	Outer Membrane
	OMVs	Outer Membrane Vesicles
	OTUs	Operational Taxonomic Units
P	**PCoA**	Principle Coordinate Analysis
	(q)PCR	(quantitative) Polymerase Chain Reaction
	PERMANOVA	Permutational Multivariate Analysis Of Variance
	pHext	Extracellular pH
	pHi	Intracellular pH
	PI	Post Infectious and/or Post Infection and/or Propidium Iodide
	PMA	Propidium MonoAzide
	pO_2	Pressure of Oxygen
	PRO	Probiotic
R	**RT**	Reverse Transcription
S	**SCFA**	Short Chain Fatty Acids
	Sc	*Saccharomyces cerevisiae* CNCM I-3856
	SD	Standard Deviation
	Sec	Secretory pathway
	SEM	Standard Error of Means
	SGF	Simulated Gastric Fluid
	SIMGI	Multicompartmental Dynamic Model of the Gastrointestinal System
	sPLS	sparse Partial Least Squares
	SSC	Side-angle light SCatter
	ST	Heat-stable toxin
	STEAC	Shiga-Toxin producing EnteroAggregative *E. coli*
	Stx	Shiga-toxin
T	**TEER**	TransEpithelial Electrical Resistance

	TIM-1	TNO gastrointestinal model
	TLR	Tool-Like Receptor
	TNF	Tumor Necrosis Factor
	TSI	The Smallest Intestine
	T1SS	Type 1 Secretion System
	T2SS	Type 2 Secretion System
U	**UPGMA**	Unweighted Pair-Grouped Method using arithmetic Averages
V	**VBNC**	Viable But Non Culturable
W	**WHO**	World Health Organization

Section I

LITERATURE REVIEW

"I am among those who think that science has great beauty. A scientist in his laboratory is not only a technician: he is also a child placed before natural phenomena which impress him like a fairy tale."

-Marie Curie (1867-1934)-

1 Enterotoxigenic *Escherichia coli* (ETEC)

1. *Escherichia coli*: a paradigm for commensalism and pathogenicity

Over 130 years have passed since the pioneer pediatrician Theodor Escherich (1857-1911) first described the *Bacterium coli commune*, known nowadays as *Escherichia coli* (*E. coli*). Since its discovery, the bacterium has arguably become the best-understood bacterial species on the planet, primarily because of its role as a model organism. For all of its importance, *E. coli* is commonly found in the lower part of the intestine of human and warm-blooded animals. Physiologically, it is a non-sporulated Gram-negative bacillus, measuring about 1 µm long by 0.35 µm wide, although this can vary depending of the strain and its culture condition (Fig. 1.1). Besides, the bacterium is oxidase-negative and a facultative anaerobe, growing happily with or without oxygen. Phylogenetically, *E. coli* belongs to *Proteobacteria* phylum and is a member of *Enterobacteriaceae* family. It typically represents only 0.1 to 5% of the total microbial community in the human gut (Hacker and Blum-Oehler, 2007; Blount 2015).

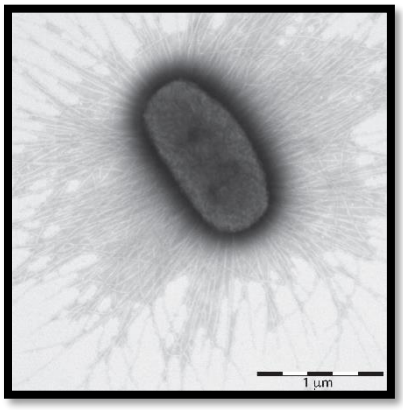

Figure 1.1. Transmission electron microscopy of *E. coli* isolate E873. The picture shows an heavily fimbriated Gram-negative bacteria by phosphotungstic staining. *Reprinted with permission from Von Mentzer, 2017.*

Notwithstanding that *E. coli* is a harmless intestinal inhabitant, horizontal gene transfer and pathogenicity islands play a major role in the evolution and gain of pathogenic properties in *E. coli* genome, contributing significantly to the burden of infectious diseases in human and animal (Messerer et al., 2017). The versatile *E. coli* pathogen is estimated to cause more than two million deaths annually through both intestinal and extraintestinal infections in humans (Nataro and Kapper, 1998; Clements et al., 2012). Thus, for taxonomic and epidemiological purposes, serotyping of O- lipopolysaccharide antigens, H- flagellar antigens and K- capsular antigens is regarded as the gold standard in classification of commensal and pathogenic *E. coli* (Fratamico et al., 2016).

Besides, on the basis of the mode of pathogenesis in humans and presence of specific sets of virulence factors, there are at least ten well recognized pathovars of pathogenic *E. coli* divided in two

groups: (i) extraintestinal pathogenic *E. coli* (ExPEC), colonizing various sites in the human body; and (ii) enteric/diarrheagenic *E. coli* (DEC).

ExPEC infections are primarily localized in the urinary tract, caused by uropathogenic *E. coli* (UPEC) or sepsis/meningitis, caused by sespsis-associated *E. coli* (SEPEC), and neonatal meningitis *E. coli* (NMEC). Among DEC group, eight pathotypes are discriminated according to their pathogenicity profiles (virulence function) and consecutive clinical diseases (Table 1.1). Collectively, DEC represent the most common bacterial pathogens worldwide and some of these pathotypes are a major cause of morbidity and mortality in low-income countries (Clements et al., 2012; Croxen et al., 2013, Gomes et al., 2016).

Table 1.1. **Summary of DEC pathotypes**

AAF: Aggregative Adherence Factor, A/E: Attaching/Effacing, BFP: Bundle Forming Pili, CFs: Colonization Factors, DAF: Decay-Accelerating Factor, EAST1: Enteroaggregative heat-stable enterotoxin 1, ER: Endoplasmic Reticulum, HUS: Hemolytic Uremic Syndrome, IECs: Intestinal Epithelial Cells, LPF: Long Polar Fimbriae, LT: Heat-Labile Toxins, ST: Heat-Stable Toxins, Stx: Shiga-Toxin, TTP: Thrombotic Thrombocytopenic Purpura. *Data reviewed from Clements et al., 2012; Croxen and Finlay 2010.*

PATHOTYPES	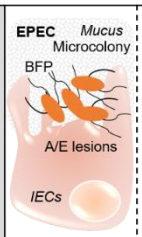	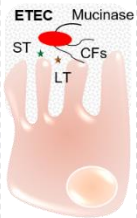	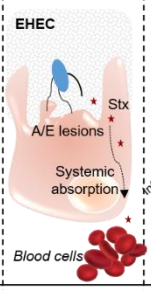	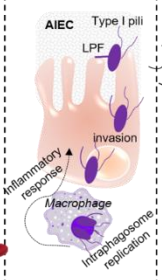	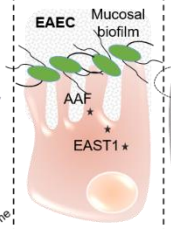	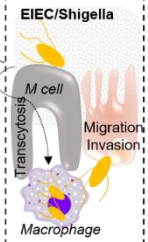	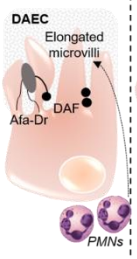	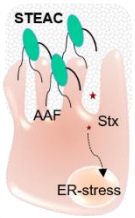
VIRULENCE FACTORS	Adhesion factors : intimin, BFP, A/E	Mucinases Colonization factors Enterotoxins (LT/ST)	Adhesion factors: A/E Shiga-toxins A & B	Adhesion factors : type 1 pili (FimH), LPF	Adhesion factors: AAF Toxin EAST1	Toxin ShET1/2	Adhesion factors: Afimbrial (Afa) or fimbrial (Dr) adhesins, DAF	Adhesion factors: AAF Shiga-toxins
GUT	Terminal ileum - colon	ileum	Colon	Ileum and colon	Colon	Colon	Unclear	Colon
DISEASE	Infant diarrhea (<6 months)	Acute watery diarrhea Infant diarrhea (<5 years) Traveler's diarrhea	Aqueous diarrhea and hemorrhagic colitis Complications: HUS, TTP	Crohn's Disease	Acute watery diarrhea with/out blood and mucus Infant diarrhea Traveler's diarrhea	Shigellosis : blood, mucus and leukocytes in stool	Acute watery diarrhea (< 5 years)	Aqueous diarrhea and hemorrhagic colitis Complications: HUS, TTP

To complete the data shown in Table 1, a brief description of each DEC pathotypes is proposed:

(i) Enteropathogenic *E. coli* (EPEC) – is the first enteric *E. coli* pathovar identified. EPEC have been associated with sporadic diarrheal illness and diarrhea outbreaks, most commonly among children less than six months of age in developing countries. The pathogen first attaches the surface of intestinal epithelial cells (IECs) by a type IV pilus, named bundle-forming pili, also involved in interbacterial

adherence. The hallmark of EPEC infection is to form "attaching and effacing" (A/E) lesions in the small intestine, disrupting the brush border cytoskeleton and leading to a proliferation of filamentous actin beneath adherent bacteria. Effacement of microvilli and intimate adherence between the bacterium and the epithelial cell are also observed. This pathotype does not produce enterotoxin and is non-invasive (Croxen et al., 2013).

(ii) Enterotoxigenic *E. coli* (ETEC) – are a leading cause of traveler's diarrhea and infant diarrhea in developing countries. The main virulence traits of ETEC are the production of adhesins that promote the attachment of bacteria to host enterocytes and the secretion of one or two enterotoxins: heat-labile (LT) / heat-stable (ST) that disrupt fluid and electrolytes homeostasis leading to abundant watery diarrhea. This pathotype has been the subject of my research and will be finely presented in part 2 of this literature review (Roussel et al., 2017).

(iii) Enterohemorrhagic *E. coli* (EHEC) – are major food-borne pathogens in industrialized countries. They are responsible for hemorrhagic colitis and bloody diarrhea that can evolve towards life-threatening age-dependent complications such as, hemolytic uremic syndrome in infant under 3 years of age, and thrombotic thrombocytopenic purpura in adult and elderly. EHEC belong to the Shiga toxin-producing *E. coli* (STEC) group, which is characterized by the production of the enterotoxin named Shiga-like toxin (Stx) or Verotoxin. In addition, intimate attachment to IECs by intimin (Eae) and adhesins long polar fimbriae (LPF) contribute largely to infection, leading to the characteristic attaching and effacing (A/E) lesions (Cordonnier et al., 2017).

(iv) Adherent invasive *E. coli* (AIEC) – are one of the causative agents for inflammatory bowel disease, including Crohn's Disease. This latter presents with abdominal pain, fever and bowel obstruction or diarrhea with presence of blood and/or mucus. AIEC strongly adhere to IECs via FimH, a mannose-binding adhesin component of the type I pilus, LPF and cell adhesion molecule 6. AIEC can also invade IECs and escape autophagy when inside macrophages, leading to extensive inflammatory cytokine secretion. However, the proinflammatory effects and invasive determinants are not yet fully understood (Sivignon et al., 2015).

(v) Enteroaggregative *E. coli* (EAEC) – are emerging pathogens, affecting children and adults worldwide, responsible for acute and persistent watery diarrhea, with or without mucus and blood. The hallmark of EAEC infection is the formation of a typical aggregative adherence (AA) pattern, characterized by adherent bacteria in a stacked-brick arrangement on the surface of intestinal epithelial cells, and also the coverslip between cells. The production of cytotoxins and enteroaggregative heat-stable enterotoxin 1 (EAST1) and other putative factors contribute to the virulence, but the pathogenesis remains complex and not yet fully established due to strain heterogeneity (Estrada-Garcia and Navarro-Garcia, 2012).

(vi) Enteroinvasive *E. coli* (EIEC) – are etiological agents of bacillary dysentery closely similar to that induced by *Shigella spp.*, especially in low-income countries. The pathogenesis is characterized by the ability of the pathogen to invade the human colonic mucosa. Following penetration, EIEC replicate in macrophages, spread to adjacent IECs, causing inflammatory destruction of the intestinal epithelial

barrier. The virulence genes have been acquired in a large F-type plasmid (pINV), but no molecular marker has been yet defined to discriminate EIEC and *Shigella*. Symptoms are self-limiting and characterized by the presence of blood, mucus and leukocytes in stools (Pasqua et al., 2017).

(vii) Diffusely adherent *E. coli* (DAEC) – are associated with watery diarrhea that can become persistent mostly in infants, but the epidemiology and site of action of this infection remain unclear. Two subclasses of DAEC exist: DAEC expressing Afa/Dr adhesins and DAEC expressing adhesin involved in diffuse adherence (AIDA-I). Besides, some Afa/Dr DAEC strains can be asymptomatic in adults, suggesting a role if the mature intestinal epithelial barrier is in a healthy condition (Servin, 2014).

(viii) Shiga toxin producing enteroaggregative *E. coli* (STEAEC) – have been described after the large-scale German outbreak in 2011 involving an unusual virulent Stx-EAEC strain of serotype O104:H4. This outbreak was associated with a high severity of illness including bloody diarrhea and complications with severe neurological symptoms and hemolytic uremic syndrome. STEAEC is not a *E. coli* pathotype with new virulence factors but rather a pathogen that, by phage acquisition, has combined the virulence properties of EAEC pathotype (AA), with the production of Stx of the STEC pathotype (Boisen et al., 2015).

Finally, to cover evolution of *E. coli*, strains are assigned phylogenetically to 5 main groups, i.e., A, B1, B2, D and E. Commensal isolates mostly group in phylogroup A, while pathogenic *E. coli* pathotypes do not group together, demonstrating thus their disparate nature (Fig. 1.2). Based on the *16S* rRNA gene, no phylogenetic difference between commensal E. coli and ETEC are displayed (phylogroup A, Croxen et al., 2013).

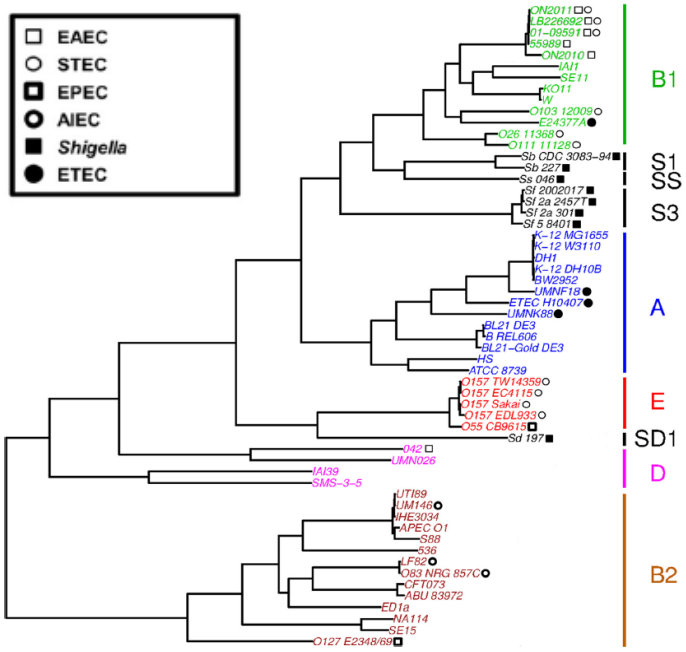

Figure 1.2. **Phylogenetic tree of DEC.** Strains of *E. coli* can be grouped into 5 main phylogenetic groups: A (blue), B1 (green), B2 (brown), D (pink), E (red). Additional phylogroups for the specific pathotype Shigella/EIEC are represented in black. The hybrid EAEC and STEC strains are denoted with both an open square and an open circle. Unmarked strains are either commensal or ExPEC. *Reprinted with permission from Croxen et al., 2013.*

2. Crossing the stage of ETEC infections

2.1. History of ETEC

The history of one of the leading causes of diarrhea in the world called ETEC, begins in 1956 in Calcutta, India. The bacterium was discovered in the course of clinical investigation of children and adult patients with *Vibrio cholerae* culture-negative stools, presenting a cholera-like syndrome, characterized by acute onset of watery diarrhea and severe dehydration. Soon after isolation of the undefined strain, investigators injected the live strain into isolated ileal loops of rabbits and found that large amounts of fluid was accumulated in the loops, similar to that seen with *Vibrio cholerae* (De et al., 1956). In the late 1960s, a subsequent study by a team of cholera investigators from Johns Hopkins University in Calcutta led to definitive identification of ETEC, notably by detecting the production of a heat-labile filterable enterotoxin from the bacteria (Carpenter et al., 1965, Sack et al., 1971). Then, the ETEC H10407 strain originally isolated in Dhaka, Bangladesh from an adult patient with acute diarrhea became the prototypical or reference strain (Evans et al., 1977). At about the same time, similar studies were being done with animals that also demonstrated ETEC strains to be responsible for diarrheal disease in several animal species (Qadri et al., 2005).

2.2. ETEC burden in the world: epidemiological data and clinical features

ETEC pathogens represent a major health concern for both humans and farm animals. There are at least 78 detectable O antigens and 34 H antigens associated with ETEC (Croxen et al., 2013). The pathogen is transmitted between humans and/or animals through the fecal-oral route, by ingestion of contaminated food and water exposed to animal and/or human sewage (Qadri et al., 2005).

In the frame of this research project, only the human conditions have been studied. This section will present briefly the data found in animals to move to a detailed description of the epidemiology and clinics in humans.

2.2.1. Animals

ETEC are commonly involved in neonatal and postweaning enteric colibacillosis, also named post-weaning diarrhea in farm animals. The pathogen is an important cause of death occurring mostly in nursery pigs, but also in calves and sheep. Such infections remain rare in poultry, horses or rabbits (Dubreuil et al., 2016). Outbreaks due to ETEC are often recurrent in the same herds. Additional factors can also contribute to the development of post-weaning diarrhea, such as deficiency of milk antibodies, dietary changes or other stresses associated to the weaning (Fairbrother et al., 2012).

ETEC causing colibacillosis results in significant economic losses in livestock industry (especially swine production) due to severe mortality, decreased weight gain and growth rate, cost for treatments, vaccinations, feed supplements and control measures. Depending on the severity of the disease and the country, the cost of post-weaning diarrhea was estimated to range from $47 to $370 per sow (Rhouma et al., 2017). Previous studies of ETEC infection models in piglets reported an incidence of diarrhea ranging from 50%–70% during the first two weeks post weaning (Madec et al., 2000; Bruins et al., 2011). A recent study from Girard et al. (2018) has shown a greater occurrence of diarrhea with a prevalence ranging from 60%–80% between day 1 and 4 post weaning in piglets (Girard et al., 2018). Not exceptionally, the infection can be recorded in older nursery pigs, until 8 weeks (Sato et al., 2016). Besides, ETEC can also be shed in feces from healthy animals. A study demonstrated that the percentage of ETEC positive in non-diarrheagenic pigs was 16.6% during the lactation period, 66% in the nursery phase and 17.3% in the finisher population (Moredo et al., 2015).

Interestingly, ETEC strains responsible for neonatal diarrhea in animals are often host-specific and rarely infect humans. Indeed, pigs and humans express the same receptors for ETEC enterotoxins binding, while they produce host-specific receptors on IECs for ETEC adhesins (Wenzel et al., 2017). Adhesins, called fimbriae mostly related to the disease in animals are F4 (K88), F5 (K99), F6 (987P), F41 and F18. The first four pili are able to mediate adhesion in both, neonates and postweaning animals, while F18 is related to postweaning only (Sun and Kim, 2017). Moreover, fimbriae F4 allows ETEC to colonize the length of jejunum and ileum, while F5, F6 and F41, to colonize the posterior jejunum and ileum. Finally, susceptibility to ETEC F5, F6 and F41 decreases with age and has been related to a reduction in the amount of active receptors on IECs with age (Zhang et al., 2007).

Regarding the clinical features in the most ETEC at-risk animals, the piglets, initial symptoms are usually characterized by abundant watery diarrhea (alkaline pH) varying in color (e.g. yellowish, grey or slightly pink) with a characteristic smell. Infected pigs are usually depressed with a reduced appetite.

Animals are rapidly dehydrated with sunken eyes and sudden death can occur. Signs are similar in pigs of various ages but tend to be more severe in younger pigs. Characteristic histopathological lesions can also be observed post-mortem including, hyperaemia of the stomach, dilatation and edema of the small intestine (Luppi, 2017).

2.2.2. Humans

2.2.2.1. Epidemiological data

Diarrheal diseases strike populations of all ages in all countries, although the relative frequency and severity differ. Over the past decade, research on diarrheal diseases has experienced a renaissance with new molecular methods, covering a larger variety of pathogens than traditional approaches where etiological agents were unidentified in up to half cases (Lääveri et al., 2017). In 2015, diarrhea caused worldwide more than 1.3 million deaths. Among the 13 recognized etiological agents (e.g. bacteria, parasites, viruses) for diarrheal diseases across all geographies, ETEC alone annually accounts for millions of diarrheal episodes over the world (GBD, 2017). In 2015, the ETEC attributable fraction of all diarrhea cases was 6%. ETEC is detected by the presence of enterotoxins LT and/or ST in stool samples thanks to molecular techniques. A systematic review of the literature across 35 countries found overall that approximately 45% of ETEC isolates expressed ST only, 25% expressed LT only, and 30% expressed both LT and ST (Isidean et al., 2011). In addition, ST is recognized as more frequently associated with diarrhea since 2015 (GBD, 2017).

The last report from the Global Burden of Diseases (GBD) study for diarrheal diseases highlights that all etiological agents gathered, the number of deaths has decreased substantially in the past 25 years, although progress has been faster in some countries than others (GBD, 2017).

Both children and adults are at-risk of getting infected, however the most vulnerable group remains children below five years of age, who may suffer from multiple diarrheal episodes each year (Qadri et al., 2005). Moreover, the epidemiology of ETEC infection attests important disparities not only according to the age-range, but also to the socioeconomic status and living conditions of the population. Thus, two at-risk groups for ETEC infections can be distinguished with (i) infants living in low and/or middle-income countries and, (ii) adults traveling and/or working occasionally in endemic countries. These two at-risk populations will be presented in the sections below. Beyond the at-risk groups, many ETEC outbreaks have occurred during natural disasters such as the floods in Bangladesh in 2004, provoking 17 000 cases of acute diarrhea due to ETEC and Cholera (Qadri et al., 2005).

2.2.2.1.1. Infant diarrhea in low and middle-income countries

In 2015, diarrhea among children under five years of age (included all etiologic agents) still pose a substantial public health burden in poor communities, killing an estimated 499 000 infants and hospitalizing millions more (Fig. 1.3). This places diarrhea as the fourth-leading cause of death in this targeted population, behind preterm birth complications, neonatal encephalopathy and lower respiratory infections (GBD, 2017).

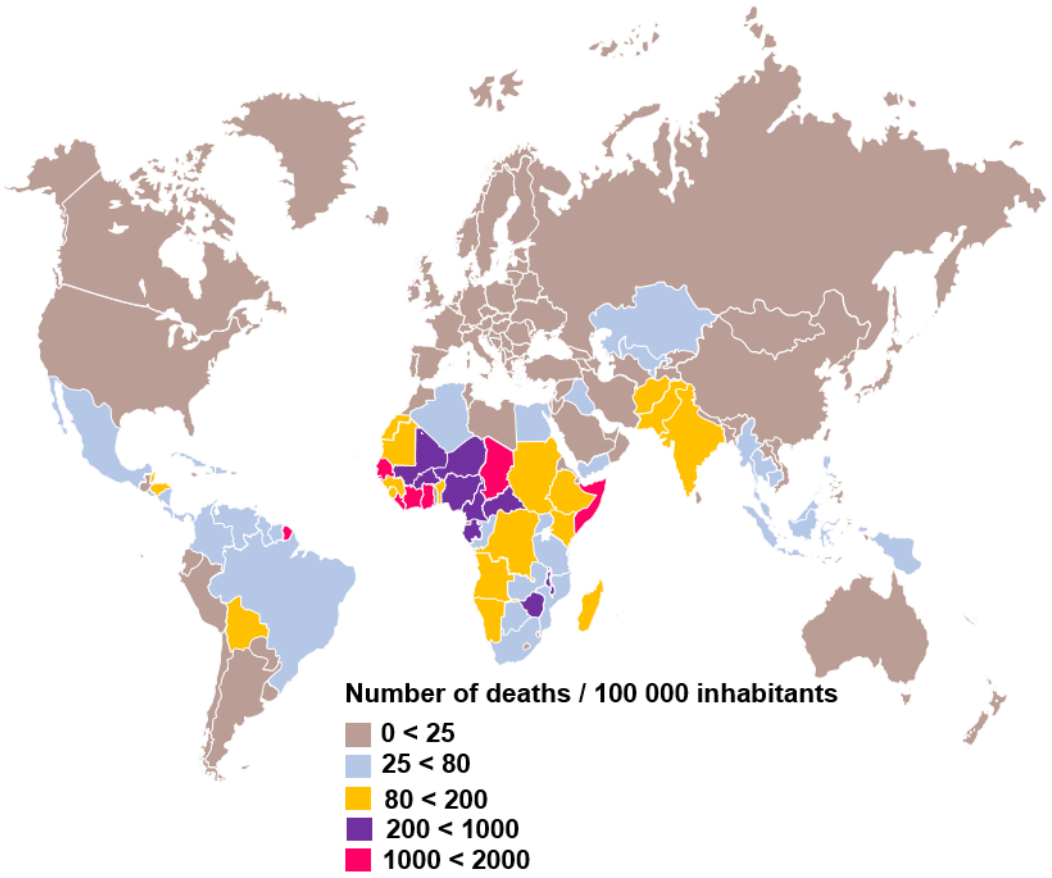

Figure 1.3. **Number of deaths due to diarrheal diseases in children under 5 years of age in 2015.** Number of deaths per 100 000 inhabitants, including all etiologic agents. *Modified from GBD, 2017.*

Regarding the surveillance network, there is no unique entity to monitor ETEC outbreaks or sporadic cases worldwide. Most of the epidemiological data are collected from multicenter, cohort or hospital-based studies carried out by the World Health Organization (WHO), the Child Health Epidemiology Reference group (CHERG), the GBD or the Global Emerging Infection Surveillance (GEIS). A local surveillance according to the country can also be implemented. So far, ETEC infection is often the first bacterial illness that infants and young children experience in endemic areas with a median of 3.2 diarrheal episodes per child during their first 3 years of life (Bourgeois et al., 2016). In 2013, 15% of the total diarrheal deaths in children under 5 years old were caused by ETEC (Fig. 1.4A) (Kotloff et al., 2013). Remarkably, even if still considerable, the number of deaths due to ETEC has strongly declined year by year, with approximately 300 000-500 000 children younger than 5 years in 2006 to 24 000 in 2015 (WHO, 2006; Walker et al., 2017) (Fig. 1.4B).

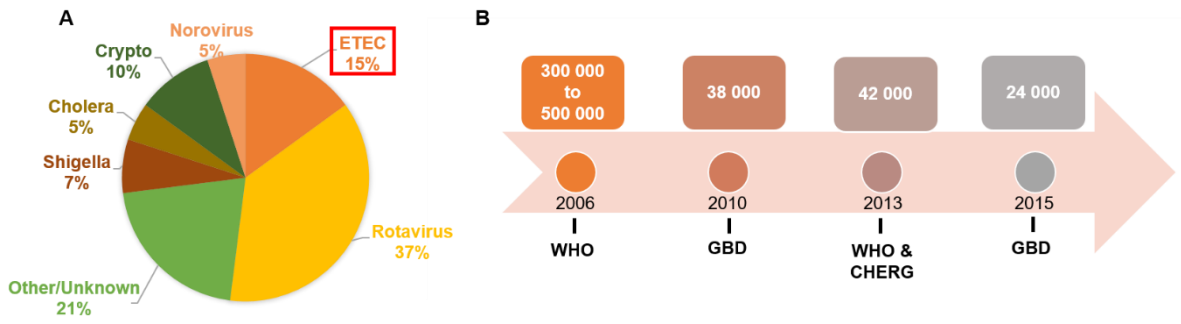

Figure 1.4. **ETEC-deaths worldwide in children under 5 years of age.** (**A**) Allocation of the main diarrheal etiologic agents associated to deaths. In 2013, Rotavirus and ETEC were the first viral and bacterial agents causing deaths in children, respectively; (**B**) Timeline of ETEC deaths in children. Different methodologies were used to assess the number of ETEC-deaths over years according to the entity in charge of the census. Bias are not excluded and can create a limitation in the interpretation. CHERG: Child Health Epidemiology Reference Group, GBD: Global Burden of Diseases, WHO: World Health Organization. *Compiled from GBD, 2017; WHO, 2006 and Kotloff et al., 2013.*

Nonetheless, high disparities due to geographic locations and ETEC serotype/virulotype (e.g. adhesin and toxin profiles) have been reported (Croxen et al., 2013). Globally, ETEC is mostly represented in south Asia, Africa and Latin America. In 2015, a meta-analysis based on stool culture and hospitalization has shown that ETEC was the first out of 13 etiologic agents, causing infant deaths in Egypt (680 deaths). This pathogen was also predominant in Central Asia (ranked 3/13) and in North Africa and Middle-East (ranked 4/13), as described in Table 1.2 (GBD, 2017). In addition to death estimates, morbidity due to ETEC was relatively unchanged between 2010-2015, with a yearly estimated 44 million cases of ETEC including all age groups, *versus* 9 million typhoid and cholera cases (6 and 3 million, respectively) (Lamberti et al., 2014; Walker et al., 2017). No morbidity data is specifically available for the children and infant populations. Finally, we must not exclude that in remote areas, the inventory of ETEC diseases and/or deaths might be difficult to assess due to data gaps or lack of health-care.

Table 1.2. **ETEC deaths in children under 5 years old ranked by geography in 2015**

Ranks given among the 13 etiological agents associated with infant diarrhea. Only the countries and geographical areas for which ETEC is in the top 6 are given. *Data reviewed from GBD, 2017.*

Geographical area	Country	Number of deaths (average)	Rank per country	Rank per geographical area
Central Asia	Kyrgyzstan	18.4	2	3
	Tajikistan	90.2	3	
Central Latin America	Nicaragua	23.8	2	6
Southeast Asia	Laos	107.9	5	6
	Myanmar	293	3	
North Africa and Middle-East	Egypt	680.1	1	4
	Afghanistan	572.8	5	
	Sudan	835	2	
South Asia	Bangladesh	251	6	6
	India	6 322.5	6	
Eastern Sub-Saharan Africa	Ethiopia	1 363.5	5	6
	Rwanda	184.2	3	
	Somalia	1 119.4	4	

2.2.2.1.2. Traveler's diarrhea and military personnel

Beyond living populations in developing countries, traveler's constitute as well a significant at-risk population in less developed tropical and subtropical areas and resource-limited destinations; especially those visiting Africa, Asia and Latin America (Fig. 1.5A). Thus, diarrheal illnesses in travelers are termed traveler's diarrhea or other non-exhaustive fanciful synonyms (e.g. Turista, Montezuma's revenge or Delhi Belly). Traveler's diarrhea is predominantly a fecal-orally transmitted disease caused by bacterial, viral or protozoal pathogens. Each etiologic agents are monitored by a global surveillance network of international travelers called GeoSentinel (Harvey et al., 2011). After ETEC and EAEC, *Campylobacter jejuni*, *Shigella* and *Salmonella* species are the most common bacterial pathogens involved. Norovirus and rotavirus are then the most common viral etiologies of traveler's diarrhea, while among protozoa, *Giardia intestinalis* and *Entamoeba histolytica* are also well represented (Giddings et al., 2016). The inconvenient traveling situations due to diarrhea required to alter planned activities in 40% of the total cases, and to stay in bed for at least one day in 20% of the cases (Steffen et al., 2005).

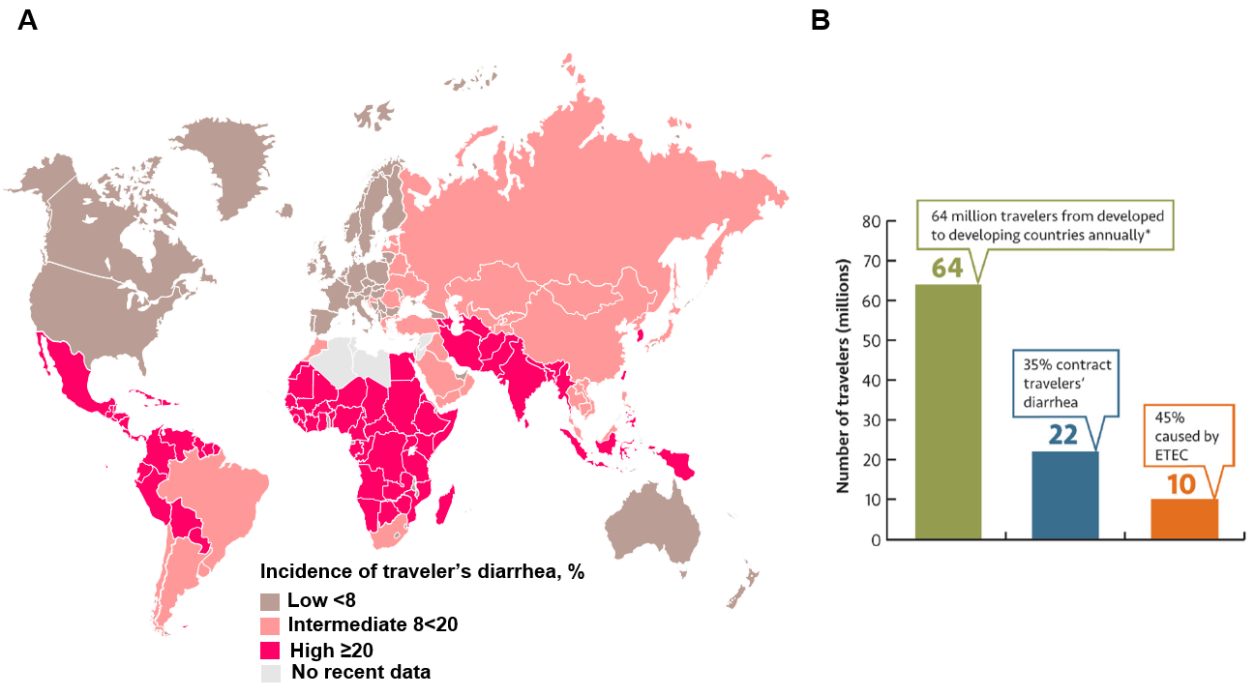

Figure 1.5. **Traveler's Diarrhea and ETEC diarrhea in the world.** (**A**) Incidence rates of traveler's diarrhea; (**B**) Estimated cases of traveler's diarrhea due to ETEC. *Modified from Steffen et al., 2015; BFGH report, 2006.*

Among 64 million people traveling to endemic countries each year, 22 million people contract a diarrheal episode. Among them, 10 million are caused by ETEC, which represents about 45% of the total traveler's diarrhea monitored. Thus, nearly 1 out of every 6 travelers to endemic regions is infected by ETEC (Path, BVGH report, 2011) (Fig. 1.5B). Although ETEC may contribute to an additional 89 000 deaths per year in Africa and South Asia, traveler's diarrhea are usually not serious regarding the million cases monitored yearly and mortality rates with proper treatment remain very low (Lamberti et al., 2014; Qadri et al., 2005). Approximately 10% of travelers with diarrhea seek medical care, and up to 3% of them require hospitalization (Giddings et al., 2016).

The problem is reinforced for military personnel deployed in such endemic areas. Around 70% of the total soldiers deployed experienced at least one ETEC-diarrheal episode. Previous studies on American forces deployed in Iraq and Afghanistan between 2001-2007 reported that among 2.3 million soldiers, more than 3.8 million cases of diarrhea have been estimated, compromising thus the unit's combat capabilities (Sanders et al., 2005; Putnam et al., 2006). Altogether, traveler's diarrhea and diarrhea in military personnel have a huge economic impact. In 2008, the global medical cost was estimated to reach $ 625 million, while the number of duty days loss amount to $ 2.2 million (Wang et al., 2008; Riddle et al., 2008).

Finally, ETEC infections represent also an emerging cause of diarrhea in industrialized countries such as USA, Denmark, Norway, South Korea and Japan. A growing number of ETEC outbreaks have

involved contaminated imported products, mostly raw fruits and vegetables from endemic regions. For example, an ETEC outbreak has been reported in Norway, in 2012. More than 200 diarrheal cases have been associated with the consumption of imported fresh chive herbals for a Christmas buffet in an hotel (MacDonald et al., 2015).

2.2.2.2. Clinical features

The symptoms from an ETEC infection are similar to those caused by many other enteric pathogens. In general, the clinical manifestations of ETEC-infected patients range from mild-watery diarrhea, without important dehydration, to profuse watery diarrhea similar to Cholera syndrome (*Vibrio cholera*e) (Qadri et al., 2005). It is usually defined by the passage of three or more unformed non-bloody stools per day, accompanied by one or more associated enteric symptom such as headaches, fever, abdominal cramping, nausea and vomiting (Dupont, 2009). The onset of diarrhea is usually quick, with an incubation period between 6-50 h after ingestion of the bacteria. Then, the duration of the illness goes from three to five days but can be prolonged beyond ten days in rare cases. The infective dose fluctuates between 8 $\log_{10}$ and 10 $\log_{10}$ cells in adults, but vulnerable populations such as infants, can be susceptible at lower dose such as 6 $\log_{10}$ cells (Levine et al., 1979; Gupta et al., 2008).

Beyond the fact that ETEC causes diarrheal diseases, it can also have long-term implications. In infants living in low-income countries, these complications include malnutrition, stunting and adverse consequences on cognitive development, as it was previously identified in infants living in Bangladesh (Qadri et al., 2007). However, it is difficult to attribute the diarrhea as a risk factor for malnutrition (cause) or a possibility to be mediated by malnutrition (consequence); making together a relentless loop (Fig. 1.6). In adult population (e.g. travelers, soldiers), it often results in post-infectious (PI) chronic sequelae ranging from functional gastrointestinal disorder to irritable bowel syndrome (IBS). A meta-analysis evaluating the risk of IBS after acute gastroenteritis revealed a 7-fold increase in the occurrence of PI-IBS (Halvorson et al., 2006). As well, in travelers recovering from ETEC-associated traveler's diarrhea, 10-14% may go on to develop IBS (Bourgeois et al., 2016).

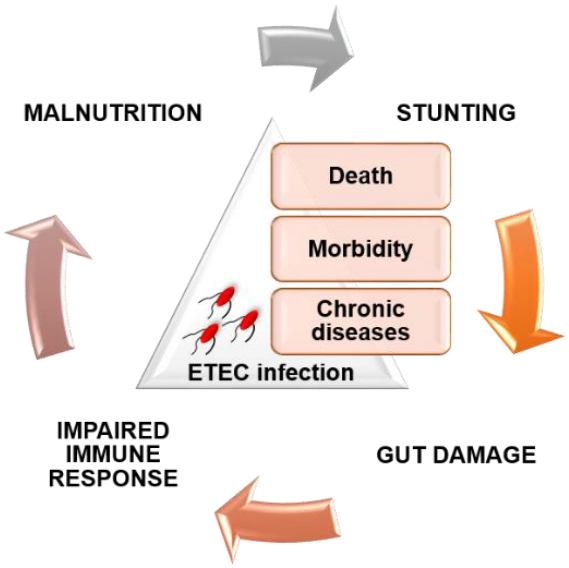

Figure 1.6. **Repeated diarrheal illnesses and malnutrition: a vicious cycle.** *Adapted from Kotloff et al., 2013.*

2.3. Exploring the virulence function of ETEC

In order to avoid being removed from the organism and initiate an enteric infection, ETEC pursue a sophisticated strategy and harbor several virulence factors to quickly and effectively attach to eukaryotic cell surface of the gut. Such adhesion is a universal prerequisite of ETEC to efficiently deploy its repertoire of virulence factors, notably by producing, secreting and delivering enterotoxins, in order to cause profuse diarrhea (Fig. 1.7).

This section will review the structure, function and genetics of the predominant and valuable ETEC proteinaceous virulence factors (e.g. colonization factors and enterotoxins), related to human infection. Due to the lack of structural and mechanistic information, putative factors (e.g. EAST1, ClyA a pore forming cytotoxin) related to few ETEC strains will be not presented.

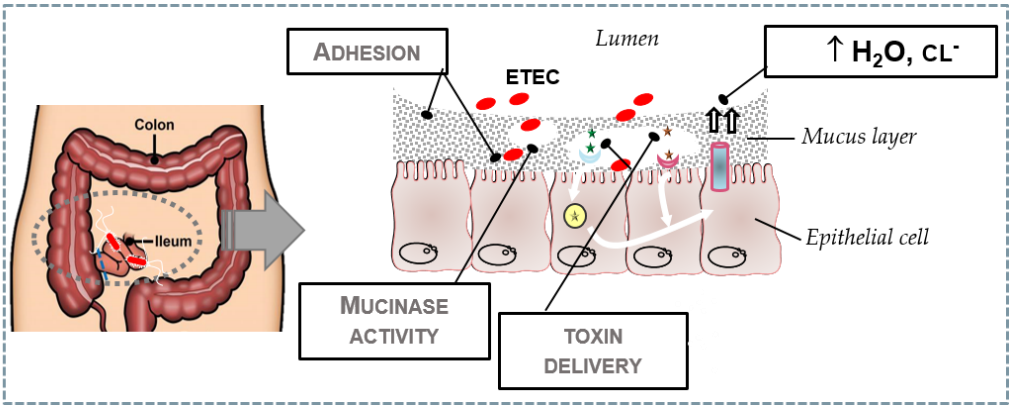

Figure 1.7. **Key steps of ETEC pathogenesis.** *Compiled from Luo et al., 2014; Qadri et al., 2005 and Turner et al., 2006.*

2.3.1. Intestinal colonization of the pathogen

ETEC colonizes the small intestine as a specific niche in the establishment of the infection. The overall colonization of the pathogen is mediated by protein adhesins, localized on its cell surface. These proteins can be ranged in two main classes according to their structures: (i) pili (fimbriae) or pili-related molecules with polymeric structures, and (ii) outer membrane proteins that do not form macromolecular structures (Madhavan and Sakellaris, 2015).

2.3.1.1. Pili and pili-related colonization factors

2.3.1.1.1. Nomenclature

Up to 25 ETEC fimbrial colonization factors (CFs) have been described in humans over the last 40 years. The nomenclature to name these adhesins has changed over decades, and a standardization has been proposed to designate the different CFs on the basis of genetic and antigenic relationships, giving a Coli Surface antigen (CS), followed by an Arabic number, that corresponds to the chronological order of identification, except for colonization factor antigen I (CFA/I). CFs are pili structures with either

homopolymeric or heteropolymeric conformations. Based on the morphology, four main types of ETEC CFs have been described: (i) fimbrial (typical rod-like morphology): CFA/I, CS1, CS2, CS4, CS8, CS12, CS14, CS17-21 and CS26; (ii) fibrillary (CS3, CS11, CS13 and CS22); (iii) helical (CS5 and CS7); and (iv) afimbrial (CS6, CS10, CS15 and CS23). Importantly, CFA/I, CS1-7, CS14, CS17 and CS21 are the most prevalent in ETEC. However, the distribution of certain CFs among ETEC strains can vary geographically and over time (e.g. seasonal occurrence). As well, an estimated number of 30-50% of ETEC strains might be still CFs uncharacterized, thus questioning the real number of CFs that the pathogen can produce (Begum et al., 2014).

2.3.1.1.2. Mechanism of CFs assembly and structure

The genes encoding ETEC CFs are organized in operons, and all the genes needed for the assembly of functional CFs are carried by plasmids; suggesting that ETEC acquired the whole operons by horizontal gene transfer (Madhavan and Sakellaris, 2015). In addition to the CFs, a recent study from Sheikh et al. (2017) displayed the contribution of type 1 pili, encoded by the highly conserved *fim* chromosomal operon in ETEC pathogenesis by promoting ETEC-host interaction. Type 1 pili usually play a critical role in virulence of UPEC, especially the FimH adhesin tipped with the pili structure. In ETEC, FimH plays a role in delivery of both enterotoxins in a rabbit ileal loop assay (Sheikh et al., 2017).

The mechanism of CFs and pili assembly is a useful criterion for grouping them into broad classes and to define them in terms of ancestry and evolutionary. Four mechanisms of pili assembly have been previously proposed: (i) conjugative pili; (ii) pili assembled by the chaperone-usher pathway; (iii) type 4 pili and (iv) pili assembled via the extracellular nucleation pathway (Nuccio and Bäumler, 2007). The majority of ETEC CFs and type 1 pili are synthesized and transported via the most extensively studied and understood pilus assembly system, the chaperone-usher pathway, except CS6, CS21 and CFA/III (Roy et al., 2011; Torres, 2010; Busch et al., 2015). In general, CFs are encoded in a four genes operon including: (i) a periplasmic chaperone; (ii) a major fimbrial subunit; (iii) an outer membrane usher protein, required for secretion of pilins and assembly of the pilus on the bacterial cell surface; (iv) a minor subunit located at the tip of the pili, with the N-terminal half of the protein responsible for the binding to the host cell receptor (Fig. 1.8A).

Then, after assembly, only the structure of CFA/I, the first identified and most predominant ETEC CF and type 1 pili, recently described are presented. Mature CFA/I consists of 2 pili subunits: a major pilin subunit CfaB, and one or a few copies of the tip-residing adhesive minor subunit CfaE. While type 1 pili are composite fibers comprised of a pilus rod, joined to a fibrillum structure tipped with the FimH adhesin, that binds mannose with stereochemical specificity (Li et al., 2009, Sheikh et al., 2017) (Fig. 1.8B).

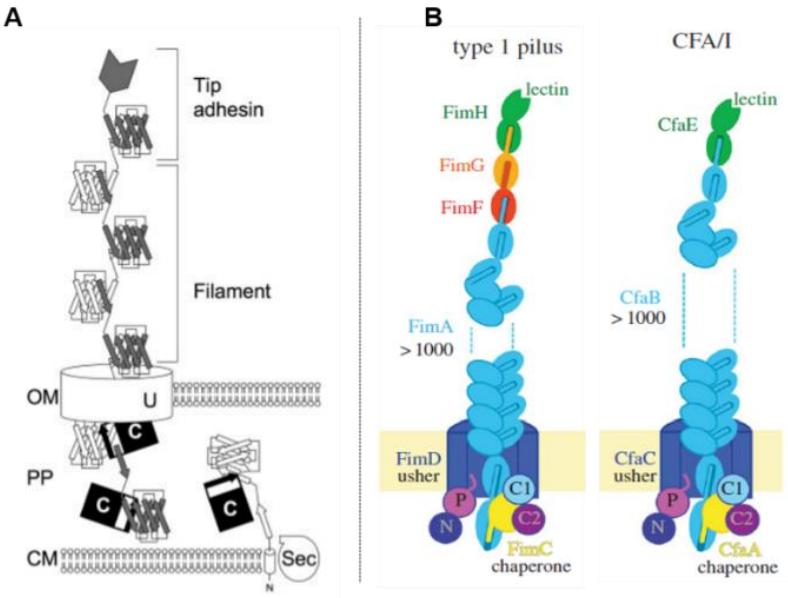

Figure 1.8. **Schematics of CFs assembly by the chaperone-usher pathway and examples of CFs structures.** (**A**) The N-terminal signal peptide of fimbrial subunits is cleaved during their transport across the cytoplasmic membrane (CM), by the general secretory pathway (Sec). In the periplasm (PP), the chaperone (C) interacts with fimbrial subunits and form a complex with the usher protein (U). Usher facilitates the replacement of the chaperone donor-strand with the N-terminal-strand of a second subunit, thereby joining subunits into a filament that is transported across the outer membrane (OM); (**B**) Each pilus is built up with a different combination of subunits (Fim, Cfa), represented by different colors. *Reprinted with permission from Nuccio and Bäumler, 2007; Busch et al., 2015.*

2.3.1.2. Nonpili adhesins

2.3.1.2.1. TibA and Tia: two non-classical virulence factors

Other uncommon non-fimbrial and pathogenicity islands (PAI) encoded adhesins have been found in some ETEC strains but remain poorly elucidated in terms of molecular structure and function. The enterotoxigenic invasion locus B (TibA) is an autotransporter glycoprotein (104-kDa) mediating bacterial attachment to IECs, autoaggregation and biofilm formation, encoded within the *tibDBCA* gene cluster, and the enterotoxigenic locus invasion A (Tia) is a 25-kDa outer membrane protein (Scherlock et al., 2005, Lindenthal and Elsinghorst, 1999). Interestingly, epidemiological studies performed in Latin America revealed that *tia* and *tibDBCA*-PAI-associated genes were found in only 17% of the total isolates (Guerra et al., 2014).

The two adhesins TibA and Tia identified in the prototypical ETEC strain H10407, promote invasion of HCT-8 cells *in vitro*. As well, expression of Tia and TibA in non-pathogenic *E. coli* HB101 and DH5α confers the invasive phenotype, suggesting that this protein would not require additional factors to exerts its function. But so far, the invasion mechanism was described in 1996-2000 by Fleckeinstein, Lindenthal and Elsinghorst and no extended investigation has been recently performed, highlighting the incertitude

of this discovery. In fact, the invasion rates of H10407 in cultured IECs are far lower than those reported for intracellular pathogens such as *Salmonella enterica* (Torres, 2016).

2.3.1.2.2. EtpA: an adhesin acting through two mechanisms of action

ETEC, and specifically the reference strain H10407 possesses a plasmid-borne two-partner secretion locus consisting of three genes, *etpBAC*. EtpA is a high-molecular weight secreted glycosylated protein sharing sequence similarities with adhesins from *Yersinia pestis* and *Y. enterocolitica* (Roy et al., 2009). A glycosylation pattern of EtpA is required to maximize its adhesion on Caco-2 and HCT-8 cells. This glycosylation might be catalyzed by EtpC, but the mechanism remains complex to understand (Fleckenstein et al., 2006). As well as conferring adherence independently, EtpA also interacts with highly conserved regions of flagellin (FliC), to promote flagellum-mediated adherence to Caco-2 and HCT-8 cells. EtpA appeared to be concentrated at the tip of flagella (Fig. 1.9). Further, this association is critical for efficient interaction of ETEC with mucosal surfaces in frozen section of mouse ileum. However, the precise contributions of both EtpA and flagella in the establishment of a critical role of ETEC colonization remain undefined (Roy et al., 2009).

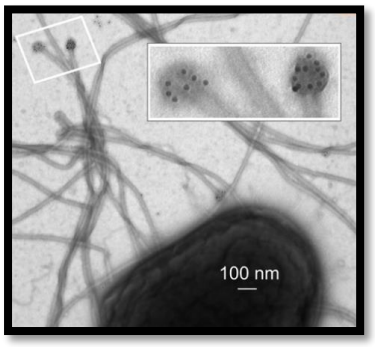

Figure 1.9. Scanning electron microscopy of EtpA at the tips of ETEC H10407 flagella. The *in situ* immunolocalization shows EtpA proteins (in white boxes) concentrated at flagellar tips of ETEC. *Reprinted with permission from Roy et al., 2009.*

2.3.1.3. Host cell receptors to ETEC adhesins

Recognition of cellular receptors by ETEC pilus and nonpilus is part of the infectious mechanism to facilitate resilient host-pathogen interaction. Nonetheless, most of the molecular receptors for ETEC CFs remain scarcely known, especially in human. Additional aspects to consider, such as receptor-binding specificity, distribution and stability of the receptors along the gut make the understanding even more complex. In general, these receptors are composed by sugars found in glycoproteins or glycolipids in the villous epithelium of the small intestine and are able to hemagglutinate (Morabito, 2014).

For example, the major subunit of CFA/I, CfaB, has been found to bind asialo-glycosphingolipids from Caco-2 cells (Madhavan et al., 2016). Remarkably, in a study using enteroids derived from healthy human intestinal stem cells, authors have shown that the adhesion of FimH, tipped on type I pili, enhanced production of highly mannosylated proteins on IECs (Sheikh et al., 2017). Besides, CS2, CS5 or CS6 bind to components of rabbit intestinal mucus and this interaction is prevented by treatment with meta-periodate, suggesting recognition of specific carbohydrates (Helander et al., 1997). Further, binding of CS6 to fibronectin has been reported, indicating that extracellular matrix proteins could also serve as a focal contact point prior to reach rabbit epithelial cells (Chatterjee et al., 2011). Finally, data

regarding nonpilus adhesins indicate that Tia interaction with the intestinal epithelium is mediated via binding to heparin sulfate proteoglycans, and that EtpA locates preferably in close proximity to mucin-producing cells in frozen section of mouse ileum (Roy et al., 2009).

2.3.2. Mucin-degrading proteins

Under healthy conditions, mucosal surfaces composed of gel-forming mucins, lining the gastrointestinal tract, prevents penetration by pathogens (see section 3.1.3.1.2). In the case of ETEC infection, two mucin-degrading enzymes have been identified over the last five years. These mucinases allow temporary access to cell membrane, then promoting close contact of the pathogen to the IECs.

EatA, a member of serine protease autotransporters of the Enterobacteriaceae (SPATE), plasmid-encoded, is able to degrade MUC2, a major protein present in the human mucus layer of the small intestine. In a model using LS174T colonic cell lines producing abundant MUC2, EatA accelerates the removal of MUC2, thereby facilitating the access of ETEC enterotoxins to the enterocyte surface (Kumar et al., 2014). Surprisingly, EatA displays another function, by degrading EtpA adhesin, thereby modulating adhesion of the pathogen in a murine colonization model, then accelerating the delivery of LT enterotoxin (Roy et al., 2011). In fact, in general adhesion by bacteria is thought to be an important prerequisite for delivery of bacterial effectors such as enterotoxins. However, the ability to negatively modify adhesion events also appears to be an important virulence trait, not yet clearly understood. Then, EatA shares structure homology with the SepA protease autotransporter identified in *Shigella flexneri*.

The second enzyme is a mucin-binding metalloprotease YghJ, highly conserved in ETEC and degrading MUC2 and MUC3, a transmembrane mucin. This protein is secreted by the type 2 secretion system (T2SS), also responsible for the secretion of LT toxin and has also been found in *Vibrio cholerae* (Luo et al., 2014).

2.3.3. Enterotoxins production

Interaction of the pathogen within the host by attaching IECs will facilitate the production, secretion and delivery of enterotoxins, considered as the main virulence feature of ETEC pathogen. By definition, the bug universally produces at least one of these plasmid-encoded enterotoxins: heat-labile (LT) and heat-stable (ST), leading to profuse watery diarrhea. As previously mentioned, ETEC strains producing the ST toxin alone or both ST and LT toxins are more likely to cause diarrhea than those producing LT alone (Isidean et al., 2011).

2.3.3.1. Heat-labile enterotoxin (LT)

2.3.3.1.1. LT molecular structure and variants

As its name suggests, LT is sensitive to heat treatment and easily breaks down at 70°C for 10 minutes (Gill et al., 1981). This large enterotoxin (84 kDa) encoded by *eltAB* gene shares 80% homology of structure and function with Cholera toxin from *Vibrio cholerae*. As illustrated by the crystal structure Fig. 1.10, LT is a multimeric AB_5 toxin, composed of a single catalytic A subunit (LT_A), associated with a ring

of five B subunits (LT_B) for binding and internalization (Dubreuil, 2012). The LT_A subunit consists of a large A1 domain and a short A2 domain (Sanchez and Holmgren, 2005).

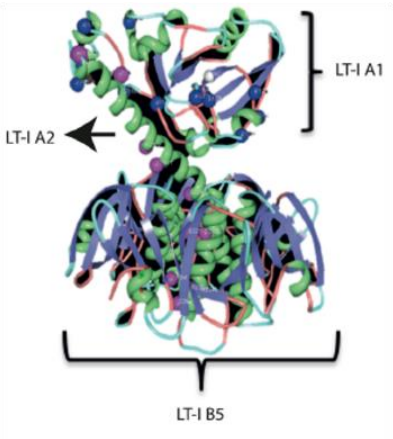

Figure 1.10. Crystal structure of the human LT enterotoxin. *Reprinted with permission from Joffré et al., 2015.*

Early studies attested the molecular heterogeneity of LT according to the host infected (e.g. LT-I human and LT-II animal origin) (Honda et al.,1981; Tsuji et al.,1982). However, the high level of LT allele variants found in ETEC strains isolated in several geographical parts of the world and over time indicated that the LT toxin was more variable than previously anticipated and not only due to the host. In total, 20 different amino acid variants of LT-I have been identified between 1980 and 2011 and all of them had binding and virulence capacity but not always at the same level (Von Mentzer et al., 2014; Joffré et al., 2015). Interestingly, two of the variants, LT1 and LT2 are often found and associated with clonal ETEC lineages that express CFs, CFA/I, CS1+CS3, CS2+CS3 and CS5+CS6 and related to diarrhea. As well, LT2 strains produce 5-fold more toxin than LT1 strains, suggesting greater virulence potential for this genetic variant (Joffré and Sjöling, 2016).

2.3.3.1.2. LT from secretion to host-binding

As illustrated in Fig. 1.11, LT secretion is initiated across the inner membrane (IM) to the periplasm by the Sec machinery. In the periplasm, monomers assemble spontaneously or by DsbA disulfide oxidoreductase activity in AB_5 toxin secreted along the periplasm to the outer membrane, involving the protein labile enterotoxin output (LeoA) (Fleckenstein et al., 2000; Brown and Hardwige, 2007). Then, in the T2SS, the outer membrane secretin GspD forms a multimeric pore for translocation of secreted LT, binding to lipopolysaccharide (LPS) on the cell surface via the LT_B subunit (Ellis and Kuehn, 2010). LT are mainly secreted associated with outer membrane vesicles (OMVs). But in some cases, LT retain in the periplasm, or stay associated with LPS of the outer membrane (Lasaro et al., 2006). Consequently, vesicles released from ETEC cells also have LT on their surface, allowing the irreversible attachment of the LT_B subunit to the monosialoganglioside (GM1) receptor on the IECs, provoking then, the internalization of OMVs (Mudrak and Kuehn, 2010). Endocytosis will be dependent of cholesterol-rich lipid rafts found on the surface of IECs (Kesty et al., 2004). Therefore, the endocytosed vesicle-associated LT will traffic through the Golgi apparatus and endoplasmic reticulum (ER) and the retrograded translocation into the cytosol. This translocation makes the A1 fragment of LT_A active. Thus, A1 domain harbors its catalytic function via ADPribosylation of G proteins, resulting in activation of

adenylate cyclase and elevated intracellular cyclic AMP (cAMP) levels. This is followed by the phosphorylation of cystic fibrosis transmembrane regulator (CFTR), a chloride channel present at the apical membrane of IECs brush-border. It subsequently leads to the hypersecretion of water (H_2O) and ions (Cl^-) from the epithelium, eliciting massive watery diarrhea (Sears and Kaper, 1996; Sanchez and Holmgren, 2005; Ellis and Kuehn, 2010).

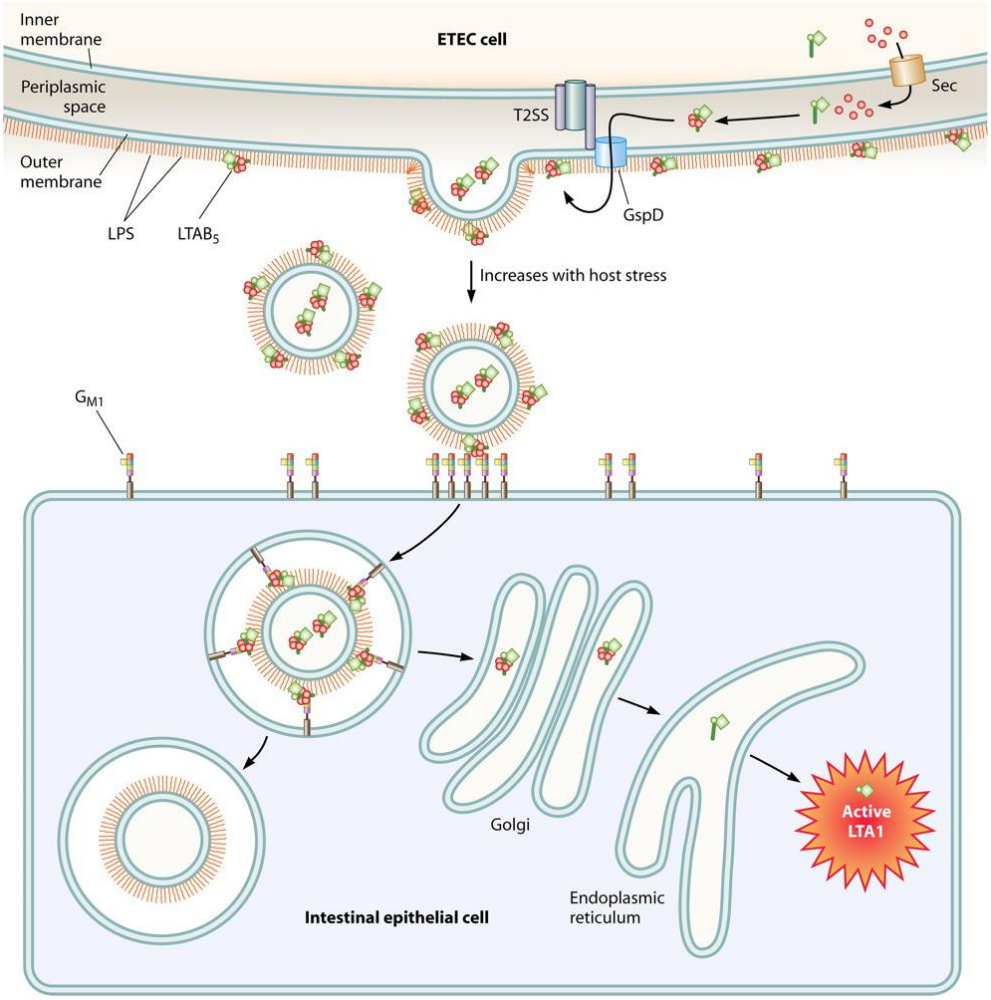

Figure 1.11. **Model of binding, secretion and vesicle-mediated LT transport into IECs.** *Reprinted with permission from Ellis and Kuehn, 2010.*

Remarkably, the GM1 receptor [Galβ1-3GalNacβ1-4(NeuAcα2-3)Gal] is predominantly found in the epithelial cells of the small intestine. Analysis of normal human intestinal epithelia found that GM1 comprises between 0.01% and 3% of the glycosphingolipid content, raising the question of whether its low concentration in enterocytes is sufficient to account for intoxication by LT (Holmgren et al., 1985; Breimer et al., 2012). Besides, a recent study has shown that human colonic epithelial cell lines contain no GM1, reinforcing that the small intestine (e.g. ileum) is considered as the main site of action in ETEC pathogenesis (Wands et al., 2015). Finally, according to the glycosylation level, some glycoproteins have been proposed to also act as LT receptors (e.g. galactoproteins, polylactosaminoglycan containing

receptors) in both small intestine and colon. But so far, this track has been poorly investigated, making it unlikely (Griffiths and Critchley, 1991; Holmgren et al., 1985).

2.3.3.1.3. Beyond the toxigenic function of LT

LT can also enhance ETEC adherence and its colonization by activating the MAPK pathway in HCT-8 cells (Johnson et al., 2009; Wang et al., 2012; Wijemanne and Moxley, 2014). The extent to which ETEC damages IECs remains unclear, however, a recent study has investigated the apoptotic effects of LT exposure on IECs (Lu et al., 2016). Authors have shown that LT decreases IECs viability, inducing then apoptosis in a dose and time dependent manner in HCT-8 cells, Caco-2 cells and mouse model. Under LT treatment, the PERK-CHOP pathway (-PERK- pancreatic ER kinase-like ER kinase; -CHOP-CCAAT-enhancer-binding protein homologous protein, a multifunctional transcription factor in the ER stress) is mostly involved in ER stress-mediated apoptosis in IECs (Lu et al., 2016).

2.3.3.2. Heat-stable enterotoxin (ST)

2.3.3.2.1. ST molecular structure and variants

ST polypeptide is non-antigenic, low molecular weight protein (2 kDa), and is encoded by *estAB* gene. ST is synthesized as 72 amino acid proteins consisting of a signal peptide, a pro peptide and a carboxy terminal region of 18-19 amino acids, forming the mature and active enterotoxin (Rasheed et al., 1990). The toxin remains active after 60 min of heating at 95°C.

ETEC isolates can express two distinct ST families, differing in structure and function: the methanol soluble protease resistant STa (synonyms ST1), found in human and the methanol insoluble and protease sensitive STb (synonyms ST2), isolated in both human and animal strains. Besides, STa and STb are ligands to different receptors expressed in the small intestine and colon, binding reversibly to guanylyl cyclase C (GC-C) and sulphatide, respectively (Dreyfus et al., 1993; Dubreuil, 2012). Interestingly, GC-C are expressed exclusively on the brush border membrane of IECs along the crypt-villus axis, and in the crypts of the colon (Weiglmeier et al., 2010; Basu et al., 2010).

In addition, within STa, the small cysteine-rich enterotoxin, two variants associated with human disease have been described, STh and STp, originally found in human and pig, respectively. These two variants have a similar crystal structure which is close to human guanylin and uroguanylin hormones (Fig. 1.12A) (Weiglmeier et al., 2010). Besides, seven subvariants (STa1-STa7) of STh and STp have been recently discovered, and ETEC isolates producing the most STa5 co-expressed with CS6 were significantly associated with disease in adults (Joffré and Sjöling, 2016). Interestingly, STa have been found in other pathogens such as *Klebsiella pneumoniae*, *Yersinia enterocolitica* and *Vibrio cholerae* O1 (Klipstein et al., 1983; Takao et al., 1984; Takeda et al., 1991).

2.3.3.2.2. ST from secretion to host-binding

Only STa secretion and release is illustrated in Fig. 1.12B as this variant is mostly involved in human pathogenesis. STa polypeptide is translocated across the IM to the periplasm via the signal peptide, and cleaved by SecA-dependent export pathway (Weiglmeier et al., 2010). Then, the toxin is folded to its mature form via the action of DsbA and is efficiently secreted into the lumen through the TolC channel,

a multidrug pump efflux system (Yamanaka et al., 2008). So far, it remains unclear how STa produced in the periplasm is moved to the TolC channel, it has been suggested that the type 1 secretion system (T1SS), resembling a large family of ATP-binding cassette (ABC) transporters might be implicated in STa translocation to the OM (Green and Mecsas, 2016). Subsequently, STa will bind the GC-C receptor on IECs (Fig. 1.12C). Such binding leads to increase intracellular formation of cyclic GMP (cGMP) that triggers signaling cascades causing activation of cGMP-dependent protein kinase II, promoting stimulation of Cl^- and fluid secretion by phosphorylation of CFTR, leading to the appearance of profuse diarrhea. Interestingly, STa can activate another pathway by inducing inhibition of phosphodiesterase 3, causes accumulation of cAMP followed by activation of protein kinase A, which activates CFTR (Weiglmeier et al., 2010).

Importantly, it has been recently proved that EtpA adhesin is required for optimal delivery of ST in T84 cell models. Indeed, cGMP activation in IECs by wild type ETEC was significantly accelerated relative to the *EtpA* mutant. (Zhu et al., 2018).

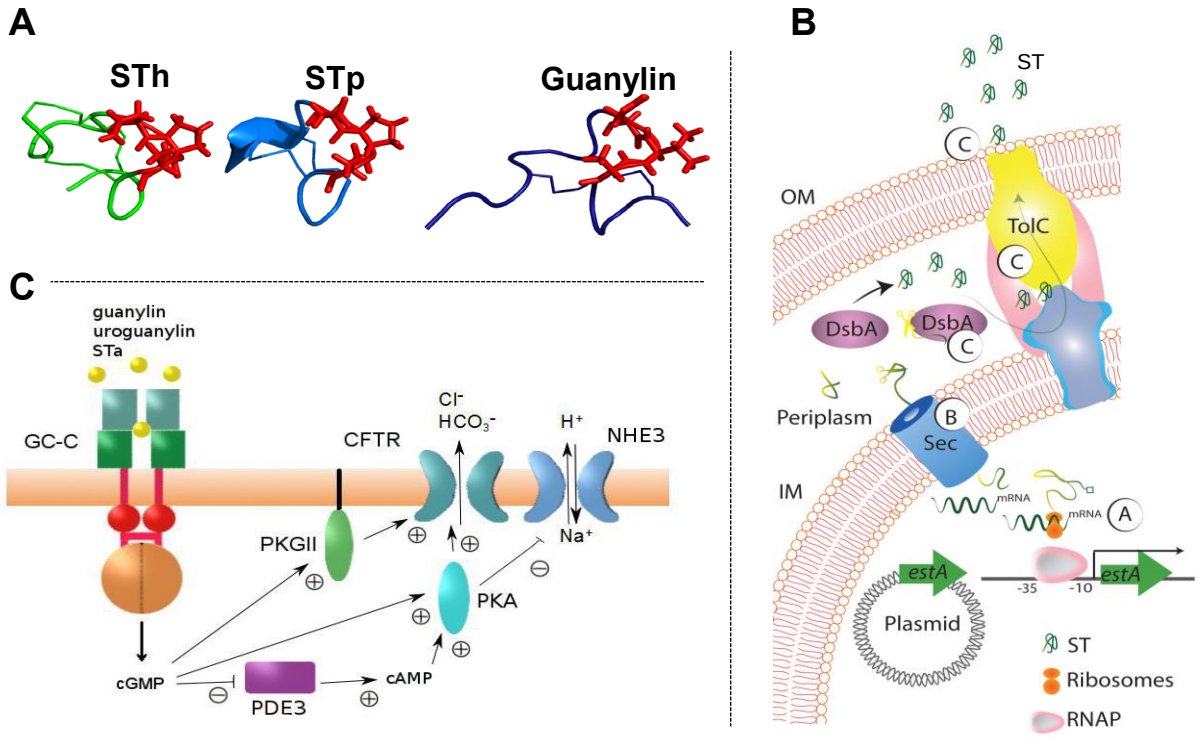

Figure 1.12. **Schematic representation of ST secretion, release and host binding mechanisms.** (**A**) Crystal structure of the 2 human variants of ST in the family of STa, and the human guanylin molecule; (**B**) STa synthesis, secretion from the inner membrane (IM) to the outer membrane (OM) of ETEC; (**C**) Release and binding of STa to the GC-C receptor from the IECs with activation of the

cGMP/cAMP signaling pathway. *Reprinted with permission from Weiglmeier et al., 2010; Joffré et al., 2015.*

2.3.4. ETEC virulence: regulatory networks

2.3.4.1. Genetic features of the reference strain ETEC H10407

ETEC H10407 serotype O78:H11:K80, originally isolated in 1973 from an adult case of severe cholera-like diarrheal illness in Dacca (Bangladesh), is to date the most extensively characterized strain of this pathovar. This isolate is LT+, ST+, CFA/I+, EtpA+, YghJ+. The complete genomic and plasmidic sequences of ETEC H10407 are available and represented in Fig. 1.13 (Evans et al., 1977; Crossman et al., 2010; EMBL database accession number FN649414, Haycocks et al., 2015). The ETEC H10407 genome consists of a circular chromosome of 5,153,435 bp and four plasmids designated pETEC948, pETEC666, pETEC58, and pETEC52. The two larger plasmids (pETEC948 and pETEC666) are reminiscent of conjugative plasmids that are often associated with the carriage of virulence factors, whereas the two smaller plasmids (pETEC58 and pETEC52) are homologous to mobilizable plasmids frequently encountered in a variety of bacterial species (Crossman et al., 2010; Haycocks et al., 2015, Hazen et al., 2017).

This reference strain has been used in the frame of my experimental works.

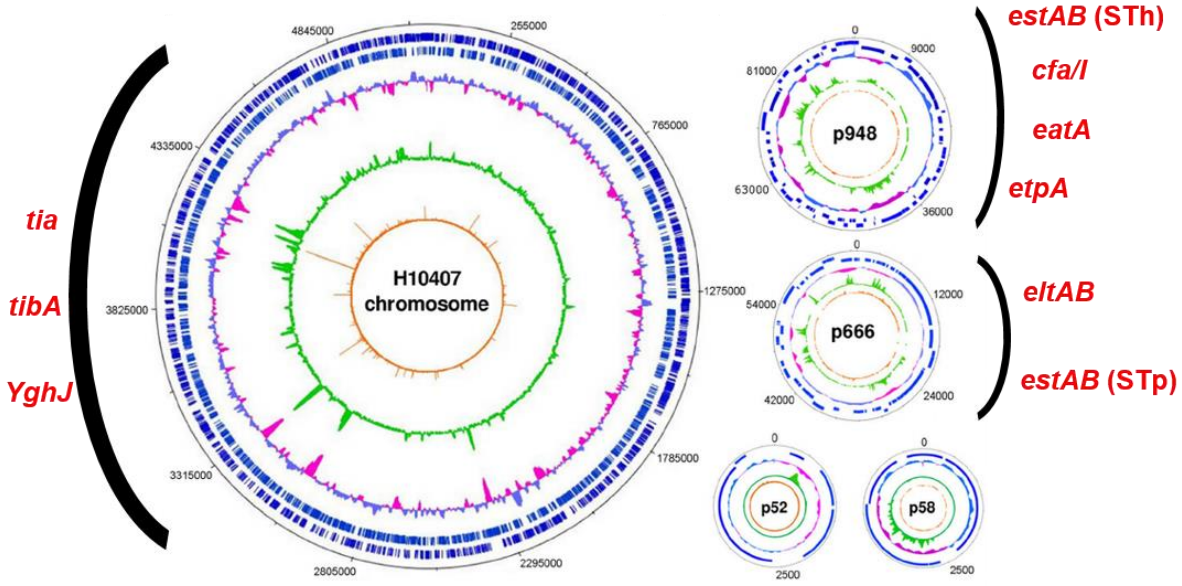

Figure 1.13. **Genome and plasmids mapping of ETEC H10407.** The main virulence genes of ETEC H10407 are represented in red. *Reprinted with permission and modified from Haycocks et al., 2015.*

2.3.4.2. Intrinsic transcriptional modulations

Pathogens in general have deployed mechanisms to sense the environment in which they evolve. In response to the signals received, they will act accordingly by turning off or on the expression of their virulence genes. Prior to regulate their genes expression according to the gastrointestinal cues (developed in section 3.2), bacteria will modulate their genes by themselves. Thus, highly complex regulatory networks exist intrinsically between virulence genes.

To date, the ETEC virulence networks are largely unknown and need to be unraveled. The majority of transcriptional studies have focused on ETEC *rns* regulon, a transcriptional regulator controlling the expression of many pili encoding genes in human ETEC. However, it has been recently shown that *rns* can also regulate non pilus adhesins, such as EtpA, by binding to upstream *etpBAC* operon (Madhavan, 2018). Besides, CFA/I is encoded by *cfaABCE* operon, which is positively controlled by the transcriptional regulator, CfaD (Caron and Scott, 1990). Beyond, CfaD appears to play a central role in the global regulation of virulence gene expression in ETEC. Indeed, a recent study has shown that the expression of *etpBAC* operon, is activated by CfaD, further highlights the importance of CfaD in inducing the production of a variety of surface adhesins (Hodson et al., 2017). Then, *leoABC* genes and *tia* locus are tightly regulated together. *LeoA* is encoded within the *tia* locus, itself within a pathogenicity island (Fleckenstein et al., 2000). Interestingly, *LeoA* is associated with the maximal secretion of LT (Michie et al., 2014; Guerra et al., 2014).

At toxin gene-encoding level, the heat-stable nucleoid-structural (H-NS) protein controls transcription of *eltAB* gene, encoding for LT toxin. H-NS regulates negatively LT transcription at low temperature by binding region downstream of the promoter. LT is secreted by the type II protein secretion pathway (T2SS), encoded by the *gspCDEFGHIJKLM* gene cluster on the chromosome of ETEC strain H10407 (Tauschek et al., 2002). Interestingly, this gene cluster and the upstream gene *yghj* (protein mucinase) are regulated by H-NS (Yang et al., 2005; Yang et al., 2007). Thus, the complete transcriptional machinery enhancing the production and secretion of LT is governed by H-NS. Lastly, a complex hierarchy of glucose-dependent regulation are involved in the control of both *eltAB* and *estAB* genes expression through the cAMP receptor protein (CRP). CRP represses transcription of *eltAB* gene while it positively regulates *estAB* gene (Haycocks et al., 2015, Bodero and Munson, 2009).

2.3.4.3. Transcriptional modulations in response to IECs interactions

Pathogen-host cell interactions are finely orchestrated by ETEC. It is featured by the coordination and sequential deployments of multiple virulence molecules. So far, only one study has investigated transcriptional modifications of ETEC H10407 on interaction with Caco-2 cells at several time points (e.g. 30, 60 and 120 min) (Kansal et al., 2013). As key information that comes out, in a total of 214 ETEC genes were consistently altered from 30 min adhesion to Caco-2 cells, while 10 to fortyish genes were expressed from 30 and 60 min, respectively. Among the genes regulated during ETEC-cell contact, *crp* expression, the repressor of *eltAB* was depressed. This downregulation was thus associated to a 7-fold overexpression of *eltAB* gene during cell contact but no expression of *estAB* gene. Likely, *hns* the transcriptional repressor of *eltAB* and its corresponding T2SS was downregulated, suggesting that attachment of ETEC to the host cells may promote the formation of OMVs vesicles, for LT excretion.

Then, an additional experiment with early time points (e.g. 15, 30, 60 min) has been done and demonstrated that multiple genes associated with the biogenesis of type 1 fimbriae were transcriptionally activated as well as *fim* operon and *eatA*. In contrast, transcription of *cfaABC* genes and those involved in synthesis and export of the *EtpA* were repressed following contact. This can be linked to the overexpression of *eltAB*. Indeed, as shown in section 2.3.2, EatA protein moderates EtpA-mediated adhesion, thus accelerating the delivery of LT toxin (Roy et al., 2011).

Finally, authors noted that ETEC undergoes morphological changes following cell contact. Indeed, at very early time points (e.g. 5 to 15 min adhesion), ETEC appears to engage host cells at a distance via long peritrichous flagella, while at later time points, flagella appear to be shortened and engulfed by the IECs (Kansal et al., 2013).

2.3.5. ETEC virulence: wrap-up of the machinery

To summarize the key steps of ETEC pathogenesis presented in the sections 2.3.1-2.3.3, a scheme of the pathogen-host interface is proposed (Fig. 1.14).

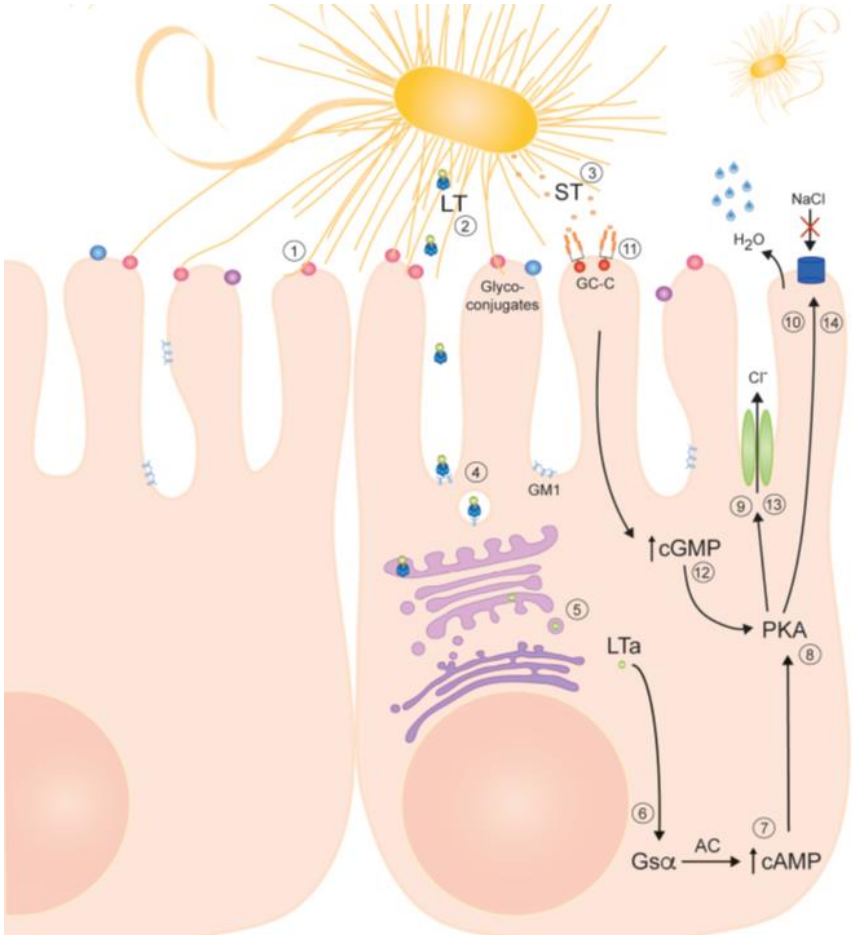

Figure 1.14. **ETEC-host interface: establishment of the virulence machinery.**
(1) ETEC colonizes the ileum via CFs adhering to host glycoconjugates. **(2 & 3)** Enterotoxins LT and/or ST are secreted, **(4)** LT binds to GM1, **(5)** LT is endocytosed and retrograded to the endoplasmic reticulum. The catalytic part of LTa is released and transported to the cytoplasm, **(6)** activating the adenylate cyclase (AC), **(7)** leading to increased levels of cyclic AMP (cAMP). **(8)** cAMP activates protein kinase (PKA), and **(9)** phosphorylates the cystic fibrosis transmembrane regulator (CFTR) resulting in efflux of chloride (Cl^-) ions, **(10)** blocking the uptake of sodium chloride (NaCl). **(11)** In parallel, STa binds to guanylate cyclase C (GC-C), **(12)** elevating the levels of cyclic GMP (cGMP) which activates PKA, and **(13)** CFTR. The effect of both LT and ST is an efflux of negatively charged ions and water, leading to the development of acute watery diarrhea. *Reprinted with permission from Von Mentzer et al., 2016.*

3. Gastrointestinal cues as regulators of ETEC survival and virulence function

The human gastrointestinal (GI) tract is a complex and tumultuous ecosystem, integrating a considerable number of biotic (living factors shaping the ecosystem) and abiotic (physicochemical parameters) that can be critical for the survival and virulence efficiency of pathogens. Such enteric bugs as ETEC have cleverly developed mechanisms to withstand sudden changes in the successive GI niches (e.g. stomach, small intestine and colon) that they will encounter. Thus, the bacteria will reach its prime site of action, the distal portion of the small intestine, the ileum and can extend to the proximal portion of the colon (Allen et al., 2006).

The following sections will first provide an overview of the abiotic and biotic factors governing the human GI tract (section 3.1). That, in order to build an initial picture of the modulation of ETEC survival and its virulence function in the human digestive ecosystem (section 3.2). However, hormonal and nervous regulation of the digestion are outside the scope of this literature review.

3.1. Defining the human gastrointestinal tract and its key functions

The human digestion is a multi-step process including mechanical and chemical breakdown by which foods are converted into organic nutrients that can be absorbed and assimilated by the body. Thus, the digestive tract is formed by a group of hollow organs from the mouth to anus and solid organs (e.g. pancreas, liver and gallbladder) (Fig. 1.15). These organs will be involved in the ingestion, digestion and elimination of foods (https://www.iffgd.org/, consulted on 07/2018). To be concise, only the biotic and abiotic factors of the GI digestion of a healthy adult, starting from the stomach to the large intestine will be detailed in the following sub-sections (3.1.1-3.1.3).

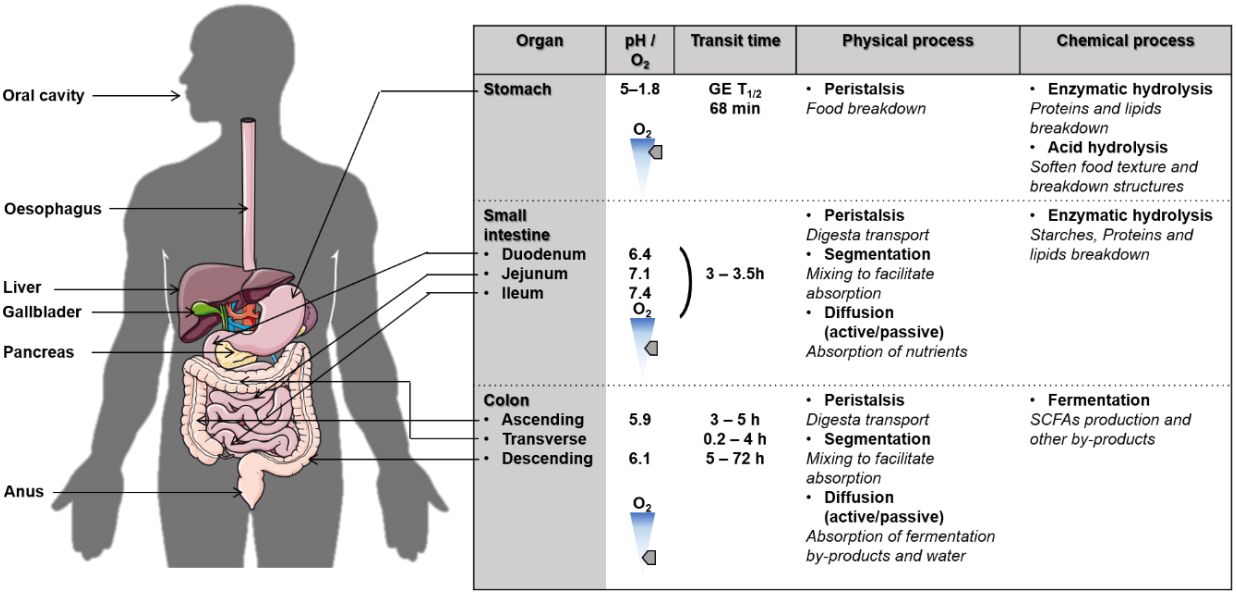

Figure 1.15. **Gastrointestinal tract of healthy adults: summary of the key physical and chemical processes.** GE $T_{1/2}$: gastric emptying half time, SCFAs: Short Chain Fatty Acids. *Modified from Bornhorst and Singh, 2014.*

3.1.1. Gastric digestion

3.1.1.1. Gastric motility

The swallowed bolus passes through the lower esophageal sphincter to enter the stomach, which is primarily comprised of the cardia, fundus and antrum. Globally, the stomach is about 25 cm length and 0.9 L volume (Ferrua and Singh, 2011). The proximal stomach is thought to act as a food reservoir, while the distal stomach is the main location of the physical breakdown of food into particles called chyme. In fact, the peristaltic movements of the gastric wall act to crush and grind food particles until they pass into the small intestine (Schulze, 2006).

Interestingly, there is an overall consensus that the peristalsis or antral contraction waves have an average speed of 1.5-3 mm s^{-1} and an average frequency of 2.6-3 waves min^{-1} for both solid and liquid meals (Bornhorst and Singh, 2014). The chyme volume, type (e.g. solid *vs* liquid) and nutrient content will influence its speed discharge (Sherwood, 2006). Magnetic resonance imaging and scintigraphy remain the most relevant approaches to determine the gastric emptying half time (GE $T_{1/2}$). For example, the GE $T_{1/2}$ mean of a glass of water is about 13 min, as reported in a study using the magnetic resonance imaging on 12 healthy volunteers (Mudie et al., 2014). While for a solid meal, GE $T_{1/2}$ mean of 68 min (45-107 min) was found in 99 healthy volunteers by scintigraphy (Vasavid et al., 2014). Values are also dependent on various factors such as meal composition and consistency, gender, ethnical origin, age-range, smoking and menstrual cycle for both gastric and GI transit time.

3.1.1.2. Gastric secretions and pH

An average of 2-3 L of gastric juice (e.g. mucus, acid, ions, enzymes, and intrinsic factors) is daily secreted by the gastric mucosa, by five different types of cells: faveolar, mucous neck, parietal, chief and G cells (Said, 2012; Sherwood, 2006).

Briefly, the faveolar cells found in the superficial phase of the gastric mucosa secrete mucus (mostly MUC5AC) and bicarbonate (HCO_3^-). This layer will allow protection of the gastric epithelium from its own acid secretion. The gastric fundus and body contain gastric crypts filled with mucous neck cells, also secreting mucus (mostly MUC6); followed by parietal and chief cells. Parietal cells play a role in the secretion of hydrochlorhydric acid (HCl) and intrinsic factor, a protein binding to vitamin B_{12}, allowing then its ileal absorption. For the HCl secretion, gastric pH decreases gradually and continuously from 5 to 1.8 during digestion (Roussel et al., 2016). However, pH fluctuates greatly according to the factors cited here above (sub-section 3.1.1.1). Then, the chief cells are involved in the enzymatic secretion of (i) pepsinogen, an inactive precursor converted into the active proteolytic enzyme pepsin upon contact with acid. Pepsin is capable of hydrolyzing peptide bonds (e.g. phenylalanine, tyrosine and leucine) of most proteins, mucin being one important exception (Seidel and Long, 2006; Hornbuckle et al., 2008); (ii) the gastric lipase, responsible for 10-30% of dietary triglyceride hydrolysis (Gallier and Singh, 2012a). Finally, deeper in the crypts, G cells secrete hormones such as gastrin, ghrelin, somatostatin or cholecystokinin mediating the overall digestion process (Vasavid et al., 2014; Sherwood, 2006).

3.1.1.3. Gastric microbial ecosystem

Contrary to old-school idea that the stomach was a sterile organ due to the acidic environment, the growth of certain bacteria and fungi is possible; making a unique community with the lowest number of microbes in the GI ranging between 1 $\log_{10}$ and 3 $\log_{10}$ colony forming units (CFU) per gram of content (Hillman et al., 2017). Nonetheless, when comparing various studies, caution is needed because gastric juice has a lower pH than the gastric mucus layer, resulting in differences in microbial composition and concentrations (Hunt et al., 2015). Thus, the gastric luminal microbiota is dominated at phylum level by *Actinobacteria* and *Firmicutes*. The main bacterial genera found are *Streptococcus*, *Prevotella*, *Helicobacter* and *Gemella* (Fig. 1.17). While mucosal biopsies of the corpus and antrum in healthy adults are dominated at phylum level by *Firmicutes*, *Bacteroides* and then *Proteobacteria*. Remarkably, half of the population is positive for *Helicobacter pylori*, recognized as a risk factor for the development of gastric carcinoma (Bik et al., 2006; Klymiuk et al., 2017). Globally, abundance and composition of luminal and mucosal gastric microbiota vary greatly between persons, especially between *Helicobacter pylori* positive or negative pattern (Klymiuk et al., 2017).

3.1.2. Small intestinal digestion and colonic fermentation

The human small intestine, separated into three sections (e.g. duodenum, jejunum, ileum), extends from the pyloric sphincter to the ileocaecal junction, representing 6-7 m long, the longest part of the digestive tract. It ensures that the partially digested chyme coming from the stomach is broken down into smaller molecules to be absorbed through the IECs and carried into the bloodstream (Vasavid et al., 2014). The small intestine receives the enzymatic secretions from the digestive glands (e.g. pancreas, liver and gallbladder). The colon, with a significant microbial mass, extends from the ileocaecal junction to the anal canal, with a larger diameter, but shorter length (1.5 m) and is divided in four sections (e.g. ascending, transverse, descending and sigmoid colon). The colon processes indigestible watery-food waste to produce fecal bulk, which in turn is an important determinant of bowel health (Said, 2012). Finally, H_2O, electrolytes and short-chain fatty acids (SCFA) by-products of the microbial fermentation are continuously absorbed along the colon.

3.1.2.1. Abiotic factors

3.1.2.1.1. Motility pattern and transit time

Non-homogeneous movements governed by segmentation, antegrade and retrograde peristalsis of intestinal chyme occur mostly in the jejunum and ileum, as the duodenum is too short. Jejunal movements are typically more rapid and intense than in the ileum, with a postprandial propagation velocity at a rate of 1.6 cm s^{-1} in the jejunum, *versus* 1.3 cm s^{-1} in the ileum (Seidl et al., 2012). By definition, small-bowel transit is considered normal if more than 40% of the chyme has progressed into terminal ileum or passed the ascending colon at 6 h (Bonapace et al., 2000). Among available studies, two separated studies have shown median orocaecal transit time of 255 min (209 to 391 min) and 231

min (± 37 min) for a solid meal, measured with a magnet tracking system and GI scintigraphy, respectively (Worsoe et al., 2011; Miller et al., 1997).

In the colon, the movements and mixing of watery waste converted into feces occur via segmentation (every 30 minutes) and mass movements (1 to 3 times day^{-1}). The colonic transit time of 87 healthy subjects showed a median of 21.6 hours (15.5-37.3 h), measured by wireless pH motility capsule (Rao et al., 2009). The transit time can also be considered according to the segment and the type of alimentation. Interestingly, the transit time fluctuates between 3 to 5 h in the ascending colon, 0.2 to 4 h in the transverse colon and 5 to 72 h in the descending and sigmoid colon, with a huge variability between individuals and food matrix (Wilson, 2010).

3.1.2.1.2. Oxygen level

A steep oxygen gradient exists within the human gut from the duodenum to the sigmoid colon. Such differences reflect a combination of oxygen sources, local metabolism and the anatomy of blood flow. Moreover, sharp contrast exists between the luminal and mucosal phase (especially serosa) of the gut. The cell layer is positioned between the low partial pressure of oxygen (pO_2) present in the lumen, and the highly vascular lamina propria, where oxygen reaches the epithelium. Thus, the pO_2 remains below 10 mmHg in the luminal colon, considered as “physiologic hypoxia”, with a rate of oxygen consumption of 8 $\mu M.h^{-1}.cm^{-2}$, while it reaches approximately 55 mmHg in the luminal ileum (Zheng et al., 2015). No data from the mucosal pO_2 are yet available in human.

3.1.2.1.3. Digestive secretions and absorption

The duodenum secretes bicarbonate that neutralizes gastric acid and provides an appropriate pH of 6.4 (5.9 to 6.8) for further enzymatic digestion to occur. It receives secretions of enzymes and bile from the pancreas and liver, respectively (Vasavid et al., 2014).

Briefly, the exocrine pancreas secretes daily 1.5 L of pancreatic juice including active (lipase) and inactive digestive enzymes (e.g. trypsin, chymotrypsin, and amylase), fluids and bicarbonate in response to food ingestion. Proteolytic and glycolytic enzymes are activated when delivered into the duodenum. Interestingly, pancreatic lipase is the unique intestinal enzyme able to digest lipids and to convert triacylglycerols in monoacylglycerols and fatty acids (Chandra and Liddle, 2014).

Bile is produced in the liver, stored in the gallbladder and 0.5 L are daily released into the duodenum. It is a complex mixture of bile acids (e.g. glyco- and/or tauro-conjugated cholate, deoxycholate, chenodeoxycholate), cholesterol, bile pigment (bilirubin and biliverdin), lecithin, mineral salts and H_2O. In the intestine, bile acids assist in the emulsification and absorption of fatty acids, monoacylglycerols and lipids. They also stimulate lipolysis by facilitating binding of pancreatic lipase with its co-lipase (Chandra and Liddle, 2014). Initially, bile salts concentrations in the duodenum range from 10 to 15 mmol L^{-1} and decrease progressively in the first 2 h following meal ingestion to 5 mmol L^{-1} (Northfield and McColl, 1973).

Then, the majority of nutrient absorption occurs in the jejunum, which is 2.5 m in length, pH 7.1 (6.6 to 7.9) and is completed in the ileum which is 3.5 m in length, pH 7.4 (6.6 to 8.1). The distal 100 cm of the ileum is the only location where vitamin B_{12} and bile salts are absorbed (Said, 2012). Bile salts

concentrations in the jejunum and ileum, are 10 mmol L^{-1} and 2 to 4 mmol L^{-1}, respectively (Northfield and McColl, 1973). All together, the digestion in the luminal phase of the small-bowel is complete for the lipids, only. While for carbohydrates and proteins, the IECs will achieve their digestion.

Subsequently, the chyme reaches the colon with the following pH and redox potential: proximal colon pH 5.9 (5.3 to 6.7), -415 mV ± -72, and the distal colon pH 6.1 (5.2 to 7), -380 mV ± 110 (Stirrup et al., 1990; Press et al., 1998). Food particles partially digested or undigested are fermented by the colonic anaerobic microbes (detailed in section 3.1.3.2.1), serving as substrates for the microbial enzymes in the colon. The lower part of the gut has also a high water-absorbing capacity (90% of the water) entering the colon. In the ascending segment, a substantial fraction of sodium (Na^+) is absorbed, but also Cl^-. Then, the colon can secrete potassium (K^+) and HCO_3^- ions (Khan et al., 1998).

3.1.2.2. Intestinal and colonic epithelial cells lining: structure and function

The small intestinal lining consists of four layers: mucosa, submucosa, muscle layer and adventia. The mucosa is the most complex layer, formed by the intestinal epithelium (Fig. 1.16A). It represents the largest epithelium of the body's mucosal surfaces, covering around 400 m^2 of surface area with a single layer of polarized cells organized into crypts and villi. The major cell types include enterocytes, goblet cells, Paneth cells and enteroendocrine cells (Fig. 1.16B). Each of them carries out specific functions, enterocytes are absorptive (adapted for metabolic and digestive function), while the 3 other types are secretory, which means that they are specialized for maintaining the digestive or barrier function of the epithelium. IECs are continuously replaced every 4-5 days, and new cells are produced by stem cells located in crypts. In addition, M cells are found in the ileum and are associated with the immune system (Peterson and Artis, 2014; Kong et al., 2018).

The functions of each cell types are succinctly described:

(i) Enterocytes – Cover 80% of the villi. They express on their apical surface hydrolytic enzymes to perform terminal digestion of polysaccharides and peptides (e.g. enterokinase, aminopeptidase), in concertation with enzymes present in the luminal phase (section 3.1.2.1.3). They play an important role in nutrient absorption (e.g. ions, water, carbohydrates, peptides and lipids), and in secreting immunoglobulins.

(ii) Goblet cells – Cover 10% of all IECs. They are specialized in the synthesis and continuous secretion of mucus (98% H_2O and 2% mucins MUC2), which lubricates the passage of food through the tract and protects the intestinal wall from digestive enzymes and prevents pathogenic entry (Birchenough et al., 2015). The structure of the small intestine mucus layer will be described in section 3.1.3.1.2.

(iii) Paneth cells – Only found in the small intestine, especially in the ileum. They synthesize and secrete antimicrobial peptides and proteins such as defensins and lysozymes.

(iv) Enteroendocrine cells – Release intestinal hormones or peptides (e.g. glucagon, cholecystokinin) into the bloodstream. They are also known to act as chemoreceptors, detecting harmful substances and initiating protective responses (Kong et al., 2018).

I-1

Histologically, there are two main differences between the small intestine and the colon. The colon lacks villi, meaning that the epithelium remains flat. Moreover, Paneth cells are absent in the colon. In this part of the gut, the absorptive cells are called colonocytes, while goblet cells keep the same denomination but are much higher in proportion (25%) to protect against hostile microenvironments (Van der Flier and Clevers, 2009) (Fig. 1.16C). The structure of the colon mucus layer will be also detailed in section 3.1.3.1.2.

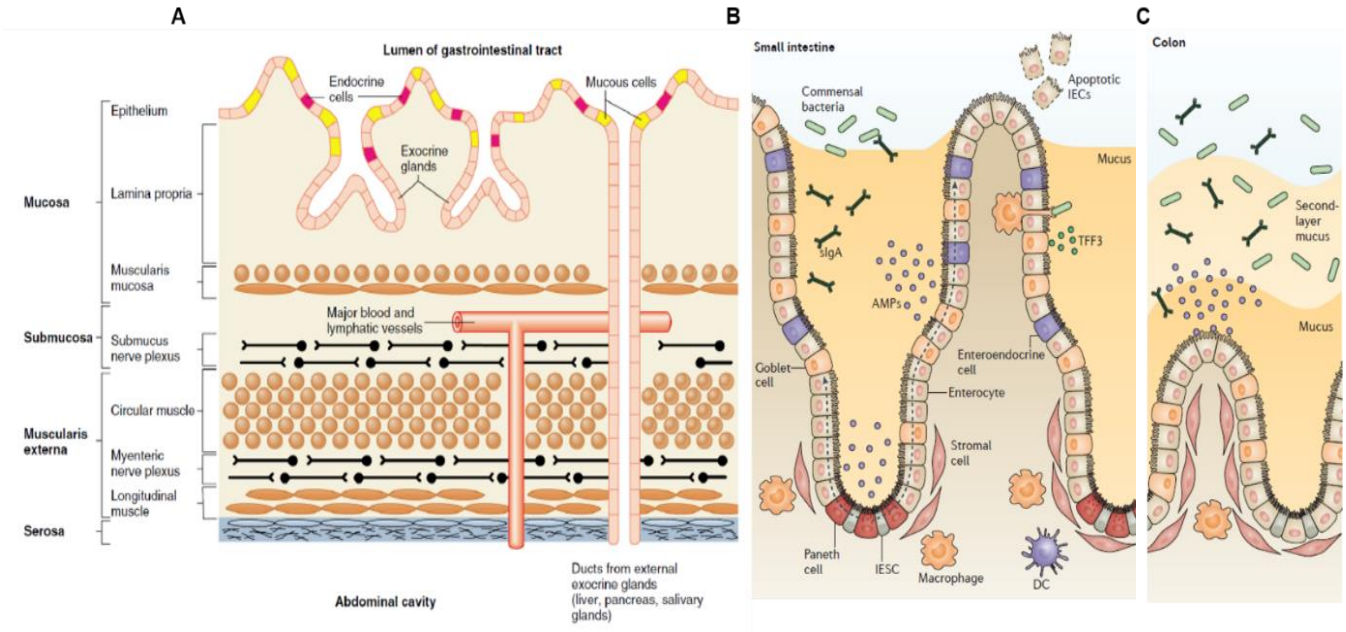

Figure 1.16. **Wall of the gastrointestinal tract (A), cell lines of the small intestine (B) and colon (C).** (**A**) The GI tract surrounds four layers: the innermost layer is the mucosa, underneath, the submucosa followed by the muscularis externa, and finally the outermost layer, the serosa; (**B** and **C**) Intestinal epithelial cells (IECs) form a biochemical and physical barrier that maintains segregation between luminal microbial communities and the mucosal immune system. The intestinal epithelial stem cell (IESC) niche controls the continuous renewal of the epithelial cell layer by crypt-resident stem cells. Secretory goblet cells and Paneth cells secrete mucus and antimicrobial proteins (AMPs) to promote the exclusion of bacteria from the epithelial surface. The transcytosis and luminal release of secretory IgA (sIgA) further contribute to this barrier function. Dendritic cells (DC), Trefoil factor 3 (TFF3), a protein involved in the maintenance and repair of the intestinal mucosa. *Reprinted with permission from Widmaier et al., 2001; Peterson and Artis, 2014.*

3.1.3. Gut microbiota

Gut microbes live in close symbiosis with the human host and play a vital role in human health. In terms of composition and abundance, the gut microbiota is characterized by pronounced regional differences (described section below 3.1.3.1.), both in the longitudinal (proximal *versus* distal) and axial direction (lumen *versus* mucus), influenced notably by physicochemical, nutritional and immunological gradients (Donaldson et al., 2016). In addition to these dissimilarities, at genus and species levels, intra- and inter-individual variability is huge, making the awareness of the gut microbiota even more complex, while the phylum level is more generally conserved. A non-exhaustive list of contributing factors can be draw up with a variation of diet, lifestyle, geographic and ethnical origin, health status, gender, menstrual cycle and age-range. Interestingly, within one individual, the microbial community (at phylum level) is fairly stable over time within a time window of up to five years (Donaldson et al., 2016). The largest shift occurs during the first 4 years of life, when the gut microbial community establishes (Hidalgo-Cantabrana et al., 2014).

To categorize an individual's gut microbial signature, several efforts were undertaken with attempts to define a core microbiota (stable and permanent bacterial members of the community) or to identify gut enterotypes. The concept of gut enterotypes emerged from a fecal metagenome analysis grouping 33 adults in three clusters based on their genus level gut microbiota composition, dominated by *Bacteroides*, *Prevotella* and *Ruminococcus* (Arumugam et al., 2011). So far, this concept remains debatable since the enterotype concept limits the identification of markers (such as diseases) associated with gut microbiota composition, and the cluster identification heavily depends on the applied statistical methodology (Jeffery et al., 2012; Knights et al., 2014).

Although not discussed in this literature update, it is important to briefly mention that in addition to bacteria, other key microorganisms are present in the gut including yeast, fungi, *Archaea*, viruses and phages, thus constituting the gut microbiome. The following sub-sections will describe only the human adult gut microbiota, excluding therefore studies on animal models.

3.1.3.1. Biogeography of the gut microbiota

With the advent of next generation sequencing technology, research studies exploring gut microbial community profiles have flourished. Nonetheless, for now, relatively little is known regarding the longitudinal and axial variation of the human gut microbiota, especially along the small intestine given the difficult accessibility of these regions *in vivo* (e.g. enteroscopic aspiration, ileostomy). Consequently, most research on host-microbes interactions are based on studies of the fecal microbiota, which are obviously most easily collected. Moreover, rare studies have started to investigate the mucosal microbiota. Changes observed in the luminal contents are unlikely representative of what is happening at the mucosal surface, where bacteria interact more intimately with the host. Thus, it is of great interest to better understand the relationship between stool and the mucosal microbiome (Hillman et al., 2018).

3.1.3.1.1. Luminal micro-environment

Most of the microbiota is found in the digestive lumen (Fig. 1.17). The adult GI tract was initially estimated to harbor 14 $\log_{10}$ bacteria, representing 10 times more cells than the human body. However,

a recent study estimated there to be 13 log_{10} bacteria, which is equivalent to the number of human cells (Sender et al., 2016). Longitudinally, the small-bowel harbors typically high levels of bile acids, antimicrobials, oxygen, and a short transit time, in comparison to the colon, limiting thereby bacterial growth of 3 log_{10} to 4 log_{10} CFU mL^{-1} of duodenal and jejunal content.

For example, in a study of only five healthy volunteers that have ingested a meal, the duodenum was aspirated 90 min post-intake. Results displayed two dominant phyla *Firmicutes* and *Actinobacteria* and four dominant genera with *Streptococcus*, *Actinomyces*, *Propionibacterium* and *Granulicatella* (Angelakis et al., 2015). In contrast, a recent study on 20 adults has shown that the jejunum is dominated by *Firmicutes*, *Proteobacteria* and *Bacteroides* phyla. It revealed also a recurring core of abundant species in the jejunum belonged to *Streptococcus*, *Prevotella*, *Veillonella*, *Haemophilus* and *Escherichia* genera (Fig. 1.17). Globally, the jejunal microbiota has a resemblance to the oral microbiota with facultative anaerobes and oxygen-tolerant obligate anaerobes (Sundin et al., 2017). Importantly, this study reported jejunal bacterial counts reaching 6.9 log_{10} CFU mL^{-1} in many subjects, 2 log_{10} higher compared to the classical concentration found in the literature.

A segment below, in the ileum, due to lower bile salts concentration, lower level of oxygen, slower transit times and possible retrograde flow by the ileocaecal valve from the colonic microbes, bacterial concentrations increase from 7 log_{10} to 8 log_{10} CFU mL^{-1} of luminal content (Booijink et al., 2010, Quigley, 2013). The ileal microbiota is dominated by the *Firmicutes* phylum and the following genera *Clostridium*, *Streptococcus, Escherichia* and *Veillonella* are most commonly found. Contrary to the duodenum and jejunum, *Bacteroidetes* phylum is found in half of the volunteers, but remains still below the levels found in the colon (Fig. 1.17) (Booijink et al., 2010; Zoetendal et al., 2012; Van den Bogert et al., 2013). These elements contradict previous studies based on samples collected by retrograde colonoscopy which indicated that the small bowel microbiota, at the level of the distal ileum was similar to the colonic microbiota (Villmones et al., 2018; Wang et al., 2005). Besides, the ileal composition from the study of Hayashi et al. (2005) differed greatly from the one described in Fig. 1.17, but effluents had been collected from three elderly individuals during an autopsy, which may explain such differences (Hayashi et al., 2005).

In contrast, colonic conditions present lower cell turnover rate and redox potential, a higher pH in the distal colon and a longer transit time. The colon supports a dense and diverse community of bacteria with 10 log_{10} to 12 log_{10} CFU mL^{-1} of colonic content according to the segment location, mainly anaerobes with the ability to utilize complex carbohydrates undigested from the small intestine. Many metagenomics analysis from fecal donations of healthy adults have shown that bacteria were predominantly members of the phyla *Firmicutes* and *Bacteroidetes*, followed by *Proteobacteria* and *Actinobacteria*. Moreover, about twenty genera belong to these cited phyla such as *Bacteroides*, *Prevotella*, *Alistipes*, *Eubacterium*, *Ruminococcus*, *Roseburia*, *Faecalibacterium*, *Lactobacillus*, *Enterococcus*, *Blautia*, *Enterobacteriaceae* (family), *Fusobacteria* and hundreds to thousands of species belonging from these genera (Eckburg et al., 2005; Ley et al., 2006; The human Microbiome Project Consortium, 2012) (Fig. 1.17). This core microbiota plays crucial roles in the gut, as explained in section 3.1.3.2.

Noteworthy, all the studies here above have so far primarily focused on proportional abundance of the gut microbes. However, if the microbial load varies substantially between samples, the relative profiling will hamper attempts to link microbiome composition to quantitative data such as physiological parameters or metabolite concentrations (Vandeputte et al., 2017). To overcome this limitation and enable genuine characterization of host microbe interactions, scientists have started to work on absolute microbial profiles by integrating microbial cell counting (flow cytometric enumeration of microbial cells) into a sequencing workflow (Vandeputte et al., 2017).

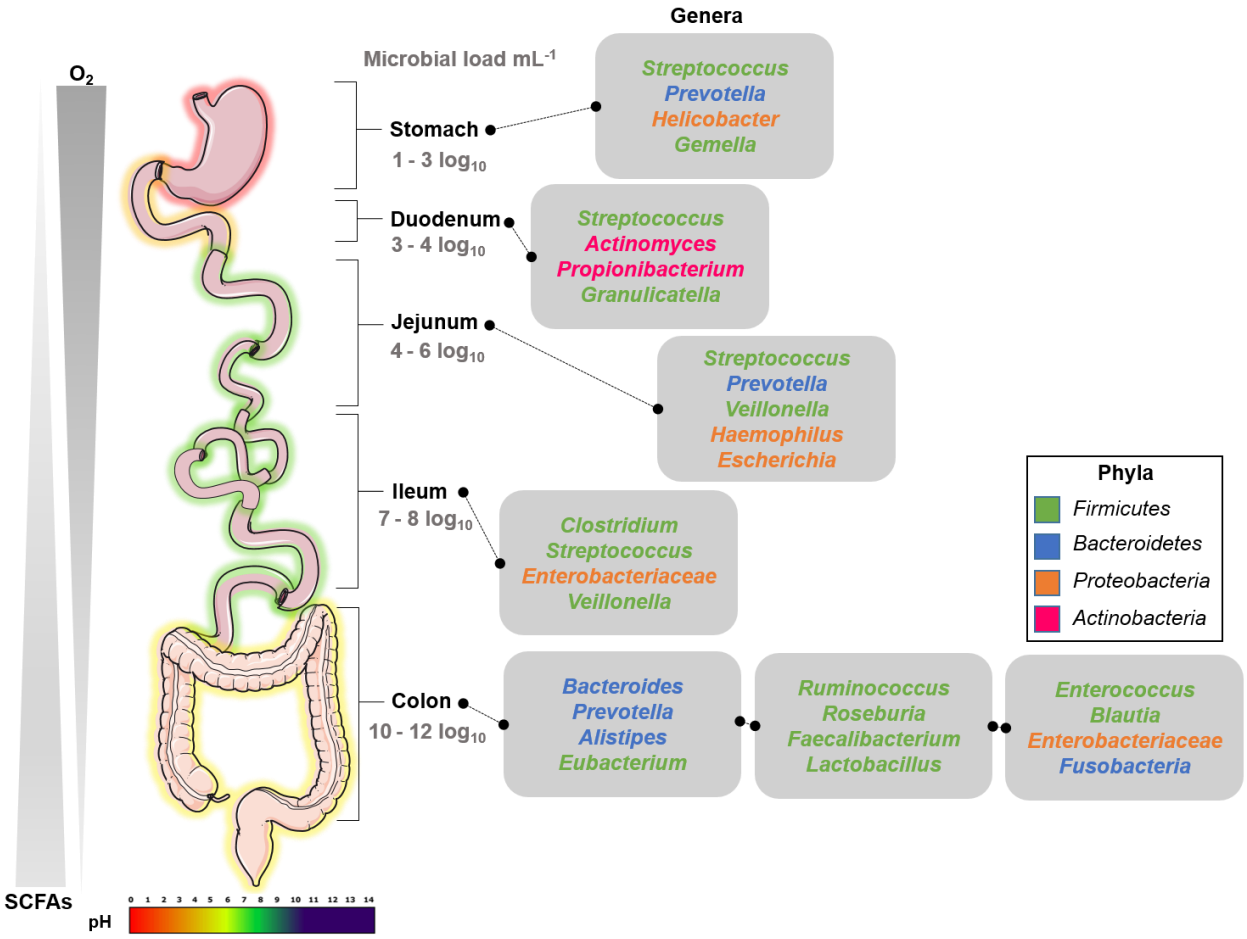

Figure 1.17. **Biogeography of the luminal microbial composition of GI tract in a healthy adult.** The most common genera in each GI tract location are represented in the rounded rectangle, belonging to a phylum represented in color (legend lower right corner). The GI tract scheme is also colored according to the pH scale shown at the bottom. *Reviewed from the data presented sections 3.1.1.3 and 3.1.3.1.1.*

3.1.3.1.2. Mucosal micro-environment

The mucus, continuously renewed by goblet cells, is a complex mixture of glycoproteins, providing a source of carbohydrates for the microbiota. This unique microbial niche tends also to push bacteria out towards the lumen, explaining the lack of bacteria directly in contact with epithelium. At least 10 distinct gel-forming and surface mucins are secreted by the intestinal epithelium, and MUC2 remains the major O-glycosylated product in mucus found in both small intestine and colon. Interestingly, organization and thickness of the mucus layer remain completely different according to the gut regions. In fact, there is a single-thin-layered mucus (123-480 µm) in the small intestine, formed by unattached mucins. This layer also has different glycosylation patterns compared to the colon; mucins are less fucosylated and more sialylated and sulfated in the ileum (Mann et al., 2016; Cecchini et al., 2013). In contrast, a two-layered mucus covers the colon, as in the stomach, with an outer loose-layer and an inner thick-layer (642-830 µm) (Johansson et al., 2013, Thursby and Juge, 2017, Atuma et al., 2001; Strugala et al., 2003). In addition, the properties of these gel-forming mucins are different. For example, in the ileum, the pore sizes are large and allow bacteria to penetrate and swim easily into the mucus. Conversely to the colon lumen, the mucosal layers are partially oxygenated due to their proximity to the blood capillaries of the gut epithelium, thus facilitating the growth of facultative anaerobes (Fig. 1.18).

These previous observations highlight the need for careful considerations of the gut mucosa microbial composition, by choosing adequate sampling methods. So far, no standardized method has emerged in humans, giving a scarce representation of the mucosa-associated bacterial populations according to the gut region. Surprisingly, two different studies have shown that the luminal jejunal microbiota displayed great similarities with microbiota of the jejunal mucosa (Sundin et al., 2017; Dlugosz et al., 2015). Sundin et al. (2017) speculate that “because of its much lower density of bacteria, the lumen is likely to remain oxygenated at similar levels to the adjoining jejunal mucosa and might explain such resemblances. It is also possible that jejunal bacteria grow endogenously in the mucosal layer, and are shed into the lumen” (Sundin et al., 2017). Then, only one work has studied the ileal mucosa, nonetheless, it was in an unhealthy volunteer, making difficult any conclusion (Patrascu et al., 2017). Finally, colonic mucosal populations are slightly better described. *Akkermansia muciniphila* is commonly found residing in the mucus layer and feeds on mucin. *Bacteroidetes* appears to be higher in luminal samples than in the mucosa. In contrast, *Firmicutes,* specifically *Clostridium cluster XIVa*, are enriched in the mucus layer compared to the lumen (Donaldson et al., 2016; Van den Abbeele et al., 2013), *Enterobacteriaceae* as well (Albenberg et al., 2014) (Fig. 1.18).

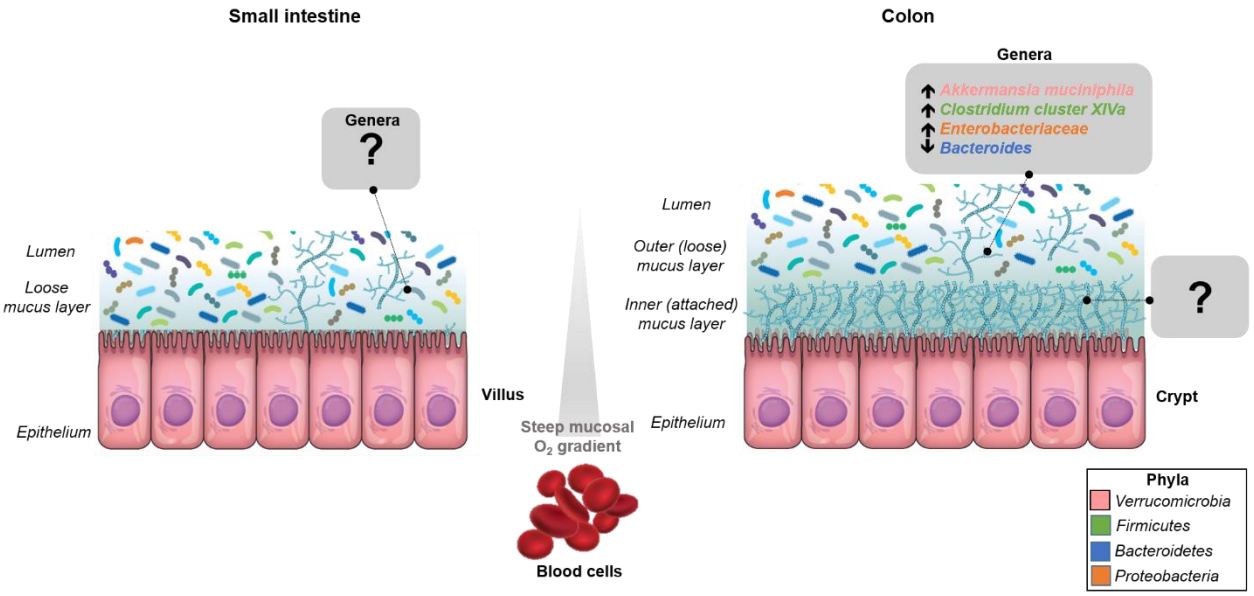

Figure 1.18. **The mucus layers of the human small intestine and colon.** *Reviewed from the data presented section 3.1.3.1.2.*

3.1.3.2. Key functions of the gut microbiota

The gut microbiota makes an important contribution to human health and metabolism. Insights into the associated mechanisms are complex and remain largely unexplored, especially for the functional repertoire contributing to human physiology. Because of this, the specific functions involving gut-brain axis and gut-liver axis crosstalk are outside the scope of this section. Only metabolic activities of the digestion, structural and protective functions of the gut are presented in the following sub-sections (O'Hara and Shanahan, 2006).

3.1.3.2.1. Metabolic activities: from substrates to end products

Bacterial cells essentially consist of a collection of macromolecules, synthesized by the catabolic breakdown of substrates and the subsequent anabolic assembly of monomers derived from the substrates, collectively termed bacterial metabolism (Madigan and Brock, 2011). Bacterial metabolism is very vast and diverse, as gut bacteria living in regionalized and changing environments with different nutrient sources, they will adopt different strategies to utilize nutrients and salvage of energy. To cite, thanks to contributing enzymes, gut microbes are involved in polysaccharides (carbohydrate-active enzymes) and polyphenols breakdown but also B and K vitamins synthesis (O'Hara and Shanahan, 2006).

Under anaerobic conditions, fermentation is the preferred metabolic strategy (Madigan and Brock, 2011; MacFarlane and MacFarlane, 2003). Prior to fermentation, complex polysaccharidic (fibers) and proteic substrates (dietary proteins partially digested or non dietary proteins such as mucins) have to be degraded to their component monosaccharides (sugars) and amino acids, which are then further oxidized (Topping and Clifton, 2001; Tremaroli and Backhed, 2012). Bacteria from the genera

Bacteroides, *Bifidobacterium*, *Ruminococcus* and *Roseburia* and some species from *Clostridium*, *Eubacterium* and *Enterococcus* are provided with hydrolytic activity for the breakdown of polysaccharides, resulting in the production of SCFA. Propionate, butyrate and acetate account for approximately 95% of colonic SCFA contents and are typically found in a proportion of 1:1:3, respectively (McNabney and Henagan, 2017; Louis et al., 2014). While the remaining 5% of SCFA are attributed to valerate, caproate, heptanoate, octanoate and branched SCFA (e.g. isobutyrate, isovalerate and isocaproate). Moreover, glycan metabolism leads to the production of intermediary metabolites such as succinate, lactate, ethanol and gases (e.g. H_2, CO_2). Acetate is predominantly produced by genera *Bacteroides*, *Clostridium*, *Ruminococcus* and *Eubacterium* and it can then be partially used for butyrate formation. Propionate is mainly produced by genera *Bacteroides*, *Propionibacterium* and *Veillonella* (Bernalier-Donadille, 2010). Despite the fact that the ileum is not known for its fermentative activity, a recent study has shown that the ileum mucosa encompasses the potential for dietary fiber degradation with a fibrolytic community belonging to *Bacteroides uniformis*, *Bacteroides cellulosilyticus* and *Eubacterium*. However, the study was performed in an unhealthy subject preventing thus any definitive conclusion (Patrascu et al., 2017).

Then, the proteolytic activity of the gut microbes (*Bacteroides, Clostridium, Propionibacterium, Fusobacterium, Streptococcus* and *Lactobacillus*) leads to the production of ammonia (NH_4^+) (Bernalier-Donadille, 2010). Besides, amino acids metabolism occurs via either deamination or decarboxylation reactions and generates SCFA or amines, respectively (Fan et al., 2015). Amines are then absorbed and transported to the liver to be converted into urea.

Overall, 99% of SCFA are absorbed by the colonic epithelium. Butyrate alone has been estimated to provide 60-70% of the colonocyte's energy needs, while acetate and propionate are energetic substrates for the liver (McNabney and Henagan, 2017). Lastly, SCFA production gradually decreases from the proximal to distal part of the colon (Bernalier-Donadille, 2010). Functions of SCFA involved in the fight against enteric pathogens are summed-up in Table 1.3.

Table 1.3. **SCFA properties against enteric infections**

SCFA in general	• Lower the pH - inhibition of pathogens growth • Regulate immune system and inflammatory responses • Increase IL-18 production – involved in maintaining and repairing epithelial integrity	*Rios-Covian et al., 2016; Correa-Oliveira et al., 2016, Morrison and Preston, 2016*
Butyrate	• Attenuates bacterial translocation - enhances gut barrier function by ✓ improving tight junction activity ✓ increasing mucin synthesis • Histone deacetylase inhibitors - regulates epigenetically genes expression	*Hamer et al., 2008; Jung et al., 2015; Morrison and Preston, 2016; Lin and Zhang, 2017*
Acetate	• Inhibits enteropathogens	*Fukuda et al., 2011*
Propionate	• Histone deacetylase inhibitors - regulates epigenetically genes expression	*Morrison and Preston, 2016*

3.1.3.2.2. Trophic effect on intestinal epithelium and regulation of host defense to infection

Shortly, gut microbes have important trophic effects on intestinal epithelia, by favoring the development of intestinal microvilli, epithelial cell differentiation and proliferation (Li et al., 2012). For example, without gut microbiota, the speed of cells renewal is diminished by 20% and mucosa thickness is also reduced in a mouse model (Alam et al., 1994).

Moreover, gut microbes can promote resistance to colonization by pathogenic species. This barrier effect can be exerted at several levels by nutrient competition and antimicrobial molecules production by both gut microbes but also IECs such as Paneth cells (Bäumler and Sperandio, 2016, Lievin-Le Moal and Servin, 2006). In addition, gut microbes play a fundamental role in the regulation and maturation of the host's innate and adaptive immune responses (Leber et al., 2008, Wu and Wu, 2012). Crosstalk between resident commensal bacteria and immune cells is vast and complex to describe and will not be discussed here.

3.2. ETEC driven by gastrointestinal cues: a proposed state of the art

Using the knowledge provided by the previous part, the section hereafter aims to unravel the numerous and complex human biotic and abiotic gastrointestinal cues that can impact ETEC pathogenesis (e.g. modulation of the survival and virulence function). Although these physiological cues are abundant, direct links with ETEC pathogenesis are so far scarcely understood and the models used are limited and remain distant from the human GI physiology.

It is worth to note that this state of the art has been published in a book chapter [1] and redrafted / updated for the present section.

3.2.1. Bacterial survival in the human GI tract

Bacterial survival in the human GI tract is a key parameter in ETEC pathophysiology. Nevertheless, how pathogens can survive in the human digestive environment remains largely unknown as studies in humans with wild type strains are obviously impossible. Until now, most of the experiments have been conducted *in vitro*, in batch systems, while almost no data are available for ETEC under dynamic human digestive simulated conditions (see section 3.3).

Physiologically, after being ingested, the pathogen must first breach the acidic barrier of the human stomach, where pH gradually decreases during digestion from around 5 to 2. Its final endpoint is to reach the small intestinal niche with pH close to the neutrality. Remarkably, no specific acid resistance system to ETEC has been found yet. Nonetheless, it has been well described that *E. coli* strains in general have intricate acid resistance (AR) systems that enable their survival in the harsh gastric

[1] ***Book chapter.*** *ROUSSEL C., CORDONNIER C., LIVRELLI V., VAN DE WIELE T., BLANQUET-DIOT S. Book chapter 1. Enterotoxigenic and enterohemorrhagic Escherichia coli : survival and modulation of the virulence in the human gastrointestinal tract. INTECH Open (2017). https://doi.org/10.5772/intechopen.68309*

environment, the glutamate-dependent AR system providing the highest level of acid protection (Zhao and Houry, 2010).

Masters et al. (1994) have shown that after static exposure to pH 2, ETEC became undetectable by plate counting after 2 hours. A study using flow cytometry indicated that there was no significant difference in the percentage of live bacteria when ETEC were subjected either to pH 5 or pH 7 (Gonzales et al., 2013). Only one study has investigated the impact of 30 g L^{-1} bile on the survival of ETEC *in vitro*. Despite the known bactericidal effect of bile in the intestine, growth curves for ETEC in Luria Bertani (LB) media and LB-bile showed similar slopes during the exponential growth phase (Sahl and Rasko, 2012).

3.2.2. Regulation of virulence genes by gastrointestinal cues

To be fully pathogenic, bacteria must not only survive in the human GI tract but also coordinate expression of virulence determinants in response to localized gut microenvironments. An increased number of *in vitro* or *animal* studies have shown that ETEC is able not only to resist the stressful conditions encountered in the gut, but rather respond or utilize various GI cues to modulate the expression of its virulence factors (Gonzales-Siles and Sjöling, 2016; Sistrunk et al., 2016), as described below (Fig. 1.19). Again, the models used to describe such effects are limited and remain far away from the human GI physiology.

3.2.2.1. Regulation by physicochemical parameters of the human gut

3.2.2.1.1. pH and oxygen gradients as chemicosensors

Studies testing GI pH on ETEC have only explored its effect on enterotoxins production and/or secretion. For example, the release of ST seems to be not pH-dependent (Johnson et al., 1978) while it is acknowledged that extracellular pH has an influence on the release of LT toxin, increasing with alkalinity (Kunkel and Robertson, 1979; Hegde et al., 2009). In fact, ETEC seems to use the pH gradient in the GI tract to modulate LT toxin production and secretion: when bacteria reach the small intestine, alkaline pH induces both transcription and maximal release of LT (Gonzales et al., 2013). Various oxygen levels can be found in the human GI tract with concentrations decreasing from the upper to the lower digestive tract and from mucosal surfaces to gut lumen, as presented section 3.1.2.1.2. A study performed in culture medium has displayed that LT was not efficiently secreted into the supernatant under anaerobic (10% CO_2, 10% H_2 and 80% N_2) or microaerobic conditions (half of the air replaced by 10% CO_2, 10% H_2 and 80% N_2) unless terminal electron acceptors (e.g. trimethylamine N-oxide dihydrate or nitrate) were available. Precisely, GspD protein, a secretin subunit of the T2SS required for LT secretion, was only assembled under anaerobic conditions and in presence of terminal electron acceptors (Lu et al., 2016). Remarkably, an additional recent and nice study has explored the effect of oxygen variations on ETEC virulence genes expression (Crofts et al., 2018). Authors used batch cultures maintained under microaerobic (85% N_2, 10% CO_2, 5% O_2) or anaerobic (95% N_2, 5% H_2, 0% O_2) atmospheres, and human feces from five volunteers infected with ETEC H10407 ($1.2x10^7$ CFU/dose). *eltAB* genes (encoding for LT toxin) and *cfa* (encoding for CFA/I adhesin) were down-regulated in infected stool samples and in anaerobic batch cultures as well and compared to the microaerobic environment. These

genes repression were relieved when the oxygen-intolerant fumarate and nitrate reduction gene (*fnr*) was inactivated near the epithelium, where oxygen seepage from IECs is sensed by *E. coli*. Thus, inactivation of *fnr* reestablishes the ETEC virulence genes expression (Crofts et al., 2018).

3.2.2.1.2. Digestive enzymes and bile salts as chemicosensors

Once the small intestine is reached, digestive enzymes form one of the challenges to pathogens to efficiently colonize the gut (section 3.1.2.1.3). Only two studies have investigated how human digestive enzymes may influence expression of virulence genes in ETEC. In the latter, *in vitro* studies have shown that trypsin, an endopeptidase secreted by duodenal epithelial cells, is able to increase LT release (Kunkel and Robertson, 1979) and its secretory activity (Rappaport et al., 1976). Then, given the length of the small intestine, bile salts are one of the more long-term exposures encountered by bacteria and pathogens such as ETEC in the human GI tract. These innate antimicrobial detergent-like compounds sequentially decrease from duodenum to colon due to re-absorption (Sistrunk et al., 2016), as described in section 3.1.2.1.3. Chatterjee and Chowdhury (2008) have shown *in vitro* that 2 g L^{-1} crude bile (porcine or bovine origin) can prevent the binding of LT toxin to GM1 and that this effect was associated to arachidonic, linoleic and oleic unsaturated fatty acids detected in crude bile. The same authors demonstrated *in vivo* in rabbit ileal loops that linoleic acid prevented LT-mediated fluid accumulation in a dose dependent manner (Chatterje and Chowdhury, 2008).

In another study conducted by Nicklasson et al. (2012), 1.5 g L^{-1} crude bile (porcine or bovine origin) and 2 g L^{-1} bile salts sodium deoxycholate and sodium glycocholate induced *in vitro* the expression of CS5 encoding gene *csfD*. Besides, a global transcriptional analysis of two ETEC strains showed that bile salts at a concentration of 30 g L^{-1} in LB medium up-regulated *estA*, *eltA* or *etpA* (encoding for STa, LTa enterotoxins and EtpA, respectively) while *csoA* and *cstA* (encoding for CS1 and CS3 colonization factors) were downregulated (Sahl and Rasko, 2012). In this study, the transcriptional response to bile salts was strain-dependent, suggesting that the results should not be extrapolated to the entire pathovar without further investigation. Finally, at the protein level, 1.5 g L^{-1} bile salts were required for surface expression of at least CS5, CS7, CS8, CS12, CS14, CS17 and CS19 (Haines et al., 2015; Grewal et al.,1997). Haines et al. (2015) have also revealed that bile salts seem not to be required for the expression of CS1, CS2 and CS3, while the opposite was demonstrated by Sjöling et al. (2007). These results suggest that both interaction of LT toxin with its receptor and expression of ETEC colonization factors may be differentially induced along the human intestine where bile acid concentrations range from 2 g L^{-1} in the terminal ileum to 20 g L^{-1} in the duodenum (see concentration in mm L^{-1} in section 3.2.2.1.2).

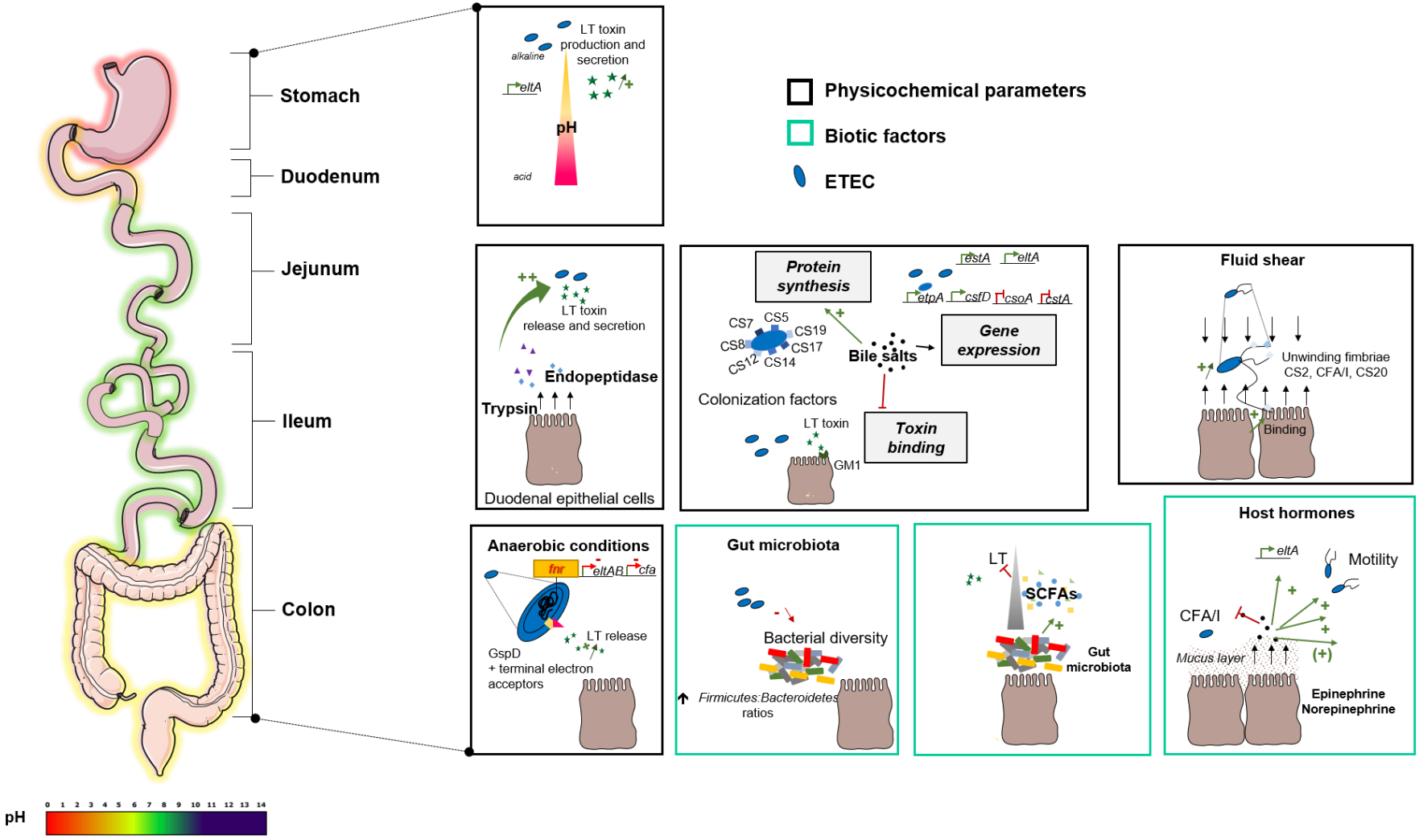

Figure 1.19. State-of-the-art on the effects of biotic and abiotic parameters of the human gut on ETEC virulence. *Modified from Roussel et al., 2017.*

3.2.2.1.3. Fluid shear as mechanosensor

Fluid shear can be defined as distribution of frictional forces due to hydrodynamic flow generated by GI peristaltic activity against the surface of intestinal epithelial cells. In the human gut, there is a decreasing gradient of fluid shear stress from duodenum to ileum. The level of fluid shear also decreases with increasing proximity to the intestinal wall (Gayer and Basson, 2009). In fact, the flow of a bolus through the center of the gut lumen creates the highest fluid-shear compared to the mucosa (Pearson and Brownlee, 2010). Moreover, the viscoelastic properties of the mucus layer further reduces the fluid shear and provides less physical perturbation and thus a protection for living cells within the mucus from high-fluid shear (Atuma et al., 2001, Nickerson et al., 2004).

It has been generally assumed that shear stress inhibits pathogen adhesion, thereby serving as a non-specific host defense against bacterial colonization (Alsharif et al., 2015). Nonetheless, sustained adhesion of pathogen to their target cells can be facilitated by a reduction in force on their tethers. Unwinding is believed to be an important biomechanical property of fimbriae, reducing thus the probability of bacteria detachment (Mortezaei et al., 2015). For ETEC this concept has been very poorly described in the literature. For instance, a study has defined the biophysical features of some ETEC fimbriae using dynamic force spectroscopy with optical tweezers. Thus, investigators have classified CS2, CFA/I and CS20 fimbriae into a low-force unwinding group of fimbriae (Mortezaei et al., 2015). In addition, Tchesnokova et al. (2010) have shown, by using *in vitro* erythrocytes and Caco-2 cell models, a shear-enhanced binding of intestinal CfaE, the tip-localized minor subunit of CFA/I, in both prototypical and clinical ETEC strains (Tchesnokova et al., 2010). These preliminary data suggest that, in addition to a range of chemical environmental signals, ETEC are capable of sensing and responding to mechanical cues in the human GI tract.

3.2.2.2. Regulation by biotic factors of the human gut

3.2.2.2.1. Gut microbiota and metabolic activities

During passage through the human gut, enteric pathogenic bacteria such as ETEC also have to face a high number of commensal bacteria that compete with them for nutrients and space, as developed in the section 3.1.3. Few studies have investigated gut microbiota changes during ETEC challenge (David et al., 2015; Pop et al., 2016; Youmans et al., 2015). In the study of David et al. (2015), the fecal samples and rectal swabs from 13 Bangladeshi patients diagnosed ETEC-positive have been longitudinally collected and followed for a month. While, in the study of Pop et al. (2016), fecal samples from 12 healthy adults that have been challenged with a low dose of ETEC H10407 (the reference strain presented in section 2.3.4.1) ranging from 5 $\log_{10}$ to 6 $\log_{10}$ CFU per dose have been followed form 3 months to evaluate the effect of the subsequent ciprofloxacin antibiotic therapy on microbial changes. However, seven subjects did not develop any symptoms due to the low dose and fecal samples were thereby not collected. Both authors conclude that ETEC infections were associated with a rapid and reversible change in gut microbial community structure as well as a significant decrease in overall bacteria diversity. In addition, a clinical study has compared the microbial composition of fecal samples from 99 individuals who developed traveler's diarrhea associated with ETEC (38 subjects), norovirus, mixed

pathogens or unidentified pathogens (Youmans et al., 2015). Samples were collected within 72 h of acute diarrhea. Regardless the etiologic agent, the authors defined the alterations of the microbiome as a dysbiosis, associated with high *Firmicutes*:*Bacteroidetes* ratios. However, when the microbiome of travelers were compared to samples from healthy travelers in the Human Microbiome Project, no difference in the microbial composition was observed, thus suggesting that the simple act of travelling resulted in a dysbiotic microbiome that was indistinguishable from those with traveler's diarrhea (Youmans et al., 2015; Rasko, 2017). Importantly, one of the limitations to these studies is the fact that fecal samples are not representative to the niche encounter in the ileum, which is recognized as the prime site of action for ETEC (previously described in sections 3.1.3.1 and 3., respectively). In addition, no data on how gut microbiota may influence ETEC virulence are yet available.

Regarding metabolic activities associated to the gut microbes, a unique study has shown that addition of SCFA from C-2 to C-7 (e.g. acetate, propionate and butyrate) at a concentration of 2 mg mL^{-1} in the culture medium significantly reduced or even abolished LT production (Takashi et al., 1989). This concentration level of SCFA is usually found in the colon and is nonetheless too high to be encountered *in vivo* in the small intestine.

3.2.2.2.2. Host hormones

Microbial endocrinology is a newly recognized microbiology research area investigating the interactions of bacteria with stress-associated hormones, such as catecholamine. Among these hormones, only epinephrine and norepinephrine have been investigated as environmental cues for ETEC. In addition, molecules involved in the quorum sensing of ETEC (autoinducers), a bacterial cell-to-cell communication mechanism are poorly investigated.

Lyte et al. (1997) demonstrated that physiological concentrations of norepinephrine increased the *in vitro* growth of an ETEC strain isolated from calf as well as the expression of the virulence factor F5 fimbrial adhesin. In contrast, Sturbelle et al. (2015) did not observe any effect of norepinephrine or epinephrine on the *in vitro* growth of a piglet ETEC strain and Haines et al. (2015) found a significant inhibition of porcine ETEC growth by norepinephrine. However, a significant increase in motility and expression of F4 fimbriae and LT toxin-encoding genes was shown in the ETEC culture supplemented with conditioned medium (containing autoinducers) and epinephrine (Sturbelle et al., 2015). Lastly, Haines et al. (2015) found that norepinephrine inhibited CFA/I expression in an ETEC strain isolated from human. So, host-derived hormones epinephrine and/or norepinephrine seem to assist ETEC in cueing their site of colonization and enhance approach to the epithelial layer through increased motility and adhesion. Nonetheless, the regionalization of these hormones in the gut and physiological concentrations remain scarcely described in human, limiting thus the development of relevant models to investigate such parameters.

Collectively, despite the scientific progresses, the data obtained until now show many gaps and inconsistencies. In particular, most of the current studies have been carried out using oversimplified *in vitro* models of the human gut and what is still missing is the integration of signals delivered in a sequential but not in an isolated fashion. Noteworthy, integration of the gastric pH drop, selection of

digestive secretion concentrations consistent to the human physiology, mimicking of the digestive dynamism, and integration of the gut microbiota are some of the most key parameters required to strengthen the conclusion of some studies described previously. Therefore, relevant alternatives to better understand how ETEC responds to these various cues in a temporal-spatial fashion may imply relevant animal models (e.g. human microbiota associated animals) or digestion models closely mimicking the human digestive tract, such as the TNO gastrointestinal model (TIM-1) or Simulator of the Human Intestinal Microbial Ecosystem (SHIME) (Blanquet-Diot et al., 2012; Van den Abeele et al., 2012).

3.3. *In vitro* models of the human gut to address knowledge gaps in ETEC pathogenesis

Further to information provided in the conclusion above, artificial digestive systems emerged as an alternative and/or a complementary tool to *in vivo* (e.g. human volunteers, animal models) studies. Prioritize *in vitro* approaches, when it is possible, is clearly encouraged by the European Partnership for Alternative Approaches to Animal Testing, the European Directive -2010/63/EU and the French decree 2013-118. As pre-requirement and according to the research topic, it is essential to assess the relevance of using these *in vitro* digestive models and make sure that they will provide complementary understanding to the *in vivo* situation. In the case of the study of ETEC pathogenesis in human, studies involving non-attenuated pathogens or physiological dose are obviously prohibited in humans. Thus, digestive *in vitro* models represent a great alternative to fully study pathogenic strains and come closer to the complexity of the GI physiology.

The simplest models are termed “static” or “batch” models. In general, most of the batch systems have been developed for specific applications and are cheap high-throughput tools, particularly relevant for large prescreening approaches (Guerra et al., 2012). Only one or two digestive conditions are fixed at start in a same bioreactor, underestimating thereby the complexity of the GI physiology. To cite, the simplest gastric model consisting in peptide hydrolysis by using a simulated gastric fluid (SGF). SGF is only composed of pepsin, stirred with the food sample of interest and can be maintained for example at pH 2 or 3 for 30 to 120 min (Egger et al., 2016). Nonetheless, in this case the complexity of the gastric physiology is undervalued since the gastric pH is not progressively dropped, and the enzymatic cocktail, classically found in the stomach is not included. In the same way, the United States Pharmacopeia apparatus also provides such static bioreactors.

When devices are then multi-compartmented, the dynamics and successive environmental niches of the GI tract can be appreciated. These models provide unlimited screening possibilities, facilitating continuous monitoring and sampling possibilities under standardized conditions. Beyond technical aspects, *in vitro* systems facilitate investigations circumventing regulatory, ethical constrains and lowering study costs. They are relevant not only for microbiological studies, but have also a huge range of applications for food processing and nutrition, pharmacology and toxicology, as well in the field of biotechnologies. According to the model considered, most of the parameters will be adjusted in terms

of food-matrix (solid *vs* liquid), group target (age-range) or health status (healthy *vs* diseased) that investigators want to reproduce.

Furthermore, simulation of the GI tract is the biotechnological core of this joint PhD gathering the expertise of two laboratories possessing the most complete simulators of the upper and lower GI tract, TIM-1 (MEDIS UMR Clermont-Auvergne University, France) and M-SHIME (CMET laboratory Gent University, Belgium), respectively. The interest of this part is not to advocate the use of these models but rather to give a brief overview of the available systems and their strengths and limits. Masticator systems or specific devices for example for infant digestion will be not described in this manuscript. Only the gastric, gastro-intestinal and colonic models, simulating the digestion and/or fermentation processes of a healthy adult will be taken into account.

3.3.1. Gastric mono-compartmental simulators

In order to cleverly appreciate the physical and/or chemical changes of food in the stomach or for microbiological applications, dynamic models have been developed. According to the *in vitro* systems, they offer a larger spectrum of parameters to follow such as: the continuous changes in pH (pH drop) and secretion flow rates (e.g. pepsin, lipase), the peristalsis, and physical breakdown or the gastric emptying as well. Four models are available and differed especially by their mixing and mechanical breakdown patterns (Table 1.4). Interestingly, the human gastric simulator (HGS) or Riddet model is the one that faithfully and precisely reproduces the contractive motility of the stomach by a series of rollers that continuously impinge and compress the compartment wall with increasing amplitude (Kong and Singh, 2010; Ferrua et al., 2015). With the dynamic gastric model (DGM) the applied grinding forces significantly differed from those observed *in vivo* (Mercuri et al., 2011). Finally, the TIM- advanced gastric compartment (TIM-agc) consists of a body part that gradually contracts to simulate gastric tone and consequent reduction of gastric volume during emptying. Two antral parts (proximal and distal) are distinguished and contracted separately to reproduce the antral contraction waves physiologically observed (Minekus, 2015). However, this device cannot simulate the mechanical breakdown of food particles.

Table 1.4. **Main dynamic gastric mono-compartmental simulators**
Antral contraction waves (ACWs). *Updated from Guerra et al., 2012.*

Gastric simulators	**Human Gastric Simulator** (HGS) *Kong and Singh, 2010*	**Gastric Digestion Simulator** (GDS) *Kobayashi et al., 2017*	**Dynamic Gastric Model** (DGM) *Mercuri et al., 2011*	**TIM-advanced gastric compartment** (TIM-agc) *Minekus, 2015*
Body T°C	+	+	+	+
pH drop	+	+	+	+
Emptying	+	+	+	+
Mixing pattern	Peristaltic motion	Peristaltic motion (ACWs)	Physiological shear (water presser piston / barrel)	Peristaltic motion proximal / distal antrum (ACWs)
Mechanical breakdown	Roller rotation system to reduce size of solid particles		Grinding forces	-
Secretions	- Saliva - HCl, HCO_{3}^{-} - Lipase, pepsin	- HCl, HCO_{3}^{-} - Lipase, pepsin, α-amylase	- HCl, HCO_{3}^{-} - Lipase, pepsin	- HCl, HCO_{3}^{-} - Lipase, pepsin,

3.3.2. Multi-compartmental simulators

3.3.2.1. Models of the upper GI tract

Although the gastric mono-compartmental simulators have started to integrate a certain number of physicochemical parameters, they give an incomplete insight of the GI digestion. For example, in order to study with precision the fate of food compounds or the fate of an enteric pathogen, it is thereby required to simulate each step of the human digestion, the digestive secretion deliveries and the associated transit time. In response to that, bio-regionalized or multi-compartmental simulators have been developed and are listed in Table 1.5. Bi-compartmental models can first be cited. They mimic only the stomach and duodenum by controlling the pH, temperature, transit time and bile concentration (Mainville et al., 2005; Levi and Lesmes, 2014; Ménard et al., 2014). For example, the In Vitro Digestive System (IViDiS) has been adapted from Mainville et al. (2005) (Thompkins et al., 2011).

Then, to increase the complexity and relevance of digesters, only few systems became innovative by combining both bio-regionalization and dynamisms of the GI digestion and/or fermentation. So far, only the TIM-1 and SHIME, the two most complete systems answer to these criteria and have been well-validated by *in vitro* / *in vivo* correlation studies (Blanquet-Diot et al., 2012; Van de Wiele et al., 2015). Noteworthy, the well-known TIM-1 faithfully reproduces the physicochemical parameters of the human upper GI tract (e.g. stomach, duodenum, jejunum and ileum) and integrates the passive absorption of small molecules thanks to a dialysis system in the jejunal and ileal compartments (Banquet-Diot et al., 2012). This system allows the mimicking of the body temperature, the temporal and longitudinal changes in gastric and intestinal pH kinetics, the dynamism of the chyme transit and mixing, and the sequential delivery of the digestive secretions. Nonetheless, this device does not integrate the anaerobiosis and the digestive microbiota, contrary to SHIME models (see section 3.3.2.2). Two additional devices, the

Engineered Stomach and small Intestinal (ESIN) and the Multicompartmental Dynamic Model of the Gastrointestinal System (SIMGI) (Guerra et al., 2016; Barroso et al., 2015) are bioregionalized. SIMGI, imitating the original SHIME, integrates the gut microbiota as well (see section 3.3.2.2). Besides, to overcome some limitations encountered in the TIM-1, ESIN allows a close imitation of real food size particles entering the stomach and reproduces a differential gastric emptying between liquid and solid particles. However, ESIN and SIMGI have only been developed recently and are still under validation.

Collectively, all existing models operate with relatively large volumes, and thus require large amounts of sample material for testing, which can increase considerably the experimental costs. Therefore, additional GI or small intestine *in vitro* models have been build-up to collect smaller volumes and increase throughput, including the Tiny-TIM (TNO) and the The Smallest Intestine (TSI), respectively (Havenaar et al., 2013; Cieplak et al., 2018). Remarkably, TSI reproduces only the small intestine and incorporates the ileal microbiota to study the microbial behavior during small intestinal passage.

3.3.2.2. Fermentation systems

The development of bioreactors able to reproduce the fermentation process of the human gut originated from the awareness that fecal microbiota significantly differ from the *in vivo* colon microbiota, both in terms of community composition and metabolic activity (Van de Wiele et al., 2015). Thus, the common purpose of fermentation systems is to cultivate a complex fecal microbiota under controlled environmental conditions for carrying out microbial modulation and metabolism studies. In practice, the bioreactors are maintained anaerobically (N_2, CO_2 or by the sole fermentative activity of the microbes), and inoculated with fresh or frozen fecal samples from one individual or pooled from several subjects. There is no consensus in the preparation of fecal samples. Aguirre et al. (2014) demonstrated comparable microbial diversity and metabolic activity between pooled and not pooled human feces (Aguirre et al., 2014), while Van de Wiele et al. (2015) revealed that “the artificially high microbial diversity in pooled inocula creates disturbances in the cross-feeding processes between microorganisms that are adapted to one another in each of the separate microbiomes”. Therefore, authors advised to study inter-individual variability through separate fecal experiments (Van de Wiele et al., 2015).

A variety of *in vitro* colonic models exists and they are listed in Table 1.5. These devices range from batch (24-48 h fermentation) to semi-continuous or continuous cultures, consisting of single or multistage setups (e.g. proximal *vs* distal colon), maintained for several weeks or months as well. Most of the dynamic multistage fermentation models are based on the Reading model, firstly described by Gibson et al. (1988). Prior to start an experiment and for a stable metabolic activity, the initial fecal inoculum needs a suitable adaptation period to the environmental conditions found in the respective colon compartments. The length of stabilization will relate to the residence time that is imposed in the bioreactor and can vary greatly between 10 to 20 days (Van de Wiele et al., 2015). To control the smooth running of the bioreactors, pH, temperature, residence time, pressure, anaerobiosis, redox potential and agitation are usually followed in addition to the nutrients availability and the microbial population dynamics (e.g. abundance, diversity and metabolic activity).

Interestingly, SHIME and SIMGI are the sole bioreactors that integrate the entire gastrointestinal transit into one system, leading to a succession of five compartments (e.g. stomach, small intestine, ascending, transverse and descending colon) (Van de Wiele et al., 2015; Barroso et al., 2015). The main difference between them is that SIMGI includes the peristaltic movements of the stomach. Nevertheless, the SHIME remains the originally and internationally known system. Special features are constantly developed in this system. This is therefore the case for the integration of the mucosal microbiome, playing a specific role in the bacterial colonization process. As explained earlier, the mucosal microbiome was already known to fundamentally differ from the luminal microbiome in composition with specific surface-attached mucosal microbes (in section 3.1.3.1.2). This niche remains difficult to access in human, and to answer that, the SHIME system was optimized for mimicking the mucosal microbial colonization, called M-SHIME. It consists of the incorporation of type 2 mucin-agar covered microcosms (polyethylene netting) within the bioreactors. To mimic mucosal desquamation and allow a physiological wash-out of mucin-adhered microbes, the microcosms are regularly replaced (Van den Abbeele et al., 2013).

Table 1.5. **Allocation of the main *in vitro* systems of the human digestion and/or fermentation**

Main features	Abiotic factors of the digestion		Abiotic + biotic factors of the digestion / fermentation		
	Upper GI tract		Upper + lower GI tract	Lower GI tract	
	Bi-compartmented 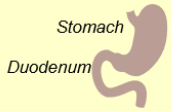	**Multi-compartmented** 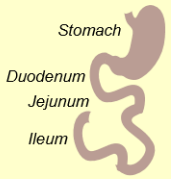	**Stomach** **Duodenum** **Jejunum** **Ileum** **Colon** 	**Single-stage** 	**Multi-stage** 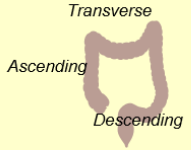
***In vitro* models**	**IViDiS** *In vitro* digestive system *Thompkins et al., 2011* *Mainville et al., 2005*	**TIM-1** TNO gastrointestinal Model *Blanquet-Diot et al., 2012* *Minekus et al., 1995*	**SHIME or M-SHIME** (Mucosal)-Simulator of the Human Intestinal Microbial Ecosystem *Van de Wiele et al., 2015* *Molly et al., 1994*	**ARCOL** ARtificial COLon *Thévenot et al., 2013*	**PolyFermS** 1-5 bioreactors *Fehlbaum et al., 2015* *Cinquin et al., 2004*
		Tiny-TIM simplified and downscaled TIM *Havenaard et al., 2013*	**SIMGI** Multi-compartmental Dynamic Model of the Gastrointestinal System *Barroso et al., 2015*		**3S-ECSIM** 3 bioreactors Environmental Control System for Intestinal Microbiota *Feria-Gervasio et al., 2014*
		ESIN Engineered Stomach and Small Intestinal *Guerra et al., 2016*			**EnteroMix** 4 bioreactors *Makivuokko et al., 2005*
		TSI The Smallest Intestine *Cielpak et al., 2018*			**CoMiniGut** 5 bioreactors Copenhagen MiniGut *Wiese et al., 2018*
					TIM-2 1-3 compartments *Minekus et al., 1999*

Regarding the other fermentation systems available, the TIM-2 developed by the TNO is very different from the traditional bioreactors (Minekus et al., 1999). It consists of an assembly of compartments, which reproduce the peristalsis and passive absorption of water and fermentation products thanks to dialysis fibers, as initially created in the TIM-1. As a drawback, this system monitors the microbiome only on a short timeframe (1 week maximum) and give therefore poor chance to the gut microbes to be well stabilized (a 48 h stabilization period has been reported). Besides, the anaerobiosis remains difficult to maintain since the system is not a bioreactor. Then, the ARtificial COLon (ARCOL), a single-stage device also integrates a passive absorption system. Another particularity of the ARCOL model, is that the anaerobiosis is maintained by the sole activity of the gut microbes (Thévenot et al., 2013). This feature is found as well in the Environmental Control System for Intestinal Microbiota (3S-ECSIM) (Feria-Gervasio et al., 2014). With originality, the bioreactors PolyFermS are seeded with immobilized fecal microbiota and used to continuously inoculate with the same microbiota different second-stage reactors mounted in parallel (Cinquin et al., 2004; Fehlbaum et al., 2015). Finally, as for the Tiny-TIM and TSI, the Copenhagen MiniGut (CoMiniGut) is composed of small bioreactor units, with a working volume of only 5 mL to increase throughput (Wiese et al., 2018). This system allows multiplying the number of tested conditions, also in a shorter period.

To conclude, it has been shown in this section that *in vitro* dynamic multi-compartmental devices of digestion and fermentation processes are highly complex, by integrating to greatest extent the physicochemical and biotic parameters of the human gut. Although some of these systems are highly sophisticated such as TIM-1 and M-SHIME, it remains impossible to reproduce *in vitro* the immune, nervous and hormonal control of the digestion, as well as the active absorption of the digestion by-products. In addition, the bioreactors reproduce only the luminal niche of the stomach or intestine, except for the M-SHIME, which integrates the mucosal niche of the colon, as explained earlier. Then, a major drawback of gut fermentation models is the limitations for simulating the host functionality. The combination of digesters / fermenters and cell cultures (e.g. intestinal or immune cells), represent therefore a common approach to reproduce *in vitro* the host responses (Déat et al., 2009; Bahrami et al., 2011; Dostal et al., 2014; Marzorati et al., 2014). Remarkably, in order to investigate the effect of a specific treatment between luminal microbial community and host surface colonization, the Host-Microbiota Interaction (HMI) module has been developed. It closely mimics the interaction and shear forces occurring at the interface of the mucus and a monolayer of human IECs. This module is maintained microaerophically and can be used in combination with dynamic gut simulator available on the market, as the SHIME system (Marzorati et al., 2014). Another device able to create anaerobic niches, the microfluidics-based co-culture device (HuMiX) allows cocultivation of human and microbial cells (Shah et al., 2014).

Of note, the two simulators that have been used in the frame of this PhD, TIM-1 and M-SHIME are presented in **Table 1.6** and better described in the experimental procedures in section II.

Table 1.6. TIM-1 and M-SHIME: parameters simulating the human adult digestion / fermentation processes

***In vitro* models**	**Compartments (volume mL) / pH / residence time**	**Digestive secretions**	**Chyme mixing**	**Level of O_2**	**Luminal gut microbes (CFU mL^{-1})**	**Mucosal gut microbes (CFU mL^{-1})**
TIM-1 (parameters simulated following ingestion of a glass of water) 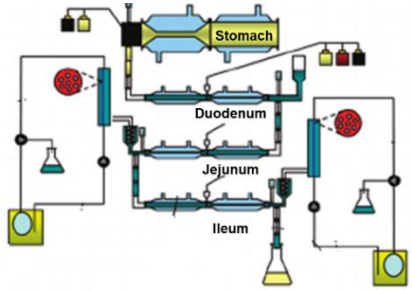 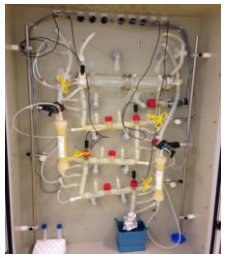	**Stomach** (200 mL) pH 6 to 1.8 $T_{1/2}$ = 15 min	• Pepsin • Lipase • HCl	Peristaltic mixing (flexible wall)	Aerobiosis	0	0
	Duodenum (30 mL) pH 6.4	• Bile salts • Pancreatic juice • $NaHCO_3$			0	0
	Jejunum (130 mL) pH 6.9	• Electrolytes • $NaHCO_3$			0	0
	Ileum (130 mL) pH 7.2 $T_{1/2}$ = 150 min	• Electrolytes • $NaHCO_3$			0	0
M-SHIME 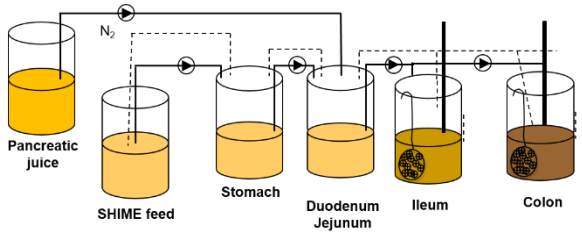 	**Stomach** pH 2 T= 60 min	• Nutritional medium • HCl	Stirrers	Anaerobiosis (N_2)	0	0
	Duodenum / Jejunum pH 5 T= 150 min	• Bile salts • Pancreatic juice • $NaHCO_3$			0	0
	Ileum pH 7 T= 180 min	• $NaHCO_3$			10^8 - 10^9	10^7 - 10^8
	Ascending colon pH 6.1 T= 8 h	• $NaHCO_3$ / HCl			10^{10} - 10^{11}	10^9 - 10^{10}

2 Therapeutics to probiotics: a choice alternative strategy in the prevention of ETEC infections

Noteworthy, several sections hereafter have been published in a review [2] and redrafted / updated for the present chapter. After shortly cite the methods used to diagnose ETEC (section 1), the following part will provide key information on the primary water control strategy to prevent ETEC oral-fecal transmission (section 2). The section 3 will list the available treatments for ETEC infections (section 3.1), highlights the growing concern of antibio-resistance phenomena (section 3.2), and describe the non-antibiotic alternatives under research (section 3.3). As the introduction of a dominant part of this PhD, the section 4 will be dedicated to the probiotic strategy as an alternative in the fight of ETEC. Then, the probiotic yeast strain used in this research work will be presented in section 4.2. Finally, this chapter will end with the main research questions (section 5).

1. ETEC diagnosis

Although advanced biomolecular techniques (DNA-based techniques) have been recently developed to identify ETEC, they are not widely available, especially in remoted areas. In such areas, the physicians may make the diagnosis only based on a patient's history and symptoms. This kind of diagnosis remains inadequate to specifically identify ETEC, where symptoms are closely related to those found in other enteric pathogens, such as *Vibrio cholerae*. In industrialized countries, when ETEC is suspected, microbiological detection is required and relies on the laboratory confirmation by stool isolation and culture and/or the identification of at least one of the two enterotoxins (e.g. LT and/or ST) that can be produced by ETEC. The use of polymerase chain reaction (PCR) to detect genes encoding for the toxin is accurate and sensitive. Commercial agglutination tests are also available for detecting LT toxins but appear to be not often used (CDC, https://www.cdc.gov/ecoli/etec.html, consulted on 08/2018). Finally, ELISA assays for detection of the toxin were commercially available in the past, but only for research use and not for the clinical diagnosis of ETEC infection.

2. Water control strategies to prevent ETEC infections

The primary control strategy for ETEC is to prevent the oral-fecal transmission. The main action that can be made is to educate the public to respect the following hygiene rules: (i) do a proper handwashing

[2] ***Review.*** *ROUSSEL C., SIVIGNON S., VAN DE WIELE T., BLANQUET-DIOT S. Foodborne enterotoxigenic Escherichia coli: from gut pathogenesis to new preventive strategies involving probiotics. Future microbiology, 12, 73-93 (2017). https://doi.org/10.2217/fmb-2016-0101*

after using the toilets, changing nappies and/or assisting another with toileting and before cooking and (ii) wash thoroughly fruits, vegetables and herbals with boiled water or water chemically treated (e.g. iodine, chlorine) and peel them when it is possible. However, the geographical inequalities in access to safe water and sanitation facilities (Fig. 2.1) make these rules suitable mainly for people living in industrialized countries. Even if it has steadily fallen over the two last decades, the number of children dying from diarrheal diseases (all pathogens included) is therefore strongly associated with poor water access, inadequate sanitation and hygiene (Mokomane et al., 2018).

In low income and/or middle income countries, the numbers are unprecedented according to the last WHO report on un-water (United Nations water, http://www.unwater.org/about-unwater/, consulted on 08/2018) global analysis assessment of sanitation and drinking water (GLASS, 2014). Indeed, at present, still 2.5 billion people lack access to improved sanitation, 1 billion practice open defecation, 748 million lack access to improve drinking water and an estimated 1.8 billion people use a source of drinking water that is fecally contaminated. Finally, hundreds of millions of people have no access to soap and water to wash their hands. Surprisingly, it has also been evidenced that piped water in the most deprived locations (e.g. Bangladesh and Ethiopia) are equally or more contaminated than non-piped supply. Thus, beyond the priority to build sanitation facilities for everyone, it is urgent to provide with an eye toward long-term sustainability, adequate water treatment at the source to prevent pathogenic contaminations such as ETEC. Reaching this goal by 2030 will require countries to spend $ 150 billion per year.

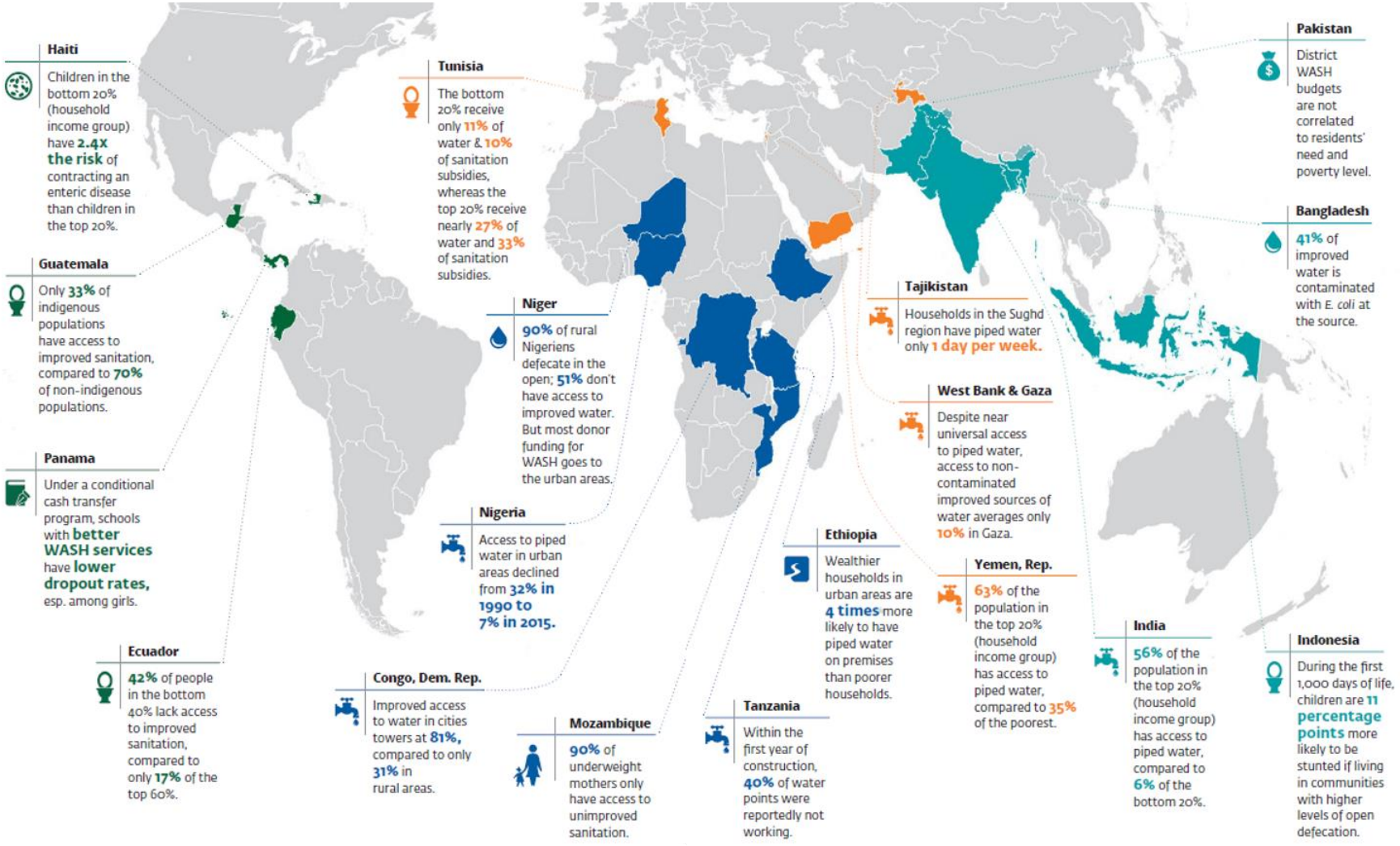

Figure 2.1. **Worldwide inequalities in water supply, sanitation and hygiene services.** Only numbers from 18 countries are shown. *Reprinted with permission from www.worldbank.org/washpdinitiative.*

3. Therapeutics in ETEC infections

Improving awareness on ETEC pathogenesis in the human GI niches, as presented in section 3.2, will help to develop novel therapeutic approaches. Ideally, such therapeutics, either prophylactic or curative must be safe, well-tolerated and respond greatly in patients. This section will draw up a state of the art of both the current and under development therapeutic strategies to prevent or cure ETEC infections in humans.

3.1. Available treatments

So far, treatments to cure ETEC infections are not specific to the pathogen, but rather follow the general recommendations given for diarrheal diseases in both children and adults. Unanimously, oral rehydration solution is the key treatment, often prescribed to prevent dehydration and loss of electrolytes. The WHO recommends low osmolarity solutions containing sodium (75 mmol L^{-1}), glucose (75 mmol L^{-1}), potassium (20 mmol L^{-1}), chloride (65 mmol L^{-1}) and citrate (10 mmol L^{-1}) (WHO, 2002; Bruzzese et al., 2018). In case of severe dehydration, a parenteral fluid therapy for replacement of free water deficit can be given (e.g. Ringer's lactate solution). Besides, whatever the type of diarrhea in children living in low-income countries and often zinc-deprived, the WHO and UNICEF recommend routine zinc therapy and if diarrhea persist, a supplementation of multi-vitamins and minerals (e.g. vitamin A, folate, copper, magnesium) as well (Table 2.1) (WHO, 2005; Galvao et al., 2013; World Gastroenterology organization, 2012). Such zinc therapy has displayed therefore to enhance both innate immunity and gut barrier function against ETEC (Galvao et al., 2013).

In the case of mild to moderate diarrhea, anti-secretory agents such as Bismuth subsalicylate or pepto-bismol© may decrease the frequency of bowel movements and the posology varies according to the age-range (Table 2.1). While for acute diarrhea, it is recommended to use antimotility drugs such as Loperamide within 48 hours, but only in adults. High dose of antimotility drugs have been associated with prolonged illness when used in highly bacterial inflammatory pathogens, which is nonetheless unlikely the case of ETEC pathogen (Lääveri et al., 2016). Antimotility agents are usually combined with a 3-day antibiotic therapy. Fluoroquinolones are primary antibiotics of choice for most destinations in traveler's diarrhea. This broad-spectrum antibiotic includes ciprofloxacin or levofloxacin for adults. Although the routine use of antimicrobials for diarrhea in children is not recommended by the WHO, azithromycin can be prescribed for severe acute diarrhea in infants and pregnant woman (WHO, 2002; Zaman et al., 2017). For example in India, pediatricians working in the government sector prescribed antibiotics to only 23% of children, while private practitioners prescribed antibiotics to 51% of children with diarrhea (Kotwani et al., 2012). Finally, rifaximin, a non-absorbable antibiotic has also been shown to be effective against ETEC (Taylor et al., 2017; Riddle et al., 2016).

Table 2.1. **Treatment recommendations in the frame of ETEC diarrhea.** *Compiled from WHO, 2002; WHO, 2005; Bruzzese et al., 2018 and Riddle et al., 2016.*

IV: intravenous, ORS: Oral rehydration solution.

	Infant	Adult
Rehydration therapy	• *Mild to moderate dehydration* **ORS** 50-100 mL Kg^{-1} body weight over 3-4h • *Severe dehydration* **Ringer's lactate solution IV** 100 mL Kg^{-1} $6h^{-1}$	• *Mild to moderate dehydration* **ORS** up to 2L day^{-1} • *Severe dehydration* **Ringer's lactate solution IV** 100 mg Kg^{-1} $3h^{-1}$
Vitamins and minerals	• **Vitamin A** 400 µg • **Folate** 50 µg • **Zinc** 20 mg • **Magnesium** 80 mg • **Copper** 1 mg *Recommended daily for 2 weeks*	*No recommendation*
Anti-secretory agents	**Pepto-Bismol©** • 2 to 24 months 44 mg every 4h • 24 to 48 months 87 mg every 4h • 48 to 70 months 175 mg every 4h	**Pepto-Bismol©** 524 mg every 30-60 min (max 8 doses/24h) up to 2 days
Anti-motility agents	*Not recommended*	**Loperamide** 4 mg immediately 2 mg after each watery stool (max 8 doses/24h) *Not recommended for mild to moderate diarrhea*
Antibiotics	*Not recommended for mild to moderate diarrhea* *For severe diarrhea* • **Azithromycin** 10-20 mg Kg^{-1} $day^{-1}$for 3 days	*For severe diarrhea* • **Ciprofloxacin** 500 mg/2xday up to 3 days • **Levofloxacin** 500 mg/day up to 3 days • **Rifaximin** 200 mg/3xday for 3 days

3.2. Antibiotherapy conflicting the growing problem of ETEC antibiotic resistance

More than 70 years of antibiotic use have already selected for diverse and highly mobile antibiotic resistance genes in human pathogens. Thus, antimicrobial drugs lose their ability to effectively inhibit pathogenic growth and have collateral effects on commensal bacteria as well. Antibiotic resistance is widely regarded as one of the major public health concerns of the 21st century, leading to longer hospital stays, higher medical costs and increased mortality. The UK government report estimated that antibiotic-resistant infections kill 700 000 people each year worldwide, and an increase of 10 million deaths per year is projected for 2050 (https://amr-review.org/). On the whole, annual losses due to antimicrobial resistance are estimated to range from 21 000 million to 34 000 million dollars in the US, and about 1500 million euros in Europe (Bulletin of WHO, 2012).

Therefore, in the case of ETEC infections, the decision to treat the population with antimicrobials remains challenging since ETEC is frequently resistant to common antibiotics, including trimethoprim-sulfamethoxazole and ampicillin (CDC, https://www.cdc.gov/ecoli/etec.html, consulted on 08/2018). The

selection of antibiotics should be then based on two major considerations: the chance of obtaining microbiological results, including resistance pattern, and the severity of clinical conditions (Bruzzese et al., 2018). Knowledge of the local pattern of resistance is crucial to reduce the number of failures, such as antibiotic-associated diarrhea, allergic reaction or complications (e.g. colitis) (https://www.mayoclinic.org/diseases-conditions, consulted on 09/2018). Solutions to alleviate the antibiotic resistance burden are multifaceted and include: (i) since 2007, the rational use of antibiotics, promoted by the action plan "Antibiotics Smart Use" and endorsed by WHO and politics (https://www.who.int/bulletin/volumes/90/12/12-105445.pdf, consulted on 12/2018); (ii) the promotion to develop alternative approaches to treat disease-causing bacterium, and not upset the other members of the host's commensal communities but rather enhance growth of beneficial gut microbes. Alternative strategies under research including prophylactic and curative approaches in the fight of ETEC infections are presented below.

3.3. Alternative strategies under research

3.3.1. Vaccines

Currently no licensed vaccines for ETEC are available on the market. Dukoral®, an oral whole-cell/recombinant B-subunit vaccine, originally directed against *Vibrio cholerae*, has been found to provide short-term efficacy (67% of protection) in some serotypes of ETEC diarrhea, involving the virulotype LT. The prescription of this vaccine is however limited to Europe, Canada and Australia (CDC, https://www.cdc.gov/ecoli/etec.html, consulted on 08/2018). Besides, protection to children populations in low and/or middle-income countries has been more difficult to demonstrate. Economically, it would be more interesting to provide a vaccine that addresses efficacy for both traveler's and children ETEC-diarrhea that is definitely not feasible with Dukoral®. Briefly, among several vaccine candidates widely reported in the literature (Zhang and Sack, 2015; Ahmed et al., 2013), the most convincing and still on course could be classified into four groups: (i) cellular candidates (ETVAX, ACE527); (ii) subunit candidates (anti-adhesin based subunit vaccine), (iii) anti-toxin candidates (dmLT) and (iv) novel antigen candidates (Flagellin, EtpA, EatA, YghJ). These vaccines are actually under development from preclinical to phase II assays, but the path seems to be long to counteract lack of protection and adverse effects in order to achieve a protective and long-term efficacy.

Even if the development of an effective ETEC vaccine is a top priority for the WHO and several public health institutions around the world, it is still limited by numerous challenges (Zhang and Sack, 2015): (i) the serological heterogeneity of ETEC and the wide variety of structurally and functionally distinct CFs ; (ii) the limited knowledge of ETEC bacterial structure and disease mechanisms ; (iii) the high costs of each vaccine program.

3.3.2. Micronutrients and medicinal plants

In accordance with the WHO recommendations in micronutrients for diarrhea in children (described in section 3.1), some efforts have been done in the assessment of new metal compounds or micronutrients as an alternative strategy to treat ETEC. For instance, the effect of metals such as iron and silver on

ETEC survival or virulence has been suggested. Addition of iron to growth media repressed the expression of CFA/I fimbriae by ETEC (Karjalainen et al., 1991) while under iron starvation, production of the CFA/I fimbriae was increased in the H10407 strain (Haines et al., 2015). Oral administration of silver nanoparticles to infant mice colonized with ETEC bacteria significantly reduced the colonization rate of the pathogen (Salem et al., 2015). None of these compounds has been however clinically investigated. Other dietary components like phenolic compounds and vitamins might also have potential as new agents against ETEC infections. *In vitro*, polyphenol extracts inhibited the LT toxin binding to its intestinal receptor GM_1 through aggregation (Verhelst et al., 2013). A placebo-controlled double-blind study has shown that vitamin A supplementation led to shorter duration of ETEC infections among children in Mexico City (Long et al., 2006). The available data highlight some beneficial effects of micronutrients in ETEC infections but the level of evidence (from *in vitro* studies to clinical trial) widely depends on the tested compound. Besides, this strategy only focused on infantile diarrhea in malnourished children and was not yet applied to traveler's diarrhea. The therapeutic benefits attributable to such micronutrients might be modulated by differential levels of nutrient deficiency in individuals or populations within developing countries.

Then, many medicinal plants and their associated bioactive compounds have been studied for their potent drug effects against ETEC in several animal models (e.g. piglet, swine or mouse) and were nicely reviewed by Dubreuil (2012). For example, Chinese medicinal herbs such as *Galla Chinensis* extract, and specifically gallic acid compounds displayed interesting properties by blocking the binding of LT_B toxin to GM_1 receptor in a mouse gut assay (Chen et al., 2006). Finally, a study not specific to ETEC but interesting in terms of mechanism, has shown that polyphenols contained in cocoa inhibit cAMP pathway- CFTR-mediated Cl^- transport across T84 colonic cells, thus limiting water efflux and diarrhea (Schuier et al., 2005).

3.3.3. Dietary fibers and prebiotics

Dietary fiber is a broad term, regrouping non-digestible carbohydrate polymers subjected to bacterial fermentation in the GI tract. Some dietary fibers can also be classified as prebiotics. Prebiotics are newly redefined as "substrate that is selectively utilized by host microorganisms conferring a health benefit" (Slavin, 2013; Gibson et al., 2017).

Although broad research on functional foods such as prebiotics has been tremendously intensified and are expected to exceed $ 7.5 billion by 2023, this field has been scarcely explored as a prophylactic substitute in the fight of ETEC infections (https://www.gminsights.com/industry-analysis/prebiotics-market/, consulted on 08/2018). In fact, most of the findings have been investigated in animal models, such as post-weaning piglets. However, a study has displayed that soluble non-starch polysaccharide from plantin (banana family *Musa spp.*) inhibits significantly ETEC adhesion on Caco-2 cells, at a concentration readily achievable in the human gut lumen (Roberts et al., 2013). Remarkably, another study conducted in 57 Bangladeshi infants (5-12 months) with persistent uncharacterized-diarrhea has shown that a week of green banana or pectin-based diets was able to reverse the abnormal mucosal permeability. Thus, improved mucosal permeability resulted in an increase of stool consistency and a reduction in frequency of defecating (Rabbani et al., 2004).

3.3.4. Probiotics

The probiotic strategy is approached in detail in section 4.

3.3.5. Bacteriophages

Viruses that affect bacteria have recently started to attract the attention as a tool used against pathogens. Phages are common in all natural environments such as the human gut and can be categorized in two types: (i) virulent or lytic phages; (ii) temperate or lysolytic phages. For therapeutic purposed, only virulent phages can be used as antimicrobial agents. They enter within the bacterial cell, replicate using the host machinery and finally lyse the host cell, allowing complete disintegration of the pathogen (Davies et al., 2016).

So far, the effectiveness of anti-ETEC phage therapy has been studied mostly in piglets (Lee et al., 2017). However, a four days oral T4-like coliphages therapy, involving 39 Bangladeshi infants (6-24 months) hospitalized with acute bacterial diarrhea (60% cases ETEC-associated) has been performed by Nestlé research centre (Sarker et al., 2016). Although coliphages showed a safe gut transit, the therapy failed to improve diarrhea outcome, possibly due to insufficient phage coverage and/or too low doses. These disappointing results should not impede new attempts to improve knowledge on *in vivo* interactions between phage and its host bacterium, and decipher if it can be considered as a viable option against antibiotic-resistant bacterial pathogens.

3.3.6. Bioactive immune compounds or immunotherapeutics

Colostrum from bovine origin contains high levels of antibodies (IgG), cytokines, growth factors and antimicrobial peptides. Its therapeutic benefit to human has been demonstrated in several studies. For instance, the colostrum of dairy cows has been immunized with antigens derived from 14 ETEC strains, belonging to the serogroups predominantly involved in traveler's diarrhea. This ETEC-hyperimmune bovine colostrum has been used in a clinical trial and a daily consumption reduced the incidence and volume of diarrheal stools in more than 90% adult volunteers challenged with 9 $\log_{10}$ CFU of ETEC H10407 (Otto et al., 2011). Thus, the product was the precursor of Travelan®, commercially available for prophylaxis of traveler's diarrhea in US, Australia and Canada (Sears et al., 2017). A similar newer product IMM-124E, indicated for ETEC infection and broader gastrointestinal health benefits is being tested in humans.

4. Probiotics in ETEC infections

4.1. The basics of probiotics

4.1.1. Definition, nomenclature and safety

Conceptually recognized for over 100 years, probiotics, translated from the Greek “for life” are defined by the FAO/WHO as “Live microorganisms that, when administered in adequate amounts, confer a health benefit on the host” (Hill et al., 2014; Syngai et al., 2016). According to the FAO/WHO guidelines, a probiotic strain should be strictly identified by the genus, species, subspecies (when applicable) and a numeric designation of the specific strain. Probiotic manufacturers should register their strain with an international depository, such as American Type Culture Collection (ATCC), National Collection of Microorganisms Cultures (CNCM), or National Collection of Industrial and Marine Bacteria (NCIMB) (http://www.worldgastroenterology.org/guidelines/global-guidelines, consulted on 08/2018).

To date, most of microorganisms recognized as probiotics are lactic acid bacteria, with *Lactobacillus* and *Bifidobacterium* being the main genera used, but yeast *Saccharomyces* and *some E. coli* and *Bacillus* species are also often used. Most probiotics commercialized are single strains. Nevertheless, the efficacy and functionality of multistrain and multispecies probiotics is not called into question since they could be more effective and consistent than monostrain probiotics (Chapman et al., 2011; Timmerman et al., 2004).

Importantly, the delivered probiotic product should meet minimum criteria, which are the following: (i) the quality of the probiotic should be defined by its maintenance of viability through the end of the product shelf-life; (ii) the probiotic cannot be stated at a general dose and can vary greatly from 8 $\log_{10}$ to 10 $\log_{10}$ CFU/serving for suitability; (iii) the probiotic should show important properties including, resistance to gastric acidity and bile acids, adherence to mucus and/or host epithelial cells and cell lines, or antimicrobial activity against potentially pathogenic bacteria or fungi and provide thus benefits for the wellbeing of the host (Hill et al., 2014; Fijan, 2014). On the whole, the regulation of probiotics differs between countries with no universally agreed framework. These products should be claimed as natural and safe either in US by the status Generally Regarded as Safe or In Europe by the Food Safety Authority (EFSA) granted Qualified Presumption of Safety. It is also important to note that to claim the health benefits of commercialized probiotics, beneficial effects should be based on *in vivo* clinical studies, and cannot be proved by *in vitro* studies only. Nonetheless, *in vitro* studies are helpful to unravel the possible mechanisms of action, and provide thereby a first step of the investigation.

4.1.2. Probiotics field of application and market

A wide variety of probiotic products and field of applications, for both animal and human health care have been introduced into the market in the past decade. Human probiotics emerged as the most significant application segment in 2016 (Fig. 2.2); compared to the animal segment. Indeed, rising concerns towards lifestyle diseases along with product efficiency may assist in developing product demand. Thus, two main forms of probiotics are delivered in the market, with the fermented or functional

food and beverages (e.g. dairy and non-dairy products) and the dietary supplements (e.g. freeze-dried powder, capsule and tablet) (Khaligi et al., 2016).

Briefly, the probiotics market is experiencing unprecedented year on year growth. For instance, the global market for human probiotics was estimated to reach $ 32 billion dollars in 2013 and $ 34 billion in 2015 (https://www.grandviewresearch.com/press-release/global-probiotics-market, consulted on 09/2018), and is projected to reach $ 46.55 billion by 2020 and $ 64.60 billion by 2023 over the world (http://www.marketsandmarkets.com, consulted on 09/2018). The notable players of the probiotic market in the world are Danone, Yakult, Nestlé, Chr. Hansen and Danisco. Other industries are taking a prominent place such as General Mills, Mother Dairy, Probi AB, Lallemand, Lesaffre and BioGaia AB (Global Market Insights data, https://www.gminsights.com/industry-analysis/probiotics-market, consulted on 09/2018). In Europe, the probiotic market is reaching $ 11.85 billion in 2018 and is estimated to grow nearly $ 15.62 billion by 2023. Germany and UK represent the largest market in Europe (Euromonitor data, https://www.euromonitor.com/probiotics-evolution-of-digestion-and-immune-support-probiotics-part-one/report, consulted on 09/2018).

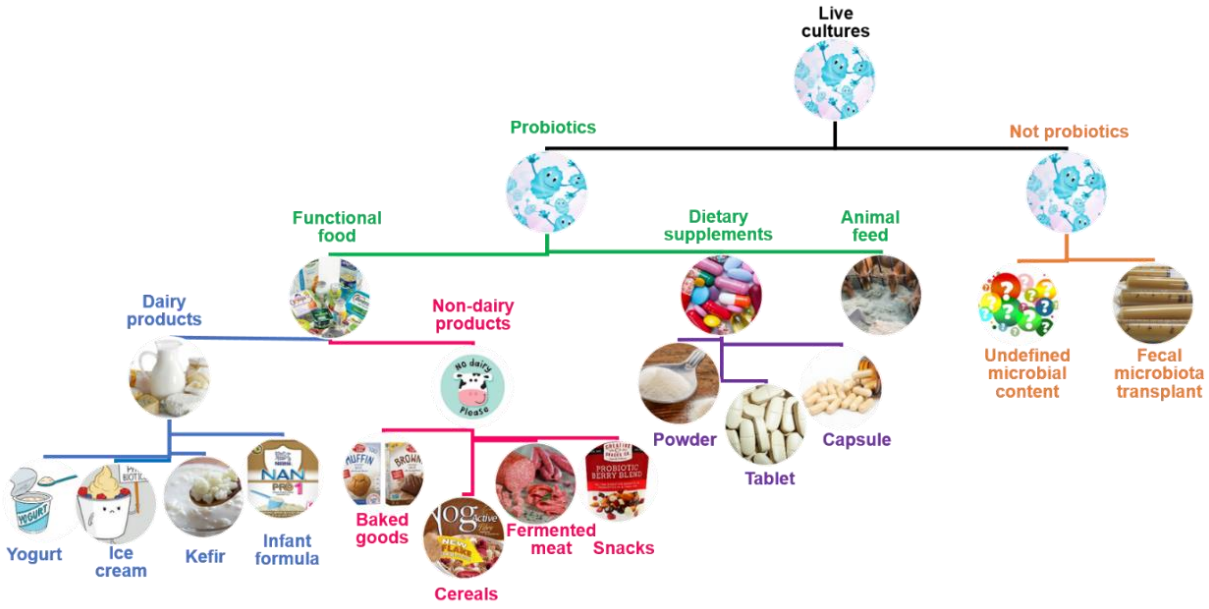

Figure 2.2. **Spectrum of products containing probiotic strains.** *Compiled from Khaligi et al., 2016.*

Although the probiotic definition is widely adopted, especially in the scientific community, since December 2012, a ban on the use of the term “probiotic” for food products remained in the European Union. This prohibition results from the interpretation of the 2006 European Commission Guidance on the implementation of the Nutritional Health Claim Regulation (NHCR, EC 1924/2006), which considered the phrase “contains probiotics” to be a health claim instead of a nutritional claim. So far, EFSA rejected all probiotic health claim applications on the basis that “increasing a healthy gut flora” is not a health benefit as such. One exception remained for the strain *Propionibacterium freudenreichij* W200 which

has been recently approved as the first legal probiotic. This probiotic contains an adequate amount of vitamin B12, resulting in an approved health claim by the EFSA (Winclove probiotics, 2017 https://www.wincloveprobiotics.com, consulted on 09/2018). Finally, yogurt has its own approved health claim in Europe as “live cultures in yogurt of fermented milk improve lactose digestion of the product in individuals who have difficulty digesting lactose” (EFSA, 2010).

4.1.3. Probiotic’s mechanism of action against ETEC

A growing concerns in the use of probiotics-based strategy against ETEC pathogens has emerged in the past 10 years as a main potential antibiotic alternative. Although the underlying mechanisms associated with probiotic prevention or alleviation of enteric pathogens are still largely unclear, the modes of action thought to contribute to human and/or animal health fall into three general classes of anti-pathogenic mechanisms: direct antagonism, immunomodulation and competitive exclusion (Preidis et al., 2011). The following sub-sections will review the *in vitro* and *in vivo* studies that have been carried out both in humans and in pigs and that show beneficial effects of probiotic bacteria and yeast against ETEC pathogens for each of the three mechanisms listed above. This part of the review was extended to studies on pigs due to scarce data in humans and to similarities between pigs and humans regarding digestive physiology and ETEC infectious process. All these studies are summarized in **Table 8** (immunomodulation), **Table 9** (direct antagonism) and **Table 10** (competitive exclusion).

4.1.3.1. Immunomodulation

Probiotics can interact with the host immune system to enhance the functionality of innate and/or adaptive immunity or to limit the ability of pathogen to induce an immune response. A large number of studies have investigated the immunomodulatory properties of probiotics in ETEC infections (Table 2.2). Most of them have been carried out *in vitro* using porcine IECs and the $F4^+$ ETEC strain (K88 old nomenclature), which is the most prevalent in pig post-weaning diarrhea. Probiotic strains from the *Lactobacillus* (Karimi et al., 2018; Wu et al., 2016; Murata et al., 2014; Zhou et al., 2014; Wachi et al., 2014) and *Saccharomyces* (Tomosada et al., 2013; Badia et al., 2012) genus significantly reduced the expression of pro-inflammatory cytokines, such as IL-1β, IL-6 and IL-8, and induced an up-regulation of the anti-inflammatory IL-10. These effects have been observed both in prophylaxis and curative treatments. Only one study displayed the same cited properties using a strain from *Enterococcus* genus (Tian et al., 2016). The mechanisms associated with the anti-inflammatory effect of probiotic strains were further explored for *Bifidobacterium* (Zanello et al., 2011; Roselli et al., 2007) and *Lactobacillus* strains (Zhou et al., 2014). These probiotics inhibited ETEC-mediated MAPK and NF-κB activation by upregulating TLR negative regulators (Zhou et al., 2014; Zanello et al., 2011; Roselli et al., 2007). In addition, immunomodulatory effects can be driven by the decrease of chemokines and complement expression, as recently shown by Kobayashi et al. (2016), using microarray analysis from the immunotranscriptome of porcine IECs. Only three studies (Qiu et al., 2017; Klingspor et al., 2015; Finamore et al., 2014) have investigated the effects of bacterial probiotics on ETEC-induced inflammatory response in human Caco-2 intestinal cells or NCM460 cells (human colonic mucosal epithelium), but still using the porcine K88 strain. Both *Enterococcus faecium* (Klingspor et al., 2015) and *Lactobacillus amylovorus* (Finamore et al., 2014) inhibited the over-production of pro-inflammatory cytokines induced by ETEC and blocked the up-regulation of heat shock protein (Hsp), especially that of Hsp72 and Hsp90 which are critical for Toll-like receptor (TLR) 4 function. Noteworthy, TLR4 is the main receptor constitutively expressed in porcine IECs for the pathogen-associated recognition. In the study by Finamore et al. (2014), both the *Lactobacillus* strain and its secreted products showed anti-inflammatory properties. In the recent study from Qiu et al. (2017), *Lactobacillus plantarum* enhanced IL-22 production in natural killer (NK) cells. Addition of NK cells pre-treated with the probiotic strain conferred protection against ETEC K88 in NCM460 cells (Qiu et al., 2017).

In vivo studies in ETEC-infected piglets confirmed the anti-inflammatory potential of probiotic strains, mainly that of *Lactobacillus spp* strains. Challenged pigs fed with *Lactobacillus* probiotic strains had lower levels of pro-inflammatory cytokines in intestinal tissues (Li et al., 2016; Khafipour et al., 2014; Zhu et al., 2014; Chytilova et al., 2013). Zhu et al. (2014) have also investigated the modulation of systemic and intestinal lymphocyte T cells subpopulations by *Lactobacillus rhamnosus* and showed that the probiotic strain can attenuate the ETEC-induced increase in CD3+ CD4+ CD8+ T cells in the small intestine. Li et al. (2012) found that the same probiotic strain reduced the increase of TLR4 expression observed both at the mRNA and protein levels in the jejunum of infected piglets. Of note, the results of these two studies suggest that pretreatment with a low dose of *Lactobacillus rhamnosus* might be more effective than with a high one.

Table 2.2. **Immunomodulatory effect of probiotics against ETEC.** *Updated from Roussel et al., 2017.*

IMMUNOMODULATION							
MODEL		**REF**	**PROBIOTIC STRAIN**	**ETEC STRAIN**	**DOSES PRO / ETEC**	**THERAPY**	**MECHANISM**
IN VITRO	CO-CULTURE IN PIGLET INTESTINAL CELLS	Karimi et al. (2018)	*L. reuteri* DSM 17938 and 1563F	853/67	$5x10^7$ to $5x10^8$ CFU/well (PRO) $5x10^6$ CFU/well (ETEC)	preventive	Down-regulation of PI cytokines expression (IL-6, TNF-α)
		Kobayashi et al. (2016)	*L. jensenii* TL2937	O9:H-:987	$5x10^7$ CFU/mL (PRO and ETEC)	preventive	Decrease expression of chemokines (CCL8, CXCL5, CXCL9, CXCL10, CXCL11), and complement (C1R, C1S, C3, CFB)
		Tian et al. (2016)	*E. faecium* HDRsEf1	F4+ac	$5x10^7$ CFU/mL (PRO and ETEC) + culture supernatant of PRO	preventive	Down-regulation of PI cytokine expression (IL-8)
		Wu et al. (2016)	*L. plantarum* CGMCC1258	O149: K91: F4+ac	$1x10^8$ CFU/well (PRO) $6.5x10^7$ CFU/well	preventive	Down-regulation of PI cytokines expression (IL-8, TNF-α) Regulation NF-κβ and MAPK
		Murata et al. (2014)	*B. breve* MCC-17	987P	$5x10^7$ CFU/mL (PRO and ETEC)	curative	AI effect by negative regulation of TLRs, NF-κβ, p38 MAPK and PI3K
		Zhou et al. (2014)	*L. reuteri* CL9	F4+ O149:K88 (JG280)	10^8 CFU/mL (PRO and ETEC)	preventive	Decrease of IL-8 (PI) and increase of IL-10 (AI) production
		Wachi et al. (2014)	*L. delbrueckii* TUA4408L and its extracellular polysaccharides	987P and F4+	$5x10^7$ CFU/mL (PRO) $5x10^7$ CFU/mL (ETEC) 100 µg/mL (NPS)	preventive	Reduction of NF-κβ, ERK, MAPK and TLRs activation. Down-regulation of PI cytokine expression (IL-6, IL-8)
		Tomosada et al. (2013)	*B. longum* BB536 *B. breve* M-16V	987P	$5x10^7$ CFU/mL (PRO and ETEC)	preventive	Reduction of TLR4, NF-κβ and MAPK activation. Decrease of PI IL-6 and IL-8
		Badia et al. (2012)	*S. cerevisiae var. boulardii* & β-galactomannan oligosaccharide	F4+ad, O8:K87:H19 (56190) GN1034 F4+	3 yeasts/cell (PRO) 10 µg/mL of βGM $1x10^7$ CFU/well (ETEC)	curative	Down-regulation of PI cytokines (TNF, IL-6) and chemokines (CCL2, CCL20, CXCL8) expression
		Zanello et al. (2011)	*S. cerevisiae* CNCM- I3856	F4+ad, O8:K87:H19 (56190)	$7.5x10^5$ yeasts/mL (PRO) $1x10^7$ CFU/well (ETEC)	curative	Decrease of PI cytokines (TNF, IL-1,6,8) production
		Roselli et al. (2007)	*L. sobrius* DSM 16698	F4+	10^9 CFU/mL (PRO) 10^8 CFU/mL (ETEC)	preventive	Down-regulation of IL-8 and activation of IL-10 expression

	CO-CULTURE IN HUMAN INTESTINAL CELLS	Qiu et al. (2017)	*L. plantarum* CGMCC1258	O149: K91: F4+ac	10^8, 5x10^8 or 10^9 CFU/mL (PRO) 10^8 CFU/mL (ETEC)	preventive	Enhance IL-22 production in natural killer cells
		Klingspor et al. (2015)	*E. faecium* NCIMB 10415	ETEC IMT 4818 O149:K91/K88 (F4+)	10^8 CFU/mL (PRO) 10^6 CFU/mL (ETEC)	preventive	Decrease of IL-8 mRNA /protein production and reduction of HSP 70 stress response
		Yu et al. (2015)	*L. fructosus* C2	F4+	Unknown	curative	Reduction of ERK and JNK activation. Decrease of IL-8 production
		Finamore et al. (2014)	*L. amylovorus* DSM 16698	F4+	5.10^7 CFU/mL (PRO) 5.10^6 CFU/mL (ETEC)	curative	Suppression of TLR4 activation, inhibition of HSP and P65 translocation : suppression of PI cytokines production
IN VIVO	ORAL ADMINISTRATION TO PIGLETS						
		Li et al. (2016)	*L. acidophilus*	ETEC K88	5.10^{10} CFU/g freeze-drying powder/ day (PRO) 10^9 CFU/kg (ETEC)	preventive	Decrease of PI cytokines (TNF-α, IL-1β, IL-8) production and increase IL-10 Downregulation of TLR2 and TLR4 Reduction of phosphorylation levels of NF-Kβ p65 and MAPK p38
		Khafipour et al. (2014)	*E. coli* UM-2, UM-7	F4+	10^9 to 10^9 CFU/mL (PRO and ETEC)	preventive / curative	Downregulation of PI cytokine expression (IL-6, TNFα) in the serum
		Zhu et al. (2014)	*L. rhamnosus* ATCC 7469	F4+ ac, O149:K91	10^9 CFU/mL (PRO) 10^9 CFU/mL (ETEC)	preventive	Attenuation of $CD3^+$ $CD4^+$ $CD8^+$ T cells increase in the small intestine
		Chytilova et al. (2013)	*L. plantarum* Biocenol LP96	O8:K88ab:H9	10^9 CFU/mL (PRO) 10^5 CFU/mL (ETEC)	preventive	Downregulation of PI cytokine expression (IL-1α, IL-8) and up-regulation of AI IL-10 in the small intestine
		Li et al. (2012)	*L. rhamnosus* ATCC 7469	F4+ ac, O149:K91	10^{10} CFU/mL (PRO) 10^9 CFU/mL (ETEC)	preventive	Decrease of TNFα and attenuation of IL-8 and TLR4 increase in the small intestine
		Zhang et al. (2010)	*L. rhamnosus* GG ATCC 53103	F4+ ac, O149:K91	10^{10} CFU/mL (PRO) 10^9 CFU/mL (ETEC)	preventive	Attenuation of IL-6 increase in the serum. Enhancement of intestinal antibody defense (IgA)

AI: Anti-inflammatory; *B.: Bifidobacterium*; *E.: Enterococcus*; *L.: Lactobacillus*; PI: Pro-inflammatory; PRO: Probiotic.

4.1.3.2. Direct antagonism

In direct antagonism, probiotics kill or inhibit the growth of pathogen to limit the spread of the infection or they down-regulate the expression of virulence factors, such as toxins or adhesins required for pathogenesis (Table 2.3). Three *in vitro* studies showed the inhibition of the growth of ETEC strains isolated from human or pig, following co-incubation of the pathogen with the culture supernatant of *Lactobacillus* species. In the study by Tsai et al. (2008), the inhibitory activity was partially affected by lactate deshydrogenase treatment showing that it may result from lactic acid production. In the works of Wang et al. (2018), they speculated the effect of hydrogen peroxide, plantacirin a bacteriocin potentially produced by *Lactobacillus plantarum* or other antimicrobial metabolites in the inhibition of ETEC growth (Wang et al., 2018). Strains of *Lactobacillus spp* also increased the rate of decline of ETEC K88 in a continuous culture of porcine intestinal bacteria, which provides a more realistic *in vitro* situation for the examination of probiotic potential than co-culture does (Hillman et al., 1995). An original study has shown that the use of the association of the probiotic strain *Lactobacillus rhamnosus* with the prebiotic fructooligosaccharide (FOS), resulting in a symbiotic combination, reduced ETEC growth in co-culture probably by lowering the pH (Anand et al., 2017).

Probiotics can lower the fecal shedding of ETEC (K88 or ECL13795), as shown in piglets orally treated with *Bifidobacterium longum subsp. infantis* (Barba-Vidal et al., 2017), *Escherichia coli* (Khafipour et al., 2014), *Lactobacillus plantarum* (Lee et al., 2012), *Lactobacillus reuteri* (Yang et al., 2015) or *Saccharomyces cerevisiae* (Trevisi et al., 2015). Similarly, *Lactobacillus sobrius* significantly reduced the prevalence of ETEC K88 in the ileum of piglets supplemented with the probiotic (Konstantinov et al., 2008). This antagonistic effect was not associated with any change in luminal pH. The reduced levels of ETEC in the ileum and feces may result from colonization of gut mucosa by the probiotic thereby reducing the attachment of the pathogen to the intestinal surface or from host microbiota modulation (see section 4.1.3.3).

Only two studies have assessed the effect of a probiotic strain on the expression of ETEC virulence genes. Zhou et al. (2014) have shown that *Lactobacillus reuteri* reduced the expression of ST encoding genes (*estA* and *estB*) but not that of LT (*elt*), in ETEC K88 strain JG280 at the early stage of its infection to porcine intestinal epithelial cells. The underlying mechanisms have not been explored by these authors but Yang et al. (2015) have shown in weaning piglets that reuteran-containing diets (an exopolysaccharide produced by *Lactobacillus reuteri*) reduced the copy number of ST gene and the toxin level in samples from the ileum, cecum and colon.

Finally, in such studies, this is the first time that the effect of probiotic was investigated on ETEC enterotoxin production. The works of Anand et al. (2017) have shown after testing the probiotic *Lactobacillus rhamnosus* with several combination of prebiotics (e.g. FOS, inulin, maltodextrin and galactooligosaccharide), that the symbiotic *Lactobacillus rhamnosus* and FOS caused the greatest inhibition of LT enterotoxin production in an ETEC culture growth medium. This study suggested that the structure of FOS plays a role in the functionality of the probiotic in terms of sugar utilization and metabolites produced (Anand et al., 2017).

Table 2.3. **Antagonistic effect of probiotics against ETEC.** *Updated from Roussel et al., 2017.*

DIRECT ANTAGONISM							
MODEL		**REF**	**PROBIOTIC STRAIN**	**ETEC STRAIN**	**DOSES PRO / ETEC**	**THERAPY**	**MECHANISM**
IN VITRO	CO-CULTURE IN CULTURE MEDIUM	Anand et al. (2017)	*L. rhamnosus* NCDC 298 + FOS	MTCC 723	10^7-10^8 CFU/mL (PRO and ETEC) +1% FOS	curative	Inhibition of ETEC growth and LT production
		Tsai et al. (2008)	*L. acidophilus* RY2 *L. salivarius* MM1 *L. paracasei* En4	BCRC 15372 & BCRC 41443 & UM4247 & EK06	10^9 CFU/mL (PRO) 10^8 CFU/mL (ETEC)	preventive	Inhibition of ETEC growth due to antimicrobial activity of lactic acid
		Hillman et al. (1995)	*Lactobacillus spp.*	F4+ac	10^7 CFU/mL (PRO) 10^8 CFU/mL (ETEC)	preventive	Inhibition of ETEC growth (continuous culture of porcine intestinal bacteria)
	CO-CULTURE IN PIGLET INTESTINAL	Wang et al. (2018)	*L. plantarum* ZLP001	F4+ac O149:K91	10^7 CFU/mL (PRO) 10^7CFU/mL (ETEC)	curative	Inhibition of ETEC growth
		Zhou et al. (2014)	*L. reuteri* CL9	F4+, O149:K88 (JG280)	10^8 CFU/mL (PRO and ETEC)	preventive	Reduction of ETEC virulence genes expression (*estA, estB*)
IN VIVO	ORAL ADMINISTRATION TO PIGLETS	Barba-Vidal et al. (2017)	*B. longum subsp. infantis CECT 7210*	F4+ O149:K91:H10	5.10^8 CFU/mL/day (PRO) 8.10^9 CFU/mL (ETEC)	preventive /curative	Reduction of ETEC fecal shedding
		Trevisi et al. (2015)	*S. cerevisiae* CNCM I-4407	F4+ac O149	5.10^{10} CFU/mL (PRO) 10^8 CFU/mL (ETEC)	preventive	
		Yang et al. (2015)	*L. reuteri* TMW1.656 *L. reuteri* LTH5794	ECL13795	10^7 CFU/mL (PRO and ETEC)	curative	Reduction of ETEC colonization and number of ST genes copies in feces /colonic digesta by feed fermentation with *L. reuteri* (reuteran and levan)
		Lee et al. (2015)	*L. plantarum* CJLP243	F4+ac	10^{10} CFU/kg (PRO) $5x10^9$ CFU/mL (ETEC)	curative	Reduction of ETEC fecal shedding
		Khafipour et al. (2014)	*E. coli* UM-2, UM-7	F4+	10^7 to 10^9 CFU/mL (PRO and ETEC)	preventive & curative	
		Zhang et al. (2010)	*L. rhamnosus* GG ATCC 53103	F4+ac O149:K91	10^{10} CFU/mL (PRO) 10^9 CFU/mL (ETEC)	preventive	
		Konstantinov et al. (2008)	*L. sobrius* DSM 16698	F4+	10^{10} CFU/mL (PRO and ETEC)	preventive	Reduction of ETEC levels in the ileum

4.1.3.3. Exclusion

Exclusion is used to describe all mechanisms that make the gastrointestinal environment less hospitable for pathogens. These mechanisms include decreasing luminal pH, modulating gut microbiota, improving epithelium barrier function, interfering with pathogen binding and translocation and stimulating production of defense-associated factors, such as mucins and defensins (Table 2.4). Even if most of the available studies have investigated the probiotic activity of lactic acid bacteria, none of them has associated their beneficial effect with a decrease in luminal pH. Only three studies in piglets have investigated how probiotics may modulate gut microbiota during ETEC infections. Oral administration of *Lactobacillus rhamnosus* counteracted the rise in the fecal shedding of coliforms in ETEC-infected animals and increased the number of *Lactobacilli* and *Bifidobacteria* (Li et al., 2012; Zhang et al., 2010). These findings suggest that treatment with specific *Lactobacillus* strains may be used in piglets to restore the homeostasis of an impaired microbial ecosystem associated with weaning (Li et al., 2012) and/or ETEC challenge (Zhang et al., 2010). Remarkably, the mix BioPlus using two *Bacillus* spore-forming strains shaped the piglet microbial colonic composition by increasing *Lactobacillus*, *Clostridium* and *Turicibacter* populations when low (8.6 $\log_{10}$ CFU d^{-1}) or moderate (8.9 $\log_{10}$ CFU d^{-1}) dose of the probiotic mixture were given. However, the study has shown that a high dose of the mix (9.6 $\log_{10}$ CFU d^{-1}) may increase the risk for enteritis by *Proteobacteria* expansion and was thus not recommended (Zhang et al., 2017). Finally, the spore-forming mixture enhanced goblet cell functions by upregulating *atoh1* gene expression, increasing MUC2 production, preserving thereby the mucosal barrier of piglets (Zhang et al., 2017).

In vitro studies using both pig and human enterocytes in culture and *in vivo* studies in piglets also showed that probiotic strains from *Lactobacillus* genus and *Enterococcus faecium* may protect the integrity of intestinal epithelial barrier damaged by ETEC. *In vitro*, treatment of intestinal cells with probiotics prevented the ETEC-induced decrease of transepithelial resistance (Karimi et al., 2018; Qiu et al., 2017; Tian et al., 2016; Klingspor et al., 2015; Wu et al., 2016; Lodemann et al., 2015) and reduced the permeation of tracers such as dextran (Karimi et al., 2018; Yu et al., 2015). Probiotic treatments are able to reestablished the intestinal barrier function, initially impaired by ETEC binding. The underlying mechanisms involved the regulation of tight junction and cytoskeleton proteins by inhibiting delocalization of zonula occludens 1, increasing the amount of occludin, rearranging F-actin and dephosphorylating occludin (Zanello et al., 2011; Wu et al., 2016; Qiu et al., 2017; Karimi et al., 2018). Such *in vitro* beneficial effects of probiotic *Lactobacillus* strains have been strengthened by an *in vivo* study in piglets. Yang et al. (2015) showed that *Lactobacillus plantarum* prevented the damage to intestinal morphology and greater intestinal permeability (measured by a functional lactulose-mannitol absorption test) induced by ETEC K88 challenge and lowered plasma endotoxin concentrations. In addition, the reduction in *zonula occludens-1* and *occludin* mRNA abundance observed in the jejunum after ETEC infections was inhibited in piglets fed *Lactobacillus plantarum*. Lastly, the study of Trevisi et al. (2017) have also shown that feeding pigs with *Saccharomyces cerevisiae* was effective in counteracting the detrimental effect of ETEC infection by limiting the early activation of genes related to the impairment of the jejunal mucosa.

In addition, several *in vitro* studies on pig (Wang et al., 2018; Badia et al., 2012) or human (Osmanagaoglu et al., 2010) intestinal cells in culture have shown that probiotic bacteria or yeast may decrease the number of adhering ETEC. In these studies, ETEC strains from both porcine and human origins have been tested. Two *in vivo* studies in piglets have also demonstrated that *Pediococcus acidilactici*, *Saccharomyces boulardii* and *Bifidobacterium longum* significantly reduced attachment of ETEC K88 to the ileal mucosa (Daudelin et al., 2011; Barba-Vidal et al., 2017). Little is known about the mechanism of inhibition of ETEC adhesion by probiotics. It has been assumed that probiotics may (i) impede the access of pathogens to tissue receptors by non-specific steric hindrance, (ii) interact with the levels of mucins produced and thus impair the adhesion of pathogens or (iii) block the binding site of ETEC to intestinal epithelial cells by receptor competition. This last hypothesis was the most studied with regards to ETEC pathogens. Purified adhesins of *Bifidobacterium adolescentis* effectively inhibit ETEC adherence to intestinal epithelial cells *in vitro* (Zhong et al., 2004). Fujiwara et al. (2001) reported that *Bifidobacterium longum* produces a proteinaceous inhibitory factor termed binding inhibitory factor (BIF), which prevents the binding of ETEC to GA1 in a dose dependant manner and also inhibits their adherence to HCT-8 human epithelial cells. Other authors rather suggest the role of carbohydrate structures in the inhibition of adhesion (Badia et al., 2012; Osmanagaoglu et al., 2010).

All the *in vitro* and *in vivo* studies described here above, and showing beneficial properties of the probiotic against ETEC have been wrapped-up in Fig. 2.3 for studies that have been carried out in humans, and in Fig. 2.4 for studies carried out in pigs.

Table 2.4. **Competitive exclusion of probiotics against ETEC**
Updated from Roussel et al., 2017.

COMPETITIVE EXCLUSION							
MODEL		**REF**	**PROBIOTIC STRAIN**	**ETEC STRAIN**	**DOSES PRO / ETEC**	**THERAPY**	**MECHANISM**
IN VITRO	CO-CULTURE IN PIGLET INTESTINAL CELLS	Karimi et al. (2018)	*L. reuteri* DSM 17938 and 1563F	853/67	$5x10^7$ to $5x10^8$ CFU/well (PRO) $5x10^6$ CFU/well (ETEC)	preventive	Maintaining E-cadherin expression and upregulation of ZO-1
		Wang et al. (2018)	*L. plantarum* ZLP001	F4+ac O149:K91	10^7 to 10^9 CFU/mL (PRO) 10^7 CFU/mL (ETEC)	preventive / curative	Inhibition of ETEC adhesion in a dose-dependent manner
		Tian et al. (2016)	*E. faecium* HDRsEf1	F4+ac	$5x10^7$ CFU/mL (PRO and ETEC)	preventive	Strengthens intestinal barrier by increasing TEER
		Wu et al. (2016)	*L. plantarum* CCGMCC1258	F4+ ac, O149:K91	10^8 CFU/well (PRO) $6.5x10^7$ CFU/well (ETEC)	preventive	Inhibition of the reduction of tight junctions proteins (claudin-1, occludins) and improvement of epithelial barrier integrity by maintaining TEER
		Badia et al. (2012)	*S. cerevisiae var. boulardii* & β-galactomannan oligosaccharide (Salmosan®, prebiotic)	F4+ ad, O8:K87:H19 (56190) GN1034 F4+	3 yeasts/cell (PRO) 10 µg/mL of βGM $1x10^7$ CFU/well (ETEC)	curative	Inhibition of bacterial adhesion
		Roselli et al. (2007)	*L. sobrius* strain DSM 16698	F4+	10^9 CFU/mL (PRO) 10^8 CFU/mL (ETEC)	preventive	Maintain of barrier integrity by inhibiting bacterial adhesion and ETEC-induced occludin dephosphorylation
	CO-CULTURE IN HUMAN INTESTINAL CELLS	Qiu et al. (2017)	*L. plantarum* CGMCC1258	O149: K91: F4+ac	10^8, $5x10^8$ or 10^9 CFU/mL (PRO) 10^8 CFU/mL (ETEC)	preventive	Partially increase of TEER ZO-1 / occludin mRNA and proteins expression
		Lodemann et al. (2015)	*E. faecium* NCIMB 10415	F4+ O149:K91:K88	10^8 CFU/mL (PRO) 10^8 CFU/mL (ETEC)	preventive	Reduction of ETEC-induced decrease of TEER
		Klingspor et al. (2015)	*E. faecium* NCIMB 10415	ETEC IMT 4818 O149:K91/K88 (F4+)	10^8 CFU/mL (PRO) 10^6 CFU/mL (ETEC)	preventive	
		Yu et al. (2015)	*L. fructosus C2*	F4+	unknown	curative	Reduction of intestinal permeability and maintain of barrier integrity
		Osmanagaoglu et al.	*Pediococcus pentosaceus* OZF	LMG 3083 (human)	10^8 CFU/mL (PRO) 10^8 CFU/mL (ETEC)	preventive	Decrease in the number of adhering ETEC

		(2010)					
		Zhong et al. (2004)	*B. adolescentis* 1027	unknown	10^8 CFU/mL (PRO and ETEC)	preventive	Competitive inhibition of ETEC adherence by adhesin production
		Fujiwara et al. (2001)	*B. longum* SBT2928 (BL2928)	Pb 176 (human)	0.5g/ml (BIF protein) 10^9 CFU/mL (ETEC)	preventive	Inhibition of interactions with ETEC receptor GA1 by BIF issued from the extracellular protein fraction of probiotic culture
IN VIVO	ORAL ADMINISTRATION TO PIGLETS	Zhang et al. (2017)	*Bacillus licheniformis* DSM 5749 and *B. subtilis* DSM 5750	F4+ac O149:K91	$3.9.10^8$ CFU/day or $7.8.10^8$ CFU/day (PRO) 1.10^{10} CFU/day (ETEC)	preventive	Increasing *Lactobacillus*, *Clostridium* and *Turicibacter* populations in the colon Improve intestinal barrier integrity by upregulating *Atoh1* gene associated to an increase in MUC2 production
		Barba-Vidal et al. (2017)	*B. longum spp infantis* CECT 7210	F4+ O149:K91:H10	5.10^8 CFU/mL/day (PRO) 8.10^9 CFU/mL (ETEC)	preventive /curative	Reduction of ileal colonization
		Trevisi et al. (2017)	*S. cerevisiae* CNCM I-4407	F4+ ac O149	5.10^{10} CFU/kg (PRO) 10^8 CFU/mL (ETEC)	curative	Limitation of early activation of genes related to the impairment of the jejunal mucosa associated with ETEC infection
		Yang et al. (2014)	*L. plantarum* CGMCC 1258	F4+ ac O149:K91	5.10^{10} CFU/kg of diet (PRO) 10^8 CFU/mL (ETEC)	preventive	Protection from ETEC-induced membrane damage, increase ZO-1 and occludin (tight junction proteins) expression in the jejunum
		Li et al. (2012)	*L. rhamnosus* ATCC 7469	F4+ ac O149:K91	10^{10} CFU/mL (PRO) 10^9 CFU/mL (ETEC)	preventive	Modulation of pig fecal microbiota composition: increase in *Lactobacilli* and *Bifidobacteria*
		Daudelin et al. (2011)	*Pediococcus acidilactici* *S. cerevisiae boulardii*	O149:F4+ (ECL8559)	10^9 CFU/pig/day (PRO) 10^9 CFU/5mL (ETEC)	preventive	Reduction of ETEC F4 attachment to the ileal mucosa
		Zhang et al. (2010)	*L. rhamnosus* GG ATCC 53103	F4+ ac, O149:K91	10^{10} CFU/mL(PRO) 10^9 CFU/mL (ETEC)	preventive	Modulation of pig fecal microbiota composition: increase in *Lactobacilli* and *Bifidobacteria*

TEER: Trans-epithelial electrical resistance; ZO-1: Zonula occludens.

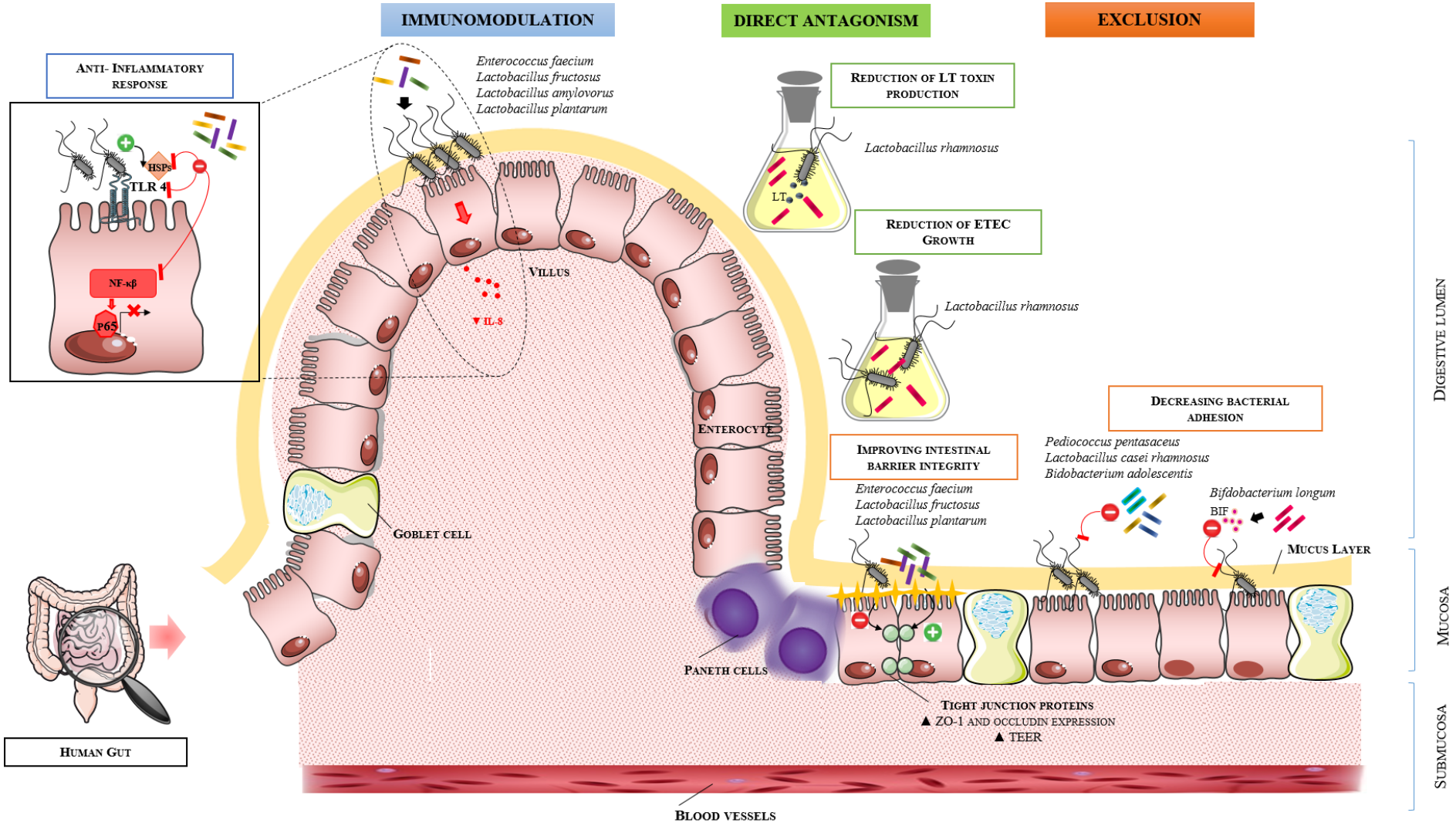

Figure 2.3. **Overview of probiotic mechanism of action against ETEC under human digestive conditions.** TEER: Transepithelial electrical resistance; TLR: Toll-like receptor; ZO: Zonula occludens. *Updated from Roussel et al., 2017.*

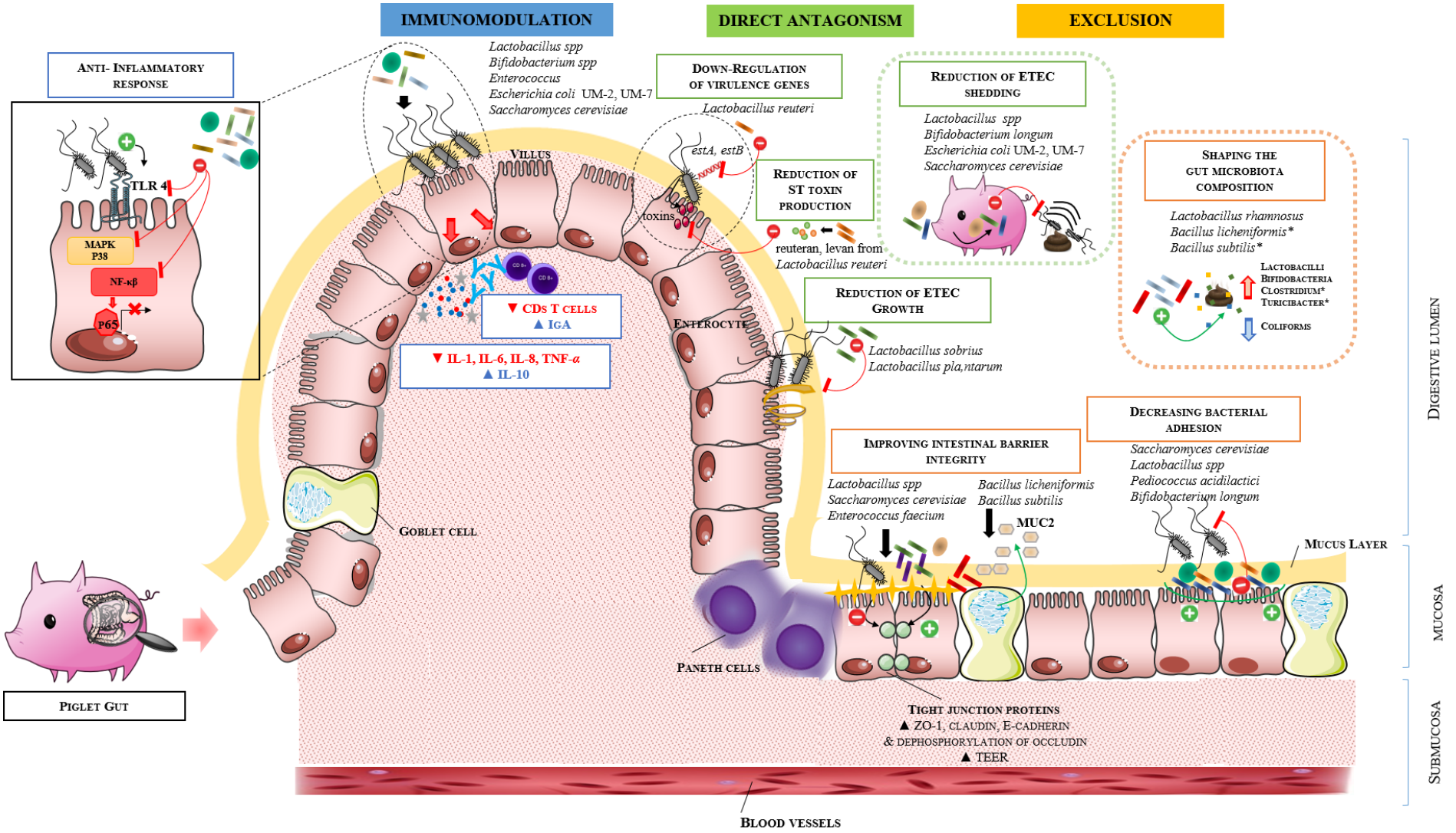

Figure 2.4. **Overview of probiotic mechanism of action against ETEC under piglet digestive conditions.** TEER: Transepithelial electrical resistance; TLR: Toll-like receptor; ZO: Zonula occludens. *Updated from Roussel et al., 2017.*

4.1.3.4. Human trials involving probiotics

As previously described, the vast majority of *in vivo* studies involving ETEC and probiotic strains have been carried out in piglets, most often in the specific context of the post-weaning phase. Only two studies have investigated the effect of probiotics in human volunteers when orally challenged with live attenuated ETEC strains. Unfortunately, these two studies showed that supplementation with either a single strain of *Lactobacillus acidophilus* (Ouwehand et al., 2014) or a blend of probiotic bacteria and yeast (Ten Bruggencate et al., 2015) were ineffective in reducing ETEC infection symptoms in healthy men. Besides, the study by Ouwehand et al. (2014) provides useful data on changes in human intestinal microbiota associated with ETEC infections, the authors showing a reduction of the fecal levels of *Bacteroides-Prevotella, Bifidobacterium* and *Clostridium clusters XIVa* and *b*. The ineffective effects of probiotics may be linked to the challenge model or to the fact that in these studies the disease mechanisms was toxin independent (ETEC attenuated strains do not produce LT and ST toxins). Other studies have shown a significant reduction in the risk of traveler's diarrhea when probiotics such as *S. boulardii* were given (McFarland et al., 2007), but ETEC strains have not been clearly involved in the diarrheal etiology. Interestingly, in 2014 the European Society for Pediatric Gastroenterology Hepatology and Nutrition recommended the use of the probiotics *Lactobacillus rhamnosus* GG or *Saccharomyces boulardii*, as routine treatment for children with acute diarrhea (Guarino et al., 2014). This recommendation has been recently reinforced by an expert panel convened by the European Pediatric Association. However, the panel highlights that in special situations such as prematurity or immunocompromised patients, these probiotic strains should be used with caution (Hojsak et al., 2018).

Then, a significant number of *in vitro* or *in vivo* studies have shown the beneficial effects of probiotics against ETEC pathogens, by interfering with their survival, adhesion to mucosa or expression of virulence genes. Nevertheless, most of these studies involved strains such as K88, which are pathogenic for piglets but not for human and the only two *in vivo* studies in humans were performed with non-toxigenic strains. As it is highly probable that the outcomes would be strain-dependent, additional studies involving strains pathogenic for humans are required.

4.2. Interest of the yeast *Saccharomyces cerevisiae* CNCM I-3856

4.2.1. Generalities on yeast cell composition and metabolism

Yeast microorganisms differ fundamentally from bacteria. Among a huge range of species, the yeast of interest in the present study belongs to the species *Saccharomyces cerevisiae*. The yeast reproduces by a budding mechanism and has specific physiological traits. This eukaryotic single cell model measures between 5-10 µm diameter, has a round to ovoid shape and a complex internal cell structure (Fig. 2.5A) (Salari and Salari, 2017). In addition, the wall consists of two layers. The mechanical strength of the wall is mainly due to the inner layer, consisting of β1,3-glucan and chitin, while the outer layer is composed of heavily glycosylated mannoproteins emanating from the cell surface and specifically

involved in cell to cell recognition (Fig. 2.5B) (Orlean, 2012). As well, the yeast cell wall materials serve as excellent substrate for microbial fermentation (Cuskin et al., 2015).

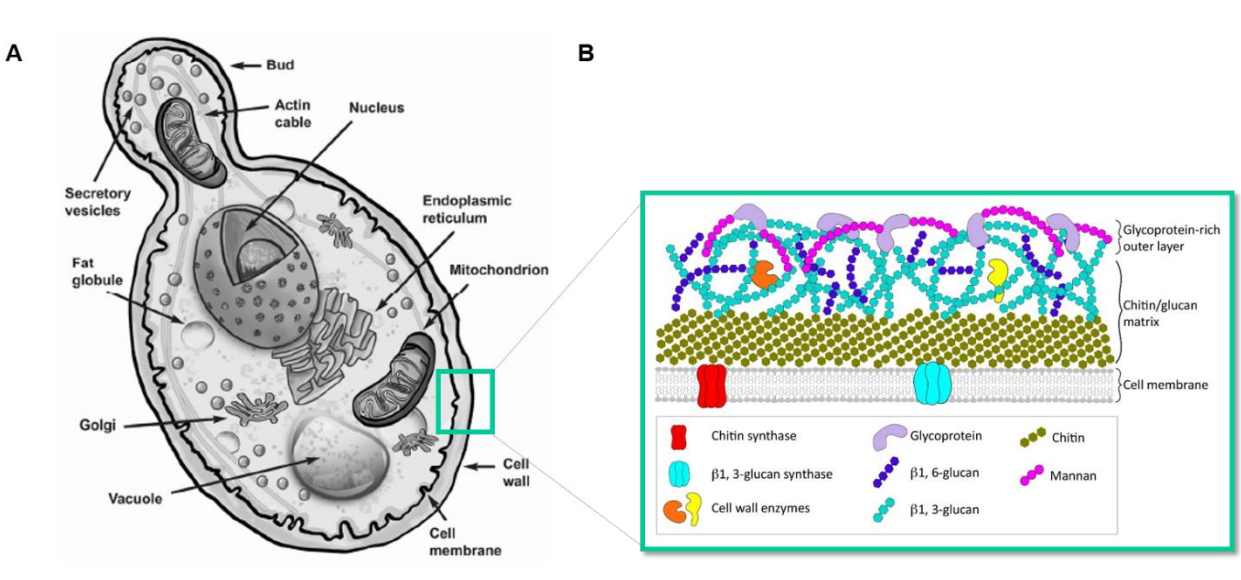

Figure 2.5. **Schematic representation of the yeast cell.** (**A**) Simplified yeast cell structure; (**B**) Schematic representation of the yeast cell wall. *Reprinted with permission from Walker and Stewart, 2016; Geoghegan et al., 2017.*

The etymology of the word *Saccharomyces cerevisiae* is the reflect of its metabolic features. The first part of the name "*Saccharomyces*" means "sugar fungus", while the second part "*cerevisiae*" means "of beer" (Salari and Salari, 2017). Indeed, *S. cerevisiae* is an heterotroph, switching to a mixed respiratory-fermentative metabolism. During fermentation and as soon as the external glucose concentration exceed 0.8 mM, ethanol is produced. Hence, *S. cerevisiae* controls fermentation *vs* respiration primarily in response to the sugar level (Otterstedt et al., 2004). Such ethanol production can have adverse effect on pathogen growth by inducing leakage of the plasma membrane (Etienne-Mesmin et al., 2011; Ingram, 1990).

4.2.2. The wild field of yeast: a market in expansion

The yeast has been successfully studied for many years to unravel biological and molecular processes of eukaryotic organisms and is also a powerful model microorganism for understanding human biology and diseases (Fig. 2.6A). Since 2001, 11 Nobel prizes have been awarded for discoveries involving yeast research. Beyond human biology and because of its fermentation capacity and ethanol production previously explained in section 4.2.1, *S. cerevisiae* is the main fermentative agent in bakery and brewery (Hatoum et al., 2012). In addition, modern applications of the yeast have been greatly expanded beyond classical applications to this microorganism. For instance, beyond its probiotic properties developed in section 4.2.3, brewer's yeast can be also used as a dietary supplement in human to enhance hair growth and nails resistance. In animals, the yeasts and derivatives (cell wall extract) are also largely used as

feed additives and ingredients for their nutritional properties and growth performance (Shurson, 2018). In pharmaceutics, *S. cerevisiae* are increasingly used for the heterologous production of enzymes and proteins. They also have wide range of applications in bioremediation or removal of heavy metals from wastewater. Finally, engineered yeast are used as biocatalyst in agriculture (Türker, 2014).

The global market of yeast represented more than $ 7 billion in 2016. Among the large sector of live yeast, baker's yeast prevailed with its $ 4 billion turnover (59% market share). The rest of the live yeast sector represented $ 624 million (9% market share) and is mainly attributed to the probiotic area (Fig. 2.6B). Probiotic market is dominated by companies including Lesaffre group (France), AB Vista (UK) and Lallemand (Canada) (BCC Research Report, 2017, https://www.bccresearch.com/market-research/food-and-beverage/probiotics-market-fod035d.html, consulted on 09/2018). But the global probiotic market remains largely dominated by the wide range of bacterial genera commercialized while the probiotic yeast are limited to *Saccharomyces* genus (Hudson et al., 2016).

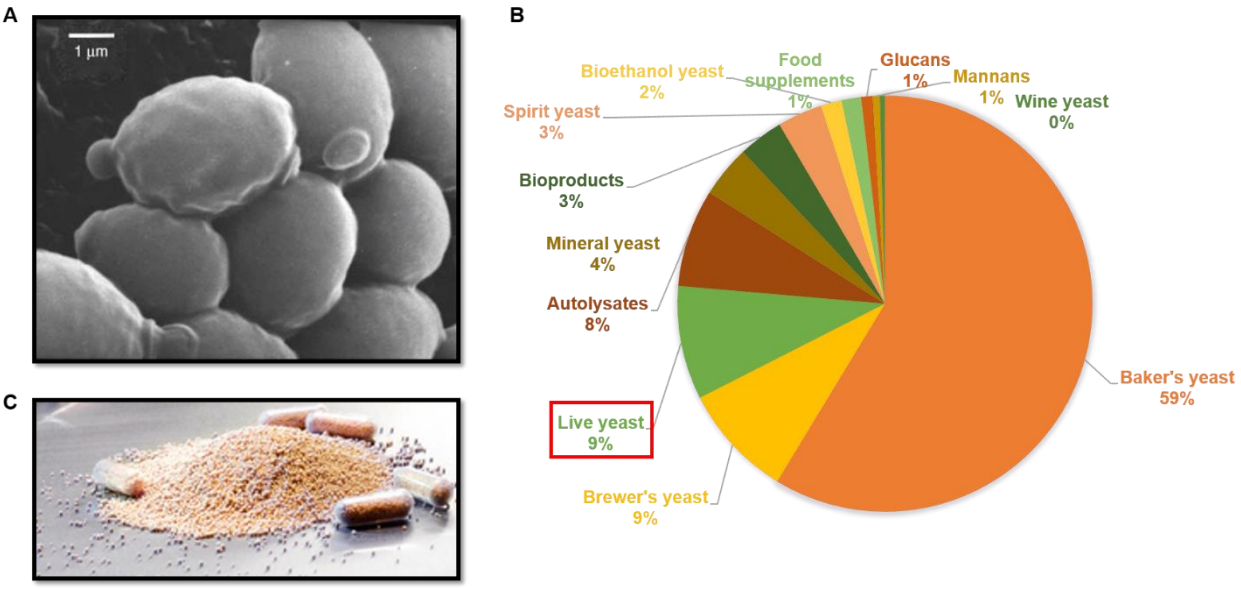

Figure 2.6. **The yeast in all its forms.** (**A**) Electron microscopy micrograph of *Saccharomyces cerevisiae* yeast cells. A typical yeast cell is around 5-10 µm diameter. The cells reproduce through a process called budding; (**B**) Global yeast market in 2016 in the world according to the type use; (**C**) Picture of active dry yeast processed by Lesaffre. *Reprinted with permission from Lesaffre; reviewed from BCC research report, 2017.*

4.2.3. The choice of the strain Saccharomyces cerevisiae CNCM I-3856

In the frame of this PhD, a partnership with Lesaffre Human Care, a business unit of Lesaffre (Marq-en-Baroeul, France) has been established in order to study the antimicrobial properties of the probiotic yeast *Saccharomyces cerevisiae* CNCM I-3856 against ETEC infection, as explained in the following section 5. In addition, Lesaffre has funded all the experimental work of this PhD.

The patented yeast *Saccharomyces cerevisiae* CNCM I-3856 from Lesaffre's collection is already known on the market under the commercial name of Ibsium® (previously named Lynside® Pro GI+), an active dry yeast (Fig. 2.6C). Indeed, in 2015, after providing strong scientific and clinical data on the benefits of the yeast in individuals with IBS, this probiotic yeast has been rewarded with the approval of a health claim by the Canadian Health Authorities. The health claim is as follow: "Helps to reduce abdominal pain and discomfort associated with irritable bowel syndrome" (https://www.lesaffre.com/health-claim-lesaffre-human-care-ibsium/, consulted on 09/2018; Cayzeele-Decherf et al., 2017; Spiller et al., 2016; Pineton de Chambrun et al., 2015).

Beyond this application area and since several years, this yeast strain is intensively studied for its probiotic properties. *Saccharomyces cerevisiae* CNCM I-3856 has already displayed recognized antagonistic characteristics through several mechanism of action in other enteropathogenic *E. coli*, reinforcing thus the interest to initiate investigation of such effects in ETEC. Remarkably, Sivignon et al. (2015) have used distinct models to investigate the antagonistic properties of *S. cerevisiae* CNCM I-3856 against AIEC infections. For instance, authors have shown in T84 cells that the yeast and its derivatives inhibited AIEC cell adhesion/invasion and restored the barrier function. In a mouse model, the yeast reduced AIEC-inflammation and colonic injuries (Sivignon et al., 2015). Thévenot et al. (2015) and Etienne-Mesmin (2011) have used *in vitro* models of the human gut, TIM-1 and ARCOL, previously described in section 3.3.2, to study the antagonistic properties of the same yeast strain on EHEC infections. Authors have shown that *S. cerevisiae* CNCM I-3856 reduced EHEC growth in the upper GI tract and inhibited the *stx* toxin gene expression in the lower GI tract (Thévenot et al., 2015; Etienne-Mesmin et al., 2011). Finally, in murine ileal loops, the pre-treatment with the probiotic yeast reduced EHEC translocation through M cells, and reduced the number of hemorrhagic Peyer's patches (Thévenot et al., 2015).

4.2.4. Saccharomyces cerevisiae versus Saccharomyces boulardii

The two strains *S. cerevisiae* and *S. boulardii* largely studied and marketed for their beneficial and probiotic effects are clearly dissociated by the manufacturers, advocating their unique reference. However, the strain difference is often misunderstood from the customers or the scientific community. Although phylogenetically closely related, *S. boulardii* is a subspecies of *S. cerevisiae,* carrying a unique and specific microsatellite allele (Mitterdorfer et al., 2002; Hennequin et al., 2001). Metabolically and physiologically, the strains displayed particularities in relation to growth yield and resistance to temperature (Fietto et al., 2003). *S. boulardii* does not produce ascospores or use galactose, while *S. cerevisiae* does (Edwards-Ingram et al., 2007).

The extensively marketed strain *S. boulardii* CNCM I-745 (Biocodex laboratory), originally extracted from lychee and mangosteen is used for its broad properties in probiotics to prevent antibiotic-associated diarrhea or to treat infant diarrhea and recurrent *Clostridium difficile* associated diarrhea. Even though the use of the yeast *S. boulardii* is recommended in prevention of traveler's diarrhea, no scientific evidence has emerged. In addition, *S. boulardii* CNCM I-745 has never been studied for its antimicrobial properties against ETEC human infections (45% of the traveler's diarrhea), contrary to *S. cerevisiae* CNCM I-3856 through this PhD research.

5. Research questions and outline of the PhD

The literature review hereinabove has redrawn the current knowledge on ETEC, one of the most redoubtable diarrheal pathogen worldwide. Throughout the alarming number of ETEC cases, its pathophysiology in the human gut, and the research initiatives undertaken to prevent or treat such infections, two main issues have been raised. Despite the fact that 70 years have passed since the first discovery of ETEC and the high number of research conducted, (i) **the bacterial pathogenesis through its survival in the human GI tract and virulence features remain still scarcely understood**, (ii) **impeding to prevent or cure properly such infections**.

Therefore, to attempt to address gaps awareness, the present European joint PhD aimed to:

(i) supply a piece of puzzle to unravel the mechanisms associated to ETEC H10407 dynamics (e.g. survival and virulence) in the human GI tract, with the use of well-controlled and bio-regionalized simulators of the human digestion and/or fermentation named TIM-1 and M-SHIME,

With the following research questions:

- *Do the stringent conditions of the human GI digestion affect ETEC survival?*
- *How the membrane integrity of ETEC is affected during the human GI passage?*
- *How ETEC interacts with the mucus-associated microbes and mucus-deprived microbes?*
- *How ETEC modulates its virulence, through the gene expression and toxin production in a spatio-temporal fashion during the human GI passage and in association with the gut microbes?*
- *Do ETEC episode modulate the human gut microbial composition and activity?*

(ii) consider the use of *S. cerevisiae* CNCM I-3856 as a prophylactic probiotic approach for traveler's diarrhea associated to ETEC, and study its inhibitory potential against ETEC H10407 in the TIM-1 and M-SHIME,

With the following research questions:

- *Does the probiotic S. cerevisiae affect the survival of ETEC during human GI passage?*
- *Does S. cerevisiae have an effect on ETEC physiological states during human GI digestion?*
- *Does S. cerevisiae modulate the virulence function of ETEC during human GI digestion?*
- *What are the potential antimicrobial mechanisms used by S. cerevisiae against ETEC?*
- *Does S. cerevisiae modulate the gut microbial composition and activity? What are the hypothetic underlying mechanisms?*

For the first time, this PhD collaboration achieved between MEDIS laboratory (Clermont-Auvergne University, France) and CMET (Gent University, Belgium), allows to combine the TIM-1 and M-SHIME, the two most complete *in vitro* systems in the world for the upper and lower GI tract, respectively. A main part of this work was also in collaboration with Lesaffre company, providing the probiotic strain.

The following chapters **in section II** will present the results of each stage of the experimental works (Fig. 2.7). **Chapter 1** presents in a methodological point of view, a series of experiments conducted in the TIM-1 to cross-compare microbiological (plate counts) and molecular based-methods (q-PCR, PMA-qPCR and Live/Dead flow cytometry) in order to assess the viability of ETEC under human simulated digestive conditions. **Chapter 2** unravels the effect of the physicochemical parameters on ETEC dynamics of survival, physiological state and virulence genes expression all along the GI tract from the stomach to the ascending colon, as well as the luminal and mucosal microenvironments. Thus, the results from the two *in vitro* models of the human digestion (TIM-1) and fermentation (M-SHIME) were combined to offer the most complete view of ETEC pathogenesis through a large set of microbiological, molecular and transcriptional analysis. **Chapter 3** elucidates through *16S* rRNA-gene sequencing, the inter-individually dependent modulation of the human gut microbiota by ETEC infection and provides the microbial and metabolic signature of the new ileum, set-up in the M-SHIME, integrating both the luminal and mucosal microbial microenvironments. **Chapter 4** evaluates the antimicrobial properties of *Saccharomyces cerevisiae* CNCM I-3856, through a series of complementary *in vitro* assays in culture media, mucin-agar layer, and Caco-2 cells, and *in vivo* assays in mice against ETEC H10407. **Chapter 5** studies the inhibitory properties of *S. cerevisiae* CNCM I-3856 against ETEC H10407 spatio-temporal survival and virulence by combining the two digestive *in vitro* systems as previously explained. This chapter explores also the capacity of the yeast to shape the microbial environment through *16S* rRNA-gene sequencing, and its metabolic activity. Finally, the **section III** summarizes and interprets the results from all chapters and will be ended by future perspectives.

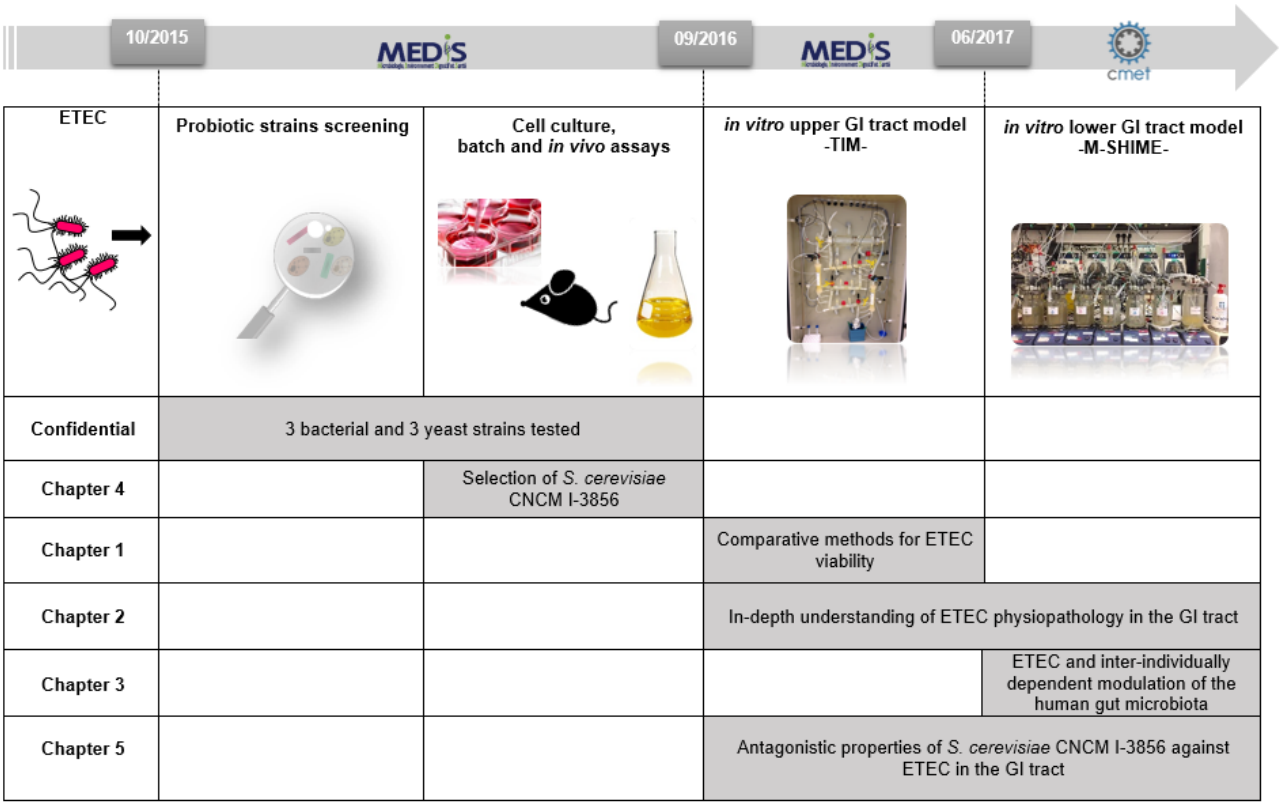

Figure 2.7. Research outline

Each stage of the experimental work has been allocated to a research chapter based-publication, presented in the next section II. The first 18 months of the PhD were conducted in MEDIS laboratory in Clermont-Auvergne University, Clermont-Ferrand, France (e.g. probiotics screening, cell culture, batch assays and TIM-1 experiments). The last 18 months were conducted in CMET laboratory in Gent University, Gent, Belgium, and ruled by the M-SHIME experiments.

Section II

EXPERIMENTAL WORK

CHAPTER 1 : COMPARISON OF CONVENTIONAL PLATING, PMA-QPCR AND, FLOW CYTOMETRY FOR THE DETERMINATION OF VIABLE ETEC ALONG THE GI TIM-1 MODEL

***

Better appreciate ETEC viability upon complex digestive environments simulated by the TIM-1 was a second purpose to this PhD. A cross-comparison of microbiological (plating) and molecular based-methods (qPCR, PMA-qPCR, flow cytometry) was thus performed in a series of experiments conducted in the TIM-1 system. A partnership with VetagroSup laboratory (Lempdes, Puy-de-Dôme, France) for flow cytometry analysis was accomplished.

The results have been subjected to the writing of a methodological article, published in Applied Microbiology and Biotechnology[3] and redrafted for the present chapter.

[3] ***Publication.*** *ROUSSEL C., GALIA W., LERICHE F., CHALANCON S., DENIS S., Van de WIELE T., BLANQUET-DIOT S. Comparison of conventional plating, PMA-qPCR, and flow cytometry for the determination of viable enterotoxigenic Escherichia coli along a gastrointestinal in vitro model. Appl. Microbiol. Biotechnol, 102, 9793-9802 (2018). https://doi.org/10.1007/s00253-018-9380-z*

1 Comparison of conventional plating, PMA-qPCR and, flow cytometry for the determination of viable ETEC along the GI TIM-1 model

Abstract Recent technological advances for bacterial viability assessment, using molecular methods or flow cytometry can provide meaningful interest for the demarcation between live and dead microorganisms. Nonetheless, these methods have been scarcely applied to foodborne pathogens and never for directly assessing their viability within the human digestive environment. The purpose of this study was to compare two methods based on membrane integrity (PMA-qPCR and Live/Dead flow cytometry) and the classical plate-count method to determine the viability of a common foodborne pathogen, ETEC, during its transit through simulated human gastro-intestinal environment. Viable ETEC counts in the gastric and small intestinal compartments of the GI TIM-1 model indicated a consensus between the three tested methods (PMA-qPCR, flow cytometry and plate counts). In a further step, flow cytometry analysis appeared as the preferred method to elucidate ETEC physiological states in the *in vitro* digestive environment by discriminating four subpopulations, while PMA-qPCR can only distinguish two. The defined viable/altered ETEC population was found during all *in vitro* digestions, but mainly in the gastric compartment. Being able to discriminate the particular physiological states of pathogenic microorganisms in the digestive environment is of high interest, because if some cells are not observable on culture media, they might keep their ability to express virulence functions.

1. Introduction

The demarcation between live and dead microorganisms is a complex and debatable feature in microbiology. In the area of food microbiology, conventional plate counting was traditionally used to indicate the level of specific microorganisms in food products. Nevertheless, recent advances in technologies for bacterial viability assessment indicate the shortcomings of the ancestral plate-count method, incapable of culturing intermediate life stages of microorganisms, such as viable but not culturable (VBNC), slow-growing or quiescent cells (Emerson et al., 2017). These different stages are important to consider during food processing and preservation, especially for safety concern (Gill, 2017; Tamburini et al., 2013). Studies from the last decade emphasized that several food-borne pathogens in VBNC state were able to express their virulence, meaning that the metabolic activity could also be associated to intermediate living steps (Li et al., 2014; Zhao et al., 2017). Consequently, in order to better tackle these intermediate life stages, plenty of tools have been developed like Live/Dead BacLight® stain by flow cytometry, viability assays based on cellular metabolism by measuring bacterial membrane potential, viability PCR-based strategies with PMA-qPCR, or other molecular approaches with pre-rRNA or rRNA sequencing (Emerson et al., 2017; Kennedy et al., 2011). Among these methods, PMA-qPCR and flow cytometry certainly remain the most studied. These multiple techniques are providing more insight into bacterial physiology, but the interpretation of results may be tricky and the respective advantages and limitations of each of these techniques remain unclear.

So far, these methods have been applied to foodborne pathogens in a quite restrictive field, i.e. to assess their viability in specific environments, such as surfaces, water or food matrices, and the effect of acidic, osmotic or desiccation stresses (Gensberger et al., 2014; Baoguang and Chen, 2013). With respect to digestive environment involving acidic pH or bile salts that are known to be challenging for microorganisms, there are very few studies that use the above-mentioned techniques to follow life stages of pathogens in the human digestive environment (Roussel et al., 2016; Villareal et al. 2013). For obvious ethical reasons, such studies involving wild-type pathogens must be conducted *in vitro*. Among available *in vitro* models of the human gut, the dynamic multi-compartmental and computer-controlled TIM-1 is currently considered as the most complete simulator of the human stomach and small intestine (Guerra et al., 2012; Roussel et al., 2016). In this work, we studied as a model of bacterial pathogen, the food and waterborne ETEC, which is responsible for hundreds of millions of diarrheal cases in young children from low-income countries and travelers over the world (Roussel et al., 2017). Even if ETEC survival in the human gut is a key parameter in the infectious process, nothing is known about cell life stages in the human digestive environment and the best way to identify them.

In this context, the aim of the present study was to compare two tools based on membrane integrity (PMA-qPCR and Live/Dead flow cytometry) and classical culture-based method for an accurate determination of ETEC viability in the complex *in vitro* human digestive environment, as simulated by the gastrointestinal TIM-1 model.

2. Materials and Methods

2.1 Bacterial strain

The prototypical ETEC strain H10407 serotype O78:H11:K80, ATCC® 35401 isolated in Bangladesh from a patient with a cholera-like syndrome (Evans et al. 1977) was used in this study. Bacteria were routinely grown under agitation (37°C, 125 rpm, overnight) in LB broth until OD_{600nm} = 0.6 (stationary phase).

2.2 TIM-1 gastrointestinal model

The TIM-1 model (The Netherlands Organization TNO, Zeist, Netherlands) consists of four successive compartments simulating the human stomach, duodenum, jejunum and ileum (Guerra et al. 2012). The main parameters of human digestion, such as body temperature, kinetics of gastric and intestinal pH, peristaltic mixing and transport, gastric, biliary and pancreatic secretions and passive absorption of small molecules and water, are reproduced as accurately as possible. Briefly, each compartment is composed of glass units with a flexible inner membrane. Peristaltic mixing and body temperature are achieved by pumping water at 37°C into the space between the glass jacket and the flexible wall at regular intervals. Mathematical modeling of gastric and ileal deliveries with the Elashoff power exponential equation ($f=1-2^{-(t/t1/2)\beta}$ where t is the time of emptying and β a coefficient describing the shape of the curve) is used for the computer control of chyme transit. Chyme transport through the TIM-1 is regulated by the peristaltic valves that connect the successive compartments. The volume in each compartment is monitored by a pressure sensor and the pH is computer-monitored and continuously controlled by adding either HCl or $NaHCO_3$. Simulated gastric, biliary and pancreatic secretions are introduced into the corresponding compartments by computer-controlled pumps. Water and products of digestion are removed from the jejunal and ileal compartments by pumping dialysis liquid through hollow fibers SF 09L (Nipro, Zaventem, Belgium, cut-off 10 KDa).

2.3 *in vitro* digestions and sampling

The TIM-1 system was programmed to reproduce, based on *in vivo* data (Roussel et al. 2016), the physicochemical digestive conditions encountered in a healthy adult when a glass of water (main source of human contamination by ETEC) is ingested (Table 1.1). The bacterial suspension (200 ml) that was introduced into the TIM system consisted of mineral water experimentally contaminated with the ETEC reference strain at a final concentration of $5x10^7$ CFU mL^{-1}. Two types of experiments were performed: gastric digestions where the gastric compartment was solely used (total duration of 60 min) and gastrointestinal digestions using the entire TIM model (total duration of 300 min). During digestion, gastric and ileal effluents were kept on ice and pooled on 0-20, and 20-60 min for gastric digestions and hour-by-hour for gastrointestinal digestions. Digestions were run in quadruplicate. Samples were taken in the initial bacterial suspension (t0) and regularly collected during digestion in each digestive compartment (stomach, duodenum, jejunum and ileum) and/or in the gastric and ileal effluents.

Table 1.1. Parameters of the TIM-1 system when simulating digestive conditions of a healthy adult after intake of a glass of water. A power exponential equation ($f= 1-2^{-(T/T_{1/2})^{\beta}}$ where f represents the fraction of water delivered, $T_{1/2}$ represents the half-time of delivery and β a coefficient describing the shape of the curve) was used for the computer control of gastric and ileal deliveries in the TIM-1.

Parameters of *in vitro* digestion of a glass of water	Gastric compartment	Duodenal compartment	Jejunal compartment	Ileal compartment
pH	from 6 (T0) to 1.5 (90 to 300 min)	maintained at 6.4	maintained at 6.9	maintained at 7.2
Volume	200 ml (T0)	30 ml	115 ml	115 ml
Secretions	(i) 130 U/min of pepsin (ii) 5 U/min of lipase (iii) HCl 0.3 M if necessary	(i) 20 mg min^{-1} of bile salts (first 30 min of digestion) then 10 mg min^{-1} (ii) 20 mg min^{-1} of pancreatic juice 4 USP (iii) $NaHCO_3$ 0.5 M if necessary	(i) $NaHCO_3$ 0.5 M if necessary	(i) $NaHCO_3$ 0.5 M if necessary
Emptying time	$T_{1/2}$ = 15 min	-	-	$T_{1/2}$ = 150 min
β coefficient	β = 1	-	-	β = 2.4

All products were purchased from Sigma (St Louis, USA). USP= United States Pharmacopeia

2.4 Bacterial numeration by plating

The number of cultivable bacteria in each digestive compartment of the TIM-1 and in the gastric and ileal effluents of the model was determined by direct plating onto LB agar (overnight incubation at 37°C), after appropriate serial dilutions in saline water.

2.5 PMA-qPCR-based quantification

PMA treatment for qPCR. Digestive samples were collected in duplicate from each compartment of the TIM-1 model and from the gastric and ileal effluents, and stained or not with 50 µM PMA (Interchim, Montluçon, France). Samples were incubated 5 min at room temperature in the dark, under agitation (100 rpm). Then, stained samples were exposed 15 min to the blue light PMA-Lite LED Photolysis (Interchim, Montluçon, France) to allow the dye photo activation. Finally, both samples (stained or not) were centrifuged (4,400 x *g*, 4°C, 10 min) and pellets were washed with milli-Q water and stored at -20°C until DNA extraction.

Genomic DNA extraction for qPCR. Total bacterial DNAs from samples treated or not with PMA were extracted using the Smart Extract Kit SK-DNEX-100 (Eurogentec, Seraing, Belgium) according to the manufacturer's instructions. Then, DNAs were stored at -20°C. DNA concentration and purity were assessed by measuring the absorbance at 260 nm and the ratio of absorbance at 260 and 280 nm (A260/A280) with a NanoDrop ND-1000 spectrophotometer (Thermo Scientific, Waltham, USA).

Quantification of bacteria by qPCR. The qPCR procedure was performed using the Mx Pro Real Time Mx 3000P system (Agilent, Les Ulis, France). The total reaction volume of 10 µL contained 5 µL of Takyon Low Rox Sybr Master Mix dTTP blue (Eurogentec, Seraing, Belgium), 0.45 µL (10 µM) of primers encoding for the 16S *Enterobacteriaceae* (F- CATGCCGCGTGTATGAAGAA, R-CGGGTAACGTCAATGAGCAAA, melting temperature 60°C) (Huijsdens et al. 2002), 3.1 µL milli-Q

water and 1 µL of template DNA from digestive samples. Non-template control was 1 µL milli-Q water. Each reaction was run in triplicate in a 96-well reaction plate sealed. The PCR reactions were amplified by an initial denaturation step at 95°C for 5 min followed by 45 cycles of 95°C (30s), 60°C (30s) and 72°C (30s). The melting curves of PCR amplicons, yielding a single melting peak, were checked to ensure primer specificity. To determine qPCR efficiency and detection limit, standard curves were generated using serial 10-fold dilutions of an ETEC pure culture (OD_{600nm} = 0.3, exponential phase, LB broth) stained or not with PMA. In parallel, each dilution was plated onto LB agar to determine ETEC concentration (CFU mL^{-1}). As a negative control, an ETEC pure culture was subjected to lethal heat-treatment (95°C, 15 min) and stained or not with PMA. The absence of viable ETEC in the heat-treated samples was confirmed on LB agar plates.

2.6 Live & Dead flow cytometry analysis

Physiological state of cells in the *in vitro* digestive samples was determined by a live/dead analysis with flow cytometry. Bacteria from gastric and ileal effluents were double stained (LIVE/DEAD BacLight®, Molecular probes, Whaltham, USA) with the green-fluorescent DNA stain SYTO 9 labelling all bacteria and the red-fluorescent Propidium Iodide (PI) only penetrating and staining cells with damaged membranes. Adequate volumes of gastric or ileal effluents were centrifuged (6,340 x *g*, 20°C, 5 min) and bacterial pellets were suspended into phosphate buffer at pH 7.3 to get a final concentration of approximately 10^6 CFU mL^{-1}. Bacterial suspensions were incubated for 15 min at room temperature in the dark with 5 µM SYTO 9 and 30 µM PI, according to the manufacturer's instructions. ETEC cells from pure culture in exponential phase and ethanol (75%)-treated cells (for 30 min) heated at 60°C (for additional 30 min) were used as controls.

Flow cytometry analyses were performed using a CyFlow® Space system (Partec GmbH, Münster, Germany). Acquisition was performed with Flowmax® (Partec GmbH, Münster, Germany) and based on light-scatter and fluorescence signals with 488 nm excitation from a blue solid-state laser delivering illumination at 100 mW. In the flow cytometer, optical filters were set up so that PI was measured above 630 nm and SYTO 9 at 520 nm. The trigger was set for the forward scatter (FSC) and data were acquired on two parameters, i.e. dot plots of green fluorescence (FL1 at 520 nm) versus red fluorescence (FL2 at 630 nm) or forward scatter versus sideward scatter (SSC). FSC, SSC and fluorescence signals of individual cells passing through the illuminated zone were collected as logarithmic signals. Data were analysed using the Flowmax® software. Following Roussel et al. (2016), the density plots obtained by flow cytometry analysis were divided into four regions (depending on gating on FL1 and FL2), each assigned to cells with different physiological properties.

2.7 Data expression and statistical analysis

Values are given as means of log_{10} cells ± SD or as mean percentages ± SD for each subpopulation when determined by PMA-qPCR and flow cytometry. Due to the TIM-1 dynamism, the results obtained were cross-compared to that of a theoretical non-absorbable transit marker provided by the computer. The concentrations of the transit marker fluctuate throughout the TIM-1 depending on the volume of each compartment, the rate of dilution by digestive secretions and the chyme flow between two

successive compartments. Normality of the data was assessed with Shapiro-Wilk test, revealing a normal distribution ($p > 0.05$). Significant differences between methods and time-points were measured using a parametric test with a two-way repeated measure ANOVA in SPSS Statistics®. In case of significant differences on dependent variable for one group compared to another, post hoc test with pairwise comparisons was performed, using Bonferonni adjustment. A probability level of $p < 0.05$ was considered to be statistically different.

3. Results

3.1 Validation of the PMA-qPCR method for ETEC quantification

Assays with heat-killed ETEC were performed in order to verify that DNA from dead cells was not amplified during the PMA-qPCR reaction (data not shown). A wide range of PMA concentrations from 10 to 50 µM has been reported in the literature to stain *E. coli* DNA from different environmental samples (Gensberger, 2013; Reyneke et al. 2017). In the present study, the final concentration of 50 µM of PMA was chosen among the range of concentrations tested (data not shown). Amplified standard curves were plotted when 10-fold dilutions of ETEC pure cultures were stained or not with 50 µM PMA before q-PCR amplification. As expected, Ct (cycle threshold) values were lower with total amplified DNA compared to DNA stained with PMA (Fig. 1.1).

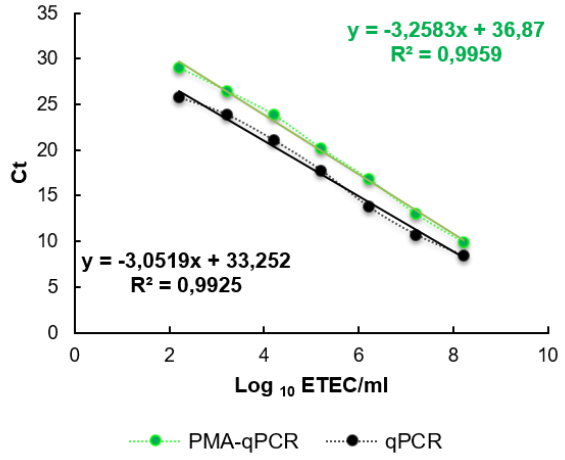

Figure 1.1. Amplification of total DNA and DNA from the PMA-treated ETEC cells by real-time PCR assay. Standard curve plot of real-time PCR generated using 10-fold serial dilutions of PMA-treated (green) and non-treated (black) ETEC H10407 culture from 10^2 to 10^8 CFU mL^{-1} . The standard curve plot, slope, Y-intercept and R^2 are shown. The detection limit was determined based on Ct of the last detectable standard, around 100 CFU mL^{-1}.

3.2 Comparison of PMA-qPCR and flow cytometry with classical plating for a quantitative detection of viable ETEC all along the *in vitro* GI tract

ETEC concentrations were determined at different time-points in the bio-regionalized TIM-1 system: (i) from the stomach to ileum to determine kinetics of bacterial survival all along the GI tract (Fig. 1.2), and (ii) in the cumulative gastric and ileal effluents, which is the resultant of what happens during gastric and gastrointestinal digestion, respectively (Fig. 1.3). In a first step, the results obtained by classical plate counts were compared to those obtained with qPCR targeting *16S* gene of *Enterobacteriaceae,* in the stomach (Fig. 1.2A), duodenum (Fig. 1.2B), jejunum (Fig. 1.2C) and ileum of the TIM (Fig. 1.2D). Not surprisingly, whatever the compartment, significantly higher bacterial concentrations (approx. 1 $\log_{10}$) were found with the molecular method compared to plating. For example, in the duodenum at T180 (Fig. 1.2B), ETEC reached 8.0 $\log_{10}$ by qPCR *vs* 6.7 $\log_{10}$ by plate counts ($p < 0.05$), and in the jejunum at 240 min (Fig. 1.2C) 9.7 $\log_{10}$ by qPCR *vs* 8.7 $\log_{10}$ by plate counts ($p < 0.05$). The differences were substantially higher in the ileum, especially at T180 where 10.3 $\log_{10}$ ETEC were found by qPCR compared to 9.2 $\log_{10}$ by plate counts ($p < 0.001$) (Fig. 1.2D). Similar tendencies were found in the gastric and ileal effluents (Fig. 1.3A and Fig. 1.3B), even if the differences (up to 1 $\log_{10}$) were not significant. On the whole, the overestimation of ETEC concentrations found by qPCR compared to plate counts might be related to DNA amplification from dead cells and/or from ETEC populations with irreversible damage to cell membranes, undetectable by classical plating technique.

In a second step, plate counts method was compared with PMA-qPCR, where DNA samples freshly collected were stained with PMA to amplify DNA from viable cells. Results have shown that whatever the small intestinal compartment (e.g. duodenum, jejunum, ileum), no statistical difference was seen between the results obtained with both methods (Fig. 1.2F, G, H). This indicates that plate counts and PMA-qPCR have the same level of sensitivity to detect viable ETEC cells. However, significant differences were found between the amounts of viable cells measured by the two methods in the stomach ($p < 0.05$), with lower levels detected with the PMA-qPCR method (Fig. 1.2E). This last method might fail to discriminate viable cells with reversible damage to the cell membrane from acidity-killed ETEC population with irreversible damage. Again, the same trends were obtained with lower levels with PMA-qPCR compared to plate counts in the gastric effluents (Fig. 1.3C), but similar ETEC populations with both methods in the ileal effluents (Fig. 1.3D).

Lastly, a third strategy using the kit Live/Dead BacLight® by flow cytometry was compared to the plating and molecular methods to analyze ETEC concentrations in the gastric and ileal effluents (Fig. 1.3). The number of total cells (as determined by qPCR and flow cytometry) or the number of viable cells (as determined by PMA-qPCR or flow cytometry) were compared to plate counts results in Fig. 1.3AB and Fig. 1.3CD, respectively. No significant difference between the three methods was observed for total cells, except a higher concentration ($p < 0.05$) of ETEC at T0-60 in the ileal effluents with qPCR (9 $\log_{10}$) and flow cytometry (9.1 $\log_{10}$) compared to plate counts (7.8 $\log_{10}$) (Fig. 1.3B). Even if the differences were not significant, similar trends were obtained for the time-points T120-300 with close levels for qPCR and flow cytometry and approx. 1 $\log_{10}$ lower for plate counts. For instance, at T240-300, 10.9 ($p = 0.054$) and 10.7 $\log_{10}$ ETEC ($p = 0.057$) were found by qPCR and flow cytometry, respectively, compared to 9.8 $\log_{10}$ by plate counts.

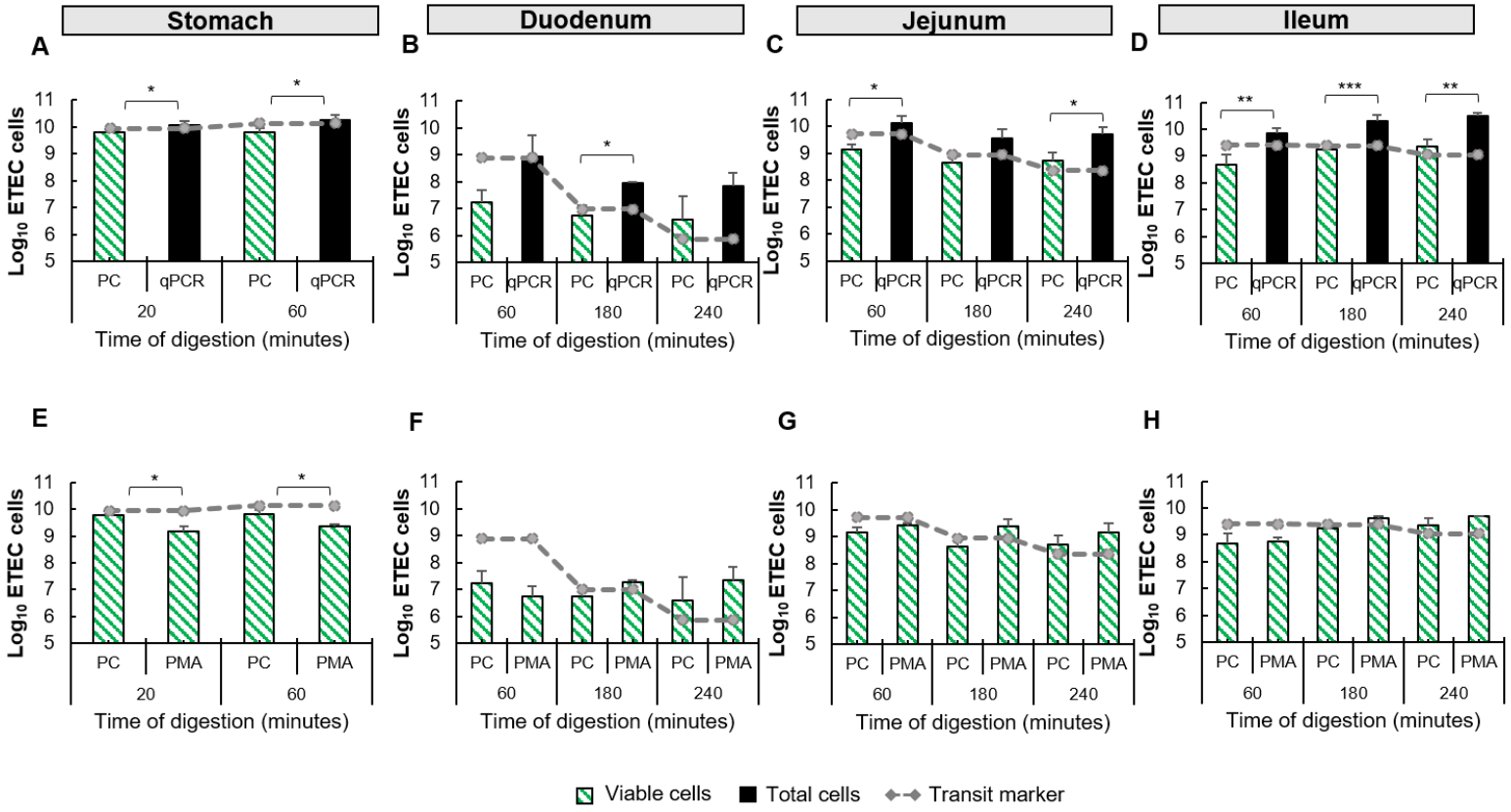

Figure 1.2. Comparison between q-PCR and classical plating to determine ETEC concentrations along the GI tract during *in vitro* digestions. Bar charts represent the mean number of log_{10} ETEC cells ± SD of four biological replicates in each compartment of the TIM-1 system. In green, viable culturable cells were measured by plate counts (PC), and cross-compared at each time-point to the number of total cells in black, measured by qPCR (**A, B, C, D**), or to viable cells in green, measured by PMA-qPCR (**E, F, G, H**). Grey line represents a theoretical non-absorbable transit marker provided by the TIM-1 system and indicating a 100% survival rate for bacteria. Bacterial curves below that of the transit marker reflect cell mortality, while curves above the transit marker are indicative of bacterial growth. Statistical differences between cross-compared methods and time points are given at $p<0.05$ (*), $p<0.01$ (**) or $p<0.001$ (***).

As expected, this higher concentration of total cells found by qPCR and flow cytometry compared to plate counts is related to damaged/dead cell quantification. With regards to viable cells (Fig. 1.3C and Fig. 1.3D), no statistical difference was found between the three methods whatever the compartment and the time-points. These results suggest that the number of viable cells, as determined by PMA-qPCR and flow cytometry, corroborates with the number of viable and culturable bacteria found by plate counts. However, in the gastric effluents, concentrations of viable ETEC remained still underestimated by flow cytometry and PMA-qPCR compared to plating (Fig. 1.3C), which calls into question if low pH might create any interferences in the proper staining.

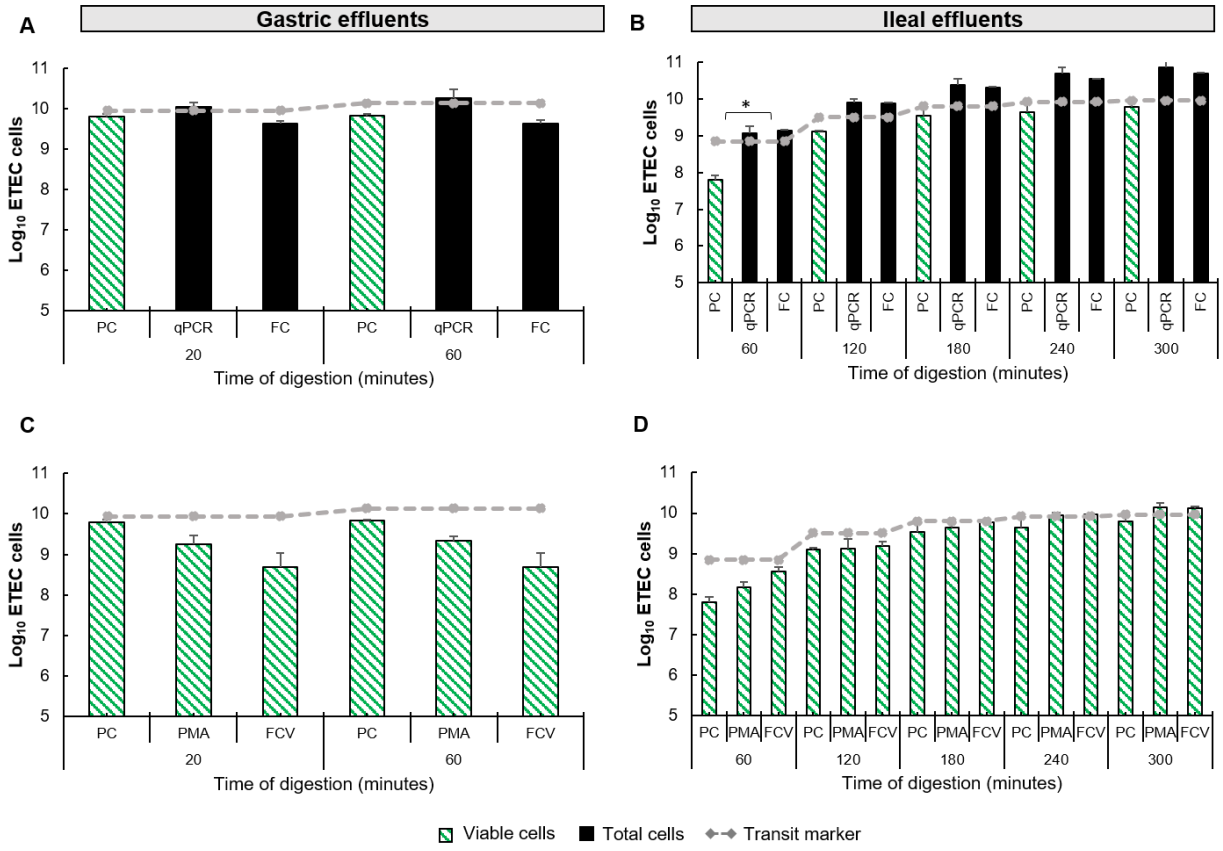

Figure 1.3. **Comparison between q-PCR, flow cytometry and classical plating to determine ETEC concentrations in the gastric and ileal effluents from the TIM-1 system.** Bar charts represent the mean number of log_{10} ETEC cells ± SD of two (FC) to four (PC and PCR) biological replicates in the digestive effluents from the TIM-1 system. In green, viable culturable cells were measured by plate counts (PC), and cross-compared at each time-point to the number of total cells in black, measured by qPCR or flow cytometry (FC) (**A, B**), or cross-compared to the number of viable cells in green, measured by PMA-qPCR or flow cytometry (FCV) (**C, D**). Grey line represents a theoretical non-absorbable transit marker provided by the TIM system and indicating a 100% survival rate for bacteria. Bacterial curves below that of the transit marker reflect cell mortality, while curves above the transit marker are indicative of bacterial growth. Statistical differences between cross-compared methods and time points are given at $p<0.05$ (*).

3.3 Flow cytometry combined with TIM-1 to cast ETEC physiological states in the digestive environment

To take the analysis one step further, the number of viable and altered/dead cells, as determined by PMA-qPCR and flow cytometry, was expressed as a percentage of total cells in the gastric (Fig. 1.4A) and ileal effluents (Fig. 1.4B). In both effluents, the percentage of viable cells represents a minority fraction, from 1.6 to 17.8% of total cells in the gastric effluents, and from 12.3 to 27.4% in the ileal effluents. No statistical difference was seen between the results obtained with PMA-qPCR and flow cytometry in both effluents. Nevertheless, the percentages of viable cells tended to be higher with flow cytometry in the ileal effluents, whatever the time-points. In addition, in the stomach at T20-60, only 1.6% of cells were detected as viable by flow cytometry compared to 13.7% by PMA-qPCR (Fig. 1.4A). Such differences were not observed at T0-20 when the pH of the stomach is higher. This result questions again the effectiveness of PMA or SYTO9/PI dyes under low pH. Another remaining question is how do we have to consider the largest fraction of ETEC cells? Is it only dead cells or a combination of dead and damaged cells such as membrane-altered bacteria?

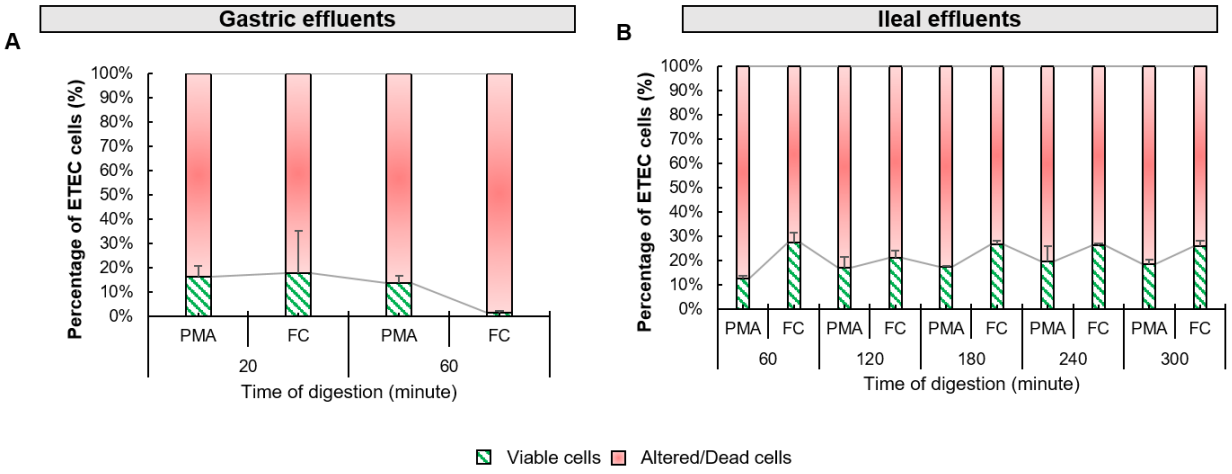

Figure 1.4. **Compared-methods to determine ETEC physiological states in the gastric and ileal effluents from the TIM-1 system.** Stacked bar charts represent the percentages of ETEC populations ± SD of two (FC) to four (PCR) biological replicates in the digestive effluents from the TIM-1. Viable cells (green) and altered/dead cells (pink) were measured by PMA-qPCR and flow cytometry (FC). Methods were cross-compared at each time point of sample collection in the gastric (**A**) and ileal (**B**) effluents.

To try to answer this question, deeper flow cytometry analysis were performed from the gastric and ileal effluents of the TIM-1 model (Fig. 1.5). As usually described and given by its name, the Live & Dead kit allows the differentiation of live and dead bacterial populations. Remarkably, by subtly gating on the cytogram according to the green (SYTO 9) and red (PI) fluorescence intensity, four populations can be discriminated, as described in our previous study (Roussel et al., 2016). Each gate was determined

based on results obtained with negative (ethanol treated and heated pure ETEC culture) and positive (pure culture in logarithmic phase) controls. Results obtained by flow cytometry were cross-compared with plate counts (e.g. killed populations were not found on agar plates and appeared in Q1 and R4). Thus, we attributed the four gates to intact membranes (viable cells, Q4), partially-altered membranes (viable/altered cells, R3 close to Q4), altered membranes (altered/dead cells, R4 close to Q1) and fully altered membranes (dead cells, Q1) (Fig. 5A). Viable/altered cells are supposed to be able to recover a viable stage compared to the altered/dead population, considered as an irreversible one.

With respect to ETEC, flow cytometry measurements revealed heterogeneity levels of ETEC subpopulations within the simulated digestive environment, probably as a result of various degrees of cell injury and differing physiological states when compared to the initial time (T0) (Fig. 1.5B). The results showed that the percentages of viable cells decreased in the gastric effluents from 0-20 to 20-60 min for the benefit of viable/altered cells (from 17.8 to 1.6% of viable cells and from 71.3 to 88.2% of viable/altered cells) (Fig. 1.5C). In the gastric effluents, the dead and altered/dead populations represented minor fractions (both less than 7%). In the ileal effluents at T0-60 (Fig. 1.4D), the distribution of the four sub-populations was the following: 27.4% of viable, 50.3% of viable/altered, 3.1% of altered/dead and 19.0% of dead cells. During the rest of *in vitro* digestions, the percentages of viable and viable/altered cells remain quite stable in the ileal effluents, while the percentages of dead cells tend to decrease toward altered/dead cells, as illustrated at T240-300, with 25.3% of viable, 60.9% of viable/altered, 7.6% of altered/dead and 6.1% of dead cells (Fig. 1.5D).

Taken together, these results indicate that in the simulated digestive environment, most of the cells are in an intermediate viability state (especially in the stomach at the end of gastric digestion), which cannot be distinguished in the analysis using plate counts, qPCR and PMA-qPCR. The defined viable/altered population seems to be in link with a VBNC state, where membrane differs morphologically from normal cells which cannot be cultured by plate counts method and might probably be challenging to identify by PMA-qPCR.

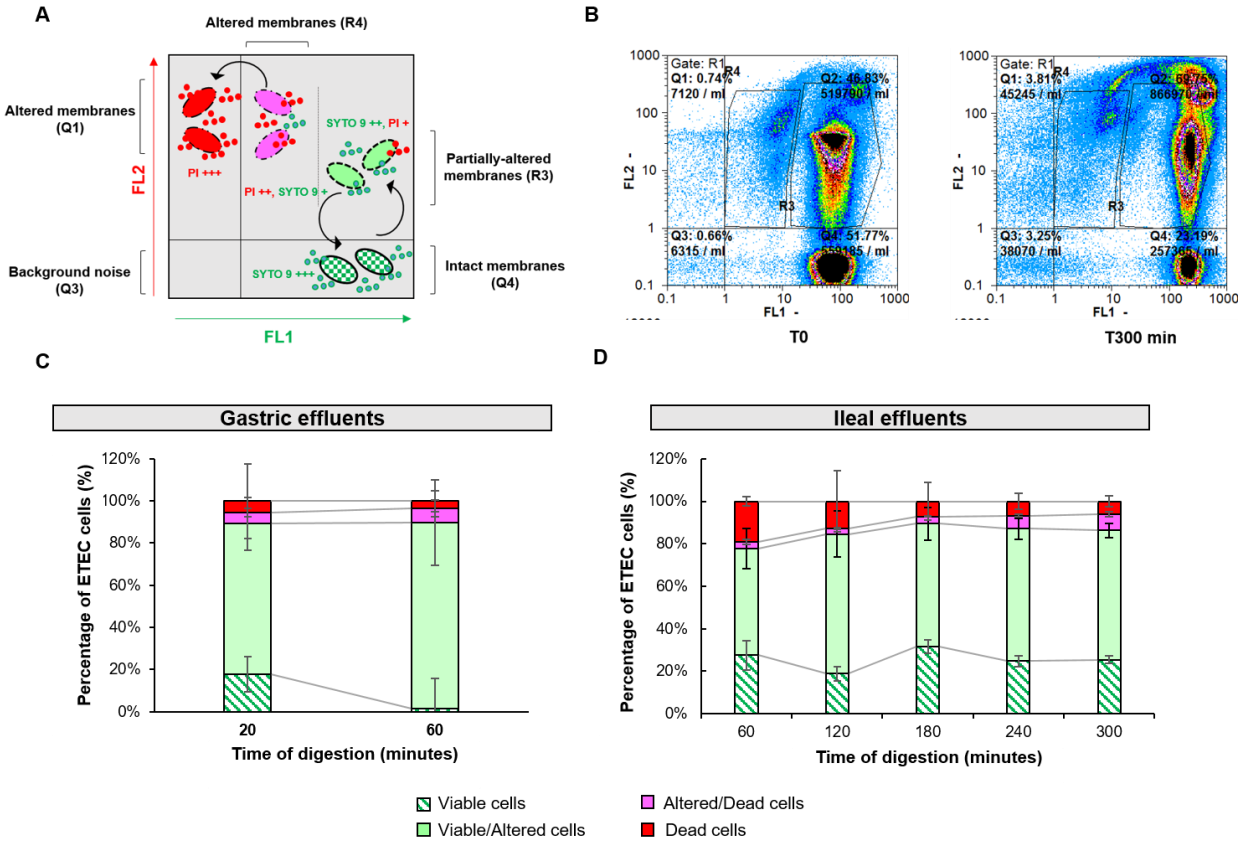

Figure 1.5. **Flow cytometry profiling of ETEC physiological states in the TIM-1 system after SYTO 9 and PI staining.** Cytogram schematic representation of the green (FL1) and red (FL2) fluorescence signals to discriminate four sub-populations (gates), assigned with different physiological properties: intact membranes (viable cells, Q4), partially-altered membranes (viable/altered cells, R3), altered membranes (altered/dead cells, R4) and fully altered membranes (dead cells, Q1) (**A**). Examples of cytograms obtained at the initial time (T0) and final time of digestion in the ileal effluents (T300 min) are shown. The cross-comparison of these two cytograms highlights the increasing amount of ETEC with partially-altered membranes (**B**). The stacked bar charts represent the percentages of each ETEC sub-populations ± SD of two biological replicates in the gastric (**C**) and ileal (**D**) effluents: viable (green), altered state able to recover viability (pale green), altered state not able to recover viability (pink) and dead state (red).

4. Discussion

Tracking viable stages of enteric pathogens in a complex niche as the human gastrointestinal tract is challenging. The key objective of the present study was to compare molecular (PMA-qPCR) and flow cytometry methods based on membrane integrity (Live/Dead) with classical culture-based method to monitor ETEC H10407 cells in the human gastrointestinal environment simulated by the TIM-1 model. PMA allows the amplification of only DNA from live cells: the dye penetrates into bacteria with compromised membranes and upon exposure to bright light, forms covalent bonds, resulting in irreversible damage to the nucleic acids after photo activation (Cangelosi and Meschke, 2014). For flow cytometry analysis, two combined fluorophores were used: Propidium Iodide (PI), a red fluorescent dye that usually does not permeate cells with intact membranes and only crosses the membrane-compromised, and SYTO 9, a green fluorescent dye, that stains both damaged and intact membranes (Berney et al., 2007).

As a first step, our results indicated a consensus between the three methods tested (PMA-qPCR, flow cytometry and plate counts) to estimate viable ETEC cells along the *in vitro* GI tract. Then, to provide deeper insight into the live and dead concept, flow cytometry analysis definitely appeared as the most accurate method to monitor ETEC subpopulations, as four physiological states were discriminated (e.g. viable, viable/altered, altered/dead, and dead). Remarkably, these results have shown that during gastrointestinal digestion (and mostly in the gastric compartment), most of the cells are in an intermediate viability state, which was not distinguished by using plate counts, qPCR or PMA-qPCR, bringing the VBNC concept up to date.

So far, this is the first time that comparative viability methods were applied to pathogenic microorganisms under simulated human digestive environment. Only one study was previously conducted under *in vitro* gastrointestinal conditions by using PMA-qPCR to evaluate viability of probiotics provided with Petit-Suisse cheeses (Villarreal et al., 2013). Other studies applied similar method comparison (PMA-qPCR, flow cytometry and plate counts) to pathogens, but not in relation with the human gastro-intestinal environment. For instance, Bankier et al. (2018) used these methods to evaluate the antimicrobial activity of engineered metallic nanoparticles combinations on *Staphylococcus aureus* and *Pseudomonas aeruginosa*, and Tamburini et al. (2013) monitored the membrane permeabilization of *E. coli*, *Listeria monocytogenes* and *Salmonella enterica* following a supercritical CO_2 treatment. In line with our conclusions, these authors showed that flow cytometry was the best method due to high-throughput, rapid and quantifiable results compared to PMA-qPCR where amplification interferences can occur. Here, we hypothesized that low pH in the stomach (< 5) might affect the proper staining by PMA or subsequent DNA amplification, as previously shown by Shi et al. (2011) for ethidium monoazide (EMA) staining. Prior to stain samples with EMA or PMA, authors recommended to thoroughly wash the cells to remove the remaining acid. However, in our experimental set-up, the washing step might be not appropriated due to the limited number of cells remaining in the stomach when the pH becomes low (the gastric compartment is almost empty).

Even if flow cytometry appeared as a method of choice in the present study, it is important to underline that the TIM model, which is particularly relevant to reproduce the physicochemical parameters of the human gut, is devoid of intestinal microbiota. With flow cytometry analysis, it should

be challenging to monitor a specific pathogen, especially at low concentration, in a complex microbial digestive environment, as the fluorescent dyes cannot be used to determine species of bacteria. Therefore, in this particular case, the use of viability PCR should be favored after designing strain-specific primers.

A unique approach in the present study was the use of flow cytometry to dynamically monitor the changing ETEC physiological states throughout its transit in the simulated digestive environment. We followed the alterations of cell membrane integrity occurring in response to abiotic stresses encountered in the *in vitro* gut (e.g. low pH, digestive enzymes or bile salts). When subjected to gastrointestinal stresses and especially under low pH, ETEC cells were found in an intermediate viability state probably associated with partially altered-membranes. This state might be related to the VBNC phenotype, even if there is yet no consensus on the relation between VBNC and cell membrane morphology (Zeng et al., 2012; Trudeau et al., 2012; Su et al., 2013). This survival state may allow the pathogen to persist and endure the digestion process, but it can no longer grow on standard culture media, reinforcing then the interest in using flow cytometry analysis. Importantly, VBNC pathogens might be able to keep their infective potential by successfully maintaining their virulence function (e.g. gene expression, enterotoxin production), but there is still conflicting data on the pathogenicity of VBNC cells (Zhao et al., 2017). In contrast with other *E. coli* pathotypes such as EHEC (Ding et al., 2017), this particular VBNC stage has not yet been extensively explored in the case of ETEC pathogen, and never under digestive conditions. Only one study has investigated the infectious potential of 6 clinical ETEC VBNC strains after a long-term incubation in sea water and freshwater (Lothigius et al., 2010). After 3 months incubation, the authors reported an expression of virulence genes encoding for toxins and colonization factors, as well as genes involved in metabolic pathways, while no enterotoxin production or secretion was observed.

To conclude, this work provides a comparison of three methods (PMA-qPCR, flow cytometry and plate counts) to determine ETEC viability under human simulated digestive conditions. Table 1.2 summarizes the main strengths and weaknesses of each method, in terms of technical requirements (e.g. sample step preparation, duration, cost and number of samples than can be analyzed simultaneously) and scientific outputs. Flow cytometry was the only real-time method that allowed accurate distinction of different physiological states of ETEC in the *in vitro* gut. In any case, there is no “gold standard” method to consider and the application should be consistent with the research question.

Table 1.2. Comparison of plating, PMA-qPCR and Live/Dead BacLight® methods. [α] Costs do not include the use of consumables or apparatus (e.g. incubator, blue light for efficient PMA dye, thermocycler, flow cytometer, etc.), [β] Time might vary according to the DNA extraction protocol used.

	Samples	Plating	PMA-qPCR	Live/Dead
Technical requirements	*Preparation steps*	2 steps (i) serial dilutions (direct) (ii) plating (direct)	3 steps (i) staining (direct) (ii) DNA extraction (indirect) (iii) qPCR (indirect)	1 step (i) staining & cytogram acquisition (direct)
	Duration of the experiment	5 min / sample	(i) 20 min (ii) 80 min [β] (iii) 180 min	45 min / sample
	Time to get final results	24h	2h	Direct
	Reagent cost[α]	25 $ / 100 agar plates (agar medium + plates)	325 $ / 100 reactions (PMA dye + kit for DNA extraction + SYBR green master mix)	755 $ / 100 reactions (BacLight® kit)
	Number of samples at the same time	Until 4 samples (excluding dilution)	Until 18 at the same time	1 by 1
	Advantages	**-** Low cost & easy to do **-** Large sampling time-points	**-** Low cost **-** Large sampling time-points	**-** Direct **-** Reduced errors / biases due to pipetting
	Limits	**-** Manipulator dependent visual interpretations / counts **-** Increased errors / biases due to serial dilutions / pipetting	**-** Indirect, get the result after 3 manipulations **-** Increased errors / biases due to pipetting / extraction / successive storages	**-** Expensive **-** Limited sampling time-points **-** Extensive training for calibration and analysis
Scientific aspects	*Expected outcomes*	- Viable-culturable bacteria only	- Specific strain(s) tracked in a complex microbial sample - Viable & Dead bacteria	**-** Specific strain tracked in a sample devoid of other microbes **-** Bacterial physiological state, including membrane altered or other intermediate states
	Interpretation limits	**-** Colony aggregation - Lack of media specificity in a complex microbial sample	**-** Proper staining according to sample type (pH/composition) - Amplification interferences	**-** Proper staining according to sample type (pH/composition) - Further phenotypic characterization of the subpopulations required

5. Conclusion

- The present study validates the use of PMA-qPCR and flow cytometry as two relevant methods to assess ETEC viability in digestive samples, though some interferences with PMA have been noticed upon gastric environment,
- Flow cytometry is a choice method to accurately distinguish ETEC subpopulations according to the membrane integrity,

The use of PMA-qPCR and flow cytometry has been pursued in the course of additional TIM-1 experiments, while only PMA-qPCR was used in the M-SHIME due to the high microbial background. The results are presented on the following chapter 2 and chapter 5.

6. Compliance with ethical standards

Conflict of Interest The authors declare that they have no conflict of interest.

Ethical approval This article does not contain any studies with human participants or animals performed by any of the authors.

7. Candidate contribution and acknowledgements

Under supervision of Stéphanie Blanquet-Diot and Tom Van de Wiele, I designed the experimental work. I carried out the *in vitro* digestions and plate counts (with technical support from Sandrine Chalancon and Sylvain Denis). I developed the new protocols for ETEC quantification by q-PCR and PMA-qPCR and carried out all the molecular-based experiments. Wessam Galia designed and carried out the flow cytometry experiments. I processed the experimental data, performed the analysis, drafted the manuscript and designed the figures. I wrote the manuscript with input from all authors. Wessam Galia and I are co-first authors of the publication.

I would like to acknowledge Sylvie Alvarez and Karine Fayolle (VetagroSup, Clermont-Ferrand, France) for welcoming us in the L3 laboratory during the TIM-1 experiments. This research was funded by Lesaffre company (Marcq-en-Baroeul, France).

CHAPTER 2 : DYNAMIC HUMAN GUT *IN VITRO* MODELS UNRAVEL THE MODULATION OF ETEC PATHOGENESIS

ROUSSEL C., De PAEPE K., GALIA W., DE BODT J., CHALANCON S., DEBOUDARD F., BALLET N., LERICHE F., DENIS S., ALRIC M., VAN DE WIELE T., BLANQUET-DIOT S.

BLANQUET-DIOT S. and VAN DE WIELE T. are co- last authors.

***

For clarity, the manuscript under preparation for submission in PLoS Pathogen journal has been redrafted and redistributed in two chapters (chapter 2 and 3), presented here after.

The chapter 2 is dedicated to the purpose of unravelling ETEC pathogenesis in the entire human GI tract, through the use of *in vitro* models of the human digestion. This chapter is therefore the reflect of 3-years close collaboration between MEDIS laboratory (France) and CMET (Belgium), where the outcomes of the two most complete *in vitro* models of the human digestion, TIM-1 (MEDIS) and M-SHIME (CMET) have been combined together. The operation of these two *in vitro* systems was also combined with a large set of techniques including plate counts, viability PCR-based methods and flow cytometry analysis (initiated in chapter 1 and pursued here), transcriptional analysis (presented in this chapter), and microbial community analysis (presented in chapter 3).

2 Dynamic human gut *in vitro* models unravel the modulation of ETEC pathogenesis

Abstract ETEC pathogen contributes substantially to the burden of diarrheal illnesses in developing countries. The hallmark of ETEC pathogenicity is the intestinal colonization (CFA/I, tia, fimH) and the production of LT and/or ST enterotoxins. During GI passage, ETEC is exposed to multiple, successive and complex GI ecosystems that have an impact on the key features of ETEC survivability and virulence. Nonetheless, the mechanisms behind such processes remain scarcely understood, owing to a lack of adequate model. With the use of complementary *in vitro* models of the human digestive environment, TIM-1 and M-SHIME, we provided the first detailed report on the spatial-temporal modulation of ETEC H10407 survival and virulence throughout the entire simulated GI tract. These systems integrate the main physicochemical parameters of the human upper digestion (TIM-1), and simulate the ileal and ascending colon microbial communities captured from six distinct fecal donors (M-SHIME). In the TIM-1, this study revealed the flexibility of ETEC to adapt its membrane physiology according to the GI environment crossed, with a die-off of the pathogen during gastric digestion, while a growth renewal at the end of the jejunal and ileal digestion was noticed and confirmed by a restoration of ETEC membrane integrity. In the M-SHIME, the remarkable capacity of ETEC to colonize the mucosal microenvironments of the ileum and ascending colon constantly seeded the gut lumen, helping to maintain high ETEC concentrations in a late post-infection stage, up till 5 days. Virulence gene expression profiles differed greatly between both systems, due to different digestive, physiological or microbial parameters that are integrated in the respective models, besides to the profound inter-individual variability. Most of the virulence genes followed were switched on in the stomach, except for *eltB* gene encoding for the enterotoxin LT, and switched off in the TIM-1 ileal effluents and in a late post-infectious stage in the SHIME ascending colon. At protein level, no LT enterotoxin production was measured in the stomach and a higher concentration was found in the ascending colon compared to the ileum of both TIM-1 and M-SHIME. A better understanding of the interplay between ETEC and the GI cues may serve to complete the scheme of the bacterial infection and may inspire novel prophylactic or therapeutic strategies for diarrheal diseases.

1. Introduction

Food and waterborne ETEC is one of the major etiological agents of traveler's diarrhea and infant diarrhea in the world (Roussel et al., 2017). Strongly associated with poor hygiene facilities, ETEC has chiefly affected low-income civilizations in south Asia, Africa and Latin America. An estimated 44 million of ETEC-related diarrheal diseases occur annually, resulting in 113,000 deaths in 2015 (Lamberti et al., 2014; Walker et al., 2017). Despite the clear preponderance of ETEC infection in developing regions, the pathogen has become sporadically epidemic in industrialized nations, mainly due to fresh products imported from endemic countries (MacDonald et al., 2015). Such diarrheal pandemic has a substantial economic impact worldwide.

In adults, once ingested at a dose of 8 to 10 $\log_{10}$ cells (Levine et al., 1979), ETEC pursues a sophisticated strategy to successfully withstand the stringent factors encountered in consecutive GI niches (e.g. acidic pH, bile acids, antimicrobial peptides and gut microbes). In the distal part of the small intestine, ETEC switches on a set of virulence factors to colonize and cause infection (Allen et al., 2006). To do so, it will effectively penetrate the mucus layer through two mucin-degrading proteins including the metalloprotease YghJ, and the serine protease EatA (Luo et al., 2014; Kumar et al., 2014). These mucinases allow temporary access to cell membranes, promoting attachment of the pathogen to the intestinal epithelial cells. Such adhesion is orchestrated by (i) fimbrial adhesins including up to 25 colonization factors such as CFA/I and FimH; and/or (ii) outer membrane proteins such as Tia, TibA and EtpA (Madhavan and Sakellaris, 2015).

ETEC adhesion in the host will facilitate the production and delivery of enterotoxins, the hallmark of ETEC pathogenesis. ETEC produces at least one of the two plasmid-encoded enterotoxins: LT and ST enterotoxins. LT enters into the ETEC periplasm by means of the Sec machinery, then is transported to the outer membrane by the protein labile enterotoxin output (LeoA) and is finally translocated into the intestinal lumen by the T2SS involving the pore-forming GspD secretin (Fleckenstein et al., 2000; Brown and Hardwige, 2007). So far, it remains unclear how ST is released into the ETEC periplasm but excretion is mediated through the TolC channel (Yamanaka et al., 2008). Upon release and binding in the small intestine, the enzymatic activity of LT and/or ST results in the opening of cystic fibrosis transmembrane regulator which creates an osmotic movement of water into the intestinal lumen, leading to profuse watery diarrhea.

Unequivocally, 70 years of intensive research has contributed to the knowledge advancement of ETEC-associated illness. Particularly, with the recent advances in molecular techniques, many studies have furthered the understanding of genomic and transcriptional regulation of ETEC (Crofts et al., 2018). However, the related pathogenesis in the human gut through ETEC survival and its virulence networks remain scarcely understood. Admittedly, in humans, ethical objections are a main constraint, precluding studies involving non-attenuated pathogens. In scarce clinical trials, the use of live but genetically attenuated ETEC strains impedes the assessment of its virulence features (Bruggencate et al., 2016). As a means of recourse, ETEC findings predominantly originate from animal models, intestinal epithelial cell cultures and simple static *in vitro* models of the human GI tract. These approaches are respectively limited by clear differences between animal and human gut physiology, the ignorance of successive GI

niches encountered by the pathogen prior to host / cell interactions, and the simplicity of *in vitro* models simulating only one digestive parameter at a time. Hence, integration and sequential delivery of GI signals are needed to model the dynamics and complexity of the human gut more closely. In particular, simulation of the gastric pH drop, representative GI transit time, and reproduction of a highly complex gut microbiota from human origin, are some of the key parameters required to strengthen the conclusion of previous studies.

Bio-regionalized and dynamic *in vitro* models are valuable alternatives to fully assess pathogenic strains and more closely approximate the complexity of the human GI physiology. Among the available models, the multi-compartmental and computer controlled TIM-1 is currently considered as the most complete simulator of the upper GI tract by simulating the main physicochemical parameters of the human digestion (Guerra et al., 2012; Roussel et al., 2016). Similarly, the M-SHIME is the most complete multistage system of the lower GI tract by simulating the gut microbial communities and mimicking the main abiotic factors of the colonic fermentation process (Molly et al., 1994; Van de Wiele et al., 2015).

Thus, the objective of the present study was to unravel the mechanisms associated with ETEC H10407 pathogenesis in the human GI tract, through the use of the complementary *in vitro* digestion models TIM-1 and M-SHIME. Hence, this study greatly contributes to assess the dynamics of ETEC survival, physiological state and its virulence features, in the successive gut niches that the pathogen will encounter in the human gut.

2. Materials and methods

2.1 ETEC strain, media and growth conditions

The prototypical ETEC strain H10407 serotype O78:H11:K80 (LT^+, ST^+, CFA/I^+) isolated from a Bangladeshi patient with a cholera-like syndrome was used in this study (Evans et al. 1977). Prior to ETEC challenge in the digestive systems, bacteria were routinely grown under agitation (37°C, 125 rpm, overnight) in Luria Bertani (LB) broth (BD Difco, New Jersey, USA) until OD_{600nm} = 0.6 (stationary phase), to achieve a final amount of 10 $\log_{10}$ CFU in the inoculum.

For a good understanding: although the host cells are lacking in both systems TIM-1 and M-SHIME, we tried to simulate the start of an infection process, and for this purpose we named in the results section the day of ETEC inoculation as “infection”.

2.2 TIM-1 gastrointestinal model

Experimental set-up is described in chapter 1 section 2.2.

Inoculation and operation of the TIM-1. Based on *in vivo* data (Roussel et al. 2016), the TIM-1 system was programmed to simulate the physicochemical digestive conditions encountered in a healthy adult when a glass of water is ingested (Table 2.1). The bacterial suspension (200 mL) introduced into the

TIM-1 system consists of mineral water experimentally contaminated with ETEC at a final amount of 10 log_{10} CFU. Two types of experiments were performed: gastric digestions where only the gastric compartment was used (total duration of 60 min) and GI digestions using the entire TIM-1 model (total duration of 300 min). Digestions were run in quadruplicate (Fig. 2.1).

TIM-1 sampling. The initial bacterial suspension (T0) was collected and samples were regularly taken during *in vitro* digestions from each digestive compartment (stomach, duodenum, jejunum and ileum) (Fig. 2.1). Gastric and ileal effluents were also collected on ice and pooled on 0-10, 10-20, 20-40 and 40-60 min for gastric digestions and hour-by-hour during 5 hours for GI digestions. Time 75 represents the fraction remaining at the end of gastric digestions in the stomach and T 330 the gastric and small intestinal residues at the end of GI digestions. Samples collected for plating and flow cytometry analysis were immediately treated. Samples used for DNA or RNA extraction were centrifuged (6,339×*g*, 10 min, 4°C). DNAs were stored at -20°C while RNAs were resuspended in 500 µL RNA*later*® (Thermo Fisher Scientific, Waltham, USA) for preservation prior to storage at -80°C. The supernatant was stored at -20°C for a subsequent enterotoxin ELISA assay.

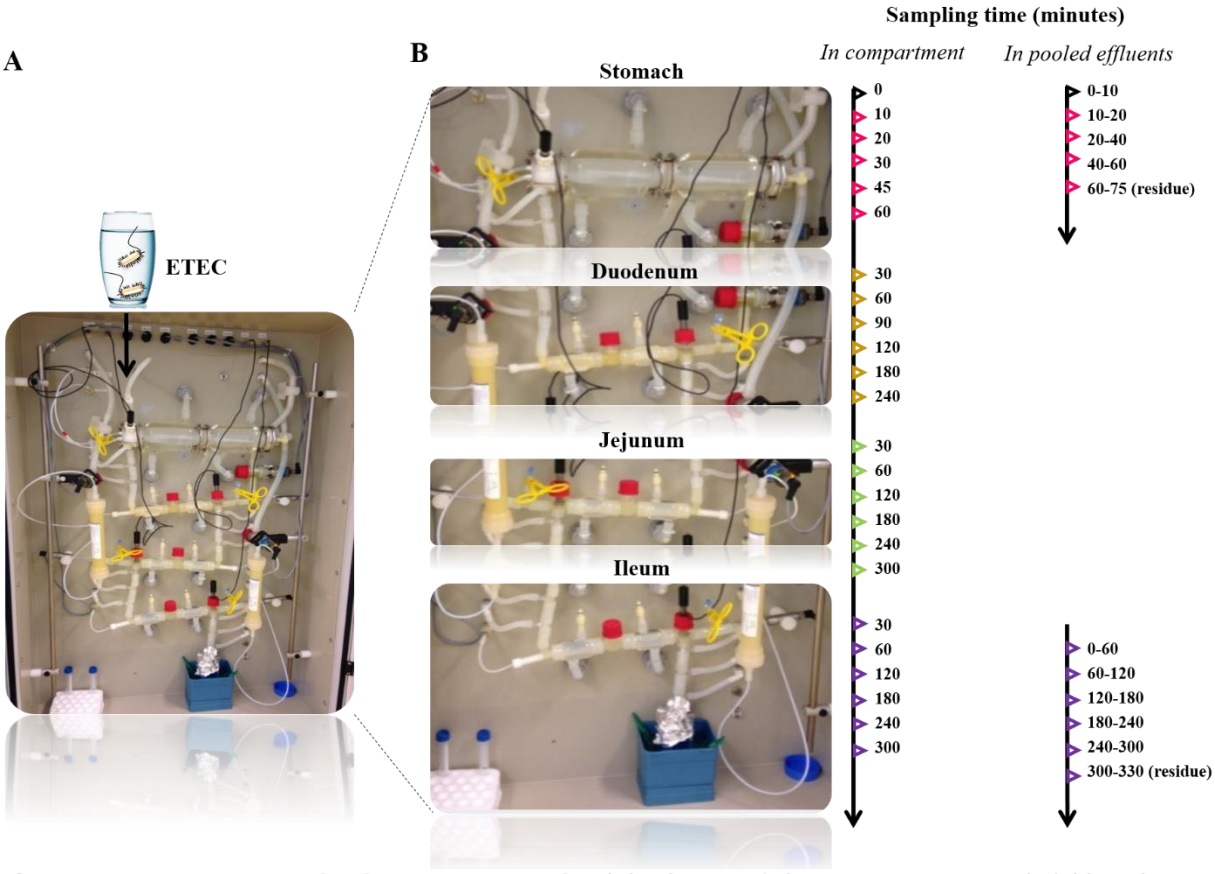

Figure 2.1. **TIM-1 set-up in the present study.** (**A**) Picture of the TIM-1 system mimicking the GI conditions of an adult ingesting a glass of mineral water contaminated with ETEC. The glass of water was introduced directly into the gastric compartment at T0; (**B**) Representation of the gut regions simulated by the TIM-1 and their associated sampling time. Two kinds of samples were taken: (i) directly in each compartment with a syringe; or (ii) indirectly by pooling the gastric effluents when the stomach compartment was solely used, or the ileal effluents when the entire system was used.

Table 2.1. Parameters of the TIM-1 system when simulating digestive conditions of a healthy adult after intake of a glass of water

A power exponential equation ($f= 1-2^{-(T/T_{1/2})^{\beta}}$ where f represents the fraction of meal delivered, $T_{1/2}$ represents the half-time of delivery and β a coefficient describing the shape of the curve) was used for the computer control of gastric and ileal deliveries in the TIM-1.

Parameters of *in vitro* digestion of a glass of water	**Gastric compartment**	**Duodenal compartment**	**Jejunal compartment**	**Ileal Compartment**
pH	from 6 (T0) to 1.5 (90 to 300 min)	maintained at 6.4	maintained at 6.9	maintained at 7.2
Volume (mL)	200 (initial)	30	115	115
Secretions	(**i**) 130 U min^{-1} of pepsin (**ii**) 5 U min^{-1} of lipase (**iii**) HCl 0.3 M	(**i**) 20 mg min^{-1} of bile salts 27.9 mM (first 30 min of digestion) then 10 mg min^{-1} of bile salts 9.3 mM (**ii**) 20 mg min^{-1} of pancreatic juice 4 USP (**iii**) Trypsin 2 mg min^{-1} (**iv**) $NaHCO_3$ 0.5 M if necessary	(**i**) $NaHCO_3$ 0.5 M if necessary	(**i**) $NaHCO_3$ 0.5 M if necessary
Half-emptying time (min)	$T_{1/2}$ = 15 min	-	-	$T_{1/2}$ = 150 min
β coefficient	β = 1	-	-	β = 2.4
Chyme mixing	water pressure	water pressure	water pressure	water pressure
Absorption	-	-	yes	Yes
[Total microbes]	sterile	sterile	sterile	Sterile
Oxygen level (%)	20	20	20	20
Temperature (°C)	37 (pumping water)	37 (pumping water)	37 (pumping water)	37 (pumping water)

2.3 M-SHIME fermentation system

Experimental set-up. The M-SHIME® consists of a series of connected double-jacketed reactors (Pierreglas, Vilvoorde, Belgium), reproducing the conditions of the upper and lower part of the human GI tract, operated in a semi-continuous mode to mimic GI transit (Molly et al., 1993; Venema and Van den Abbeele, 2013). Three successive compartments simulating the stomach / combined duodenum-jejunum, the ileum and the ascending colon were used in the set-up as shown in Fig. 2.2. The mucosal environment was reproduced in both the ileum and ascending colon compartments, incorporating 40, respectively, 80 microcosms (AnoxKaldnes K1 carrier, AnoxKaldnes AB, Lund, Sweden) coated with type III porcine mucin-agar (Sigma-aldrich, St. Louis, USA), as described by Van den Abbeele et al. (2012). All seven SHIME vessels were attached to a warm water bath (Julabo, Seelbach, Germany) at

37°C, mixed using magnetic stirrer at 300 rpm and connected with pumps (ProMinent, Heidelberg, Belgium). The ascending colon was pH controlled (Consort, Turnhout, Belgium) and connected with pumps regulating the dosage of 0.5 M NaOH or 0.5 M HCl. Next to the acid and base in- and outlets, all ileum and colon vessels have a feed inlet, gas in- and outlets and a sampling port.

Inoculation and operation of the M-SHIME. Fresh fecal samples were collected from three female and three male adults (25 to 36 years old, including Belgian, African, Turkish and French origins with two vegetarians) (Table 2.2) in sterile airtight containers comprising an Anaerocult® A strip (Merck, Darmstadt, Germany) to maintain anoxic conditions until processing. A 20% (w/v) fecal slurry was prepared as described by De Boever et al. (2000) and inoculated in the ascending colon vessels pre-filled with 500 mL nutritional medium (Prodigest, Zwijnaarde, Belgium) in order to obtain a final concentration of 1% (w/v) fecal material (De Boever et al., 2000; Van den Abbeele et al., 2012). All vessels were flushed with N_2 for 15 min immediately after inoculation to generate anaerobic conditions and subsequently the system was left to incubate overnight without flow-through. After the initial overnight incubation of the fecal sample in the ascending colon, a semi-continuous feeding pattern with nutritional SHIME medium, simulated gastric, biliary and pancreatic secretions was established (Tables 2.3 and S2.1) by pumping feed into the stomach/combined duodenum-jejunum vessel three times a day. Subsequently, this mixture was transferred to the ileum vessels, followed by the ascending colon vessels. After a residence time of 3 h in the ileum and 20 h in the ascending compartments, the entering volume was discharged. The ileum vessels were inoculated two times at day 3 and 8 by injection of 100 µL microbial suspensions from the ascending colon in order to maintain a low microbial biomass concentration. From day 3 onwards, the nutritional SHIME medium was supplemented with simple sugars to enhance the growth of bacteria usually found in the small intestine (Table S2.2). To mimic the lower turnover rate of the mucus environment and avoid wash-out of mucus adherent bacteria, half of the mucus beads were replaced every 2-3 days in each of the ileum and ascending colon vessels (Geirnaert et al., 2015).

The six fecal donors were evaluated in two M-SHIME runs, each involving three individuals over the course of 20 days. After a stabilization period (adaptation to the *in vitro* conditions) of 12 days, the system was challenged in the SHIME ileum vessels with ETEC by inoculation of 10 $\log_{10}$ CFU at day 13, followed by a post-infectious period from day 14 to 20. Prior to the challenge, ETEC was pre-digested 3 h under batch conditions, to reproduce the gastro-jejunal digestion of a glass of contaminated mineral water, where physicochemical conditions were closer to those found in TIM-1 (without nutritional medium, under aerobic conditions) (Table S2.3).

M-SHIME sampling. SHIME suspensions from ileum and ascending colon vessels were sampled daily for SCFA analysis. After each sampling, the vessels were flushed with N_2 for 8 min, to ensure anaerobic conditions. Samples were also regularly collected from fermentation medium for DNA and RNA extractions and ELISA measurement, and stored as previously explained for TIM-1 sampling. Mucus samples were obtained every 2-3 days, during mucus carrier replacement and were washed by rinsing

four times with 0.1M phosphate buffer at pH 6.8, as described by Geirnaert et al. (2015) to remove luminal bacteria. Then, 250 mg mucus were aliquoted and stored at -20°C before DNA extraction.

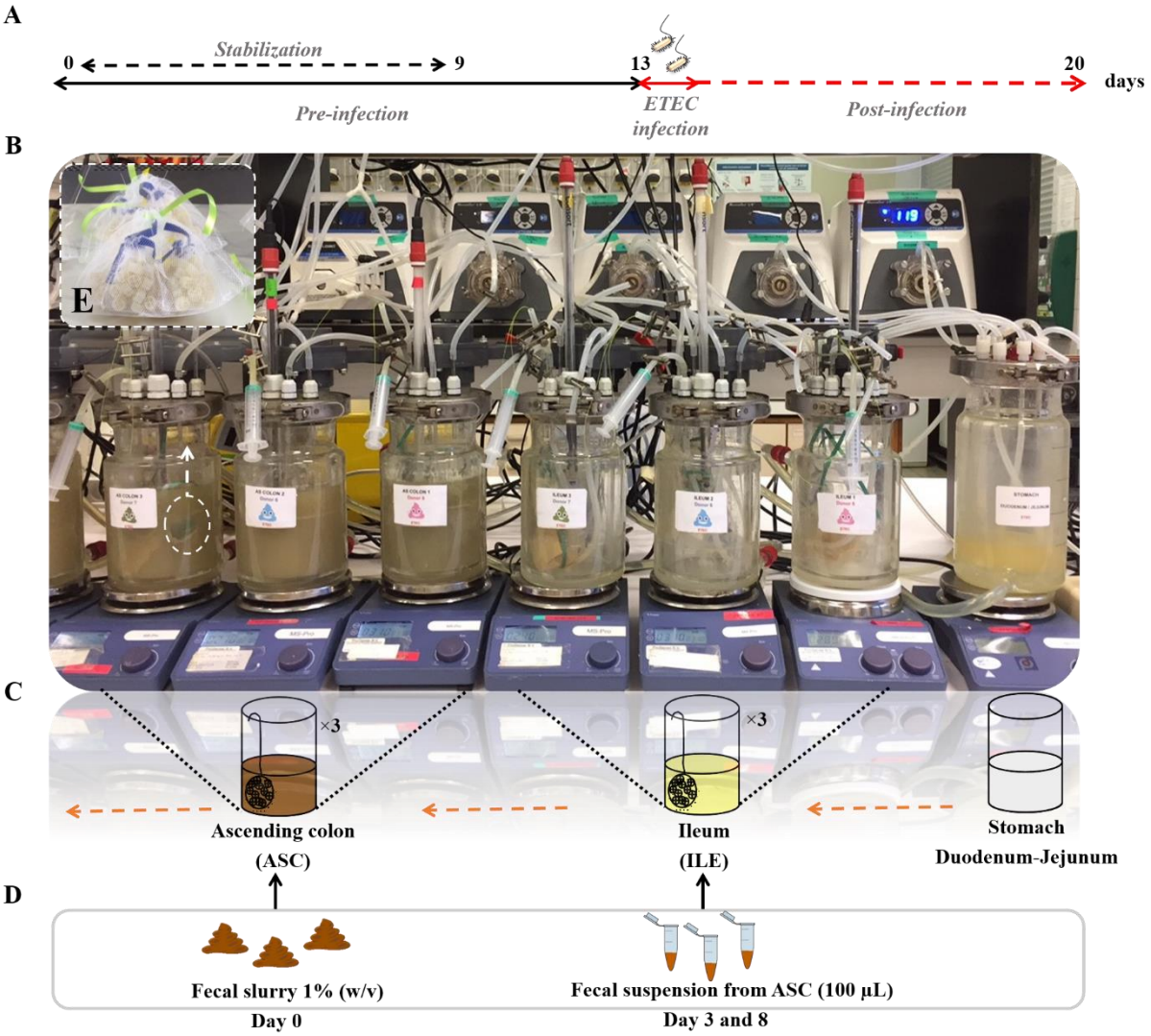

Figure 2.2. M-SHIME set-up in the present study. (**A**) Time course (days) of the M-SHIME run; (**B**) Picture of the M-SHIME system mimicking the digestive and fermentative conditions of three individuals. In total, the run has been performed twice to get a representative population of six distinct individuals; (**C**) The stomach/combined duodenum-jejunum vessel was connected with three ileum (ILE) bioreactors coupled to three ascending colon (ASC) vessels; (**D**) Upon start-up (day 0), the ASC were inoculated with the fecal samples obtained from three individuals. The fecal inoculation of the ILE started at day 3, by introducing a small amount of the fecal suspension collected in the ASC for each individual. To maintain such population levels, this inoculation was repeated at day 8; (**E**) Picture of the tulle bags stored in a sterile environment and containing the microcosms coated with type III mucin-agar. To reproduce the mucosal phase, the bags were introduced in each ILE and ASC vessel under N_2 flow to ensure anaerobic conditions.

Table 2.2. **General characteristics of the fecal donors for the M-SHIME experiments**

	Run 1			Run 2		
	Donor 1	**Donor 2**	**Donor 3**	**Donor 4**	**Donor 5**	**Donor 6**
Gender	female	female	male	male	female	Male
Age	27	28	32	36	25	29
Nationality	French	Turkish	Belgian	African	Belgian	Belgian

Table 2.3. **Parameters of the M-SHIME system when simulating a cycle of digestive and fermentative conditions of a healthy adult**

The cycle of entering and emptying secretions described below is repeated 3 times per day.

Parameters of *in vitro* digestion / fermentation	**Gastric compartment**	**Duodenal-jejunal compartment**	**Ileal compartment**	**Ascending colon Compartment**
pH	2	5	6	maintained at 6.2-6.4
Volume (mL)	140	200	200	500 to 700
Secretions	(**i**) 14 ml min^{-1} of nutritional medium (**ii**) HCl 0.5 M	(**i**) 12 ml min^{-1} of pancreatic juice and bile salts mixture (**ii**) $NaHCO_3$ 0.5 M	(**i**) NaOH 0.5 M if necessary	(**i**) NaOH 0.5 M if necessary
Residence time (hours)	1 h	2h30	3 h	20 h
Chyme mixing	magnetic stirrer	magnetic stirrer	magnetic stirrer	magnetic stirrer
Absorption	-	-	-	-
[Total microbes]	sterile	sterile	9-10 log_{10}	11-12 log_{10}
Oxygen level (%)	< 3	< 3	< 3	< 3
Mucosal phase	-	-	40 microcosms	80 microcosms
Temperature (°C)	37 (pumping water)	37 (pumping water)	37 (pumping water)	37 (pumping water)

2.4 DNA extraction

Total DNAs from the TIM-1 and M-SHIME experiments were extracted according to a protocol adopted from Geirnaert et al. (2015). Briefly, cells were lysed with 1 mL lysis buffer (100 mM Tris/HCl pH 8, 100 mM EDTA pH 8, 100 mM NaCl, 1% (m/v) polyvinylpirolidone and 2 % (m/v) sodium dodecyl sulphate) and 200 mg glass beads (0.11 mm, Sartorius, Göttingen, Germany) in a FastPrep 96 instrument (MP Biomedicals, Santa Ana, USA) for two times 40 s at 1600 rpm. Following removal of glass beads by centrifugation (5 min, 13,000×*g,* 4°C), DNA was extracted from the supernatant using a phenol-chloroform extraction. The DNA was precipitated at -20°C with 1 volume of ice-cold isopropyl alcohol and 0.1 volume of 3 M sodium acetate for at least 1 h. After removal of isopropyl alcohol by centrifugation (30 min, 13,000×*g,* 4°C), the DNA pellet was dried and resuspended in 100 µL 1x TE (10 mM Tris, 1 mM EDTA) buffer. The DNA samples were immediately stored at -20°C. The quality of DNA samples was analyzed by gel electrophoresis (1.2% (w/v) agarose) (Life technologies, Madrid, Spain). The DNA samples were diluted 1:10 in 1X TE for further ETEC quantification.

2.5 ETEC quantification

Enumeration by plating. The number of cultivable bacteria in each digestive compartment of the TIM-1 was determined by direct plating onto LB agar (overnight incubation at 37 °C), after appropriate serial dilutions in sterile saline water. Due to the TIM-1 dynamism, the results obtained for the pathogen were cross-compared to that of a theoretical non-absorbable transit marker provided by the computer representing a 100% survival rate. The concentration of the transit marker fluctuates throughout the TIM-1 model depending on the volume of each compartment, the rate of dilution by digestive secretions and the chyme flow between two successive compartments.

qPCR and PMA-qPCR-based quantification. Digestive samples from TIM-1 and M-SHIME were collected in duplicate and stained or not with 50 µM propidium monoazide (PMA, Interchim, Montluçon, France) according to the recommendations made by Roussel et al. (2018). Pellets were washed one time with filtered milli-Q water and stored at -20°C. After DNA extractions, the qPCR procedure was performed using the Mx Pro Real Time Mx 3000P system (Agilent, Les Ulis, France) for TIM-1 samples and StepOnePlus Real-Time PCR system (Applied Biosystems, Carlsbad, USA) for M-SHIME. The total reaction volume of 10 µL contained 5 µL of Takyon Low Rox Sybr Master Mix dTTP blue (Eurogentec, Seraing, Belgium), 0.45 µL (10 µM) of *gspD* primers (Table 2.4), 3.1 µL nuclease-free water (Sigma-aldrich, St. Louis, USA) and 1 µL of template DNAs. The non-template control consisted of 1 µL nuclease-free water. Each reaction was performed in triplicate in a sealed 96-well plate. The qPCR thermal cycling amplification procedure consisted of a pre-denaturation step (5 min, 95°C), followed by repeated denaturation (30 s, 95°C), annealing (30 s, 60°C) and extension (30 s, 72°C), during 45 cycles and a final stage to allow for the construction of step and hold melt curves, initiated by 15 s at 95°C, followed by 1 min at 60°C with a gradual temperature increment of 0.3°C. The melting curves of PCR amplicons were checked to ensure primer specificity and yielded a single melting peak.

Table 2.4. **Primers for ETEC reference and pathogenicity related genes**

CFA: Colonization factor antigen, F: forward, GAPDH: Glyceraldehyde 3-phosphate dehydrogenase, LT: Heat-labile enterotoxin, R: reverse, ST: Heat-stable enterotoxin.

Gene	Target	Primer sequence 5'-3'	Amplicon length (pb)	Reference
Gene to monitor ETEC by qPCR				
gspD	Type II secretion system for LT delivery	F- CGGATACCAACGGCGATCT R- CCGCTAAAGCCGGAAAGAA	55	Kansal et al. (2013)
16S rRNA	16S *Enterobacteriaceae*	F- CATGCCGCGTGTATGAAGAA R- CGGGTAACGTCAATGAGCAAA	96	Huijsdens et al. (2002)
Virulence genes for qRT-PCR				
eltB	LT toxin	F- GGCAGGCAAAAGAGAAATGG R- TCCTTCATCCTTTCAATGGCT	117	Lothigius et al. (2008)
estA	ST toxin	F- TCTTTCCCCTCTTTTAGTCAG R- ACAGGCAGGATTACAACAAAG	165	Rodas et al. (2009)
leoA	Labile enterotoxin output	F- AAACGGTGCATATCCTCGTC R- AAATGCTGCCACCGAAATAC	168	This study
tolC	TolC outer membrane protein	F- AAGCCGAAAAACGCAACCT R- CAGAGTCGGTAAGTGACCATC	101	Swick et al. (2011)
cfa/Ib	CFA/Ib Adhesin	F- TCAGTGTGTCATGGGGAGG R- CAGTTTTAGGTGCAGCGCTA	138	This study
tia	Tia Adhesin	F- ACAGGCTTTTATGTGACCGGTAA R- GACGGAAGCGCTGGTCAGT	67	Kansal et al. (2013)
fimH	Minor component of Type I pili	F- GTGCCAATTCCTCTTACCGTT R- TGGAATAATCGTACCGTTGCG	164	Hojati et al. (2015)
rpoS	Sigma 38 protein	F- GCGCGGTAGAGAAGTTTGAC R- GGCTTATCCAGTTGCTCTGC	229	Rahman et al. (2006)
Reference genes screened for qRT-PCR				
rpoS	Sigma 38 protein	F- GCGCGGTAGAGAAGTTTGAC R- GGCTTATCCAGTTGCTCTGC	229	Rahman et al. (2006)
arcA	Aerobic respiration control	F- GTTCTTACCCGGCAGATTGA R- CAGACCCCGCACATTCTTAT	180	This study
gapA	*E. coli* GAPDH	F- CGTTGAAGTGAAAGACGGTCATC R- CAACACCAACTTCGTCCCATTT	101	Nicklasson et al. (2012)
16S rRNA	16S *Enterobacteriaceae*	F- CATGCCGCGTGTATGAAGAA R- CGGGTAACGTCAATGAGCAAA	96	Huijsdens et al. (2002)

ETEC pure cultures (OD_{600nm}=0.3, exponential phase, LB broth) stained or not with PMA were used as DNA templates. Standard curves were thus generated by PCR amplification of the *Enterobacteriaceae 16S* rRNA and ETEC *gspD* genes for TIM-1 and M-SHIME samples, respectively. The PCR products were purified using the QIAquick PCR purification kit (Qiagen, Hilden, Germany). Concentrations were measured with a NanoDrop spectrophotometer (Thermo Fisher Scientific, San José, USA) and calculated back to the *16S* rRNA and *gspD* gene copy numbers, which amounted 11 log_{10} and 11.1 log_{10} copies μL^{-1}, respectively. Tenfold serial dilutions of the standard were prepared in TE buffer and stored at -20°C until further use. As a negative control, an ETEC pure culture was subjected to lethal heat-treatment (95 °C, 15 min) and stained or not with PMA. The absence of viable ETEC in the heat-treated samples was confirmed on LB agar plates.

2.6 Flow cytometry analysis

Adequate volumes of gastric or ileal effluents (Live/Dead and membrane potential kits) or specific time points (intracellular pH assay) from TIM-1 were centrifuged (9,000×*g*, 5 min, 20°C). Pellets were resuspended into PBS at pH 7.3 to obtain approximately 6 log_{10} cells mL^{-1}. Flow cytometry analysis was performed on a CyFlow SL cytometer and data were collected with FlowMax software version 2.3 (Partec, Sainte-Geneviève-des-Bois, France). The cytometer was equipped with a solid blue laser emitting at 488 nm, and four band-pass filters: a forward-angle light scatter (FSC) combined with a diode collector, a side-angle light scatter (SSC) and two fluorescence signals collected with photomultiplier tubes, a 530-nm band-pass filter (515–545) to collect green fluorescence (FL1 channel), and a 630-nm long pass filter to collect the red fluorescence (FL2 channel). The flow cytometry analysis was performed using logarithmic gains and specific detector settings were adjusted on a sample of unstained cells in order to eliminate cellular auto-fluorescence. Gating on FSC/SSC was used to discriminate bacteria from the background. In order to investigate the physiological states of ETEC, three different flow cytometry staining cell protocols were used, as described hereafter.

Live/Dead ETEC quantification. Bacteria were double stained (Live/Dead BacLight™ Kit L34856 Molecular Probes, Whaltham, USA) with the green-fluorescent DNA stain SYTO 9 labeling all bacteria and the red-fluorescent propidium iodide (PI) only penetrating and staining cells with damaged membranes according to the protocol described in Roussel et al. (2018), chapter 1.

ETEC membrane potential. The membrane potential probe 3,3'-diethyloxacarbocyanine iodide ($DiOC_2(3)$, BacLight™ Kit B34950 Thermo Fisher Scientific, Waltham, USA) has been developed for ETEC H10407, using fluorescence emission ratio detection. $DiOC_2(3)$ at low concentration exhibits green fluorescence in all bacterial cells. However, the dye becomes more concentrated in healthy cells that are maintaining a membrane potential, causing the dye to self-associate and the fluorescence emission to shift to red. The proton ionophore carbonyl cyanide m-chlorophenyl hydrazone (CCCP) supplied by the kit, was used as a control to eradicate the proton gradient, eliminating thus the bacterial membrane potential.

According to the kit protocol, red/green fluorescence ratios were calculated using population mean fluorescence intensities for bacteria incubated with 30 µM $DiOC_2(3)$ for 30 min at room temperature in the dark in either the presence or absence of 5 µM CCCP.

ETEC intracellular pH (pHi). The carboxyfluorescein diacetate succinimidyl ester (CFDA-SE, Vybrant Kit CFDA SE cell Tracer, Kit V12883 Thermo Fisher Scientific, Waltham, USA) is a pH-dependent fluorescent probe. Upon entering a live cell, the acetate groups of CFDA-SE are cleaved by intracellular esterase to create the fluorescent carboxyfluorescein succinimidyl ester (CFSE) compound. CFSE forms covalent bonds with free amino groups and is retained in the cytosol of cells. The fluorescence intensity of CFSE is thus proportional to the intracellular pH. In order to efficiently stain ETEC cells with CFDA-SE, the bacterial pellets were resuspended in McIlvaine buffer at pH 7.3 (citric acid: 0.1M; disodium hydrogenophosphate: 0.2M), supplemented with 1 mM EDTA. EDTA permeabilizes the outer membrane of Gram-negative bacteria by chelating divalent cations from their binding sites in lipopolysaccharides (Vaara, 1992; Breeuwer et al., 1994). Subsequently, samples were incubated with CFDA-SE (5 µL mL^{-1}) 10 min, 40°C under slight agitation in the dark and centrifuged 2 min 10,000×*g* at room temperature. The supernatant was discarded and the remaining pellet was resuspended in McIlvaine's buffer without EDTA at the pH value equal to the pH of the sample (gastric or ileal samples) before flow cytometry analysis, as described by Bouix and Ghorbal (2015). The fluorescence intensity of the cells was directly linked to the pHi in the range of the calibration curves (from pH 3 to 8). Calibration curves were determined for each cell sample. Five microliters of nigericin (Molecular Probes, Waltham, USA) (0.2 mM in DMSO) and 5 µL of valinomycin (Sigma, Saint-Quentin-Fallavier, France) (0.2 mM in DMSO) were added to equilibrate the pHi and the external pH (pHext) and kept at room temperature for 2 min before flow cytometry analysis. Valinomycin renders plasma membranes permeable to potassium ions, and nigericin exchanges potassium for protons.The combined actions of these compounds result in equilibration of both potassium ions and protons across the membrane. Finally, the fluorescence intensity from each sample (e.g. initial inoculum, T20 in the stomach, T180 in the duodenum and T300 in the ileum) was obtained from the calibration curves expressed according to the pHi.

2.7 RNA isolation and transcriptional analysis by quantitative real-time qPCR

RNA extraction. Total RNAs were extracted from TIM-1 and SHIME digestive samples using the TRIzol® reagent method (Invitrogen, Thermo Fisher Scientific, Waltham, USA) adapted from Toledo-Arana et al. (2009). Bacterial pellets were suspended into 400 µL of lysis A solution containing 10% glucose, 12.5 mM Tris pH 7.6, and 10 mM EDTA. The bacterial cell suspension was transferred into Lysing Matrix B tubes containing 500 µL of acid phenol:chloroform (5:1, v/v) and mixed. Bacteria were mechanically lysed using the Fastprep apparatus (Mixer Mill MM 400, Verder Scientific, USA) at speed 6.0 during 1 min at 4°C. After lysis, tubes were centrifuged (21,900×*g*, 10 min, 4°C) and the aqueous phase was transferred into 1 mL TRIzol. Tubes were incubated for 5 min at room temperature before 100 µL chloroform were added. After additional incubation at room temperature during 3 min, another centrifugation step (21,900×*g*, 10 min, 4°C) was performed and the aqueous phase was collected. This

last separation step was reiterated using 200 µL chloroform. After centrifugation (21,900×*g*, 5 min, 4°C), RNAs contained in the aqueous phase were precipitated by addition of 500 µL isopropanol and incubated 15 min at room temperature. After centrifugation (21,900×*g*, 15 min, 4°C), RNA pellets were washed twice with 75% ethanol. Samples were centrifuged (21,900×*g*, 5 min, 4°C) and dried RNA pellets were resuspended in DEPC-treated water (Invitrogen, Thermo Fisher Scientific, Waltham, USA) and stored at -80°C.

DNAse treatment. DNAse treatment with the TURBO DNA-free™ Kit (Invitrogen, Thermo Fisher Scientific, Waltham, USA) was performed to remove any contaminating genomic DNA. 43.3 µL of RNAs were mixed with 5 µL of 10X turbo DNase buffer, 1.5 µL of turbo DNase 2 IU μL^{-1} and 0.2 µL of RNase inhibitor 20 IU μL^{-1} (SUPERase In™ RNase Inhibitor, Invitrogen, Thermo Fisher Scientific, Waltham, USA). Samples were incubated 45 min at 37°C and the reaction was stopped by adding 5 µL of DNAse inactivation reagent according to the manufacturer's recommendation (TURBO DNA-free™ Kit, Invitrogen, Thermo Fisher Scientific, Waltham, USA). After centrifugation (21,900×*g*, 2 min, 4°C), supernatants containing RNAs were stored at -80°C until analysis. In parallel, the efficiency of DNAse treatment was checked by PCR and the following reaction mixture was used: 4 µL of dNTPs 2 mM, 2.5 µL of buffer 10X containing 2.5 mM $MgCl_2$, 0.5 µL of each primers at 500 nM, 1 unit of Taq DNA polymerase, 15.4 µL of ultrapure Milli-Q water and 2 µL of RNA samples. *eltB* gene-specific primers (Table 3.4) were used to evidence bacterial DNA. PCR assays were performed using a thermal cycler T100™ (Biorad, Hercules, USA) under the following conditions: a pre-denaturation (5 min, 95°C), followed by repeated denaturation (30 s, 92°C), and annealing (1 min, 72°C), during 35 cycles and a final extension for 5 min at 72°C. PCR products were analyzed by gel electrophoresis (1.2 % (w/v) agarose).

Quality control. Three quality controls were performed to determine the quantity, purity and integrity of the RNA extracts. RNAs were quantified using UV absorption (at a wavelength ranging from 200 to 350 nm) with the NanoDrop ND-1000 (Thermo Fisher Scientific, Waltham, USA). The ratio of the absorbance at 260 and 280 nm (A260/A280) was used to assess the RNAs purity. RNAs were considered as pure when A260/A280 ratio ranged from 1.8 to 2.1. A minimal concentration of 10 ng μL^{-1} was required to carry out the Reverse Transcription Polymerase Chain Reaction (RT-PCR). RNA integrity was checked using the 2100 Bioanalyzer and the RNA 6000 Nano kit (Agilent Technologies, Ratingen, Germany) according to the manufacturer's instructions. The RNA integrity number (RIN) software algorithm allows for the classification of total RNA based on a numbering system from 1 to 10 with 1 being the most degraded profile and 10 the most intact. Only high-quality RNAs with a RIN between 8.7 and 10 were retained for subsequent transcriptional analysis.

qRT-PCR. RNAs were reverse transcribed into complementary DNAs (cDNAs) by using the PrimeScript™ RT Reagent Kit (TAKARA Bio Inc., Otsu, Japan) according to the manufacturer's instructions. The following RT-PCR reaction mixture (final volume of 20 µL) was used: 4 µL of buffer PrimeScript 5X, 2.5 µL of dNTPs 1 mM, 6.5 µL RNAse free water 40 IU μL^{-1}, 1 µL of random primer 6-

mer, 1 µL of reverse transcriptase Prime Script and 1 µg of RNA matrix. The reaction mixture was incubated at 42°C for 30 min and then at 70°C for 15 min. qPCR was performed on the cDNAs as outlined in the section above. All the primers used at a concentration of 300 nM (except *tia* and *leoA* primers at 100 nM) are listed in Table 2.4. The specificity and usefulness of each primer were verified in two different ways. Firstly, specific PCR amplification was confirmed by the presence of a single reaction product of the expected size in a 2% (w/v) agarose gel after electrophoresis. Secondly, the specificity of amplification was demonstrated by the presence of single melting curve point obtained by real-time PCR, followed by a melting curve analysis of the synthetized product.

To calculate the relative fold changes in ETEC virulence gene expression in the TIM-1 and SHIME, the qPCR data were analyzed using the comparative $E^{-\Delta\Delta Ct}$ method and normalized to the selected reference genes, described here after. Four candidate reference genes (e.g. *16S rRNA, arcA, gapA and rpoS*), listed in Table 2.4 were selected. The delta Ct approach (Silver et al., 2006) and BestKeeper excel-based tool (Pfaffl et al., 2004) were used to rank and determine the stability of the selected reference genes between samples. Of the original candidates, only the geometric means of *arcA* and *gapA* reference genes were considered for the normalization. The amplification efficiency of each reference gene was determined by the generation of a standard curve based on a ten-fold dilution series of a set of cDNA samples from each compartment of the TIM-1 and SHIME models. The efficiency was calculated from the slope of the standard curves generated for each run using the following equation $E = 10^{(-1/slope)}$, where E corresponds to high/acceptable amplification efficiency equals to 90-110 %. Differences in the relative expression levels of each virulence gene were calculated as follows: $\Delta\Delta Ct = (Ct_{target\ gene} - Ct_{reference\ gene})_{at\ time\ t} - (Ct_{target\ gene} - Ct_{reference\ gene})_{at\ time\ t0}$ and data were derived from $E^{-\Delta\Delta Ct}$.

2.8 LT-monosialoganglioside (GM1) ELISA

The protocol was modified from Salimian et al. (2010). All incubations were performed at 37°C and between each step the 96-well plates (Nunc MaxiSorp™ flat-bottom, Thermo Fisher Scientific, Waltham, USA) were washed four times with 400 µL PBST (pH 7.2, 0.010 mg mL^{-1} tween 20%) (Sigma-aldrich, St. Louis, USA). First, the plates were coated with 3 µg mL^{-1} of GM1 dissolved in sodium carbonate-bicarbonate buffer (50 mM, pH 9.6, G7641, Sigma-aldrich, St. Louis, USA) and incubated for at least 2 h. Then, the plates were blocked for 1 h with a PBS blocking buffer containing 1% (w/v) filtered BSA. Consecutively, wells were loaded with 100 µL of serially diluted LT subunit B standard (E8656, Sigma-aldrich, St. Louis, USA) and undiluted supernatants collected from the TIM-1 and SHIME experiments. After 1 h of incubation, 100 µL of the rabbit anti-cholera toxin antibody (1:500 dilution in PBST, CTXB C3062, Sigma-aldrich, St. Louis, USA) were covered and incubated for the same duration. Then, 100 µL of the goat anti-rabbit IgG, conjugated with horseradish peroxidase (1:5000 dilution in PBST, A0545, Sigma-aldrich, St. Louis, USA) were added and incubated for 1 h. As a final reaction, 200 µL o-Phenylenediamine dihydrochloride (SIGMAFAST™ OPD, Sigma-aldrich, St. Louis, USA) dissolved in filtered distilled water were added. After 20 min incubation at room temperature in the dark, the plate was read at 450 nm using the multiscan Tecan Infinite® 200 PRO (Tecan Group Ltd, Männedorf , Switzerland). LT toxin concentrations were expressed in pg mL^{-1}.

2.9 Statistical analysis

All statistical analyses were performed in R studio, version 3.5.1. All formal hypothesis tests were conducted on the 5% significance level ($p \leq 0.05$). The assumptions of normality and heterogeneity of variances were verified based on visual inspection of QQ-plots and shapiro-Wilk (stats4_3.4.2) and Levene's Test (car_2.1-5), preceding statistical hypothesis testing to assess pairwise comparison of: (i) ETEC survival at t time in comparison with the transit marker of the TIM-1 system; (ii) ETEC survival at T time in comparison with the initial inoculum (T0) in the M-SHIME; (iii) ETEC survival between luminal and mucosal microenvironments at T time; (iv) the $\log_2$ fold change gene expression at T time in comparison with the T0; and (v) the LT enterotoxin production at T time in comparison with T0. The assumptions were not met for most variables, in which a non-parametric Mann-Whitney (Wilcoxon-Rank-Sum) test with Holm correction was performed for (i, ii, iii hypothesis), and Nemenyi post-hoc test conducted after significant results for the Friedman test was performed for (iv and v hypothesis), using PMCMR package.

3. Results

3.1 Dynamics of ETEC survival along different GI regions

ETEC survival is influenced by the harsh conditions of the upper GI tract. The TIM-1 was used to simulate the effect of physicochemical parameters and upper GI transit on ETEC survival. At time point T0, upon introduction of a glass of ETEC-contaminated water in the stomach compartment, the average ETEC concentration amounted 7.7 ± 0.1 log_{10} mL^{-1}. During *in vitro* digestion, ETEC counts dropped below 5 log_{10} mL^{-1} after 45 min in the stomach and remained between 6 and 4 log_{10} mL^{-1} all along the duodenal digestion. In contrast, ETEC concentrations were maintained above 6 log_{10} mL^{-1} over time during the jejunal and ileal digestion (Fig. 2.3A).

In order to interpret these changes in ETEC viability, the regionalized kinetics of ETEC survival were compared to a non-absorbable inert transit marker, representing a 100% survival (Fig. 2.3B, C, D, E). In the stomach (Fig. 2.3B), ETEC survival rapidly and drastically decreased by several orders of magnitude in comparison with the transit marker from 45 min digestion. A mean of 1.4 ± 0.6 log_{10} mL^{-1} difference with the transit marker was observed after 45 min of gastric digestion increasing up to 3.5 ± 0.9 log_{10} mL^{-1} after 60 min. This increased loss of viability corresponded to a rapid and real-time drop of pH in the gastric compartment, as denoted in Fig. 2.3B. In the duodenum (Fig. 2.3C), ETEC concentrations gradually decreased until 120 min digestion, with about 1 log_{10} mL^{-1} difference with the transit marker. Remarkably, after 180 min in the duodenum, though not statistically significant, ETEC tended to recover (ETEC curve above that of the transit marker). Conversely, in the jejunum and ileum (Fig. 2.3D, E), ETEC kinetics paralleled that of the transit marker during the first 180 min of digestion. Afterwards, the survival of ETEC was distinguishable from the marker with a slight re-growth observed in both gut regions. The pathogen reached 6.6 ± 0.6 log_{10} mL^{-1} and 7.3 ± 0.3 log_{10} mL^{-1} at the end of the jejunal (T300 min) and ileal (T240 min) digestion, respectively. Taken together, at the end of the upper digestion, a global ETEC survival percentage of 65% ± 31% (6.9 ± 0.1 log_{10} mL^{-1}) was found in the TIM-1.

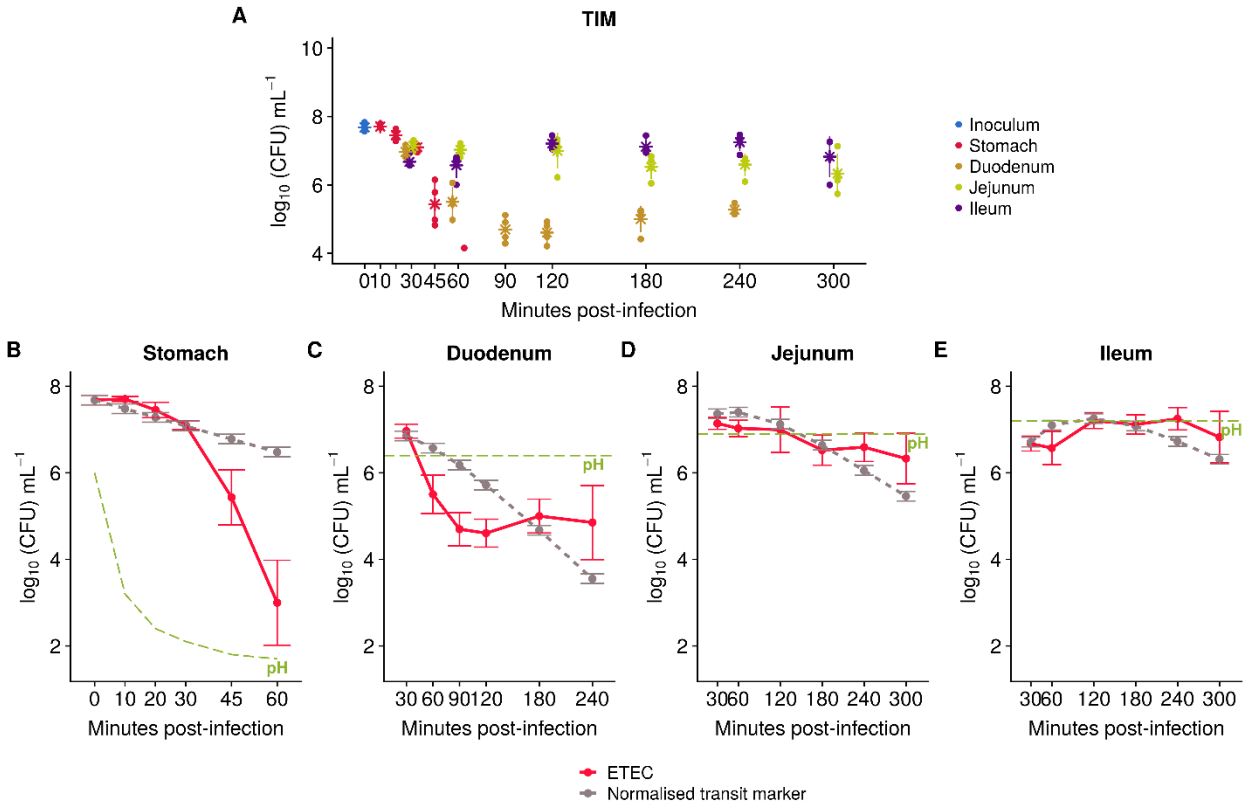

Figure 2.3. **Dynamics of ETEC survival in different GI regions in the TIM-1 system (stomach, duodenum, jejunum and ileum) as determined by plate counts.** After introduction of a glass of ETEC-contaminated water in the TIM-1 stomach, the number of cultivable cells in each compartment was determined by plating. The experiment was repeated in four independent replicates. (**A**) ETEC survival in each GI region of the TIM-1 system. The four replicates are represented by the circles. The average is indicated with a * and the SD is shown; (**B, C, D, E**) Average regionalized survival of ETEC in the four compartments of the TIM-1 system (red line), compared with an inert and non-absorbable transit marker indicating 100% survival (grey dashed line). Bacterial curves below that of the transit marker reflect cell mortality, while curves above the transit marker are indicative of bacterial growth. The level of the pH in each compartment is illustrated in green. Results are expressed as mean concentrations in $\log_{10}$ CFU mL^{-1} ± SD (n=4). No statistical significant differences were found between ETEC and the transit marker kinetics, as determined by Pairwise Wilcoxon Rank Sum Tests with Holm correction.

ETEC persists in the luminal and mucosal microbial niches of the ileum and ascending colon in a late post-infection stage. The impact of the ileal and ascending colon environments on ETEC colonization was assessed in the M-SHIME *in vitro* model. To account for individual variability in gut microbiota composition and metabolic activity, the microbial communities of six fecal healthy donors were tested in two separate M-SHIME runs. The luminal and mucosal microbial composition and metabolic activity are presented in chapter 3. Given the complex microbial background, the *gspD* gene was used to characterize the dynamics of ETEC survival in the different gut regions. The pre-digested ETEC was inoculated in the SHIME ileum and a mean *gspD* copy number of 8.8 ± 0.3 $\log_{10}$ mL^{-1} was noticed upon inoculation (Fig. 2.4A). Already 1 h post-infection (PI) in the ileum, ETEC reached a mean *gspD* copy number of 9.7 ± 0.2 $\log_{10}$ mL^{-1} in the carbohydrate-rich medium. These high levels were maintained for the six donors 3 h PI. Then, 5 h PI the ileal content was emptied within the ascending colon and the concentration of ETEC significantly decreased compared to the initial inoculum (p= 0.016). Nonetheless, the *gspD* copy number remained above 6 $\log_{10}$ mL^{-1} 96 h PI for four donors in the ileum, and for all donors 98 h PI in the ascending colon (Fig. 2.4A). At the endpoints of follow-up, 120 and 122 h PI in the ileum and ascending colon respectively, ETEC *gspD* copy number amounted 5.5 ± 1.4 and 6.1 ± 0.8 $\log_{10}$ *gspD* copy number mL^{-1}, respectively, with an increasing variability between donors (Fig. 2.4A).

As ETEC is known to attach to the intestinal mucus layer, the latter environment was reproduced in both ileum and ascending colon compartments in the M-SHIME by incorporation of type-III mucin agar coated microcosms (Fig. 2.4B, C). ETEC *gspD* copy numbers were significantly higher in the luminal *vs* mucosal phases in ileum and ascending colon at 3 h (p= 0.03), respectively 7h PI (p= 0.03), with an exceptionally low variability between the six donors (Fig. 2.4B, C). In contrast, at a later stage (96 h PI), ETEC *gspD* copy numbers were significantly higher in the mucosal *vs* luminal phase with 7.3 ± 1.0 $\log_{10}$ mL^{-1} compared to 6.8 ± 0.9 $\log_{10}$ mL^{-1} (p= 0.03) in the ileum (Fig. 2.4B). In the colon (98 h PI), however the luminal and mucosal niches did not display a significant difference (p= 0.18), an ETEC *gspD* copy number of 7.4 ± 0.6 $\log_{10}$ mL^{-1} persisted in the mucus niche compared to a 7.0 ± 0.36 $\log_{10}$ mL^{-1} in the luminal phase (Fig. 2.4C).

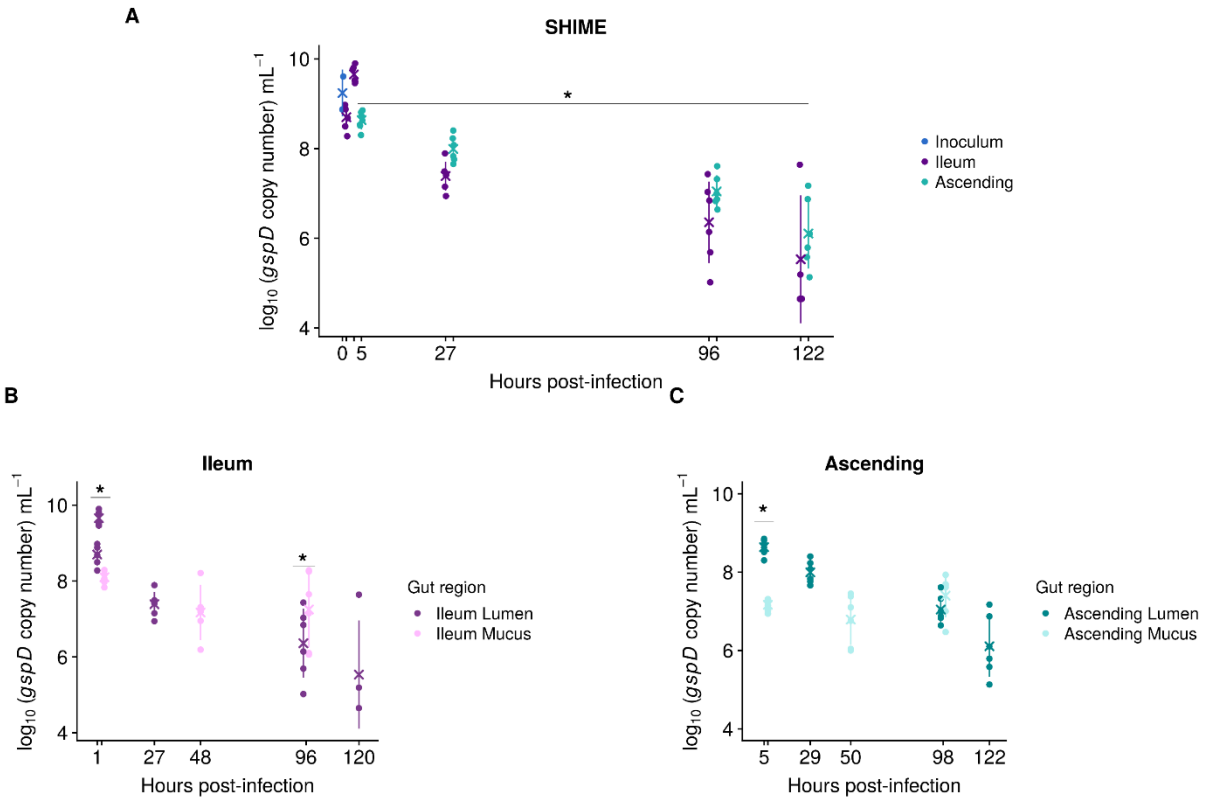

Figure 2.4. Dynamics of ETEC survival in different GI regions in the M-SHIME system (ileum and ascending colon) as determined by ETEC specific qPCR (*gspD* gene). After digestion of a glass of ETEC-contaminated water under static batch *in vitro* conditions mimicking the gastro-jejunal conditions found in the TIM-1 system, the pre-digested ETEC inoculum was introduced in the M-SHIME ileum. Both the ileum and ascending colon compartments hosted a complex microbial community derived from a fecal sample provided by a healthy donor. The experiment was repeated with the fecal microbial communities from six different donors (biological replicates), represented by the circles. The average of these biological replicates is indicated with a '**x**' and the SD is shown. The survival of ETEC was estimated by qPCR and expressed in $\log_{10}$ *gspD* copy number mL^{-1}. (**A**) ETEC survival in the luminal ileum and ascending colon compartments; (**B, C**) Comparison of ETEC numbers in the luminal and mucosal environments, in the ileum (**B**) and ascending colon (**C**). Statistically significant differences over time compared to the initial inoculum (T0) (**A**), or between ETEC survival in the luminal *vs* the mucosal phases (**B, C**) are denoted at $p < 0.05$ (*), as determined by Pairwise Wilcoxon Rank Sum Tests with Holm correction.

3.2 Dynamics of ETEC physiological states along different GI regions

ETEC membrane integrity is affected by upper GI passage in the TIM-1. Maintaining cell membrane integrity is critical for bacterial physiology. ETEC physiological states in the TIM-1 were monitored by PMA-qPCR and flow cytometry (Fig. 2.5). Two and four ETEC subpopulations were discriminated by PMA-qPCR and flow cytometry, respectively, as described in chapter 1 and shown in Fig. 2.5C. Digestion in the stomach altered ETEC membrane integrity. At initial time T0, 64% of the population was detected as viable by PMA-qPCR and 48% by flow cytometry (Fig. 2.5A, B). With the latter technique, three additional membrane states, with different physiological properties were discriminated by gating on the cytogram. 37% had partially-altered membranes but was still able to recover a viable state, 9% was altered/dead and 6% dead (Fig. 2.5B). During gastric digestion, the ETEC fraction with altered membranes (Fig. 2.5A) or partially-altered membranes (Fig. 2.5B) increased over time and that of viable cells decreased (Fig. 2.5A, B). After 60 min, 86% of ETEC cells detected by PMA-qPCR were dead and/or damaged, and 14% remained viable (Fig. 2.5A). A clear difference was seen using flow cytometry technique where only 1% of ETEC preserved an intact cell membrane, while 86% entered an intermediate viability state which was however not categorized as dead cells. This latter remained stable compared to initial time (Fig. 2.5B). These results indicate that most of the cells reaching the small intestine were at least partially-damaged.

In the ileal effluents, reflecting all the stresses endured by ETEC along the gastric then intestinal digestion, flow cytometry analysis displayed a restoration of ETEC physiology as soon as 60 min digestion (Fig. 2.5B). At the final time point (T300 min), 31% of the total population was viable, 58% had partially-altered membranes, 6% had altered membranes and, 5% was dead (Fig. 2.5B). ETEC membrane restoration was less evident with PMA-qPCR analysis since the 78% displayed at 300 min represent a mixed of both dead and damaged membranes (Fig. 2.5A), not finely distinguishable as discussed in chapter 1. Consequently, at the end of the GI digestion, about 1/4 of the total ETEC cells entering in the colon had an intact membrane (Fig. 2.5).

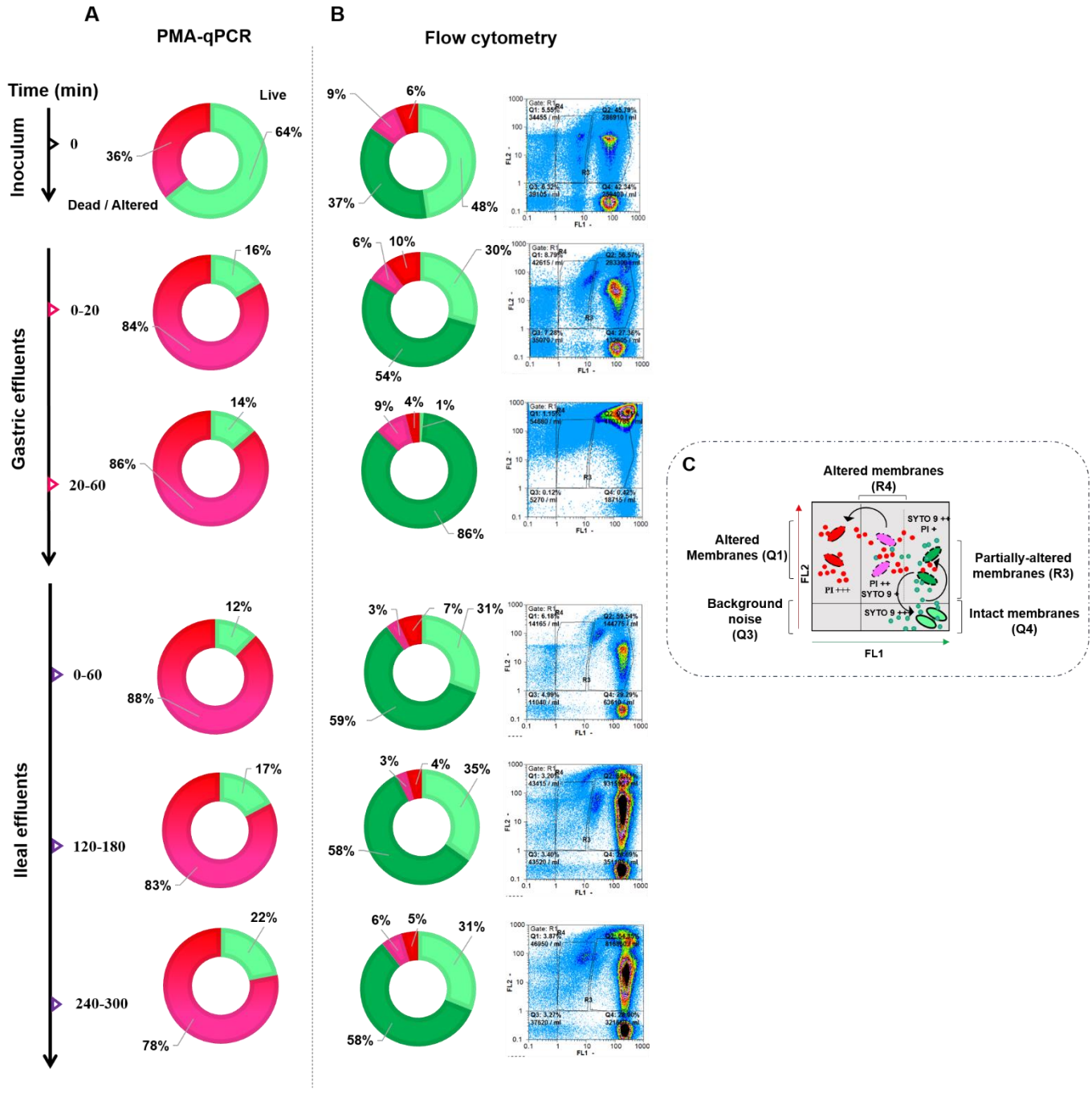

Figure 2.5. **Dynamics of ETEC physiology in the gastric and ileal effluents of the TIM-1 system as determined by PMA-qPCR and flow cytometry.** ETEC membrane integrity was measured over time in the gastric and ileal effluents (**A**) PMA-qPCR shows the live (green) and dead/altered (shade of red) cells. The latter was obtained after deducting the number of intact cells from the total ETEC cells measured by qPCR. (**B**) Flow cytometry shows four subpopulations discriminated after SYTO9 and PI staining, according to the green (FL1) and red (FL2) fluorescence signals, as depicted in the schematic representation (**C**): intact membranes in pale green (viable cells, Q4), partially altered membranes in green (viable/ altered cells, R3), irreversibly altered membranes in pink and red (dead). The doughnut charts represent the average percentages from two independent replicates over time (**A, B**), and cytograms are shown for only one replicate (**B**).

ETEC membrane integrity is affected by the niche-specific gut microbiota in the M-SHIME. The use of flow cytometry to evaluate the physiological state was impossible due to the complex microbial background in the M-SHIME (the microbial composition is given in chapter 3). PMA-qPCR was the sole technique employed to track ETEC viability only in the luminal phase of the M-SHIME (Fig. 2.6). Interindividual variability is given Fig. S2.1. At early post-infection stage, 3 h in the ileum and 5 h in ascending colon, the number of viable ETEC tended to increase in comparison with the pre-digested ETEC inoculum containing approximately 24% live cells (p= 0.03) (Fig. 2.6A). The ratio of viable ETEC progressively decreased along the fermentation with an important donor variability displayed in the ileum (Fig. 2.6B). For instance, 27 h post-infection, only 10% of ETEC cells was viable for 5 donors, while 42% was still viable for donor 3 (Fig. 2.6B). In the ascending colon, all donors displayed a low number of viable ETEC cells with 13% at T29 h PI (Fig. 2.6C).

ETEC membrane potential and intracellular pH are affected by gastric passage in the TIM-1. To further investigate the physiology of ETEC membranes during GI transit, membrane potential was measured by means of flow cytometry analysis in combination with $DiOC_2(3)$ staining (Fig. 2.7A). According to the fluorescence intensity (FI) ratio (FL1/FL2), membranes are considered to be polarized when above a FI ratio exceeding 1, and depolarized below 1. In comparison to the initial inoculum, the membrane potential of ETEC was higher in the gastric and ileal effluents (especially at the beginning of digestion) and had the highest value (FI ratio of 2.5 ± 0.6) after 60 min digestion in the ileal effluents. These values were maintained up till 120 min but drastically decreased afterwards to a value (FI ratio of 1.3 ± 0.1) similar to that of the inoculum after 300 min. No depolarization of ETEC membrane was observed.

The low stomach pH is one of the main stress factors during GI passage. The influence of this low pH on the intracellular cytoplasmic pH, was examined through flow cytometry analysis with a pH-dependent fluorescent probe CFDA-SE (Fig. 2.7B). Importantly, ETEC pHi closely followed the changes in pHext encountered in each GI region. For instance, 20 min after inoculation in the stomach, when the external pH was 2.5, the pHi of ETEC sharply decreased to 3.0 ± 0.1. In contrast, at later time points in the duodenum (pHext= 6.4) and ileum (pHext= 7.2), the pHi was maintained at 5.8 ± 0.2 and 6.0 ± 0.1, respectively (Fig. 2.7B).

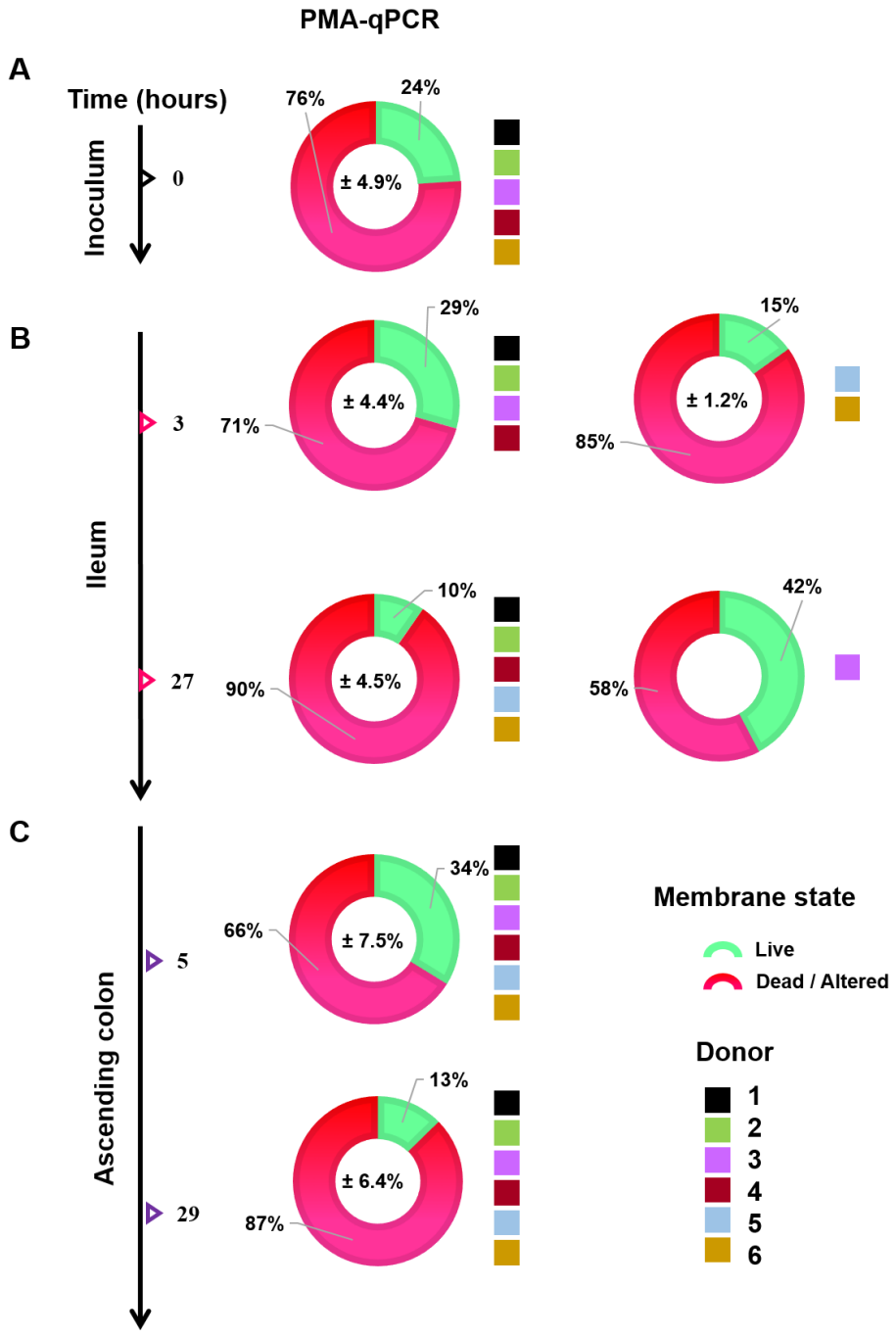

Figure 2.6. **Dynamics of ETEC physiology in the ileum and ascending colon regions of the SHIME as determined by PMA-qPCR.** ETEC membrane integrity was measured over time in the ileum and ascending colon. The number of altered/dead cells was obtained after deducting the number of intact cells from the total ETEC cells measured by qPCR. (**A, B, C**) The viable and altered/damaged ETEC populations are depicted in green and shade of red, respectively. The doughnut charts represent the average percentages from six different donors over time, ± SD. When inter-individual variability is important, a second doughnut is represented, as displayed in (**B**). The inoculum (T0), represents the pre-digested ETEC in batch, prior to introduction in the ileum.

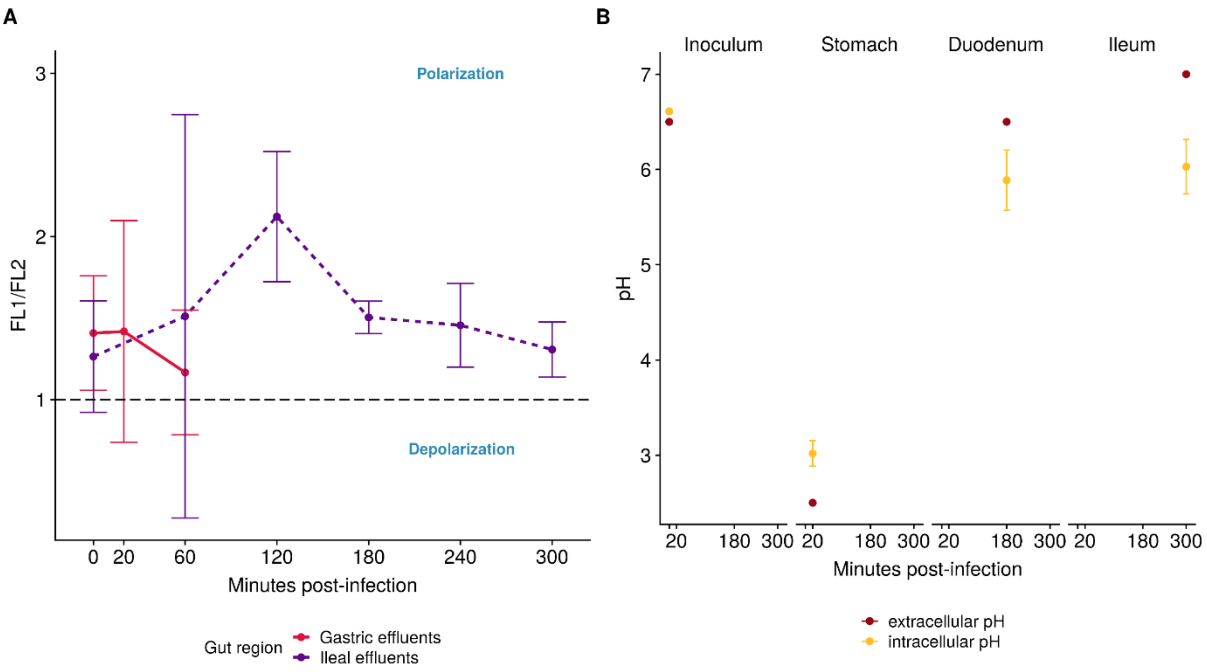

Figure 2.7. Dynamics of ETEC membrane potential and intracellular (pHi) in the gastric and ileal effluents of the TIM-1 system as determined by flow cytometry. (**A**) ETEC membrane potential was measured in the gastric and ileal effluents using flow cytometry analysis with the membrane potential probe $DiOC_2(3)$. According to the fluorescence intensity (FI) ratio (FL1/FL2), membranes are considered to be polarized when above a FI ratio exceeding 1, and depolarized below 1; (**B**) ETEC pHi measured in digestive samples from the TIM-1 using flow cytometry analysis with the pH-dependent fluorescent probe CFDA-SE. The graphs show the mean of two independent replicates ± SD.

II-2

3.3. Dynamics of ETEC virulence along different GI regions

The expression of the main ETEC H10407 virulence genes encoding for attachment and colonization (*cfa/Ib, tia, fimH*), enterotoxin production (*eltB, estAB*), and the release of these enterotoxins (*leoA, tolC*) within the host was followed up over time in the TIM-1 and luminal phase of the SHIME. The log_2 fold change of each gene at any time point was thereto compared with the T0 and results are shown for each replicate individually (Fig. 2.8, 2.9 and Tables S2.4, S2.5). A large variability was observed between replicates in both the TIM-1 and M-SHIME, resulting in few statistically significant differences.

ETEC virulence profiles are affected by upper GI passage in the TIM-1. In general, in comparison with the T0, the virulence gene expression was more induced in the gastric effluents and repressed in the ileal effluents, particularly from 120 min digestion (Fig. 2.8). Two distinct expression profiles were discerned for the enterotoxins *eltB* and *estAB* in both gastric and ileal effluents (Fig. 2.8). The mean expression of *estAB* significantly increased by 2.2 ± 1.0 log_2 fold (p= 0.03) upon exposure to gastric conditions in the first 10 min (pH 3.2), while *eltB* expression was not significantly changed. However, from 20 to 60 min digestion, when pH remained below 2.4, *eltB* gene tended to be repressed, while *estAB* was basally expressed (Fig. 2.8). Thus, *eltB* was positively correlated with the pH, confirming that

LT production is pH dependent as already shown in the literature (Fig. 2.9A). Overall, poor correlations were found in the stomach, in comparison with the ileal effluents. Such results are moreover highly time-dependent, making difficult the interpretation of each correlations (Fig. 2.9). In the ileal effluents, on the other hand, *eltB* tended to be induced in half of the replicates in the first 180 min of the digestion. During the two last hours of digestion *eltB* expression reverted back to the levels measured at T0. *estAB* was repressed from T120 to T300 min in the ileal effluents, with a significant -7 ± 0.6 log_2 fold repression at T240 min (p= 0.05). The two genes carried by the plasmid P948, *estAB* and *cfa/Ib* genes displayed similar expression profiles, especially in ileal effluents. Positive and significant Spearman correlations between both genes confirmed the similarity in the ileal effluents (Fig. 2.9B, C). As for *estAB*, *cfa/Ib* exhibited a significant -6 ± 2 log_2 fold repression in the ileum at T240 min (p= 0.05) (Fig. 2.8).

We also examined the transcriptional response of the *leoA* and *tolC* genes that are contributing to the release of LT and ST enterotoxins, respectively. Both genes were expressed at low level in the gastric effluents and tended to be under-expressed in the ileal effluents, but less than *estAB* and *cfa/Ib*. For instance, *tolC* displayed a mean -2.2 log_2 fold repression at T300 min compared to T0 (Fig. 2.8). *leoA* and *tia* genes that are encoded within the same pathogenicity island in ETEC H10407, showed similar expression profiles especially in the ileal effluents, resulting in a positive correlation (Fig. 2.9B). Although *leoA* encodes for the release of the LT toxin, the gene was negatively correlated with the *eltB* gene in the ileal effluents (Fig. 2.9B, C). Then, the *tolC* gene responsible for the release of ST was positively correlated with *estAB*, but only at T300 min (Fig. 2.9C).

The *fimH* gene encoding for type 1 pili, was slightly over-expressed in the gastric effluents at T20, as for *tia* gene with a 1.2 ± 0.3 and 1.6 ± 0.4 log_2 fold over-expression, respectively (Fig. 2.8). Surprisingly, *rpoS* gene which is known to be activated in response to environmental stresses, was not over-expressed in the stomach, displaying a negative correlation with the pH, and tended to be repressed in the ileal effluents from 120 min digestion (Fig. 2.8 and Fig. 2.9A).

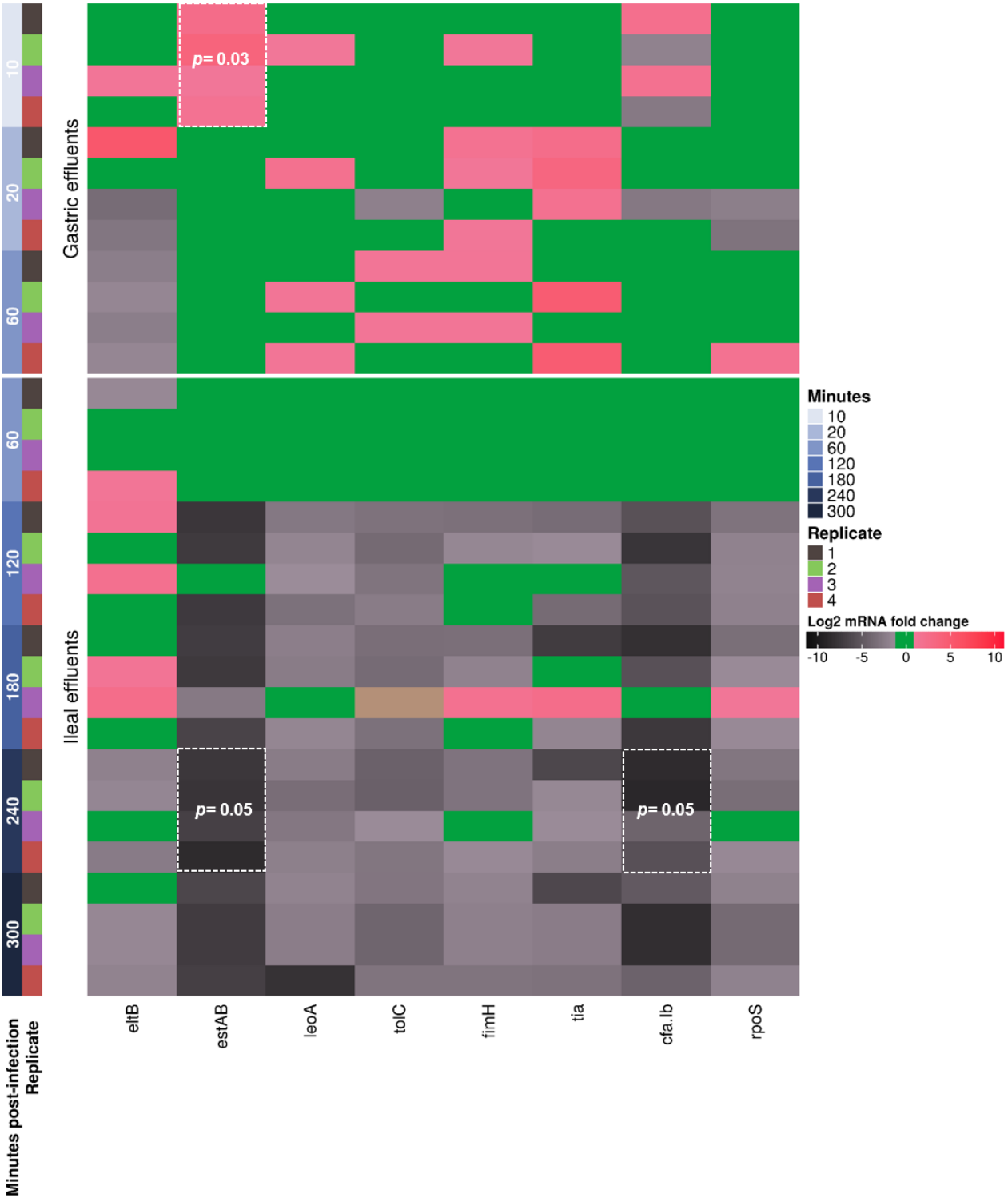

Figure 2.8. **Dynamics of ETEC virulence gene expression in the gastric and ileal effluents of the TIM-1 system as determined by RT-qPCR.** Results are expressed and colored according to the $\log_2$ fold-change. For reasonable statements, statistically significant differential expression had to meet two criteria: a mean $\log_2$ fold change expression of ≥ 1 (induction denoted in shade of pink) or ≤ -1 (repression denoted in shade of black/grey) and, a $p \leq 0.05$. The statistically significant differences in average of $\log_2$ gene expression at each time points are compared to the initial inoculum (T0) and marked by the white frames in the heatmap, as determined by the friedman post-hoc Nemenyi test.

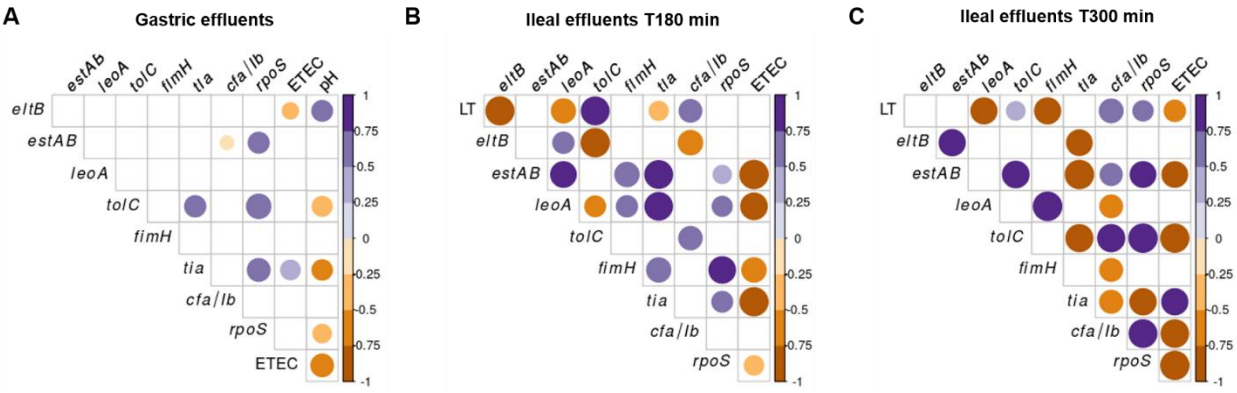

Figure 2.9. **Spearman correlation between virulence gene expression, LT toxin production and/or ETEC survival in the gastric and ileal effluents of the TIM-1 system.** The size and color of the circles correspond to the magnitude and sign of the correlation. Only significant correlations are shown (p< 0.05).

ETEC virulence gene expression is affected by the abiotic factors and niche-specific gut microbiota in the M-SHIME. The same set of ETEC virulence genes (except *rpoS* gene) was analyzed in the ileum and ascending colon lumen of the six distinct donors (Fig. 2.10). In general, in comparison with the initial inoculum, the virulence genes were significantly (p= 0.01) under-expressed at late time points of fermentation in both gut regions (T27 and 29 h PI). The enterotoxin encoding genes *eltB* and *estAB* displayed a somewhat similar expression profile but with donor dependent differences. *eltB* was significantly over-expressed 5 h PI in the colon in 5 donors with a 2 fold to 3 $\log_2$ fold induction in donors 2, 3, 4 and 6 and, a 7 $\log_2$ fold induction in donor 5 (Fig. 2.10). *estAB* was over-expressed in the ileum at 3 h PI and in the ascending colon 5 h and 20 h PI but in overall was not significant compared to T0. This is due to inter-individual differences as *estAB* was over-expressed in 3 donors (donors 1, 2 and 3) at T3 h in the ileum and the same 3 donors at T20 h in the ascending colon. The genes encoding for the export of LT (*leoA*) and ST (*tolC*) enterotoxins did not follow the same expression pattern and were also characterized by high donor variability. In the colon, *leoA* was predominantly repressed, for most donors over time. For example, at T5 h PI (p= 0.03) and T29 h PI (p= 0.01), a donor-dependent -3 to -13 $\log_2$ fold repression was noticed (Fig. 2.10). *tolC* expression did not substantially change compared to the T0 inoculum, especially in the ileum. In contrast, the *tia* gene expression was consistently repressed in the ASC with a mean of -13 $\log_2$ fold repression and at T27 h in the ileum as well (Fig. 2.10).

cfa/Ib mRNA was not detectable (not amplified) either in the ileum and colon. It is possible that the appropriate environmental conditions have not been met for optimal gene expression in this case. Finally, correlations between genes were mostly found in the ileum than the colon (Fig. 2.11). Interestingly, in the ileum *eltB* was positively correlated with *leoA*, *estAB*, *fimH* and *tia* genes, as well as with ETEC survival, while all of them were negatively correlated with the LT production (Fig. 2.11). Such results confirmed that post-transcriptional regulation are key determinants in the LT toxin production, presented here after.

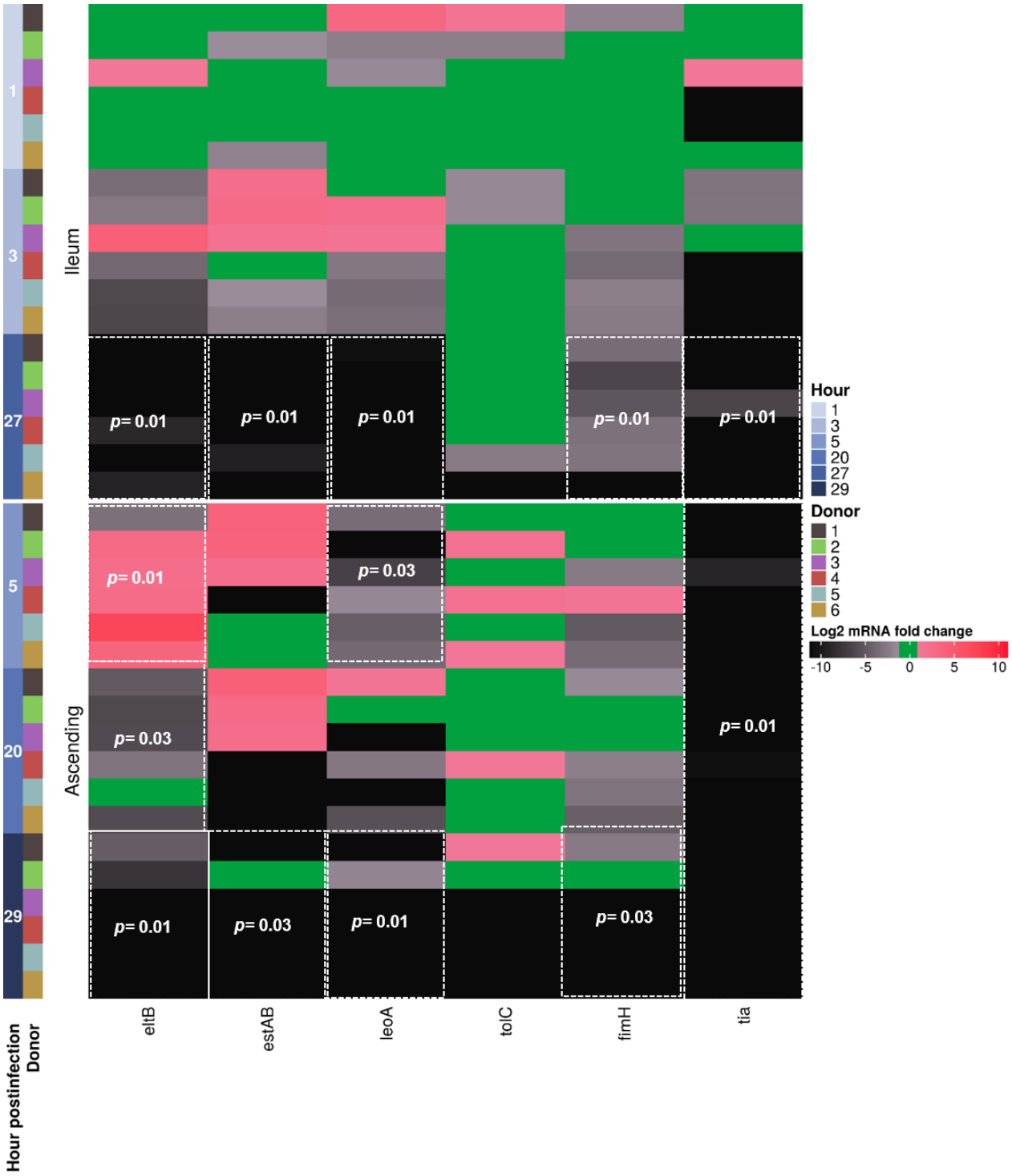

Figure 2.10. **Dynamics of ETEC virulence gene expression in the ileum and ascending colon regions of the M-SHIME as determined by RT-qPCR.** Results are expressed and colored according to the log_2 fold-change. For reasonable statements, statistically significant differential expression had to meet two criteria: a mean log_2 fold change expression of ≥ 1 (induction denoted in shade of pink) or ≤ -1 (repression denoted in shade of black/grey) and, a $p \leq 0.05$. The statistically significant differences in log_2 gene expression are compared to the initial inoculum (T0) and marked by the white frames in the heatmap, as determined by the friedman post-hoc Nemenyi test.

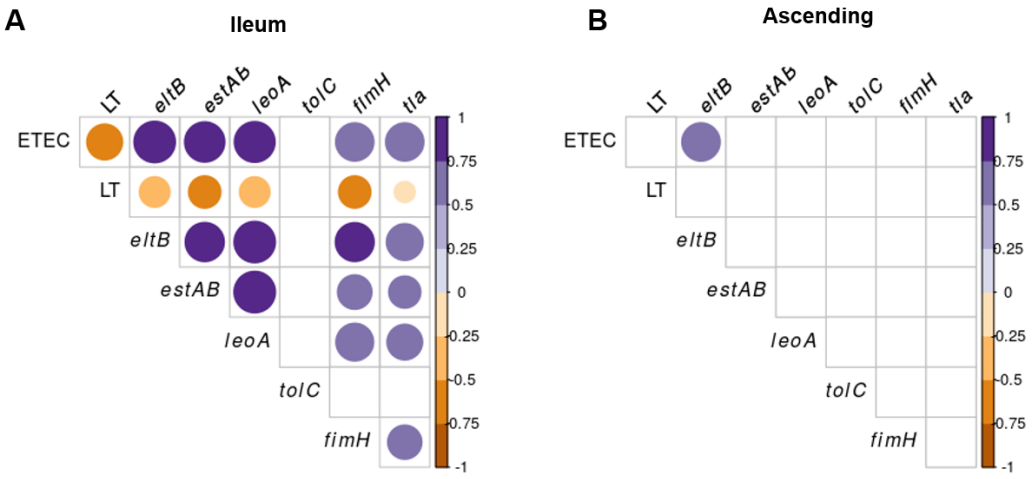

Figure 2.11. **Spearman correlation between virulence genes expression, LT toxin production and/or ETEC survival in the ileum and ascending colon regions of the M-SHIME system.** The size and color of the circles correspond to the magnitude and sign of the correlation. Only significant correlations are shown (p< 0.05).

II-2

LT enterotoxin production is influenced by the GI tract passage in the TIM-1 and M-SHIME. In addition to following the enterotoxin encoding *eltB* and *leoA* gene expression, LT enterotoxin production was quantified at the protein level in both the TIM-1 and M-SHIME systems (Fig. 2.12). LT enterotoxin was absent from the gastric effluents, probably due to the low pH (transient activation of *eltB* when pH was low), while LT was detected in the ileal effluents of the TIM-1 at all-time points (Fig. 2.12A). The production of LT was maximal and significantly increased compared with T0 after T120 min digestion, with a mean of production of 185 ± 72 pg mL^{-1} (p= 0.014). Afterwards, the LT concentration gradually decreased below to the detection limit value at T300 (Fig. 2.12A). Surprisingly no toxin was measured in the SHIME ileum during the first 3 h PI in all donors (Fig. 2.9B), while LT was produced at high levels varying between 3500 to 7200 pg mL^{-1} in the ascending colon, 5 h PI in three (donors 1, 2 and 3) out of the six donors (p= 0.042). Although lower, LT production was still achieved 20 h PI in the ileum, by 3 (donors 1, 2 and 3) of the 6 donors, and persisted in donor 1, 29 h PI in the ascending colon (Fig. 2.12B). Remarkably, the donors displaying the highest *estAB* gene expression level (donors 1 to 3) in the M-SHIME ascending colon, were also those who produced highest amount of the LT toxin (Fig. 2.10 and 2.12B). As for the TIM-1 at the end of the ileal effluents, LT toxin production was found to be negatively correlated with the ETEC survival in the ileum of the M-SHIME (Fig. 2.9C and 2.11A).

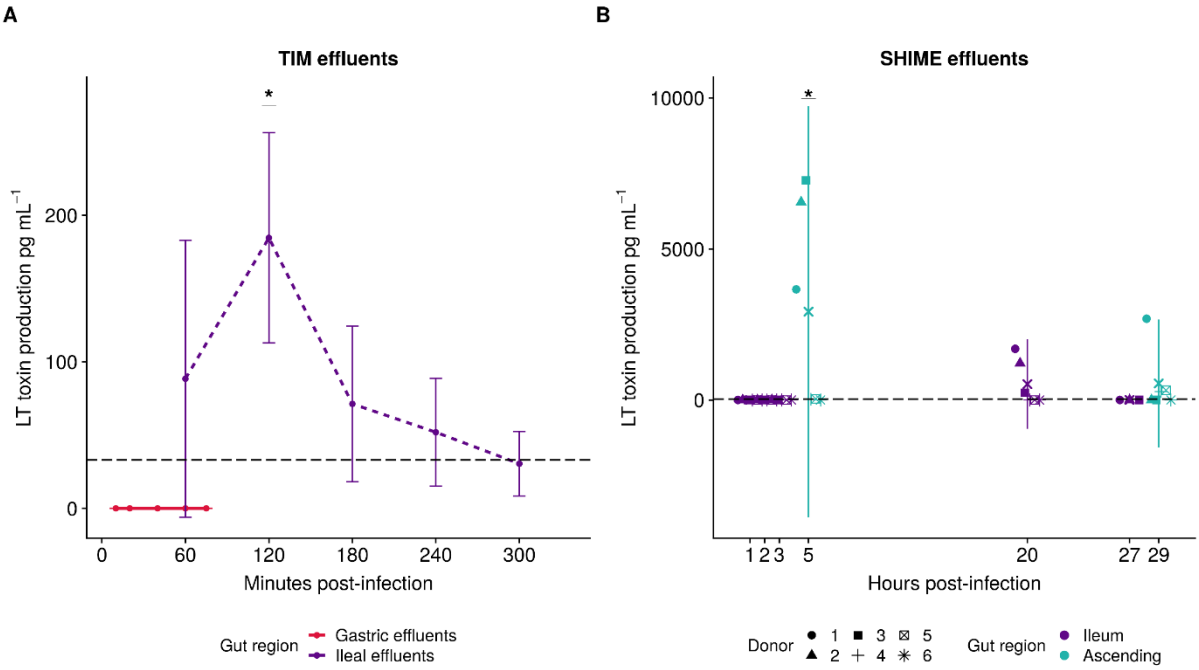

Figure 2.12. **Dynamics of LT toxin production in different GI tract regions in the TIM-1 (gastric and ileal effluents) and M-SHIME (ileum and ascending colon) as determined by a GM1 ELISA.** (**A**) LT toxin production in the gastric and ileal effluents of the TIM-1 is expressed as a mean of four independent replicates in pg mL^{-1} ± SD; (**B**) LT toxin production in pg mL^{-1} in the luminal ileum and ascending colon compartments of the M-SHIME for six different donors (denoted by the different shapes). The average of the 6 biological replicates is shown as a '**x**'. The horizontal black dashed line represents the detection limit. Statistically significant differences in LT toxin production over time compared to the initial inoculum (T0) are denoted at $p < 0.05$ (*), as determined by the friedman post-hoc Nemenyi test.

4. Discussion

ETEC survival and virulence in the human GI tract are scarcely understood due to the multiple, successive and complex GI ecosystems crossed by the pathogen to reach its prime site of action, the distal part of the small intestine. With the use of complementary *in vitro* models of the human digestive environment, TIM-1 and M-SHIME, the key objective of the present study was to unravel the dynamics of ETEC H10407 survival and virulence throughout the entire simulated GI tract.

Overall, our data suggested in the TIM-1 an ETEC die-off during gastric digestion. This was supported by an increased number of ETEC with membrane-damaged and a very low cytoplasmic pH (close to 3). Then, an improved survival of ETEC was noticed in the *in vitro* small intestine with growth renewal at the end of jejunal and ileal digestion. This was characterized by a restoration of ETEC membrane integrity and the return to a slight alkaline pHi. In the M-SHIME, ETEC persisted in both luminal and mucosal microbial niches of the ileum and ascending colon in a late post-infectious stage, up till 5 days. Moreover, a marked survival of ETEC in the mucosal niche of the ileum was noticed compared to the luminal one. For ETEC virulence gene expression profiles, global differences between virulence genes, GI tract regions and, donors were observed. Most of the virulence genes were switched on in the stomach and switched off in the TIM-1 ileal effluents and at late post-infectious stage in the SHIME ileum and ascending colon. The *eltB* gene was mainly over-expressed in the ascending colon, while *estAB* gene expression was displayed in the stomach and ascending colon. At protein level, no LT enterotoxin production was measured in the stomach and a higher concentration was found in the ascending colon compared to the ileum of both TIM-1 and M-SHIME.

The first challenge for the pathogen when entering the stomach is the acidic pH. Scientific research on susceptibility to infection has primarily focused on gastric pH, while the contribution from gastric enzymes (e.g. lipase and pepsin) is rarely investigated as the activity of these enzymes is intricately related to low pH (Tennant et al., 2008). The (drinking) water in which ETEC often resides, has no buffering properties itself to help sustaining the pathogen viability in the stomach. From physiological perspective it is important to understand that water ingestion elicits a stronger early gastric secretory response resulting in a faster acidification and a shorter gastric emptying time than for a solid meal (Malagelada and Summerskill, 1979). Our TIM-1 system is able to capture such dynamics in pH drop and transit time, resulting in ETEC only exposed for a short time to low pH (gastric emptying time of 15 min). This parameter is often over-estimated when using static *in vitro* models. For instance, Masters et al. (1994) claimed ETEC cells to be undetectable upon 2 h static exposure at pH 2 (Masters et al., 1994). This is non-representative for adult *in vivo* conditions. Our data show that culturable ETEC cells were drastically decreased upon 45 min gastric digestion at pH below 2, but far from undetectable. For further understanding, we investigated the physiological state of the bacterium by PMA-qPCR and flow cytometry analysis. The integrity of ETEC membranes dynamically changed upon prolonged exposure to low pH. At the end of the gastric digestion (pH 1.8), 99% of the remaining ETEC fraction displayed partially-compromised membranes as measured by flow cytometry. This altered viability state was clearly distinguishable from the dead sub-populations on the cytogram and might be related to a VBNC physiological state as previously discussed in chapter 1 (Roussel et al., 2018). In addition, this

intermediate state implies that the decline in ETEC viability is reversible, as confirmed in the subsequent digestive compartments.

After passing the stomach, ETEC reaches the proximal part of the small intestine, the duodenum. Bicarbonate secretion neutralizes the acidity from the gastric digestion resulting in a progressively increasing pH from 6.4 in the duodenum to 7.2 in the ileum. Despite this duodenal pH increase in TIM-1, we found a progressive decrease of ETEC until halfway duodenal digestion, to eventually observe ETEC survival in the jejunum and ileum with even a growth renewal found at the end of the digestion. This initial duodenal decline in ETEC viability can be explained by the level of duodenal bile salts which are initially high. Bile is an innate antimicrobial detergent-like compound essential for lipid digestion and nutrient absorption, and is thus one of the more long-term challenges encountered by ETEC (Sistrunk et al., 2016; Urdaneta and Casadesus, 2017). Concentrations of bile salts are physiologically higher during the first hour of duodenal digestion (15 mmol L^{-1}) and then decreases to 5 mmol L^{-1}, resulting in a 95% reabsorption by the end of the ileal digestion (2 mmol L^{-1}) (Roussel et al., 2016; Northfield and McColl, 1973). As digestion progresses in TIM-1 the pH and dilution level further increases, contributing to ETEC's increased survival in the jejunum and ileum compartments. This is the first time that the dynamics of ETEC viability in the upper digestive tract has been monitored in such detail. Interestingly, ETEC seems to be quite robust as our previous TIM-1 work on the EHEC pathotype only displayed re-growth at the end of the ileum (Cordonnier et al., 2017; Roussel et al., 2016). A unique step in the present study was the use of an adapted M-SHIME to study ETEC's colonization ability in the ileum in the presence of the human gut microbiota (8-9 log_{10} bacteria mL^{-1}) from six fecal donors and under anaerobiosis, features that are not present in TIM-1. We found high levels of ETEC in both luminal and mucosal phases in a late post-infectious stage (120 h PI). In line with our previous study where ETEC was highly attaching the mucin proteins in a deprived microbial environment (Roussel et al., 2018), the same properties were found in the presence of the ileal microbiota. The mucus layer is a nutrient rich environment, helping to maintain high ETEC concentrations in the mucosal phase and constantly seeding the gut lumen upon each consecutive emptying cycle. We further discuss the nutrient utilization capacity of ETEC in chapter 3, in relation with the gut microbial communities. Altogether, the number of viable ETEC was restored in the TIM-1 ileum compared to that found in the stomach. At final time point in the ileal effluents, 1/3 remained viable, as estimated by PMA-qPCR and flow cytometry techniques. In the microbial environment of the M-SHIME ileum, 10% of the remaining ETEC was still viable the day upon infection with however a variability between donors.

As a final step, ETEC will transit in the colonic part. Although most of the studies displayed the ileum as the main site of action for ETEC, others assume that it can be extended to the proximal part of the colon, or at least colonize this region in a mouse model (Allen et al., 2006, Rodea et al., 2017; Gonzales et al., 2013; Roussel et al., 2018). At this site, ETEC will encounter a mildly acidic environment, while most of the bile acids have been recycled back into the small intestine. In addition, the colon is largely devoid of oxygen which enhances the growth of anaerobic bacteria. A mean 10-11 log_{10} bacteria mL^{-1} are classically found in the colonic environment. These anaerobic microbes display a high metabolic activity (SCFA production) through the fermentation of partially-digested / undigested food particles (Sender et al., 2016; MacFarlane and MacFarlane, 2003). Successful ETEC colonization will require the

bacterium to gain a growth advantage over the intestinal microbiota. Our study shows that, similar to the M-SHIME ileal compartment, ETEC can persist in both the luminal (5 days post-infection still 6 log mL^{-1}) and mucosal phase of a simulated colon environment. We attribute ETEC's high survival to its high adhesion capacity to the mucus layer, a property that is even more pronounced than the AIEC pathotype (Van den Abbeele et al., 2016).

A new approach to studying ETEC's physiological state was the assessment of its membrane potential and the pHi. The membrane potential is established by multiple ion gradients across the cytoplasmic membrane: it is involved in numerous processes of bacterial physiology and is strongly associated with bacterial viability (Novo et al., 1999). We observed a low membrane polarization in the small fraction of viable ETEC remaining in the stomach. In sharp contrast with other studies reporting a reverse electrical potential in acid resistant *E. coli* using static *in vitro* models (Richard and Foster, 2004; Foster, 2004; Yang et al., 2015) we found no depolarization at all. We therefore assume that the low membrane potential found upon gastric conditions may be linked to the altered-damaged ETEC membranes, which is a temporary state to withstand the stringent conditions encountered. Such hypothesis was supported in a study using $DiOC_2(3)$ dye as well to investigate the impact of decontamination treatments on *E. coli* membrane polarization (Fröhling and Schlüter, 2015). In the ileal effluents, ETEC-membranes were hyperpolarized (higher negative charge at the intracellular side of the cytoplasmic membrane) during the first 2 h following GI digestion. A time-dependent loss of polarization occurred in the second part of the digestion to reach back the polarization level found in the inoculum. Interestingly, recent studies have concluded that hyperpolarization primarily occurs due to an increase in pH (from acidic to neutral), which is in line with our study, resulting in a higher diffusion of K^+ out of the ETEC cell membrane (Bot and Prodan., 2010; Castaneda-Garcia et al., 2011). There is no consensus in the literature of the consequence of this hyperpolarization. Spindler et al. (2011) stated that a transient hyperpolarization can result in a non-lethal destabilization of the cytoplasmic membrane, while other authors highlighted that this phenomenon can be associated with the formation of superoxide radicals, associated with bacterial viability loss (Kohanski et al., 2007; Vanhauteghem et al., 2013; Sanchez et al., 2010). In our case, when comparing results obtained from the Live/Dead flow cytometry, we did not notice a clear loss of viable ETEC when the membrane was hyperpolarized. The oxygen depletion play also a role on the protein localization at the membrane and modulate the membrane potential, but this parameter was not integrated in the TIM-1 system.

The capacity of cells to maintain a pH gradient (higher cytoplasmic pH than external pH) can also supply information about cellular viability (Richard and Foster, 2004). Even though it is a bioenergetic challenge, bacteria in general are able to maintain a fairly constant pHi which is not necessarily similar to the pHext. Our results show a sharp decrease of ETEC pHi, when exposed to a pHext of 2.5 in the stomach. This result was in line with the very low survival rate of ETEC in this compartment, and also in agreement with earlier analysis showing that in non-pathogenic *E. coli* exposed to a pHext of 2.5, the pHi may drop as low as 3.5 in case inducible acid resistance (AR) systems were not operational (Richard and Foster, 2004, Yang et al., 2015). *E. coli* contains several acid resistance systems, but most of them require extracellular metabolites to be inducible. To cite, AR2 requires extracellular glutamate and is known to be the most effective system to relieve the acid stress (e.g. stomach), while AR3 requires

extracellular arginine. Through the amino acid decarboxylation they will consume intracellular protons in order to re-equilibrate the pHi of the bacterium (Lund et al., 2014; Richard and Foster, 2004; Zhao and Houry, 2010). In our case, the operation of such systems in ETEC was not possible due to the absence of these amino-acids in the TIM-1 stomach. Even when these systems are operative, the pHi was reported to drop below 5, suggesting that the threshold internal pH value is not the sole important factor for survival (Richard and Foster, 2004). The AR systems have never been described in ETEC, while better studied in other *E. coli* pathotypes such as EHEC to justify the fact that the low infectious dose of the pathogen was attributed to its robust survival in the stomach. Then, an increased ETEC pHi closely related to pHext was found in the duodenum and ileum, compared to the stomach. Such results demonstrated explicitly the flexibility of the pathogen to adapt the successive stress-inducing environmental changes and its potential to recover within its main site of action, the ileum.

The potency of ETEC H10407 to infect its host depends on its virulence gene expression profiles that are in turn determined by many GI cues. So far, ETEC gene regulation has never been investigated in upper and lower GI conditions in such detail as in this study. It is important to note that gene expression profiles differed between TIM-1 and M-SHIME, due to different digestive, physiological or microbial parameters that are integrated in the respective models. This chapter discusses the effects on ETEC virulence from the abiotic digestive factors, while the effect from gut microbiota and their metabolic activity will be discussed in chapter 3.

With respect to the genes encoding for the enterotoxins, the *eltB* gene was not induced during the gastric digestion (especially at low pH) and at protein level no production of the LT enterotoxin was observed in the gastric effluents, which is largely consistent with previous studies, and strengthen the pH-dependency of LT for optimal toxin production (Gonzales-Siles et al., 2016; Gonzales et al., 2013; Kunkel and Robertson, 1979; Hegde et al., 2009). Gonzales et al. (2013) have shown in static *in vitro* batch and in mice models that LT secretion gradually increases from pH 7 to pH 9 (this latter is however not physiologically found in the human GI tract), while *eltB* transcription levels are pH independent between pH 5 to 9 (Gonzales et al., 2013). In the TIM-1 ileal effluents, *eltB* tended to be slightly overexpressed in the first 180 min of the digestion, with an increasing production of LT protein during the first 2 h of the digestion. In contrast, in the SHIME ileum, the LT toxin was measured only in a late post-infectious stage, while its corresponding *eltB* gene was significantly repressed. Remarkably, in the ascending colon, the *eltB* gene was over-expressed only 5 h post-infection, which corresponds with the observed maximal production of LT toxin at that time point. For the other time points in the SHIME, we did not find a correlation between LT production and *eltB* gene expression. Altogether, two arguments are proposed to explain the differential pattern observed for LT toxin production and *eltB* gene expression in the TIM-1 and M-SHIME: (i) induction of the *eltB* gene does not necessarily indicates a production at protein level since transcriptional and post-transcriptional regulations are key determinants in the LT toxin production. For instance, the global transcription factor cAMP receptor protein (CRP) is a repressor of *eltB* expression while, it is a positive regulator of LT secretion, as shown in *in vitro* and *in vivo* models (Gonzales et al., 2013); (ii) due to the transit of the *in vitro* systems, the toxin produced in a higher compartment, can simply recover in a lower compartment without any production at this site (e.g. ileum *vs* ascending colon); and (iii) the possibility that the LT toxin was released upon ETEC cell

lysis is often affirmed and refuted from several studies. However, given that LT can be associated with the LPS of the outer membrane of ETEC cells, it is likely to affirm this hypothesis and can justify the fact that we found high production of the LT still 20 h post-infection when ETEC survival decreases (Lasaro et al., 2006). Next, our results displayed that the LT toxin can be produced either under aerobic or anaerobic conditions, as confirmed by Lu et al. (2016). Authors have shown that LT secretion depends on the integrity of the respiratory chain and demonstrated that in the Type-II secretion system, the GspD protein, a secretin of ETEC was assembled under anaerobic conditions and was accompanied by LT secretion (Lu et al., 2016). The *estAB* gene encoding the ST enterotoxin was overexpressed during the first minutes of the TIM-1 gastric digestion and repressed in the ileum while it was overexpressed for 3 out of 6 donors in the ileum and ascending colon of the SHIME. These findings support the fact that *estAB* and *eltB* do not follow the same regulation pattern. Interestingly, the CRP regulator represses transcription of *eltAB* gene while it positively regulates *estAB* gene (Haycocks et al., 2015, Bodero and Munson, 2009). Even if the production of ST enterotoxin was not investigated, older studies have shown that the production of ST and activity were not pH-dependent in contrast with LT (Sriranganathan et al., 1983; Johnson et al., 1978), while we found in the present study that *estAB* gene expression seemed to be pH-dependent, with a significant over-expression during the 10 first minutes in the stomach, when pH is not too low. With respect to the likely effect of oxygen level, it has been recently shown that *eltB* and *estAB* genes were under-expressed in human stool samples and in anaerobic batch culture compared to microaerobic and aerobic cultures. Such repressions were dependent on the oxygen-sensitive transcriptional regulator fumarate nitrate reduction (FNR) regulator, and authors made the assumption that the inactivation of *fnr* near the epithelium reestablished the ETEC virulence genes expression (Crofts et al., 2018). In our cases, we observe the expression of *eltB* and *estAB* upon both aerobic (TIM-1) and anaerobic (SHIME) conditions, assuming therefore that other unknown regulation networks might explain the observed gene expression patterns.

Next, we followed *leoA* and *tolC* genes, that are encoding the proteins contributing to the secretion and delivery of LT and ST, respectively (Brown and Hardwidge, 2007). No significant induction of both genes was observed in the gastric and ileal effluents of the TIM-1, while distinguishable profiles were found in the M-SHIME. The *leoA* gene was repressed all along the M-SHIME anaerobic compartments. This contrasts a recent study demonstrating a significant gene induction in human stool and anaerobic batch cultures compared to microaerobic cultures (Crofts et al., 2018). *tolC* maintained a basal expression in the ileum and a tendency to be over-expressed in the ascending colon in a donor dependent manner. The latter suggests that the anaerobic and/or the microbial environments might help to enhance *tolC* expression contrary to *leoA*. Interestingly, beyond the role of TolC in the expel of ST enterotoxin, this component of the MDR efflux complexes is one of the main regulators for bile salts resistance and to overcome bile acid toxicity in *E. coli,* but also a member of the EvgA acid-resistance regulon and is required for expression of the AR2 system and for the growth of *E. coli* under acid conditions (Deininger et al., 2011, Masuda and Church, 2002 ; Sengupta et al., 2014).

With respect to the genes encoding for the adhesins CFA/Ib, tia and FimH, promoting the attachment to the IECs, so far their respective genes regulation in general have been scarcely investigated. Here we showed that *fimH* and *tia* genes tended to be over-expressed in the stomach, while repressed in

both ileum and the ascending colon. The *fimH* gene is located on the chromosomal *fim* operon in ETEC and is highly conserved. Even though far from our models, previous studies have shown in uropathogenic *E. coli* that pH 5.5 repressed type 1 pili encoding gene *in vitro* and in murine urinary tract (Sheikh et al., 2017; Schwan et al., 2002; Schwan and Ding, 2017). The *cfa/Ib* gene displayed a basal expression in the gastric environment and a repression in the TIM-1 ileum and surprisingly, the gene was not amplified under the experimental conditions of the M-SHIME, leading us to believe that the presence of the IECs could be required for the gene induction. In a contradictory study, *cfaD* (encoding for another subunit of CFA/I adhesin, in the same operon than *cfa/Ib*) was under-expressed in stool samples and in anaerobic batch culture compared to microaerobic and aerobic environments, while *fimH* was significantly induced (Crofts et al., 2018). Globally during the digestion, *cfa/Ib* gene displayed a similar expression profile than *estAB* gene with a significant positive correlation. Both genes are carried by the same plasmid in ETEC H10407 (p948) but the existing co-regulation of *cfa/Ib* and *estAB* is unknown. As another correlation, we have found similar profiles for *leoA* and *tia* genes in the stomach. This result is in line with the fact that *leoA* is encoded in the same pathogenicity island, within *tia* locus and are assumed to be tightly regulated together (Fleckenstein et al., 2000). Although bile salts are important signal for inducing colonization factor genes expression, as previously shown (Sahl and Rasko, 2012; Nicklasson et al., 2012), the effect on *cfa/Ib* gene expression has not been investigated, as well as for *tia* and *fimH* genes (Sistrunk et al., 2016). Finally, we followed in the TIM-1 only, the sigma factor σ^S *rpoS* gene known as the general stress-response regulator in *E. coli* that contributes to the bacterial survival, for example under acidic pH conditions (Seo et al., 2015; Sun et al., 2012). In our study we did not observed an induction of *rpoS* gene during the gastric digestion. Altogether, ETEC virulence gene expression profiles in the successive gut regions offer a dynamic and representative overview on ETEC pathogenicity. Nonetheless, the complexity of the gene networks as well as the lack of information in the regulation of the virulence genes bring up to date the great interest to better decode such networks. Further adding the complexity are the profound variation in negative and positive correlations between the different virulence genes followed over time and in the different gut regions, questioning therefore how to improve the exploitation of such complex data?

5. Conclusion

In summary, the present study provides for the first time significant insights into the temporal and spatial modulation of ETEC survival and virulence in the human GI tract by combining the two most complete and well-controlled TIM-1 and M-SHIME systems worldwide. In particular we showed that:

- ETEC displays high capacity to modulate its membrane physiology according to the GI niches and is able to enter in an intermediate viability state to withstand the stringent acid conditions,
- The pathogen is attuned to the small intestinal conditions resulting in a growth renewal at the end of the jejunal and ileal digestion, confirmed by a restoration of ETEC membrane integrity and the return to a slight alkaline intracellular pH,
- The microbial bulk encountered in the M-SHIME ileum and ascending colon does not impede ETEC to colonize with success these gut regions in luminal and even more in mucosal microenvironments for all the six donors tested,
- At gene level, although the complexity in the regulation of the virulence network and the profound inter-individual variability, most of the virulence genes are switched on in the stomach and switched off in the TIM-1 ileal effluents and in a late post-infectious stage in the M-SHIME ascending colon,
- At protein level, ETEC is not able to produce the LT enterotoxin upon gastric condition while the toxin is produced in the ileum and at highest amount in the ascending colon, with however an inter-individual variability,

Further interactions of the pathogen with the gut microbiota and its metabolic activity are presented in the following chapter, chapter 3.

6. Candidate contribution and acknowledgements

Under supervision of Stéphanie Blanquet-Diot and Tom Van de Wiele, I designed the experimental work. I carried out the *in vitro* digestions (with technical support from Sandrine Chalancon, Sylvain Denis or my intern Florelle Deboudard) and *in vitro* fermentations (with technical support from Jana de Bodt). I carried out all the molecular-based experiments (q-PCR and PMA-qPCR) and developed the new protocols for the reverse transcription experiments according to the MIQE guidelines. Wessam Galia carried out the flow cytometry experiments. I processed the experimental data and performed the analysis in collaboration with Kim de Paepe. I drafted the manuscript and designed the figures. I wrote the manuscript with input from all authors. I will be first author of the future publication.

I would like to acknowledge Sylvie Alvarez and Karine Fayolle (VetagroSup) for welcoming us in the L3 laboratory during the TIM-1 experiments. I thank Pieter Van den Abbeele and Massimo Marzorati (Prodigest) for sharing their expertise in the set-up of the new ileum in the M-SHIME; Tim Lacoere (CMET) for assistance in the molecular techniques and Frederiek-Maarten Kerckhof for statistical support. I also thank the team of Prof. Filip Van Nieuwerburgh and especially Sarah De Keulenaer

(Department of Pharmaceutics) for welcoming me during the RNA quality control experiments and for providing me the Bioanalyzer. This research was funded by Lesaffre company (Marcq-en-Baroeul, France).

7. Supplementary data

Table S2.1. Daily secretion regime of the M-SHIME

The residence time in each simulated gut region is indicated in grey. Ⓟ: pumps

Gut region	Secretion delivery	1st cycle	2nd cycle	3rd cycle
Stomach	Nutritional medium 14mL min^{-1}	Ⓟ 9 – 9:30 9a.m – 10a.m	Ⓟ 5 – 5:30 5p.m – 6p.m	Ⓟ 1 – 1:30 1a.m – 2a.m
Duodenum-Jejunum	pancreatic juice and bile salts mixture 12mL min^{-1}	Ⓟ 10 – 10:15 10a.m – 12:30a.m	Ⓟ 6 – 6:15 6p.m – 8:30p.m	Ⓟ 2 – 2:15 2a.m – 4:30a.m
Ileum	5mL min^{-1}	Ⓟ 12 – 12:30 12:30a.m – 3:30p.m	Ⓟ 8 – 8:30 8:30p.m – 11:30p.m	Ⓟ 4 – 4:30 4:30a.m – 7:30a.m
Ascending colon	5mL min^{-1}	In Ⓟ 3:30 – 4:30 3:30p.m – +∞ Out Ⓟ 5:30 – 6:30	In Ⓟ 11:30 – 0:30 11:30p.m – +∞ Out Ⓟ 1:30 – 2:30	In Ⓟ 7:30 – 8:30 7:30a.m – +∞ Out Ⓟ 9:30 – 10:30

Table S2.2. Chemical composition of the nutritional medium delivered in the M-SHIME

Components	Amount (g L^{-1})
Monosaccharides	
Glucose	0.4
Fructose	0.5
Galactose	0.5
Disaccharides	
Maltose	0.5
Sucrose	0.5
Complex carbohydrates	
Pectin	2
Starch	3
Xylan	0.5
Glycosylated proteins	
Arabinogalactan	1.2
Mucin	3
Amino-acids and proteins	
L-cystein	0.5
Pepton	1
Yeast extract	3

Table S2.3. **Static *in vitro* gastro-jejunal digestion procedure**

Prior to introduction of the pathogen in the SHIME ileum, ETEC was pre-digested in a static batch incubation (Erlenmeyer), to reproduce the physicochemical parameters of a gastro-jejunal digestion, found in the TIM-1 system. Secretions were manually added and pH was manually controlled during the 180 min digestion.

Parameters of static *in vitro* digestion	**Gastric compartment**	**Duodenum-Jejunum**
pH	from 6 (T0) to 2.1	maintained at 6.8
Volume (mL)	50	90
Secretions	(**i**) 5.36 mg pepsin (727 U mg^{-1}) (**ii**) 4.28 mg lipase (32 U mg^{-1}) (**iii**) HCl 0.3 M (**iv**) $NaHCO_3$ 0.5 M if necessary	(**i**) 0.657 g bile extract + 0.168 g sodium cholate + 81 mg sodium deoxycholate (27.9 mM in solution) (**ii**) 1.8 g of pancreatin 4 USP (**iii**) Trypsin 2 mg mL^{-1} (**iv**) $NaHCO_3$ 0.5 M if necessary
Residence time (min)	30	150
Chyme mixing	magnetic stirrer	magnetic stirrer
[Total microbes]	sterile	sterile
Oxygen level (%)	20	20
Temperature (°C)	37 (incubator)	37 (incubator)

Table S2.4. **Log_2 fold change virulence genes expression in the TIM-1**

ILE: ileal effluents; STO: gastric effluents.

Replicate	Minutes post-infection	Gut Region	*eltB*	*estAB*	*leoA*	*tolC*	*fimH*	*tia*	*cfa/Ib*	*rpoS*
1	10	STO	-0,82	2,43	-0,19	-0,39	-0,19	0,04	2,10	0,14
1	20	STO	5,00	-0,47	0,89	0,99	1,73	2,32	0,54	0,83
1	60	STO	-1,87	0,06	-0,79	1,27	1,24	0,62	0,47	0,44
2	10	STO	0,08	3,54	1,04	0,96	1,04	-0,04	-1,61	0,81
2	20	STO	-0,38	0,79	1,86	0,22	1,18	3,19	0,61	0,07
2	60	STO	-1,36	0,87	1,28	0,23	-0,20	4,49	-0,01	0,48
3	10	STO	1,21	1,09	0,28	-0,12	0,28	-0,30	1,76	-0,45
3	20	STO	-3,03	0,69	0,08	-1,73	0,91	1,81	-2,26	-1,85
3	60	STO	-1,87	0,06	-0,79	1,27	1,24	0,62	0,47	0,47
4	10	STO	-0,47	1,65	-0,27	-0,35	-0,27	0,36	-2,19	-0,42
4	20	STO	-2,40	-0,65	0,08	-0,83	1,18	-0,75	0,75	-2,61
4	60	STO	-1,36	0,87	1,28	0,23	-0,20	4,49	-0,01	1,71
1	60	ILE	-1,24	-0,39	-0,63	-0,95	-0,63	-0,58	-0,11	-0,66
1	120	ILE	1,48	-6,78	-2,27	-2,64	-2,78	-3,02	-4,87	-2,59
1	180	ILE	-0,46	-6,33	-1,85	-2,89	-2,84	-6,35	-7,22	-2,88
1	240	ILE	-1,68	-6,70	-2,04	-3,75	-2,56	-5,58	-7,57	-2,42
1	300	ILE	-0,59	-5,65	-1,58	-2,44	-1,58	-5,54	-4,29	-1,66
2	60	ILE	0,01	0,71	0,91	0,76	0,91	0,53	-0,24	0,46
2	120	ILE	0,07	-6,49	-1,46	-3,18	-1,33	-1,11	-6,87	-1,62
2	180	ILE	1,36	-6,58	-2,00	-3,08	-1,60	-0,58	-4,93	-1,10
2	240	ILE	-1,37	-6,90	-2,95	-3,83	-2,56	-1,26	-7,89	-2,94
2	300	ILE	-1,30	-6,39	-1,92	-3,51	-1,73	-1,98	-7,38	-3,17
3	60	ILE	0,01	0,03	0,91	0,76	0,91	0,53	-0,24	0,46
3	120	ILE	1,92	0,02	-1,01	-2,55	-0,51	0,37	-4,54	-1,58
3	180	ILE	2,33	-2,19	0,94	1,00	1,80	2,32	0,78	1,18
3	240	ILE	0,11	-6,06	-2,32	-1,04	-0,65	-1,07	-3,59	-0,82
3	300	ILE	-1,30	-6,39	-1,92	-3,51	-1,73	-1,98	-7,38	-3,17
4	60	ILE	1,25	0,03	0,43	0,26	0,43	0,37	0,43	0,23
4	120	ILE	-0,98	-6,53	-2,75	-2,01	-0,91	-3,12	-4,78	-1,67
4	180	ILE	-0,55	-5,87	-1,40	-2,74	-0,54	-1,46	-6,61	-1,19
4	240	ILE	-2,05	-7,63	-1,77	-2,41	-1,17	-1,91	-4,92	-1,25
4	300	ILE	-1,55	-6,09	-7,10	-2,55	-2,55	-2,64	-3,68	-1,65

Table S2.5. **Log_2 fold change virulence genes expression in the M-SHIME**

ASC: Ascending colon; ILE: ileal effluents.

Donor	Hours post-infection	Gut Region	*eltB*	*estAB*	*leoA*	*tolC*	*fimH*	*tia*
1	1	ILE	-0.43	0.81	3.00	1.47	-1.62	-0.53
2	1	ILE	-0.74	-1.02	-1.83	-1.85	0.73	-0.64
3	1	ILE	1.17	0.21	-1.17	-0.13	0.89	1.17
4	1	ILE	-0.82	-0.26	-0.86	-0.68	-0.29	-13.29
5	1	ILE	0.82	0.26	0.86	0.68	0.29	-13.38
6	1	ILE	-0.92	-1.70	0.91	0.46	0.31	-0.74
1	3	ILE	-2.91	2.30	0.81	-1.24	0.19	-2.61
2	3	ILE	-2.25	2.68	2.19	-1.25	0.36	-2.50
3	3	ILE	3.94	1.67	1.51	0.31	-2.54	0.14
4	3	ILE	-3.23	0.83	-2.31	0.46	-3.20	-13.33
5	3	ILE	-5.45	-1.08	-3.10	0.97	-1.83	-13.09
6	3	ILE	-5.58	-1.84	-2.83	0.65	-2.06	-13.29
1	27	ILE	-9.99	-13.29	-9.72	0.95	-3.01	-13.12
2	27	ILE	-12.25	-17.61	-13.29	0.09	-5.67	-12.29
3	27	ILE	-10.44	-11.48	-13.81	0.35	-4.53	-5.73
4	27	ILE	-7.86	-13.28	-11.29	-0.45	-2.72	-11.48
5	27	ILE	-11.70	-8.43	-11.58	-2.07	-2.55	-12.77
6	27	ILE	-8.29	-10.57	-13.22	-11.29	-14.00	-13.29
1	5	ASC	-2.76	3.72	-2.98	0.18	-0.02	-13.38
2	5	ASC	2.77	3.58	-13.29	1.79	0.25	-13.02
3	5	ASC	2.22	2.24	-5.95	-0.24	-2.17	-8.08
4	5	ASC	2.49	-13.27	-1.34	1.78	1.37	-11.28
5	5	ASC	6.88	0.56	-3.99	0.37	-4.27	-11.29
6	5	ASC	3.36	0.91	-3.22	1.13	-3.09	-13.44
1	20	ASC	-4.28	4.00	1.43	0.19	-1.16	-13.29
2	20	ASC	-5.44	2.71	0.55	0.01	-0.35	-13.29
3	20	ASC	-5.36	2.26	-13.29	0.23	-0.85	-12.24
4	20	ASC	-2.56	-13.29	-2.32	1.06	-1.84	-9.72
5	20	ASC	-0.46	-13.21	-13.29	-0.02	-2.56	-13.80
6	20	ASC	-5.30	-13.25	-4.91	-0.39	-3.92	-13.01
1	29	ASC	-4.11	-13.19	-13.29	1.06	-2.15	-12.44
2	29	ASC	-6.92	0.82	-1.49	0.38	-0.75	-11.96
3	29	ASC	-13.29	-12.27	-16.34	-13.33	-11.46	-13.33
4	29	ASC	-16.61	-13.29	-14.49	-13.24	-13.29	-11.28
5	29	ASC	-19.95	-12.47	-19.29	-13.78	-13.67	-13.29
6	29	ASC	-19.93	-12.68	-11.29	-13.29	-13.80	-13.66

CHAPTER 3 : ETEC BEHAVIOR IN A SIMULATED DYNAMIC GUT MODEL IS MODULATED BY GUT MICROBIOTA IN AN INTER-INDIVIDUAL DEPENDENT WAY

ROUSSEL C., De PAEPE K., GALIA W., DE BODT J., CHALANCON S., DEBOUDARD F., LERICHE F., DENIS S., BALLET N., ALRIC M., BLANQUET-DIOT S., VAN DE WIELE T.

VAN DE WIELE T. and BLANQUET-DIOT S. are co- last authors.

***

For clarity, the manuscript under preparation for submission in PLoS Pathogen journal has been redrafted and redistributed in two chapters (chapter 2 and 3), presented here after.

To complete the data from the chapter 2 where ETEC colonization was displayed in the M-SHIME ileum and ascending colon, this chapter provides information on the microbial community composition and metabolic activity preceding and following ETEC infection; with an attempt to correlate the main ETEC virulence features with the microbial composition. In addition, the chapter gives a short description of the microbial community variation according to the donors and the gut region simulated (e.g. ileum and ascending colon).

3 ETEC behavior in a simulated dynamic gut model is modulated by gut microbiota in an inter-individual dependent way

Abstract ETEC is considered one of the leading pathogens associated with traveler's diarrhea. Diarrheal illnesses have been correlated with alterations in the human gut microbial composition, but up to now scarce studies have explored gut microbial changes during ETEC infection. Reversely, nothing is known on how gut microbiota may influence ETEC virulence. Since complex gut niches are difficult to access *in vivo* in humans, we used in the present study the sophisticated *in vitro* M-SHIME model to address these issues. The M-SHIME system was operated in order to monitor the microbial succession over the course of an ETEC infection in both the ileal and ascending colon compartments, using next-generation *16S* rRNA gene-based amplicon sequencing. Microbial populations of both luminal and mucosal microenvironments were characterized and inter-individual differences were captured by using six distinct fecal healthy donors. For the first time, the ileal signature was reproduced in the M-SHIME, characterized with a low community diversity and a low metabolic activity compared to the ascending colon. ETEC infection had no effect on the microbial diversity index but led to the bloom of opportunistic pathogens in the ileum such as *Klebsiella*, *Achromobacter* and *Mycobacterium* and decreased the species with potential health promoting functions in the ascending colon such as *Bifodobacterium* and *Fusicatenibacter*. At metabolic level, infection led to the increase of propionate concentration. Our study also provides for the first time a regression analysis between ETEC virulence features and gut microbiota populations in an attempt to better consider the susceptibility of ETEC infection for the six donors. Although the model was limited to the 5 h post-infection in the ascending colon, we observed that *eltB* encoding LT toxin co-occurred with *Coprococcus* and *Allisonella* genera, while at the opposite the LT toxin and the *estAB* gene encoding for the ST toxin strongly co-occurred with *Enterobacteriaceae*. LT production and *estAB* gene were also negatively associated with acetate and propionate production, while butyrate was positively correlated with LT production. With respect to traveler's diarrhea, there is mounting evidence that following a diarrheal episode, people may experience post-infectious irritable bowel syndrome (PI-IBS). As a relevant perspective to this work, we showed that ETEC infection significantly decreased the abundance of the actinobacterium *Collinsella aerofaciens* and *Bifidobacterium* members as often observed in the course of PI-IBS.

1. Introduction

Diarrheal illnesses related to ETEC annually affect millions of people worldwide. ETEC is considered one of the leading pathogens associated with traveler's diarrhea and severe diarrhea in children living in resource-limited settings (Giddings et al., 2016). In the classical paradigm for ETEC pathogenesis, the bacterium produces adhesins (e.g. CFA/I, Tia, FimH) promoting its attachment and colonization to host enterocytes in the distal part of the small intestine. At this site, ETEC delivers LT and/or ST enterotoxins that disrupt fluid and electrolytes homeostasis, leading to profuse watery diarrhea (Roussel et al., 2017; Fleckenstein et al., 2016). With respect to traveler's diarrhea, there is mounting evidence that following a diarrheal episode, people may experience post-infectious (PI) chronic sequelae ranging from functional GI disorder to irritable bowel syndrome (IBS) (Connor and Riddle, 2013; Barrett and Brown, 2016), to such extent that 10-14% of traveler's diarrhea associated ETEC cases result in IBS (Bourgeois et al., 2016).

During the last decade, high throughput *16S* rRNA gene-based sequencing technologies have been extensively used to profile the human intestinal microbiota in healthy and diseased individuals. A certain number of diarrheal illnesses have been correlated with alterations in the human gut microbial composition, a state known as dysbiosis. Such dysbiotic state is often characterized by an increase of some members in the *Firmicutes* and *Proteobacteria* phyla, and fewer members of *Bacteroidetes* (Schippa and Pia Conte, 2014). The overall decrease of bacterial diversity is another hallmark of dysbiosis. Next, a growing number of studies are exploring the duality of the gut microbiota component that can offer either resistance or assistance to colonization by enteric pathogens and may play a direct role in activating or inactivating virulence of pathogenic bacteria. Such microbial studies have predominantly involved *Clostridium difficile* and *Salmonella typhimurium*, to the detriment of other *E. coli* pathogens such as ETEC (Bäumler and Sperandio, 2016). In this respect, only three recent studies have explored the human gut microbial changes during the initiation and progression of ETEC diarrhea (Youmans et al., 2015; David et al., 2015; Pop et al., 2016). Moreover, no data are available at all on how the gut microbiota may influence ETEC virulence. The few studies available all relied on fecal samples and rectal swabs collected from patients that experienced an ETEC episode, or in the course of a clinical trial where healthy adults have been challenged with an infra-physiological dose of ETEC (5 to 6 $\log_{10}$ CFU per dose) compared to the classical infectious dose ranging from 6 to 8 $\log_{10}$ (Youmans et al., 2015; David et al., 2015; Pop et al., 2016).

While fecal samples are most often used to study the human gut microbiota, it is generally accepted that fecal microbial communities fundamentally differ from microbial communities residing in other locations in the GI tract. Indeed, the microbial abundance, composition and metabolic activity is regionalized and orchestrated by the chemical, nutritional, and immunological gradients along the gut. In addition to this longitudinal axis, the human gut microbiota varies in the cross-sectional direction from the mucosal to the luminal microbiota with considerable differences in composition and abundance (Thursby and Juge, 2017). On top of the regional variations, the gut microbiota is unique to each

individual and highly variable between individuals, especially at genus and species levels (The human microbiome project consortium, 2012; Turnbaugh et al., 2007).

Taken together, these unique and complex gut niches are difficult to access *in vivo* in humans. Therefore, sophisticated *in vitro* dynamic gut models can address such issues. The M-SHIME, a series of bioreactors can for instance be used to cultivate a complex fecal microbiota under controlled environmental conditions. The M-SHIME reproduces the physiological conditions in the distal part of the small intestine, the proximal and distal part of the colon, as well as the luminal and mucosal microbial niches.

In the present study, we operated the M-SHIME system in order to monitor the regionalized gut microbial succession over the course of an ETEC infection, using next-generation *16S* rRNA gene-based amplicon sequencing. Microbial populations of both luminal and mucosal part of the ileum and ascending colon were characterized and inter-individual differences were captured by assessing six distinct fecal healthy donors. Finally, we also attempted to give insights into ETEC-disease susceptibility by matching the microbial profiles and virulence profiles (virulence profiles were shown in chapter 2).

2. Materials and methods

2.1 ETEC strain, media and growth conditions

The strain serotype and culture conditions are described in chapter 2, section 2.1.

2.2 M-SHIME fermentation system

The experimental set-up, the inoculation and operation of the M-SHIME and the sampling are described in chapter 2, section 2.3.

For a good understanding: although the host cells are lacking, we tried to simulate the start of an infection process, and for this purpose we named the day of ETEC inoculation into the SHIME as “infection”.

2.3 Gut microbes quantification

Gut microbes were quantified in both the ileum and ascending colon: (i) the number of cultivable bacteria was determined by direct plating onto Brain Heart Infusion (BHI) agar (Sigma, Diegem, Belgium) at 37°C aerobically and anaerobically, after appropriate dilution in sterile saline water; (ii) total bacterial *16S* rRNA gene copy number was quantified by qPCR with 338F and 518R total bacterial primers amplifying the V3 region, synthesized by Biolegio (Nijmegen, The Netherlands) (Ovreas et al., 1997). The qPCR procedure was performed as described by Geirnaert et al., 2015. A standard was generated by cloning the 63F-1378R amplicon obtained from *Bifidobacterium breve* JCM 7019 into a pCR2.1®-TOPO®TA vector in *E. coli* by means of the TOPO®TA kit for subcloning (Promega, Madison, WI, US) (Lane, 1991). Transformed colonies were selected based on ampicillin resistance and lacZ blue-white screening and clones with a correct insert were cultured overnight in liquid LB medium containing 50 ppm ampicillin at 37°C. Plasmid DNA was extracted with the PureYield*TM* Plasmid Miniprep kit (Promega, Madison, WI, US) and the concentration was measured with a NanoDrop spectrophotometer (Thermo Fisher

Scientific, San José, US) and calculated back to the *16S* rRNA gene copy number, which amounted $2x10^{10}$ copies μL^{-1}. A tenfold dilution series of the standard (10^3 to 10^8) was analyzed in a preliminary test. The 10^8 standard dilution was omitted, because the amplification curves coincided with those of a negative control (PCR mix without addition of a sample). The quantification limit was 10^3 copies μL^{-1}.

2.4 SCFA production

Luminal samples from the M-SHIME were diluted 1:2 with miliQ water to a total volume of 2 mL. SCFA production was measured using capillary gas chromatography coupled to a flame ionization detector after diethyl ether method extraction, as described by Andersen et al. (2014). The concentrations of acetate, propionate, butyrate, isobutyrate, valerate, isovalerate, caproate and isocaproate were determined in each sample. The sum of all SCFA was noted “total amount of SCFA” and the total of isobutyrate, isovalerate and isocaproate was called “total branched”. SCFA concentrations were expressed in mM.

2.5 Microbial community analysis

Next-generation *16S* rRNA gene amplicon sequencing of the V3-V4 region (341F-785R) was performed by LGC Genomics (Teddington, Middlesex, UK), on an Illumina MiSeq platform using Illumina V3 chemistry (Illumina, Hayward, CA, US), as detailed in De Paepe et al. (2017).

Bioinformatics analysis of amplicon data. The mothur software package (v.1.40.5) and guidelines were used to process the Illumina amplicon sequencing data generated by LGC Genomics (Kozich et al., 2013). In short, after assembling forward and reverse reads, contigs with a length between 400 and 428 bases were aligned to the mothur formatted silva_seed release 123 alignment database, trimmed between positions 6388 and 25,316, to be compatible with the 341F-785R primers (Quast et al., 2013). After removing non-aligning sequences as well as sequences containing homopolymer stretches of more than 12 bases, sequences were pre-clustered allowing up to 4 differences. UCHIME was applied to remove chimera (Edgar et al., 2011). Subsequently, sequences were classified, by means of a naive Bayesian classifier, against the silva taxonomy database, version v132 with a 80% cutoff for the pseudobootstrap confidence score. Only bacterial sequences were retained and binned into Operational Taxonomic Units (OTUs) within each order identified by the preceding classification step, using the splitmethod “classify” option (Chen et al., 2013; Schloss and Westcott, 2011; Schloss et al., 2009). The 3% dissimilarity level shared file was selected for further analysis. An OTU is, hence, defined in this manuscript as a collection of sequences with a length between 400 and 428 nucleotides that are found to be more than 97% similar to one another in the V3-V4 region of their *16S* rRNA gene (Schloss et al., 2009; Schloss and Westcott, 2011; Wang et al., 2012; Chen et al., 2013). About 40,088 OTUs were identified in the 224 samples. Finally, taxonomy assignment was obtained according to the silva.nr_v132 database (Wang et al., 2012; Quast et al., 2013). Figures in this manuscript display the RDP taxonomy. The shared file, containing the number of reads observed for each OTU in each sample, was loaded into R version 3.5.1 (2018-09-04) (R Core Team, 2016). Singletons, that is reads occurring only once in all samples were considered noise and were removed (McMurdie and Holmes, 2014). From the 40,088 reads, 7,877 were retained. For the most abundant OTUs the sequences retrieved from the 3%

dissimilarity level fasta file, obtained in mothur, were classified through the RDP web interface using the RDP SeqMatch tool. This restricts the database search to type strains with only near-full-length good quality sequences and blasted in NCBI against the *16S* rRNA gene sequences, selecting only type material, with optimization of the BLAST algorithm for highly similar sequences (accession date: September 2018) (Altschul et al., 1990; Wang et al., 2007; Cole et al., 2014). Although a certain level of uncertainty is introduced by classification to the species level based on short 300 bp reads, the best hit returned by both databases is used to refer to interesting OTUs in the results section of this article. In case inconsistencies were seen between the RDP SeqMatch tool and NCBI BLAST, no species level classification was mentioned. A more detailed overview of the RDP Seqmatch and NCBI BLAST results for the most abundant and significant OTUs (best hit as well as the next best hits) can be found in Table 3.1.

Table 3.1. **RDP Seqmatch and NCBI BLAST results for the most abundant species in the M-SHIME**
The similarity score (Sab), as calculated by RDP, and the NCBI BLAST output for the best hit and next best hit(s) is shown. The NCBI maximal score (not shown) equalled the total score for all displayed entries. Indicated in bold, the OTU numbers for which they have been replaced by the species names for the microbial analysis. NA= Not Available

		RDP	NCBI BLAST			
OTU	**Species**	**Sab**	**Total score**	**Query coverage (%)**	**E-value**	**Identity (%)**
1	*Escherichia/Shigella fergusonii*	1.000	787	100	0.0	100
	Escherichia/Shigella flexneri	1.000	787	100	0.0	100
	Shigella sonei	1.000	787	100	0.0	100
	Escherichia coli	1.000	787	100	0.0	100
	Escherichia vulneris	1.000	787	100	0.0	100
2	*Anaerovibrio lipolyticus*	0.771	638	99	0.0	94
	Selenomonas bovis	0.752	614	100	1e-175	93
3	***Klebsiella pneumoniae***	**0.969**	**782**	**100**	**0.0**	**99**
	Klebsiella quasipneumoniae	0.969	776	100	0.0	99
	Klebsiella variicola	0.964	NA	NA	NA	NA
	Serratia liquefaciens	NA	776	100	0.0	99
4	*Leclercia adecarboxylata*	1.000	787	100	0.0	100
	Enterobacter cloacae	0.983	787	100	0.0	100
	Enterobacter ludwigii	1.000	787	100	0.0	100
	Pantoea agglomerans	NA	787	100	0.0	99
	Enterobacter kobei	0.983	784	100	0.0	99
	Salmonella enterica	0.983	782	100	0.0	99
5	***Mitsuokella multacida***	**0.983**	**784**	**100**	**0.0**	**99**
	Mitsuokella jalaludinii	0.954	754	100	0.0	99
	Selenomonas bovis	0.814	630	99	1e-180	93
6	***Faecalibacterium prausnitzii***	**0.982**	**736**	**100**	**0.0**	**99**
	Gemmiger formicilis	0.716	569	100	7e-159	92
7	*Succinivibrio dextrinosolvens*	0.919	688	100	0.0	98
	Anaerobiospirillum succiniciproducens	0.646	540	100	2e-153	91
8	***Clostridium bolteae***	**1.000**	**741**	**100**	**0.0**	**100**
	Clostridium asparagiforme	0.923	986	100	0.0	98

9	***Veillonella dispar***	**0.968**	**776**	**100**	**0.0**	**99**
	Veillonella tobetsuensis	0.949	760	100	0.0	99
	Veillonella parvula	0.929	754	100	0.0	99
10	***Bacteroides fragilis***	**1.000**	**778**	**100**	**0.0**	**100**
	Bacteroides ovatus	NA	649	100	0.0	95
11	*Mitsuokella jalaludinii*	0.983	782	100	0.0	99
	Mitsuokella multacida	0.937	750	100	0.0	98
12	***Bacteroides dorei***	**1.000**	**778**	**100**	**0.0**	**100**
	Bacteroides vulgatus	0.951	756	100	0.0	99
13	***Pseudomonas aeruginosa***	**1.000**	**787**	**100**	**0.0**	**100**
	Pseudomonas guezennei	NA	776	100	0.0	99
14	***Faecalibacterium prausnitzii***	**0.918**	**713**	**100**	**0.0**	**99**
	Gemmiger formicilis	0.735	592	100	7e-169	93
15	***Bacteroides thetaiotaomicron***	**1.000**	**778**	**100**	**0.0**	**100**
	Bacteroides faecichinchillae	0.947	756	100	0.0	99
	Bacteroides faecis	0.935	739	100	0.0	98
16	***Bacteroides uniformis***	**1.000**	**778**	**100**	**0.0**	**100**
	Bacteroides rodentium	0.906	717	100	0.0	97
17	*Acidaminococcus fermentans*	0.925	737	100	0.0	98
	Acidaminococcus intestini	NA	671	100	0.0	95
18	***Clostridium butyricum***	**1.000**	**741**	**100**	**0.0**	**100**
	Clostridium saccharobutylicum	0.941	719	100	0.0	99
19	*Citrobacter freundii*	0.990	782	100	0.0	99
	Citrobacter brakii	0.971	771	100	0.0	99
20	***Acidaminococcus intestine***	**1.000**	**787**	**100**	**0.0**	**100**
	Acidaminococcus fermentans	0.885	704	100	0.0	96
21	***Gemmiger formicilis***	**1.000**	**741**	**100**	**0.0**	**100**
	Subdoligranulum variabile	0.959	719	100	0.0	99
22	*Bacteroides timonensis*	NA	761	100	0.0	99
	Bacteroides cellulosilyticus	0.934	750	100	0.0	99
	Bacteroides intestinalis	0.888	739	100	0.0	98
23	***Eubacterium rectale***	**0.949**	**741**	**100**	**0.0**	**100**
	Roseburia faecis	0.941	713	100	0.0	99
	Roseburia intestinalis	0.892	939	100	0.0	98
24	***Parabacteroides distasonis***	**0.971**	**778**	**100**	**0.0**	**100**
	Parabacteroides gordonii	0.672	756	100	2e-174	93
	Parabacteroides faecis	0.613	601	100	1e-171	92
25	*Bacteroides ovatus*	0.978	773	100	0.0	99
	Bacteroides xylanisolvens	NA	730	100	0.0	98
26	***Phascolarctobacterium faecium***	**1.000**	**787**	**100**	**0.0**	**100**
	Phascolarctobacterium succinatutens	0.734	632	100	0.0	93
27	***Clostridium perfringens***	**1.000**	**741**	**100**	**0.0**	**100**
	Eubacterium tarantellae	NA	691	100	0.0	98
28	*Mitsuokella jalaludinii*	0.935	704	100	0.0	96
	Mitsuokella multacida	0.886	673	100	0.0	95
	Selenomonas bovis	NA	675	100	0.0	95
29	*Bilophila wadsworthia*	0.973	NA	NA	NA	NA

	Desulfovibrio simplex	NA	604	100	9e-173	92
	Blautia faecis	**1.000**	**741**	**100**	**0.0**	**100**
30	*Blautia glucerasea*	0.926	726	100	0.0	99
35	***Bifidobacterium longum***	**0.985**	**750**	**100**	**0.0**	**100**
	Bifidobacterium breve	0.918	NA	NA	NA	NA
	Prevotella copri	0.851	717	100	0.0	97
40	*Prevotella oulorum*	0.751	640	100	0.0	94
	Prevotella salivae	0.749	606	100	2e-173	93
44	*Prevotella shahii*	0.712	NA	NA	NA	NA
	Bifidobacterium faecale	1.000	758	100	0.0	100
47	*Bifidobacterium adolescentis*	1.000	758	100	0.0	100
	Phascolarctobacterium succinatutens	**0.958**	**765**	**100**	**0.0**	**99**
49	*Phascolarctobacterium faecium*	0.724	638	100	0.0	94
	Eubacterium ventriosum	**0.961**	**726**	**100**	**0.0**	**99**
52	*Lachnospiraceae bacterium*	0.765	628	99	5e-180	95
	Marivita hallyeonensis	**0.964**	**730**	**100**	**0.0**	**99**
53	*Marivita roseacus*	0.940	719	100	0.0	99
	Enterococcus hirae	1.000	787	100	0.0	100
	Enterococcus villorum	1.000	787	100	0.0	100
55	*Enterococcus ratti*	1.000	787	100	0.0	100
	Enterococcus durans	1.000	787	100	0.0	100
	Achromobacter denitrificans	0.978	776	100	0.0	99
	Achromobacter pulmonis	0.978	776	100	0.0	99
60	*Achromobacter agilis*	NA	776	100	0.0	99
	Achromobacter xylosoxidans	0.958	776	100	0.0	99
	Clostridium aldenense	**0.964**	**730**	**100**	**0.0**	**99**
66	*Clostridium algidixylanolyticum*	0.835	NA	NA	NA	NA
	Lachnoclostridium pacaense	NA	708	100	0.0	99
	Fusicatenibacter saccharivorans	**1.000**	**741**	**100**	**0.0**	**100**
70	*Murimonas intestine*	0.856	669	100	0.0	97
	Synergistetes bacterium	**1.000**	**NA**	**NA**	**NA**	**NA**
72	*Cloacibacillus porcorum*	0.916	730	100	0.0	99
	Collinsella aerofaciens	**1.000**	**743**	**100**	**0.0**	**100**
79	*Collinsella bouchesdurhonensis*	NA	675	100	0.0	97
	Paraprevotella clara	**0.969**	**765**	**100**	**0.0**	**99**
81	*Paraprevotella xylaniphila*	0.685	604	100	0.0	93
	Sutterella wadsworthensis	**1.000**	**787**	**100**	**0.0**	**100**
85	*Sutterella stercoricanis*	NA	654	100	0.0	94
	Roseburia sp.	1.000	NA	NA	NA	NA
88	*Eubacterium eligens*	NA	625	100	6e-179	95
	Clostridium scindens	**1.000**	**741**	**100**	**0.0**	**100**
90	*Dorea longicatena*	NA	669	100	0.0	97
	Clostridium chromiireducens	NA	725	100	0.0	99
91	*Clostridium butyricum*	0.982	719	100	0.0	99
	Clostridium saccharobutylicum	NA	708	100	0.0	99
94	*Clostridium celerecrescence*	0.860	686	100	0.0	98
	Clostridium xylanolyticum	0.857	NA	NA	NA	NA

	Clostridium colinum	0.830	658	100	0.0	96
102	*Clostridium piliforme*	0.828	NA	NA	NA	NA
	Ruminococcaceae bacterium	1.000	NA	NA	NA	NA
103	*Oscillibacter ruminantium*	NA	573	100	2e-163	92
	Bacteroides caccae	**1.000**	**778**	**100**	**0.0**	**100**
104	*Bacteroides faecis*	0.850	723	100	0.0	98
	Klebsiella variicola	**0.983**	**782**	**100**	**0.0**	**99**
115	*Klebsiella pneumonia*	0.959	776	100	0.0	99
	Clostridium tertium	**1.000**	**741**	**100**	**0.0**	**100**
117	*Clostridium chauvoei*	0.985	736	100	0.0	99
	Oscillibacter valericigenes	0.778	617	100	1e-176	94
120	*Oscillibacter ruminantium*	0.745	606	100	2e-173	94
	Blautia luti	**0.987**	**736**	**100**	**0.0**	**99**
124	*Blautia stercoris*	0.926	691	100	0.0	98
	Alistipes shahii	**0.968**	**773**	**100**	**0.0**	**99**
127	*Alistipes finegoldi*	0.924	739	100	0.0	98
	Blautia obeum	**1.000**	**737**	**100**	**0.0**	**99**
131	*Blautia wexlerae*	0.916	686	100	0.0	98
	Bifidobacterium angulatum	**1.000**	**754**	**100**	**0.0**	**100**
151	*Bifidobacterium merycicum*	0.974	737	99	0.0	99
	Victivallis vadensis	**1.000**	**743**	**100**	**0.0**	**100**
160	*Caloramator proteoclasticus*	NA	331	99	2e-90	82
	Ruminococcus faecis	**1.000**	**741**	**100**	**0.0**	**100**
163	*Ruminococcus torques*	0.985	682	100	0.0	97
	Bacteroides eggerthii	**1.000**	**778**	**100**	**0.0**	**100**
166	*Bacteroides uniformis*	0.857	712	100	0.0	97
	Blautia coccoides	0.867	680	100	0.0	97
175	*Muricome intestine*	0.824	675	100	0.0	97
	Clostridium oroticum	0.810	669	100	0.0	97
	Mycobacterium moriokaense	0.915	701	100	0.0	98
201	*Mycobacterium grossiae*	NA	701	100	0.0	98
	Mycobacterium aquaticum	NA	701	100	0.0	98

OTU corresponding ETEC strain H10407. A phylogenetic placement analysis was performed, comparing the *16S* rRNA gene Illumina amplicon sequences to the ETEC H10407 *16S* rRNA gene reference sequence, downloaded from the NCBI database (FN649414.1). In a first step, the *16S* rRNA gene reference sequence was trimmed to the V3-V4 region (341F-785R), which was used for Illumina MiSeq *16S* rRNA gene amplicon sequencing. The trimmed ETEC reference sequence was subsequently aligned to the amplicon sequences in mothur (align.seqs), yielding a report with the closest OTU based on kmer searching (Schloss et al., 2009). This report was loaded into R, version 3.5.1 (2018-07-02) (R Core Team 2016). From the report, the top 20 OTUs with the highest SearchScores were selected. A fasta file was constructed containing these OTUs, as well as, the trimmed ETEC reference sequence. RAxML was used to construct a maximum likelihood phylogenetic tree with the General Time

Reversible model of nucleotide substitution under the Gamma model of rate heterogeneity (GTRGAMMA) with the parsimony random seed set to 12345 (Stamatakis, 2014). A rapid bootstrap analysis starting from N=1000 distinct randomized maximum parsimony trees and search for best scoring ML tree was performed with rapid bootstrap random number seed 123. The best scoring ML tree was visualized in interactive Tree of Life (iTOL) (Letunic and Bork, 2016).

Statistical analysis of amplicon and metabolic data. All statistical analyses were performed in R, version 3.5.1 (2018–09-04) (R Core Team, 2016). All formal hypothesis tests were conducted on the 5% significance level. To visualize differences in microbial community composition between donors, ordination and clustering techniques were applied. For these purposes, the shared file was further processed to remove OTUs with too low abundance according to the arbitrary cutoffs described by McMurdie and Holmes (2014). An OTU should be observed in 5% of the samples and read counts should exceed 0.5 times the number of samples (McMurdie and Holmes, 2014). Rarefaction curves were constructed to assure that the samples were sequenced in sufficient depth (Oksanen et al., 2016). To deal with differences in sampling depth, proportional data transformed on the common scale to the lowest number of reads was used (McMurdie and Holmes, 2014).

Principle Coordinate Analysis (PCoA; package stats4_3.3.1) (Gower, 1966; Cailliez, 1983; Becker et al., 1988; Cox, 2001; Ramette, 2007) was conducted based on the abundance based jaccard dissimilarity matrix (package vegan_2.4–0) (Anderson et al., 2006; Borcard et al., 2011; Oksanen et al., 2016) and visualized with ggplot2_2.1.0 (Wickham, 2009). This procedure was repeated on species and genus levels focusing on the comparison between gut region (e.g. ileum lumen, ileum mucus, ascending lumen and ascending mucus), donor samples and the comparison between period (e.g. pre and post-infection). The pre-infection was from day 3 to 12 for the ileum, and 2 to 12 for the ascending colon. The post-infection in both gut regions was from day 13 to 20. On the genus level, weighed averages of genera abundances were a *posteriori* added to the ordination plot using the wascores function in vegan (Oksanen et al., 2016). To confirm the trends, observed data was clustered by means of an Unweighted Pair-Grouped Method using arithmetic Averages (UPGMA) clustering method (cluster_2.0.4) (Maechler et al., 2016). The significance of the observed group separation between gut region, donor and period conditions in the PCoA was assessed with a Permutational Multivariate Analysis of Variance (PERMANOVA) using distance matrixes (package vegan_2.4–0) (Ramette, 2007; Oksanen et al., 2016). Prior to this formal hypothesis testing, the assumption of similar multivariate dispersions was evaluated.

When comparing the effects, the influence of the gut region donor and period conditions was determined by applying a distance based redundancy analysis (db RDA) (Vardakou et al., 2007) using the abundance based jaccard distance as a response variable (vegan) (Ramette, 2007; Oksanen et al., 2016). The factor donor is used as a constraint with the effect of the gut region or period is being partialled out. Interpretation of the results is preceded by a permutation test of the RDA results to confirm that a linear relationship exists between the response data and the exploratory variables. The constrained fraction of the variance, explained by the exploratory variables is adjusted by applying Ezekiel's formula (Borcard et al., 2011).

In order to find statistically significant differences in species abundance between the different treatments (pre and post-infection), the DESeq package was applied as suggested by McMurdie and Holmes (2014) (Love et al., 2014; McMurdie and Holmes, 2014). The factors period, gut region and donor were used in the design formula. Statistical differences between the pre and post-infection were determined using a Wilcoxon Signed Rank Test on the proportional data. Statistical hypothesis testing to assess the effect of ETEC infection on the metabolic activity (SCFA) was performed by using the Kruskal–Wallis rank sum test, followed by Pairwise Wilcoxon Rank Sum Tests with Holm correction for multiple testing.

The evolution of the microbial community structure throughout the SHIME run was followed-up by computing richness (Chao 1) and diversity measures (Shannon, Simpson, inverse Simpson and Fisher α) on the DESeq normalized, unfiltered data (package vegan_2.4–4). To make an ecological choice, only Simpson index is shown since it gives more interpretable results than the others and is less sensitive to species richness and rare OTUs than Shannon index.

Sparse Partial Least Squares (sPLS) regression implemented in the R-package mixOmics was performed to select the taxonomic entities most predictive of LT toxin production and *eltB*, *estAB* gene expression. The initial model was built in regression mode with the LT toxin, *eltB*, *estAB* gene expression as response (Y) variables in function of the proportional read counts only at time point 5 h post-infection in the ascending colon (X). To ensure a predictive regression, this time point (5 h) was the only one having in common the *16S* illumina MiSeq, LT toxin production and virulence gene expression data. 2 Dimensions, 3 Y variables and 15 or 10 X variables at species, respectively, genus level were selected on each of the 2 components in the sparse model.

3. Results

This is the first report where the ileum part of the M-SHIME was developed to obtain a specific ileal microbial population that clearly differentiates from that in the ascending colon. The microbial populations in the different simulated environments all originated from the fecal microbiota from one human individual, but experimental set-up (detailed in chapter 2, section 2.3) allowed to discriminate transversally and longitudinally: ileum lumen, ileum mucus, ascending lumen and ascending mucus. The evolution of the microbial community composition preceding and following ETEC infection (on day 13) was therefore assessed in these four gut regions of six different fecal donors.

3.1 Microbial community signatures of the Ileum and ascending colon luminal/mucosal gut regions reproduced by the M-SHIME and inter-individual differences in donor gut microbiota

Gut regions determine microbial community variations. This section presents the results before ETEC infection, from day 2 to 12. The gut regionalization into the ileum and ascending colon compartments resulted in profound differences in microbiota composition and relative abundance, respectively dominated by *Proteobacteria* phylum in ileum lumen and *Firmicutes* and *Bacteroidetes* in ascending colon lumen (Fig. S3.1). In the mucosal niches, the ileum was dominated by *Proteobacteria* in donors 1, 2 and 5, while *Firmicutes* were dominant in donors 3, 4, 6 and in all donors in the ascending colon as well (Fig. S3.2A). At family and/or genus level, the ileum lumen was characterized by a high relative abundance of *Enterobacteriaceae* and *Klebsiella*, while donors 4 and 6 displayed an increase of *Anaerovibrio* (Fig. 3.1A). In contrast, the ascending colon lumen was dominated by *Bacteroides*, *Faecalibacterium*, *Lachnoclostridium* and *Prevotella* in most of the donors, except for donors 4 and 6 who displayed a high abundance of *Succinivibrio* genus. Interestingly, the mucosal niches had more variations in the relative abundance between donors, especially in ileum. For instance, donors 1 and 2 were dominated by *Klebsiella*, donor 3 by *Mitsuokella*, donors 4 and 6 by *Anaerovibrio* and donor 5 by *Enterobacteriaceae* (Fig. 3.1B). In the ascending mucus, a high relative abundance of *Lachnoclostridium* and *Bacteroides* was observed in donors 1, 2, 3 and 5, while donors 4 and 6 were dominated by *Succinivibrio* (Fig. 3.1B). Results at species level are presented in supplementary data (Fig. S3.1B, Fig. S3.2B). All donors displayed a remarkable less diverse microbial community in both ileum lumen and mucus compared to the ascending colon lumen and mucus, as shown by the Simpson diversity estimator (Fig. 3.2). In the ileum, even though we performed a retrograde low dose microbial inoculation from the ascending colon, we found a surprising high bacterial concentration based on *16S* rRNA gene quantification with about 10 $\log_{10}$ copy number mL^{-1} over time for all donors (2h30 after feed arrives in the ileum) (Fig. S3.3), while the number of culturable bacteria was near to 8 $\log_{10}$ CFU mL^{-1}. However, the ileal samples taken at earlier time points of the fed state (30 min after feed arrives in the ileum), displayed lower concentrations (7.2 $\log_{10}$ copy number mL^{-1}, data not shown) compared to the 2h30 post-feeding.

Statistical analysis with first PCoA performed at genus and species levels indicated that gut region and donor are important factors determining the grouping of samples (Fig. S3.4). Further test applying

a db-RDA analysis, a robust method for testing group dissimilarities confirmed that gut region accounted largely and significantly (19.5%, *p*= 0.001) to the observed patterns in microbial community variability at genus level (Fig. 3.3A and B). *Bifidobacterium*, *Faecalibacterium* and *Bacteroides* genera were mostly represented in the ascending colon centroids, while *Enterobacteriaceae*, *Veillonella*, *Mitsuokella*, *Clostridium* and *Anaerovibrio* displayed higher abundance in the ileum centroids (Fig. 3.3A). The factor 'donor' was the second most important contributor (5.8%, *p*= 0.001) to the microbial composition dissimilarities (Fig. 3.3B). Among the six donors, the centroids of the two vegetarians (donors 3 and 5) are distant and displayed different community composition. *Veillonella* was primarily related with donor 5, which displayed no similarity to the other donors. The centroid of donor 3 is closer to the donors 1 and 2 (two women) where *Mitsuokella*, *Bacteroidetes* and *Enterobacteriaceae* were predominantly retrieved. Finally the close proximity of the two men (donors 4 and 6) displayed similar community composition with a preponderance for *Succinivibrio* and *Anaerovibrio* genera compared to the other donors (Fig. 3.3B, Fig. S3.4). Further information on donor characteristics are found in chapter 3, Table 2.

Gut regions determine metabolite profiles. The observed changes in microbial community composition between ileum and ascending colon is also indicative of a differential bacterial metabolism displaying over time a significantly low SCFA concentration in the ileum compared to the ascending colon (Fig. S3.5). Total SCFA concentration in the ileum remained below 20 mM and acetate contributed essentially to this production, while the ascending colon displayed high total SCFA concentration ranging from 40 to 60 mM with about 25 mM acetate, 13 mM propionate, 8 mM butyrate and 1.5 mM total branched (Fig. S3.5). Interestingly, higher concentration of propionate was observed in donor 4 and 6, while the concentration of valerate was slightly higher in donor 2 (Fig. S3.5).

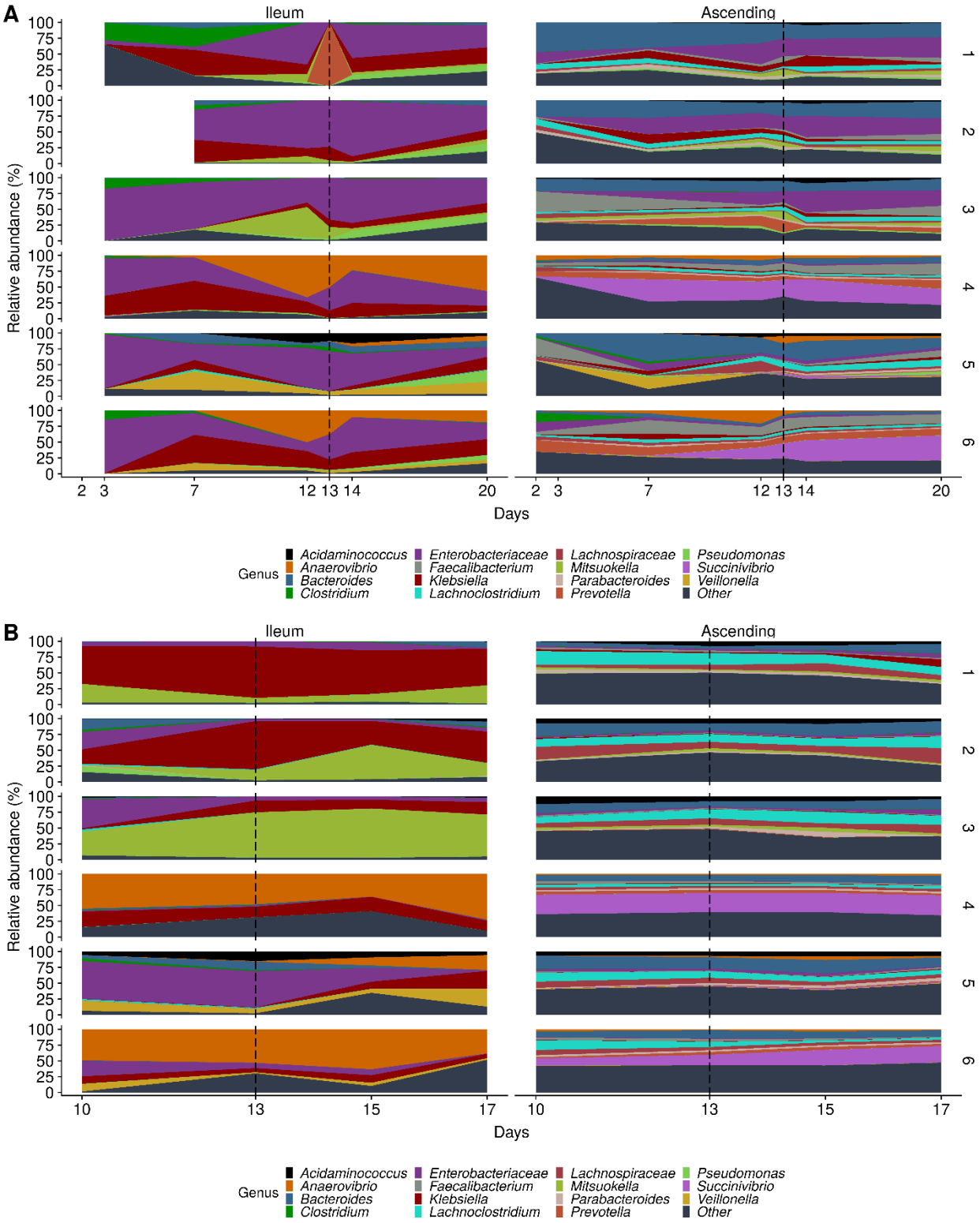

Figure 3.1. **Genus level microbial community composition of the ileum and ascending colon environments preceding and following ETEC infection, as determined by amplicon sequencing.** The area graphs show the relative abundance of the 15 most abundant genera in the (**A**) luminal, and (**B**) mucosal ileum and ascending colon from six different donors over the course of 20 days fermentation. ETEC infection is demarcated by the dashed line at day 13.

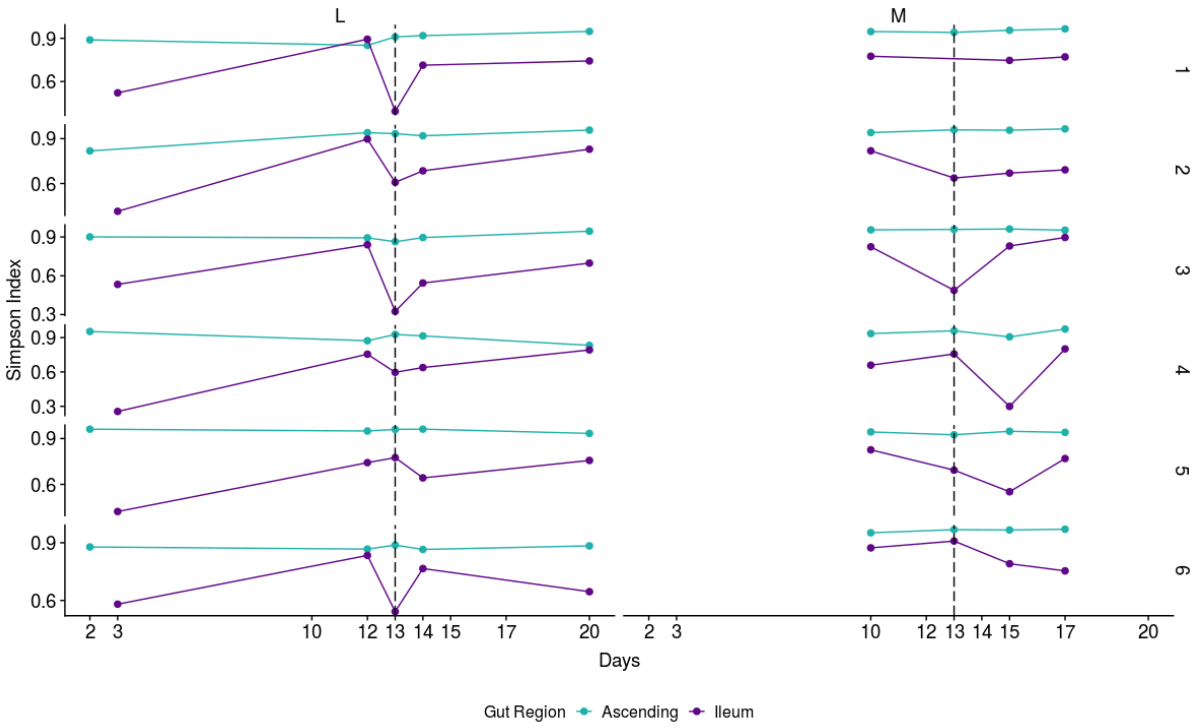

Figure 3.2. **Simpson diversity index over time for the six donors according to the luminal (L) and mucosal (M) gut regions, as determined by amplicon sequencing.** Simpson's Diversity Index is a measure of diversity which takes into account the number of species present, as well as the relative abundance of each species. It gives more weight to common or dominant species. The diversity index ranges between 0 (no diversity) and 1 (infinite diversity). ETEC infection is demarcated by the dashed line at day 13.

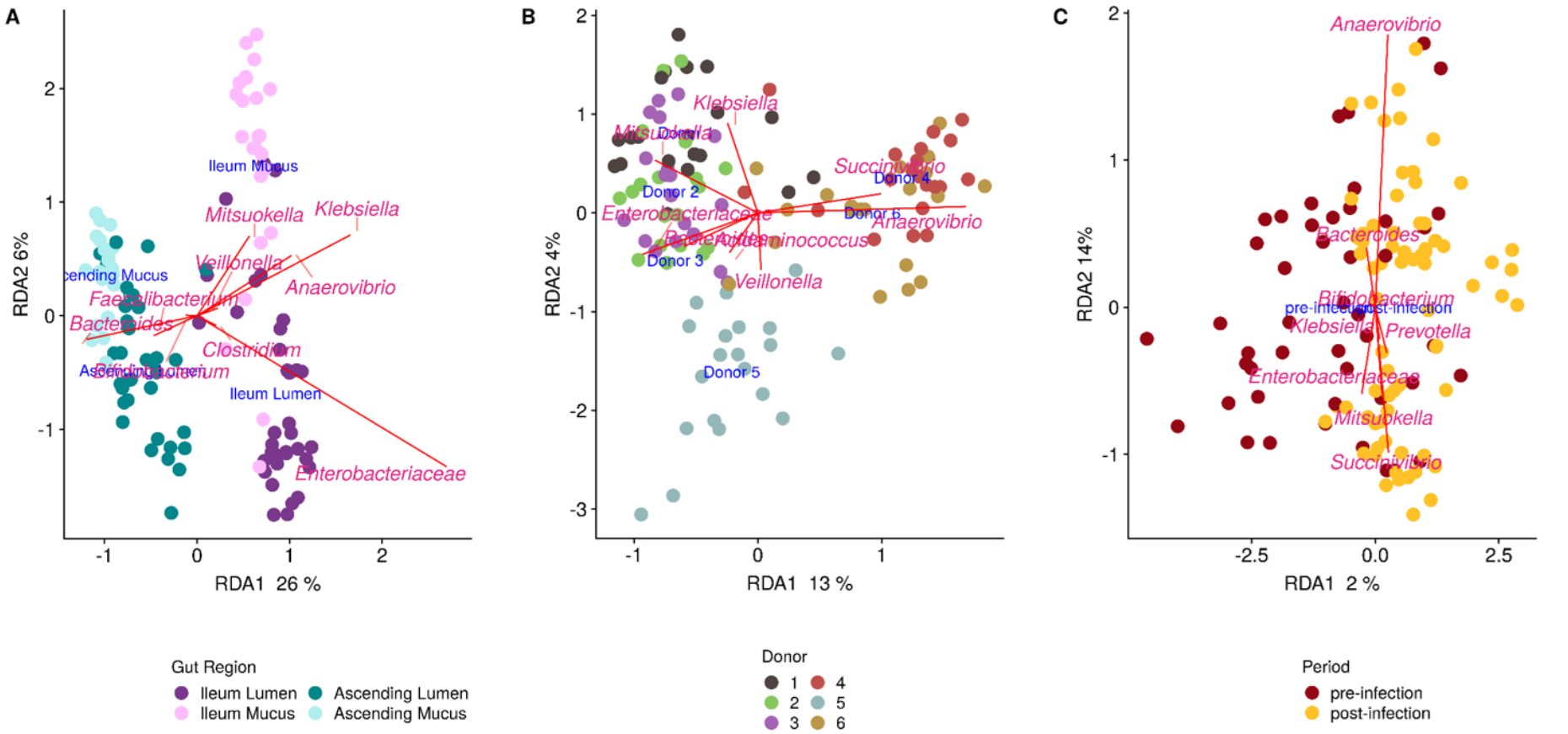

Figure 3.3. **Distance-based redundancy analysis (db-RDA) triplots showing the relationship of gut regions (A), donors (B) and period pre- *vs* post-infection (C) as explanatory variables to the microbial community structure at genus level.** Factor levels are represented as centroids in blue. Genus scores in pink show the direction of higher abundance of a particular genus. All factors significantly contributed to the variation of the microbial community structure at (**A**) 19.5% (p= 0.001); (**B**) 5.8% (p= 0.001); (**C**) 1.7% (p= 0.036).

3.2 Interactive effects of ETEC with the gut microbial niches

ETEC infection displays a significant effect on microbial community composition. Following ETEC infection (from day 13), an increase of *Enterobacteriaceae* was unsurprisingly observed in the ileum lumen for all donors. Interestingly, in donor 1 this was concomitant with a particularly sharp rise of *Prevotella* genus (Fig. 3.1A). In ascending lumen and mucus, as well as in ileum mucus the shift of microbial communities and/or the increase of *Enterobacteriaceae* was less evident, except for donors 1, 2, and 3 in ascending lumen (Fig. 3.1A and B). The supplementary figures also show the increase of *Proteobacteria* and OTU1 at phylum and species levels, respectively, in the ileum lumen from day 13 (Fig. S3.1A and B). In order to retrieve ETEC H10407 within the OTU catalog, a phylogenetic placement analysis was performed. As a confirmation to the previous paragraphs, OTU1 showed the highest similarity with ETEC and a clear upsurge of OTU1 was noticed at day 13 in ileum lumen (Fig. S3.6). In donors 1, 2 and 3 in the ileum strangely enough a sequence 100% identical to ETEC was already present before infection. However, *16S* rRNA gene of *Enterobacteriaceae* are phylogenetically very close and donors 1, 2 and 3 could have had a commensal species similar to ETEC H10407 prior to infection (Fig. S3.6B). Similar to gut region and donor, ETEC supplementation was an explanatory variable for dissimilarities in microbiota composition. It did so in a limited yet significant way (1.7%, p= 0.046) (Fig. 3.3C). The centroids pre and post-infection remain closely related which indicates that ETEC presence did not shift the overall microbiota composition (Fig. 3.3C).

ETEC infection leads to a bloom of opportunistic pathogens in the ileum. We used DESeq2 analysis to further investigate the changes in genus and species abundance between pre and post-infection periods in the different gut regions (Fig. 3.4, 3.5 and 3.6). Although ETEC infection has no direct effect on the microbial diversity in the different gut regions (Fig. 3.2), it resulted in a significant (12%, p< 0.05) global decrease of microbial species in all gut regions, and only 3.9% of the species were increased following ETEC infection (Fig. 3.4). In the ileum at species level, ETEC infection significantly stimulated, *Achromobacter* (OTU60), *Klebsiella variicola* (OTU115) and *Mycobacterium* (OTU201), while *Clostridium tertium* (OTU117) abundance was dropped (Fig. 3.6). In the ascending colon, ETEC infection was associated with an upsurge of *Prevotella* (OTU40, 44), *Paraprevotella clara* (OTU81), *Clostridium scindens* (OTU90), *Victivallis vadensis* (OTU160), *Bacteroides eggerthii* (OTU166) and *Gastranaerophilales* family (OTU248) (Fig. 3.6). Many OTUs were significantly decreased such as *Gemmiger formicilis* (OTU21), *Eubacterium ventriosum* (OTU52), *Fusicatenibacter saccharivorans* (OTU70), *Bacteroides caccae* (OTU104), *Oscillibacter* (OTU120), *Blautia luti* (OTU124), *Alistipes shahii* (OTU127), *Blautia obeum* (OTU131), *Bifidobacterium angulatum* (OTU151), *Ruminococcus faecis* (OTU163) (Fig. 3.6). Only *Escherichia* (OTU1) was stimulated in the ileum and ascending colon, while *Clostridium butyricum* (OTU18), *Citrobacter* (OTU19), *Bifidobacterium* (OTU47), *Collinsella aerofaciens* (OTU79) and *Clostridium* (OTU91) were decreased in both gut regions (Fig. 3.6).

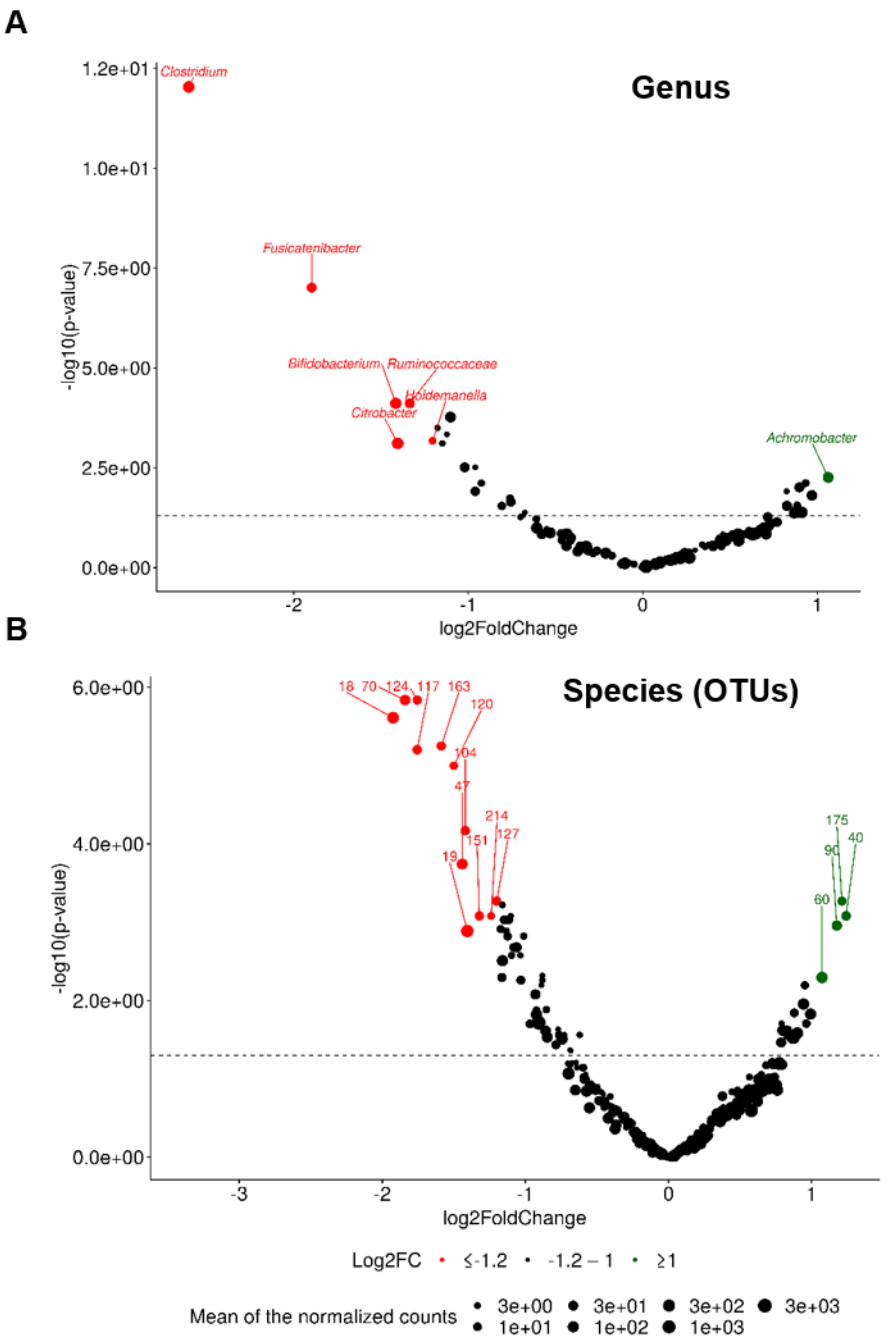

Figure 3.4. **Log_2 Fold Change of normalized (A) genus and (B) species abundances between the pre and post-infection phases microbial community composition under the control condition.** A positive log_2 Fold Change indicates a stimulation of the genera in the post-infection period (in green) compared to a negative log_2 Fold Change which indicates a stimulation of the genera in the pre-infection period (in red). The log transformed adjusted p-value is displayed on the y-axis and the $\alpha = 0.05$ significance level is indicated by a dashed line.

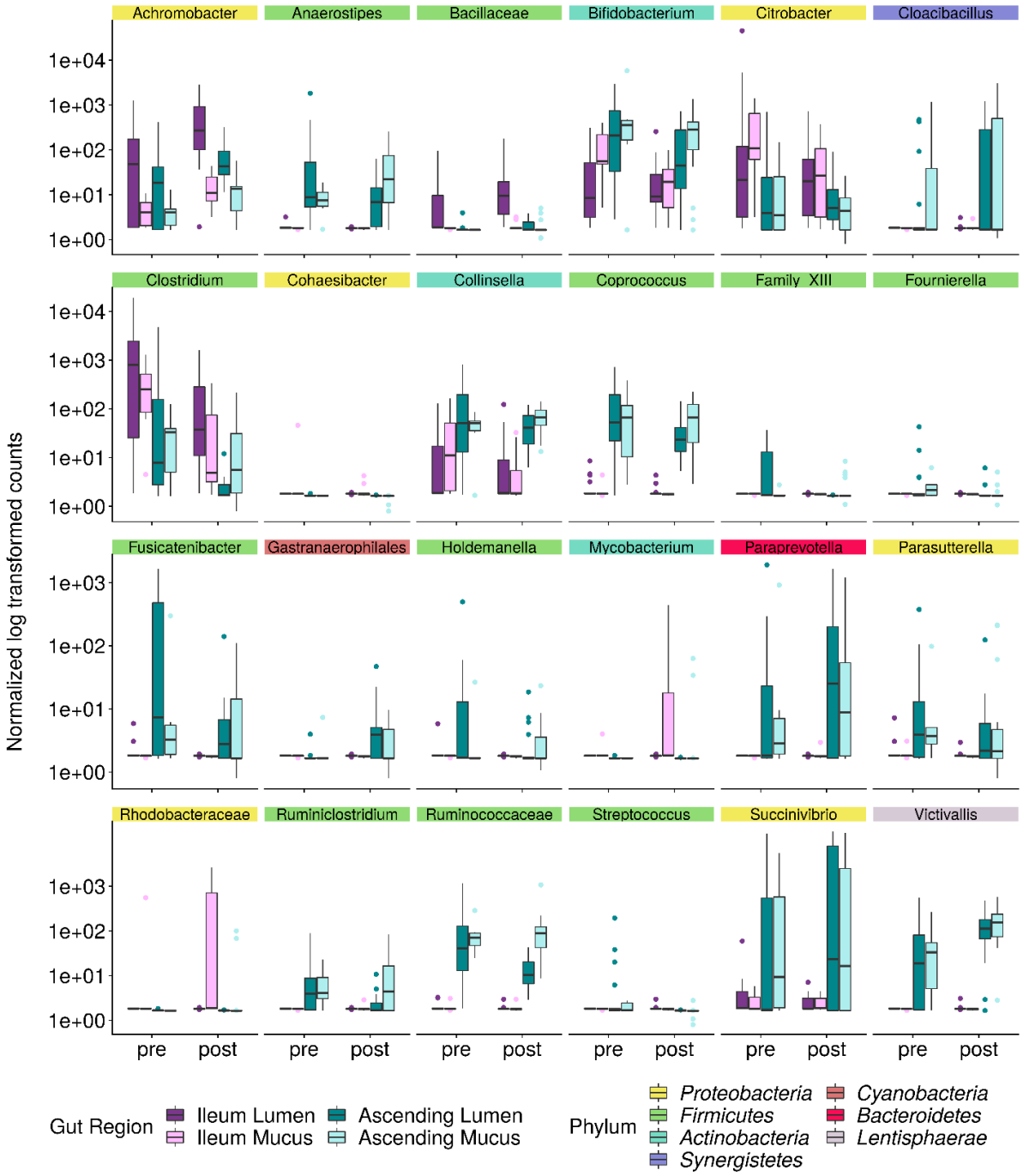

Figure 3.5. **Significant differences in genus level abundance between pre and post infection period.** The abundance is displayed for the different gut regions. Coloured labels indicate the phylum classification of the respective genera.

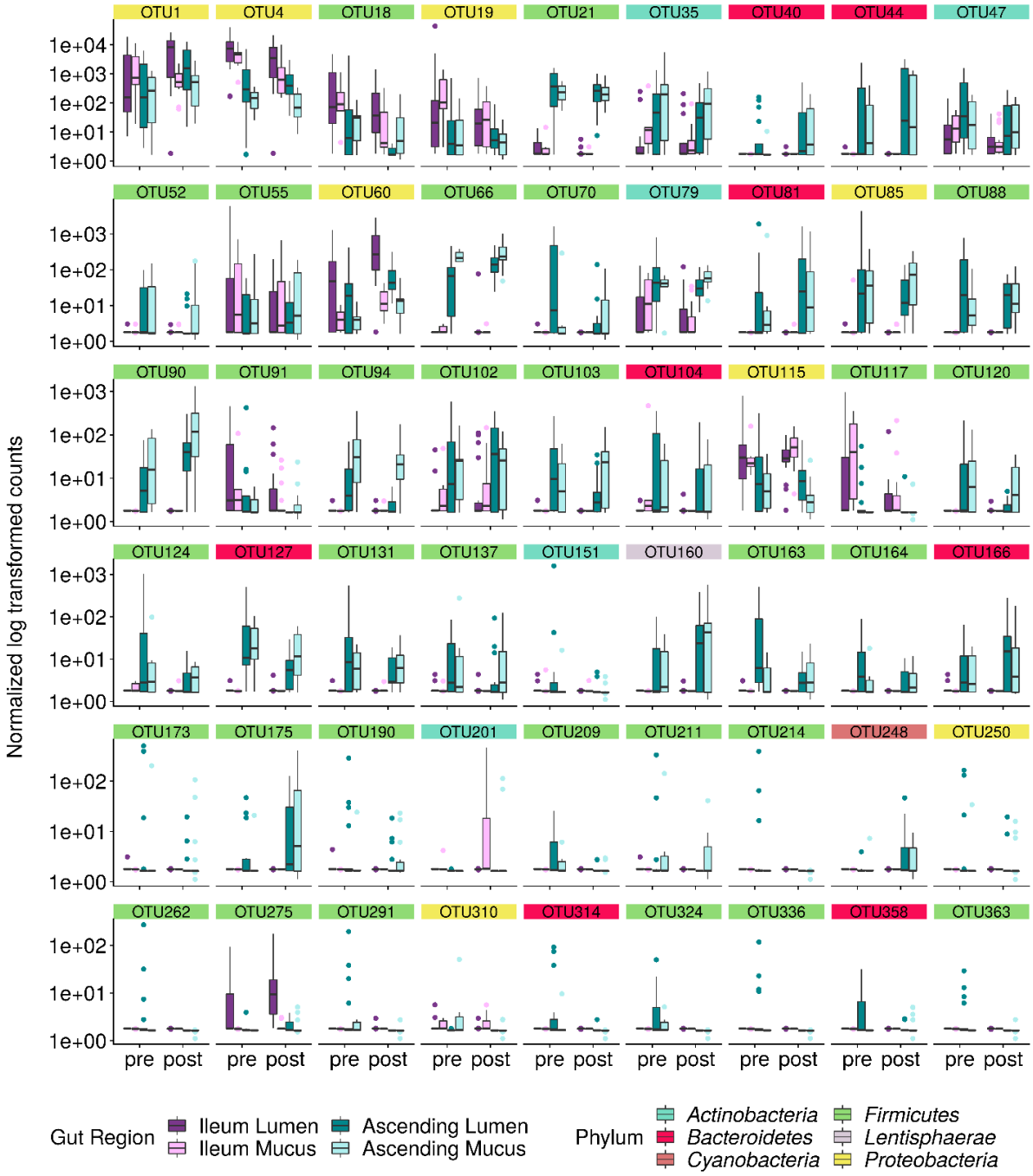

Figure 3.6. **Significant differences in species level abundance between pre and post infection period.** The abundance is displayed for the different gut regions. Coloured labels indicate the phylum classification of the respective OTU.

ETEC infection modulates the microbial metabolic activity by increasing the propionate concentration in ileum and ascending colon. Besides effects on community composition, ETEC infection had an impact on the fermentation activity in both ileum and ascending colon (Fig. 3.7 and 3.8). Following infection, a significant increase of the average propionate ratio was observed in both gut regions (p= 0.07), with a decrease of the average acetate ratio (p= 0.01) only noticed in the ileum (Fig. 3.7). Figure 4.8 shows the inter-individual variability of the difference average of SCFA concentrations between pre- and post-infection. Following ETEC infection in the ileum, a significant increase of propionate levels (p= 0.003) was noticed for donors 4, 5 and 6. In contrast, a slight increase of acetate was seen for donors 1, 2, 3. Next in the ascending colon, the infection displayed stronger changed on SCFA concentrations, especially a significant increase of propionate for donors 2, 4 and 5 (p= 0.01) up to 5.6 mM increase. In contrast, acetate tended to decrease and butyrate concentration was significantly decreased (p= 0.04) especially for donors 1, 5 and 6. Finally, no change in the branched fatty-acid concentration was seen (Fig. 3.8). Next, we examined the existing correlations between SCFA concentrations and ETEC survival and virulence (Fig. 3.9). No significant correlations were found in the ileum. In the ascending colon, acetate and propionate displayed significant and negative correlations with LT toxin production and *estAB* gene expression (encoding for the ST toxin); while butyrate was positively correlated with LT production (Fig. 3.9).

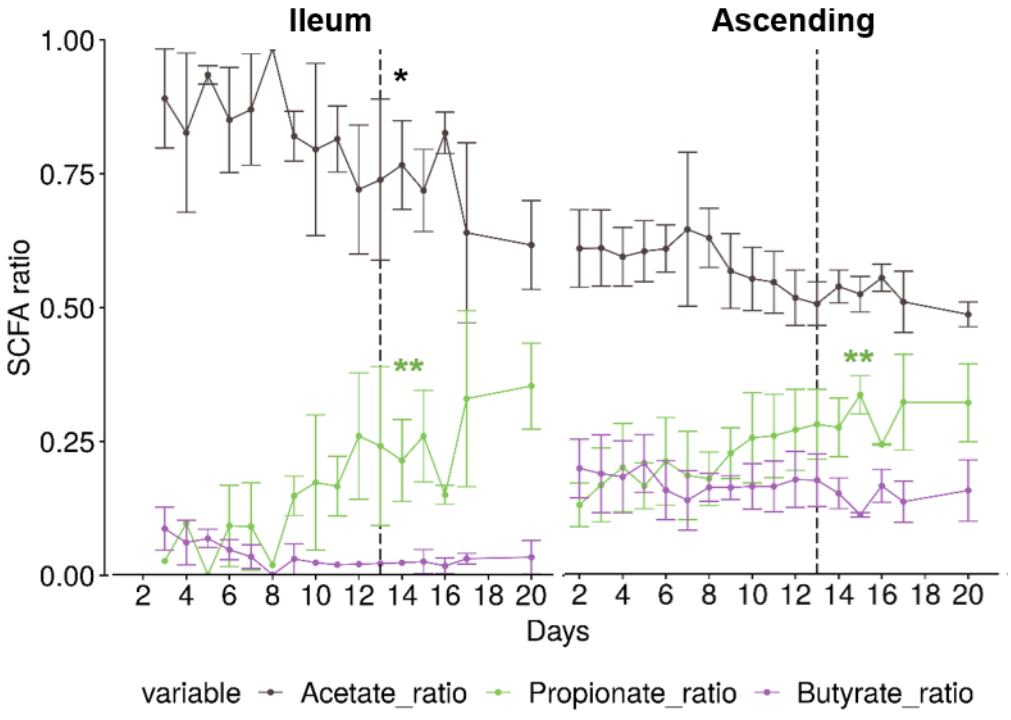

Figure 3.7. **Mean SCFA ratios in the ileum and ascending colon compartments over time.** For the statistics, SCFA concentrations displaying stability from day 9 to 12 were retained as the pre-infection period, and from day 13 to 20 as the post-infection period. The figure represents the mean of 6 donors ± SD. Statistically significant differences between pre and post-infection periods are denoted for at p< 0.05 (*) and p< 0.01 (**) as determined by Pairwise Wilcoxon Rank Sum Tests with Holm correction.

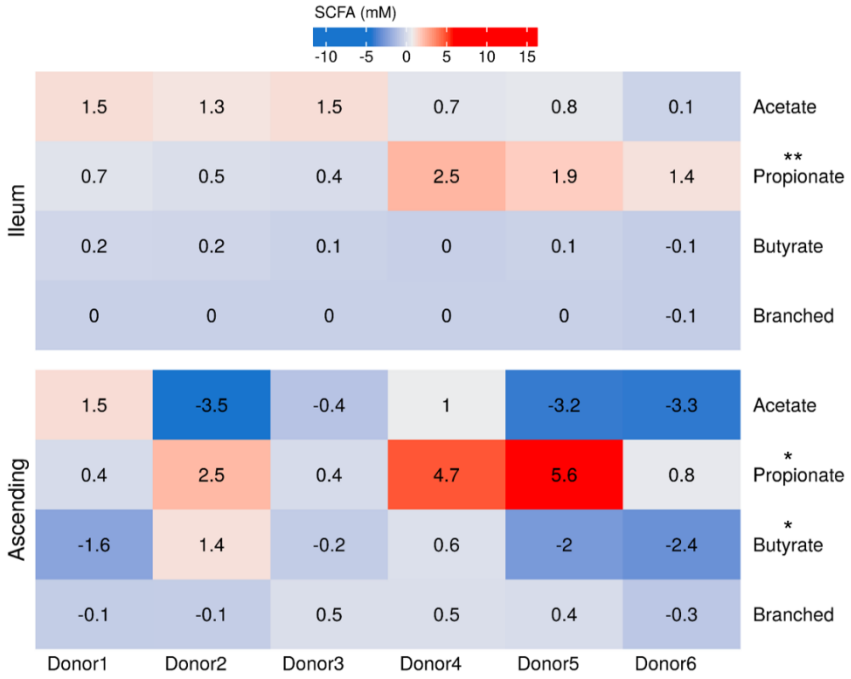

Figure 3.8. **Difference in average concentration of SCFA between pre and post-infection periods in the ileum and ascending colon for the six donors.** For the statistics, SCFA concentrations (mM) displaying stability from day 9 to 12 were retained as the pre-infection period, and from day 13 to 20 as the post-infection period. Statistically significant differences between pre and post-infection periods are denoted at $p< 0.05$ (*) and $p< 0.01$ (**) as determined by Pairwise Wilcoxon Rank Sum Tests with Holm correction.

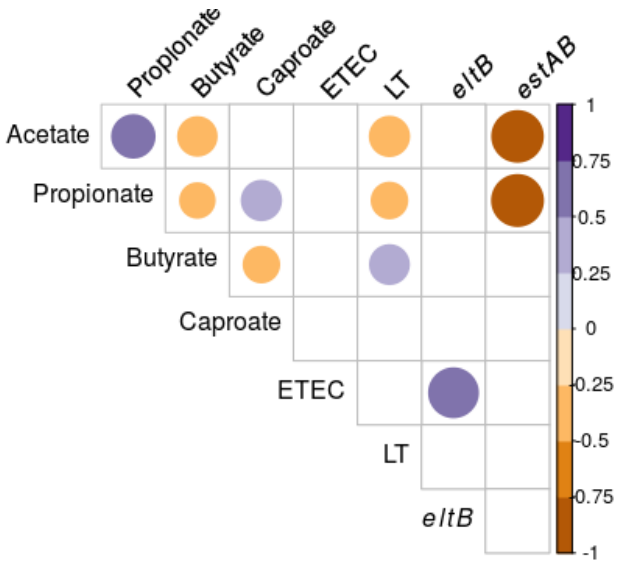

Figure 3.9. **Spearman correlations between the main SCFA produced in the ascending colon and ETEC survival, LT toxin production, and the expression of virulence genes encoding for the enterotoxins.** The correlation is made only for the post-infection period. Significant negative and/or positive correlations are denoted by the circles ($p< 0.05$).

Co-occurrence between virulence features and gut microbiota as an attempt to predict susceptibility to ETEC infection. Combining microbial community composition data and ETEC virulence profiles applying PLS regression, confirmed the donor-based clustering of samples. To give a more representative picture and ensure a predictive model, only the time point 5 h post-infection in the ascending colon was retained in the model. This time point corresponds to the most interesting response in term of virulence gene expression and toxin production for the six donors, as previously shown in chapter 2. An sPLS model, retaining three virulence factors (LT enterotoxin, *eltB* and *estAB* genes), was used to select the 20 genera and 30 OTUs most predictive for the expression and/or production of the enterotoxin (Fig. 3.10, S3.7 and S3.8). *Enterobacteriaceae* (OTU1, ETEC), *Mitsuokella* (OTU11, OTU28), *Gastranaerophilales (*OTU248*)*, *Parabacteroides* and *Klebsiella* (OTU115, *Klebsiella variicola*) were associated with high LT toxin production and *estAB* gene over-expression, whereas *Coprococcus*, *Allisonella* and *Anaerovibrio* (OTU2) were positively correlated with *eltB* gene over-expression (Fig. 3.10, S3.7 and S3.8).

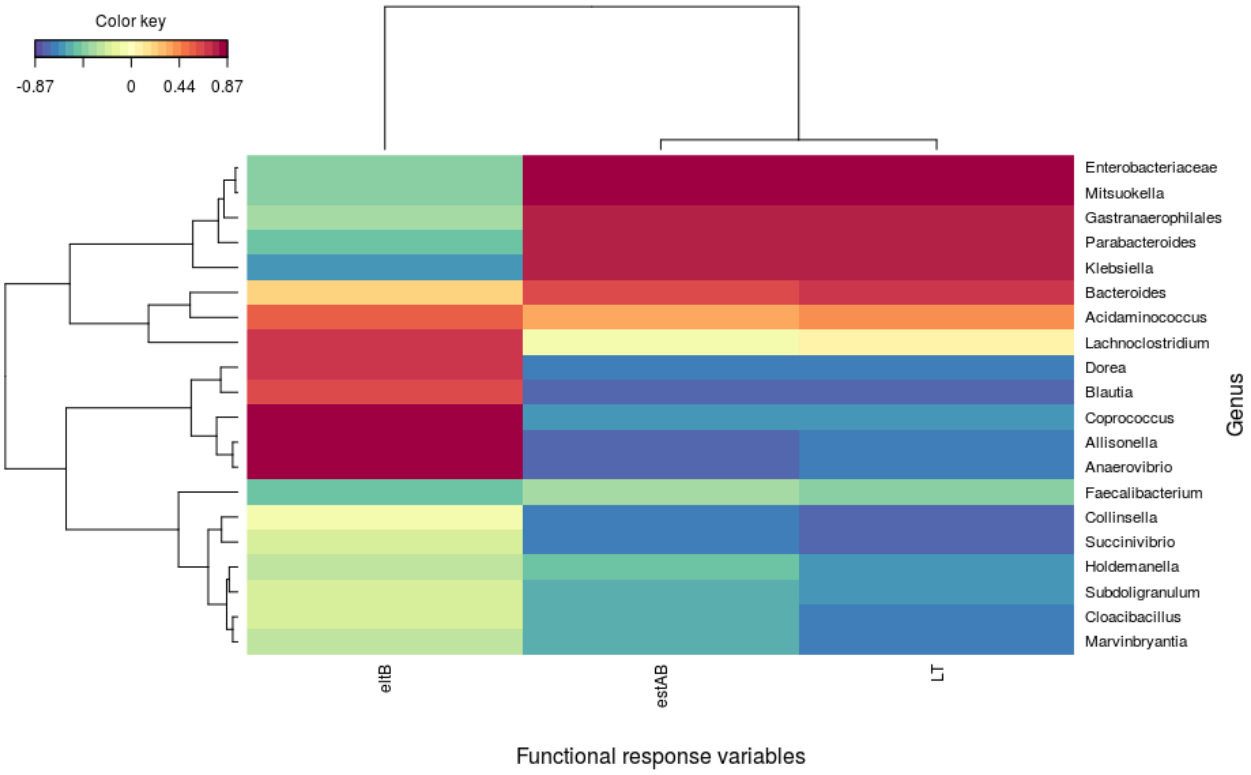

Figure 3.10. Heatmap representation of a sparse Partial Least Squares (sPLS) regression analysis of the ascending colon luminal microbial community composition data at genus level and the main virulence features of ETEC 5 h post-infection for the six donors, as determined by amplicon sequencing.

4. Discussion

During passage through the human GI tract, concurrently to the abiotic factors, ETEC has to face successive and complex microbial communities with which the pathogen enters competition for nutrients and space. Despite the fact that ETEC successfully colonizes the ileum and ascending colon of the M-SHIME (as described in chapter 2), it is barely investigated how the human gut microbiota is impacted in the course of an ETEC episode. In this study, we first examined the effect of ETEC challenge on the microbial community composition and activity in a new M-SHIME set-up, consisting of distinct gut regions (ileum and ascending colon) and microenvironments (luminal and mucosal) originated from six fecal donors. In a second instance, we identified specific microbial populations that can be correlated with ETEC virulence profiles.

The ileum microbiota is specialized in fast uptake and conversion of relatively simple carbohydrates, in contrast to the colonic microbiota which is efficient in the degradation of complex carbohydrates (Zoetendal et al., 2012). Based on physiological evidence, we attempted to recreate the specific ileal niche which was derived from the M-SHIME ascending colon through a low dose retrograde inoculation. In line with previous studies in human ileostomies, our *in vitro* ileum displayed a less diverse microbial community in both microenvironments (lumen and mucus) in comparison to the ascending colon (Zoetendal et al., 2008; Booijink et al., 2010). Despite the subject-specific phylogenetic composition of the microbiota, the dominant bacterial groups belonging to the genera *Enterobacteriaceae*, *Veillonella*, *Clostridium*, *Mitsuokella* and *Klebsiella* were found in the ileum, while *Bacteroides*, *Faecalibacterium* and *Bifidobacterium* prevailed in the ascending colon. Most of these observations are consistent with previous works on human ileostoma samples (Oh et al., 2012; Booijink et al., 2010; Zoetendal et al., 2012; Van den Bogert et al., 2013). However, the previous studies highlighted that ileum was dominated at phylum level by *Firmicutes* followed by *Proteobacteria*, while *Proteobacteria* predominated in our study (Oh et al., 2012). In addition, *Streptococcus* was not found in the top 15 most abundant genera in our case, but its abundance can vary substantially from 1 to 88% in human ileostoma samples, as observed in unpublished work from Van den Bogert (PhD dissertation, 2013). *Streptococcus* and *Veillonella* are also abundant in other parts of the upper GI tract and likely originate from the oral cavity (Walter and Ley, 2011). *Mitsuokella* observed in high abundance in the *in vitro* ileum is commonly retrieved in the oral cavity as well (Peterson et al., 2013). Collectively the distinct microbial community composition and diversity between ileum and ascending colon was also reflected in two distinct metabolite profiles. Most bacterial activity occurred in the colon where substrate availability was highest and fermenters like *Bacteroidetes* prevailed (Besten et al., 2013). In contrast, the ileum displayed total SCFA concentrations below 20 mM as previously observed (Cummings et al., 1987). As last remark to the ileum set-up, we intriguingly found a higher bacterial concentration than expected with about 10 $\log_{10}$, while most studies assure that the ileum does not exceed 8 $\log_{10}$. However, it has to be noted that most of the time, the modalities of the procedure to perform the ileostomy or collect the luminal content by means of a catheter remains unclear, as well as the type of samples (lumen *vs* mucus) and site of collection (proximal *vs* distal ileum). All these aspects can greatly influence the estimation of the microbial concentration. Moreover, most of these surgeries were performed at fasted state which limits the growth of the bacterial community (nutrients deprivation). In sharp contrast, we took samples from

the simulated ileal environment during fed conditions. This may explain the higher bacterial levels found in the ileum in our study compared to the other data found in the literature. It must be noted that ileal samples taken at earlier time points of the fed state (30 min after feed arrives in the ileum) displayed lower bacterial levels that are in line with literature.

Following ETEC infection, the microbial successions were first examined. Succession is a widely used ecological concept describing a course of changes in species composition over time in response to environmental perturbations (Connell and Slatyer, 1977). In our study, although limited, the unique administration of ETEC (~10 $\log_{10}$) in the ileum of six donors was enough to observe a microbial succession in both gut regions (ileum and ascending colon) and microenvironments (lumen and mucus) when comparing the pre-infection period (until day 12) to the post-infection period (from day 13 to 20). As key changes, the blooms of taxa recognized as opportunistic pathogens in previous studies were noted. For instance, *Klebsiella variicola* recently involved in bloodstream infections, species belonging to *Achromobacter* involved in nosocomial infections and acute necrotizing pancreatitis, non-tuberculous *Mycobacterium*, *Prevotella* and *Paraprevotella* genera were stimulated upon ETEC microbial assault (Chin'ombe et al., 2016; Otta et al., 2014; debata et al., 2014; Martin and Bachman, 2018; Edwards et al., 2017; Larsen, 2017). It is indeed acknowledged that opportunistic pathogens are often associated with stress conditions for the host, which can be related in this case to ETEC infection (Stecher et al., 2013). Conversely, microbes with potential health promoting functions were decreased in the ascending colon: *Bifidobacterium angulatum*, the butyrate producers *Gemmiger formicilis*, the species *Clostridium butyricum* and *Fusicatenibacter saccharivorans,* which helps to suppress intestinal inflammation in a colitis model (Kanai et al., 2015, Sarkar and Mandal, 2016; Takeshita et al., 2016, Rivière et al., 2016). Overall in the ascending colon, although the microbial diversity was not altered following infection, a reduced abundance of some obligate anaerobic bacteria and an expansion of some facultative anaerobic bacteria members were observed. These ecological features reflect an imbalance in the microbiota, which might be associated to a dysbiotic state (Walker et al., 2011; Bäumler and Sperandio, 2016). Nonetheless, such definition needs to be carefully considered as highlighted in the review of Hooks and O'Malley (2018) where dysbiosis is broadly associated with any change in microbiota composition without particular normal-abnormal distinction, limiting thus the comprehensive interest to use this term (Hooks and O'Malley, 2018). For example, a clinical study has suggested that the increase of *Firmicutes*:*Bacteroidetes* ratios in human fecal samples 72 h post-ETEC infection resulted in a dysbiotic microbiota, even though in line with our study, authors did not observed significant difference in the microbial diversity when comparing ETEC-free travellers to ETEC-infected travelers (Youmans et al., 2015). Interestingly, when the microbial diversity was compared with those from healthy travelers, they did observe a significant difference in the diversity, suggesting that the simple fact to travel might result in a dysbiotic signature. Two longitudinal studies performed on fecal samples of Bangladeshi patients diagnosed ETEC-positive or experimentally infected adults, limited their conclusions to a rapid and reversible change in gut microbial community structure and as well did not observed a significant decrease in overall bacteria diversity, which is in line with our study (Pop et al., 2016; David et al., 2015). The use of fecal samples in the latter studies is nonetheless not representative for the successive microbial ecosystems encountered by the pathogen in the gut, which justifies even more the purpose of

our study. In close relationship with dysbiosis, evidence suggested that post traveler's diarrhea associated with ETEC triggered chronic functional GI disorder named PI-IBS (Principi et al., 2017; Nair et al., 2014; Connor and Riddle, 2014). No microbial markers have so far been attributed to the PI-IBS, but a decreased percentage of *Lactobacillus* and *Bifidobacterium* genera has been described in the IBS microbiota and a decreased abundance of the actinobacterium *Collinsella aerofaciens* was often associated with PI-IBS status (Bag et al., 2017; Lee and Bak, 2011; Malinen et al., 2010; Malinen et al., 2005; Rodino-Janeiro et al., 2018). Interestingly, in our study the relative abundance of *Collinsella aerofaciens* and *Bifidobacterium* genus were among those significantly decreased in the ileum and ascending colon following ETEC infection. However this result is too restrictive to make any conclusion in this respect.

Beyond the microbial successions enhanced in the course of ETEC infection, the pathogen has to obtain a benefit from the microbial niches crossed, by means of successful competition for nutrients with the gut microbes (Bäumler and Sperandio, 2016). We have already shown in the previous chapter (chapter 2) that ETEC brought to fruition its long-term colonization in the luminal and mucosal part of the ileum and ascending colon. The intricate nature of interactions with the distinct microbial niches which allows a growth benefit to ETEC remains nonetheless largely unknown. In the case of our fermentation experiments, we supplemented the nutritional medium in the ileum with simple sugars fructose, glucose, maltose, sucrose and galactose to reproduce the *in vivo* situation. ETEC will utilize these carbon sources to grow but we don't know the degree of competition with the other gut microbes. We can speculate that commensal *E. coli* are important competitors because they will utilize the same source of carbon than ETEC. As key clue to circumvent this competition, it has been shown in the case of EHEC that other source of sugars can be exploited by the pathogen such as mannose, ribose, galactose and hexuranates that commensal *E. coli* do not optimally catabolize (Fabich et al., 2008; Autieri et al., 2007). In our study, ETEC was found in high quantity attaching the mucosal niche (chapter 2 and chapter 4) in line with several studies in animals (calves, piglets, mice) and *in vitro* using human secreting HT-29 cell (Kumar et al., 2016; Kerneis et al., 1994; Mouricout and Julien, 1987). The mucus layer is composed of fucose, galactose, mannose, sialic acid, N-acetylgalactosamine or N-acetylglucosmaine (Rakoff-Nahoum et al., 2014). The possibility that ETEC can exploit certain compounds of the mucus layer for its growth benefit is however yet unknown. Even though ETEC by itself is able to degrade the human intestinal mucin compounds MUC2 and MUC3 thanks to two mucin-degrading enzymes YghJ and EatA, it is not to exclude that the pathogen also acts in dialogue with saccharolytic members of the microbiota such as *Bacteroidetes thetaiotaomicron* or *Akkermansia muciniphila* to better exploit the availability of sugars and promote its expansion (Kumar et al., 2014; Luo et al., 2014; Sonnenburg et al., 2005; Van Herreweghen et al., 2017). Indeed it has been shown in previous studies with other enteric pathogens that *Bacteroidetes thetaiotaomicron* cleaved fucose residues from the mucus, generating thus a free pool of fucose in the lumen that was catabolized by EHEC, *Clostridium difficile* and *Salmonella typhimurium* (Ng et al., 2013).

Another aspect to discuss is the exploitation of microbiota-derived molecules as signals for the successful ETEC infection. Bacteria are together capable to exchange chemical signaling molecules to communicate and regulate their behaviors. This cell-to-cell communication process is called quorum

sensing and is involved in production of chemical signals that are called autoinducers (Bivar, 2018). Even though not investigated in the present study, we found an interesting example with respect to *Vibrio cholerae*, sharing 80% homology with ETEC for the LT toxin production. The presence of *Ruminococcus obeum* reclassified as *Blautia obeum* can hamper *V. cholerae* colonization through the production of a furanone signal autoinducer-2, causing the repression of several *V. cholerae* colonization factors (Hsiaso et al., 2013). Interestingly, in our study the relative abundance of *Blautia obeum* was significantly decreased in the ascending colon following ETEC infection.

Reflecting the microbial metabolic activity, SCFA are important determinants of interactions between the microbiota and enteric pathogens. In our study, SCFA concentrations in the ileum and ascending colon displayed significant changes following ETEC infection mainly through the increase of the propionate concentration, though inter-individual variations. Propionate is acknowledged to be a health-promoting microbial metabolite, but direct interaction between enteric pathogens and propionate production has been not yet documented in the literature (Hosseini et al., 2011). However, other studies have shown that SCFA can regulate expression of virulence genes, as already observed in EHEC and *Salmonella typhimurium* (Barnett Foster et al., 2013; Herold et al., 2009; Lawhon et al., 2002, Takao et al., 2014). In ETEC, only one study has shown that addition of high concentrations (2 mg mL^{-1}) of C-2 to C-7 SCFA in a culture medium abolished LT production (Takashi et al., 1989). However, this supra-physiological SCFA concentration gives speculative conclusion on the regulation of the LT toxin production. Our study revealed a significantly negative correlation in the ascending colon between the LT toxin production and acetate and propionate, while LT was positively correlated with butyrate. In addition, *estAB* gene expression (encoding for the ST enterotoxin) was negatively correlated with acetate and propionate. The detailed mechanism of this regulation is yet to be unraveled. In addition, SCFA can have indirectly an effect on ETEC pathogenicity by enhancing for instance the expression of enterotoxin host receptors. This was reported in the case of EHEC infection where an enhanced production of butyrate through a high-fibre diet was associated with an increase host's expression of the Shiga toxin receptor in a mouse model (Zumbrun et al., 2013). In our case it was impossible to exploit this clue as the fermenters cannot directly integrate the IECs for cytotoxicity issues. But this example give additional perspectives of research to explore.

This is also the first report on the possible correlation between ETEC virulence features and gut microbiota populations under simulated ileum and colon conditions. Although our model was restricted to only one time point in the ascending colon following ETEC infection, the sPLS regression revealed the strongest association of LT toxin production and *estAB* gene expression with *Enterobacteriaceae* (ETEC, OTU1), as well as *Mitsuokella* (OTU11, OTU28) for all donors. Remarkably, the *eltB* gene expression co-occurred with other microbial communities, and predominantly with *Coprococcus*, and *Allisonella* (OTU2). These results strengthen the fact that *eltB* does not correlate in a similar manner with the metabolites in comparison with *estAB* and LT toxin. However, the association between virulence profiles and susceptibility to infection according to the microbial communities represents a real knowledge gaps which deserves more attention in future scientific research.

5. Conclusion

- The ileal signature was reproduced for the first time in the M-SHIME, resulting in low community diversity as well as a low metabolic activity compared to the ascending colon,
- ETEC infection had no effect on the microbial diversity index,
- ETEC infection encouraged the bloom of opportunistic pathogens in the ileum and decreased the species with potential health promoting functions were decreased in the ascending colon,
- ETEC infection significantly decreased the abundance of *Bifidobacterium* genus and the actinobacterium *Collinsella aerofaciens*, as generally accepted in the course of PI-IBS,
- ETEC infection led to the increase of propionate concentration though inter-individual variations.

As a summary of the results obtained from the complementary *in vitro* systems TIM-1 and M-SHIME on the dynamics of ETEC survival, physiological state and virulence (chapter 2) and the microbial successions following ETEC infection (chapter 3), the Figure 3.11 is proposed.

6. Candidate contribution and acknowledgements

Under supervision of Stéphanie Blanquet-Diot and Tom Van de Wiele, I designed the experimental work. I carried out the *in vitro* fermentations (with technical support from Jana de Bodt). I carried out all the molecular-based experiments (DNA and SCFA extractions). Tim Lacoere carried out the gas chromatography measurements and generated the OTU tables. All the microbial community analyses and statistical analyses were performed in close collaboration with Kim de Paepe (she supervised me at each steps of the data processsing). I drafted the manuscript. I designed the figures in collaboration with Kim de Paepe. I wrote the manuscript with input from all authors. I will be first author of the future publication.

I would like to acknowledge Pieter Van den Abbeele and Massimo Marzorati (Prodigest) for sharing their expertise in the set-up of the new ileum in the M-SHIME, and also Tim Lacoere (CMET) for technical assistance. This research was funded by Lesaffre company (Marcq-en-Baroeul, France).

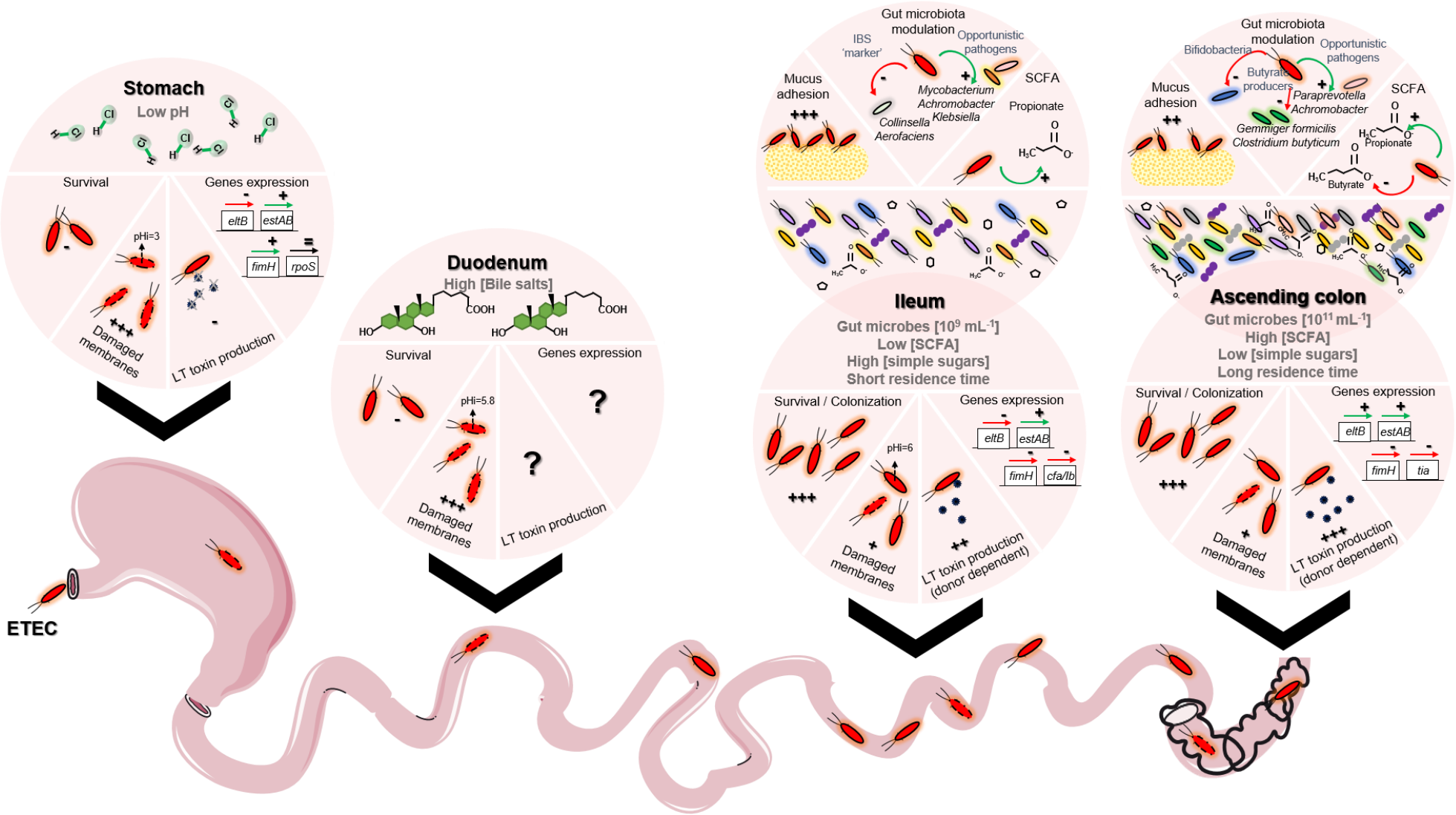

Figure 3.11. Biogeography of ETEC H10407 pathogenesis in the human *in vitro* systems TIM-1 and M-SHIME

7. Supplementary data

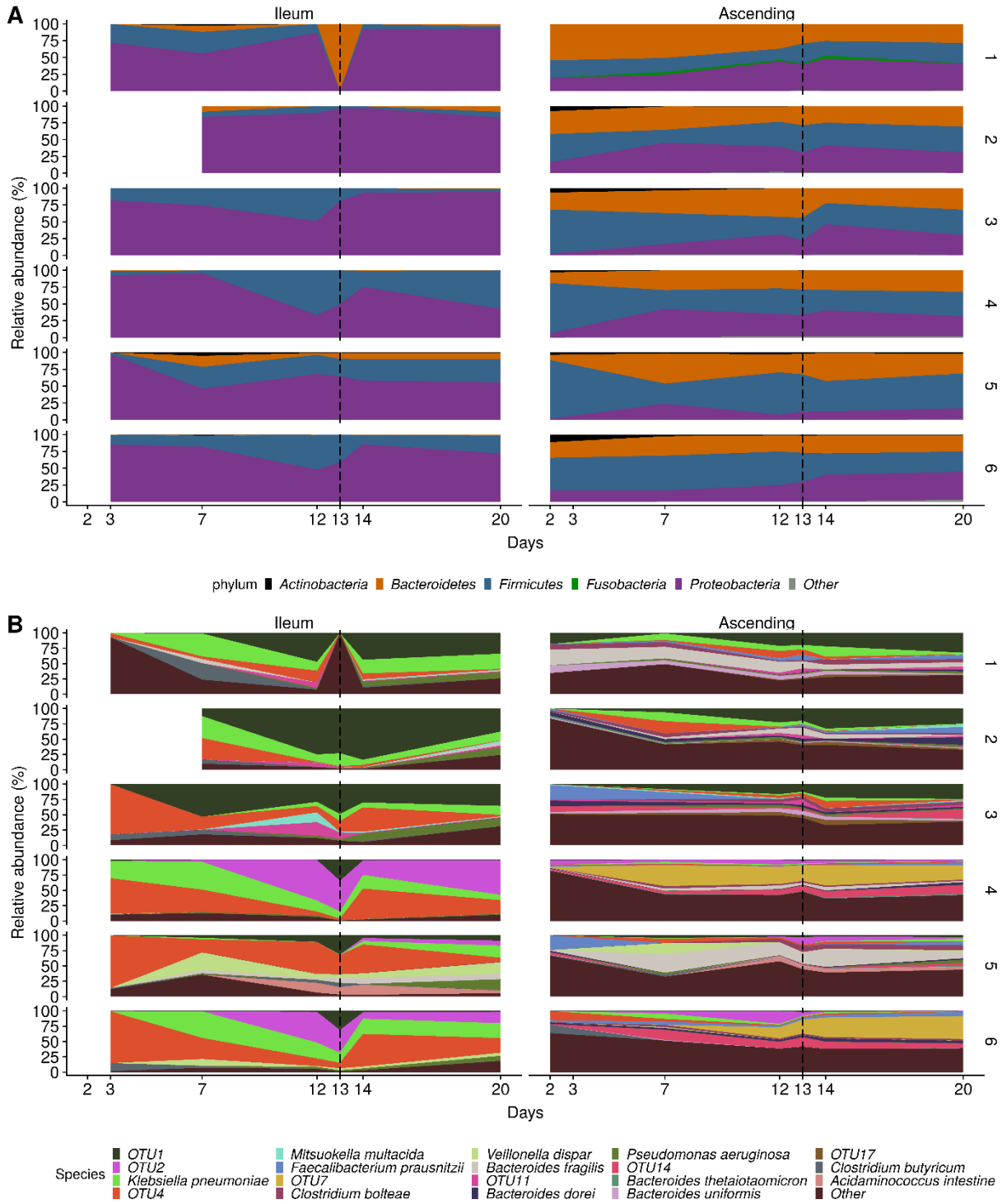

Figure S3.1. **Phylum and species levels microbial community composition of the luminal gut regions preceding and following ETEC infection, as determined by amplicon sequencing.** The area graphs show the relative abundance of the (**A**) 5 most abundant phyla, and (**B**) 19 most abundant species in the luminal ileum and ascending colon from six different donors over the course of 20 days fermentation. ETEC infection is demarcated by the dashed line at day 13. Species were annotated using the RDP SeqMatch and NCBI BLAST. For species that could not unambiguously be identified at species level, the OTU identifier is displayed.

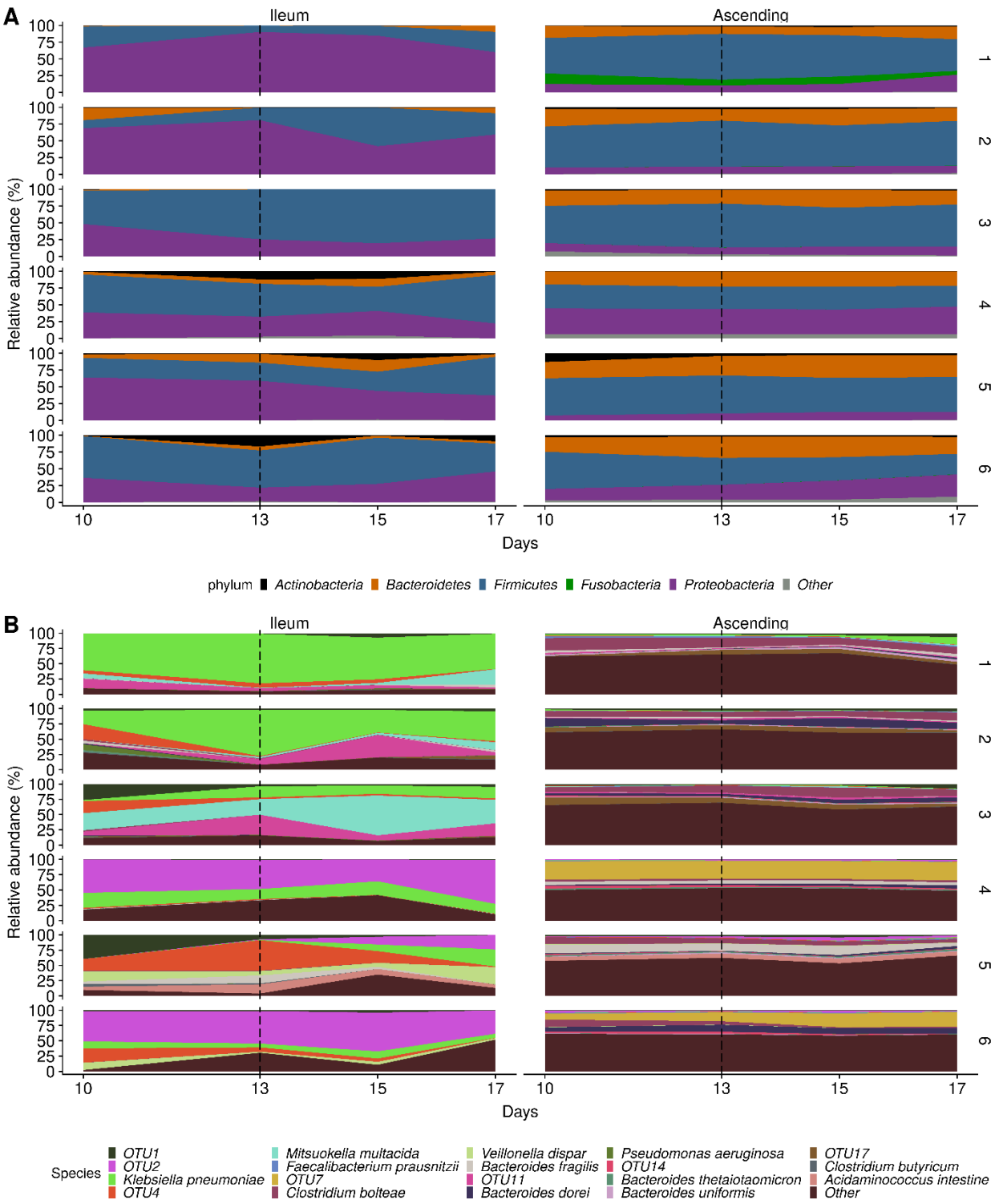

Figure S3.2. **Phylum and species levels microbial community composition of the mucosal gut regions preceding and following ETEC infection, as determined by amplicon sequencing.** The area graphs show the relative abundance of the (**A**) 5 most abundant phyla, and (**B**) 19 most abundant species in the mucosal ileum and ascending colon from six different donors over the course of 20 days fermentation. ETEC infection is demarcated by the dashed line at day 13. Species were annotated using the RDP SeqMatch and NCBI BLAST. For species that could not unambiguously be identified at species level, the OTU identifier is displayed.

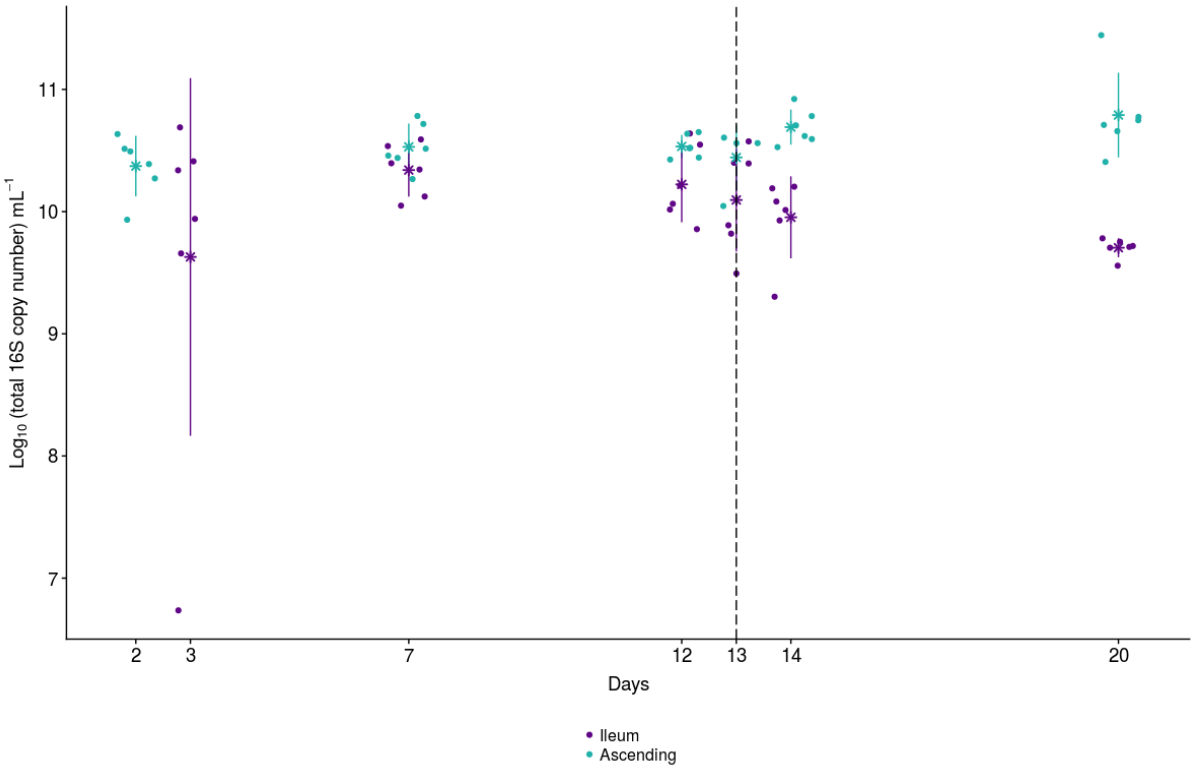

Figure S3.3. **Gut microbes concentration in the ileum and ascending colon lumen determined by total *16S* rRNA gene quantification**

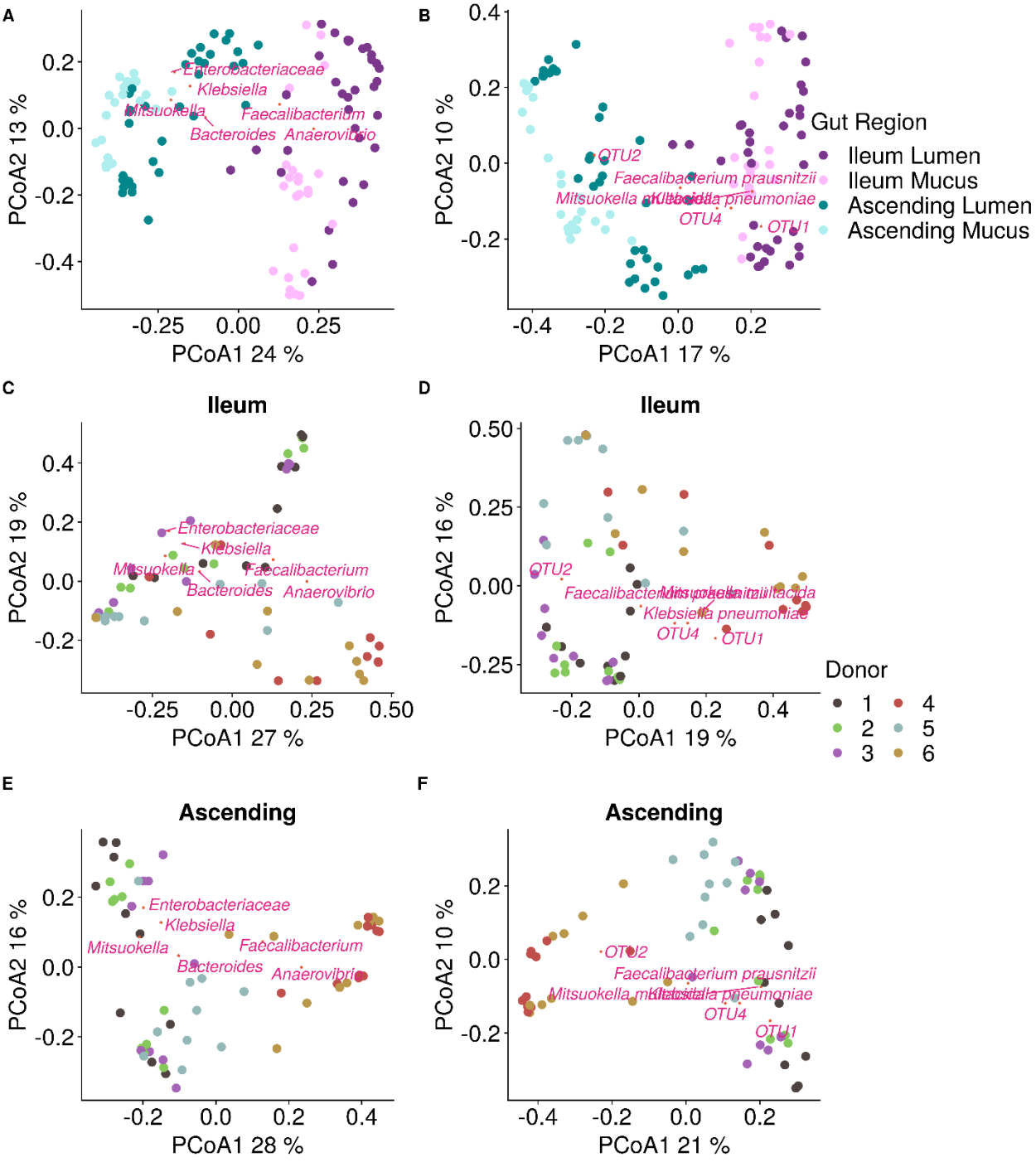

Figure S3.4. **PCoA biplot showing distinct microbial community according to the gut regions and the inter-individual variability represented by the six donors.** Weighted average scores of the six most abundant genera (**A, C, E**) and species (**B, D, F**) microbial community were indicated in pink according to the gut region (**A, B**) and donor (**C, D, E, F**) subtypes.

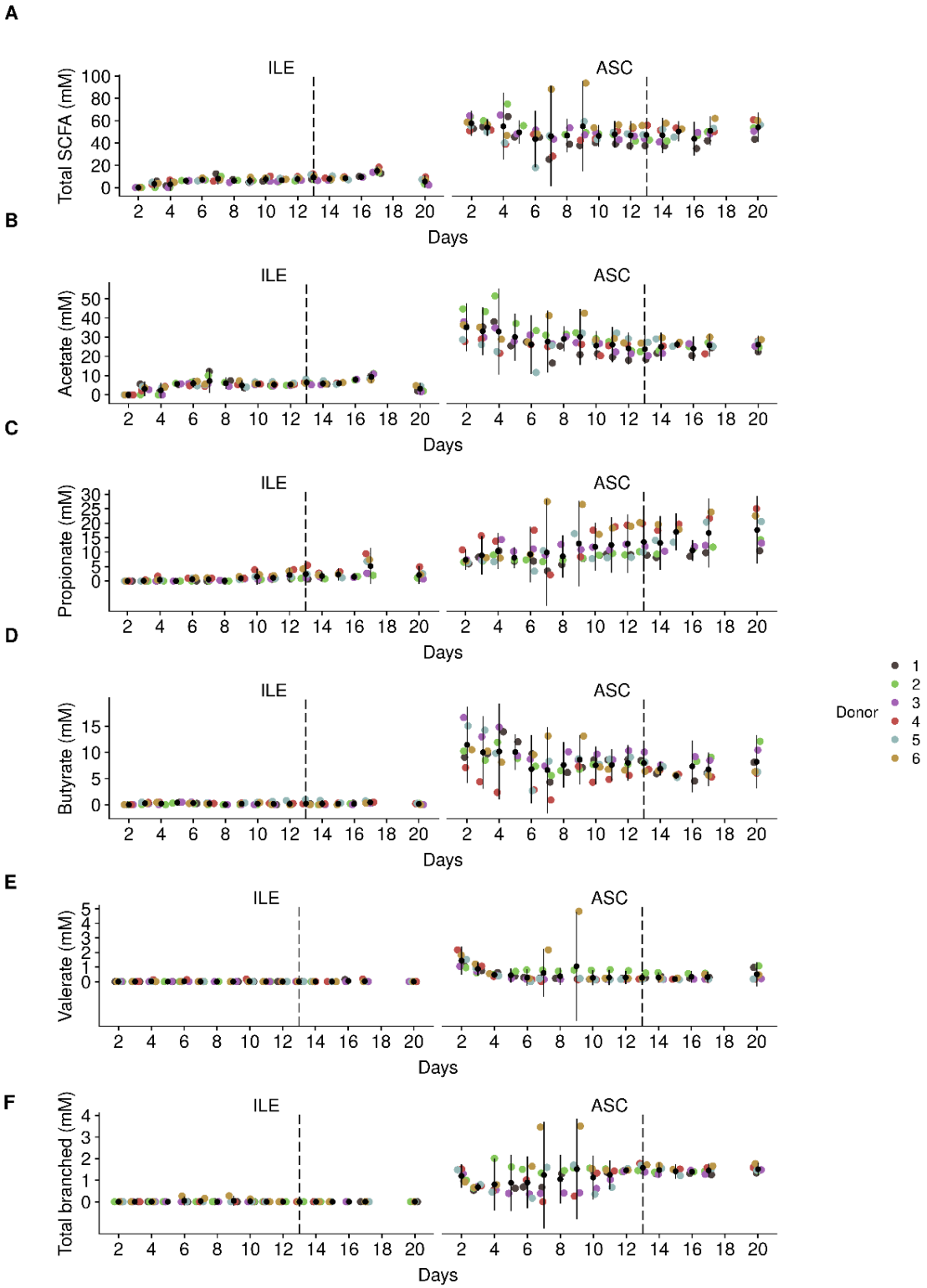

Figure S3.5. **Short chain fatty acid (SCFA) concentrations (mM) in the ileum (ILE) and ascending colon (ASC) compartments, inoculated with the microbial community derived from six different donors in the course of 20 days fermentation.** The pre-infection period is represented from day 2 to 12, ETEC infection is demarcated by the dashed line at day 13 and, the post-infection until day 20.

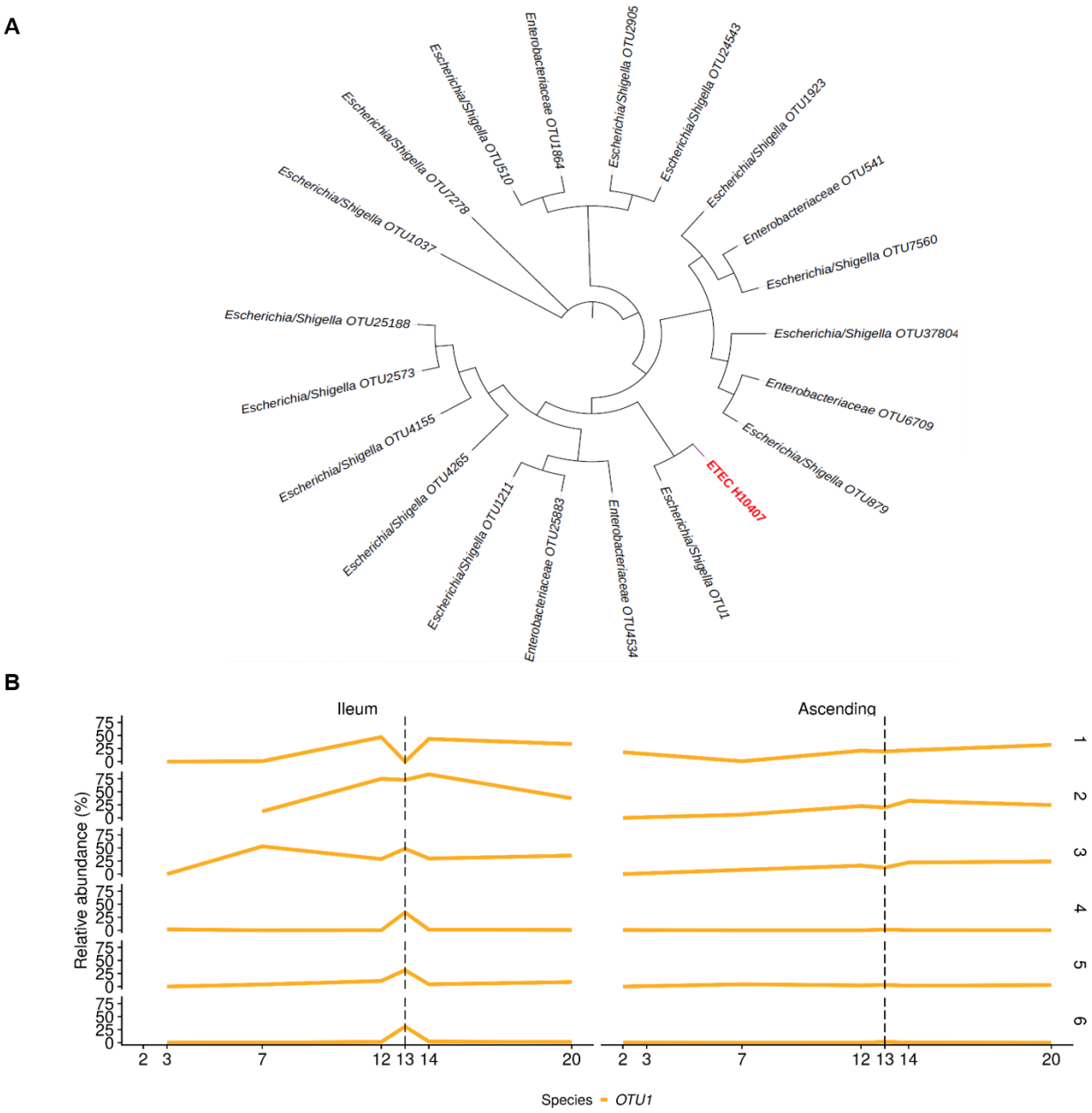

Figure S3.6. **OTU corresponding ETEC strain H10407.** (**A**) Maximum Likelihood phylogenetic tree showing the relatedness of the amplicon *16S* rRNA sequences with the ETEC H10407 *16S rRNA* gene reference sequence, downloaded from the NCBI database; (**B**) Relative abundance of OTU1 corresponding to ETEC H10407.

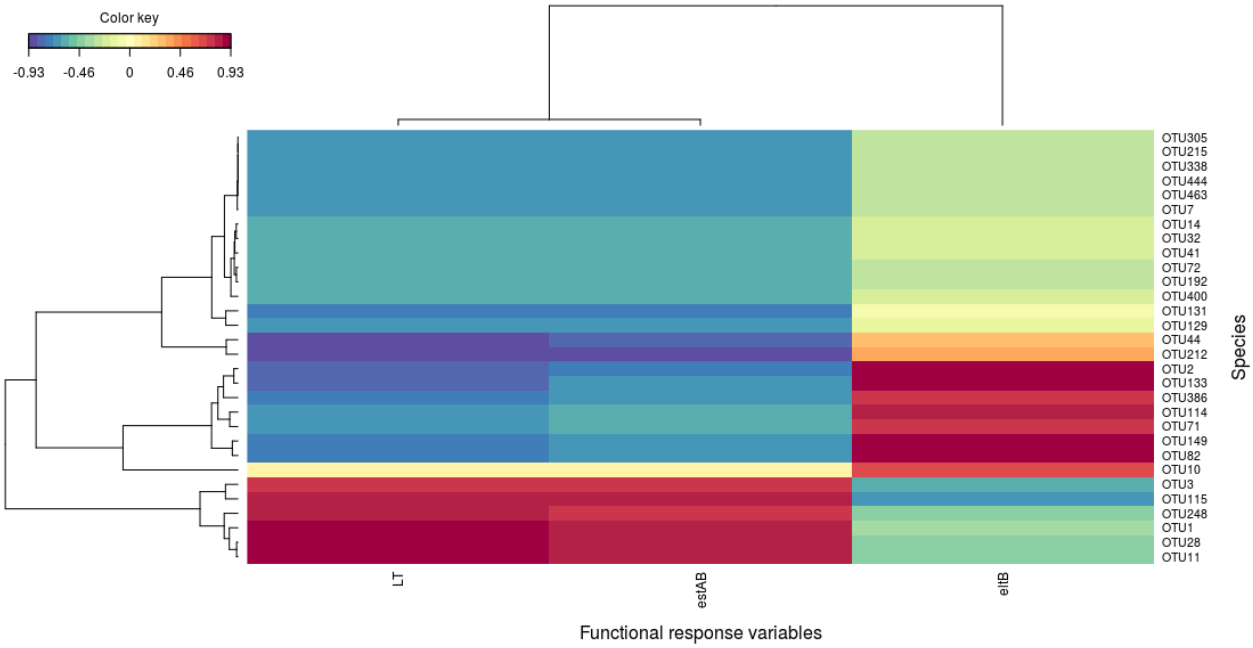

Figure S3.7. **Heatmap representation of a sparse Partial Least Squares (sPLS) regression analysis of the ascending colon-luminal microbial community composition data at species level and the main virulence features of ETEC 5 h post-infection for the six donors, as determined by amplicon sequencing.**

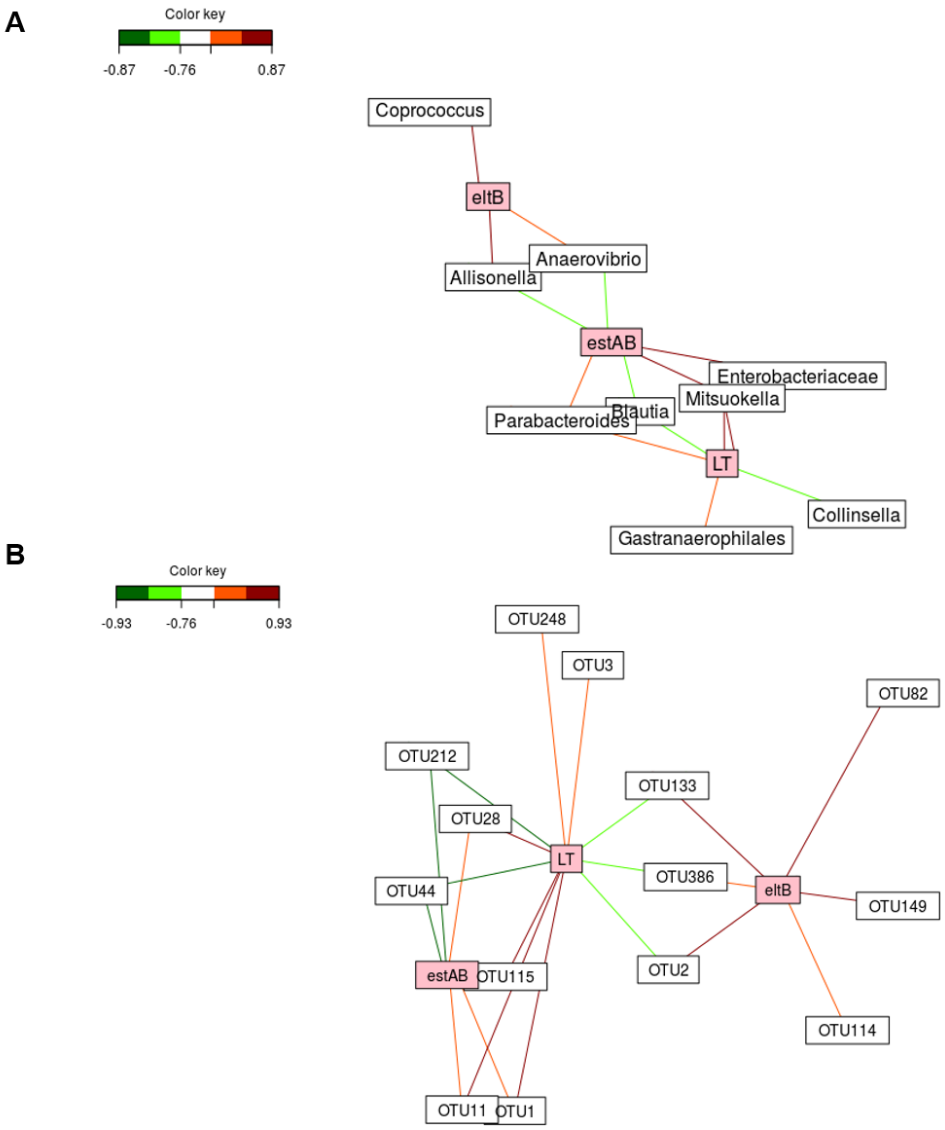

Figure S3.8. Co-occurrence network representation of the ASC-luminal microbial community composition data at (A) genus and (B) species levels and the main virulence features of ETEC 5 h post-infection for the six donors, as determined by sPLS regression analysis.

CHAPTER 4 : ANTI-INFECTIOUS PROPERTIES OF THE PROBIOTIC *SACCHAROMYCES CEREVISIAE* CNCM-3856 ON ETEC STRAIN H10407

***

As chief concern for the industrial partner Lesaffre, a probiotic screening has been performed during the first 6 months of this research project. The main purpose of the screening phase was to evaluate through rapid and complementary *in vitro* testing methods, the antimicrobial properties of six probiotic strains supplied by Lesaffre (e.g. 3 bacteria and 3 yeasts) against ETEC H10407. At the end of the screening, in the interest of Lesaffre, the yeast *Saccharomyces cerevisiae* CNCM I-3856 was retained to pursue the study and improve the knowledge on the associated mechanism of action (chapter 4 and chapter 5). Of note, Lesaffre requested to keep confidential the results of the five non-retained strains as well as their names. With their consent, we propose to give a brief overview on the results obtained with the six strains that are renamed P1, P2, P3 (*S. cerevisiae* CNCM I-3856), P4, P5 and P6 through co-cultures and mucin adhesion tests. Results are available in supplementary data (Fig. S4.1, Fig. S4.2) and the methods used are described in section 2.3 and 2.5, respectively.

To better exploit the preliminary observed antagonistic properties of *S. cerevisiae* against ETEC, further *in vitro* (cell culture) and *in vivo* (mice) experiments were executed in collaboration with M2iSH (Microbes, Intestine, Inflammation and Host Susceptibility) laboratory (Clermont-Auvergne University, France).

These works have been published in Applied Microbiology and Biotechnology[4] and redrafted for the present chapter 4.

[4] ***Publication.*** *ROUSSEL C., SIVIGNON A., de VALLEE A., GARRAIT G., DENIS S., TSILIA V., BALLET N., VANDEKERCKOVE P., VAN DE WIELE T., BARNICH N., BLANQUET-DIOT S. Anti-infectious properties of the probiotic Saccharomyces cerevisiae CNCM I-3856 on enterotoxigenic E. coli (ETEC) strain H10407. Appl. Microbiol. Biotechnol, 102, 6175-6189 (2018). https://doi.org/10.1007/s00253-018-9053-y*

4 Anti-infectious properties of the probiotic *Saccharomyces cerevisiae* CNCM I-3856 on ETEC strain H10407

Abstract ETEC are major food borne pathogens responsible for traveler's diarrhea. The production of adhesins and the secretion of enterotoxins constitute the major virulence traits of the bacteria. Treatments are mainly symptomatic and can involve antibiotherapy. However, given the rise of antibiotic resistance worldwide, there is an urgent need for the development of new preventive strategies for the control of ETEC infections. Among them, a promising approach is the use of probiotics. The aim of this study was to investigate, using complementary *in vitro* and *in vivo* approaches, the inhibitory potential of the yeast *Saccharomyces cerevisiae* CNCM I-3856 against the human ETEC reference strain H10407. In conventional culture media, *S. cerevisiae* significantly reduced ETEC growth and toxin production. The yeast also inhibited bacterial adhesion to mucin-agar and intestinal Caco-2/TC7 cells in a dose dependent manner. Lastly, pre-treatment with *S. cerevisiae* inhibited Interleukin-8 production by ETEC-infected intestinal cells. In streptomycin-treated mice, the probiotic yeast decreased bacterial colonization, mainly in the ileum, the main site of ETEC pathogenesis. For the first time, this study shows that the probiotic yeast *S. cerevisiae* CNCM I-3856 can exert an anti-infectious activity against a human ETEC strain through a multi-targeted approach, including inhibition of bacterial growth and toxin production, reduction of bacterial adhesion to mucins and intestinal epithelial cells and suppression of ETEC-induced inflammation. Interestingly, the highest activity was obtained with a prophylactic treatment. Further studies will aim to assess the effect of the yeast on ETEC survival and virulence under human simulated digestive conditions.

1. Introduction

The food and water-borne pathogen ETEC is responsible for hundreds of millions of diarrheal episodes worldwide in people visiting endemic countries (traveler's diarrhea) and in infant under 5 years of age living in low-income countries where sanitation is poor (Kotloff et al. 2013; de la Cabada Bauche and DuPont 2011). In humans, ETEC infection is characterized by two major virulence traits which are: (i) the adhesion of the bacteria to epithelial cells of the small intestine orchestrated by fimbrial or non-fimbrial adhesin colonization factors (CFs), and (ii) the production of heat-labile (LT) and/or heat-stable (ST) enterotoxins leading to hypersecretion of H_2O and Cl^- at the root of watery cholera-like diarrhea (Quadri et al. 2005; Turner et al. 2006). Following travelers' diarrhea, persistent changes in GI function may occur and extend to post-infectious (PI) irritable bowel syndrome (IBS) (Spiller and Garsed 2009; Connor and Riddle 2013).

The treatment of diarrheal disease due to ETEC is mainly symptomatic with oral rehydration and use of antimotility agents. Antimicrobials are of definite benefit in particular in the treatment of traveler's diarrhea, but their use is limited by the associated cost, common adverse-effects and raise in antibiotic resistance worldwide. Non-antibiotic alternative strategies are then widely encouraged by the European Union and World Health Organization (CDC, 2014). Additionally, there is yet no commercially available prophylactic treatment (in particular no vaccine) that specifically addresses ETEC infections or PI-IBS. Among promising solutions, strategies using probiotic microorganisms are an extensive field of research (Roussel et al., 2017). The internationally endorsed definition of probiotics is "Live microorganisms that, when administered in adequate amounts, confer a health benefit on the host" (Hill et al. 2014). A large panel of strains has been acknowledged as probiotics, including lactic acid bacteria from *Lactobacillus* and *Bifidobacterium* genera, and *Saccharomyces* yeast strains.

Among them, *Saccharomyces cerevisiae* CNCM I-3856 has already recognized probiotic properties. The strain displayed beneficial effects against enteric *E. coli* pathogens, such as EHEC or AIEC. When co-administered with EHEC O157:H7, this probiotic yeast significantly reduced bacterial growth observed in the distal part of the human small intestine, as simulated by the TIM-1 (Etienne Mesmin et al., 2011). Thévenot et al. (2015) also demonstrated that *S. cerevisiae* CNCM I-3856 inhibited Shiga toxin gene expression under human simulated colonic conditions and EHEC O157:H7 interactions with intestinal Peyer's patches and subsequent hemorrhagic lesions in mice. In addition, the probiotic yeast reduced colonization, decreased pro-inflammatory cytokine production and prevented colitis in AIEC-infected mice (Sivignon et al., 2015). Lastly, in clinical studies, *S. cerevisiae* CNCM I-3856 has been reported to benefit IBS symptoms through reduction of abdominal pain, bloating and constipation (Pineton de Chambrun et al., 2015; Cayzeele-Decherf et al., 2017).

Therefore, it would be of high interest to investigate the inhibitory potential of *S. cerevisiae* CNCM I-3856 against the well characterized human ETEC strain H10407 in order to evaluate its ability to prevent travelers' diarrhea but also associated PI-IBS. Here, we report the use of complementary *in vitro* and *in vivo* approaches to assess the antagonistic effects of the probiotic yeast against the human reference strain ETEC H10407 and try to describe the underlying mechanisms.

2. Material and Methods

2.1 Strains and growth conditions

The prototypical ETEC strain H10407 (LT+, ST+, CFA/I+, EtpA+, EatA+, YghJ+, ATCC® 35401), serotype O78:H11:K80, isolated in Bangladesh from a patient with a cholera-like syndrome (Evans et al. 1977), was used in this study. Then, spontaneous mutations in ETEC H10407 that confer resistance to streptomycin were selected onto LB agar BD Difco (Fisher, Waltham, USA) containing streptomycin (1 mg mL^{-1}) (Sigma, St Louis, USA). Bacterial growth and adhesion to intestinal epithelial cells of the selected ETEC Str^R mutant was equivalent to the wild type ETEC strain.

ETEC wild type was routinely grown at 37°C in LB or in CFA media. For mouse infection, ETEC Str^R mutant was grown at 37°C in LB broth with streptomycin (25 µg mL^{-1}). ETEC and ETEC Str^R mutant were plated onto LB agar and LB agar supplemented with streptomycin (25 µg mL^{-1}), respectively, and incubated at 37°C for 24h under aerobic conditions.

The probiotic yeast strain *S. cerevisiae* CNCM I-3856 (Lesaffre Human Care, Marcq-en-Baroeul, France) was supplied in its active dried powder form. Before experiments, yeasts were resuspended in sterile saline water and mixed with an ultra-turrax yellow line (IKA, Rawang, Malaysia). Yeasts were plated onto Sabouraud agar BD Difco (Fisher, Waltham USA) with chloramphenicol (50 mg L^{-1}) (Sigma, St Louis, USA) and incubated at 30°C for 48h under aerobic conditions.

2.2 Human intestinal cell lines

TC7 cells, a sub-clone obtained after a late passage of the Caco-2 human colonic cell line (P-198), was provided from the ATCC and maintained in an atmosphere containing 5% CO_2 at 37°C in DMEM (Dulbecco's Modified Eagle's medium). The Caco-2/TC7 polarized epithelial cell line, mimicking structurally and functionally an intestinal barrier, has been previously recommended for its performance and reproducibility (Liévin-Le Moal and Servin, 2013). Cells were seeded in 24-well culture plate at a density of 5 x 10^4 cells/well and incubated at 37°C for 14 days. Experiments were performed 14 days post-seeding, after complete morphological and functional differentiation of Caco-2/TC7 cells.

2.3 Co-cultures in LB media

In a first series of experiments (n=3), ETEC H10407 (10^7 CFU mL^{-1}) and *S. cerevisiae* CNCM I-3856 were co-cultured in LB broth media during 6h at 37°C in a rotary shaker (80 rpm). Before co-culture phase, *S. cerevisiae* (10^7 yeasts mL^{-1}) was pre-incubated in LB media for 3h. Samples were collected every two hours to determine ETEC culturability by plating onto LB and viability by PMA-qPCR (propidium monoazide). Briefly, samples were stained with 50 µM PMA (Interchim, Montluçon, France) in the dark, incubated 5 min at room temperature, and exposed 15 min to the blue light PMA-Lite LED Photolysis (Interchim, Montluçon, France). Samples were then pelleted (1000 g, 10 min, 4°C) and stored at -20°C until DNA extractions, that were performed using the Smart Extract Kit SK-DNEX-100 (Eurogentec, Seraing, Belgium) according to the manufacturer's instructions. The qPCR procedure was carried out using the StepOnePlus Real Time PCR (ThermoFisher, Waltham, USA) in a total reaction volume of 10 µL, containing 5 µL of Takyon Low Rox Sybr Master Mix dTTP blue (Eurogentec, Seraing, Belgium), 0.45 µl (10 µM) of primers encoding for the 16S *Enterobacteriaceae* (F-

CATGCCGCGTGTATGAAGAA, R- CGGGTAACGTCAATGAGCAAA) (Huijsdens et al. 2002), 3.1 µL milli-Q water and 1 µL of template DNA sample. Non-template control was 1 µL milli-Q water. The PCR reactions were amplified by an initial denaturation step at 95°C for 5 min followed by 45 cycles of 95°C (30s), 60°C (30s) and 72°C (30s).

In a second series of experiments (n=3), LT toxin production was measured after an overnight co-culture (14h) of ETEC and *S. cerevisiae* in LB broth media (37°C, 80 rpm). The yeast ability to remove LT toxin was also studied by incubating the supernatant from an ETEC overnight culture (containing LT toxin) with *S. cerevisiae* suspended into Phosphate Buffer Saline -PBS- (14 h, 37°C, 80 rpm). At the end of the assays, culture supernatants (centrifugation at 1000 g, 15 min, 4°C) were collected to measure the final LT toxin concentrations and cell pellets from the co-culture experiments were used to follow *eltB* gene expression. Control experiments were performed in each condition without probiotic (n=3).

2.4 Agglutination assays

Serial dilutions (from undiluted to 1/360) of an ETEC H10407 bacterial suspension in PBS (10^7 CFU mL^{-1}) were added in a 96-well plate (U bottom) at a final volume of 50 µL/well. A suspension of yeasts was prepared in PBS (10^8 yeasts mL^{-1}) with or without α-D-mannose 1% (Sigma, St Louis, USA) and was distributed in each well (50 µL/well). Microplates were shaken for 10 min at 300 rpm and visually analyzed to determine the agglutination titer after 2 h incubation at room temperature. Agglutination titer was determined according to the last bacterial dilution allowing yeast agglutination. Agglutination assays in microplates were completed by microscopic observations of agglutinates. Co-culture of ETEC and yeasts (1:1), with or without α-D-mannose 1%, were observed after 1 h incubation (37°C, 45 rpm) by using the Axioskop phase contrast microscope at a magnification x 1000 (Zeiss, Thornwood, USA). Negative controls were performed without ETEC and all experiments were performed in triplicate.

2.5 Mucin adhesion assay

Adhesion experiments were adapted from Tsilia et al. (2016). Mucin agar consisted of 5% porcine mucin type II (Sigma, St Louis, USA) and 1% bacteriological agar (Sigma, St Louis, USA). The pH of mucin agar was adjusted at 6.8 with 10 M NaOH to closely mimic small intestinal pH. In the pre-incubation phase, a suspension of *S. cerevisiae* CNCM I-3856 (10^7 yeasts mL^{-1}) was added onto 12-wells plates containing 1.2 mL of autoclaved mucin agar. Plates were incubated at 37°C on a rotary shaker (45 rpm) for 1 h. Then, the infection phase was started by adding ETEC H10407 (10^7 CFU mL^{-1}). After 1-h co-incubation, non-adhered bacteria were removed and each well was rinsed three times with PBS. Extraction of adhered bacteria was mechanically performed by transferring aseptically the whole mucin layer with a sterilized spatula in a sterile bag containing 8.8 mL PBS. The mixture was homogenized for 10 min in a 400P BagMixer® (Interscience, Woburn, USA). Non-adhered ETEC/*S. cerevisiae* and adhered ETEC/*S. cerevisiae* extracted were quantified by plating. Percentages of adherent bacteria or yeasts onto mucus were calculated as follows: $(X_{\text{adhered to mucus}}) / (X_{\text{adhered to mucus}} + X_{\text{lumen}}) \times 100$. Lumen represents the liquid part upon the mucus layer with non-adhered bacteria. The experiments were performed in triplicate and agar without mucin was used as negative control (NC).

2.6 *In vitro* digestions in the TIM-1 model

In vitro digestions were performed in the TIM-1 model (TNO Triskelion, Zeist, Netherlands) as described in chapter 1 section 2.2. The TIM-1 system was programmed to reproduce, based on *in vivo* data, the digestive conditions observed in a healthy adult after ingestion of a glass of water (see table Table 1.1). At the beginning of digestion, a hydroxypropylmethylcellulose (HPMC) capsule containing 2 x 10^9 yeasts *S. cerevisiae* CNCM I-3856 (Lesaffre Human Care, Marcq-en-Baroeul, France) was introduced into the TIM-1 stomach with a glass of mineral water (initial concentration 10^7 yeasts mL^{-1}). In a first series of digestion (n=3), ileal effluents were collected on ice and pooled at 0-60, 60-120, 120-180, 180-240 and 240-300 min. Samples were taken in each collection to evaluate by plating yeast survival rate during gastrointestinal passage. Results were expressed as percentages of initial intake and were compared to that of a theoretical non-absorbable transit marker which models a 100% survival rate. In a second series of digestion, the overall content of the ileal compartment was collected at 120 min digestion for adhesion assays on intestinal Caco-2/TC7 cells.

2.7 Experiments on intestinal Caco-2/TC7 cells

In a first series of experiments (n=3), Caco-2/TC7 cells were infected at a MOI of 100. Different concentrations of *S. cerevisiae* CNCM I-3856 were used: 10^5, 10^6, 5 x 10^6 and 10^7 yeasts mL^{-1}. Three modes of treatment were tested for the probiotic yeasts: (i) pre-incubation: Caco-2/TC7 cells were pre-treated for 3 h with yeasts then, they were infected with ETEC bacteria in the presence of yeasts for 3 h; (ii) co-incubation: ETEC and yeasts were co-incubated for 3 h with intestinal cells and; (iii) post-incubation: Caco-2/TC7 cells were first infected with ETEC for 3 h, non-adherent bacteria were eliminated by three washes with PBS and intestinal cells were further incubated with yeasts for 3 additional hours. At the end of the experiments, Caco-2/TC7 cells were lysed with 1% Triton X-100 (Sigma, St Louis, USA) and serial dilutions were plated onto LB agar to determine the number of ETEC bacteria associated to the cells. Control experiments (n=3) were performed without yeast (“not treated”) to determine the level of ETEC adhesion to Caco-2/TC7 cells (considered as 100%) and with yeast alone. Effect of yeasts on ETEC adhesion was compared to the non-treated condition and results were expressed in percentages of residual adhesion.

In a second series of experiment (n=3), Caco-2/TC7 cells were pre-incubated with *S. cerevisiae* CNCM I-3856 (at different doses: 10^5, 10^6 and 10^7 yeasts mL^{-1}) before ETEC infection using a 3 h pre-incubation with yeast and 3 h infection at MOI 100. At the end of experiments, cell supernatants (centrifugation at 1000 g, 15 min, 4°C) were collected to measure the pro-inflammatory cytokine IL-8 secreted by the intestinal cells and LT production by ETEC. Control experiments (n=3) were performed without probiotic (“not treated”) and with non-infected cells (“not infected”).

In a third series of experiments (n=3), digested yeasts collected from the TIM-1 ileal compartment were washed twice in PBS (2500 g, 15 min, 4°C), numerated in Malassez cells and resuspended in DMEM to obtain different cell concentrations (10^5, 10^6, 5 x 10^6 and 10^7 yeasts/well). Caco-2/TC7 cells were pre-incubated for 3 h with the different concentrations of *S. cerevisiae* CNCM I-3856 before ETEC infection (3 h at MOI 100). At the end of experiments, Caco-2/TC7 cells were treated as described above

to determine the percentages of adherent bacteria. Control experiments (n=3) were performed without probiotic ("not treated") and with non-digested *S. cerevisiae* that were washed or not.

2.8 Determination of *eltB* expression and LT production

Reverse transcription (RT)-PCR was used to follow *eltB* gene expression. Total RNAs from overnight co-cultures in LB media were extracted using TRIzol reagent (Fisher, Waltham, USA). RNAs were reversely transcribed using the PrimeScript RT reagent kit (Takara Bio, Korea, Japan). q-PCR was performed using Takyon low Rox SYBR master mix (Eurogentec, Seraing, Belgium) on a MxPro qPCR system (Agilent, Les Ulis, France) with the primers *eltB*-F: GGCAGGCAAAAGAGAAATGG and *eltB*-R: TCCTTCATCCTTTCAATGGCT (Lothigius et al. 2008). *Enterobacteriaceae* rRNA 16S (16S-F: CATGCCGCGTGTATGAAGAA and 16S-R: CGGGTAACGTCAATGAGCAAA) was used as housekeeping gene for quantification of mRNA expression (Huijsdens et al. 2002). Fold-induction was calculated using the cycle threshold (Ct) method as follows: $\Delta\Delta Ct = (Ct_{\text{target gene}} - Ct_{\text{housekeeping gene}})$ at time t – $(Ct_{\text{target gene}} - Ct_{\text{housekeeping gene}})$ at t0.

LT concentrations in supernatants from co-cultures in LB media or Caco-2/TC7 cells were measured by an Enzyme Linked Immunosorbant Assay (ELISA) according to the manufacturer's instructions (human heat-labile enterotoxin B subunit ELISA kit, MyBiosource, San Diego, USA). Optical density was read at 450 nm using a multi-scan spectrum (Fisher, Waltham, USA).

2.9 Interleukin-8 ELISA

Pro-inflammatory IL-8 cytokines were dosed in supernatants from Caco-2/TC7 cells according to the manufacturer's instructions (DuoSet ELISA, human CXCL8/IL-8 ref DY208, RnDSystems, Minneapolis, USA). Optical density was read at 450 nm using a multi-scan spectrum (Fisher, Waltham, USA).

2.10 Mouse infection experiments and ethics statement

According to the validated murine model of small intestinal colonization with ETEC from Allen et al. (2006), 5 to 7 immunocompetent adult (5 to 7 weeks old) female mice ICR (Institute of Cancer Research) were provided by Charles River Laboratories (Ecully, France). Mice were housed in specific-pathogen-free conditions in the animal care facility of the University of Clermont Auvergne (Clermont-Ferrand, France). Animal protocols used in this study were approved by the CEMEA Auvergne committee for ethical issues (N° agreement 00730.02). Briefly, mice were forced-fed with *S. cerevisiae* CNCM I-3856 (5×10^7 yeasts/day from day 0 to day 3). At day 2, they were orally treated with 20 mg/mouse of the broad spectrum antibiotic streptomycin (Euromedex, Souffelweyersheim, France) to disrupt normal resident intestinal microbiota. At day 3, cimetidine (Sigma, St Louis, USA) was administered by intra-peritoneal injection (50 mg Kg^{-1}) to ablate gastric secretions. On the same day, 1 h after the last administration of the probiotic, mice were orally challenged with 10^8 CFU of Str^R ETEC. Body weight was measured at days 1 and 4. At day 4, mice were anesthetized with isofluorane (Sigma, St Louis, USA) and euthanized by cervical dislocation. Bacterial colonization of fecal samples and intestinal tissues was assessed at day 4. Fresh feces were suspended in sterile saline solution and serial dilutions were plated onto LB agar supplemented with streptomycin. Ileal tissue (3 cm-segment) and entire colon were collected, weighted and cut longitudinally, washed and homogenized in PBS with an Ultra-Turrax

before plating on streptomycin LB agar. The amount of adherent bacteria was expressed in CFU mg^{-1} of tissue.

2.11 Statistical analysis

Values are given as means ± standard deviation (SD) for *in vitro* experiments (n=3) and as medians and means ± standard errors of the means (SEM) for *in vivo* experiments (n=5 to 7). Significant differences between treatments were tested using a non-parametric Mann-Whitney test. Statistical analysis was performed with R 3.3.2 and R studio. A probability level of $p< 0.05$ was considered to be statistically different.

3. Results

3.1 *S. cerevisiae* reduces ETEC H10407 growth and LT toxin concentrations in culture media

As the inhibitory properties of *S. cerevisiae* CNCM I-3856 against the human prototypical ETEC strain H10407 have never been evaluated, the effect of the probiotic yeast on ETEC growth and toxin production was first studied in conventional culture media. When *S. cerevisiae* was pre-incubated 3 h in LB media before ETEC inoculation, the probiotic yeast induced a significant decrease in bacterial growth ($p<0.01$, n=3), as assessed by plating (Fig. 4.1A) and confirmed by PMA-qPCR (Fig. S4.3). The highest inhibitory effect was noticed at 4 h, with ETEC concentrations of 3.4 x 10^8 CFU mL^{-1} with probiotic treatment compared to 1.2 x 10^9 CFU mL^{-1} under control conditions. In addition, LT toxin production and the expression of the corresponding *eltB* gene were measured after an overnight culture of ETEC H10407 when the probiotic was added or not. LT production was significantly reduced with *S. cerevisiae* CNCM I-3856 with concentrations decreasing from 136 ± 31 pg mL^{-1} under control conditions to 69 ± 8 pg mL^{-1} with probiotics ($p<0.01$, n=3) (Fig. 4.1B on the left). This decrease in LT production was associated to a removal by the yeast of LT toxin ($p<0.001$, n=3) (Fig. 4.1B on the right) and to a reduction in *eltB* gene expression ($p=0.063$, n=3) (Fig. 4.1C).

3.2 *S. cerevisiae* directly interacts with ETEC bacteria in a mannose-related manner

In a later step, the ability of the probiotic strain to directly interact with ETEC through a trapping mechanism at the cell surface called agglutination (Tiago et al., 2012) was investigated. *S. cerevisiae* CNCM I-3856 and ETEC H10407 were co-incubated and agglutinates were macro- and microscopically observed. Agglutination between probiotic yeast and ETEC H10407 occurred until bacterial dilution of 1/24 (Fig. S4.4). To further investigate the mechanisms of action, we evaluated the effect of α-D-mannose, a major compound from *S. cerevisiae* cell walls, on yeast-bacteria agglutination. In presence of 1% α-D-mannose, ETEC H10407 lost their ability to agglutinate probiotic yeasts (Fig. 4.1D). Additional images from phase contrast microscopy are shown Fig. S4.5. These results suggest that yeasts interact directly with ETEC bacteria in a mannose-related manner.

3.3 Pre-incubation with *S. cerevisiae* reduces ETEC H10407 adhesion to mucin-agar layer

As the gut mucus layer is critical in limiting contact between host and enteric pathogens (Linden et al., 2008), the ability of ETEC H10407 to adhere to a mucin-agar layer and the antagonistic effect of *S. cerevisiae* CNCM I-3856 was assessed in a next step. In preliminary tests, we evaluated the effect of incubation times (60, 90 and 120 min) on ETEC adhesion to mucin-agar and showed that the maximal percentage of adherent bacteria was obtained as soon as 60 min (data not shown). Therefore, 1 h incubation was chosen for later experiments. The probiotic yeast was only slightly adherent (less than 4% adhesion, Fig. S4.6A). In sharp contrast, ETEC highly adhered to the mucin-agar layer with percentages of adhesion of 51 ± 6% (n=3) (Fig. 4.1E). When the probiotic yeast was added, the adhesion was significantly reduced with residual percentages of 35 ± 11% (p<0.01, n=3). Interestingly, adhesion of the pathogen was found to be mucin-dependent as the negative control incubation with agar alone (no mucin) resulted only in 1.5 ± 1.2 % of adherent bacteria. Further information on ETEC strain specificity to attach mucin and respond to Sc treatment are displayed in Fig. S4.7, by testing a strain isolated from a Brazilian child, serotype ETEC O6:H16. Although less adherent to the mucin than ETEC H10407, the serotype O6:H16 displayed no response to the probiotic treatment, which call into question the ETEC strain-specificity on probiotic effects. This aspect is further discussed in section III, General discussion.

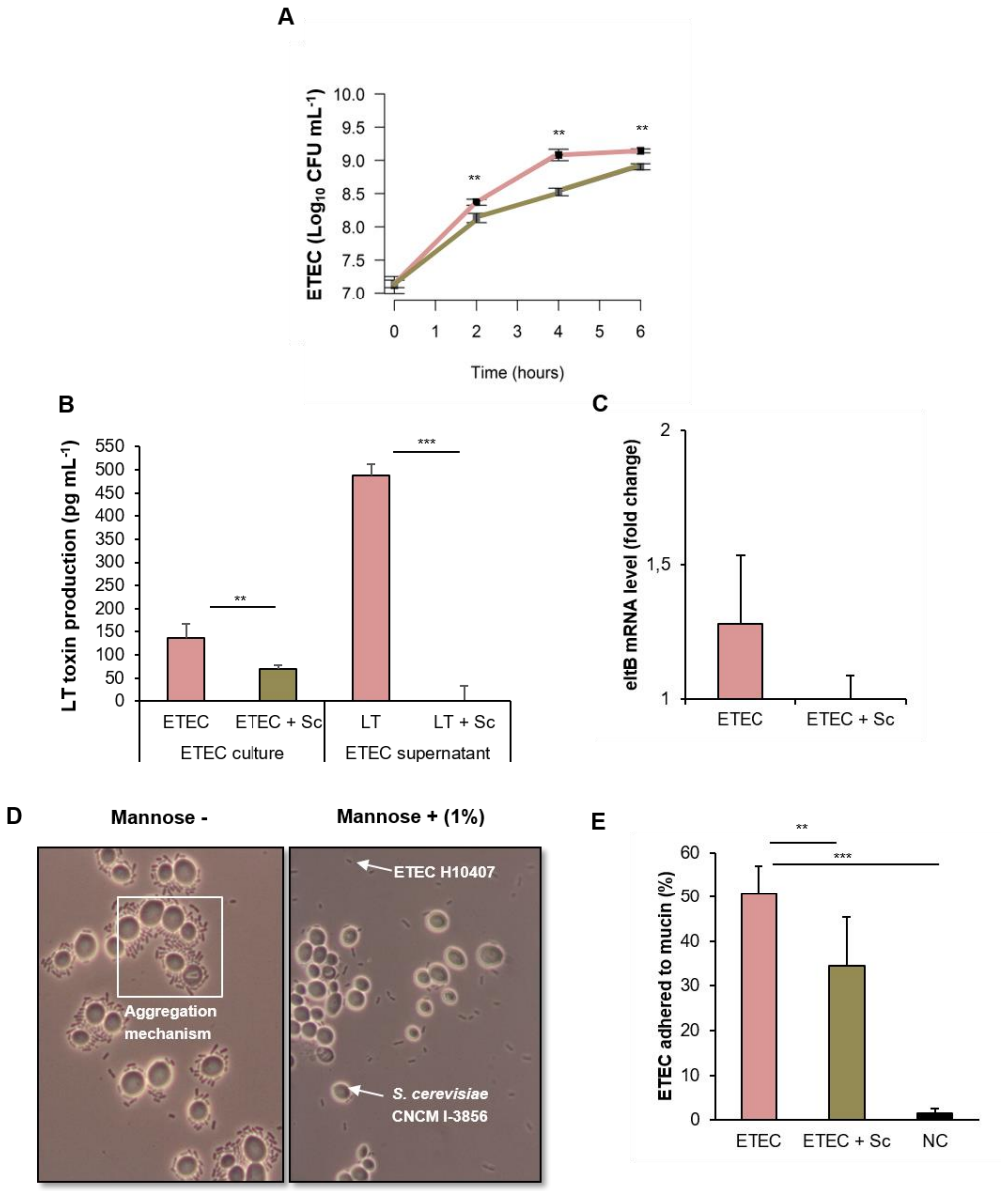

Figure 4.1. ***In vitro*** **effect of** ***S. cerevisiae*** **CNCM I-3856 on ETEC growth, toxin production, agglutination and adhesion to mucin.** (**A**) ETEC H10407 growth in LB media (10^7 CFU mL^{-1}), as determined by plating, without probiotic (pink) or after 3 h pre-incubation with 10^7 yeasts mL^{-1} of *S. cerevisiae* CNCM I-3856 (Sc) (brown). (**B**) on the left: LT toxin production (in pg mL^{-1}) after an overnight culture of ETEC or ETEC + Sc in LB media inoculated with 10^7 CFU mL^{-1} bacteria and/or yeasts. The results were normalized with the number of viable cells as determined by plating on LB ; on the right: LT toxin concentration (in pg mL^{-1}) in the supernatant from an ETEC culture treated or not with 10^7 CFU mL^{-1} Sc . (**C**) *eltB* gene expression (fold changes compared to the initial time T0 set at 1) after an overnight culture of ETEC or ETEC + Sc in LB media inoculated with 10^7 CFU mL^{-1} bacteria and/or yeasts. (**D**) Microscopic observation of ETEC/Sc agglutinates after 1 h co-culture with or without 1% α-D mannose (magnification x 1000). (**E**) ETEC (10^7 CFU mL^{-1}) adhesion to mucin-agar layer without probiotic or after 1 h pre-incubation with 10^7 yeasts mL^{-1} Sc. Agar without mucin was used as negative control (NC). The data represent the means ± SD of three independent replicates. ETEC+Sc statistically different from ETEC at $p<0.05$ (*), $p<0.01$ (**) or $p<0.001$ (***).

3.4 Pre-incubation with *S. cerevisiae* reduces ETEC H10407 adhesion to Caco-2/TC7 intestinal cells in a dose-dependent manner

Adhesion to host tissue surfaces is another fundamental step in the infection process of enteric pathogens. In this study, we therefore tested if *S. cerevisiae* CNCM I-3856 can modulate *in vitro* adhesion of ETEC H10407 to Caco-2/TC7 human intestinal cells. The probiotic yeast was added at different concentrations to intestinal cells through different treatment modalities (pre, co-and post-incubation in Fig. 4.2A, 2B, 2C respectively). *S. cerevisiae* CNCM I-3856 only slightly adhered to intestinal epithelial cells (less than 3% adhesion, Fig. S4.6B). Adhesion of ETEC without yeast was assigned as 100%. ETEC residual adhesion was unchanged (except for concentrations of 10^6 yeasts mL^{-1}, $p<0.05$) when *S. cerevisiae* CNCM I-3856 was post-incubated with the pathogen (Fig. 4.2C). In co-incubation experiments, ETEC adhesion tended to reduce with increasing doses of probiotic, but this effect was only significant at the highest concentration of 10^7 yeasts mL^{-1} (residual adhesion of 38 ± 4 %, n=3) (Fig. 4.2B). The greatest impact of the probiotic yeast was observed during pre-incubation assays (Fig. 4.2A). ETEC adhesion was significantly reduced in a dose-dependent manner from 10^6 to 10^7 yeasts mL^{-1} ($p<0.05$). At the highest probiotic dose, residual adhesion was very low (6 ± 3 % $p<0.01$). Thus, prophylactic strategy seems to be the most effective one to limit ETEC H10407 adhesion to Caco-2/TC7 cells.

3.5 Pre-incubation with *S. cerevisiae* decreases IL-8 production in a dose dependent manner and LT production in ETEC-infected Caco-2/TC7 intestinal cells

ETEC infection may elicit a mild inflammatory response as the result of pathogen interactions with host epithelial cells (Mercado et al. 2011). In the present study, we confirmed that ETEC H10407 induced secretion by Caco-2/TC7 intestinal cells of the Interleukin-8 (IL-8) pro-inflammatory cytokine (Fig. 4.3). For a better understanding of the immunomodulatory potential of *S. cerevisiae* CNCM I-3856, the ability of a 3 h pre-treatment with probiotic to reduce IL-8 production by ETEC-infected cells was investigated. Fig. 4.3 shows that *S. cerevisiae* CNCM I-3856 effectively inhibited IL-8 production in a dose-dependent manner, from 10^6 yeasts mL^{-1} ($p<0.05$). At the highest probiotic dose (10^7 yeasts mL^{-1}), IL-8 production was reduced by 97% (20 ± 19 *vs* 692 ± 352 pg mL^{-1}). LT production was also measured in supernatants from Caco-2/TC7 cultures (data not shown). Under untreated conditions, LT was found only after an overnight ETEC infection at a concentration of 10 ± 2 pg mL^{-1}. This suggests that 3 h infection was not enough to induce enterotoxin production in our experimental conditions. When the probiotic was added, whatever the dose, LT amounts fell under the detection limit of the ELISA kit ($p<0.01$). This result confirms the inhibitory effect of *S. cerevisiae* CNCM I-3856 on LT production already observed in LB media.

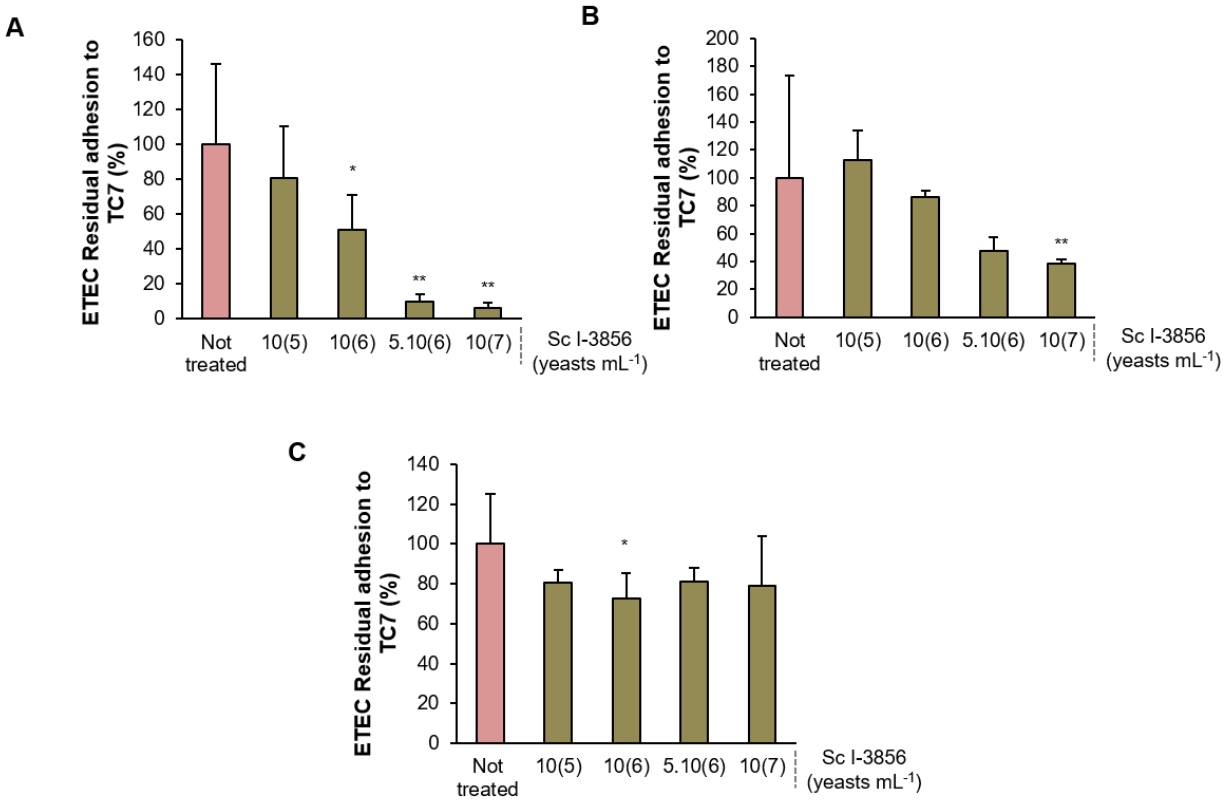

Figure 4.2. Effect of treatment modalities and *S. cerevisiae* CNCM I-3856 concentrations on ETEC adhesion to Caco-2/TC7 intestinal cells. Intestinal cells were infected during 3 h with 5 x 10^6 CFU/well of ETEC H10407 (MOI 100). The probiotic was added with different treatment modalities (pre-, co- and post-incubation) and doses (10^5, 10^6, 5 x 10^6 and 10^7 yeasts mL^{-1}). (**A**) ETEC residual adhesion to Caco-2/TC7 cells (%) after 3 h pre-incubation with *S. cerevisiae* CNCM I-3856 (Sc) followed by 3 h infection. (**B**) ETEC residual adhesion to Caco-2/TC7 cells (%) when co-incubated 3 h with Sc. (**C**) ETEC residual adhesion to Caco-2/TC7 cells (%) after 3 h infection, wash and 3 h post-incubation with Sc. The data represent the means ± SD of three independent replicates. ETEC+Sc statistically different from ETEC at $p<0.05$ (*) or $p<0.01$ (**).

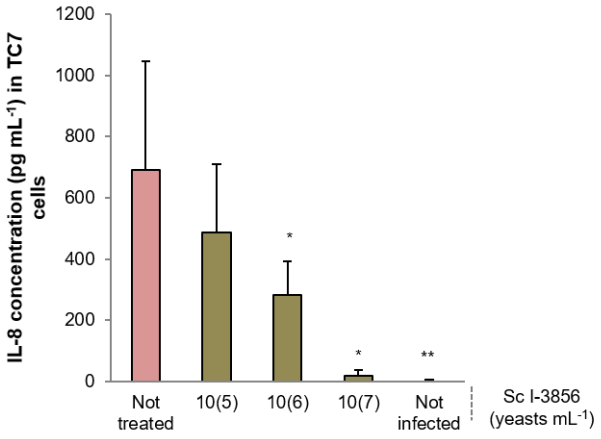

Figure 4.3. Effect of pre-incubation with *S. cerevisiae* CNCM I-3856 at different concentrations on IL-8 production by ETEC-infected Caco-2/TC7 intestinal cells. Intestinal cells were pre-incubated with the probiotic yeast during 3 h at different doses (10^5, 10^6 and 10^7 yeasts mL^{-1}). Then, Caco-2/TC7 cells were infected during 3 h with 5 x 10^6 CFU mL^{-1} (MOI 100) of ETEC H10407. Interleukin-8 (IL-8) concentrations (in pg mL^{-1}) were determined in culture supernatants at the end of assays. Control experiments were performed without ETEC and probiotic (not infected) and without probiotic (not treated). The data represent the means ± SD of three independent replicates. Statistically different from untreated cells under similar experimental conditions at $p<0.05$ (*) or $p<0.01$ (**).

3.6 *In vitro* digestion in the gastrointestinal TIM-1 model does not impair *S. cerevisiae* ability to inhibit ETEC adhesion to Caco-2/TC7 intestinal cells

One major challenge for probiotics is to remain viable and keep their antagonistic properties in the stringent conditions found in the human gut. Then, the effect of transit through the upper human gastrointestinal tract (as simulated by the TIM-1 model) on *S. cerevisiae* CNCM I-3856 viability and anti-adhesive property was assessed. Yeast survival percentages in the TIM-1 ileal effluents are shown in Fig. 4.4A. The curve obtained for *S. cerevisiae* CNCM I-3856 perfectly fits that of the non-absorbable transit marker, showing that the probiotic yeast was not impacted by gastrointestinal stresses such as acid pH in the stomach or bile salts in the small intestine. At the end of digestion, a global survival percentage of 94.8 ± 4.9 % was found, confirming the high resistance of *S. cerevisiae* CNCM I-3856 to human gastrointestinal conditions. In a second stage, in order to assess the effect of *in vitro* digestion on yeast anti-adhesive properties, the whole content of the ileal compartment was collected at 120 min, washed to remove digestive secretions and inoculated onto Caco-2/TC7 intestinal cells at different concentrations. ETEC residual adhesion to epithelial cells was determined after 3 h pre-incubation with the probiotic and 3 h infection at MOI 100, based on the results obtained in Fig. 4.2. As previously observed with non-digested yeast (Fig. 4.2A and Fig. 4.4B), anti-adhesive properties of digested and washed *S. cerevisiae* CNCM I-3856 remained effective from a concentration of 10^6 yeasts mL^{-1} ($p<0.01$). Whatever the probiotic dose, ETEC residual adhesion was similar for non-digested, non-digested / washed or digested / washed cells, suggesting that gastrointestinal passage does not impair the ability of *S. cerevisiae* CNCM I-3856 to inhibit ETEC adhesion to intestinal epithelial cells.

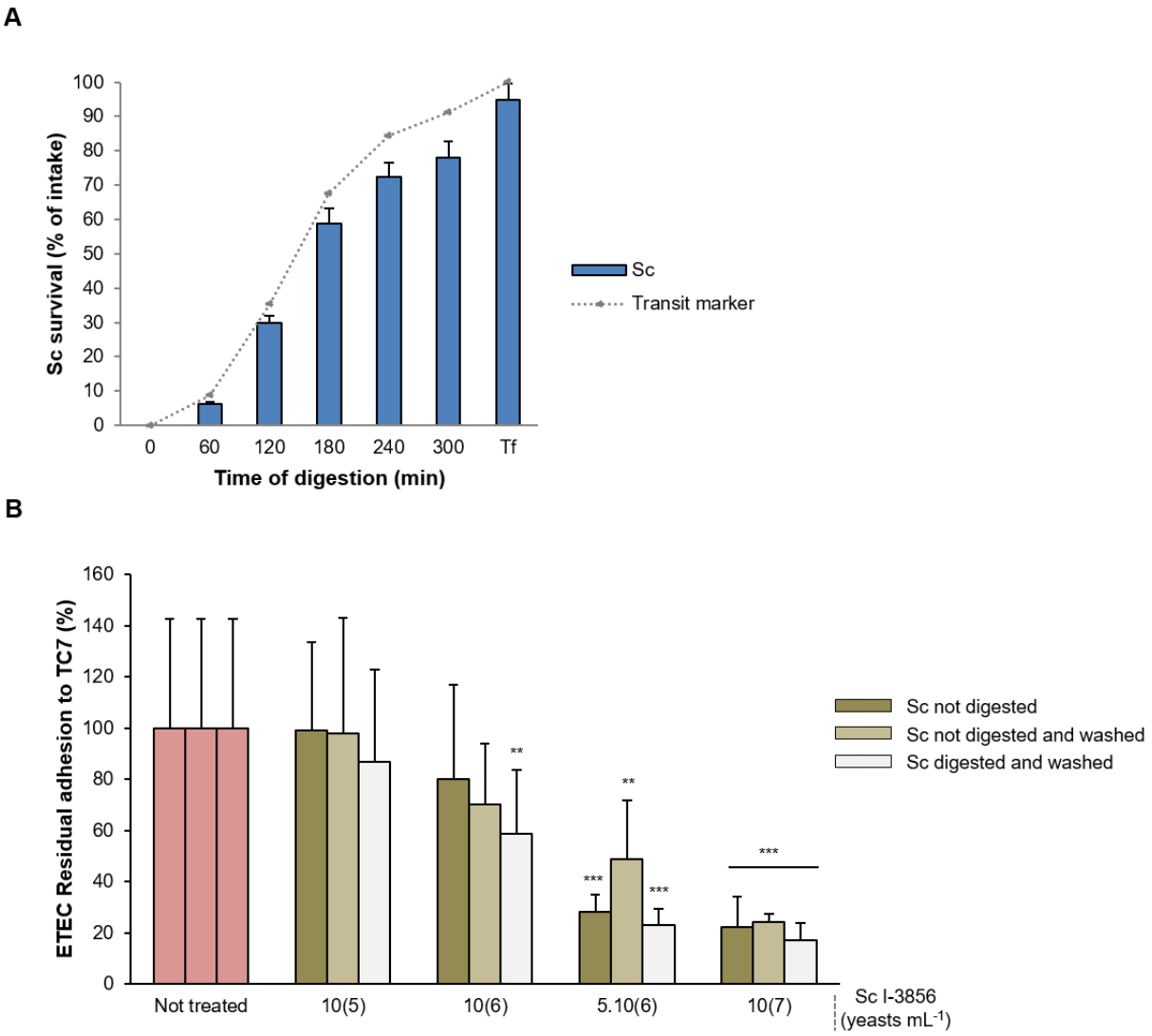

Figure 4.4. Effect of *in vitro* digestion in the gastrointestinal TIM-1 model on anti-adhesive properties of *S. cerevisiae* CNCM I-3856 against ETEC. Gastrointestinal digestions of probiotic yeasts (initial concentration in the glass of water: 10^7 yeasts mL^{-1}) were performed in the TIM-1 model. (**A**) In a first series of digestion, digestive samples were regularly collected in the ileal effluents and plated onto selective medium. Probiotic survival kinetic was expressed in cumulative percentages of intake. At the end of digestion, cumulative ileal effluents and final gastrointestinal residue were pooled (Tf). Survival percentages of the probiotic were compared to that of a non-absorbable transit marker. The data represent the means ± SD of three independent replicates. (**B**) In a second series of digestion, the whole content of the ileal compartment was recovered at 120 min, yeast cells were washed and added to Caco-2/TC7 intestinal cells at different concentrations (10^5, 10^6, 5 x 10^6 and 10^7 yeasts mL^{-1}). Yeasts were pre-incubated for 3 h before an additional period of 3 h infection with ETEC H10407. ETEC residual adhesion to Caco-2/TC7 cells (in %) was determined. The data represent the means ± SD of three independent replicates. Statistically different from untreated cells under similar experimental conditions at $p<0.01$ (**) or $p<0.001$ (***).

3.7 *S. cerevisiae* reduces ETEC colonization in streptomycin-treated mice

Finally, we used an *in vivo* model of ETEC infection in ICR mice to examine the ability of a 3-days pre-treatment with *S. cerevisiae* CNCM I-3856 to reduce bacterial colonization. Administration of the yeast significantly reduced weight loss associated with ETEC infection (-8.1 ± 3.2% *vs* -12.8 ± 4.4%, $p<0.05$), as shown in Fig. 1.5A. The number of ETEC bacteria in mice feces (Fig. 1.5B) as well as the number of colonic mucosa-associated ETEC bacteria (Fig. 1.5C) tended to decrease with probiotic treatment, but the differences were not found to be significant (182 000 *vs* 9050 bacteria mg^{-1} of feces, p=0.0745 ; 6085 *vs* 251 bacteria mg^{-1} of colonic tissue, $p=0.0530$). The most striking effect of the probiotic yeast was observed in ileal tissues (Fig. 1.5C) where ETEC was no more detected in 4 out of 7 mice ($p<0.05$).

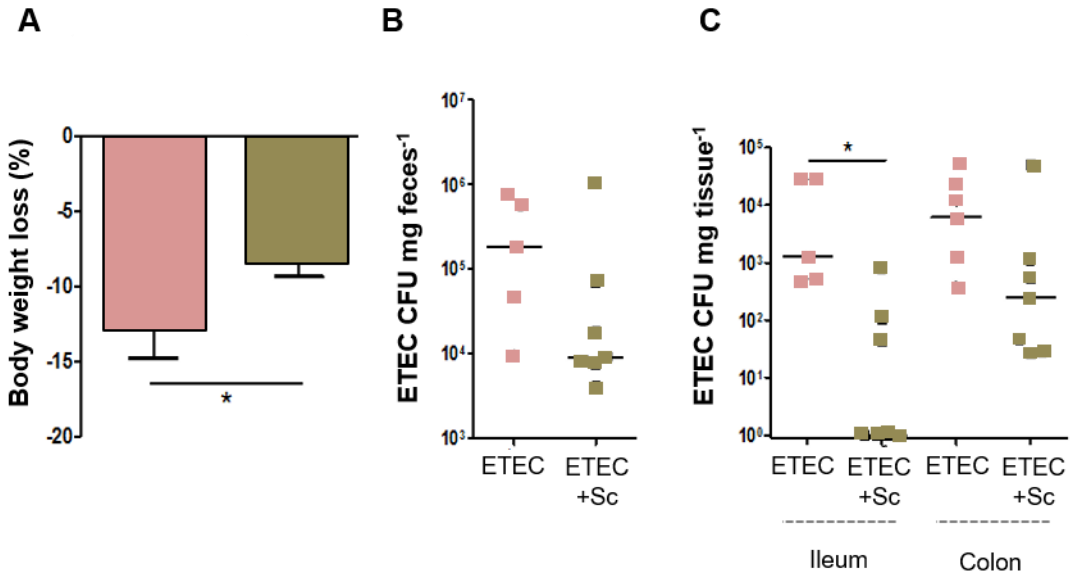

Figure 4.5. **Effect of *S. cerevisiae* CNCM I-3856 on ETEC colonization in ICR mice.** Five to seven ICR mice were forced-fed three days with 5 x 10^7 yeasts/day before infection with ETEC H10407 (10^8 CFU). (**A**) Body weight loss (in %) of mice at day 4 (24h after ETEC challenge) compared to day 1. The data represent the means ± SEM of 5 (ETEC in pink) to 7 (ETEC+Sc in brown) mice per group. ETEC+Sc statistically different from ETEC at $p<0.05$ (*). (**B**) Number of ETEC bacteria at day 4 (in CFU mg^{-1} of feces) in feces of infected mice treated or not with Sc. Individual results are indicated by each point and lines represent medians. (**C**) Number of ETEC bacteria at day 4 (in CFU mg^{-1} of tissue) associated to the ileal or colonic mucosa of infected mice treated or not with Sc. Individual results are indicated by each point and lines represent medians. ETEC+Sc statistically different from ETEC at $p<0.05$ (*).

4. Discussion

The present study shows for the first time that the probiotic yeast *S. cerevisiae* CNCM I-3856 exerts an antagonistic effect against the prototypical human ETEC strain H10407. Thanks to a large range of complementary *in vitro* and *in vivo* assays, we tried to describe associated mechanisms of action, in relation with the three modes of action described for probiotics against enteric pathogens (Cordonnier et al., 2017; Preidis et al., 2011): (i) direct antagonism defined as probiotic inhibition of pathogen growth or down-regulation of the expression of virulence genes, such as adhesins or toxins required for pathogenesis; (ii) competitive exclusion where probiotics alter the microenvironment to prevent pathogens from gaining access to their appropriate receptors, limit their attachment, colonization, entry or translocation, or improve intestinal barrier function; (iii) and immunomodulation where probiotics elicit a variety of responses from immune cells to limit infection and inflammation.

4.1 Direct antagonism

Here, we showed that prophylactic treatment with *S. cerevisiae* CNCM I-3856 was able to significantly reduce ETEC growth in culture media. This was assessed by plating and confirmed by PMA-qPCR to ensure that the lower number of culturable ETEC was not due to agglutination (see below). This work is the first study reporting the growth inhibition of an ETEC strain from human origin by probiotic yeasts, while previous works only involved *Lactobacillus* spp (Tsai et al., 2008). Inhibition of pathogen growth has been mainly linked to the ability of probiotics to produce anti-microbial compounds. Nevertheless, in contrast to probiotic bacteria (particularly lactic acid bacteria), which are known to produce bacteriocins (Dobson et al., 2012), probiotic yeasts are rarely known to diffuse specific antagonistic compounds (Tiago et al., 2012).

In ETEC infections, the secretion of enterotoxins represents the major virulence trait leading to watery diarrhea. In the present study, we demonstrated that *S. cerevisiae* down-regulated *eltB* mRNA gene expression and LT enterotoxin production by ETEC in culture media as well as LT production in intestinal cells. Only one study by Zhou et al. (2014) has previously shown a decrease in *estA* gene expression (encoding ST enterotoxin) by *Lactobacillus reuteri* in piglet intestinal cells. The present work is then the first one performed with human intestinal epithelial cells and providing results on both LT toxin production and *eltB* gene expression. In addition to a reduction in LT gene expression, we showed that such a decrease in toxin amounts can be also related to its removal by the probiotic yeast. This removal might be explained by toxin degradation or binding to yeast surface. Similarly, Pothoulakis et al. (1993) have previously shown that a 54-kDa serine protease from another strain of *S. cerevisiae, S.boulardii* effectively hydrolyzes the toxin A produced by *Clostridium difficile*. Brandao et al. (1998) also indicated the presence of a specific receptor on the surface of *S. cerevisiae* W303 able to bind to the cholera toxin, which is structurally very close to LT toxin. Lastly, with regard to gene expression, in a previous study by our team, we have already shown that *S. cerevisiae* CNCM I-3856 is able to decrease *stx* gene expression encoding for Shiga-toxins in EHEC, another pathotype of *E. coli* (Thévenot et al., 2015). This could be mediated through the quorum sensing that has been recently shown to modulate the expression of important virulence genes in ETEC (Sturbelle et al., 2015).

4.2 Exclusion

Enteric pathogens have evolved a wide range of specific strategies to disseminate through the digestive lumen, cross mucus layer to reach intestinal epithelial cells and spread the infection. For example, it has been recently discovered that ETEC H10407 produces two mucinase proteins YghJ and EatA (Luo et al., 2014; Kumar et al., 2014) that degrade intestinal mucins and should promote bacterial access to enterocytes. It is acknowledged that adhesion of bacteria to host surfaces is a crucial aspect of colonization as it prevents the mechanical clearing of pathogens and confers a selective advantage towards bacteria of the endogenous microbiota (Ribet and Cossart 2015). Probiotics can favor the exclusion of pathogens by competing for binding sites. Therefore, in a second part of this work, we investigated the ability of *S. cerevisiae* CNCM I-3856 to reduce ETEC colonization in a mice model and inhibit bacterial adhesion to mucins and intestinal Caco-2/TC7 cells.

We demonstrated in our model of immunocompetent mice that *S. cerevisiae* CNCM I-3856 effectively reduces ETEC ileal loading. This is the first work reporting the inhibition by a probiotic yeast of ETEC colonization *in vivo* in animals. Up to date, only one study has described in a murine model a reduction in bacterial fecal shedding after oral administration of *Lactobacillus casei*, but the intestinal loading of the pathogen was not measured (Mirnejad et al., 2010). This result is particularly striking as the ileum is known to be the main site of infection by ETEC in the human body (Deneke et al., 1983). Interestingly, the tropism of ETEC for the mice ileum has been also recently confirmed by using *in vivo* bioluminescence imaging (Rodea et al., 2017).

In further experiments, we showed that the probiotic *S. cerevisiae* reduced the number of adherent bacteria *in vitro* both to mucus layer and human intestinal epithelial cells. In the last case, the effect was found to be dose-dependent and maximized by a prophylactic treatment. There was no documented study reporting the inhibition of ETEC adhesion to mucins by probiotics. On the contrary, anti-adhesive properties of lactic acid bacteria and probiotic yeast strains have been already evidenced in *in vitro* cultures of human (Osmanagaoglu et al., 2010, Zhong et al., 2004) and piglet (Badia et al., 2012; Roselli et al., 2007) intestinal cells. Little is known about the mechanism of inhibition of ETEC adhesion by probiotics. It has been assumed that probiotics may (i) impede the access of pathogens to host intestinal tissue by non-specific steric hindrance (particularly relevant for yeast cells that are 10 times bigger than bacteria), (ii) stimulate mucin production and thus impair the adhesion of pathogens to enterocytes or (iii) block the binding site of ETEC to mucins or epithelial cells by receptor competition (Turner et al., 2006). In accordance with previous studies on various strains of *S. cerevisiae* (Klingberg et al. 2008), we found that our probiotic yeast was slightly adherent to both mucus and intestinal epithelial cells, making unlikely the adhesive competition between the yeast and ETEC. We further investigated the ability of *S. cerevisiae* CNCM I-3856 to trap ETEC cells at their surface. We showed that the probiotic yeast effectively agglutinates the human ETEC strain H10407, as it has been previously observed by Zanello et al. (2011) for the pig K88 ETEC strain. Agglutination between ETEC and the probiotic *S. cerevisiae* was inhibited by mannose. *S. cerevisiae* contains mannan in the outer layer of their cell wall and it has been shown that ETEC strains express at their surface mannose-sensitive (type 1) fimbrial lectins (Knutton et al. 1984). We therefore propose that ETEC bind to the mannan on the surface of yeast cells through type-1 fimbriae, thereby limiting interactions with mannose residues from mucins or

intestinal epithelial cells. A very recent study by Sheikh et al. (2017) confirms our hypothesis. The authors have shown that *fimH* ETEC mutants (with no type 1 pili activity) were unable to agglutinate yeast and have a reduced ability to adhere to intestinal epithelial cells. Interestingly, *fimH* mutants were also impaired in delivery of both LT and ST toxins.

Overall, we hypothesized that the reduced ETEC colonization observed in mice after the yeast treatment might be correlated to an inhibition of ETEC adhesion to mucin and intestinal epithelial cells, as a possible consequence of probiotic-pathogen agglutination. It might be also related to (i) the reduction of ETEC growth which in turn diminishes the number of adherent ETEC or to (ii) the decrease in LT toxin production due to direct antagonism, as Allen et al. (2006) have already shown that the enterotoxin provides a significant advantage in colonization of the small intestine.

4.3 Immunomodulation

The epithelium is a crucial regulator of intestinal immune homeostasis and the modulation of inflammatory responses is thought to be an important mechanism by which probiotics modify the outcome of enteric infections. The synthesis and secretion of pro-inflammatory cytokines are initiated by bacterial interactions with cellular receptors such as Toll-like receptors (TLR) (Mongensen 2009) and orchestrated by the well-known inflammatory signaling pathways Nuclear Factor Kappa B (NF-κB), Extracellular Signal-Regulated Kinases (ERK1/2) or p38 Mitogen Activated Protein Kinase (p38-MAPK) (Schmitz et al., 2011). ETEC induce a mild inflammatory response (Pawlowski et al., 2009) and IL-1β, IL-8, IL-6 and TNF-α pro-inflammatory cytokines were detected in fecal samples of infected patients (Mercado et al., 2011; Long et al., 2010). Here, we showed that pre-incubation with *S. cerevisiae* CNCM I-3856 inhibited in a dose-dependent manner IL-8 production by ETEC-infected human intestinal cells. Our results are in accordance with the work from Klingspor et al. (2015) who demonstrated that IL-8 expression was considerably increased in ETEC-infected human Caco-2 cells and that of Zanello et al. (2011) who showed in infected porcine intestinal epithelial cells (IPEC-J2) that *S. cerevisiae* CNCM I-3856 inhibited IL-8 gene expression. The effect of the probiotic yeast has been linked to its ability to decrease ERK1/2 and p38 MAPK phophorylation. Another hypothesis is that the yeast could interfere with TLR signaling as previously described for *Lactobacillus rhamnosus* by Li et al. (2012). Lastly, the decrease in IL-8 concentration could be related to a lower number of bacteria adhered to epithelial cells, as described above, or to IL-8 degradation by the yeast or binding to its cell surface. Nevertheless, this last hypothesis seems unlikely, as only one previous study has shown in a murine colitis model that a probiotic strain of *Lactobacillus* was able to degrade IP-10 chemokine through the secretion of a protease called lactocepin (Von Schillde et al., 2012).

Taken together, our results suggest that *S. cerevisiae* CNCM I-3856 seems to exert an anti-infectious activity against the human reference strain ETEC H10407 through a multi-targeted approach, namely inhibition of bacterial growth and toxin production, reduction of adhesion to mucins and intestinal epithelial cells and suppression of ETEC-induced inflammation (Fig. 4.6). We also highlighted that the most efficient way to administer the probiotic treatment would be the use of prophylactic measures. *In vivo* studies in humans have already shown that *S. cerevisiae* CNCM I-3856 significantly improved abdominal pain/discomfort and bloating in IBS patients (Cayzeele-Decherf et al., 2014). Besides, traveler's diarrhea have been associated with a higher risk of developing IBS (Connor and Riddle, 2013).

Therefore, *S. cerevisiae* CNCM I-3856 may be used not only to prevent ETEC infections but also associated PI-IBS. Next steps will be dedicated to the study of probiotic/ETEC interactions in a more complex and physiologically relevant digestive environment by using dynamic multi-compartmental models of the human gastrointestinal tract, such as the TIM-1 or the SHIME. In particular, for a deeper understanding of probiotic mode of action, we will investigate how *S. cerevisiae* CNCM I-3856 may modulate human gut microbiota and the subsequent impact on ETEC colonization.

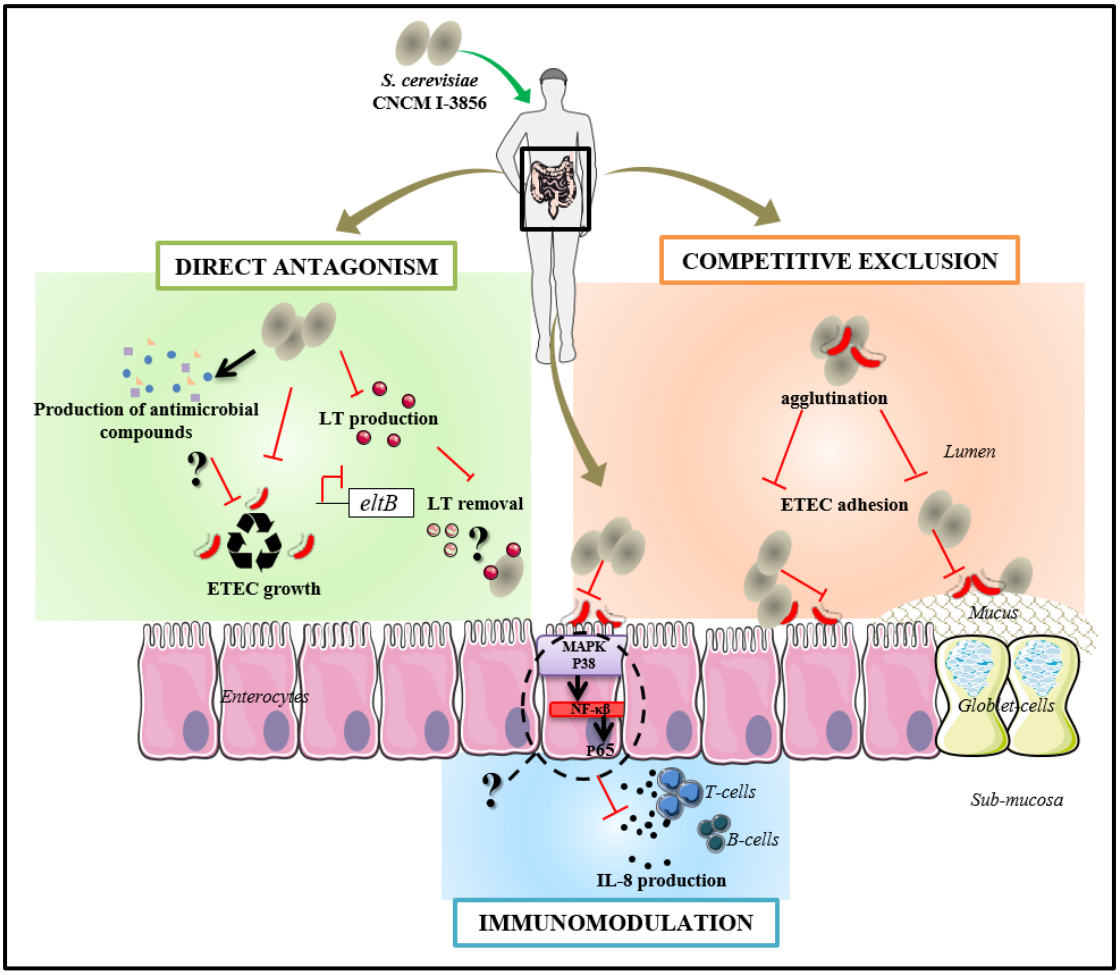

Figure 4.6. **Overview of *S. cerevisiae* CNCM I-3856 potential modes of action in ETEC infection.** *S. cerevisiae* CNCM I-3856 exerts inhibitory effects (red line) against ETEC H10407 through direct antagonism, competitive exclusion and immunomodulation.

5. Conclusion

Collectively, we have shown in the present chapter that the pre-administration of the probiotic yeast *S. cerevisiae* CNCM I-3856 can exert an anti-infectious activity against ETEC H10407 through complementary *in vitro* / *in vivo* models.

The yeast:

- limits ETEC growth in simple culture medium,
- reduces ETEC adhesion to type II-mucin-agar,
- inhibits ETEC adhesion to IECs and exerts an immunomodulatory effect by decreasing IL-8 cytokines in a dose-dependent manner,
- down-regulates *eltB* mRNA gene expression and the associated LT enterotoxin production,
- reduces ETEC loading in mice ileum (after a repeated treatment),

We also identified an agglutination mechanism between yeast and ETEC which could be mannose related.

Finally, *S. cerevisiae* CNCM I-3856 withstands greatly the GI passage and keep its inhibitory properties once digested in the TIM-1 system. To gain knowledge on the probiotic mechanism against ETEC in the human GI tract, further investigations testing the co-administration of the yeast and ETEC in the TIM-1 system; and testing the prolonged pre-, co-, and post- administration of the yeast in the M-SHIME ileum and ascending colon on ETEC survival and virulence function have been performed. These results are provided in chapter 5.

6. Compliance with ethical standards

Conflict of Interest The authors declare that they have no conflict of interest.

Ethical of approval Animal protocols used in the study were approved by the committee for ethical issues, CEMEA Auvergne (N° agreement 00730.02).

7. Candidate contribution and acknowledgements

Under supervision of Stéphanie Blanquet-Diot and Tom Van de Wiele, I designed the experimental work. I carried out the following experiments: the co-cultures, agglutination and mucin adhesion assays as well as the reverse transcription and ELISA assays. The cell culture experiments were performed in collaboration with Adeline Sivignon. The mouse infection experiments were performed by Adeline Sivignon and the TIM-1 experiments by Sylvain Denis. I processed the experimental data, performed the analysis, drafted the manuscript and designed the figures. I wrote the manuscript with input from all authors. Adeline Sivignon and I are co-first authors of the publication.

I would like to acknowledge M2iSH laboratory for their collaboration, for the realization of the mice experiments and for sharing their expertise in the cell culture and ELISA assays. This research was funded by Lesaffre company (Marcq-en-Baroeul, France).

8. Supplementary data

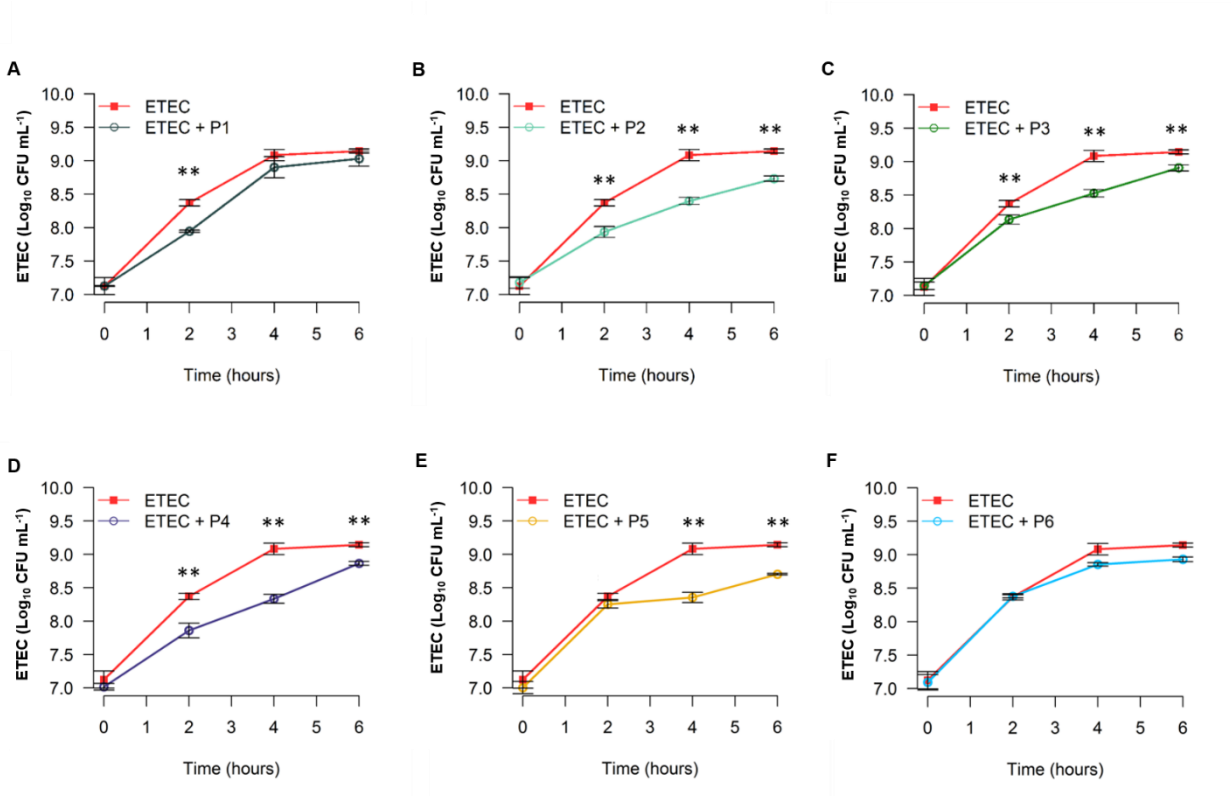

Figure S4.1. ETEC growth inhibition tests in the course of a probiotic screening including six different strains. ETEC H10407 growth in LB media (10^7 CFU mL^{-1}), as determined by plating, without probiotic (red) or after 3 h pre-incubation with (A, B, C) 10^7 yeasts mL^{-1}; (D, E, F) 10^7 bacteria mL^{-1}. P3 corresponds to the probiotic *S. cerevisiae* CNCM I-3856 that has been retained all along the PhD project. The data represent the means ± SD of three independent replicates. Statistical differences between ETEC and probiotic treatment are given at $p \leq 0.05$ (*) and $p \leq 0.01$ (**), applying a Mann-Whitney Wilcoxon test.

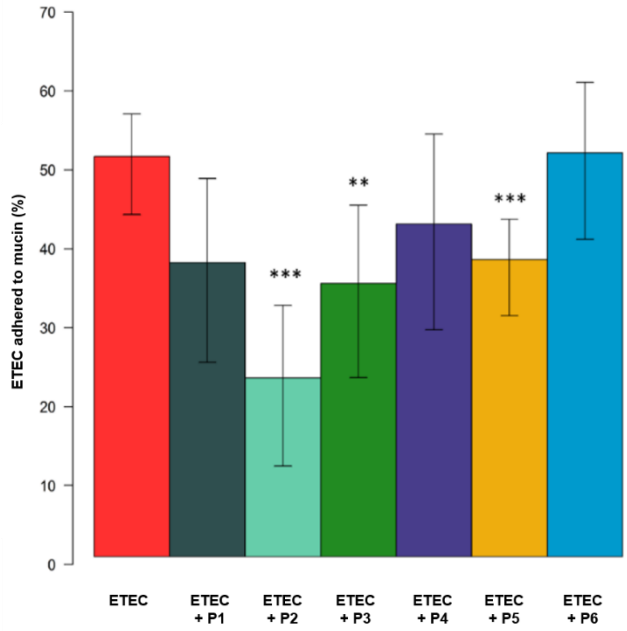

Figure S4.2. ETEC-mucin adhesion inhibition tests in the course of a probiotic screening including six different strains. ETEC (10^7 CFU mL^{-1}) adhesion to mucin-agar layer without probiotic (red) or after 1 h pre-incubation with 10^7 yeasts mL^{-1} (P1, P2, P3), or 10^7 bacteria mL^{-1} (P4, P5, P6). The data represent the means ± SD of three independent replicates. Statistical differences between ETEC and probiotic treatment are given at $p \leq 0.05$ (*) and $p \leq 0.01$ (**), applying a Mann-Whitney Wilcoxon test.

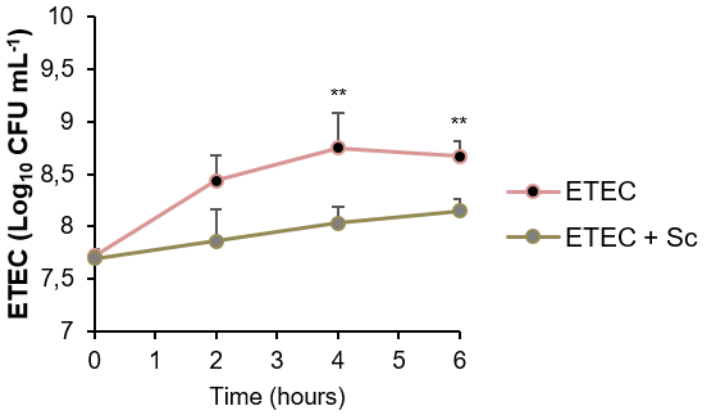

Figure S4.3. ***In vitro* effect of *S. cerevisiae* CNCM I-3856 on ETEC viability as determined by PMA-qPCR.** ETEC H10407 growth in LB media, as determined by PMA-qPCR , without probiotic (pink) or after 3 h pre-incubation with 10^7 yeasts mL^{-1} (Sc, brown).

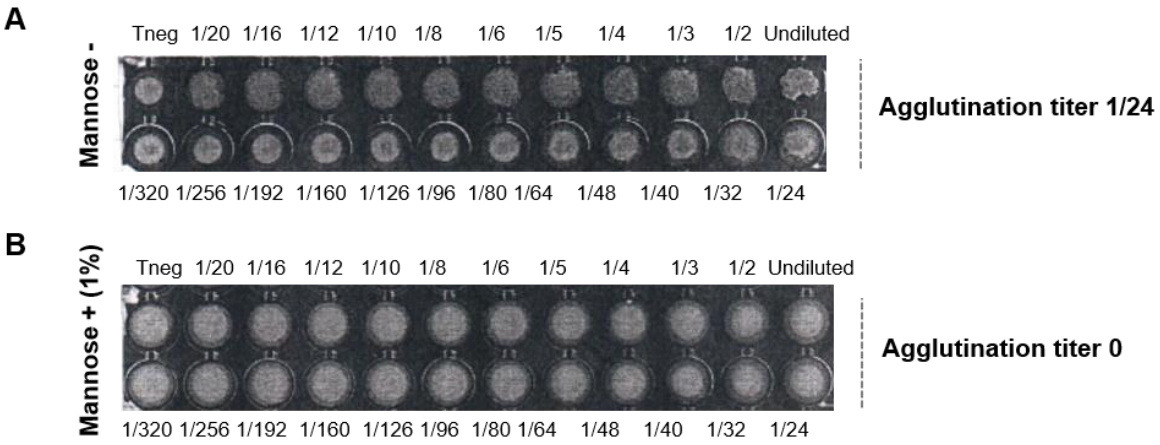

Figure S4.4. Microplate agglutination of ETEC and Sc. A suspension of yeasts ($2x10^8$ CFU mL^{-1} in PBS) was prepared with or without α-D mannose 1% and distributed in 96-wells microplates. In each well, serial dilutions (from undiluted to 1/320) of ETEC suspension yeasts ($2x10^8$ CFU mL^{-1} in PBS) were added. Titer agglutination was visually determined after at least 1 h incubation at room temperature. Control wells (Tneg) were performed without ETEC.

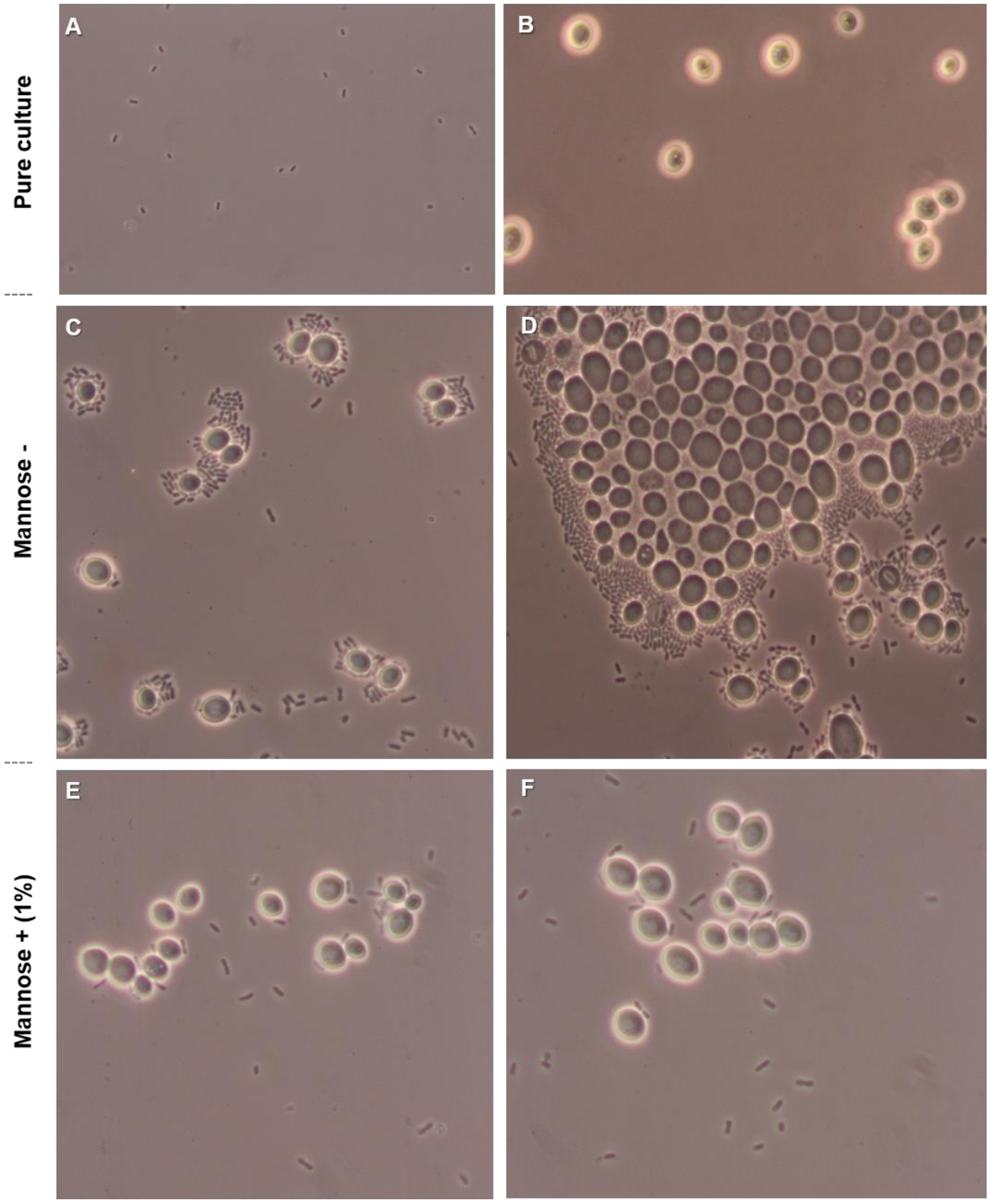

Figure S4.5. **Phase contrast microscopy images.** Microscopic observation (magnification x 1000) of a pure culture of (**A**) ETEC, (**B**) Sc, (**C, D**) ETEC/Sc agglutinates after 1 h co-culture without any treatment and, (**E, F**) ETEC/Sc with 1% α-D mannose.

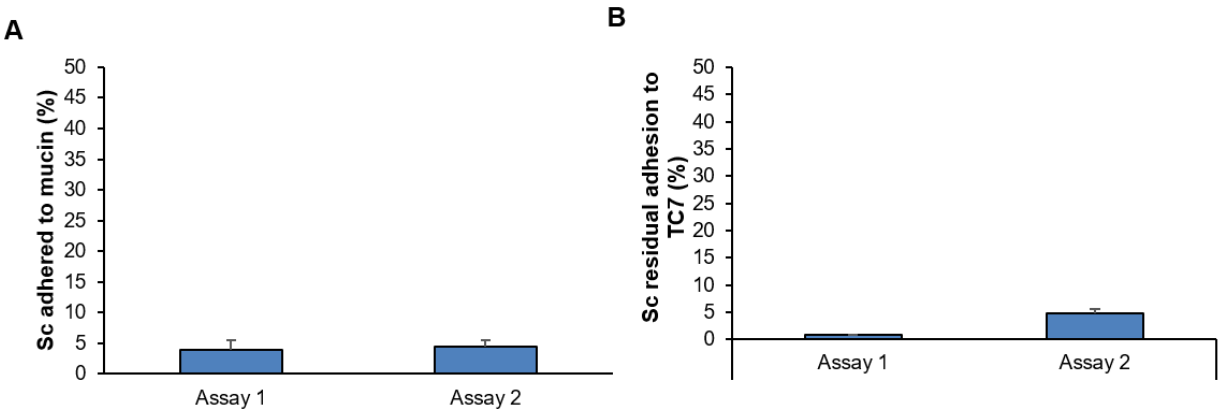

Figure S4.6. **Adhesion capacity of Sc probiotic to mucin and TC7 cells.** (**A**) Sc (10^7 yeasts mL^{-1}) adhesion to mucin-agar layer after 1 h incubation; (**B**) Sc ($5x10^6$ yeasts mL^{-1}) adhesion to TC7 cells ($5x10^4$ cells mL^{-1}) after 3 h incubation.

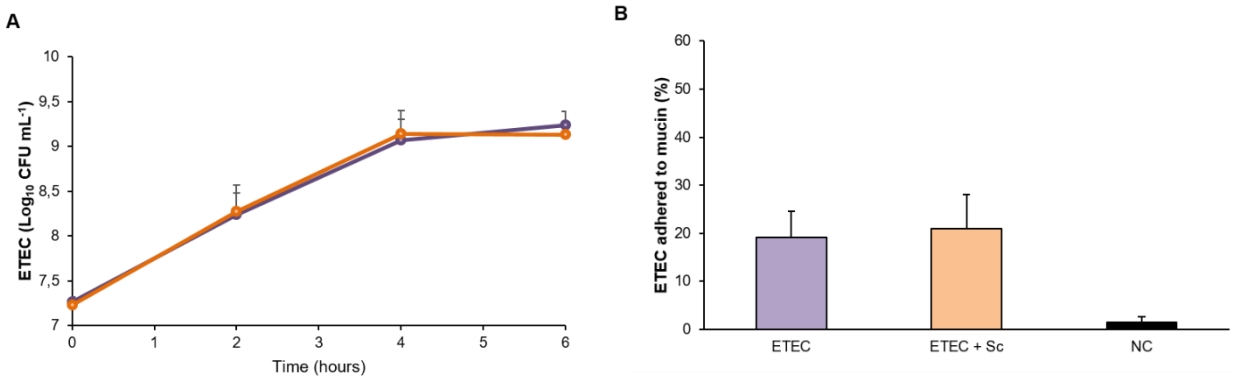

Figure S4.7. ***In vitro*** **effect of** ***S. cerevisiae*** **on ETEC O6:H16 growth in LB medium (A) and adhesion to mucin-agar (B).** The graphs show no effect of the probiotic on the serotype O6:H16, which confirms the strain-specificity of *S. cerevisiae* in the induction of inhibitory effects. Agar without mucin was used as negative control (NC).

CHAPTER 5 : MARRY TIM-1 AND M-SHIME FOR AN IN-DEPTH UNDERSTANDING OF THE ANTI-INFECTIOUS PROPERTIES OF *S. CEREVISIAE* CNCM I-3856 AGAINST ETEC PATHOGEN IN THE HUMAN GUT

ROUSSEL C., De PAEPE K., GALIA W., DE BODT J., LERICHE F., BALLET N., VAN DE WIELE T., BLANQUET-DIOT S.

BLANQUET-DIOT S. and VAN DE WIELE T. are co- last authors. Manuscript under preparation for submission in mBio journal.

***

In chapter 4, the antagonistic properties of the probiotic *S. cerevisiae* CNCM I-3856 against ETEC H10407 were assessed *in vivo* in mice and in simple *in vitro* models. In addition, GI digestions in the TIM-1 system combined to ETEC-infected intestinal epithelial cells were set out in order to evaluate the immunomodulatory and anti-adhesive properties of the digested yeasts. The encouraging outcomes have merited to be further explored in this chapter, through the use of the two most relevant models of digestion TIM-1 and M-SHIME which reproduce closely the human GI and colonic environments.

5 Marry TIM-1 and M-SHIME for an in-depth understanding of the anti-infectious properties of *S. cerevisiae* CNCM I-3856 against ETEC pathogen in the human gut

Abstract ETEC is one of the most common cause of acute traveler's diarrhea. The production of adhesins and the secretion of enterotoxins constitute the major virulence traits of the bacterium. Treatments are mainly symptomatic and can involve antibiotherapy. However, given the rise of antibiotic resistance worldwide, there is an urgent need for the development of new preventive strategies for the control of ETEC infections. Among them, a promising approach is the use of probiotics. The objective of the present study was to further examine the antimicrobial properties of the probiotic *S. cerevisiae* CNCM I-3856 against ETEC H10407 in complex *in vitro* models TIM-1 and M-SHIME. This study revealed that the probiotic had no effect on the survivability of ETEC all along the digestion. However, the functionality of the pathogen through its virulence activity was significantly altered under the probiotic treatment with a repression of the virulence genes encoding for the enterotoxins, especially in the TIM-1 system, as well as the tendency to decrease at protein level the LT enterotoxin production. The *fimH* gene, encoding for the type 1 pili, exhibited a profound over-expression all along the digestion in ileal effluents under probiotic condition. From mechanistic perspectives, we can assume that the *fimH* over-expression could be associated to the mannose related agglutination between ETEC and the yeast, as previously observed in batch medium (chapter 4). An overall increased concentrations of the main SCFA acetate, propionate, and butyrate was shown under probiotic condition and could be associated to the stimulation of *Faecalibacterium*, *Butyricicoccus* and *Roseburia* genera for butyrate production. Acetate producers *Bifidobacterium* and *Veillonella* were stimulated as well. The probiotic tended to counteract the blooming of opportunistic species such as *Achromobacter* and *Klebsiella* induced in the course of ETEC infection in the ileum and ascending colon. The promising ETEC H10407-inhibitory properties displayed by the probiotic yeast *S. cerevisiae* CNCM I-3856 merit more attention. Thus, complementary investigations by coupling the digestive systems with human intestinal cell cultures could serve to an improved understanding of *S. cerevisiae* anti-microbial properties.

1. Introduction

Prevailing in people living in resource-limited countries, diarrheal diseases related to ETEC represent thus far one of the leading cause of morbidity, amounting to 44 million diarrheal cases annually (Giddings et al., 2016). As well, ETEC is part of the most frequent bacterial causes of diarrhea for people traveling in Asia, Africa and Latin America, including military personnel deployed in these areas, and such infections extend sporadically to industrialized nations (Lamberti et al., 2014; Walker et al., 2017; MacDonald et al., 2015). As critical virulence traits, ETEC mediates attachment to the IECs in the distal part of the small intestine through a large set of colonization factors and adhesins (e.g. CFA/I, Tia, EtpA). Then, the release of LT and/or ST enterotoxins leads to the onset of profuse watery diarrhea and dehydration (Roussel et al., 2017; Fleckenstein et al., 2016; Qadri et al., 2005). Recent data strongly suggest that following ETEC diarrheal episodes, people may experience post-infectious (PI) chronic sequelae ranging from functional GI disorder to irritable bowel syndrome (IBS) (Connor and Riddle, 2014; Barrett and Brown, 2016). To such extent that 10-14% of traveler's diarrhea associated ETEC cases result in IBS (Bourgeois et al., 2016).

So far, no prophylactic or curative treatments specific to the ETEC etiologic agent are available on the market. As a means of recourse, the general clinical recommendations given for diarrheal episodes are therefore followed for ETEC infection, including the prescription of antibiotic therapy in the case of acute diarrhea (WHO, 2002; Zaman et al., 2017; Taylor et al., 2017; Riddle et al., 2016). Nonetheless, such measures remain inadequate to overcome the burden, further highlighting the importance to speed up the development of prophylactic approaches (Bruzzese et al., 2018; CDC, 2016). In the context of the dramatic increase of antibiotic-resistance and its concomitant health repercussions, probiotics are considered as a wholesome alternative approach to address this problem (Roussel et al., 2016).

Over the last two decades, initial efforts have been centered on establishing scientific support for the efficacy of several bacterial and yeast probiotic strains to combat ETEC pathogen by interfering with its survival, adhesion to intestinal mucosa or expression of virulence genes (Roussel et al., 2016). However, the majority of these studies have been carried out in piglets, involving ETEC $F4^+$ or $F5^+$ strains, that are strongly associated with neonatal and post-weaning enteric colibacillosis in the animals, but unlikely pathogenic in humans (Dubreuil et al., 2016; Fairbrother et al., 2012). As it is obvious that the outcomes will be strain-dependent, studies involving human strains require the use of adequate human gut models. Only two human clinical trials have investigated the effect of probiotics when orally challenged with live attenuated human ETEC strains (Ouwehand et al., 2014; Ten Bruggencate et al., 2015). Unfortunately, these studies using a single strain of *Lactobacillus acidophilus* or a blend of probiotic bacteria and yeast displayed low level of evidence for the treatment of ETEC-associated symptoms. Other studies have shown a significant reduction in the risk of traveler's diarrhea when probiotics such as *S. boulardii* were given (McFarland et al., 2007; Bae, 2018), but ETEC strains have not been clearly involved in the diarrheal etiology. As recently published by an expert panel of the International Society of Travel Medicine, insufficient evidence to recommend the use of the actual commercially available pre- or probiotics to prevent or treat traveler's diarrhea was highlighted (Riddle et al., 2017). We previously set out the assessment of the anti-infectious properties of the probiotic *Saccharomyces cerevisiae* CNCM I-3856 against ETEC H10407 (chapter 4, Roussel et al., 2018). This

strain which already displayed beneficial effects against other enteric *E. coli* pathogens (Etienne Mesmin et al., 2011; Sivignon et al., 2015; Thévenot et al., 2015) has proven in ETEC H10407 as well, its effective inhibitory properties through *in vitro* batch cultures, IECs cultures and *in vivo* mouse model (Roussel et al., 2018).

Therefore, the purpose of the present study was to further examine the inhibitory properties of the probiotic *S. cerevisiae* CNCM I-3856 against ETEC H10407 through the use of the complementary *in vitro* digestive models TIM-1 and M-SHIME, closely reproducing the human GI and colonic environments (as previously described in chapters 2, 3 and 4). Hence, this study greatly contributes to elucidate modulatory effects of the probiotic yeast on the dynamics of ETEC survival, physiological state and its virulence features, in the successive human GI niches from the stomach to the ascending colon. Finally, using next-generation *16S* rRNA gene-based amplicon sequencing, the capacity of *S. cerevisiae* to shape or maintain the functioning of the gut microbial ecosystems was explored. The inter-individual differences were captured by assessing six distinct fecal donors.

2. Materials and methods

2.1 ETEC and probiotic strains, media and growth conditions

ETEC serotype and culture conditions are described in chapter 2, section 2.1. The probiotic yeast strain *S. cerevisiae* CNCM I-3856 (Lesaffre Human Care, Marcq-en-Baroeul, France) was supplied in its active dried powder form, aliquoted and stored at room temperature. Before experiments, yeasts were resuspended in sterile saline water and mixed with an ultra-turrax yellow line (IKA, Rawang, Malaysia). Yeasts were plated onto Sabouraud agar (BD Difco Fisher, Waltham USA), supplemented with chloramphenicol (50 mg L^{-1}) (Sigma, St Louis, USA) and incubated at 30°C for 48h under aerobic conditions, as described in chapter 4 section 2.1.

For a good understanding: although the host cells are lacking in both systems TIM-1 and M-SHIME, we tried to simulate the start of an infection process, and for this purpose we named in the results section the day of ETEC inoculation as “infection”.

2.2 TIM-1 gastrointestinal model

The experimental set-up, operation of the TIM-1 system and sampling procedure were described in chapter 2, section 2.2. Two series of experiments were performed according to the treatment condition (control *vs* probiotic). The control condition consists of mineral water (200 mL) experimentally contaminated with ETEC (7.5 $\log_{10}$ CFU mL^{-1}) introduced into the stomach of the TIM-1 system; while during the probiotic condition, both ETEC (7.5 $\log_{10}$ CFU mL^{-1}) and the probiotic yeast *S. cerevisiae* (7.5 $\log_{10}$ CFU mL^{-1}) were co-administered in the TIM-1 stomach. Under both conditions, two experimental set-up of the TIM-1 were used: gastric digestions where only the gastric compartment was used (total duration of 60 min) and GI digestions using the entire TIM-1 model (total duration of 300 min). Digestions were run in quadruplicate (Fig. 2.1).

2.3 M-SHIME fermentation system

The experimental set-up and operation of the M-SHIME were described in chapter 2, section 2.3. The same gut regions were reproduced, only the number of vessels was changed and included two sets of seven SHIME vessels according to the treatment condition tested (probiotic *vs* control) (Fig. 5.1). The same six fecal donors were tested under both control and probiotic-treated conditions, as described in chapter 2, section 2.3, Table 2.2. The probiotic condition consists of the introduction of the yeast *S. cerevisiae* CNCM I-3856 resuspended in 30 mL sterile water (7.5 $\log_{10}$ CFU mL^{-1}) in the SHIME stomach, twice a day (9 a.m and 5 p.m) from day 2 to 20. The control condition consists in the introduction of 30 mL sterile water in the SHIME stomach, twice a day (9 a.m and 5 p.m) from day 2 to 20 (Fig. 5.1). Under both conditions, the system was challenged in the SHIME ileum vessels with ETEC by inoculation of 7.5 $\log_{10}$ CFU mL^{-1} at day 13, followed by a post-infectious period from day 14 to 20, resulting in a pre-, co- and post-incubation of the probiotic and the pathogen. Prior to the challenge, ETEC and *S. cerevisiae* were pre-digested 3 h under batch conditions, to reproduce the gastro-jejunal digestion of a glass of mineral water, where physicochemical conditions were closer to those found in TIM-1 as described in chapter 2, section 2.3, Table S.2.3.

2.4 DNA extraction

DNA was extracted and the quality was verified as described in chapter 2, section 2.4.

2.5 ETEC and probiotic quantification

All the plating, qPCR and PMA-qPCR procedures for ETEC were described in chapter 2, section 2.5. The number of cultivable probiotic yeast *S. cerevisiae* CNCM I-3856 in each digestive compartment of the TIM-1 was determined by direct plating onto Sabouraud agar, supplemented with chloramphenicol (50 mg L^{-1}) (48h incubation, 30°C), after appropriate serial dilutions in sterile saline water. Due to the TIM-1 dynamism, the results obtained for the yeast were cross-compared to that of a theoretical non-absorbable transit marker provided by the computer representing a 100% survival rate. The concentration of the transit marker fluctuates throughout the TIM-1 model depending on the volume of each compartment, the rate of dilution by digestive secretions and the chyme flow between two successive compartments.

2.6 Flow cytometry analysis

Three different flow cytometry staining cell protocols were used to study ETEC membrane integrity, ETEC membrane potential and ETEC intracellular pH. All the procedures were described in chapter 2, section 2.6.

2.7 RNA isolation and transcriptional analysis by quantitative real-time qPCR

RT-qPCR was used to follow the expression of seven virulence genes encoding for enterotoxins (*eltB* and *estAB*), enterotoxin release (l*eoA* and *tolC*), adhesins (*cfa/Ib, tia, fimH*), and for the stress response

(*rpoS*). RNA extraction, DNAse treatment, quality control of the RNA and RT-qPCR were described in chapter 2, section 2.7. The primers are referenced in chapter 2, Table 2.4.

2.8 LT-monosialoganglioside (GM1) ELISA

The procedure to measure the LT enterotoxin was described in chapter 2, section 2.8.

2.9 Statistical analysis

All statistical analyses were performed in R studio, version 3.5.1. All formal hypothesis tests were conducted on the 5% significance level ($p \leq 0.05$). The assumptions of normality and heterogeneity of variances were verified based on visual inspection of QQ-plots and shapiro-Wilk (stats4_3.4.2) and Levene's Test (car_2.1-5), preceding statistical hypothesis testing to assess pairwise comparison of: (i) *S. cerevisiae* survival at T time in comparison with the transit marker given by the TIM-1 system; (ii) ETEC survival under control condition at T time in comparison with ETEC survival under probiotic condition in the TIM-1 and M-SHIME; (iii) the $\log_2$ fold change gene expression under control condition at T time in comparison with the probiotic condition; and (iv) the LT enterotoxin production under control condition at T time in comparison with the probiotic condition. The assumptions were not met for most variables, in which a non-parametric Mann-Whitney (Wilcoxon- Rank-Sum) test with Holm correction was performed for (i, ii hypothesis); Nemenyi post-hoc test conducted after significant results for the friedman test was performed for (iii hypothesis), Fisher post-hoc test conducted after significant results for the Friedman test was performed for (iv hypothesis), using PMCMR package.

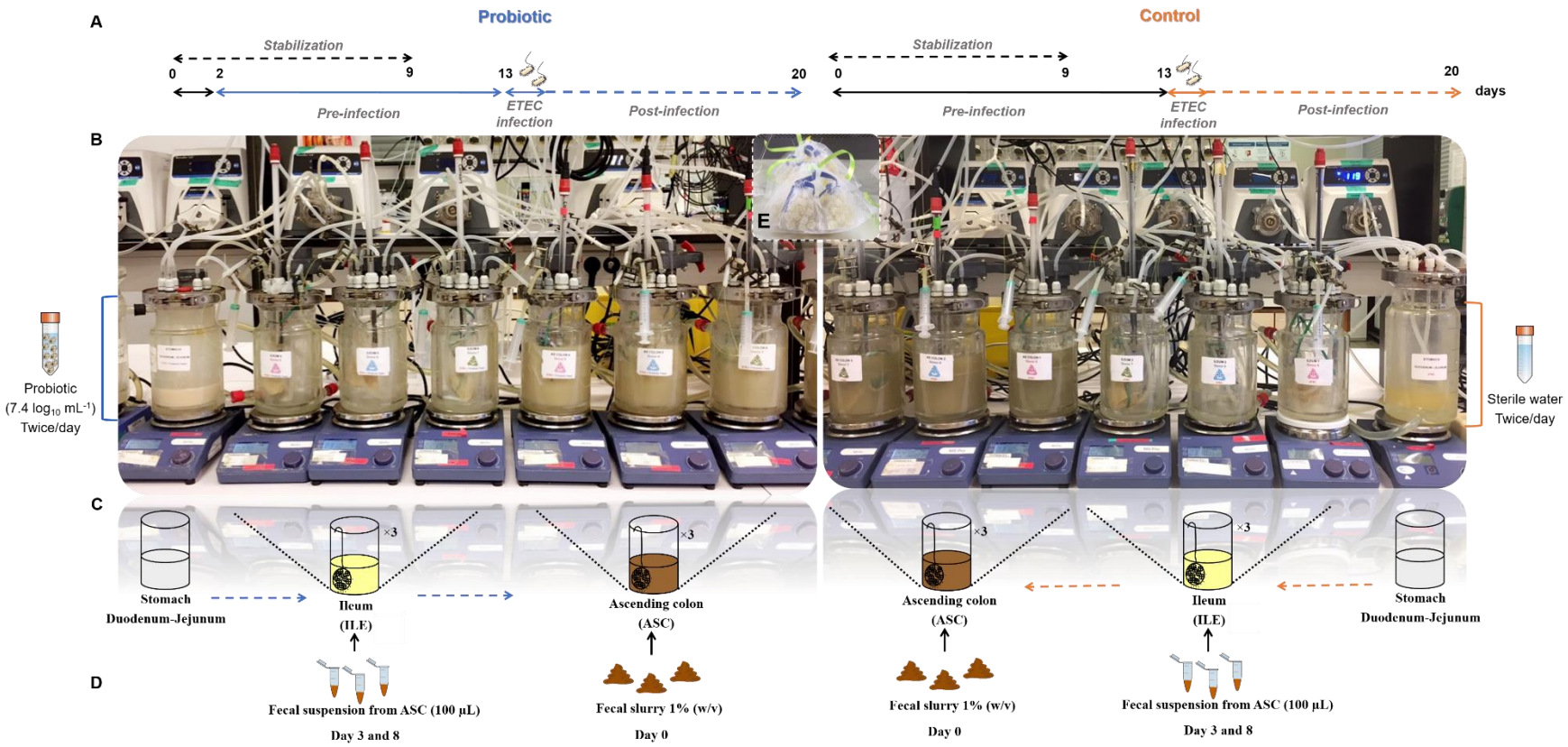

Figure 5.1. **M-SHIME set-up under probiotic and control conditions.** (**A**) Time course (days) of the M-SHIME run; (**B**) Picture of the M-SHIME system mimicking the digestive and fermentative conditions of three individuals under both treatment conditions. In total, the run has been performed twice to get a representative population of six distinct individuals; (**C**) The stomach/combined duodenum-jejunum vessel was connected with three ileum (ILE) bioreactors coupled to three ascending colon (ASC) vessels; (**D**) Upon start-up (day 0), the ASC were inoculated with the fecal samples obtained from three individuals. The fecal inoculation of the ILE started at day 3, by introducing a small amount of the fecal suspension collected in the ASC for each individual. To maintain such population levels, this inoculation was repeated at day 8; (**E**) Picture of the tulle bags stored in a sterile environment and containing the microcosms coated with type III mucin-agar. To reproduce the mucosal phase, the bags were introduced in each ILE and ASC vessel under N_2 flow to ensure anaerobic conditions.

2.10 Microbial community analysis

Next-generation *16S* rRNA gene amplicon sequencing of the V3-V4 region (341F-785R) was performed by LGC Genomics (Teddington, Middlesex, UK), on an Illumina MiSeq platform using Illumina V3 chemistry (Illumina, Hayward, CA, US), as detailed in De Paepe et al. (2017). The bioinformatics processing of amplicon data was performed as described in chapter 3, section 2.5. Although a certain level of uncertainty is introduced by classification to the species level based on short 300 bp reads, the best hit returned by both databases -RDP SeqMatch tool and NCBI BLAST- is used to refer to interesting OTUs in the results section of this article. In case of inconsistencies were seen between the RDP SeqMatch tool and NCBI BLAST, no species level classification was mentioned. A more detailed overview of the RDP Seqmatch and NCBI BLAST results for the most abundant and significant OTUs (best hit as well as the next best hit) can be found in Table S5.1.

Statistical analysis of amplicon and metabolic data. All statistical analyses were performed in R, version 3.5.1 (2018–09-04) (R Core Team, 2016). All formal hypothesis tests were conducted on the 5% significance level. To visualize differences in microbial community composition between donors, ordination and clustering techniques were applied. For these purposes, the shared file was further processed to remove OTUs with too low abundance according to the arbitrary cutoffs described by McMurdie and Holmes (2014). An OTU should be observed in 5% of the samples and read counts should exceed 0.5 times the number of samples (McMurdie and Holmes, 2014). Rarefaction curves were constructed to assure that the samples were sequenced in sufficient depth (Oksanen et al., 2016). To deal with differences in sampling depth, proportional data transformed on the common scale to the lowest number of reads was used (McMurdie and Holmes, 2014).

Principle Coordinate Analysis (PCoA; package stats4_3.3.1) (Gower, 1966; Cailliez, 1983; Becker et al., 1988; Cox, 2001; Ramette, 2007) was conducted based on the abundance based jaccard dissimilarity matrix (package vegan_2.4–0) (Anderson et al., 2006; Borcard et al., 2011; Oksanen et al., 2016) and visualized with ggplot2_2.1.0 (Wickham, 2009). This procedure was repeated on species and genus levels focusing on the comparison between treatment (e.g. control and probiotic), gut region (e.g. ileum lumen, ileum mucus, ascending lumen and ascending mucus), donor samples and the comparison between period (e.g. pre- and post-infection). On the genus level, weighed averages of genera abundances were a *posteriori* added to the ordination plot using the wascores function in vegan (Oksanen et al., 2016). To confirm the trends, observed data were clustered by means of an Unweighted Pair-Grouped Method using arithmetic Averages (UPGMA) clustering method (cluster_2.0.4) (Maechler et al., 2016). The significance of the observed group separation between treatment, gut region, donor and period conditions in the PCoA was assessed with a Permutational Multivariate Analysis of Variance (PERMANOVA) using distance matrixes (package vegan_2.4–0) (Ramette, 2007; Oksanen et al., 2016). Prior to this formal hypothesis testing, the assumption of similar multivariate dispersions was evaluated.

When comparing the effects, the influence of the treatment, gut region, donor and period conditions was determined by applying a distance based redundancy analysis (db RDA) (Vardakou et al.) using the abundance based jaccard distance as a response variable (vegan) (Ramette, 2007; Oksanen et al.,

2016). The factor treatment is used as a constraint with the effect of the gut region, period or donor are being partialled out. Interpretation of the results is preceded by a permutation test of the RDA results to confirm that a linear relationship exists between the response data and the exploratory variables. The constrained fraction of the variance, explained by the exploratory variables is adjusted by applying Ezekiel's formula (Borcard et al., 2011).

In order to find statistically significant differences in species abundance between the different treatments (control and probiotic), the DESeq package was applied as suggested by McMurdie and Holmes (2014) (Love et al., 2014; McMurdie and Holmes, 2014). The factors treatment, gut region, donor and period were used in the design formula. Statistical differences between the control and probiotic treatment were determined using a Wilcoxon Signed Rank Test on the proportional data. Statistical hypothesis testing to assess the effect of the products on the functional parameters was performed by using the Kruskal–Wallis rank sum test, followed by Pairwise Wilcoxon Rank Sum Tests with Holm correction for multiple testing.

2.11 Metabolites production

The procedure of SCFA extraction and measurement is described in chapter 3, section 2.4. Ethanol was measured from SHIME samples under both treatment conditions. After a ten-fold dilution in mili-Q sterile water, ethanol concentrations were determined using a HPLC system (Shimadzu Prominence HPLC system, Columbia, MD, USA) (Gildemyn et al., 2017).

3. Results

3.1 Survival capacity of *S. cerevisiae* CNCM I-3856 along the different GI regions

As a prerequisite to exert its antimicrobial properties in the course of ETEC infection, the probiotic yeast *S. cerevisiae* CNCM I-3856 must withstand the harsh conditions found in the upper and lower GI tract simulated by the TIM-1 and M-SHIME systems, respectively (Fig. 5.2).

The fate of the probiotic *S. cerevisiae* upon the upper digestive tract was followed when co-administered with ETEC, at the same dose in the TIM-1 system. The regionalized kinetics of survival of *S. cerevisiae* are first shown, and compared with a non-absorbable inert transit marker, representing a 100% survival (Fig. 5.2A, B, C, D). At time point T0, upon introduction of a glass of water in the stomach compartment, containing both the probiotic and ETEC, the average probiotic concentration amounted 7.4 ± 0.2 $\log_{10}$ mL^{-1}. Remarkably, the survival of *S. cerevisiae* was not impacted by the GI stresses such as the low pH encountered in the stomach (Fig. 5.2A) or the high bile salts concentration in the duodenum (Fig. 5.2B) since the probiotic kinetics paralleled that of the transit marker in all the digestive compartments. For instance, *S. cerevisiae* reached 6.0 ± 0.1 $\log_{10}$ mL^{-1} and 5.2 ± 0.8 $\log_{10}$ mL^{-1} at the end of the gastric (60 min) and ileal (300 min) digestion, respectively (Fig. 5.2A, D).

In the M-SHIME system, to simulate a usual posology, the probiotic was administered twice a day (from day 2 to 20) at a dose of 7.5 $\log_{10}$ mL^{-1} in the SHIME stomach. The impact of the ileal and ascending colon microbial populations derived from six distinct fecal donors, as well as the luminal and mucosal microenvironments were assessed on *S. cerevisiae* survival (Fig. 5.2E). The results show that 6 h after its first administration in the M-SHIME, the probiotic yeast maintained each day a higher concentration in the ileum lumen (6.5 $\log_{10}$ mL^{-1}) and mucus (5.8 $\log_{10}$ mL^{-1}) than in the ascending lumen (6 $\log_{10}$ mL^{-1}) and mucus (5 $\log_{10}$ mL^{-1}). Following ETEC infection at day 13, the yeast concentration was significantly decreased below 4 $\log_{10}$ mL^{-1} in the ascending colon mucus, while not significantly changed in the ileum compared to the pre-infection (Fig. 5.2E).

3.2 Effect of *S. cerevisiae* treatment on the dynamics of ETEC survival and physiological states along the different GI regions

The probiotic treatment has no direct inhibitory effect on ETEC survival in the gut. Beyond the impact of the physicochemical parameters and upper GI transit on ETEC survival, as studied in chapter 3, the effect of the co-administration of *S. cerevisiae* (T0 7.4 ± 0.2 $\log_{10}$ mL^{-1}) on ETEC survival (T0 7.7 ± 0.1 $\log_{10}$ mL^{-1}) was also investigated in the TIM-1. Collectively, the probiotic displayed no significant effect on ETEC survival over time from the stomach to the ileum (Fig. 5.3). Although the decrease of ETEC concentrations was less exacerbated with the probiotic treatment in the stomach (Fig. 5.3A), reverse trends were found in the duodenum (from 180 min), jejunum and ileum (from 240 min) in the non-treated condition with a tendency of higher ETEC growth recovery than under probiotic condition (Fig. 5.3B, C, D). The pre-, co- and post- administration of *S. cerevisiae* were then tested against ETEC in the M-SHIME gut regions (ileum and ascending colon), and microenvironments (luminal and mucosal)

with the six distinct fecal donors (Fig. 5.4). Given the complex microbial background, the *gspD* gene was used to characterize the dynamics of ETEC survival in the different gut regions from the M-SHIME. Following infection, no significant change was found in both conditions, suggesting that the yeast treatment did not display direct inhibitory effect on ETEC survival (Fig. 5.4).

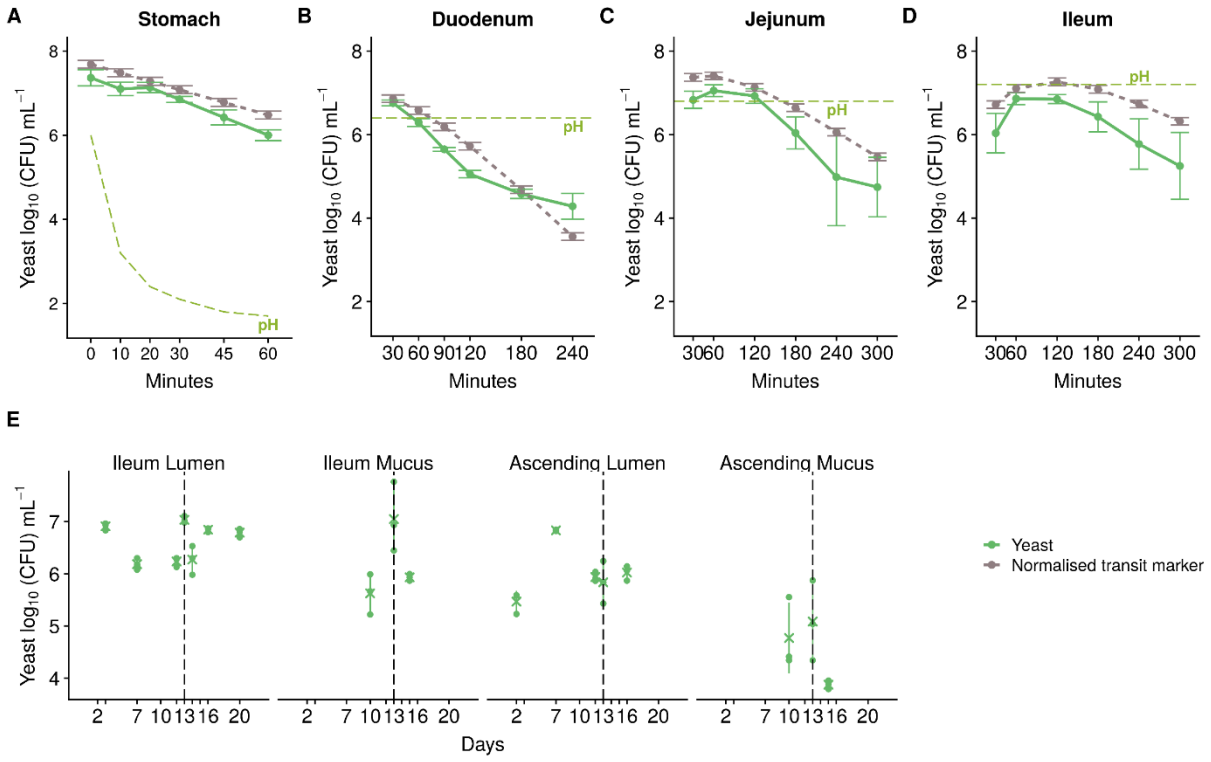

Figure 5.2. **Dynamics of *S. cerevisiae* survival in the different GI regions of the TIM-1 and M-SHIME systems as determined by plate counts.** Results are expressed as mean concentrations in $\log_{10}$ CFU mL^{-1} ± SD, as determined by plate counts. (**A, B, C, D**) The number of *S. cerevisiae* cultivable cells in the four compartments of the TIM-1 system (green line) was compared to the results obtained for an inert and non-absorbable transit marker indicating 100% survival (grey dashed line). Probiotic curves below that of the transit marker reflect cell mortality, while curves above the transit marker are indicative of a growth. The level of the pH in each compartment is illustrated in green dashed line. The experiment was repeated in four independent replicates. No statistically significant differences over time between yeast and the transit marker were found, as determined by Pairwise Wilcoxon Rank Sum Tests with Holm correction. (**E**) The average survival of *S. cerevisiae* from day 2 to 20 in the luminal and mucosal microenvironments of the ileum and ascending colon compartments hosted by a complex microbial community derived from a fecal sample is shown. The average of six biological replicates is indicated with a '**x**' and the SD is shown.

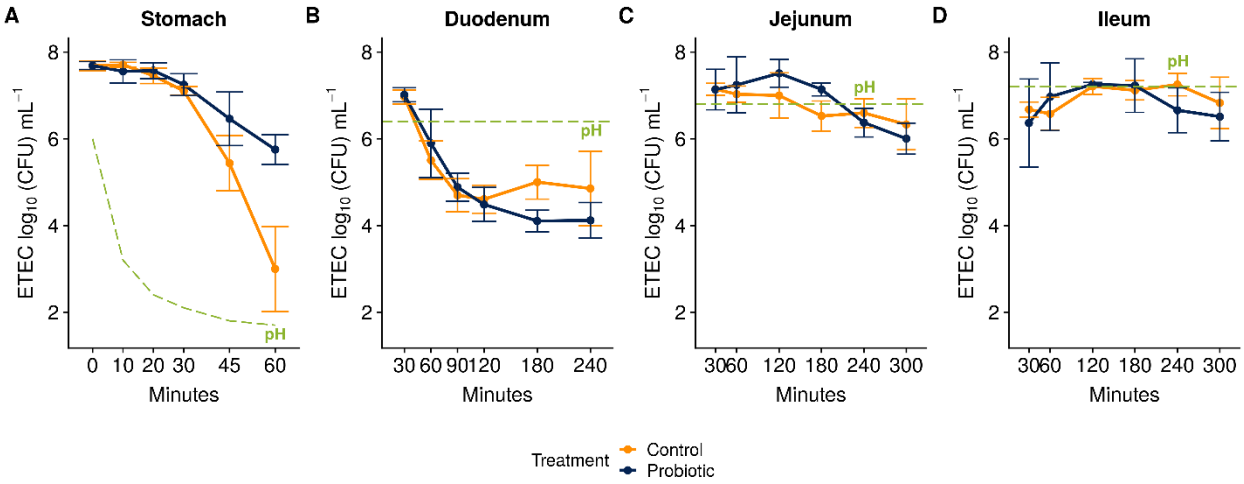

Figure 5.3. **Effect of *S. cerevisiae* treatment on ETEC survival in the different GI regions of the TIM-1 system (stomach, duodenum, jejunum and ileum) as determined by plate counts.** Average regionalized survival of ETEC (orange line) in $\log_{10}$ CFU mL^{-1} ± SD, compared to ETEC co-administered with the probiotic (blue line) in the four compartments of the TIM-1 system. The level of the pH in each compartment is illustrated by a green dashed line. The experiment was repeated in four independent replicates.

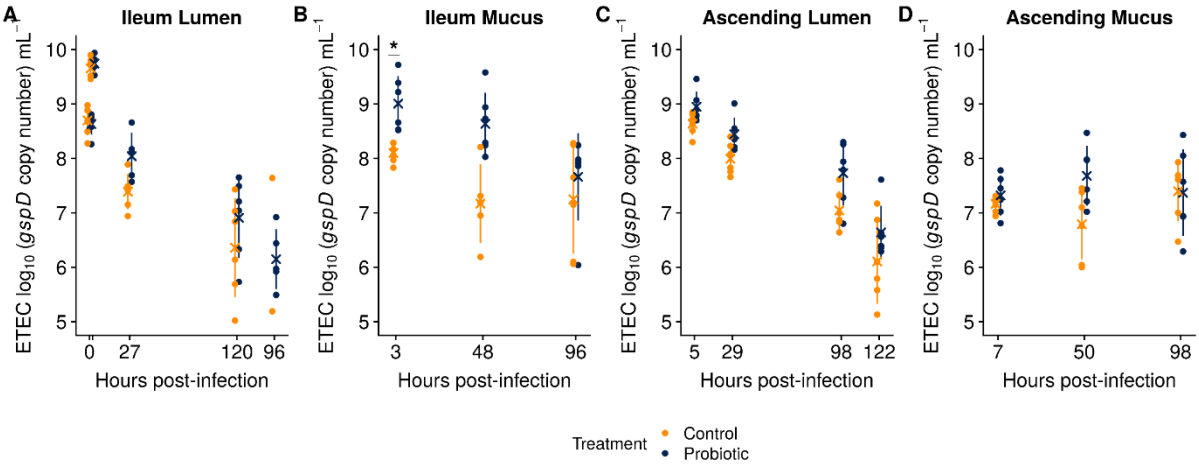

Figure 5.4. **Effect of *S. cerevisiae* treatment on ETEC survival in the different GI regions of the M-SHIME system (ileum and ascending colon) as determined by ETEC specific qPCR (*gspD* gene).** The survival of ETEC (orange line) or ETEC treated with the probiotic (blue line) was estimated by qPCR and expressed in $\log_{10}$ *gspD* copy number mL^{-1}. The experiment was repeated with the fecal microbial communities from six different donors (biological replicates), represented by the circles. The average of these biological replicates is indicated with a '**x**' and the SD is shown. Statistical significant differences between the treatment conditions are denoted at $p < 0.05$ (*), as determined by Pairwise Wilcoxon Rank Sum Tests with Holm correction.

The probiotic treatment contributes to the disruption of ETEC membrane integrity in the upper part of the GI tract. ETEC physiological states in the TIM-1 were monitored by PMA-qPCR and live/dead flow cytometry (Fig. 5.5). Two and four ETEC subpopulations were discriminated by PMA-qPCR and flow cytometry, respectively, as described in chapters 1 and 2. *S. cerevisiae* treatment tended to increase over-time the number of damaged and dead ETEC cells compared to the untreated condition, in both gastric and ileal effluents (Fig. 5.5). For instance, during the first hour of GI digestion (T0-60 in the ileal effluents), 15% of the total ETEC cells were viable under control condition, while 2% only under probiotic condition, as estimated by PMA-qPCR (Fig. 5.5A). With the flow cytometry technique, three additional membrane states, with different physiological properties were discriminated (Fig. 5.5B). Thus at T20-60 min in the stomach, 28% of the total ETEC cells were viable, 50% had partially-altered membranes but were still able to recover a viable state, 3% had altered membranes and, 19% were dead under control condition; whereas under probiotic treatment, 15% of the total ETEC cells were viable, 24% partially-altered membranes, 21% had altered membranes and, 40% were dead (Fig. 5.5B). Consequently, at the end of the GI digestion (T240-300 in the ileal effluents), about 25% of the total ETEC cells entering in the colon had an intact membrane under control condition, compared to 19% under probiotic condition (Fig. 5.5B). In the luminal phase of the SHIME, PMA-qPCR was the sole possible technique to track ETEC viability (Fig. 5.6). Under *S. cerevisiae* treatment, the ratio of live/dead ETEC cells did not display significant change compared to the control condition in both ileum (Fig. 5.6A) and ascending colon (Fig. 5.6B). However, donor variability was observed in the ileum (Fig. 5.6A). For example, donor 3 responded well to the probiotic treatment where the number of viable ETEC was decreased by half from 45 to 23%, 27 h post-infection (Fig. 5.6A).

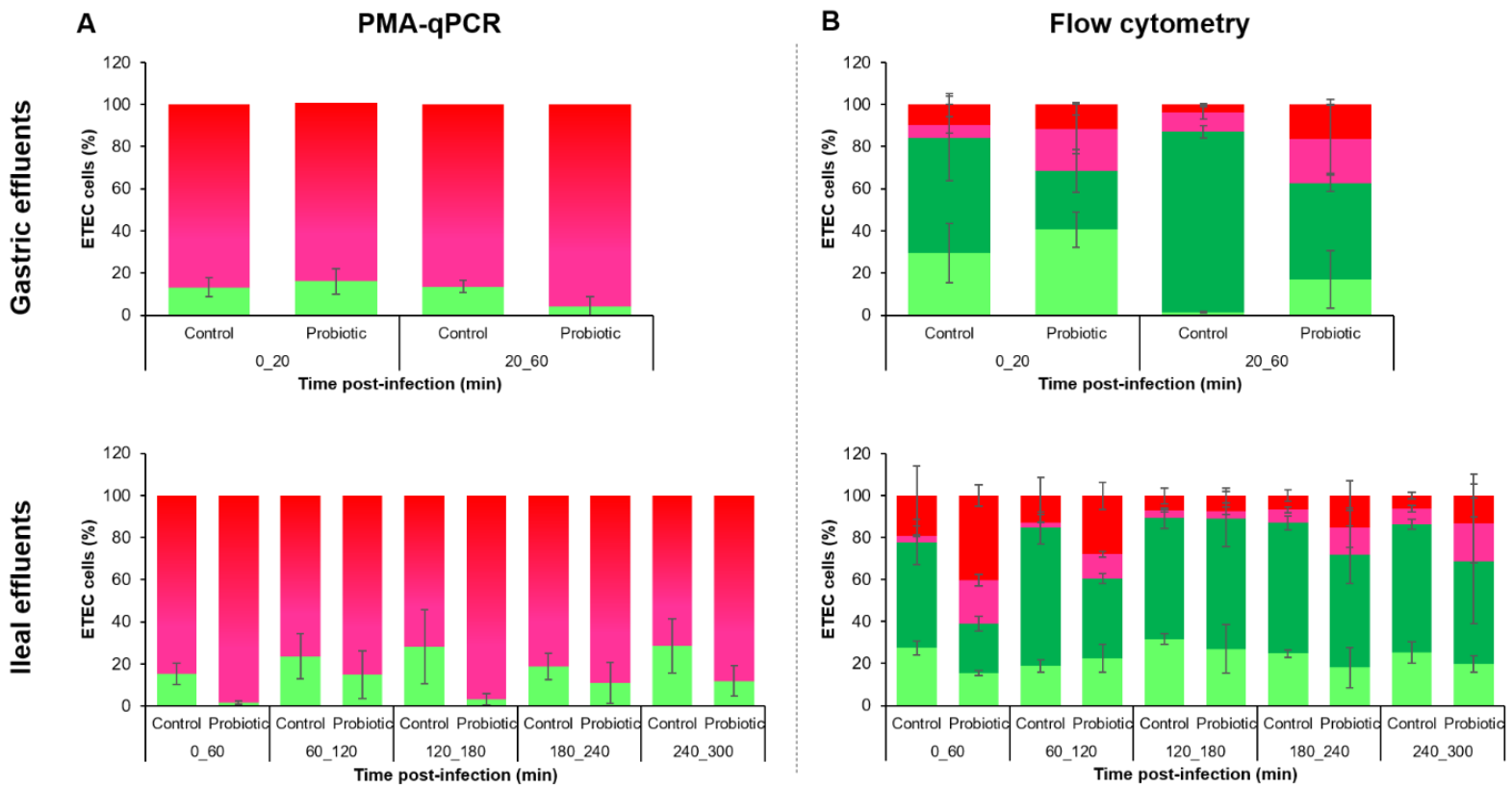

Figure 5.5. **Effect of *S. cerevisiae* treatment on ETEC physiology in the gastric and ileal effluents of the TIM-1 system as determined by PMA-qPCR and flow cytometry.** ETEC membrane integrity was measured over time in the gastric and ileal effluents under control and probiotic conditions. (**A**) PMA-qPCR shows the live (green) and dead/altered (shade of red) cells. The latter was obtained after deducting the number of intact cells from the total ETEC cells measured by qPCR. (**B**) Flow cytometry shows four subpopulations discriminated after SYTO9 and PI staining, according to the green (FL1) and red (FL2) fluorescence signals : intact membranes (pale green), partially altered membranes (green), irreversibly altered membranes (pink) and dead cells (red). The barplots represent the average percentages from two independent replicates over time under each condition (**A, B**).

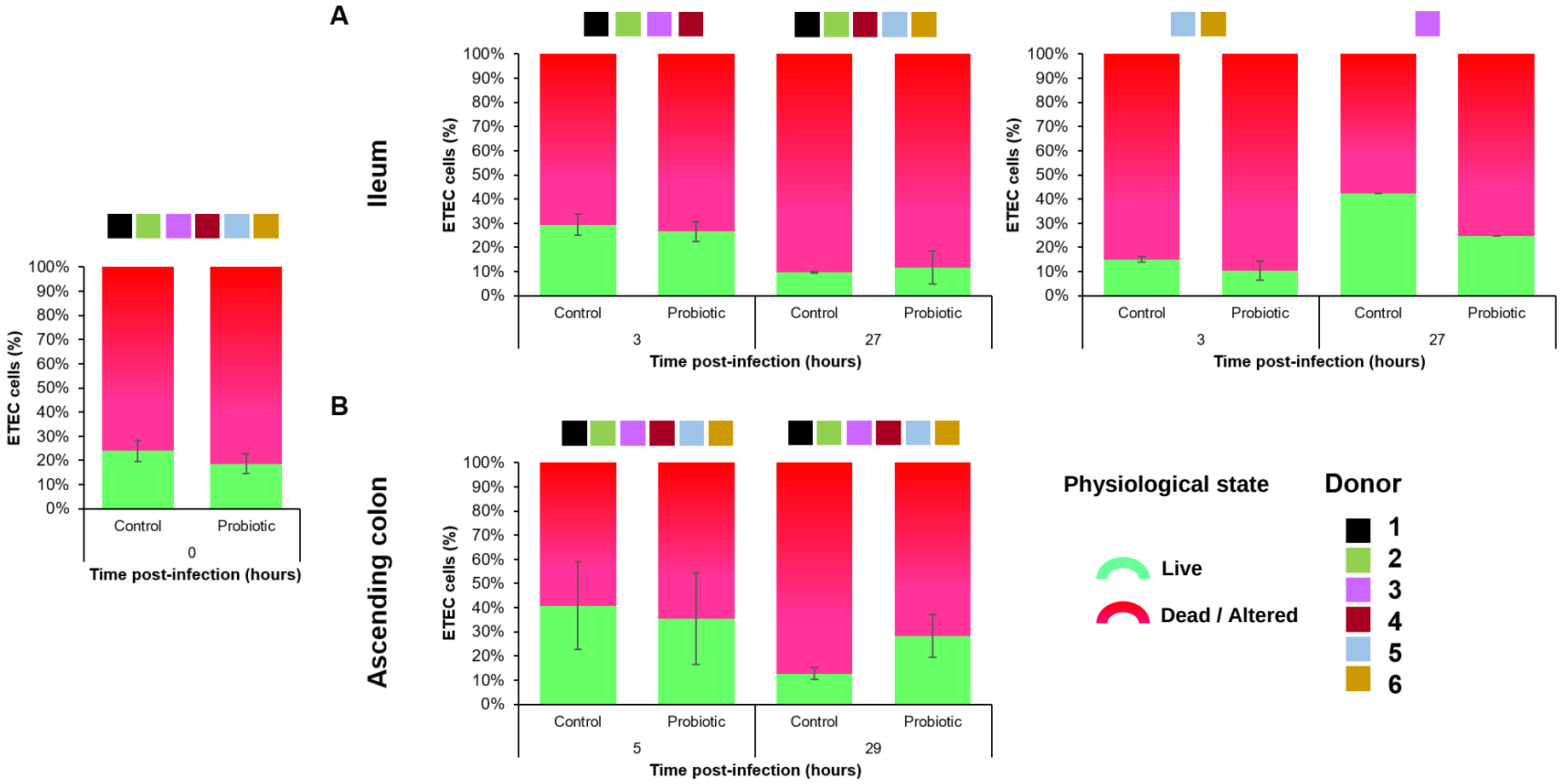

Figure 5.6. **Effect of *S. cerevisiae* treatment on ETEC physiology in the ileum and ascending colon regions of the M-SHIME as determined by PMA-qPCR.** (**A, B**) ETEC membrane integrity was measured over time in the ileum and ascending colon under control and probiotic conditions, after the *in vitro* batch gastro-jejunal digestion (T0, on the left). PMA-qPCR shows the live (green) and dead/altered (shade of red) cells. The latter was obtained after deducting the number of intact cells from the total ETEC cells measured by qPCR. The barplots represent the average percentages from six different donors over time, ± SD. When inter-individual variability is important, a second barplot is represented, as displayed in (**A**).

The probiotic treatment leads to a modest depolarization of ETEC membrane potential in the TIM-1. To further study the physiology of ETEC membranes during upper GI transit, intracellular pH of the pathogen cells was first measured in response to the treatment condition through flow cytometry analysis with a pH-dependent fluorescent probe CFDA-SE (Fig. 5.7A). *S. cerevisiae* treatment displayed no change in the intracellular pH of ETEC in comparison to the untreated condition in all GI regions simulated by the TIM-1 (Fig. 5.7A). As a second tool, ETEC membrane potential was followed in the gastric and ileal effluents by means of flow cytometry analysis in combination with $DiOC_2(3)$ staining (Fig. 5.7B, C). According to the fluorescence intensity (FI) ratio (FL1/FL2), membranes are considered to be polarized when above a FI ratio exceeding 1, and depolarized below 1. In response to the probiotic treatment, ETEC membranes were less polarized in the gastric effluents (Fig. 5.7B). Remarkably, a profound depolarization of ETEC membranes was noticed after 60 min GI digestion in the ileal effluents under probiotic treatment, in comparison with the untreated condition (Fig. 5.7C).

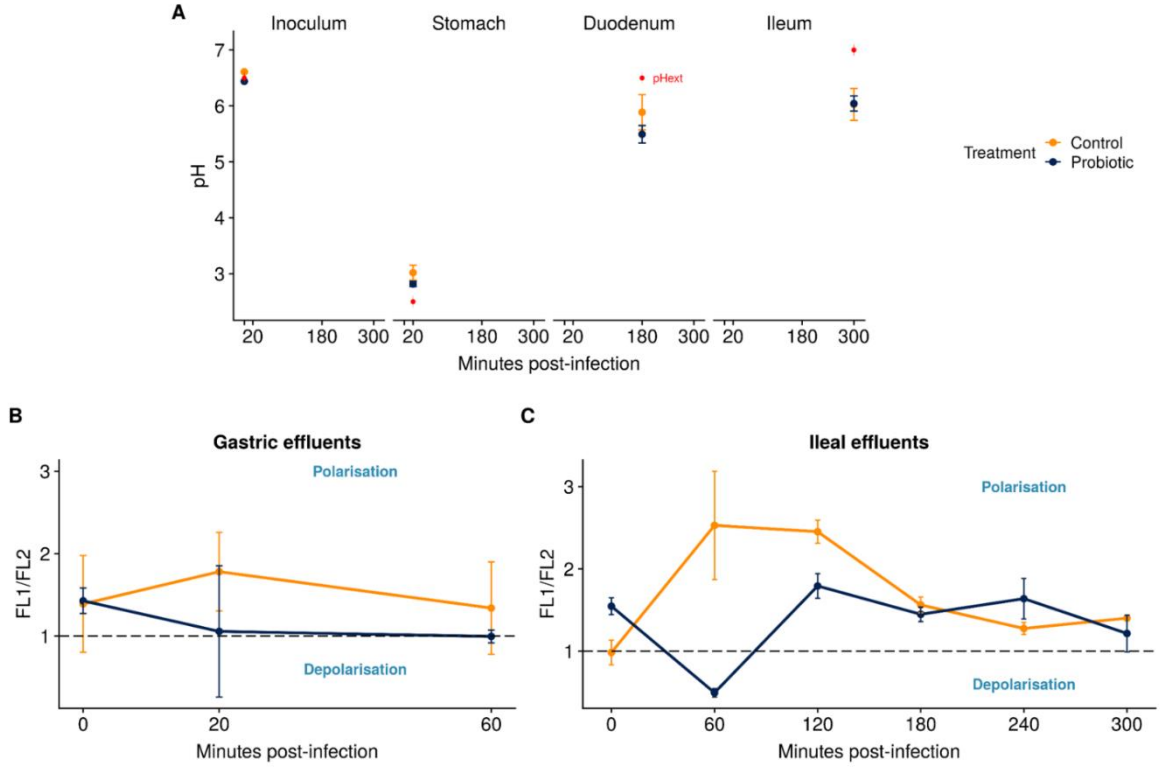

Figure 5.7. Effect of *S. cerevisiae* treatment on ETEC intracellular (pHi) and membrane potential and in the TIM-1 system as determined by flow cytometry. The graphs show the mean of two independent replicates ± SD, (**A**) ETEC pHi measured in digestive samples from the TIM-1 under control and probiotic treatment, using flow cytometry analysis with the pH-dependent fluorescent probe CFDA-SE. The external pH is shown in red dot. (**B, C**) ETEC membrane potential was measured in the gastric and ileal effluents under control and probiotic treatment, using flow cytometry analysis with the membrane potential probe $DiOC_2(3)$. According to the fluorescence intensity (FI) ratio (FL1/FL2), membranes are considered to be polarized when above a FI ratio exceeding 1, and depolarized below 1.

3.3 Effect of *S. cerevisiae* treatment on the dynamics of ETEC virulence along different GI regions

The expression of the main ETEC H10407 virulence genes encoding for attachment and colonization (*cfa/Ib, tia, fimH*), enterotoxin production (*eltB, estAB*), and the release of these enterotoxins (*leoA, tolC*) within the host was followed up over time in the TIM-1 and in the luminal phase of the M-SHIME under both treatment conditions, control and probiotic. The log_2 fold change of each gene is shown for each replicate individually (Fig. 5.8 for TIM-1 and 5.9 for M-SHIME).

The probiotic treatment triggers a profound ETEC-virulence change in the gastric and ileal effluents of the TIM-1. Remarkably, *S. cerevisiae* treatment led to a significant mean of -4-fold repression of the *estAB* gene all along the gastric digestion, while an opposite profile was found in the ileal effluents with a mean of 1-fold induction of the *estAB* gene at the end of the digestion (T240 and 300 min) (Fig. 5.8). Although the *eltB* gene tended to be more induced under control condition in both GI regions with for example a 1.8-fold over-expression noticed in two replicates at T180 min in the ileal effluents, no significant changes were found between both treatment conditions. The *leoA* gene, encoding for the delivery of the LT enterotoxin was irregularly over or under-expressed with the probiotic treatment in both gastric and ileal effluents. The gene was significantly over-expressed at T20 min and T300 min, with a mean of 1.5-fold induction. Interestingly, the *tolC* gene, encoding for a protein involved in the delivery of ST enterotoxin displayed globally the same expression pattern than *estAB* gene under probiotic treatment. With respect to the genes encoding for ETEC adhesins, the *fimH*, *tia*, *cfa/Ib* genes were all significantly repressed in the gastric effluents (especially at T20 min) under probiotic condition, and significantly over-expressed in the ileal effluents. Particularly, the *fimH* gene encoding for type 1 pili, exhibited a profound over-expression until T240 min in the ileal effluents (a mean of 3.6-fold induction at T240 min) with the probiotic treatment, while in comparison the *fimH* gene was largely repressed under control condition (a mean of -1.7-fold repression at T240 min) (Fig. 5.8). Finally, the stress-response *rpoS* gene was switched on (1.2-fold induction) only at the final time point of the GI digestion at T300 min under the probiotic treatment, and basally expressed or repressed for all the other time points under both conditions (Fig. 5.8).

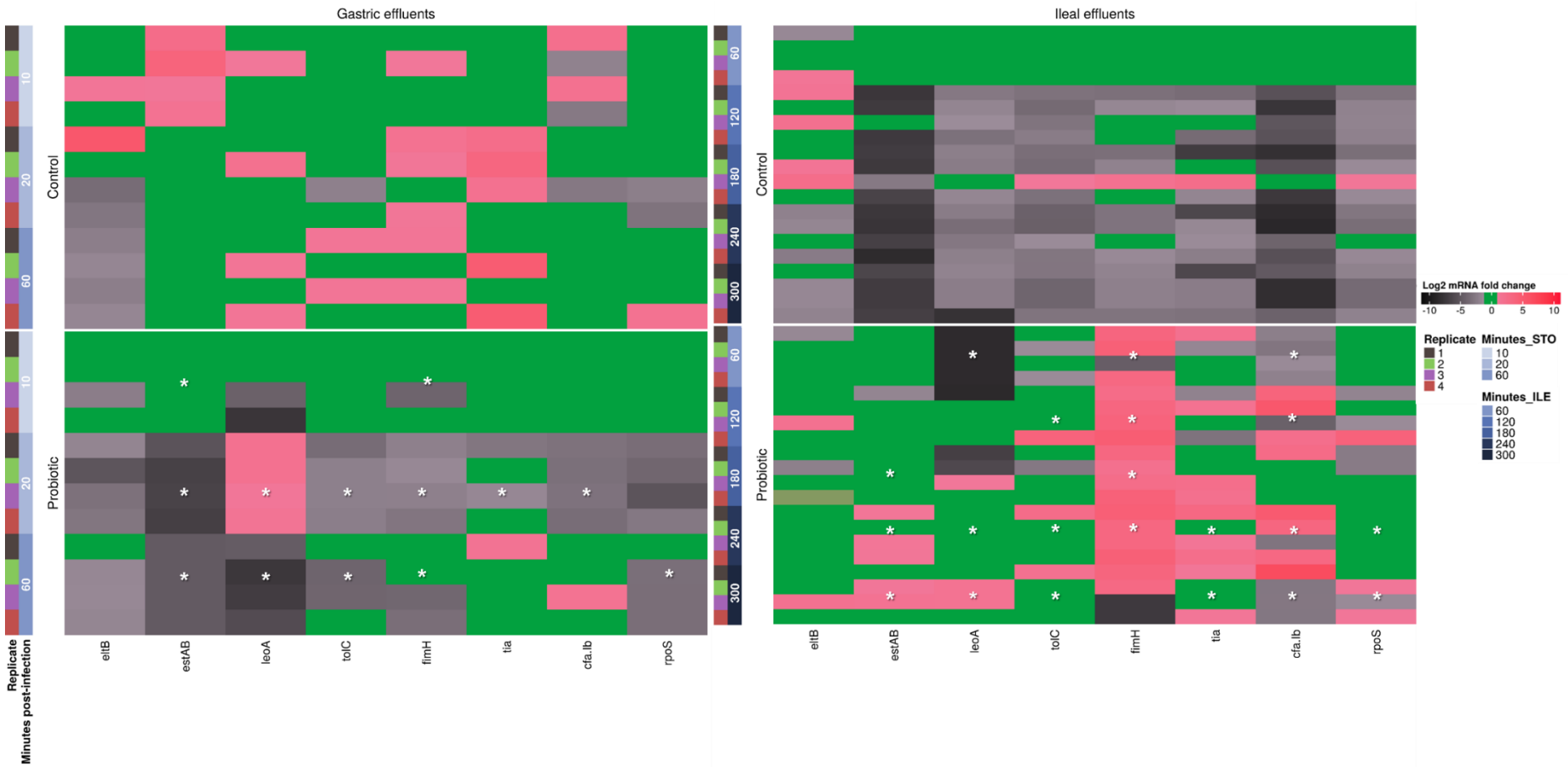

Figure 5.8. **Effect of *S. cerevisiae* treatment on ETEC virulence gene expression in the gastric and ileal effluents of the TIM-1 system as determined by RT-qPCR.** Results are expressed and colored according to the $\log_2$ fold-change. For reasonable statements, statistically significant differential expression had to meet two criteria: a mean $\log_2$ fold change expression of ≥ 1 (induction denoted in shade of pink) or ≤ -1 (repression denoted in shade of black/grey), and a $p \leq 0.05$. The statistically significant differences in average of $\log_2$ gene expression between the treatment conditions are marked by a ***** in the heatmap, as determined by the friedman post-hoc Nemenyi test.

Effect of the probiotic treatment on the modulation of ETEC virulence genes expression in the ileum and ascending colon of the M-SHIME. The same set of ETEC virulence genes (except *rpoS* gene) was followed in the luminal ileum and ascending colon of the six distinct donors (Fig. 5.9). A variability was observed among donors, resulting in no statistically significant differences between the probiotic and control conditions over time. Globally in the ileum, the *eltB, leoA, tia* and *fimH* gene expression patterns were unchanged between the control and probiotic conditions. In contrast, the *estAB* gene was slightly over-expressed only for donor 3 (1.3-fold), 3 h post-infection in the ileum under probiotic treatment, while a mean of 2.3-fold induction was noticed for donors 1, 2 and 3 under control condition. This was also observed in the ascending colon, 20 h post-infection where the *estAB* gene was 3-fold over-expressed for 3 donors out of 6 (donors 1, 2, 3) under control condition. Consequently to the probiotic treatment, *estAB* gene stayed over-expressed only in donor 2 (2.6-fold induction T20 h post-infection) (Fig. 5.9). The *eltB* gene displayed also a reduced expression in the ascending colon 5 h post-infection under probiotic treatment for 2 donors (donors 1 and 2) with a 1.9-fold induction, while 5 donors exhibited a mean of 3.5-fold over-expression under control condition (Fig. 5.9). Interestingly, the two donors 2 and 3 displayed simultaneous over-expression of the *estAB*, *leoA*, *tolC* and *fimH* genes 5 h post-infection in the ascending colon with the probiotic. Finally, *cfa/Ib* mRNA was not detectable (not amplified) either in the ileum and ascending colon contrary to the TIM-1 system.

The probiotic treatment contributes to the reduction of the LT toxin production in the TIM-1 and M-SHIME. The LT toxin production under control and probiotic-treated conditions was examined in the TIM-1 gastric and ileal effluents, as well as in the luminal phase of the M-SHIME ileum and ascending colon (Fig. 5.10). As displayed in chapter 2, upon gastric digestion no production of the LT toxin was noticed. This result was reaffirmed here, under *S. cerevisiae* treatment. In the cumulated ileal effluents, though high variation between replicates, the probiotic globally tended to reduce the LT toxin production compared to the control condition. At T240 min GI digestion, a significant decrease was observed (p= 0.044), with a mean of production of 393 ± 114 pg mL^{-1} and 238 ± 62 pg mL^{-1} under control, respectively, probiotic condition (Fig. 5.10A). In the SHIME ileum, the LT toxin output was achieved with high variability between donors, but was diminished under probiotic condition in comparison with the control condition (Fig. 5.10B). An approximate 4-fold decrease of the LT production was measured 20 h post-infection in the ileum for all donors that originally experienced a high production (donors 1, 2 and 3). For example, a production of 1693 pg mL^{-1} and 401 pg mL^{-1} was achieved for donor 1 under control, respectively probiotic condition. In the ascending colon, 5 h post-infection and upon *S. cerevisiae* treatment, a 3-fold decrease was noticed for donors 1, 3 and 4, with a decrease from 3660 to 1315 pg mL^{-1} for donor 3 (Fig. 5.10C). As an exception, donor 2 was the only one not responding to the probiotic treatment: to the contrary, an increase of the LT toxin production reaching 9910 pg mL^{-1} was observed 5 h post-infection in the ascending colon compared to the control condition (Fig. 5.10C).

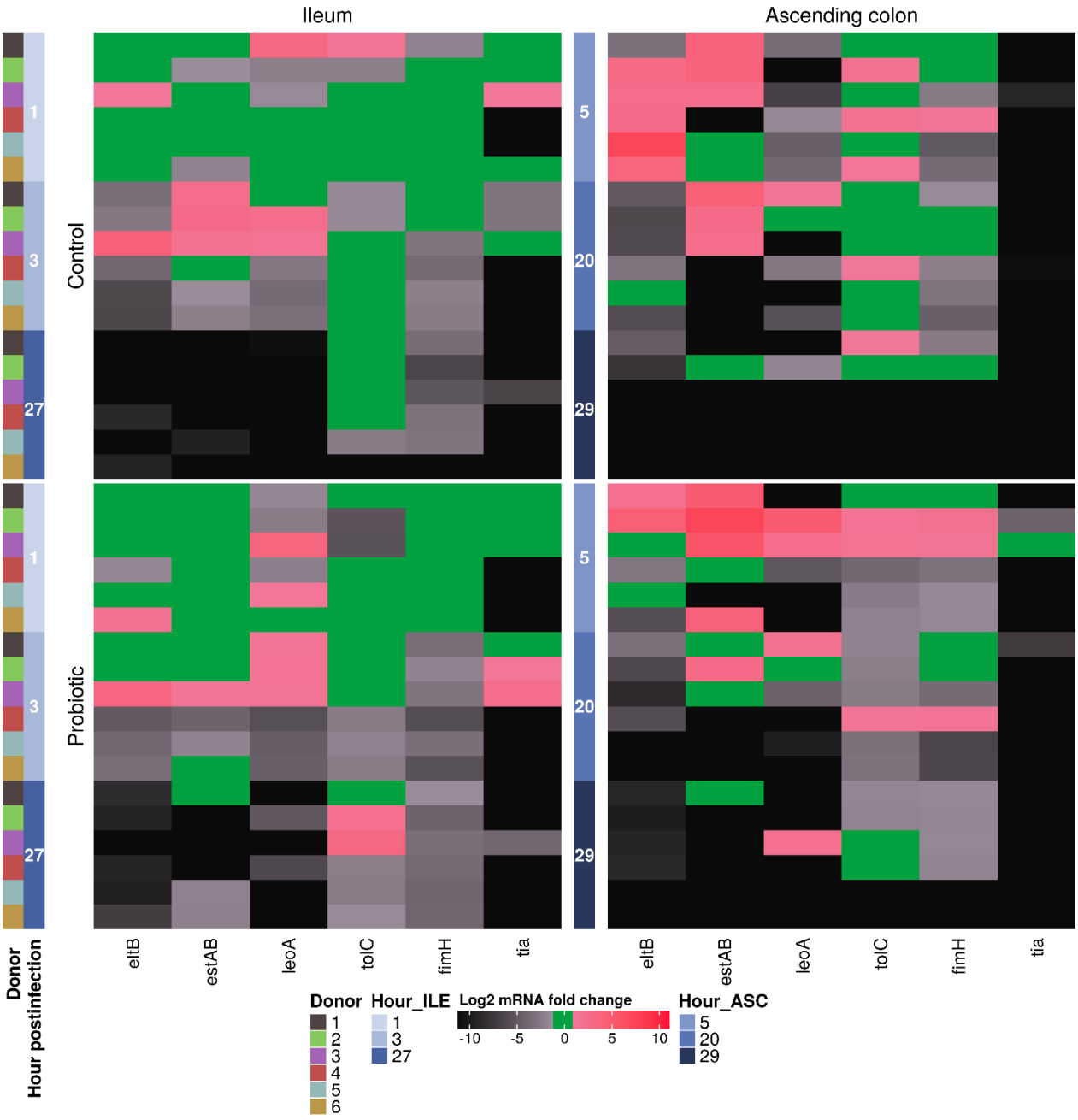

Figure 5.9. **Effect of *S. cerevisiae* treatment on ETEC virulence gene expression in the ileum and ascending colon regions of the M-SHIME as determined by RT-qPCR.** Results are expressed and colored according to the log2 fold-change. For reasonable statements, statistically significant differential expression had to meet two criteria: a mean log2 fold change expression of ≥ 1 (induction denoted in shade of pink) or ≤ -1 (repression denoted in shade of black/grey), and a $p \leq 0.05$. No statistically significant differences in log2 gene expression were found between the treatment conditions, as determined by the friedman post-hoc Nemenyi test.

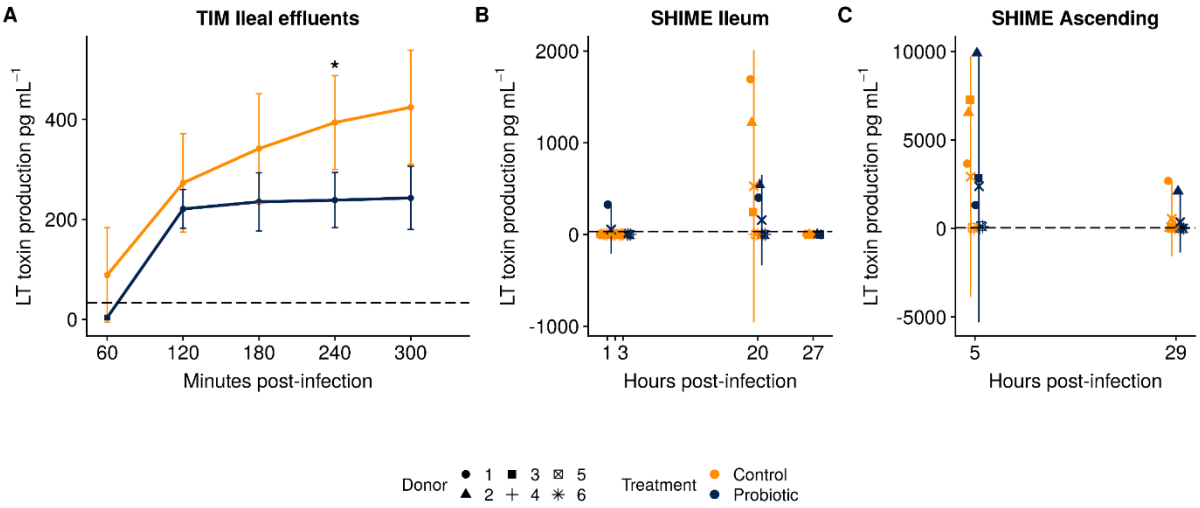

Figure 5.10. **Effect of *S. cerevisiae* treatment on LT toxin production in the different GI regions in the TIM-1 (cumulated ileal effluents) and SHIME (ileum and ascending colon) as determined by a GM1 ELISA.** (**A**) LT toxin production in the gastric and ileal effluents of the TIM-1 is expressed as a mean of four independent replicates in pg mL^{-1} ± SD; (**B, C**) LT toxin production in pg mL^{-1} in the luminal ileum (ILE) and ascending colon (ASC) compartments of the SHIME for six different donors (denoted by the different shapes). The average of the 6 biological replicates is shown as a '**x**'. The horizontal black dashed line represents the detection limit. Statistically significant differences in LT toxin production over time between the treatment conditions are denoted at $p< 0.05$ (*), as determined by the friedman post-hoc Fisher test.

3.4 *S. cerevisiae* treatment induces specific changes on the gut microbial community composition and activity

The evolution of the microbial community composition preceding and following ETEC infection under both control and probiotic treatment conditions was assessed in the four gut regions of the M-SHIME: ileum lumen, Ileum mucus, ascending lumen and ascending mucus, for the six different fecal donors. The detailed profiles of microbial community composition per donor are shown according to the gut regions and treatment conditions in supplementary data (Fig. S5.1 to S5.6).

The 3-weeks probiotic treatment intervention displays a significant effect on the overall microbial community composition. *S. cerevisiae*, besides serving a role in the modulation of ETEC physiological states and virulence, induced significant changes in the gut microbial community structure compared to the control condition (Fig. S5.7, Fig. 5.11 and 5.12). Applying first a db-RDA analysis, the group dissimilarities "control" and "probiotic" were first discriminated. Globally, the treatment condition significantly accounted for the observed patterns in microbial community variability at genus (5.2%, p= 0.001) and species (7.7%, p= 0.001) levels (Fig. S5.7). Other factors were also tested to verify their impact on the microbial dissimilarity patterns. For instance, the donor factor between both control and probiotic treatments explained at a similar level (~5%, p= 0.001) the global dissimilarities, as shown in supplementary data (Fig. S5.8). Further information on donor characteristics are found in chapter 2,

Table 2.2. The gut region also largely accounted for the microbial community dissimilarities as described in chapter 3. The specific effect of *S. cerevisiae* treatment was further investigated according to the gut region (Fig. S5.9). Remarkably, the probiotic condition displayed a strong effect in the luminal and mucosal microenvironments of the ascending colon, where the probiotic explained 5.1%, respectively, 11.3% (p= 0.001) of the microbial community composition dissimilarities (Fig. S5.9C and D). In the ileum lumen and mucus, the probiotic condition accounted to a lesser extent but still significantly for the microbial community dissimilarities (lumen 3.2%, p= 0.005; mucus 2.5%, p= 0.009) (Fig. S5.9A and B). The pronounced abundance of certain taxa according to the treatment condition are shown Fig. 5.11, applying DESeq2 analysis. 6% (p< 0.05) of the microbial genera were increased under probiotic condition compared to the control one (Fig. 5.11). To further describe the community change, the same DESeq2 analysis was performed by discriminating the four gut regions (Fig. 5.12). Most of the genera belonging to the *Firmicutes* phylum were enriched under the probiotic treatment, particularly in the luminal and mucosal phase of the ascending colon (Fig. 5.12). For instance, *Butyricicoccus*, *Clostridiales* (order), *Dorea*, *Faecalibacterium*, *Fusicatenibacter*, *Fusobacterium* and *Roseburia* prevailed under the probiotic condition in the ascending colon compared to the control condition. In addition, a large increase in *Lactobacillus*, *Enteroccoccus* and *Veillonella* abundance were found either in the ileum or ascending colon under the probiotic condition, while *Akkermansia* and *Klebsiella* were decreased (Fig. 5.12).

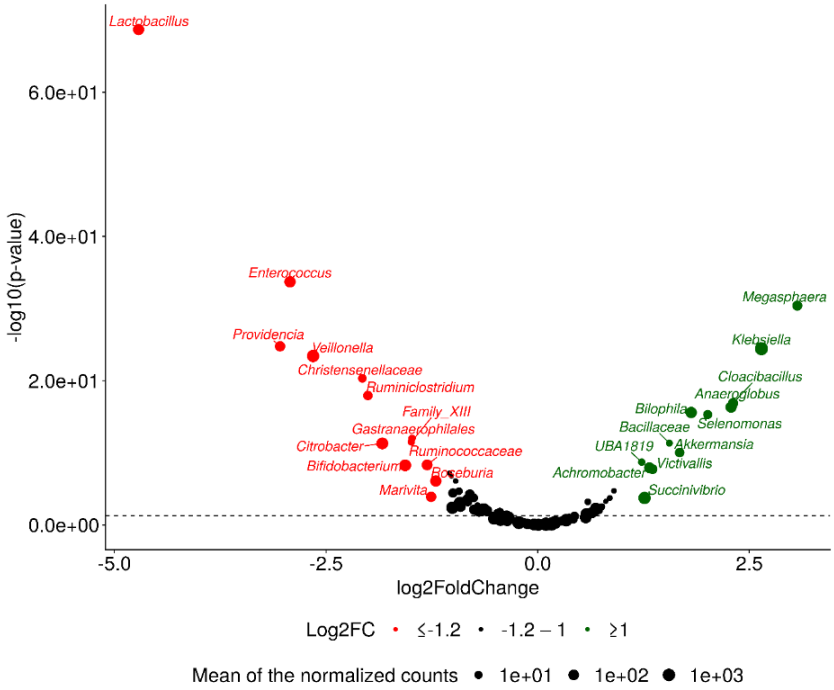

Figure 5.11. Log_2 Fold Change of normalized genus abundances of the overall (ileum and ascending colon) microbial community composition under probiotic (red) and control (green) condition. A positive log_2 Fold Change indicates a stimulation (in green) of the genera in the control condition compared a negative log_2 Fold Change which indicates a stimulation of the genera in the probiotic condition (in red). The log transformed adjusted p-value is displayed on the y-axis and the α = 0.05 significance level is indicated by a dashed line. Only the genera with an absolute log_2 Fold Change value exceeding 1.2 are represented.

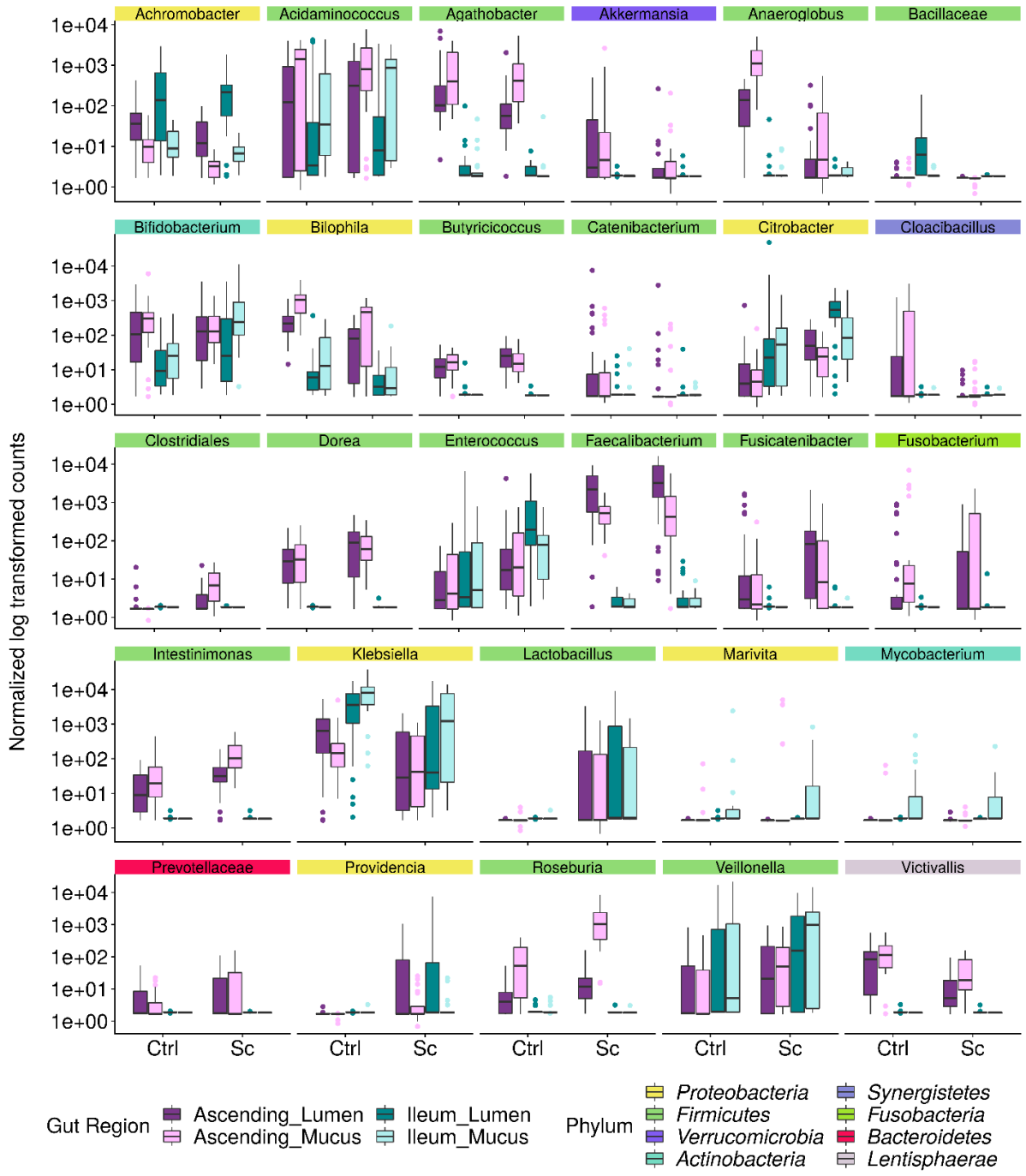

Figure 5.12. Significant differences in genus level abundance between control (Ctrl) and probiotic (Sc for *S. cerevisiae*) conditions, as assessed by DESeq analysis. The abundance is displayed for the different gut regions. Coloured labels indicate the phylum classification of the respective genera. Only the genera with an absolute $\log_2$ Fold Change value exceeding 1.2 are represented.

Effect of the probiotic treatment on the microbial communities following ETEC infection. The pre-infection (from day 2 to 12) and post-infection (from day 13 to 20) were characterized to examine the effect of the probiotic condition on the microbial community compared to the control condition, applying DESeq2 analysis (Fig. 5.13, 5.14, 5.15 and S5.10). Under control condition, following ETEC infection 12% of the genera were decreased and 6.4% increased $p< 0.05$ (Fig. 5.13A), and under probiotic condition, 9.6% of the genera were decreased and 5.8% increased $p< 0.05$ (Fig. 5.13B).

To obtain a more precise overview of the microbial changes between pre- and post-infection under the probiotic treatment are shown in Fig. 5.14 at genus and 5.15 at species levels. Of note, these results are compared to those described in chapter 3 in the untreated control condition (Fig. 3.4 and 3.5). In chapter 3 we have shown following ETEC infection a bloom of opportunistic pathogens in the ileum: *Achromobacter* (OTU60), *Klebsiella variicola* (OTU115) and *Mycobacterium* (OTU201), while *Clostridium tertium* (OTU117) abundance was dropped. Under the probiotic condition the bloom of opportunistic pathogens seemed to be more limited except for *Achromobacter* (OTU60) which was significantly increased as well (Fig. 5.15).

In the ascending colon, under control condition ETEC infection was associated with an upsurge of *Prevotella* (OTU40, 44), *Paraprevotella clara* (OTU81), *Clostridium scindens* (OTU90), *Victivallis vadensis* (OTU160), *Bacteroides eggerthii* (OTU166) and *Gastranaerophilales* suborder (OTU248) (Fig. 3.5). Still under control condition, many OTUs were significantly decreased such as *Gemmiger formicilis* (OTU21), *Eubacterium ventriosum* (OTU52), *Fusicatenibacter saccharivorans* (OTU70), *Bacteroides caccae* (OTU104), *Oscillibacter* (OTU120), *Blautia luti* (OTU124), *Alistipes shahii* (OTU127), *Blautia obeum* (OTU131), *Bifidobacterium angulatum* (OTU151), *Ruminococcus faecis* (OTU163) (Fig. 3.5). Only *Escherichia* (OTU1) was stimulated in the ileum and ascending colon, while *Clostridium butyricum* (OTU18), *Citrobacter* (OTU19), *Bifidobacterium* (OTU47), *Collinsella aerofaciens* (OTU79) and *Clostridium* (OTU91) were decreased in both gut regions (Fig. 3.5).

Under the probiotic treatment in the ascending colon (Fig. 5.15), many species belonging to the *Firmicutes* phylum were decreased such as *Ruminococcus faecis* (OTU163), *Ruminococcus bromii* (OTU245), *Dialister invisus* (OTU173), *Streptococcus salivarius* (OTU291) and other species non-identified by RDP-seqmatch (OTU214, OTU216, OTU225, OTU251, OTU262, OTU270, OTU293, OTU336). Still in the ascending colon, *Akkermancia muciniphila* (OTU107) was dropped following infection, while species belonging to *Prevotella* genus (OTU40, OTU41, OTU44) prevailed as for the control condition (Fig. 5.15). In both gut regions, ileum and ascending colon, an upsurge of *Stenotrophomonas maltophilia* (OTU31), *Enterococcus faecalis* (OTU77), *Providencia vermicola* (OTU80) was noticed, with a decrease of *Clostridium tertium* (OTU117) and *Burkholdenia cepacia* (OTU177) (Fig. 5.14 and Fig. S5.10).

Finally, under the control condition, ETEC infection significantly decreased the abundance of the actinobacterium *Collinsella aerofaciens* , a 'marker' of PI-IBS (chapter 3), while under probiotic condition the abundance of this species was not altered following ETEC infection.

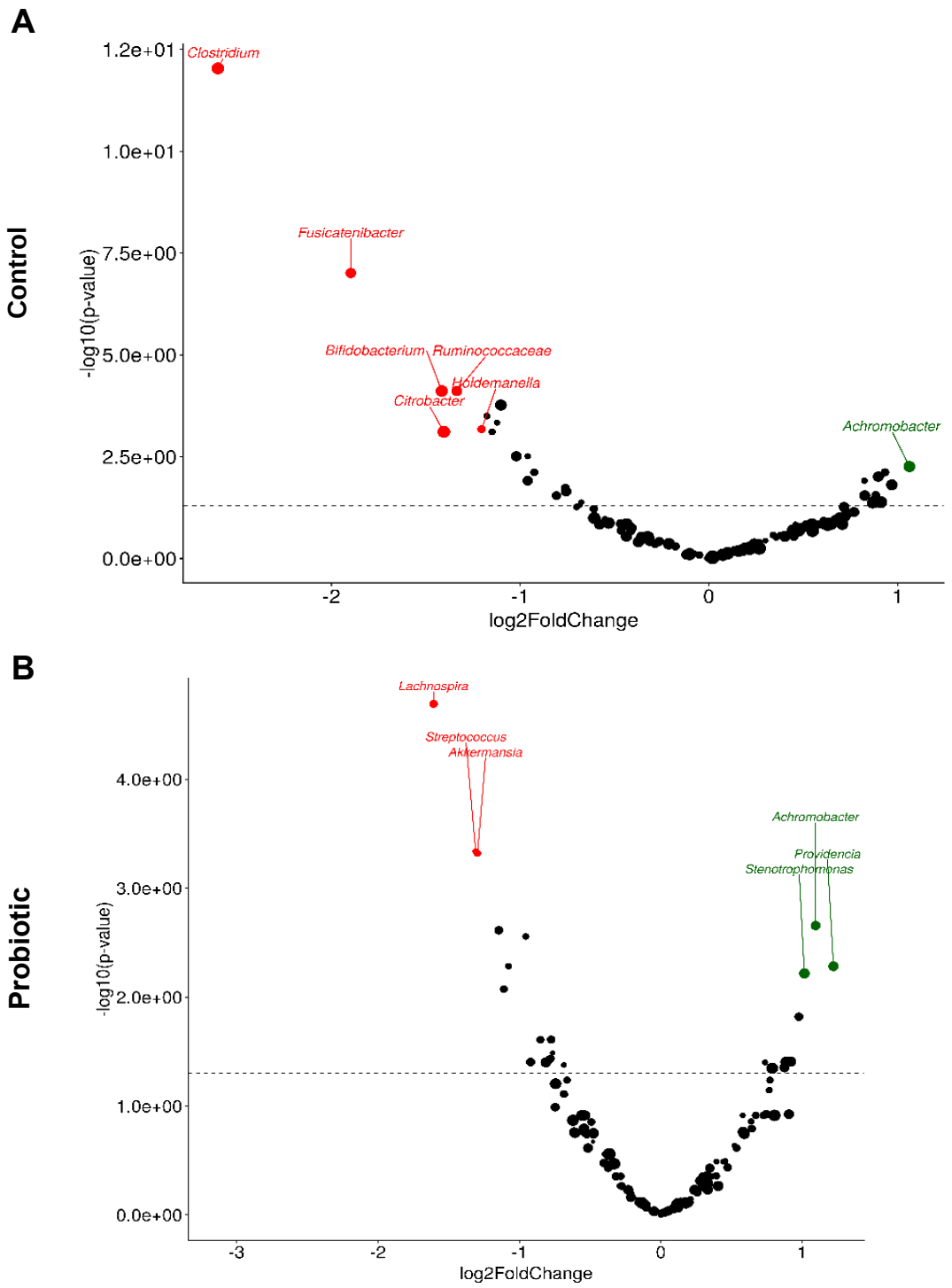

Figure 5.13. **Log_2 Fold Change of normalized genus abundances (A) in the control and (B) probiotic conditions between the pre- (red) and post-infection (green) phases microbial community composition.** A positive log_2 Fold Change indicates a stimulation (in green) of the genera in the post-infection period compared to a negative log_2 Fold Change which indicates a stimulation of the genera in the pre-infection period (in red). The log transformed adjusted p-value is displayed on the y-axis and the $\alpha = 0.05$ significance level is indicated by a dashed line.

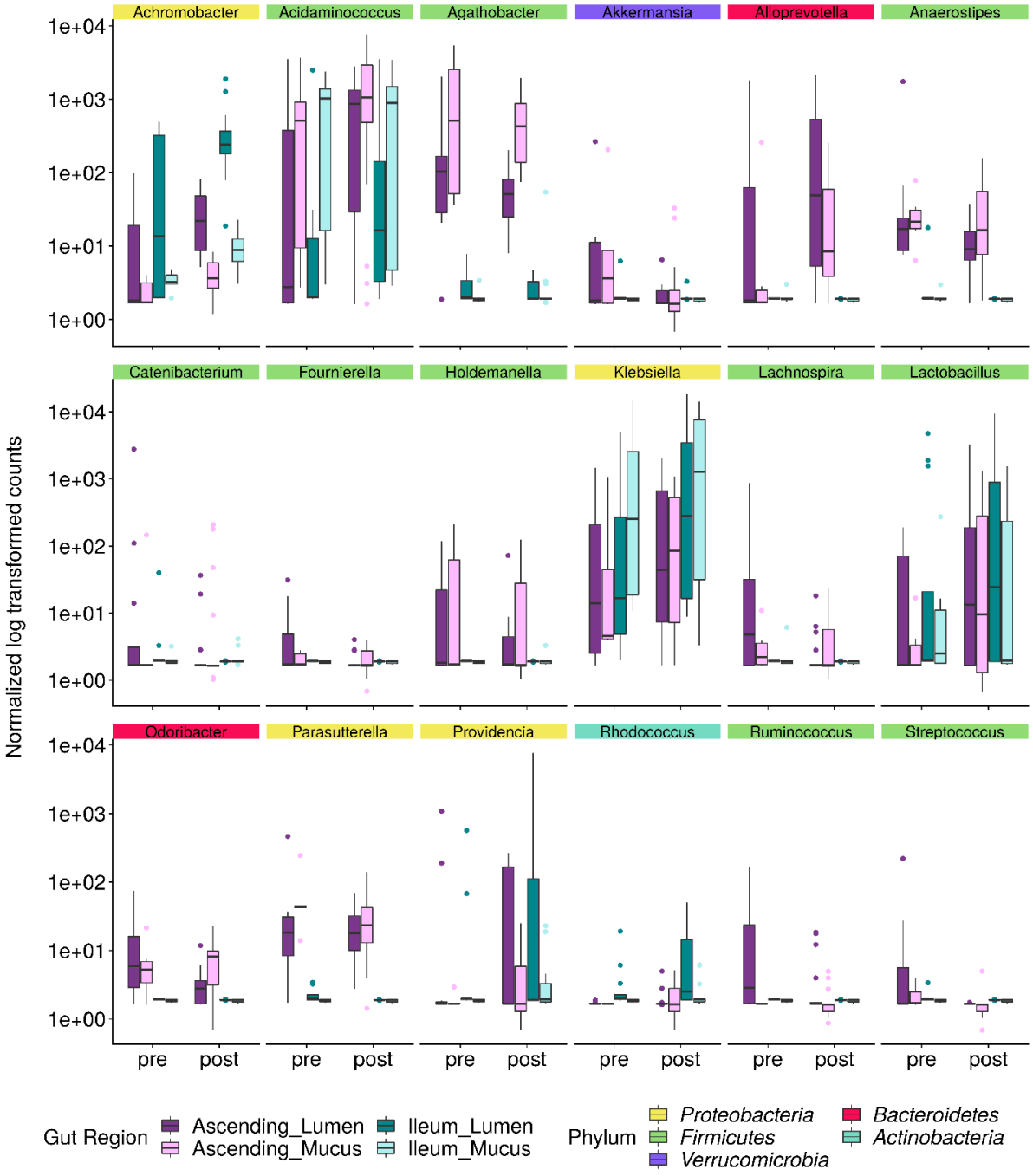

Figure 5.14. **Significant differences in genus level abundance between pre- and post-infection under the probiotic condition, as assessed by DESeq analysis.** The abundance is displayed for the different gut regions. Coloured labels indicate the phylum classification of the respective genera.

II-5

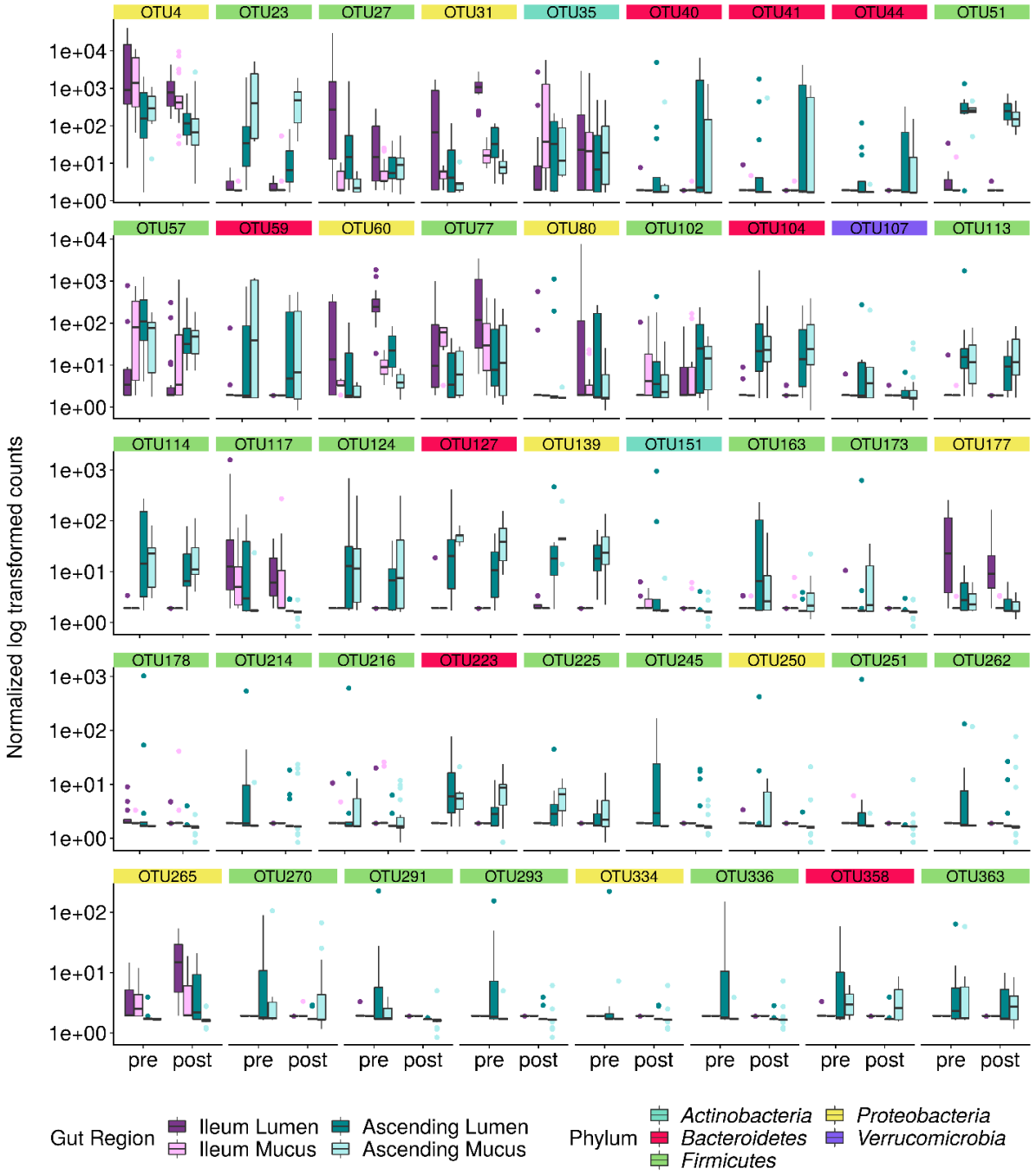

Figure 5.15. **Significant differences in species level abundance between pre- and post-infection under the probiotic condition, as assessed by DESeq analysis.** The abundance is displayed for the different gut regions. Coloured labels indicate the phylum classification of the respective OTU.

The probiotic treatment stimulates a rich microbial metabolic activity predominantly in the ascending colon. Ultimately, we focused on the impact of *S. cerevisiae* treatment towards microbial functionality through SCFA production as markers for carbohydrate and protein fermentation. The probiotic yeast significantly increased the absolute metabolite concentrations in the ascending colon for all donors, while the effect in the ileum remained limited due to the initial low metabolic activity, as previously described in chapter 4 (Fig. 5.16, 5.17, S5.10 to S5.12). In the ileum, only the acetate displayed increased concentration under the probiotic treatment (Fig. 5.17), which was more pronounced with a 4 mM increase for donors 4, 5 and 6, while a 1.6 mM increase was observed in donor 1, 2 and 3 (Fig. 5.17). Remarkably, in the ascending colon an approximate 2-fold increase of the total SCFA was observed for all donors (Fig. 5.16). All the SCFA followed during the 20 days fermentation (e.g. acetate, propionate, butyrate, caproate, valerate and branched-fatty acids) were significantly increased compared to the untreated control condition in the ascending colon (Fig. 5.17). The increases were even more pronounced for acetate and propionate, displaying a mean of 20 mM, respectively 8.5 mM increase, except for donor 6 where the propionate concentration was decreased upon treatment (Fig. 5.17). With respect to the valerate, caproate and branched-fatty acids, a mean of 4, 3 and 2 mM were respectively noticed still in the ascending colon with an exceptionally low donor variability. On the contrary, a higher donor variability was displayed for the butyrate concentration with a high increase for donors 4 and 6, compared to the low increase for donors 1, 2, 3 and 5 (Fig. 5.17). Lastly, ethanol which is known to be produced by *S. cerevisiae* was measured under both treatment conditions (Fig. S5.13). Not surprisingly, high concentrations were found under the probiotic treatment, reaching 1.6 g L^{-1} and 0.7 g L^{-1} in the ileum, respectively ascending colon; while under the control condition, ethanol remained below 0.4 g L^{-1} in both gut regions (Fig. S5.13).

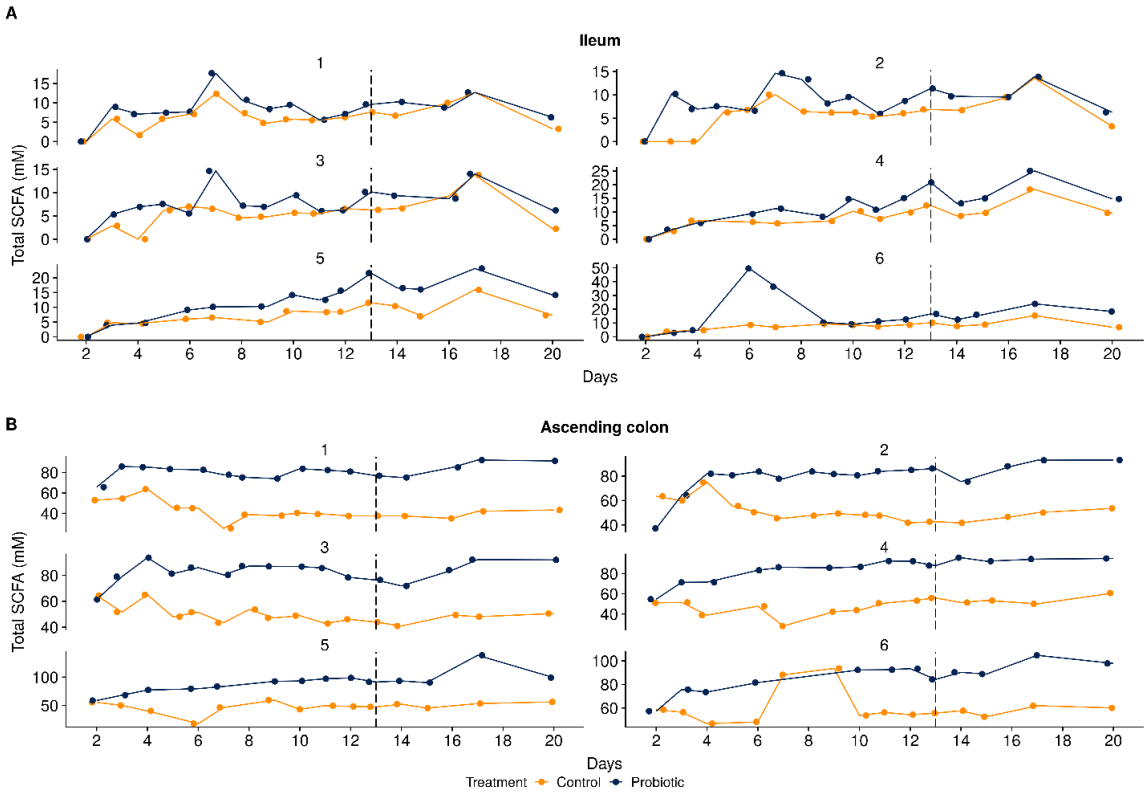

Figure 5.16. **Total short chain fatty acid (SCFA) concentrations (mM) in the (A) ileum and (B) ascending colon, inoculated with the microbial community derived from six different donors, under control and probiotic treatment conditions.** The pre-infection period is represented from day 2 to 12, ETEC infection is demarcated by the dashed line at day 13 and, the post infection run until day 20.

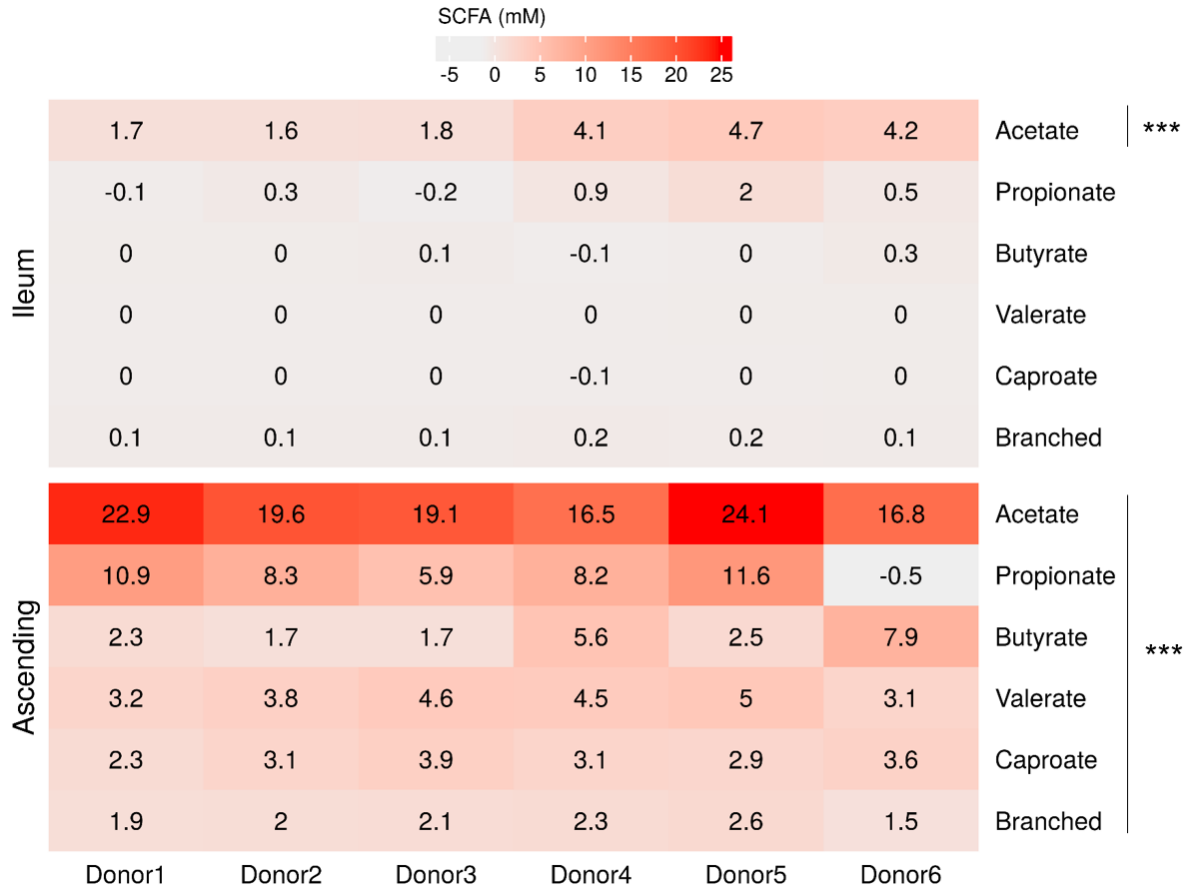

Figure 5.17. Effect of the probiotic treatment on the SCFA concentrations compared to the control condition in the ileum and ascending colon for the six donors. The differential average concentrations (mM) of each metabolite were obtained after deducting the concentrations found over time (day 2 to 20) under probiotic condition to those found under control condition. Statistically significant differences between treatments are denoted at $p < 0.001$ (***) as determined by Pairwise Wilcoxon Rank Sum Tests with Holm correction.

4. Discussion

The lack of specific treatment for ETEC infections, as well as the growing threat of antibiotic-resistance and its detrimental side effects in humans, has prompted research on alternative treatment strategies. The probiotic strategy fits with the increasing awareness of consumers to increase gut health and their request for safe alternatives and functional foods for controlling foodborne illnesses. Among potential bacterial and yeast probiotic candidates, the yeast cells offer the advantage to be antibiotic resistant and do not exchange DNA with bacteria (Moré and Swidsinski, 2015). Due to the scientific support set out for the probiotic *S. cerevisiae* CNCM I-3856 (chapter 4, Roussel et al., 2018), we further examine its antimicrobial properties against ETEC in the human upper and lower GI tract, as simulated by the TIM-1 and M-SHIME, respectively. Two modalities of probiotic administration were performed. On one hand, due to the unique administration possible at the beginning of the digestion in the TIM-1 system, it makes impossible to evaluate the pre- and post-administration modalities. The yeast was therefore co-administered with ETEC in the TIM-1 system. On the other hand, the prolonged pre-, co- and post-administration of the yeast were tested in the M-SHIME system over the course of 20 days fermentation.

As beneficial value, the probiotic must stay metabolically active, which implies surviving the adverse conditions found all along the GI transit. In our study, the viability of *S. cerevisiae* was not disrupted by the upper GI stresses during its transit in the TIM-1. The acid, bile acids and protease tolerance of this *S. cerevisiae* strain was in line with a previous study from our laboratory exploring its fate in another experimental condition, after intake of a solid meal (Etienne-Mesmin et al., 2011). In colonic *in vitro* models, previous multiple lines of evidence have shown that the genus *Saccharomyces* may not readily colonize the colonic environment (Auchtung et al., 2018; Thévenot et al., 2015). In the M-SHIME, we applied a posology with a repeated administration of the probiotic, twice a day, at a dose of 7.5 $\log_{10}$ mL^{-1} (with a height hours dosage interval), allowing therefore the maintenance of the yeast at high concentration in the ileum, while lower concentration remained in the ascending colon. Especially, the yeast displayed low capacity to attach the mucus in the ascending colon. This result is in line with our previous study displaying the slight adherence properties of the yeast to mucins in absence of gut microbes (chapter 4, Roussel et al., 2018).

These last years, the mechanisms of action of probiotics in a context of enteric diseases have been clarified and resulted in three main mechanisms of action including direct antagonism, competitive exclusion and immunomodulatory properties (Preidis et al., 2011; Roussel et al., 2016). This latter was not explored in the present study (unlike in chapter 4) as the IECs cannot be directly integrated into the *in vitro* digestive environments.

With respect to direct antagonism, the co-administration of the probiotic with ETEC (TIM-1), as well as its pre-, co-, and post-administration (M-SHIME) displayed no direct inhibitory properties on ETEC survival (total ETEC) all along the *in vitro* digestive environments. This lack of effect on enteric pathogen survival in the colon was also claimed in a study on EHEC, using the same probiotic strain (Thévenot et al., 2015). In sharp contrast, a significant reduction of ETEC growth was observed in LB medium, which is nonetheless a non-representative model to capture the physiological parameters of the human digestion (chapter 4, Roussel et al., 2018). For further insights, the viability of the pathogen under probiotic treatment was assessed by PMA-qPCR (TIM-1 and M-SHIME), and flow cytometry (TIM-1).

Remarkably, *S. cerevisiae* treatment contributed to the disruption of ETEC membrane integrity, through the increase of dead and damaged ETEC cells. This result was observed mainly in the gastric and ileal effluents of the TIM-1, while in the microbiota containing ileum and ascending colon compartments of the M-SHIME, a high variability between donors was noticed making difficult any conclusion. However, compared to the control condition, the number of dead/damaged ETEC cells was markedly increased for the donor 3 under probiotic treatment in the ileum, while a high concentration of ethanol was noticed (1.5 g L^{-1}) at this site. Although not measured in the TIM-1, the assumption that ethanol production by *S. cerevisiae* might be one of the explanatory effects to the disruption of ETEC membrane integrity cannot be refuted and was already observed for EHEC in the TIM-1 system as well as in other studies (Etienne-Mesmin et al., 2011; Chiou et al., 2004; Gyurova and Zhivkov, 2009). To go deeper into the mechanism of action, the membrane potential and the intracellular pH of ETEC were measured in the gastric and ileal effluents of the TIM-1 only. A modest depolarization of ETEC membrane potential was observed under the probiotic condition. A unique study has shown that two strains of *Lactobacillus casei* induced the membrane depolarization of *Salmonella typhimurium* in culture medium through undetermined mechanism of action (Liévin-Le Moal et al., 2013). We hypothesize that ETEC membrane depolarization might be linked to the ethanol production displayed in *S. cerevisiae*. In support of this hypothesis, Gyurova and Zhivkov (2009) have shown a linear decrease of the *E. coli* K12 polarization when ethanol concentration was increased in standard LB medium. With respect to the pH measurements, probiotics, especially bacterial strains can exert antimicrobial effects by reducing the pH of the luminal microenvironment (Anand et al., 2017). However in our study this feature was impossible to explore since the pH was controlled all along the *in vitro* GI tract. In accordance, no change at all of ETEC pHi between the control and probiotic condition was observed.

Next, probiotics can exert direct antagonistic properties through the modulation of the virulence gene expression. For the first time, this study provides the spatial-temporal virulence expression profile of ETEC under *S. cerevisiae* treatment in the two simulators of the human GI tract. We found that *S. cerevisiae* co-administration triggered profound changes in ETEC virulence in the gastric and ileal effluents of the TIM-1. In the M-SHIME, effects of the pre-, co- and post-administration were more limited due to the microbiota interference, the inherent variability across individuals and the lack of dynamic sampling where transitory expression pattern may have been missed. Only the most relevant changes in ETEC virulence gene expression are therefore discussed. In the stomach, the probiotic yeast led to the repression of the genes encoding the enterotoxins (*eltB* and *estAB*), as well as for some donors in the ascending colon between T5 to 20 h post-infection, though not significant, while *estAB* remained significantly over-expressed in the TIM-1 ileum compared to the control condition. In addition to the *eltB* gene expression, *S. cerevisiae* treatment encouraged the decrease of the LT enterotoxin production in both TIM-1 and M-SHIME ileum, though inter-individual variability persisted. These outcomes validate our previous observations in batch culture (chapter 4, Roussel et al., 2018), and are particularly relevant as the enterotoxin secretion trigger the diarrheal symptoms. The underlying mechanisms to such inhibitory properties from the probiotic remain however unidentified. Based on previous research on enteric pathogens, we can speculate at gene level that the probiotic secretes molecule(s) that either act(s) as a quorum sensing signal inhibitor, or directly interact(s) with bacteria transcriptional regulators

(Medellin-Pena et al., 2007; Sturbelle et al., 2015). At protein level, several possibilities are to consider: the LT enterotoxin might have been degraded by the probiotic through the production of proteolytic molecules, as already observed for the toxin A produced by *Clostridium difficile* which was hydrolyzed upon treatment with *S. boulardii* (Pothoulakis et al., 1993). LT might also bind to specific receptor on the surface of *S. cerevisiae* as identified for the cholera toxin of *Vibrio cholerae*, which shares 80% homology with the LT enterotoxin (Brandao et al., 1998). With respect to the genes encoding for adhesins (*tia*, *fimH* and *cfa/Ib*), under the probiotic treatment, they were globally repressed in the stomach, but reverse trends were observed in the ileum of the TIM-1, with a significant over-expression of the genes. Remarkably, the *fimH* gene, which is encoding for the type 1 pili, exhibited a profound over-expression all along the digestion in ileal effluents under probiotic condition. From mechanistic perspectives, we can assume that the *fimH* over-expression could be associated to the mannose related agglutination between ETEC and the yeast, as previously observed in batch medium (chapter 4, Roussel et al., 2018). More in particular, ETEC through the expression of type 1 pili and its FimH subunit protein can bind the mannan on the surface of yeast cells (Knutton et al., 1984; Sheikh et al., 2017). In contrast, the *fimH* gene was either basally expressed or repressed in both control and treated conditions when interacting with the microbial ecosystem of the SHIME ileum and ascending colon, indicating a possible role of the microbial bulk in the modulation of the *fimH* gene expression profile. No studies have yet explored ETEC adhesin gene expression profiles under probiotic treatment condition.

The last class of mechanism of action explored in this study is the competitive exclusion, where probiotics make the GI microenvironments less hospitable for pathogens. These mechanisms include decreasing luminal pH, modulating gut microbiota, improving epithelium barrier function, interfering with pathogen binding and translocation and stimulating production of defense-associated factors, such as mucins and defensins (Roussel et al., 2016; Preidis et al., 2011). Only the assumption that *S. cerevisiae* can modify the composition and activity of the gut microbiota to counteract ETEC was explored in the present study. Following ETEC infection, an imbalanced of the gut microbiota was suggested in chapter 3. Indeed under control condition, the bloom of opportunistic pathogens as well as the decrease of microbes with potential health effect was displayed in chapter 3. Subsequently to the probiotic treatment and in comparison with the control condition, this bloom of opportunistic pathogens such as *Klebsiella*, *Achromobacter* and *Mycobacterium* seemed to be more limited, and we found a general higher abundance of the microbial communities with potential health effect reported in the literature such as *Bifidobacterium*, *Faecalibacterium*, *Lactobacillus* or *Fusicatenibacter* genera (Sokol et al., 2009; Sarkar and Mandal, 2016; Takeshita et al., 2016, Rivière et al., 2018). In addition, no change of the predominant members of the gut microbial community (probiome) was observed after infection even though some species displaying controversial role in the human gut, such as *Enterococcus faecalis* and *Providencia vermicola* were increased upon infection (Almeida et al., 2018). Evidence suggested that post traveler's diarrhea associated with ETEC triggered chronic functional GI disorder named PI-IBS (Principi et al., 2018; Nair et al., 2014; Connor and Riddle, 2014). No microbial marker are so far attributed to the PI-IBS, but decreased abundance of *Bifidobacterium* and *Lactobacillus* members as well as the actinobacterium *Collinsella aerofaciens* were often associated with PI-IBS status (Bag et al., 2017; Lee and Bak, 2011; Malinen et al., 2010; Malinen et al., 2005; Rodino-Janeiro et al., 2018). Remarkably,

under the probiotic treatment this microbial change was counteracted and a significant increase of *Bifidobacterium* and *Lactobacillus* genera was found compared to the control condition (ETEC without probiotic treatment). In addition, no significant change of the abundance of *Collinsella aerofaciens* was observed between the pre and post-infection under the probiotic treatment while decreased under control condition. Although further markers are lacking to affirm any conclusion, we can suggest that *S. cerevisiae* treatment might help in the prevention of the development of PI-IBS.

Surprisingly and contrary to the control condition, a significant reduced abundance of the two mucin-degrading bacteria, *Akkermansia muciniphila* and *Cloacibacillus porcorum* was noticed under the probiotic treatment in the luminal and mucosal ascending colon (Van Herreweghen et al., 2017; Looft et al., 2013).

Finally, the observed changes in microbial composition over time under the probiotic treatment were indicative of metabolic shifts taking place predominantly in the ascending colon. At this site, an overall increase of the SCFA concentrations was shown, dominated by acetate and propionate, and secondary by butyrate, caproate and valerate. We can hypothesize that a duality exists in the increase of the SCFA production pattern upon *S. cerevisiae* treatment. On the one hand the observed stimulation of genera such as *Faecalibacterium*, *Butyricicoccus* and *Roseburia* may have contributed to the butyrate production, while *Bifidobacterium* and *Veillonella* are often associated with the production of acetate. In addition, the yeast cell wall material can serve as a substrate for bacterial fermentation and can therefore favor the increased production of SCFA. This was observed with the yeast *S. boulardii* α-mannan which was utilized by *Bacteroides thetaiotaomicron* to increase the butyrate production (Moré and Swidsinski, 2015; Cuskin et al., 2015; Schneider et al., 2005). On the other hand, *S. cerevisiae* itself physiologically produces acetate (Tang et al., 2015). In addition, we observed an unusual increase of caproate levels in the ascending colon while caproate producers in the gut remain poorly known. Another possibility to explain such increase could be the elongation of n-butyric acid to n-caproic acid through the use of ethanol, abundantly produced under the yeast treatment (Ge et al., 2015). Among these metabolites, some have already displayed interesting properties such as the butyrate, which is considered as a health marker (Hamer et al., 2008, Rios-Covian et al., 2016). SCFA are also important determinants of interactions between the microbiota and enteric pathogens. So far, controversial effects have been generally shown in other enteric pathogens either by enhancing or impeding the virulence gene expression in EHEC or *Salmonella typhimurium* (Barnett Foster, 2013; Herold et al., 2009). Such mechanisms have however never been assessed in ETEC and remain to be unraveled.

5. Conclusion

For the first time, the present study provides significant insights with respect to the anti-pathogenic approaches of the probiotic *S. cerevisiae* CNCM I-3856 against ETEC in the two most relevant *in vitro* systems of the human GI tract. In particular we have shown under the probiotic treatment that:

- Although no direct changed in ETEC survival, the functionality of the pathogen through its virulence activity was significantly altered under the yeast probiotic treatment with a valuable repression of the virulence genes encoding for the enterotoxins as well as the tendency to decrease at protein level the LT enterotoxin production,
- The probiotic tended to counteract the blooming of opportunistic bacteria affiliated to *Klebsiella*, *Achromobacter* and *Mycobacterium* genera induced in the course of ETEC infection,
- The probiotic promoted the microbial communities with potential heath effect such as *Bifidobacterium*, *Faecalibacterium*, *Lactobacillus* or *Fusicatenibacter* genera,
- A higher metabolic activity was displayed especially in the ascending colon under the probiotic treatment.

6. Candidate contribution and acknowledgments

Under supervision of Stéphanie Blanquet-Diot and Tom Van de Wiele, I designed the experimental work. I carried out the *in vitro* digestions (with technical support from Sandrine Chalancon or Sylvain Denis) and *in vitro* fermentations (with technical support from Jana de Bodt). I designed and carried out all the molecular-based experiments (DNA and RNA extractions, q-PCR, PMA-qPCR, RT-qPCR). Wessam Galia carried out the flow cytometry experiments. Tim Lacoere carried out the gas chromatography measurements and generated the OTU tables. All the microbial community analysis and statistical analysis were performed in close collaboration with Kim de Paepe (she supervised me at each steps of the data processsing). I drafted the manuscript. I designed the figures in collaboration with Kim de Paepe. I wrote the manuscript with input from all authors. Kim de Paepe and I will be co-first authors of the future publication.

I would like to acknowledge Sylvie Alvarez and Karine Fayolle (VetagroSup) for welcoming me in the L3 laboratory during the TIM-1 experiments. I thank Pieter Van den Abbeele and Massimo Marzorati (Prodigest) for sharing their expertise in the set-up of the M-SHIME ileum; Tim Lacoere (CMET) for assistance in the molecular techniques and Frederiek-Maarten Kerckhof for statistical support. I also thank the team of Prof. Filip Van Nieuwerburgh and especially Sarah De Keulenaer (Department of Pharmaceutics) for welcoming me during the RNA quality control experiments and for providing me the Bioanalyzer. This research was funded by Lesaffre company (Marcq-en-Baroeul, France).

7. Supplementary data

Table S5.1. RDP Seqmatch and NCBI BLAST results for the most abundant species in the M-SHIME.

The similarity score (Sab), as calculated by RDP, and the NCBI BLAST output for the best hit and next best hit(s) are shown. The NCBI maximal score (not shown) equalled the total score for all displayed entries. Indicated in bold, the OTU numbers for which they have been replaced by the species names for the microbial analysis. NA= Not Available

		RDP	NCBI BLAST			
OTU	**Species**	**Sab**	**Total score**	**Query coverage (%)**	**E-value**	**Identity (%)**
1	*Escherichia/Shigella fergusonii*	1.000	787	100	0.0	100
	Escherichia/Shigella flexneri	1.000	787	100	0.0	100
	Shigella sonei	1.000	787	100	0.0	100
	Escherichia coli	1.000	787	100	0.0	100
	Escherichia vulneris	1.000	787	100	0.0	100
2	*Anaerovibrio lipolyticus*	0.771	638	99	0.0	94
	Selenomonas bovis	0.752	614	100	1e-175	93
3	***Klebsiella pneumoniae***	**0.969**	**782**	**100**	**0.0**	**99**
	Klebsiella quasipneumoniae	0.969	776	100	0.0	99
	Klebsiella variicola	0.964	NA	100	0.0	99
	Serratia liquefaciens	NA	776	NA	NA	NA
4	*Leclercia adecarboxylata*	1.000	787	100	0.0	100
	Enterobacter cloacae	0.983	787	100	0.0	100
	Enterobacter ludwigii	1.000	787	100	0.0	100
	Pantoea agglomerans	NA	787	100	0.0	99
	Enterobacter kobei	0.983	784	100	0.0	99
	Salmonella enterica	0.983	782	100	0.0	99
5	***Mitsuokella multacida***	**0.983**	**784**	**100**	**0.0**	**99**
	Mitsuokella jalaludinii	0.954	754	100	0.0	99
	Selenomonas bovis	0.814	630	99	1e-180	93
6	***Faecalibacterium prausnitzii***	**0.982**	**736**	**100**	**0.0**	**99**
	Gemmiger formicilis	0.716	569	100	7e-159	92
7	*Succinivibrio dextrinosolvens*	0.919	688	100	0.0	98
	Anaerobiospirillum succiniciproducens	0.646	540	100	2e-153	91
8	***Clostridium bolteae***	**1.000**	**741**	**100**	**0.0**	**100**
	Clostridium asparagiforme	0.923	986	100	0.0	98
9	***Veillonella dispar***	**0.968**	**776**	**100**	**0.0**	**99**
	Veillonella tobetsuensis	0.949	760	100	0.0	99
	Veillonella parvula	0.929	754	100	0.0	99
10	***Bacteroides fragilis***	**1.000**	**778**	**100**	**0.0**	**100**
	Bacteroides ovatus	NA	649	100	0.0	95
11	*Mitsuokella jalaludinii*	0.983	782	100	0.0	99
	Mitsuokella multacida	0.937	750	100	0.0	98
12	***Bacteroides dorei***	**1.000**	**778**	**100**	**0.0**	**100**
	Bacteroides vulgatus	0.951	756	100	0.0	99
13	***Pseudomonas aeruginosa***	**1.000**	**787**	**100**	**0.0**	**100**
	Pseudomonas guezennei	NA	776	100	0.0	99

	Faecalibacterium prausnitzii	**0.918**	**713**	**100**	**0.0**	**99**
14	*Gemmiger formicilis*	0.735	592	100	7e-169	93
	Bacteroides thetaiotaomicron	**1.000**	**778**	**100**	**0.0**	**100**
15	*Bacteroides faecichinchillae*	0.947	756	100	0.0	99
	Bacteroides faecis	0.935	739	100	0.0	98
	Bacteroides uniformis	**1.000**	**778**	**100**	**0.0**	**100**
16	*Bacteroides rodentium*	0.906	717	100	0.0	97
	Acidaminococcus fermentans	0.925	737	100	0.0	98
17	*Acidaminococcus intestini*	NA	671	100	0.0	95
	Clostridium butyricum	**1.000**	**741**	**100**	**0.0**	**100**
18	*Clostridium saccharobutylicum*	0.941	719	100	0.0	99
	Citrobacter freundii	0.990	782	100	0.0	99
19	*Citrobacter brakii*	0.971	771	100	0.0	99
	Acidaminococcus intestine	**1.000**	**787**	**100**	**0.0**	**100**
20	*Acidaminococcus fermentans*	0.885	704	100	0.0	96
	Gemmiger formicilis	**1.000**	**741**	**100**	**0.0**	**100**
21	*Subdoligranulum variabile*	0.959	719	100	0.0	99
	Bacteroides timonensis	NA	761	100	0.0	99
22	*Bacteroides cellulosilyticus*	0.934	750	100	0.0	99
	Bacteroides intestinalis	0.888	739	100	0.0	98
	Eubacterium rectale	**0.949**	**741**	**100**	**0.0**	**100**
23	*Roseburia faecis*	0.941	713	100	0.0	99
	Roseburia intestinalis	0.892	939	100	0.0	98
	Parabacteroides distasonis	**0.971**	**778**	**100**	**0.0**	**100**
24	*Parabacteroides gordonii*	0.672	756	100	2e-174	93
	Parabacteroides faecis	0.613	601	100	1e-171	92
	Bacteroides ovatus	0.978	773	100	0.0	99
25	*Bacteroides xylanisolvens*	NA	730	100	0.0	98
	Phascolarctobacterium faecium	**1.000**	**787**	**100**	**0.0**	**100**
26	*Phascolarctobacterium succinatutens*	0.734	632	100	0.0	93
	Clostridium perfringens	**1.000**	**741**	**100**	**0.0**	**100**
27	*Eubacterium tarantellae*	NA	691	100	0.0	98
	Mitsuokella jalaludinii	0.935	704	100	0.0	96
28	*Mitsuokella multacida*	0.886	673	100	0.0	95
	Selenomonas bovis	NA	675	100	0.0	95
	Bilophila wadsworthia	0.973	NA	NA	NA	NA
29	*Desulfovibrio simplex*	NA	604	100	9e-173	92
	Blautia faecis	**1.000**	**741**	**100**	**0.0**	**100**
30	*Blautia glucerasea*	0.926	726	100	0.0	99
35	***Bifidobacterium longum***	**0.985**	**750**	**100**	**0.0**	**100**
	Bifidobacterium breve	0.918	NA	NA	NA	NA
	Prevotella copri	0.851	717	100	0.0	97
40	*Prevotella oulorum*	0.751	640	100	0.0	94
44	*Prevotella salivae*	0.749	606	100	2e-173	93
	Prevotella shahii	0.712	NA	NA	NA	NA
	Bifidobacterium faecale	1.000	758	100	0.0	100
47	*Bifidobacterium adolescentis*	1.000	758	100	0.0	100

	Phascolarctobacterium succinatutens	**0.958**	**765**	**100**	**0.0**	**99**
49	*Phascolarctobacterium faecium*	0.724	638	100	0.0	94
	Eubacterium ventriosum	**0.961**	**726**	**100**	**0.0**	**99**
52	*Lachnospiraceae bacterium*	0.765	628	99	5e-180	95
	Marivita hallyeonensis	**0.964**	**730**	**100**	**0.0**	**99**
53	*Marivita roseacus*	0.940	719	100	0.0	99
	Enterococcus hirae	1.000	787	100	0.0	100
	Enterococcus villorum	1.000	787	100	0.0	100
55	*Enterococcus ratti*	1.000	787	100	0.0	100
	Enterococcus durans	1.000	787	100	0.0	100
	Achromobacter denitrificans	0.978	776	100	0.0	99
	Achromobacter pulmonis	0.978	776	100	0.0	99
60	*Achromobacter agilis*	NA	776	100	0.0	99
	Achromobacter xylosoxidans	0.958	776	100	0.0	99
	Clostridium aldenense	**0.964**	**730**	**100**	**0.0**	**99**
66	*Clostridium algidixylanolyticum*	0.835	NA	NA	NA	NA
	Lachnoclostridium pacaense	NA	708	100	0.0	99
	Fusicatenibacter saccharivorans	**1.000**	**741**	**100**	**0.0**	**100**
70	*Murimonas intestine*	0.856	669	100	0.0	97
	Synergistetes bacterium	**1.000**	NA	NA	NA	NA
72	*Cloacibacillus porcorum*	0.916	730	100	0.0	99
	Collinsella aerofaciens	**1.000**	**743**	**100**	**0.0**	**100**
79	*Collinsella bouchesdurhonensis*	NA	675	100	0.0	97
	Paraprevotella clara	**0.969**	**765**	**100**	**0.0**	**99**
81	*Paraprevotella xylaniphila*	0.685	604	100	0.0	93
	Sutterella wadsworthensis	**1.000**	**787**	**100**	**0.0**	**100**
85	*Sutterella stercoricanis*	NA	654	100	0.0	94
	Roseburia sp.	1.000	NA	NA	NA	NA
88	*Eubacterium eligens*	NA	625	100	6e-179	95
	Clostridium scindens	**1.000**	**741**	**100**	**0.0**	**100**
90	*Dorea longicatena*	NA	669	100	0.0	97
	Clostridium chromiireducens	NA	725	100	0.0	99
91	*Clostridium butyricum*	0.982	719	100	0.0	99
	Clostridium saccharobutylicum	NA	708	100	0.0	99
	Clostridium celerecrescence	0.860	686	100	0.0	98
94	*Clostridium xylanolyticum*	0.857	NA	NA	NA	NA
	Clostridium colinum	0.830	658	100	0.0	96
102	*Clostridium piliforme*	0.828	NA	NA	NA	NA
	Ruminococcaceae bacterium	1.000	NA	NA	NA	NA
103	*Oscillibacter ruminantium*	NA	573	100	2e-163	92
	Bacteroides caccae	**1.000**	**778**	**100**	**0.0**	**100**
104	*Bacteroides faecis*	0.850	723	100	0.0	98
	Klebsiella variicola	**0.983**	**782**	**100**	**0.0**	**99**
115	*Klebsiella pneumonia*	0.959	776	100	0.0	99
	Clostridium tertium	**1.000**	**741**	**100**	**0.0**	**100**
117	*Clostridium chauvoei*	0.985	736	100	0.0	99
120	*Oscillibacter valericigenes*	0.778	617	100	1e-176	94

	Oscillibacter ruminantium	0.745	606	100	2e-173	94
124	***Blautia luti***	**0.987**	**736**	**100**	**0.0**	**99**
	Blautia stercoris	0.926	691	100	0.0	98
127	***Alistipes shahii***	**0.968**	**773**	**100**	**0.0**	**99**
	Alistipes finegoldi	0.924	739	100	0.0	98
131	***Blautia obeum***	**1.000**	**737**	**100**	**0.0**	**99**
	Blautia wexlerae	0.916	686	100	0.0	98
151	***Bifidobacterium angulatum***	**1.000**	**754**	**100**	**0.0**	**100**
	Bifidobacterium merycicum	0.974	737	99	0.0	99
160	***Victivallis vadensis***	**1.000**	**743**	**100**	**0.0**	**100**
	Caloramator proteoclasticus	NA	331	99	2e-90	82
163	***Ruminococcus faecis***	**1.000**	**741**	**100**	**0.0**	**100**
	Ruminococcus torques	0.985	682	100	0.0	97
166	***Bacteroides eggerthii***	**1.000**	**778**	**100**	**0.0**	**100**
	Bacteroides uniformis	0.857	712	100	0.0	97
175	*Blautia coccoides*	0.867	680	100	0.0	97
	Muricome intestine	0.824	675	100	0.0	97
	Clostridium oroticum	0.810	669	100	0.0	97
201	*Mycobacterium moriokaense*	0.915	701	100	0.0	98
	Mycobacterium grossiae	NA	701	100	0.0	98
	Mycobacterium aquaticum	NA	701	100	0.0	98

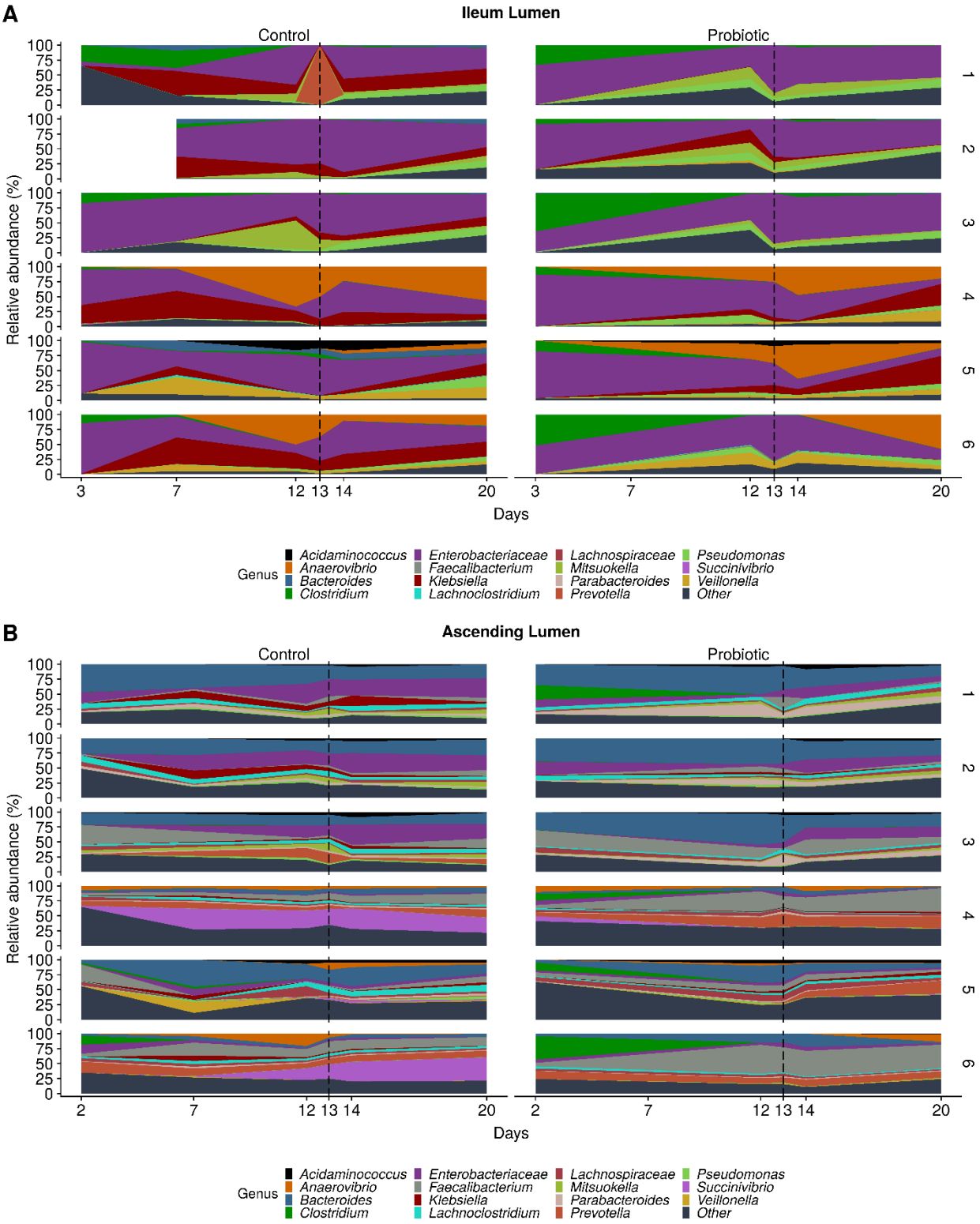

Figure S5.1. **Genus level microbial community composition of the ileum and ascending luminal environments under control and probiotic conditions, as determined by amplicon sequencing.** The area graphs show the relative abundance of the 15 most abundant genera in the luminal (**A**) ileum and (**B**) ascending colon, from six different donors over the course of 20 days fermentation. ETEC infection is demarcated by the dashed line at day 13.

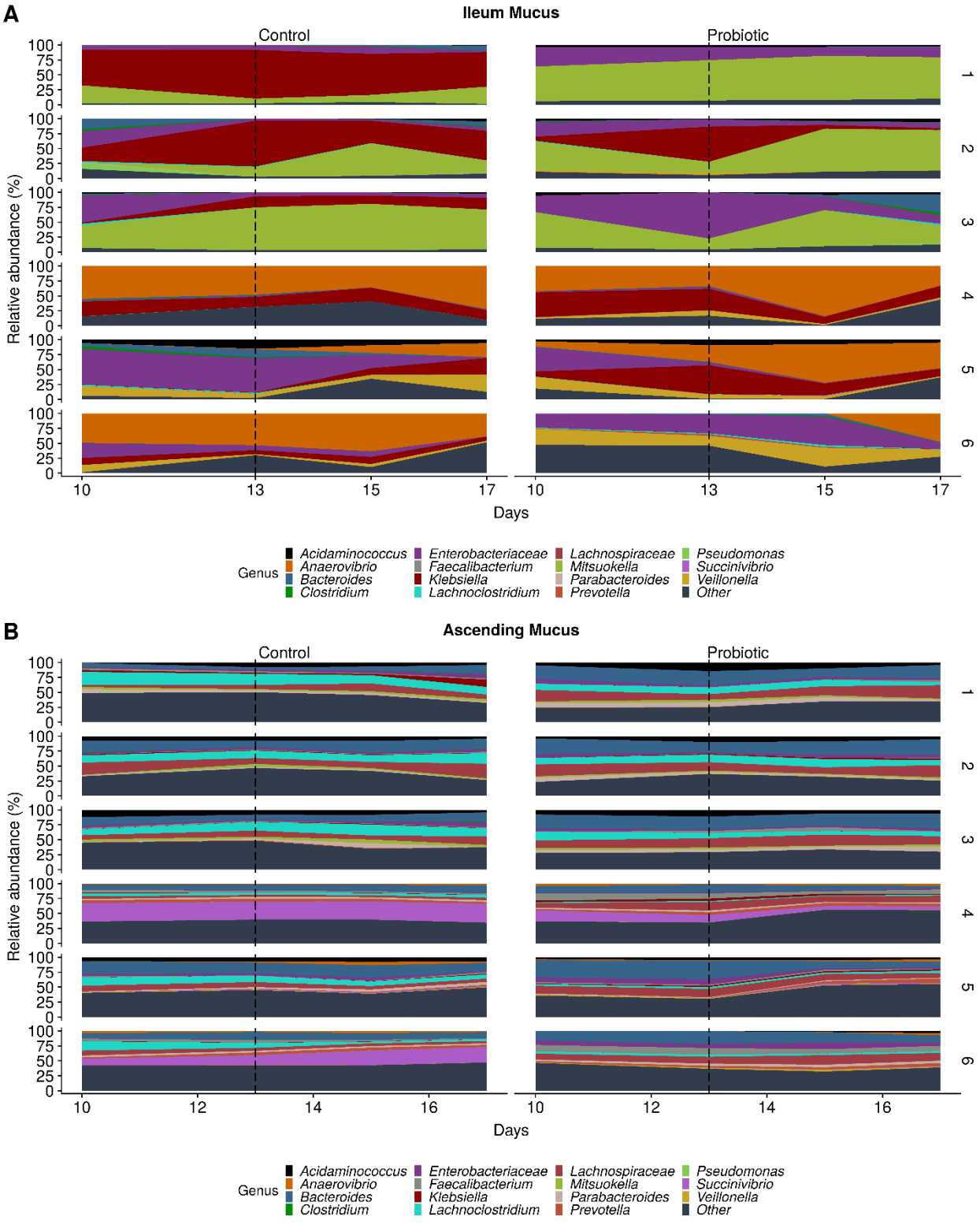

Figure S5.2. **Genus level microbial community composition of the ileum and ascending mucosal environments under control and probiotic conditions, as determined by amplicon sequencing.** The area graphs show the relative abundance of the 15 most abundant genera in the mucosal (**A**) ileum and (**B**) ascending colon, from six different donors over the course of 20 days fermentation. ETEC infection is demarcated by the dashed line at day 13.

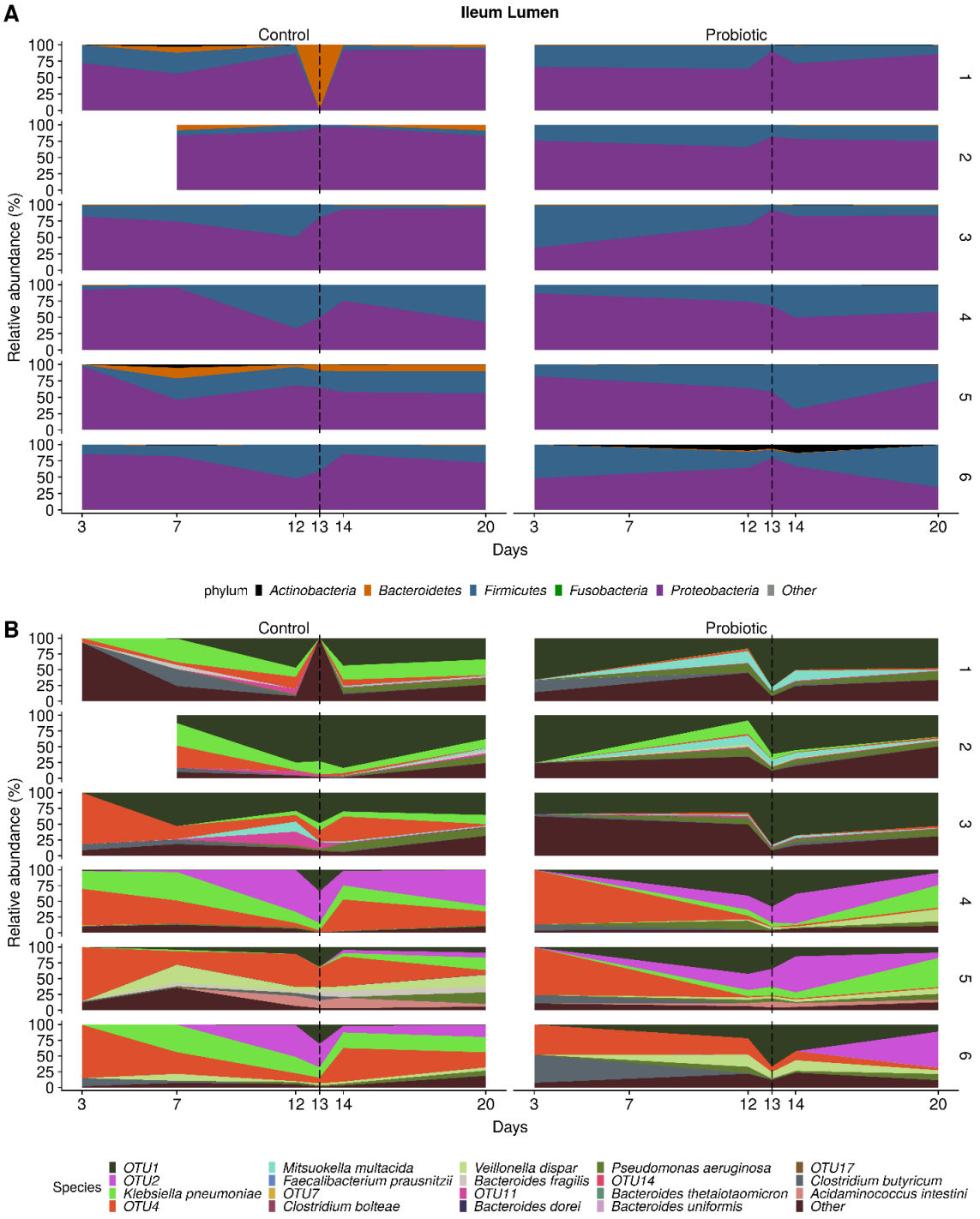

Figure S5.3. **Phylum and species levels microbial community composition of the luminal ileum region under control and probiotic conditions, as determined by amplicon sequencing.** The area graphs show the relative abundance of the (**A**) 5 most abundant phyla and, (**B**) 19 most abundant species in the luminal ileum from six different donors over the course of 20 days fermentation. ETEC infection is demarcated by the dashed line at day 13. Species were annotated using the RDP SeqMatch and NCBI BLAST. For species that could not unambiguously be identified at species level, the OTU identifier is displayed.

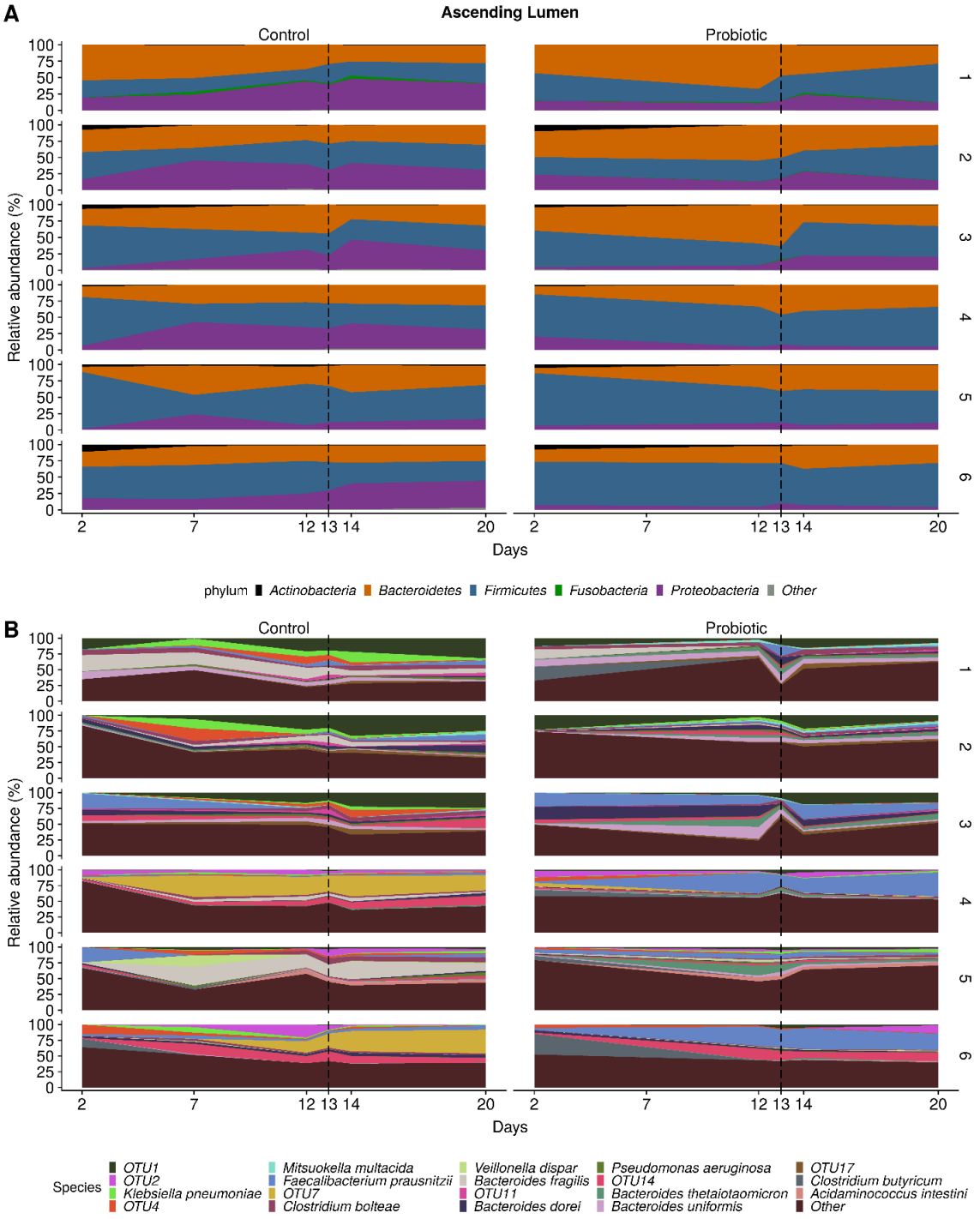

Figure S5.4. **Phylum and species levels microbial community composition of the luminal ascending colon region under control and probiotic conditions, as determined by amplicon sequencing.** The area graphs show the relative abundance of the (**A**) 5 most abundant phyla and, (**B**) 19 most abundant species in the luminal ascending colon from six different donors over the course of 20 days fermentation. ETEC infection is demarcated by the dashed line at day 13. Species were annotated using the RDP SeqMatch and NCBI BLAST. For species that could not unambiguously be identified at species level, the OTU identifier is displayed.

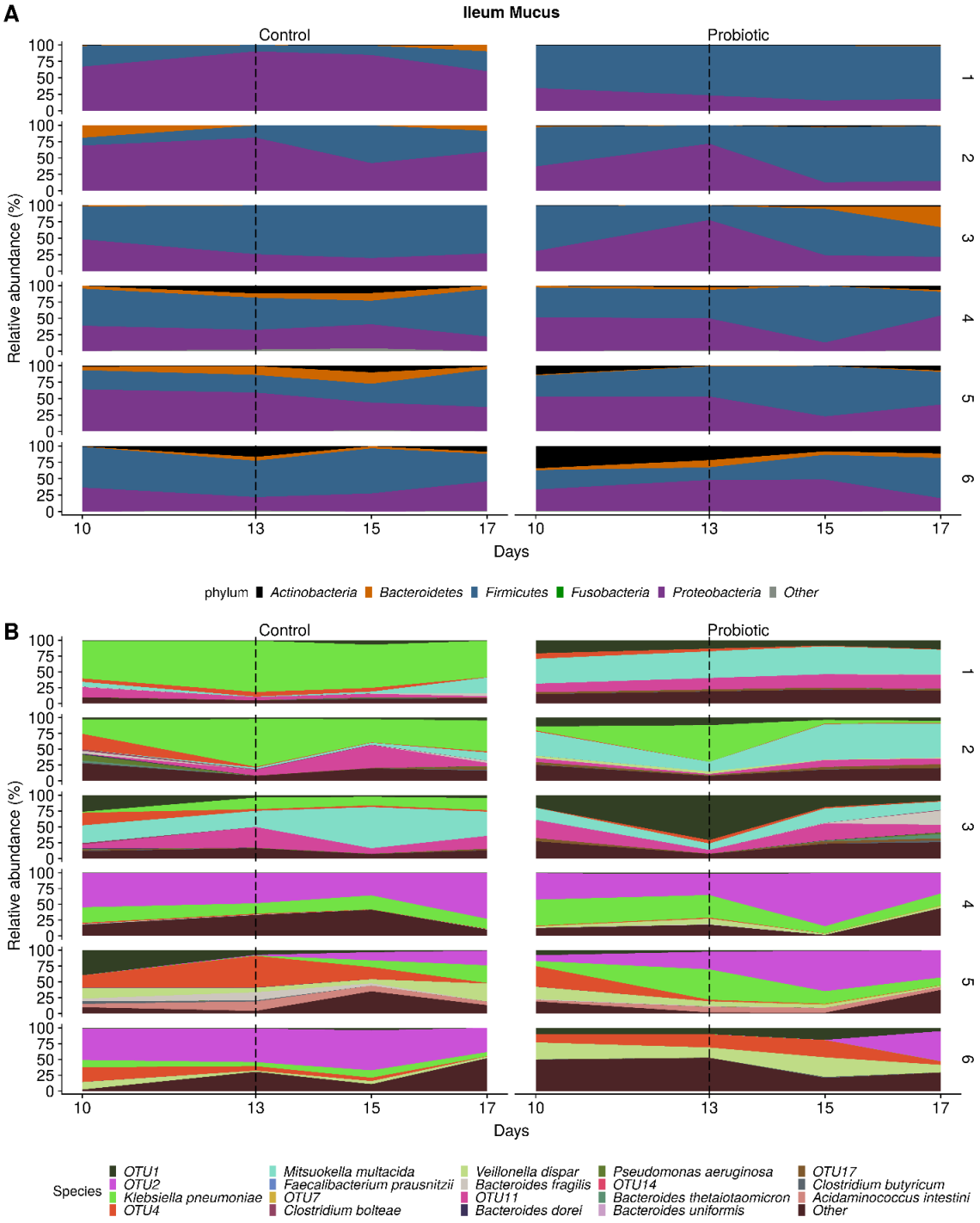

Figure S5.5. Phylum and species levels microbial community composition of the mucosal ileum region under control and probiotic conditions, as determined by amplicon sequencing. The area graphs show the relative abundance of the (**A**) 5 most abundant phyla and, (**B**) 19 most abundant species in the mucosal ileum from six different donors over the course of 20 days fermentation. ETEC infection is demarcated by the dashed line at day 13. Species were annotated using the RDP SeqMatch and NCBI BLAST. For species that could not unambiguously be identified at species level, the OTU identifier is displayed.

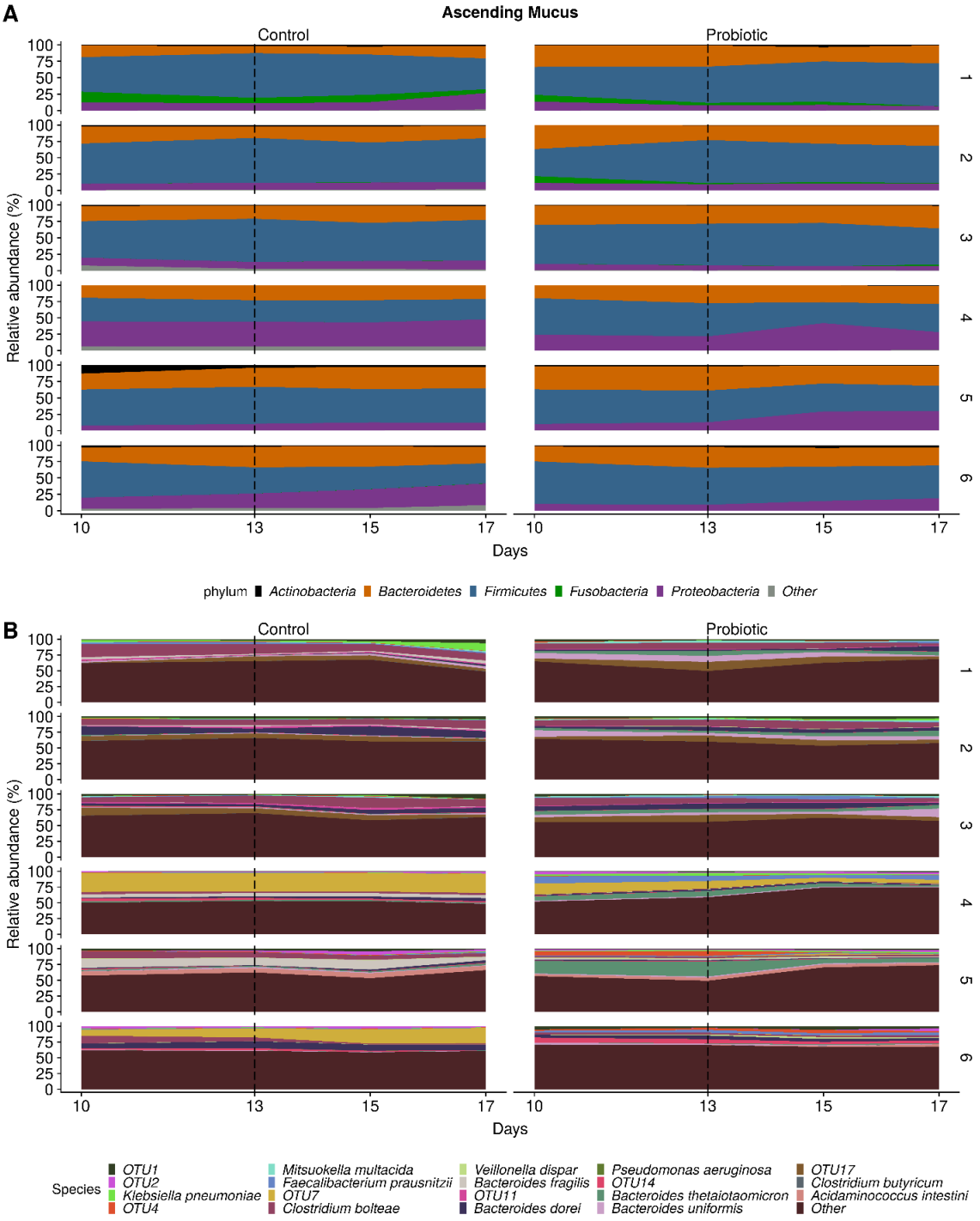

Figure S5.6. Phylum and species levels microbial community composition of the mucosal ascending colon region under control and probiotic conditions, as determined by amplicon sequencing. The area graphs show the relative abundance of the (**A**) 5 most abundant phyla and, (**B**) 19 most abundant species in the mucosal ascending colon from six different donors over the course of 20 days fermentation. ETEC infection is demarcated by the dashed line at day 13. Species were annotated using the RDP SeqMatch and NCBI BLAST. For species that could not unambiguously be identified at species level, the OTU identifier is displayed.

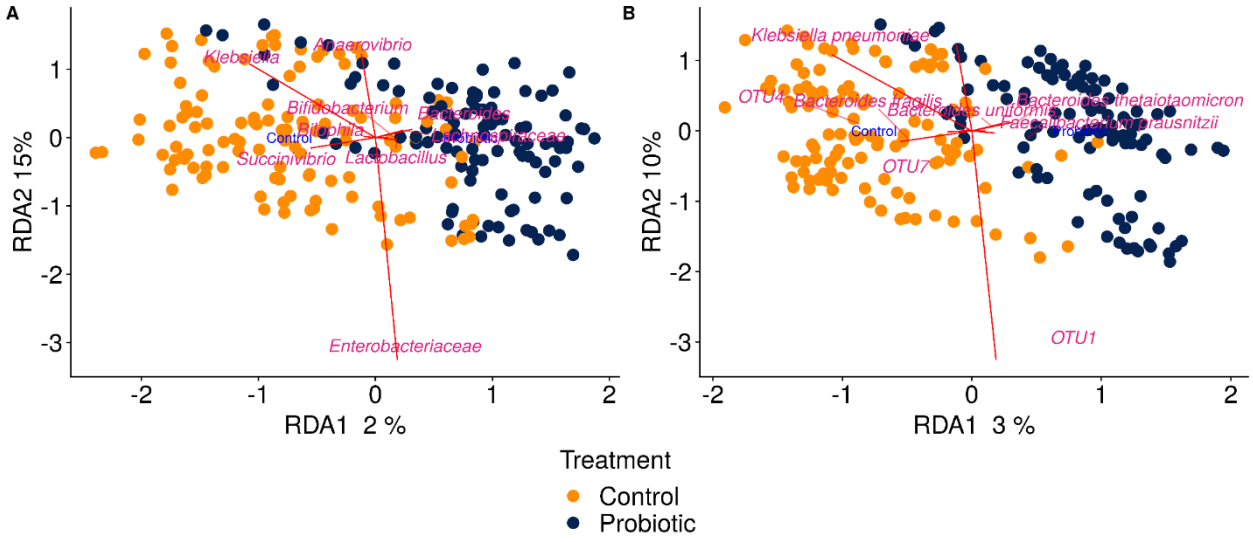

Figure S5.7. **Distance-based redundancy analysis (db-RDA) triplots showing the relationship of the treatment condition as explanatory variable to the microbial community structure at genus (A) and species (B) levels.** Factor levels are represented as centroids in blue. Genus scores in pink show the direction of higher abundance of a particular genus. The factor treatment significantly contributed to the variation of the microbial community structure at (**A**) 5.2% (*p*= 0.001); (**B**) 7.7% (*p*= 0.001).

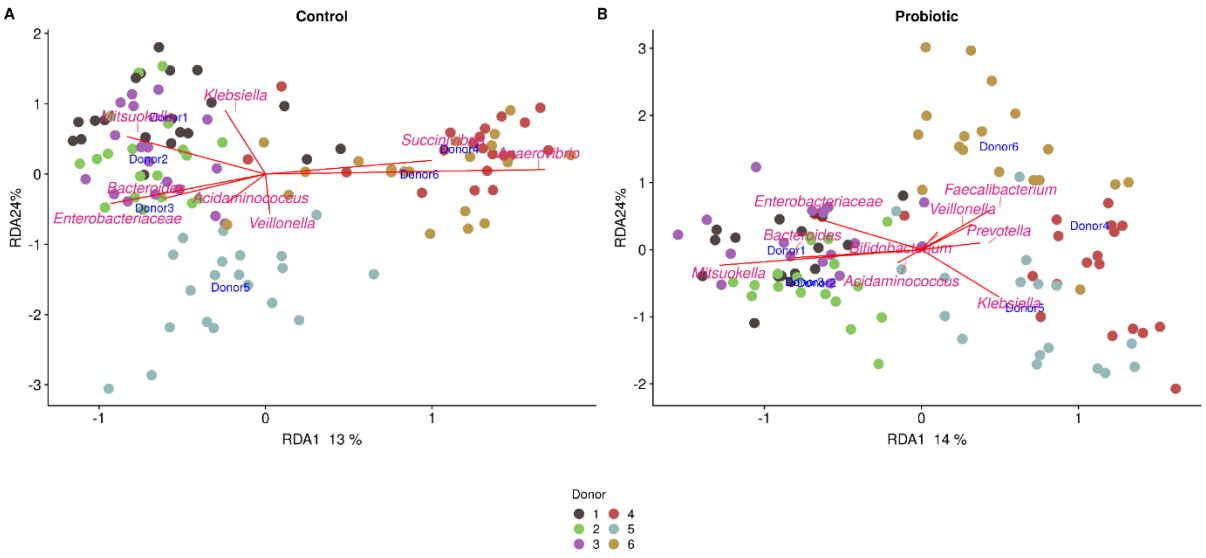

Figure S5.8. **Distance-based redundancy analysis (db-RDA) triplots showing the relationship of the donor condition as explanatory variable to the microbial community structure at genus level under control (A) and probiotic (B) conditions.** Factor levels are represented as centroids in blue. Genus scores in pink show the direction of higher abundance of a particular genus. The factor donor significantly contributed to the variation of the microbial community structure at (**A**) 5.8% (*p*= 0.001); (**B**) 5.2% (*p*= 0.001).

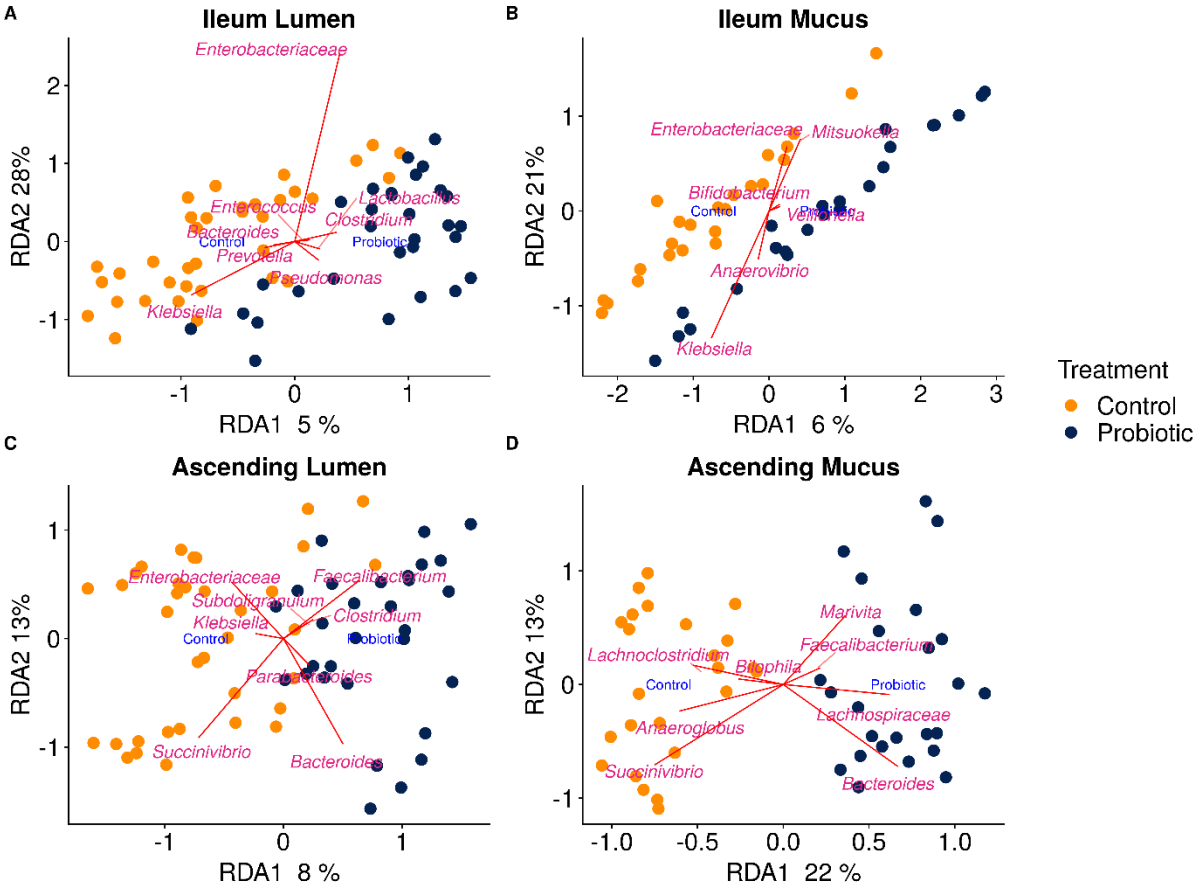

Figure S5.9. **Distance-based redundancy analysis (db-RDA) triplots showing the relationship of the treatment condition as explanatory variable to the microbial community structure at genus level in ileum lumen (A), ileum mucus (B), ascending colon lumen (C) and ascending colon mucus (D).** Factor levels are represented as centroids in blue. Genus scores in pink show the direction of higher abundance of a particular genus. The factor treatment significantly contributed to the variation of the microbial community structure in each gut region and microenvironment (**A**) 3.2% (p= 0.005); (**B**) 2.5% (p= 0.009); (**C**) 5.1% (p= 0.001); (**D**) 11.3% (p= 0.001).

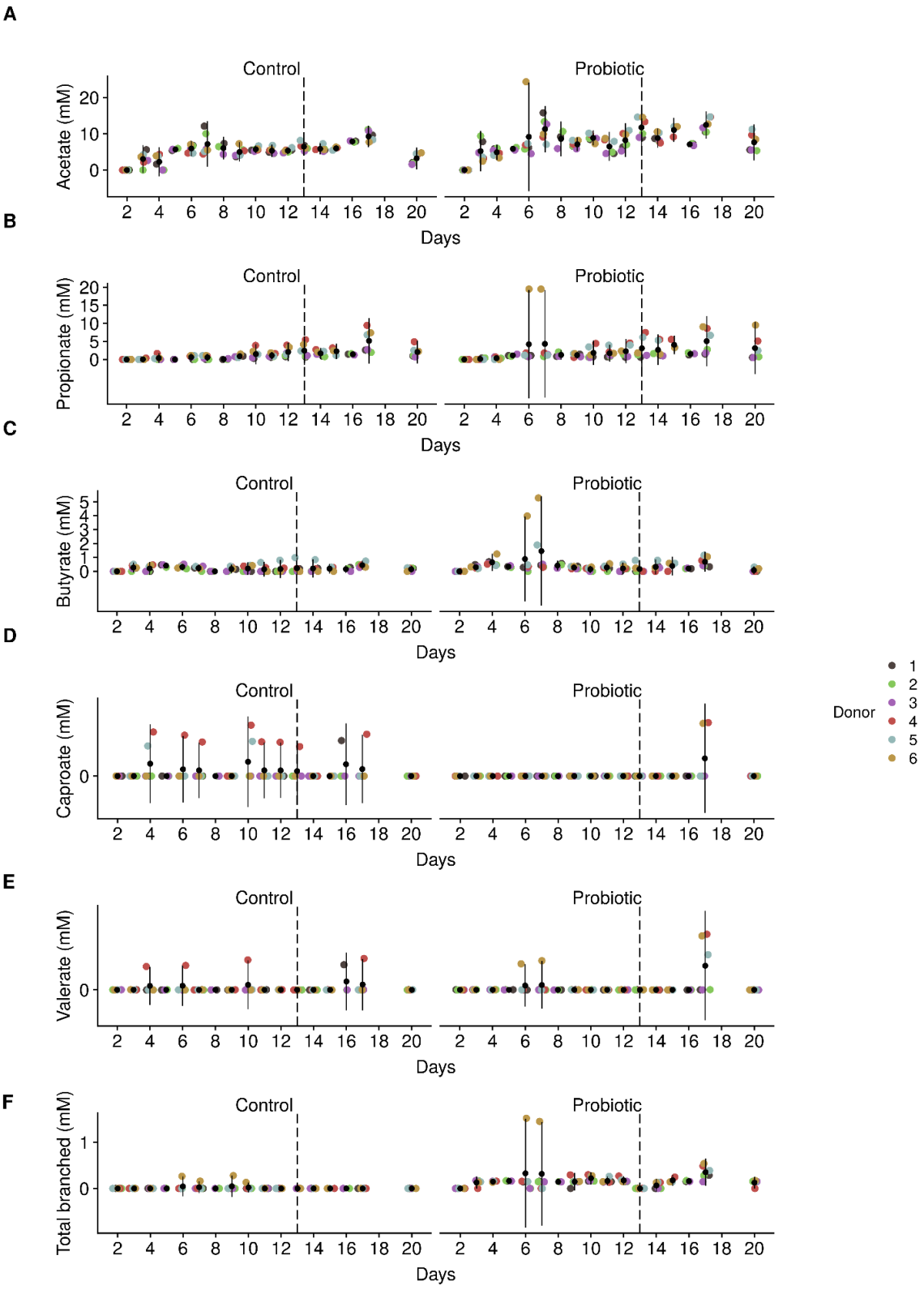

Figure S5.10. **Short chain fatty acid (SCFA) concentrations (mM) in the ileum, inoculated with the microbial community derived from six different donors, under control and probiotic treatment conditions.** The pre-infection period is represented from day 2 to 12, ETEC infection is demarcated by the dashed line at day 13 and, the post infection until day 20.

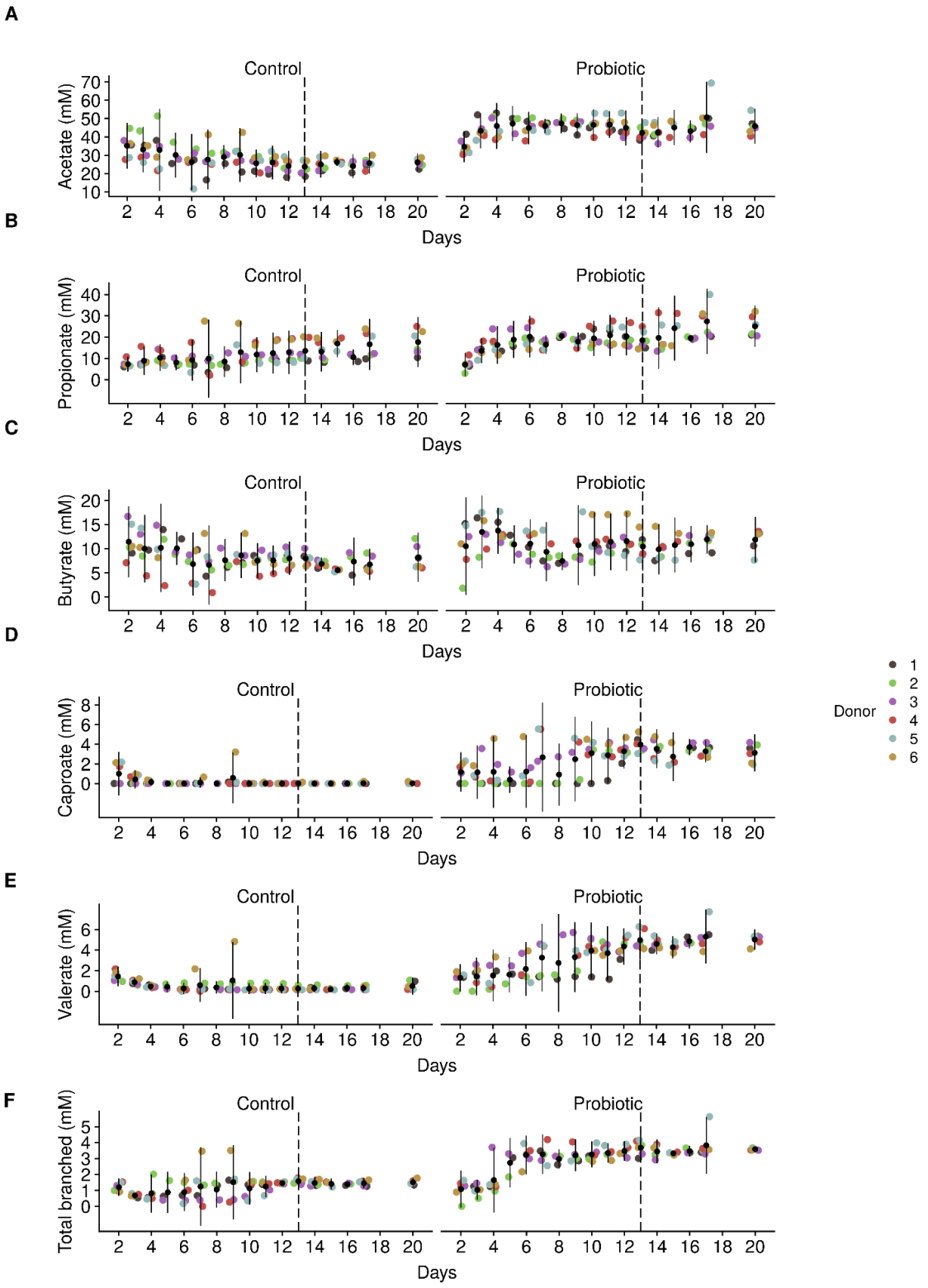

Figure S5.11. **Short chain fatty acid (SCFA) concentrations (mM) in the ascending colon, inoculated with the microbial community derived from six different donors, under control and probiotic treatment conditions.** The pre-infection period is represented from day 2 to 12, ETEC infection is demarcated by the dashed line at day 13 and, the post infection until day 20.

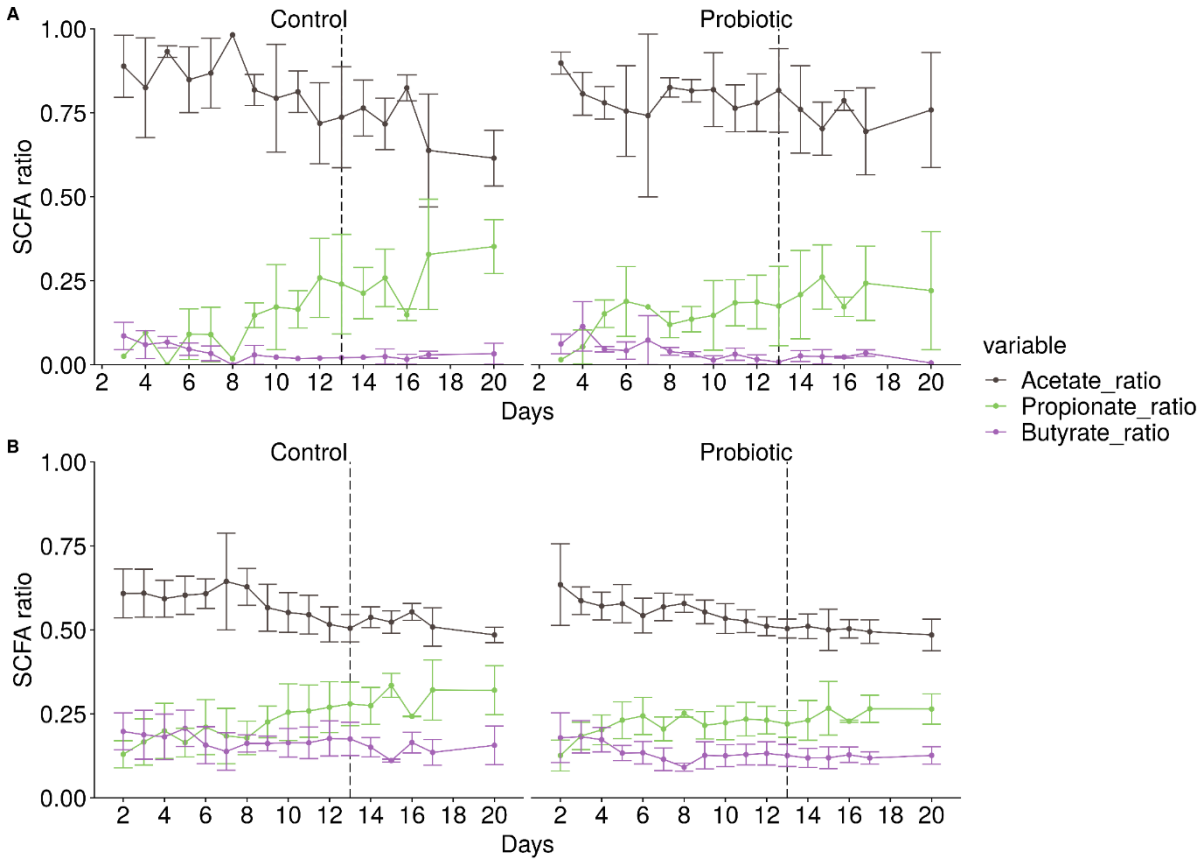

Figure S5.12. **Mean concentration of the SCFA ratio in the ileum (A) and ascending colon (B) compartments over time and between treatment conditions.** No significant differences between treatments were observed as determined by Pairwise Wilcoxon Rank Sum Tests with Holm correction.

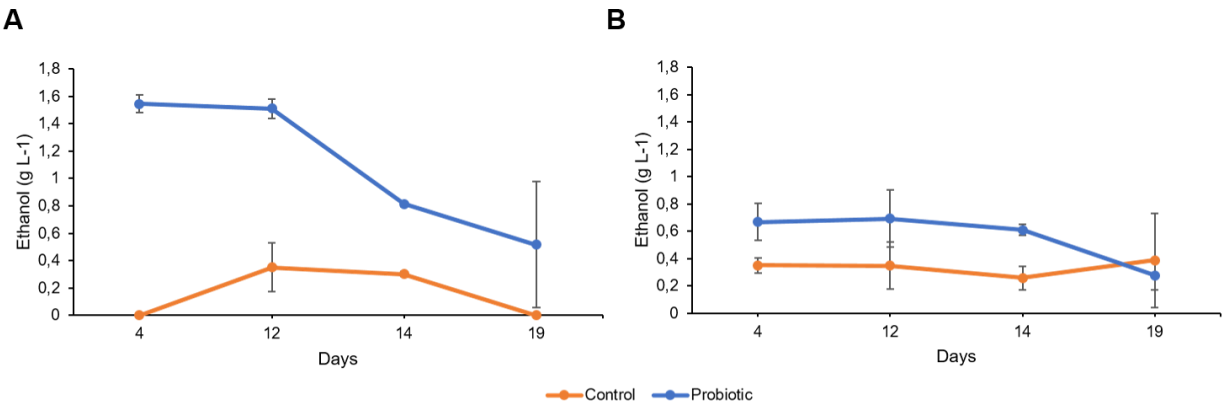

Figure S5.13. **Mean concentration of ethanol in the ileum (A) and ascending colon (B) luminal compartments over time and between treatment conditions.** Only the average concentrations of donors 1, 2 and 3 are represented under both conditions.

Section III

GENERAL DISCUSSION

1. Positioning of the research

Diarrheal diseases strike populations of all ages and across all geographies, although the relative frequency and severity differ. In 2015, diarrhea caused worldwide more than 1.3 million deaths (GBD, 2017). Among the 13 recognized etiological agents for diarrheal diseases (*Clostridium difficile*, *Shigella spp.*, *Campylobacter*, **ETEC**, *Vibrio cholerae*, enteropathogenic *E. coli*, *Salmonella*, *Aeromonas*, *Entamoeba histolytica*, *Cryptosporidium spp.*, adenovirus, rotavirus, norovirus), the ETEC attributable fraction of all diarrhea cases was 6% in 2015, resulting in 113,000 deaths and an estimated 44 million of cases occurring annually (Lamberti et al., 2014; Walker et al., 2017). Noteworthy, **ETEC burden** attests considerable disparities according to the age-range as well as the socioeconomic status and living conditions of the population. Two at-risk groups for ETEC infections are distinguished with (i) infants living in resource-limited countries, and (ii) adults traveling in endemic zones such as Asia, Africa and Latin America. **Traveler's diarrhea** impacts annually over 20 million tourists, business travelers and military troops in a worldwide basis. Among them, 10 million are caused by **ETEC**, which **represents about 45% of the total traveler's diarrhea** monitored (Harvey et al., 2013; Path, BVGH report, 2011; Giddings et al., 2016; Putnam et al., 2006). Beyond diarrheal symptoms, ETEC can have long-term implications, resulting in post-infectious chronic sequelae ranging from functional gastrointestinal disorder to **irritable bowel syndrome (IBS)**, to such extent that 10-14% of traveler's diarrhea associated ETEC cases result in IBS (Connor and Riddle, 2014; Barrett and Brown, 2016; Bourgeois et al., 2016).

These epidemiological and clinical observations give rise to two major and concomitant issues: (i) the **understanding of ETEC behavior in the human GI tract** through the survival of the pathogen and its virulence features is crucially missing, and consequently results to (ii) the **lack of prophylactic and/or curative treatments** specific to ETEC infections. These limitations are further discussed hereafter.

First, in humans, ethical objections are a main constraint, precluding studies involving non-attenuated pathogens. In scarce clinical trials, the use of infra-physiological dose of ETEC and/or live but genetically attenuated strains impedes the proper assessment of the pathogen survivability and its virulence features in the human gut (Bruggencate et al., 2016). As a means of recourse, ETEC findings predominantly originate from animal models (especially piglets), human and pig intestinal epithelial cell cultures and simple static *in vitro* models of the human GI tract. Nonetheless, these approaches remain respectively far distant from the human physiology, ignore the successive GI niches encountered by the pathogen prior to host / cell interactions and, simulate *in vitro* only one digestive parameter at a time. Hence, integration and sequential delivery of GI signals are needed to model the dynamics and complexity of the human gut more closely. In particular, simulation of the gastric pH drop, representative GI transit time, and reproduction of a highly complex gut microbiota from human origin, are some of the key parameters required to strengthen the conclusion of previous studies. The use of **dynamic multi-compartmented *in vitro* model**s of the human digestion (**TIM-1**) and colonic fermentation (**M-SHIME**) represent therefore a great alternative to fully study pathogenic strains and come closer to the complexity of the GI physiology, as already shown for EHEC and AIEC pathogens (Thévenot et al., 2013; Thévenot et al., 2015; Van den Abbeele et al., 2016).

Second, as an attempt to prevent or treat ETEC infections, the general clinical recommendations for diarrheal episodes are followed and include rehydration or the use of anti-motility and/or anti-secretory agents (WHO, 2002; Bruzzese et al., 2018). In addition, the use of **antibiotic therapy has been overdone** in the past years, carrying consequences nowadays to the increased **resistance of ETEC** to the most common antibiotics prescribed (Zaman et al., 2017; Taylor et al., 2017; Riddle et al., 2016; CDC, 2016). The lack of treatments highlight the importance to **speed up the development of prophylactic approaches** to overcome the burden gaining ground to the extent of industrialized countries (MacDonald et al., 2015; Beatty et al., 2004). To address this shortcoming, several **alternative strategies** are currently under research including vaccines, micronutrients, pre- and **probiotics**, bacteriophages as well as immunotherapeutic (Zhang and Sack, 2015; Verhelst et al., 2013; Roberts et al., 2013; Sarker et al., 2016; Sears et al., 2017; Roussel et al., 2016). With respect to the probiotic approach, over the last two decades, initial efforts have been centered on establishing scientific support for the efficacy of several bacterial and yeast probiotic strains (Roussel et al., 2016). However, the majority of these studies have been carried out in piglets with specific ETEC strains unlikely pathogenic in humans (Dubreuil et al., 2016; Fairbrother et al., 2012). Other studies have shown a significant reduction in the risk of traveler's diarrhea when probiotics such as *S. boulardii* were given (McFarland et al., 2007; Bae, 2018), but ETEC strains have been rarely involved in the diarrheal etiology. As recently published by an expert panel of the International Society of Travel Medicine, insufficient evidence to recommend the use of the actual commercially available pre- or probiotics to prevent or treat traveler's diarrhea was highlighted (Riddle et al., 2017), which implies that the research on probiotics need to be continued. The use of the yeast ***Saccharomyces cerevisiae* CNCM I-3856** patented by Lesaffre has already displayed fruitful antagonistic characteristics through several mechanism of action in other pathogenic *E. coli* such as EHEC and AIEC (Thévenot et al., 2015; Etienne-Mesmin et al., 2011; Sivignon et al., 2015), making interesting to extend the research to ETEC.

In this context, this joint doctoral research aimed to **(i) unravel the dynamics of survival and virulence of the reference strain ETEC H10407 in the human GI tract**, with the use of well-controlled and validated multi-compartmented systems of the human digestion and fermentation, respectively TIM-1 and M-SHIME; and **(ii) examine the antimicrobial properties of the probiotic *S. cerevisiae* CNCM I-3856 against ETEC H10407** from simple to complex *in vitro* models TIM-1 and M-SHIME, and evaluate this probiotic as a prophylactic approach for traveler's diarrhea.

This research on ETEC thematic was initiated for the first time in the two laboratories in partnership MEDIS UMR, Clermont-Auvergne University, France (18 months) and CMET laboratory, Gent University, Belgium (18 months). The simulation of the GI tract represents the biotechnological core of this joint PhD gathering the expertise of the two laboratories possessing the most complete simulators of the upper and lower GI tract, TIM-1 (MEDIS) and M-SHIME (CMET), respectively. In addition, a partnership with Lesaffre company, who provided the probiotic and funded the experiments was achieved.

Prior to initiate the experimental work on ETEC pathophysiology in the TIM-1 and M-SHIME, it was required to dress an inventory from the literature on the interplay between ETEC survival / virulence and the main biotic / abiotic factors of the human gut, as published in a book chapter presented in chapter 1 of the literature review (section I). This inventory allowed us to clearly identify the missing pieces of the puzzle to further exploit them in this PhD experimental works. The impact of the biotic and abiotic GI factors on the dynamics of ETEC survival, physiological state and virulence in the TIM-1 and M-SHIME were assessed (chapter 2), and the microbial community composition and metabolic activity preceding and following ETEC infection were examined (chapter 3). A set of techniques to estimate the viability of ETEC and its physiological states were compared: PCR-based methods and flow cytometry analyses (chapter 1) and applied in the ETEC experiments (chapters 2 and 5).

In parallel, we centered our research with respect to the available studies relating the probiotic mechanisms of action against ETEC for which a review has been published and presented in chapter 2 of the literature review (section I). We realized that the mechanisms of action were much more documented for the piglets, while scarcely investigated under human digestive conditions. The experimental work for the probiotic part has started with a 6 months probiotic screening phase. After selection of the probiotic yeast *S. cerevisiae* CNCM I-3856, its anti-microbial properties were further assessed in a series of tests using simple *in vitro* assays in culture medium, human IECs, mucin adhesion assays and *in vivo* tests in a mouse model (chapter 4). The encouraging outcomes allowed to further investigate the inhibitory properties of the probiotic against ETEC in complex and representative models of the human digestive physiology, using the TIM-1 and the M-SHIME (chapter 5).

The research outcomes and perspectives of these chapters are discussed according to the two aims of this PhD work in two separate sections hereafter.

2. ETEC H10407 pathophysiology in the *in vitro* human GI tract: to provide some of the missing pieces of the puzzle

2.1 Dynamics of survival and physiological states

- **Acid pH and bile acids: enemy or ally for ETEC?**

The first stress that food and waterborne pathogens find upon ingestion is the very acidic pH of the stomach. Such dynamics in pH drop, transit time and exposure observed physiologically in the human GI tract were captured by the TIM-1 system (chapter 2). After inoculation of ETEC-contaminated water at a physiological dose of 10 $\log_{10}$ in the TIM stomach, a die-off of the pathogen, estimated by plate counts, was observed at this site. As culturable cells do not provide the complete picture of the viability concept, in a further step ETEC physiological states were discriminated by PMA-qPCR and Live/Dead flow cytometry (chapter 1 and 2). These analyses confirmed that most of the ETEC cells (99%) entered in a reversible state with membrane damage upon low pH, as estimated by flow cytometry.

New approaches using other cellular characteristics, i.e. membrane potential and pHi were assessed (chapter 2). Strengthening our previous results, a low pHi (close to 3) was observed already after 20

min gastric digestion (pHext 2.4). For the membrane potential, surprisingly no depolarization of the membrane was observed, contrary to other studies performed in other enteric pathogens, such as EHEC under acid pH (Richard and Foster, 2004; Foster, 2004; Yang et al., 2015). For a methodological aspect, it was difficult to interpret and compare the membrane potential results obtained with other studies. In our case, $DiOC_2(3)$ method gives a ratiometric value calculated according to the fluorescence intensity (between 0 and 1), while many studies used other fluorophores (e.g. $DiBAC_4(3)$) and developed a calibration procedure based on the Nernst equation which gives an absolute value of the membrane polarization in mV (Suzuki et al., 2003; Breeuwer and abee, 2004; Klapperstück et al., 2009). To improve interpretability and cross-compare the studies, the same normalization method should be used in the future. Although we already employed a large set of techniques to describe ETEC cellular characteristics, other kits assessing the bacterial respiration (e.g. RedoxSensor, CTC) based on detecting activity of bacterial oxidases and reductases, can be interesting to complete our data to distinguish healthy and membrane-compromised cell populations (Sieracki et al., 1999; Thomas et al., 2011). Another way of detecting ETEC and visualize it dynamically would be the bioluminescence imaging, as recently achieved in a mouse model (Rodea et al., 2017). Bioluminescent images provide in real-time spatial information regarding the labeled bacteria and their metabolic activities.

In the duodenum, bile acids are one of the more long-term challenges encountered by ETEC following gastric passage. These antimicrobial detergent-like are present in higher concentrations during the first hour of digestion (15 mmol L^{-1}) and then decrease to 5 mmol L^{-1} (Northfield and McColl, 1973). This feature correlates with the low concentration of ETEC found until halfway of the duodenal digestion. The decrease of bile salts concentration was then more in favor to the growth of ETEC, from 180 min duodenal digestion onwards (chapter 2). Although ETEC pHi was assessed in the duodenum and was remarkably increased to a slight alkaline pHi compared to the stomach, it could be even more interesting to assess the membrane integrity and/or membrane potential in this compartment. For the membrane integrity (chapter 1), only three time points in the duodenum were assessed by PMA-qPCR and displayed a low number of viable ETEC compared to the total concentration. Nevertheless providing deeper insight to finely monitor ETEC subpopulations through the use of flow cytometry will be required. In practice, this was not possible in the present study due to the large amount of sample necessary to collect in the compartment, which can therefore disrupt the duodenal transit. However, due to the compartmentalization of the system, it offers several possibilities in perspective. For this purpose, it will be interesting to run only two compartments (stomach and duodenum), as a window of the most stringent conditions found in the upper digestive tract, and therefore collect higher quantity in the cumulated duodenal effluents (compared to a sample collected directly in the compartment) for further analysis of membrane integrity (but also follow the virulence genes expression, see section 2.2).

Altogether, these data displayed the flexibility of ETEC to modulate its membrane integrity, as well as pHi. To answer the question: does ETEC armed to withstand the gastro-duodenal conditions? We followed ETEC in the lower GI compartments here below.

- **Ileum and ascending colon harbor ETEC pathogen**

The prime site of action for ETEC originally described was the distal part of the small intestine, as for many other enteric pathogens such as EPEC, *Vibrio cholerae* or *Salmonella enteritidis*, though it was investigated in animal model for most of the studies (Allen et al., 2006; Gorbach, 1996). As digestion progresses, the pH and dilution level further increase in the jejunum and ileum, while 95% of the bile salts are reabsorbed by the end of the ileal digestion (2 mmol L^{-1}), making this gut region a playground for enteric pathogens (Roussel et al., 2016; Northfield and McColl, 1973). Our results confirmed an improved survival of ETEC with a growth renewal at the end of the jejunal and ileal digestion in the TIM-1. This was characterized by a restoration of ETEC membrane integrity and the return to a slight alkaline pHi, as assessed by flow cytometry (chapter 2). In addition, an adapted M-SHIME was used to study ETEC's colonization ability in the ileum and ascending colon in the presence of the complex human gut microbiota from six unique fecal donors and under anaerobiosis, features that are not present in TIM-1. We found high levels of ETEC in the lumen of both ileum and ascending colon in a late post-infectious stage until 5 days post-infection in the M-SHIME (chapter 2), which corroborates with our previous findings in the ileum and colon of the mouse model (chapter 4). The differential follow-up of ETEC in TIM-1 and M-SHIME validated that ETEC can be maintained upon both aerobic and anaerobic conditions and in presence of 9-10 log_{10} and 10-11 log_{10} microbial bulk mL^{-1}, respectively in the ileum and ascending colon (chapter 2). It remains however speculative to extend the site of action of the pathogen to the colon as no GM1 receptors to the LT toxin are displayed in the human colon based on rare human studies (Holmgren et al., 1985; Breimer et al., 2012). With respect to the ST toxin, it has been however recently shown that GC-C receptors of the ST enterotoxin are homogeneously expressed from the ileum to the human colon (Wands et al., 2015; Waldman and Camilleri, 2018). Further studies merit to explore this purpose and clarify whether the ileum is the only important site of action for ETEC.

Several limits to our experimental work subsist. For instance prior to ETEC infection in the M-SHIME ileum, we performed a gastro-jejunal digestion in *in vitro* batch as an attempt to reproduce the physicochemical conditions found in the TIM-1, i.e. without nutritional medium, under aerobic conditions, with pancreatin and bile salts that differed compared to the SHIME system. However, the gastro-jejunal batch system did not fairly reproduce what happened in the TIM-1 in terms of dynamism, sequential delivery as well as the lack of absorption process. Therefore, collection and storage of samples from the TIM-1 jejunal effluents in order to directly introduce them into the SHIME ileum was another option, but non-investigated for three main reasons: (i) during the experimental work in the TIM-1 we only did two kinds of set-up, gastric digestion where the gastric effluents were collected and full TIM digestion, where the ileal effluents were taken, so to collect the jejunal effluents, another set-up should have been required; (ii) geographical and time intervals between TIM-1 and M-SHIME experiments may compromise the storage of the samples collected in the TIM-1; and, (iii) the collection of jejunal effluents means that we could not use the SHIME in its entire configuration but start the digestion process only in the ileum, which is impossible.

- **ETEC interplay with cellular and/or mucosal microenvironments**

To adhere to the intestinal epithelium, ETEC must penetrate the complex mucus layer overlying the epithelium. Some carbohydrates can be cleaved from mucins by ETEC thanks to two mucinase EatA and YghJ to better reach IECs (Kumar et al., 2014; Luo et al., 2014). Although not yet investigated in our mucin adhesion assays (chapter 4) and M-SHIME experiments (chapter 2), this feature merits further investigation in our *in vitro* models. The mucin carbohydrates can also be cleaved by members of the gut microbiota and become available as nutrients for themselves or surrounding bacteria such as ETEC. The competition for such nutrients was also not assessed. Besides, nothing is known in the literature on the nutrient utilization by ETEC compared to other enteric pathogens. This would merit further assays. In our study, we observed remarkable ETEC-attaching properties to the Type-II mucin (crude mixture of glycoproteinsand with bound sialic acid ≤ 1.2%, chapter 4) and Type-III mucin (partially purified mucins with bound sialic acid 0.5-1.5%, chapter 2). ETEC was also tested for its high adhesive properties to the human TC7/Caco-2 cells and the induction of IL-8 pro-inflammatory production was observed (chapter 4). Globally these outcomes offer large future perspectives as discussed in section 2.3.

- **ETEC interplay with the gut microbes community and activity**

Gut microbes contribute to human health through different ways, by stimulating the development of the immune system, by providing colonization resistance to pathogens, through the production of anti-microbial components (bacteriocins, H_2S, H_2O_2), through the synthesis of essential vitamins (vitamin K, folate) or through the degradation of xenobiotics or deconjugation of bile acids (Sekirov et al., 2010).

The M-SHIME provides for the first time the successive interactions of the ileal and ascending colon microbial niches with ETEC. For this purpose, the ileal signature in the M-SHIME was set-up for the first time, resulting in low community diversity and metabolic activity compared to the ascending colon (chapter 3). A unique physiological dose of 10 $\log_{10}$ ETEC was enough to encourage the bloom of opportunistic pathogens in the ileum and decreased the species with potential health promoting functions in the ascending colon. For further understanding on ETEC and its impact on microbial communities, it will be interesting to play with the dose and/or the frequency of ETEC inoculum. For instance, inoculate the bioreactors with a repeated dose, which is likely the case when people are consuming water in resource-limited countries.

Although we observed a change in microbial composition following ETEC infection, we did not observe a marked decrease of the biodiversity index (chapter 3). In the chapter, we decided to not use the term “dysbiosis” since doubts about the current usefulness of this state to explain research finding have been nicely raised in the review of Hooks and O’Malley (2017). So far, there is no consensus in the definition of the term dysbiosis. It is broadly associated with almost any change in the gut microbiota with often negative consequences for the health. We agree with the authors that such term should be employed with care. In addition, dysbiosis can not only be the consequence of one pathogen (ETEC) but rather come from the association of other pathogenic species that live and interact together, all generating and participating in complex interactions that might contribute to the disease process. In addition, other host-related factors i.e. antibiotic use, genetic predisposition, immune depression, etc. may contribute to the establishment of a dysbiotic state, increasing the susceptibility of the microbiome

to colonization and proliferation of a pathogen. Morever, the recently introduced concept of pathobiome breaks down the initial concept of “one pathogen leads to one disease” (Vayssier-Taussat et al., 2014).

Beyond to closely reproduce the microbial communities longitudinally (ileum *vs* ascending colon) and in the cross-sectional direction (luminal *vs* mucosal), the inter-individual variability from six donors was captured. This individual signature represents a new concept of interpreting the results, by emancipating from an “average” individual. Indeed, it is crucial to investigate at what level the interpersonal variability is also important for ETEC susceptibility. For example, a previous study performed at the laboratory and testing a nutritional compound on 51 fecal females from the same age-range group displayed high inter-individual variabilities leading to a clustering of 3 groups for results interpretability (Possemiers et al., 2006). This approach is not well incorporated in certain subsections of the scientific community, seeking to minimize inter-individual variation through the preparation of standardized fecal slurry by pooling fecal samples from different individuals (O’Donnell et al., 2016). Such approach is therefore in contradiction with the reasoning behind this present study.

The level of SCFA produced by the gut microbes can impact the susceptibility to infection. Indeed, SCFA will play major roles for the barrier function and the immune system (Ciarlo et al., 2016; Sun and O’Riordan, 2013). A duality subsist in SCFA production, they can mediate antimicrobial host defenses through mechanism largely unknown, while they can also act as a signal for virulence gene regulation in many enteric pathogens, as explained in section 2.2 (Bäumler and Sperandio, 2016). Even if the propionate concentration was enhanced following ETEC, no related mechanism is yet documented in the literature.

2.2 Successive environmental cues regulate ETEC virulence factor expression

As a mark of pathogenicity, enteric bacteria must not only survive and/or colonize the human GI tract but also use various and complex virulence regulation strategies to sense the local (micro)environment. Although a myriad of molecules exist as virulence factors, in this PhD work we restricted the follow-up to the main virulence genes of ETEC H10407 for time and cost reasons. In total, seven virulence genes encoding for enterotoxins (*eltB* and *estAB*), enterotoxin release (l*eoA* and *tolC*), adhesins (*cfa/Ib, tia, fimH*), and for the stress response (*rpoS*), as well as the enterotoxin LT production were profiled in the dynamic and successive GI regions simulated by the TIM-1 and M-SHIME. This is so far the unique study reporting ETEC virulence genes expression in such details and in complex human digestive environments (chapters 2 and 3). Although complex, for a correct representation, the variability between biological replicates (TIM-1) and distinct fecal donors (M-SHIME) were captured. The following GI cues for ETEC virulence are discussed here after: gastric pH, bile acids, oxygen level, gut microbes and their metabolites (SCFA).

We would like first to engage the discussion on the following aspect: “pathogen stay avirulent before reaching their colonization sites […], and express only virulence factors upon reaching the destination sites” (Kitamoto et al., 2016). This is one of the statements recently published. This theory can be refuted because it suppresses all the complexity and dynamism in the transient expression of genes, and

contradict all the concept that enteric pathogens use various GI cues to modulate their virulence function all along the GI tract and not only in a unique site of action. Besides, induction of genes at earlier stage does not necessary mean that the pathogen will be incapable to express the gene again.

The following outcomes of our research will give therefore examples to show that ETEC was not only able to express its virulence genes in the ileum, but already in the stomach as well as in lower compartments, such as the ascending colon.

- **Gastric pH**

Acid pH was the first physicochemical stimuli sensed by ETEC in the TIM stomach. Interestingly, we found that most of the virulence genes followed were switched on in the stomach, except for the *eltB* gene encoding the LT toxin which was repressed below pH 3.6. Strikingly, at protein level, no production of the LT toxin was observed. This pH-dependency for *eltB* gene and LT protein is in line with previous *in vivo* (mice) and simple *in vitro* batch studies (Gonzales et al., 2013; Gonzales-Siles et al., 2017). This outcome also confirmed that genes encoding the enterotoxins *eltB* and *estAB* are differently regulated since the expression of *estAB* gene is pH-independent (Sriranganathan et al., 1983; Johnson et al., 1978). With respect to the genes encoding the adhesins, there is so far no available data on their regulation at acid pH (chapter 2). It will be interesting to start with simple *in vitro* batch cultures with only a gradient pH control to assess the *cfa/Ib*, *tia* and *fimH* genes expression, then transfer the culture medium on Caco-2 cells (after adequate treatment) to investigate whether the genes can still be effectively expressed in the host after acidic passage (leading to adhesion) and compared to a control condition. We can consider the same experiments using gastric effluents from the TIM-1. A nice example in EHEC O157:H7 give us also other perspectives to exploit for ETEC: the virulence gene *fliC* encoding for the motility was slightly increased in EHEC in acute acid-stress conditions compared with no acid stress (House et al., 2009). We can indeed imagine that as an adaptation effect to escape the stringent conditions of the stomach, EHEC motility is enhanced. It will be therefore interesting to follow *fliC* gene in ETEC and see whether same conclusion can emerge.

In addition, *E. coli* contains five acid resistance systems (AR1 to AR5) as well as acid tolerance response (CadC) (Lund et al., 2014; Richard and Foster, 2004; Zhao and Houry, 2010). These systems generally depend on the regulators of stress response such as the sigma factor *rpoS* or *crp* (Sun et al., 2013). In the course of the gastric digestion we followed the *rpoS* gene expression and surprisingly the gene remained basally expressed (chapter 2). Most of the acid resistance system require extracellular metabolites (e.g. glutamate, lysine) to be inducible, as well as for *rpoS* which requires polyamines (Chattopadhyay et al., 2015). In our case, the operation of such systems in ETEC was not possible due to the absence of these amino-acids in the TIM-1 stomach as only a glass of water was introduced in the system. It would be therefore of high interest to use complex food matrix for ETEC vehicule (further discussed at the end of the section), that provides such metabolites to re-examine the regulation of *rpoS* during the gastric digestion and assess other regulators such as *crp* or *cadC* systems. Finally, it is not to exclude that additional acid resistance or tolerance systems specific to ETEC exist, but this track has been not yet explored.

- **Bile acids**

As previously explained, bile acids are delivered into the duodenum and remained at high concentration during the first hour of digestion in adults. Although this parameter was fairly reproduced in the TIM-1, the complexity of the system did not allow to directly observe the specific effect of bile acids as a metabolite cue for ETEC virulence. Indeed the transcription analysis was performed only in the cumulated gastric and ileal effluents. In the small intestinal compartments, the digestive complexity is that not only the bile acids but also other factors may greatly modulate virulence genes expression, such as bicarbonate, pancreatin or electrolytes. In addition, reaching the ileum, 95% of the bile acids have been reabsorbed thanks to a dialysis system which does not give a good representation of what happened in the duodenum where high bile salts concentrations are found. As suggested earlier in the discussion, it would be helpful to run the stomach-duodenum as a bi-compartment in order to collect the duodenal effluents for transcription analysis. Bile acids were also present in the small intestinal part of the SHIME set-up but as for the TIM-1 not directly investigated, as we performed sample collection only in the ileum and ascending colon for the purpose of the study. It is also important to note that different bile salts were used between TIM-1 (porcine origin supplemented with sodium cholate and deoxycholate) and M-SHIME (bovine origin). This might greatly influence the virulence genes expression.

We can however make a small comment on the observed virulence profiles found in the ileal effluents compared to those found in the gastric effluents from the TIM-1. In both ileum of TIM-1 and M-SHIME, most of ETEC virulence genes were switched off and the consecutive exposure to the different physicochemical parameters of the small intestine, including bile salts did not impede or even favored the LT enterotoxin production.

Another perspective would be to test separately in batch culture the influence of glyco- and tauroconjugated human bile acids on ETEC virulence (Chiang, 2013). Few studies have already shown that upon high concentration of bile acids (30 g L^{-1} in LB medium), *eltB* and *estAB* were up-regulated (Sahl and Rasko, 2012). One of the main limitations to this study is that the choice of such supra-physiological concentration was not justified as well as the information on the type of bile and bile acids are missing. This impedes therefore proper comparison between studies. Finally, the *tolC* gene, responsible for the expel of ST enterotoxin constitutes also one of the main regulators for bile salts resistance, it could be interesting to see in which order of magnitude this gene would be expressed in batch culture or in the duodenal effluents from the TIM-1 (Deininger et al., 2011).

- **Oxygen levels, gut microbes and their metabolites**

Oxygen level is decreasing from the stomach towards the distal colon. In the TIM-1, the system remains “open” and does not allow to simulate anaerobiosis, while the bioreactors in the M-SHIME are all maintained under anaerobic condition but so far does not allow to play with oxygen gradients according to the gut region. This oxygen difference between both systems can induce large disparities in ETEC gene expression patterns or toxin production. As for the bile acids, due to the multiplicity and complexity of parameters, we cannot directly relate ETEC virulence genes expression to the oxygen level. Strikingly, we showed that the LT toxin was produced in both systems in the ileum, so under both aerobic

and anaerobic conditions, in line with the results from *in vitro* batch culture (Lu et al., 2016) (chapter 2). In addition, *cfa/Ib* was not amplified all along the SHIME ileum and ascending colon, while the gene was repressed in the TIM ileum. At first, this leads us to believe that such difference in oxygen between both systems might explain these differences. However, another cue is important to consider as an explanatory factor between TIM-1 and M-SHIME: the microbial environment and metabolic activity of the SHIME system, lacking in the TIM-1, as well as the bile salts as explained earlier.

Indeed, activities of microbial species from the gut microbiota influence the nature and concentrations of metabolites present in the gut ecosystem and may therefore affect ETEC virulence (Jubelin et al., 2018). For this purpose, our study provide for the first time a regression analysis between ETEC virulence features and gut microbiota populations in an attempt to better consider the susceptibility of ETEC infection for the six donors. Although the model was limited to the 5 h post-infection in the ascending colon, as explained in chapter 3, we found that *eltB* co-occurred with *Coprococcus* and *Allisonella* genera, while at the opposite the LT toxin and *estAB* gene strongly co-occurred with *Enterobacteriaceae*. At metabolites level, LT production and *estAB* gene were negatively associated with acetate and propionate production, while butyrate was positively correlated with LT production. Our results strengthen the fact that both genes *eltB* and *estAB* do not follow the same regulatory pattern, as already evidenced in the stomach. With respect to the role of the gut microbes and metabolites that were co-occurring, at the present time there is no explanation for their relation with ETEC virulence. Indeed no data are available in the literature on the effect of complex gut microbiota, selective strains from microbiota nor metabolic products such as SCFA on ETEC virulence. We therefore pointed out that such analysis need to be further explored by integrating more time points and gut regions to obtain a dynamic profile as the reflect of the human physiology. It would also be interesting to test separately in batch cultures, as we previously proposed for the bile acids, the main SCFA on ETEC virulence profile.

Briefly, other GI cues that were not investigated in our current study need however further attention for the future. The quorum sensing, involving microbiota-derived molecules for a communication process between bacteria can be another cue sensed by ETEC (Bivar, 2018). Finally, the sensing of mechanical stimuli such as viscosity to the mucus layer, attachment to the IECs as well as fluid shear might modulate ETEC virulence. Although the mucosal microenvironment was integrated in the M-SHIME, unfortunately due to the poor amount (especially in the ileum), the viscosity properties and the complex glycoprotein matrix, it was difficult to collect the supernatants for LT toxin measurement, or to extract the RNA with good quality for transcriptional analysis of the virulence genes. Technical optimizations are required to better exploit the potential to such microenvironments.

Finally, we attempted to make several correlations between virulence genes expression over time and in the different gut regions (chapter 2), we did not see consistencies between genes except for *estAB* and *eltB* genes that were mostly negatively correlated as highlighted earlier. Moreover, correlations between virulence genes were highly variable depending on the sampling time, certainly as a reflect of the variable effect of the dynamic and complex digestion process on ETEC virulence.

Collectively, the *in vitro* digestive systems give us the possibility to dynamically observe the modulation of ETEC virulence through the dependency of multiple environmental cues. So far, we dispose of scarce information on ETEC virulence process in simple *in vitro* batch systems, this information could be advantageously combined to better interpret and exploit the original data of this PhD work (chapters 2 and 3).

2.3 Future perspective to study ETEC pathophysiology

Other long-term perspectives to this PhD work merit further attention, as listed here below and sum-up in Figure 2.

- **Impact of saliva on ETEC virulence**: A recent study has shown that the salivary peptide histatin-5 binds ETEC type I pili, thereby blocking adhesion of ETEC to intestinal epithelial cells (Brown et al., 2018). In this respect, a new set of TIM-1 or M-SHIME experiments can be imagined by co-introducing human saliva with ETEC in the TIM stomach and see if the saliva has an added value to ETEC pathogenicity,

- **Impact of food matrices on ETEC fate in the GI tract**: At MEDIS laboratory, the influence of several food matrices on the survivability and virulence properties of EHEC has been already tested (Etienne-Mesmin et al., 2011; Thévenot et al., 2015). It will be interesting to explore this aspect in the case of ETEC, secondly found in fresh fruits, vegetables and herbs (McDonalds et al., 2015; Beatty et al., 2004). It could complete our data, especially to examine whether the buffering properties of a food matrix might enhance ETEC survival to gastric acid,

- **Examination of additional human at-risk populations for ETEC infection**: Several protocols according to the age-range have already been set-up in MEDIS and CMET laboratories. For example, during the course of my master thesis, an exhaustive survey of the literature was made to identify the physicochemical parameters unique to the child (6 months – 2 years old) in healthy state and implemented into the TIM-1 system. The final purpose was to study EHEC pathophysiology upon infant digestion, compared to the adult one (Roussel et al., 2016, appendix 1[5]). We can therefore conceive of the same set-up for ETEC. As well, in the M-SHIME, it would be interesting to test the feces collected from infants as well as from those displaying acute malnutrition (Kane et al., 2015; Monira et al., 2011), and evaluate the impact of ETEC in these particular situations. Finally, to complete the current study with the six adult fecal donors, it will be pertinent to proceed the same type of M-SHIME with feces collected from traveler's, recently acknowledged to have a unique gut microbiome, displaying a dysbiotic signature which might predispose to enteric infections (Riddle and Connor, 2016),

[5] ***Publication. Appendix 1.*** ROUSSEL C., CORDONNIER C., GALIA W., LE GOFF O., THEVENOT J., CHALANCON S., THEVENOT-SERGENTER D., LERICHE F., ALRIC M., VAN DE WIELE T., LIVRELLI V., BLANQUET-DIOT S. Increased EHEC survival and virulence gene expression indicate an enhanced pathogenicity upon simulated pediatric gastrointestinal conditions. *Pediatric research, 80, 734-743 (*2016). *https://doi.org/10.1038/pr.2016.144*

- **Assessment of ETEC interplay with human intestinal cells and mucus**: The study of such interactions was limited in the present PhD to the adhesive properties of ETEC to TC7/Caco-2 cells (chapter 4), as shown earlier in the discussion. A disadvantage of the monocultures Caco-2 is that they do not closely simulate the composition of the normal epithelial layer. For instance, a mucus layer is lacking in the Caco-2 cells (Hidalgo, 1996). This specificity is however important to assess for ETEC, as we already shown its remarkable adhesive properties to the Type-II mucin (chapter 4) and Type-III mucin comprising the microbial ecosystem (chapter 2). Several *in vitro* models are therefore possible to investigate, including both the host cell part and the mucus layer. For instance, we can consider comparing ETEC adhesion and virulence by using co-culture cell lines Caco-2 and HT-29MTX with different ratio (e.g. 70:30, or 90:10) with monoculture of Caco-2 cells. HT-29MTX cells are derived from goblet cells, secreting the membrane bound MUC1 and the gel forming MUC5. The co-cultivation of enterocyte and goblet cells will form a layer on top of the epithelial cells, as physiologically observed (Kleiveland, 2015). Although Caco-2 colonic cells exhibit many properties of the small intestinal epithelium, it would be relevant to strengthen the model by using cells isolated from human ileum for ETEC purpose. The cell line HilEpC, isolated from a normal healthy human ileum is available on the market. However, the cell viability remained short and no published protocol or data are yet available (https://www.cellapplications.com/human-ileum-epithelial-cells-hilepc). Then, for suitable enterocytic cell culture of the ileum, the use of primary cells isolated from intact crypts from human intestines (Fig. 1) and cultivated with appropriate culture medium allowing cell differentiation and the formation of villi that resemble intestinal epithelium viable for at least 60 days (Castellanos-Gonzalez et al., 2013) can be useful. Lastly, based on the same principle, the use of enteroids constitutes the final approach to study ETEC interactions with the host in a 3-D multiple intestinal epithelial cell types (Zachos et al., 2016; Saxena et al., 2016). Beyond the adhesive properties of ETEC to test, these different models allow to investigate barrier dysfunction, inflammation, virulence genes expression and enterotoxin production and binding,

- **Coupling the digestive systems with human cell culture**: At MEDIS laboratory, digestive samples collected from the TIM-1 system were added to Caco-2 cells after appropriate treatments to test the absorption of carotenoids (Déat et al., 2009). The coupling of ETEC in digesta with Caco-2/HT-29MTX cells would be therefore possible. At CMET laboratory, in combination with the SHIME, the Host Microbiota Interaction module can be used to evaluate the effect of ETEC challenge at the level of luminal microbial community and host surface colonization and signaling (Marzorati et al., 2014). This module consists of two compartments separated by a functional double-layer composed of an upper mucus layer and a lower semi-permeable membrane. The upper compartment represents the luminal side of the GI tract (SHIME effluents), whereas the lower compartment contains enterocytes representing the host (Caco-2 cells). This module allows the study of shear stress effect encountered in the intestinal epithelium during peristalsis and oxygen availability on the adhesion of ETEC. Microaerophilic conditions and medium shear stress are characteristics that can be adapted to the specific ileal conditions.

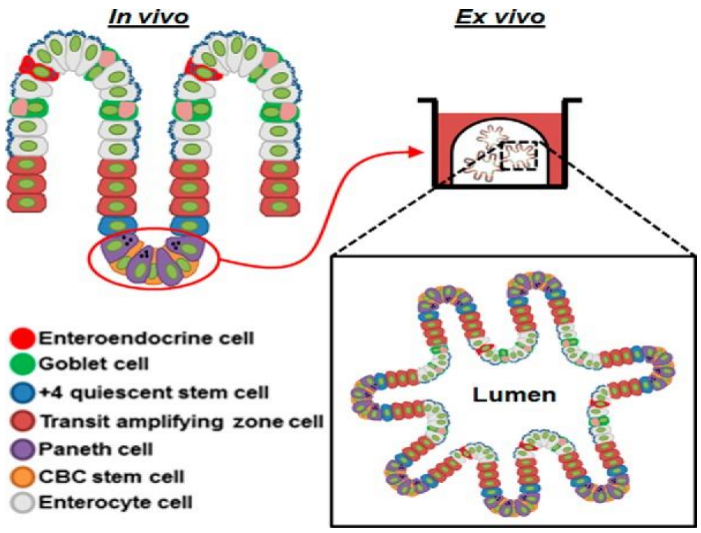

Figure 1. **Intestinal primary cells located at the base of the crypts can be cultured *ex vivo* to generate indefinitely propagating enteroid cultures.** The enteroid epithelium is composed of the same intestinal cell types that exist *in vivo*. *Reprinted with permission from Zachos et al., 2016*.

↳ **Development of methods for detection and quantification of the ST enterotoxin**: ST is recognized to be more frequently associated with diarrheal symptoms than LT enterotoxin since 2015, based on the virulence gene expression (GBD, 2017). However, for physiological perspectives, no dose of both proteins ST and LT susceptible to provoke the diarrheal symptoms are yet available in the literature. Although several protocols for LT ELISA assays are found in the literature (e.g. GM1 ELISA sandwich, capture), such procedures remain poorly investigated for the ST enterotoxin (Rocha et al., 2013). As a promising alternative to ELISA assays using polyclonal antibodies, where specificity and detection are often affected, the use of Liquid Chromatography Mass Spectrometry (LC-MS/MS) following tryptic digestion to measure unique peptides of LT or ST would be conceivable (Tsilia et al., submitted; Andjelkovic et al., 2016).

↳ **From transcriptome to proteome analysis of ETEC**: In the frame of this PhD we only followed a specific set of ETEC virulence genes for time and cost reasons (chapters 2 and 5). For tackling the transcriptome, the use of high-throughput techniques such as RNA sequencing or microarrays of ETEC strain would be relevant. But global analyses of transcripts-proteins have displayed modest correlations due to post-transcriptional and post-translational modification and regulations (Pettersen et al., 2018). For instance, RNA interference (RNAi) or small interfering RNA (siRNA) will initiate a transcript-specific destruction resulting in the subsequent decrease of the corresponding protein (Curtis and Nardulli, 2009). To our interest, shifting more towards a more targeted approach by focusing on proteins of interest for ETEC would provide functional insights into ETEC virulence in the successive GI environments.

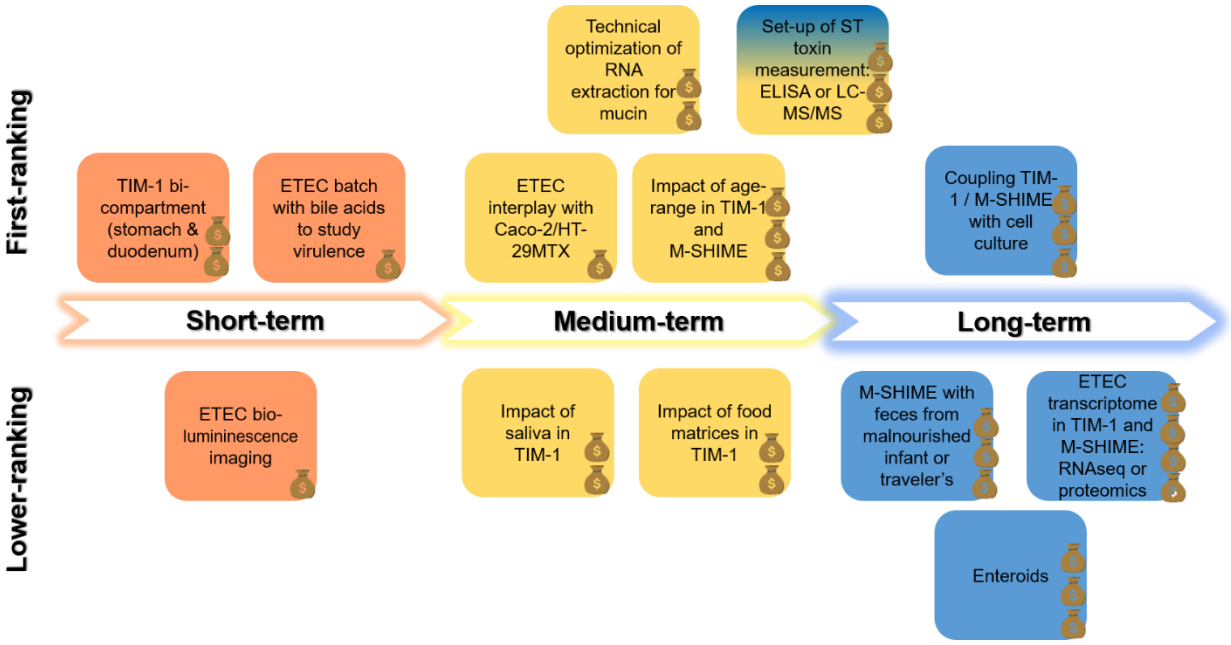

Figure 2. Future conceptual research framework to further improve awareness on ETEC pathophysiology in the human GI tract. Experiments are ranked in terms of: (i) priority according to the scientific interest (first *vs* lower-ranking); (ii) timeline (short-term: in the coming weeks or months, medium-term: a year and long-term: 1 to 3 years); and (iii) cost ($ low, $$ medium, $$$ expensive, $$$$ highly expensive).

3. The probiotic *S. cerevisiae* CNCM I-3856 against ETEC H10407 in the *in vitro* human GI tract

3.1 Identification of the main mechanism of action of *S. cerevisiae*

After a six months screening phase with six probiotic strains (3 bacteria, 3 yeasts) supplied by Lesaffre company, the yeast *S. cerevisiae* CNCM I-3856 was retained by the company to pursue the study and identification of its mechanistic properties against ETEC H10407. The final aim would be to consider this *S. cerevisiae* strain as a future prophylactic approach for traveler's diarrhea. In the difficult context of European regulation, as discussed here below, many years of research are required to provide stepwise relevant scientific supports for the efficacy and safety of the probiotic, or in the opposite refute its efficacy.

- **European Regulatory deadlock of probiotic claims**

The probiotic market has grown into a global multi-billion dollar industry these last years. As a result, probiotics encompass a range of regulatory infrastructures with varying requirements for demonstrating safety and efficacy. In Europe, due to the current regulatory system for pharmaceutical products, no

"probiotic" claims other than lactose intolerance relief, have been approved by the EFSA, and the word probiotic itself for health claim is banned from use in marketing and on consumer products (NHCR, EC 1924/2006). So far, none of the 422 applications for probiotics submitted under the Health Claims Regulation to EFSA received a positive evaluation (http://www.ipaeurope.org/, consulted on 11/2018). The main reasons for unfavorable opinions are the following: (i) insufficient strain characterization, (ii) non defined and/or beneficial claims, (iii) not all measurable outcomes reflect a direct benefit for humans, (iv) pertinent human studies are lacking as well as the quality. In another hand, "some fragmented national measures on probiotics have been adopted which create discrepancies and difference of treatment between Member States", highlighted the international probiotic association (IPA). The term probiotic should not fall necessarily within a definition of a health claim. The whole category may be in search of a new identity. Indeed, other terms including live bacteria, bio- or strain-specific terms have become common on label packaging to replace the use of the word "probiotic".

- **Promote awareness on *S. cerevisiae* survival**

Prior to going towards the mechanistic insight of the probiotic yeast against ETEC, it is necessary to provide more information on the functional characteristic of the strain of interest itself. For the patented strain *S. cerevisiae* CNCM I-3856, many years of internal research have been performed for its characterization. The safety of the use of this yeast strain has been validated, and is already known on the market under the commercial name of Ibsium® (previously named Lynside® Pro GI+). Indeed, in 2015, after providing strong scientific and clinical data on the benefits of the yeast in individuals with IBS, this probiotic yeast has been rewarded with the approval of a health claim by the Canadian Health Authorities (https://www.lesaffre.com/health-claim-lesaffre-human-care-ibsium/, consulted on 12/2018; Cayzeele-Decherf et al., 2017; Spiller et al., 2016; Pineton de Chambrun et al., 2015).

For a probiotic strain, the first pre-requisite is to show its ability to survive human GI conditions. In this PhD research, we demonstrated in the TIM-1 the *S. cerevisiae* CNCM I-3856 robustness to upper digestive tract conditions after a unique administration of 10 $\log_{10}$ yeasts (chapters 4 and 5). This administration was in accordance with the routine dosage used for human clinical studies involving probiotics (Desreumaux et al., 2011). In the M-SHIME, obviously *S. cerevisiae* cannot establish in the colonic environment for 20 days fermentation with a unique dose. The posology was therefore adapted with a repeated administration, twice a day at a dose of 10 $\log_{10}$ yeasts (with a height hours dosage interval). *S. cerevisiae* was thus maintained at high concentration in the ileum, while at lower concentration in the ascending colon, as long as it was administered. Using a mucin adhesion assay and TC7/Caco-2 cell culture we found a low capacity of the yeast to attach to the mucus layer and the IECs (chapter 4). In line with the mucin adhesion assay (chapter 4), the yeast displayed even less attaching properties to the mucus in presence of gut microbes (chapter 5). To go further, it will be interesting to better investigate the physiological state of the yeast itself in the gut, as performed for ETEC. In this respect, we already designed specific primers of the yeast for the PMA-qPCR analyses for future experiments. The use of flow cytometry kits analysis specific to the yeast is also another possibility.

- **Identify the mechanistic properties of *S. cerevisiae* CNCM I-3856 against ETEC H10407**

As a brief reminder, three main mechanisms of action in the fight of enteric pathogens are acknowledged for probiotics: (i) **immunomodulation** through interaction between the probiotic and the host immune system to enhance innate and/or adaptive immunity, or to limit the ability of pathogen to induce an immune response; (ii) **direct antagonism** where probiotics inhibit the growth of pathogen and/or down-regulate the expression of virulence factors and; (iii) **competitive exclusion** where probiotics make the GI environment less hospitable for pathogens by modulating the gut microbiota, improving the epithelium barrier function, interfering with pathogen binding by stimulating the production of defense-associated factors, as described in the review from Roussel et al., 2016.

This 3-year PhD had greatly contributed to the identification at a first stratum to such anti-microbial properties in *S. cerevisiae* CNCM I-3856. The most striking outcomes are discussed here. We have gathered evidence that the **probiotic acts by impairing ETEC functionality** in terms of virulence genes expression and LT toxin production yet does not affect the survival of the pathogen *in vitro* in both the TIM-1 and M-SHIME (direct antagonism, chapter 5). With respect to the **decrease of the LT toxin production**, it will be important to investigate the underlying mechanism of the probiotic, such as better describe toxin degradation for instance by testing yeast supernatant, or assess the possible binding of the toxin to yeast surface by assessing the surface properties. For instance, even if the yeast in general are rarely known to produce antimicrobial compounds, Pothoulakis et al. (1993) refuted this hypothesis. Authors have previously shown that a 54-kDa serine protease from another strain of *S. cerevisiae, S. boulardii* effectively hydrolyzes the toxin A produced by *Clostridium difficile*. Brandao et al. (1998) also indicated the presence of a specific receptor on the surface of *S. cerevisiae* W303 able to bind to the cholera toxin, which is structurally very close to LT toxin.

We observed the **disruption of ETEC membrane integrity** through the increase of dead and damaged ETEC cells under the probiotic treatment only in the TIM-1 effluents (direct antagonism, chapter 5). We made the assumption that the high **ethanol** production measured in *S. cerevisiae* might be one of the explanatory effect to the membrane disruption, since this organic solvent was already recognized for its anti-bacterial properties through the membrane disruption (Chiou et al., 2004). It will be interesting in our case to test a range of ethanol concentrations in ETEC batch cultures and investigate whether the ethanol itself can alter the membrane integrity of ETEC.

With respect to the virulence genes, we found interesting the **over-expression of the *fimH* gene**, encoding for the type 1 pili, all along the TIM ileal effluents, deprived of microbial bulk under probiotic condition (direct antagonism, chapter 5). From mechanistic perspectives, we assumed that the *fimH* over-expression could be associated to the remarkable **cell-to-cell interaction** between the yeast and ETEC, that we observed at the beginning of the PhD. Indeed, a **mannose related agglutination** between the yeast and ETEC was observed, as previously observed in batch medium (competitive exclusion, chapter 4). Precisely, ETEC through the expression of type 1 pili and its FimH subunit protein can bind the mannan on the surface of yeast cells (Knutton et al., 1985; Sheikh et al., 2017). Further explorations of the cell-to-cell mechanism should be performed in order to see for instance whether the yeast could be capable to block the binding site of ETEC to mucins or epithelial cells (Turner et al. 2006). For this purpose, other sugars such as mucin-bound fucose or galactose could be tested for

agglutination. Additional tests will be useful to better describe the surface properties by measuring the critical aggregation concentration or the hydrophobic interactions between the yeast and ETEC as well as the interactions with mucins.

In the SHIME ileum and ascending colon under the probiotic treatment, the microbial environment was **enriched with species for which a beneficial health effect has been reported in the literature** such as *Bifidobacterium*, *Faecalibacterium*, *Lactobacillus* or *Fusicatenibacter* genera (Sokol et al., 2009; Sarkar and Mandal, 2016; Takeshita et al., 2016, Rivière et al., 2018), while **a tendency to a decrease of opportunistic pathogens** such as members of *Klebsiella*, *Achromobacter* and *Mycobacterium* genera were found. Besides, a **remarkable increase of the SCFA concentration** in the ascending colon was noticed, especially for **acetate** and **propionate** (competitive exclusion, chapter 5). As a general statement, most of these observed effects were inter-individual dependent meaning that the conclusion should be taken with care. SCFA metabolites constitute an environmental cue for enteric pathogens, and can be used to modulate the virulence genes expression (Rolhion and Chassaing, 2016). Such concentration of SCFA can lead to lower the environmental pH. However this observation was not possible in our experimental conditions since the pH was controlled. It would be therefore interesting to assess in anaerobic batch fecal inoculation supplemented or not with the probiotic, or in M-SHIME without pH control, in which order of magnitude the pH would be decreased. Besides, it remains unclear whether the probiotic can itself produce or not these metabolites or merely stimulate the gut microbe producers such as *Faecalibacterium*, *Butyricicoccus*, *Roseburia* (butyrate producers) or *Bifidobacterium* and *Veillonella* (acetate producers) as observed in chapter 5. We can conceive to do separate batch cultures using the SHIME nutritional medium deprived in gut microbes to evaluate the capacity of the yeast to ferment sugars and produce such metabolites.

We also provided few outcomes on the interaction of *S. cerevisiae* with the host human IECs. We showed that **ETEC adhesion to both the type-II mucin and TC7/Caco-2 cells was decreased in a dose-dependent manner** with the probiotic. It has been assumed that probiotics may (i) impede the access of pathogens to host intestinal tissue by non-specific steric hindrance (particularly relevant for yeast cells that are 10 times bigger than bacteria), (ii) stimulate mucin production and thus impair the adhesion of pathogens to enterocytes or (iii) block the binding site of ETEC to mucins or epithelial cells by receptor competition (Turner et al. 2006). It will be also interesting to investigate whether the probiotic treatment can improve the barrier function, which is particularly disturbed upon ETEC infection (Noel et al., 2018). Measurement of the trans-epithelial electrical resistance and tight junction proteins expression, is some of the additional techniques to provide. The immunomodulatory effect of *S. cerevisiae* was poorly investigated in our study but we observed an **inhibition in a dose-dependent manner of the IL-8 production**, a pro-inflammatory cytokine. The decrease of IL-8 might be related to a lower number of bacteria adhered to the IECs. The measurement of other pro- and anti-inflammatory cytokines such as IL-1β, IL-6, IL-10 should be considered to reinforce this last conclusion.

Finally, the experimental perspectives previously discussed for ETEC (section 2.3) such as: to test the impact of food matrices, to investigate other at-risk populations for ETEC, or to better assess the interplay between ETEC and IECs or mucus; can be advantageously applied to further study the antimicrobial properties of the probiotic *S. cerevisiae*.

3.2. Future perspectives for probiotics in the treatment of ETEC infections

↳ ***S. cerevisiae* CNCM I-3856 from research to potential commercialization for the prevention of traveler's diarrhea**: These encouraging results merit further research at several levels by completing the missing *in vitro* tests as discussed above and designing new *in vivo* assays, in animals prior to test it in humans. For instance, the piglet seems to be a pertinent model as digestive conditions are close to the human in comparison with other models such as the mouse or rabbit. The final probiotic galenic form need to be defined (e.g. active dried powder, capsule or tablet) and the posology need to be adjusted according to the type of strategy targeted (curative *vs* prophylactic) as well as the population (traveler's but maybe also infants). In our study, we demonstrated that the prophylactic strategy was the most efficient. If we conceive to extend the commercialized probiotic to other populations, additional ETEC strains need to be tested. Indeed, some strains have been predominantly found in infants, while other in adults (Gyles and Fairbrother, 2008).

With respect to our probiotic strain, a hypothetic scenario is presented here after. According to the galenic forms tested in Lesaffre, it is most likely that a capsule of hydroxypropylmethylcellulose containing active dried yeast powder (as tested in the TIM-1, chapter 4) could be positioned on the market. The targeted population will be the adults traveling in endemic areas for which a prophylactic treatment will be proposed. As posology schedule, the oral intake of the probiotic twice a day, 12 days preceding the travel could be conceivable. For final validation, these modalities should be tested in ETEC-infected humans, over the course of a clinical trial. To address this, access to infected patients with a non-attenuated ETEC strain and at a physiological dosage is required, in order to test the antagonistic properties of the yeast strain in an "unbiased" way. Recently, such controlled human ETEC-infection study was achieved by testing the oral administration of a virulent ETEC strain at a dose of 8 $\log_{10}$ to follow the development of diarrheal symptoms (Vedoy et al., 2018).

The expectations of the consumer are also important to consider and can influence the commercialization of the final product. Nowadays, a common perception among consumers is that probiotics are safe and not associated with risks compared to the antibiotic therapy (Schultz et al., 2011). It remains however important to inform the consumer of the potential side-effect engendered by a probiotic intake. For instance, some safety concerns must be specified in the case of immunocompromised travelers.

Finally, the process of manufacturing controls to ensure high-quality products is costly, and to make benefit with a reasonable cost for the consumer, the company should sell the probiotic approximately to 1€ per day and per consumer.

↳ **Varying the probiotic therapy to increase human responsivity**: Two preponderant factors are often pointed-out in choosing the appropriate probiotic: the strain-specificity and disease-specificity or efficacy (McFarland et al., 2018). Although non applicable for all diseases, in the case of traveler's diarrhea for which many other etiologic agents are involved in, varying the probiotic treatments displaying "gut health properties" for instance between travels might help to increase the human responsivity. In addition, the use of probiotic mixture could be relevant, for example by mixing *S. cerevisiae* strain with a *Lactobacillus rhamnosus* GG strain. This latter has been already successfully

tested in the treatment of traveler's diarrhea in 245 American tourists. The mean daily risk of developing diarrhea was reduced by 50% compared to travelers who received the placebo (DuPont, 1997; Hilton et al., 1997).

↳ **Postbiotic as an emerging alternative**: A secondary function of probiotics is to form postbiotics including soluble factors (metabolic byproducts) and/or cell-wall components secreted by probiotics or released after lysis (Fig. 2). Even if the exact mechanisms of postbiotic activities have not been fully elucidated, they have drawn attention because of their clear chemical structure, long shelf life and safety dose parameters (Aguilar-Toala et al., 2018). The main advantages to the postiobics compared to the probiotics could be the higher product stability, the more convenient processing and formulation and the fact that we do not have to rely on maintenance of probiotic viability.

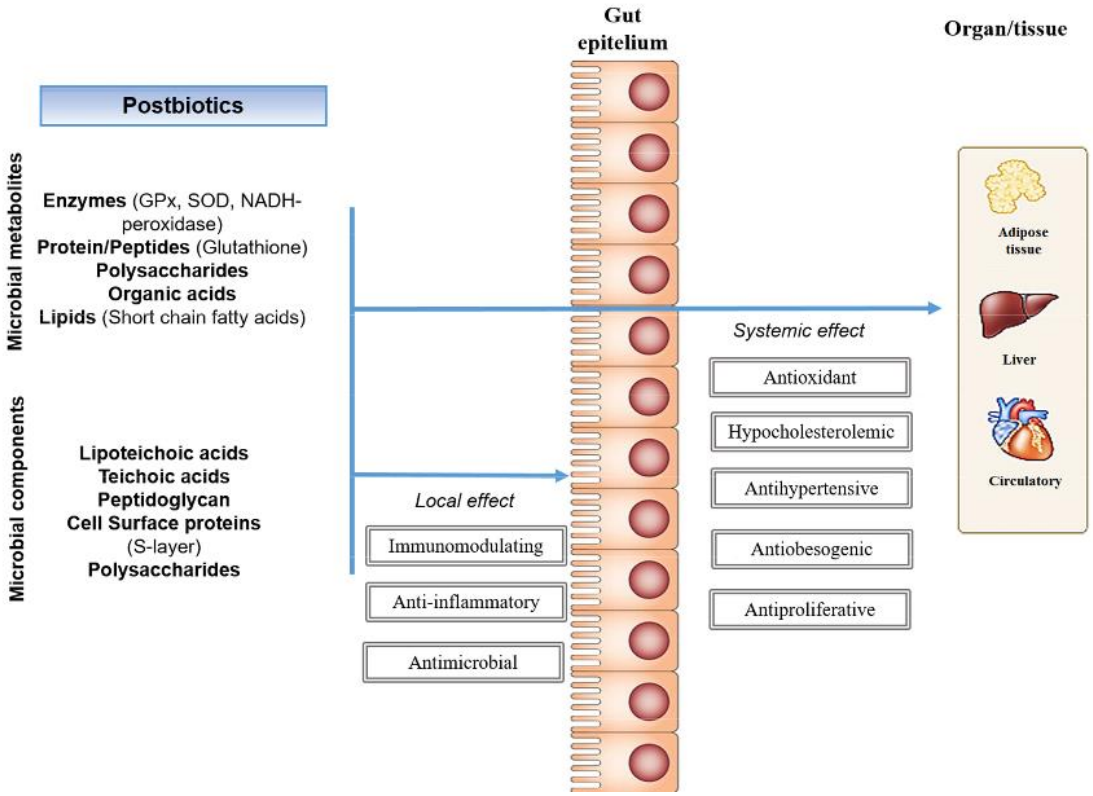

Figure 2. **Postbiotics and their potential local and systemic positive effect in the host.** *Reprinted with permission from Aguilar-Toala et al., 2018*.

↳ **Future treatments to tackle post-infectious IBS**: Beyond the diarrheal episodes induced by ETEC, we have previously discussed the increased incidence of the development of chronic intestinal disorders following ETEC infection, the post-infectious IBS. Although not in a post-infectious context, a 2-months supplementation with *S. cerevisiae* CNCM I-3856 has displayed significant properties to relieve abdominal pain and bloating in IBS patients (Cayzeele-Decherf et al., 2017). The development of fecal microbiome transplants for this purpose is extensively investigated these last years and is

promising (Halkjaer et al., 2018; Stern and Brenner; 2018). The optimization of the transplant formulation with synthetic microbiome transplants appears also to be an effective approach to treat PI-IBS associated with *Clostridium difficile* (Van der Lelie et al., 2017). We can imagine for example to supplement the synthetic microbiome transplant formulation with the yeast *S. cerevisiae* for future research.

- **Prebiotic approach**: Prebiotics are defined as “substrates that are selectively utilized by host microorganisms conferring a health benefit” (Slavin, 2013; Gibson et al., 2017). In the continuity to this PhD work on ETEC pathophysiology, the prebiotic approach in the prevention of ETEC infection has been retained for the next PhD project. In this objective, the experimental work on interaction between ETEC and intestinal mucins will be emphasized.

REFERENCES

A

Aguilar-Toalá, J.E., Garcia-Varela, R., Garcia, H.S., Mata-Haro, V., González-Córdova, A.F., Vallejo-Cordoba, B., and Hernández-Mendoza, A. (2018). Postbiotics: An evolving term within the functional foods field. Trends in Food Science & Technology *75*, 105–114.

Aguirre, M., Ramiro-Garcia, J., Koenen, M.E., and Venema, K. (2014). To pool or not to pool? Impact of the use of individual and pooled fecal samples for *in vitro* fermentation studies. J. Microbiol. Methods *107*, 1–7.

Ahmed, T., Bhuiyan, T.R., Zaman, K., Sinclair, D., and Qadri, F. (2013). Vaccines for preventing enterotoxigenic *Escherichia coli* (ETEC) diarrhoea. Cochrane Database Syst Rev CD009029.

Alam, M., Midtvedt, T., and Uribe, A. (1994). Differential cell kinetics in the ileum and colon of germfree rats. Scand. J. Gastroenterol. *29*, 445–451.

Albenberg, L., Esipova, T., Judge, C., Bittinger, K., Chen, J., Laughlin, A., Grunberg, S., Baldassano, R., Lewis, J., Li, H., et al. (2014). Correlation Between Intraluminal Oxygen Gradient and Radial Partitioning of Intestinal Microbiota in Humans and Mice. Gastroenterology *147*, 1055-1063.e8.

Allen, K.P., Randolph, M.M., and Fleckenstein, J.M. (2006). Importance of Heat-Labile Enterotoxin in Colonization of the Adult Mouse Small Intestine by Human Enterotoxigenic *Escherichia coli* Strains. Infect Immun *74*, 869–875.

de Almeida, C.V., Taddei, A., and Amedei, A. (2018). The controversial role of *Enterococcus faecalis* in colorectal cancer. Therap Adv Gastroenterol *11*.

Alsharif, G., Ahmad, S., Islam, M.S., Shah, R., Busby, S.J., and Krachler, A.M. (2015). Host attachment and fluid shear are integrated into a mechanical signal regulating virulence in *Escherichia coli* O157:H7. Proc Natl Acad Sci USA *112*, 5503–5508.

Altschul, S.F., Gish, W., Miller, W., Myers, E.W., and Lipman, D.J. (1990). Basic local alignment search tool. J. Mol. Biol. *215*, 403–410.

Anand, S., Mandal, S., and Tomar, S.K. (2017). Effect of *Lactobacillus rhamnosus* NCDC 298 with FOS in Combination on Viability and Toxin Production of Enterotoxigenic *Escherichia coli*. Probiotics Antimicrob Proteins.

Andersen, S.J., Hennebel, T., Gildemyn, S., Coma, M., Desloover, J., Berton, J., Tsukamoto, J., Stevens, C., and Rabaey, K. (2014). Electrolytic membrane extraction enables production of fine chemicals from biorefinery sidestreams. Environ. Sci. Technol. *48*, 7135–7142.

Anderson, M.J., Ellingsen, K.E., and McArdle, B.H. (2006). Multivariate dispersion as a measure of beta diversity. Ecol. Lett. *9*, 683–693.

Andjelkovic, M., Tsilia, V., Rajkovic, A., De Cremer, K., and Van Loco, J. (2016). Application of LC-MS/MS MRM to Determine Staphylococcal Enterotoxins (SEB and SEA) in Milk. Toxins (Basel) *8*, 118.

Angelakis, E., Armougom, F., Carrière, F., Bachar, D., Laugier, R., Lagier, J.-C., Robert, C., Michelle, C., Henrissat, B., and Raoult, D. (2015). A Metagenomic Investigation of the Duodenal Microbiota Reveals Links with Obesity. PLOS ONE *10*, e0137784.

Arumugam, M., Raes, J., Pelletier, E., Le Paslier, D., Yamada, T., Mende, D.R., Fernandes, G.R., Tap, J., Bruls, T., Batto, J.-M., et al. (2011). Enterotypes of the human gut microbiome. Nature *473*, 174–180.

Atuma, C., Strugala, V., Allen, A., and Holm, L. (2001). The adherent gastrointestinal mucus gel layer:

thickness and physical state *in vivo*. Am. J. Physiol. Gastrointest. Liver Physiol. *280*, G922-929.

Auchtung, T.A., Fofanova, T.Y., Stewart, C.J., Nash, A.K., Wong, M.C., Gesell, J.R., Auchtung, J.M., Ajami, N.J., and Petrosino, J.F. (2018). Investigating Colonization of the Healthy Adult Gastrointestinal Tract by Fungi. MSphere *3*.

Autieri, S.M., Lins, J.J., Leatham, M.P., Laux, D.C., Conway, T., and Cohen, P.S. (2007). l-Fucose Stimulates Utilization of d-Ribose by *Escherichia coli* MG1655 ΔfucAO and *E. coli* Nissle 1917 ΔfucAO Mutants in the Mouse Intestine and in M9 Minimal Medium. Infect Immun *75*, 5465–5475.

B

Badia, R., Zanello, G., Chevaleyre, C., Lizardo, R., Meurens, F., Martínez, P., Brufau, J., and Salmon, H. (2012). Effect of *Saccharomyces cerevisiae var. Boulardii* and β-galactomannan oligosaccharide on porcine intestinal epithelial and dendritic cells challenged *in vitro* with *Escherichia coli* F4 (K88). Vet Res *43*, 4.

Bae, J.-M. (2018). Prophylactic efficacy of probiotics on travelers' diarrhea: an adaptive meta-analysis of randomized controlled trials. Epidemiol Health *40*.

Bag, S., Ghosh, T.S., and Das, B. (2017). Complete Genome Sequence of *Collinsella aerofaciens* Isolated from the Gut of a Healthy Indian Subject. Genome Announc *5*.

Bahrami, B., Macfarlane, S., and Macfarlane, G.T. (2011). Induction of cytokine formation by human intestinal bacteria in gut epithelial cell lines. Journal of Applied Microbiology *110*, 353–363.

Bankier, C., Cheong, Y., Mahalingam, S., Edirisinghe, M., Ren, G., Cloutman-Green, E., and Ciric, L. (2018). A comparison of methods to assess the antimicrobial activity of nanoparticle combinations on bacterial cells. PLoS One *13*.

Barba-Vidal, E., Castillejos, L., López-Colom, P., Rivero Urgell, M., Moreno Muñoz, J.A., and Martín-Orúe, S.M. (2017). Evaluation of the Probiotic Strain *Bifidobacterium longum subsp. Infantis* CECT 7210 Capacities to Improve Health Status and Fight Digestive Pathogens in a Piglet Model. Front Microbiol *8*.

Barnett Foster, D. (2013). Modulation of the enterohemorrhagic *E. coli* virulence program through the human gastrointestinal tract. Virulence *4*, 315–323.

Barrett, J., and Brown, M. (2016). Travellers' diarrhoea. BMJ *353*, i1937.

Barroso, E., Cueva, C., Peláez, C., Martínez-Cuesta, M.C., and Requena, T. (2015). The Computer-Controlled Multicompartmental Dynamic Model of the Gastrointestinal System SIMGI. In The Impact of Food Bioactives on Health: *In Vitro* and *Ex Vivo* Models, K. Verhoeckx, P. Cotter, I. López-Expósito, C. Kleiveland, T. Lea, A. Mackie, T. Requena, D. Swiatecka, and H. Wichers, eds. (Cham: Springer International Publishing), pp. 319–327.

Basu, N., Arshad, N., and Visweswariah, S.S. (2010). Receptor guanylyl cyclase C (GC-C): regulation and signal transduction. Molecular and Cellular Biochemistry *334*, 67–80.

Bäumler, A.J., and Sperandio, V. (2016). Interactions between the microbiota and pathogenic bacteria in the gut. Nature *535*, 85–93.

Beatty, M.E., Bopp, C.A., Wells, J.G., Greene, K.D., Puhr, N.D., and Mintz, E.D. (2004). Enterotoxin-producing *Escherichia coli* O169:H41, United States. Emerging Infect. Dis. *10*, 518–521.

Becker, R.A., Chambers, J.M., and Wilks, A.R. (1988). The News Language: A Programming Environment for Data Analysis and Graphics (Pacific Grove, Calif: Chapman & Hall).

Begum, Y.A., Baby, N.I., Faruque, A.S.G., Jahan, N., Cravioto, A., Svennerholm, A.-M., and Qadri, F.

(2014). Shift in phenotypic characteristics of enterotoxigenic *Escherichia coli* (ETEC) isolated from diarrheal patients in Bangladesh. PLoS Negl Trop Dis *8*, e3031.

Bernalier-Donadille, A. (2010). [Fermentative metabolism by the human gut microbiota]. Gastroenterol. Clin. Biol. *34 Suppl 1*, S16-22.

Berney, M., Hammes, F., Bosshard, F., Weilenmann, H.-U., and Egli, T. (2007). Assessment and interpretation of bacterial viability by using the LIVE/DEAD BacLight Kit in combination with flow cytometry. Appl. Environ. Microbiol. *73*, 3283–3290.

den Besten, G., van Eunen, K., Groen, A.K., Venema, K., Reijngoud, D.-J., and Bakker, B.M. (2013). The role of short-chain fatty acids in the interplay between diet, gut microbiota, and host energy metabolism. J Lipid Res *54*, 2325–2340.

den Bogert, B. van, Erkus, O., Boekhorst, J., Goffau, M. de, Smid, E.J., Zoetendal, E.G., and Kleerebezem, M. (2013). Diversity of human small intestinal *Streptococcus* and *Veillonella* populations. FEMS Microbiol Ecol *85*, 376–388.

Bik, E.M., Eckburg, P.B., Gill, S.R., Nelson, K.E., Purdom, E.A., Francois, F., Perez-Perez, G., Blaser, M.J., and Relman, D.A. (2006). Molecular analysis of the bacterial microbiota in the human stomach. Proc Natl Acad Sci U S A *103*, 732–737.

Birchenough, G.M.H., Johansson, M.E.V., Gustafsson, J.K., Bergström, J.H., and Hansson, G.C. (2015). New developments in goblet cell mucus secretion and function. Mucosal Immunol *8*, 712–719.

Bivar Xavier, K. (2018). Bacterial interspecies quorum sensing in the mammalian gut microbiota. Comptes Rendus Biologies *341*, 297–299.

Blanquet-Diot, S., Denis, S., Chalancon, S., Chaira, F., Cardot, J.-M., and Alric, M. (2012). Use of artificial digestive systems to investigate the biopharmaceutical factors influencing the survival of probiotic yeast during gastrointestinal transit in humans. Pharm. Res. *29*, 1444–1453.

Blount, Z.D. The unexhausted potential of *E. coli*. ELife *4*.

Bodero, M.D., and Munson, G.P. (2009). Cyclic AMP receptor protein-dependent repression of heat-labile enterotoxin. Infect. Immun. *77*, 791–798.

Boever, P.D., Deplancke, B., and Verstraete, W. (2000). Fermentation by Gut Microbiota Cultured in a Simulator of the Human Intestinal Microbial Ecosystem Is Improved by Supplementing a Soygerm Powder. J Nutr *130*, 2599–2606.

Boisen, N., Melton-Celsa, A.R., Scheutz, F., O'Brien, A.D., and Nataro, J.P. (2015). Shiga toxin 2a and Enteroaggregative *Escherichia coli* – a deadly combination. Gut Microbes *6*, 272–278.

Bonapace, E.S., Maurer, A.H., Davidoff, S., Krevsky, B., Fisher, R.S., and Parkman, H.P. (2000). Whole gut transit scintigraphy in the clinical evaluation of patients with upper and lower gastrointestinal symptoms. Am. J. Gastroenterol. *95*, 2838–2847.

Booijink, C.C.G.M., El-Aidy, S., Rajilić-Stojanović, M., Heilig, H.G.H.J., Troost, F.J., Smidt, H., Kleerebezem, M., De Vos, W.M., and Zoetendal, E.G. (2010). High temporal and inter-individual variation detected in the human ileal microbiota. Environ. Microbiol. *12*, 3213–3227.

Borcard, D., Gillet, F., and Legendre, P. (2011a). Numerical Ecology with R (New York: Springer-Verlag).

Bornhorst, G.M., and Paul Singh, R. (2014). Gastric digestion *in vivo* and *in vitro*: how the structural aspects of food influence the digestion process. Annu Rev Food Sci Technol *5*, 111–132.

Bot, C.T., and Prodan, C. (2010). Quantifying the membrane potential during *E. coli* growth stages. Biophys. Chem. *146*, 133–137.

Bouix, M., and Ghorbal, S. (2015). Rapid assessment of Oenococcus oeni activity by measuring intracellular pH and membrane potential by flow cytometry, and its application to the more effective control of malolactic fermentation. Int. J. Food Microbiol. *193*, 139–146.

Bourgeois, A.L., Wierzba, T.F., and Walker, R.I. (2016). Status of vaccine research and development for enterotoxigenic *Escherichia coli*. Vaccine *34*, 2880–2886.

Brandão, R.L., Castro, I.M., Bambirra, E.A., Amaral, S.C., Fietto, L.G., Tropia, M.J., Neves, M.J., Dos Santos, R.G., Gomes, N.C., and Nicoli, J.R. (1998). Intracellular signal triggered by cholera toxin in *Saccharomyces boulardii* and *Saccharomyces cerevisiae*. Appl. Environ. Microbiol. *64*, 564–568.

Breimer, M.E., Hansson, G.C., Karlsson, K.-A., Larson, G., and Leffler, H. (2012). Glycosphingolipid composition of epithelial cells isolated along the villus axis of small intestine of a single human individual. Glycobiology *22*, 1721–1730.

Breeuwer, P., and Abee, T. (2000). Assessment of viability of microorganisms employing fluorescence techniques. Int. J. Food Microbiol. *55*, 193–200.

Breeuwer, P., Drocourt, J.L., Rombouts, F.M., and Abee, T. (1994). Energy-dependent, carrier-mediated extrusion of carboxyfluorescein from *Saccharomyces cerevisiae* allows rapid assessment of cell viability by flow cytometry. Appl. Environ. Microbiol. *60*, 1467–1472.

Brown, E.A., and Hardwidge, P.R. (2007). Biochemical characterization of the enterotoxigenic *Escherichia coli* LeoA protein. Microbiology (Reading, Engl.) *153*, 3776–3784.

Brown, J.W., Badahdah, A., Iticovici, M., Vickers, T.J., Alvarado, D.M., Helmerhorst, E.J., Oppenheim, F.G., Mills, J.C., Ciorba, M.A., Fleckenstein, J.M., et al. (2018). A Role for Salivary Peptides in the Innate Defense Against Enterotoxigenic *Escherichia coli*. J. Infect. Dis. *217*, 1435–1441.

Bruins, M.J., Vente-Spreeuwenberg, M. a. M., Smits, C.H., and Frenken, L.G.J. (2011). Black tea reduces diarrhoea prevalence but decreases growth performance in enterotoxigenic *Escherichia coli*-infected post-weaning piglets. J Anim Physiol Anim Nutr (Berl) *95*, 388–398.

Bruzzese, E., Giannattasio, A., and Guarino, A. (2018). Antibiotic treatment of acute gastroenteritis in children. F1000Res *7*.

Busch, A., Phan, G., and Waksman, G. (2015). Molecular mechanism of bacterial type 1 and P pili assembly. Philosophical Transactions of the Royal Society A: Mathematical, Physical and Engineering Sciences *373*, 20130153–20130153.

C

de la Cabada Bauche, J., and Dupont, H.L. (2011). New Developments in Traveler's Diarrhea. Gastroenterol Hepatol (N Y) *7*, 88–95.

Cailliez, F. (1983). The analytical solution of the additive constant problem. Psychometrika *48*, 305–308.

Cangelosi, G.A., and Meschke, J.S. (2014). Dead or alive: molecular assessment of microbial viability. Appl. Environ. Microbiol. *80*, 5884–5891.

Caron, J., and Scott, J.R. (1990). A rns-like regulatory gene for colonization factor antigen I (CFA/I) that controls expression of CFA/I pilin. Infect Immun *58*, 874–878.

Carpenter, C.C.J., Barua, D., Wallace, C.K., Sack, R.B., Mitra, P.P., Werner, A.S., Duffy, T.P., Oleinick, A., Khanra, S.R., and Lewis, G.W. (1965). Clinical and physiological observations during an epidemic outbreak of non-vibrio cholera-like disease in Calcutta. Bull World Health Organ *33*, 665–671.

Castañeda-García, A., Do, T.T., and Blázquez, J. (2011). The K+ uptake regulator TrkA controls membrane potential, pH homeostasis and multidrug susceptibility in *Mycobacterium smegmatis*. J

Antimicrob Chemother *66*, 1489–1498.

Castellanos-Gonzalez, A., Cabada, M.M., Nichols, J., Gomez, G., and White, A.C. (2013). Human Primary Intestinal Epithelial Cells as an Improved *In Vitro* Model for *Cryptosporidium parvum* Infection. Infect Immun *81*, 1996–2001.

Cayzeele-Decherf, A., Pélerin, F., Leuillet, S., Douillard, B., Housez, B., Cazaubiel, M., Jacobson, G.K., Jüsten, P., and Desreumaux, P. (2017). *Saccharomyces cerevisiae* CNCM I-3856 in irritable bowel syndrome: An individual subject meta-analysis. World J Gastroenterol *23*, 336–344.

Cecchini, D.A., Laville, E., Laguerre, S., Robe, P., Leclerc, M., Doré, J., Henrissat, B., Remaud-Siméon, M., Monsan, P., and Potocki-Véronèse, G. (2013). Functional metagenomics reveals novel pathways of prebiotic breakdown by human gut bacteria. PLoS ONE *8*, e72766.

Chandra, R., and Liddle, R.A. (2014). Recent Advances in the Regulation of Pancreatic Secretion. Curr Opin Gastroenterol *30*, 490–494.

Chapman, C.M.C., Gibson, G.R., and Rowland, I. (2011). Health benefits of probiotics: are mixtures more effective than single strains? Eur J Nutr *50*, 1–17.

Chatterjee, A., and Chowdhury, R. (2008). Bile and Unsaturated Fatty Acids Inhibit the Binding of Cholera Toxin and *Escherichia coli* Heat-Labile Enterotoxin to GM1 Receptor. Antimicrobial Agents and Chemotherapy *52*, 220–224.

Chatterjee, R., Ghosal, A., Sabui, S., and Chatterjee, N.S. (2011). Three dimensional modeling of C-terminal loop of CssA subunit in CS6 of Enterotoxigenic *Escherichia coli* and its interaction with the 70 KDa domain of Fibronectin. Bioinformation *6*, 307–310.

Chattopadhyay, M.K., Keembiyehetty, C.N., Chen, W., and Tabor, H. (2015). Polyamines Stimulate the Level of the σ38 Subunit (RpoS) of *Escherichia coli* RNA Polymerase, Resulting in the Induction of the Glutamate Decarboxylase-dependent Acid Response System via the gadE Regulon. J Biol Chem *290*, 17809–17821.

Chen, J.-C., Ho, T.-Y., Chang, Y.-S., Wu, S.-L., and Hsiang, C.-Y. (2006). Anti-diarrheal effect of Galla Chinensis on the *Escherichia coli* heat-labile enterotoxin and ganglioside interaction. Journal of Ethnopharmacology *103*, 385–391.

Chen, W., Zhang, C.K., Cheng, Y., Zhang, S., and Zhao, H. (2013). A comparison of methods for clustering 16S rRNA sequences into OTUs. PLoS ONE *8*, e70837.

Chiang, J.Y.L. (2013). Bile Acid Metabolism and Signaling. Compr Physiol *3*, 1191–1212.

Chin'ombe, N., Muzividzi, B., Munemo, E., and Nziramasanga, P. (2016). Molecular Identification of Nontuberculous Mycobacteria in Humans in Zimbabwe Using 16S Ribosequencing. Open Microbiol J *10*, 113–123.

Chiou, R.Y.-Y., Phillips, R.D., Zhao, P., Doyle, M.P., and Beuchat, L.R. (2004). Ethanol-Mediated Variations in Cellular Fatty Acid Composition and Protein Profiles of Two Genotypically Different Strains of *Escherichia coli* O157:H7. Appl Environ Microbiol *70*, 2204–2210.

Chytilová, M., Mudroňová, D., Nemcová, R., Gancarčíková, S., Buleca, V., Koščová, J., and Tkáčiková, L. (2013). Anti-inflammatory and immunoregulatory effects of flax-seed oil and *Lactobacillus plantarum* - Biocenol™ LP96 in gnotobiotic pigs challenged with enterotoxigenic *Escherichia coli*. Res. Vet. Sci. *95*, 103–109.

Ciarlo, E., Heinonen, T., Herderschee, J., Fenwick, C., Mombelli, M., Le Roy, D., and Roger, T. (2016). Impact of the microbial derived short chain fatty acid propionate on host susceptibility to bacterial and fungal infections *in vivo*. Sci Rep *6*.

Cieplak, T., Wiese, M., Nielsen, S., Van de Wiele, T., van den Berg, F., and Nielsen, D.S. (2018). The

smallest intestine (TSI) - a low volume *in vitro* model of the small intestine with increased throughput.

Cinquin, C., Le Blay, G., Fliss, I., and Lacroix, C. (2004). Immobilization of infant fecal microbiota and utilization in an *in vitro* colonic fermentation model. Microb. Ecol. *48*, 128–138.

Clements, A., Young, J.C., Constantinou, N., and Frankel, G. (2012). Infection strategies of enteric pathogenic *Escherichia coli*. Gut Microbes *3*, 71–87.

Cole, J.R., Wang, Q., Fish, J.A., Chai, B., McGarrell, D.M., Sun, Y., Brown, C.T., Porras-Alfaro, A., Kuske, C.R., and Tiedje, J.M. (2014). Ribosomal Database Project: data and tools for high throughput rRNA analysis. Nucleic Acids Res. *42*, D633-642.

Connell, J.H., and Slatyer, R.O. (1977). Mechanisms of Succession in Natural Communities and Their Role in Community Stability and Organization. The American Naturalist *111*, 1119–1144.

Connor, B.A., and Riddle, M.S. (2013). Post-infectious sequelae of travelers' diarrhea. J Travel Med *20*, 303–312.

Consortium, T.H.M.P., Huttenhower, C., Gevers, D., Knight, R., Abubucker, S., Badger, J.H., Chinwalla, A.T., Creasy, H.H., Earl, A.M., FitzGerald, M.G., et al. (2012). Structure, function and diversity of the healthy human microbiome. Nature *486*, 207–214.

Cordonnier, C., Etienne-Mesmin, L., Thévenot, J., Rougeron, A., Rénier, S., Chassaing, B., Darfeuille-Michaud, A., Barnich, N., Blanquet-Diot, S., and Livrelli, V. (2017). Enterohemorrhagic *Escherichia coli* pathogenesis: role of Long polar fimbriae in Peyer's patches interactions. Scientific Reports *7*, 44655.

Cox, T.F. (2001). Multidimensional scaling used in multivariate statistical process control. Journal of Applied Statistics *28*, 365–378.

Crofts, A.A., Giovanetti, S.M., Rubin, E.J., Poly, F.M., Gutiérrez, R.L., Talaat, K.R., Porter, C.K., Riddle, M.S., DeNearing, B., Brubaker, J., et al. (2018). Enterotoxigenic *E. coli* virulence gene regulation in human infections. Proc. Natl. Acad. Sci. U.S.A. *115*, E8968–E8976.

Crossman, L.C., Chaudhuri, R.R., Beatson, S.A., Wells, T.J., Desvaux, M., Cunningham, A.F., Petty, N.K., Mahon, V., Brinkley, C., Hobman, J.L., et al. (2010). A commensal gone bad: complete genome sequence of the prototypical enterotoxigenic *Escherichia coli* strain H10407. J. Bacteriol. *192*, 5822–5831.

Croxen, M.A., and Finlay, B.B. (2010). Molecular mechanisms of *Escherichia coli* pathogenicity. Nat. Rev. Microbiol. *8*, 26–38.

Croxen, M.A., Law, R.J., Scholz, R., Keeney, K.M., Wlodarska, M., and Finlay, B.B. (2013). Recent advances in understanding enteric pathogenic *Escherichia coli*. Clin. Microbiol. Rev. *26*, 822–880.

Cummings, J.H., Pomare, E.W., Branch, W.J., Naylor, C.P., and Macfarlane, G.T. (1987). Short chain fatty acids in human large intestine, portal, hepatic and venous blood. Gut *28*, 1221–1227.

Curtis, C.D., and Nardulli, A.M. (2009). Using RNA Interference to Study Protein Function. Methods Mol Biol *505*, 187–204.

Cuskin, F., Lowe, E.C., Temple, M.J., Zhu, Y., Cameron, E., Pudlo, N.A., Porter, N.T., Urs, K., Thompson, A.J., Cartmell, A., et al. (2015). Human gut Bacteroidetes can utilize yeast mannan through a selfish mechanism. Nature *517*, 165–169.

D

Darkoh, C., Lichtenberger, L.M., Ajami, N., Dial, E.J., Jiang, Z.-D., and DuPont, H.L. (2010). Bile Acids Improve the Antimicrobial Effect of Rifaximin. Antimicrob Agents Chemother *54*, 3618–3624.

Daudelin, J.-F., Lessard, M., Beaudoin, F., Nadeau, E., Bissonnette, N., Boutin, Y., Brousseau, J.-P., Lauzon, K., and Fairbrother, J.M. (2011). Administration of probiotics influences F4 (K88)-positive enterotoxigenic *Escherichia coli* attachment and intestinal cytokine expression in weaned pigs. Vet. Res. *42*, 69.

David, L.A., Weil, A., Ryan, E.T., Calderwood, S.B., Harris, J.B., Chowdhury, F., Begum, Y., Qadri, F., LaRocque, R.C., and Turnbaugh, P.J. (2015). Gut microbial succession follows acute secretory diarrhea in humans. MBio *6*, e00381-00315.

Davies, E.V., Winstanley, C., Fothergill, J.L., and James, C.E. (2016). The role of temperate bacteriophages in bacterial infection. FEMS Microbiol. Lett. *363*, fnw015.

De, S.N., Bhattacharya, K., and Sarkar, J.K. (1956). A study of the pathogenicity of strains of Bacterium coli from acute and chronic enteritis. J Pathol Bacteriol *71*, 201–209.

Déat, E., Blanquet-Diot, S., Jarrige, J.-F., Denis, S., Beyssac, E., and Alric, M. (2009). Combining the dynamic TNO-gastrointestinal tract system with a Caco-2 cell culture model: application to the assessment of lycopene and alpha-tocopherol bioavailability from a whole food. J. Agric. Food Chem. *57*, 11314–11320.

Debata, N.K., Panigrahy, R., Otta, S., Panda, K., and Swain, B. (2014). Achromobacter xylosoxidans: a rare pathogen for community-acquired acute pancreatitis. JMM Case Reports *1*.

Deininger, K.N.W., Horikawa, A., Kitko, R.D., Tatsumi, R., Rosner, J.L., Wachi, M., and Slonczewski, J.L. (2011). A Requirement of TolC and MDR Efflux Pumps for Acid Adaptation and GadAB Induction in *Escherichia coli*. In PloS One, p.

Deneke, C.F., McGowan, K., Thorne, G.M., and Gorbach, S.L. (1983). Attachment of enterotoxigenic *Escherichia coli* to human intestinal cells. Infect Immun *39*, 1102–1106.

De Paepe, K., Kerckhof, F.-M., Verspreet, J., Courtin, C.M., and Van de Wiele, T. (2017). Inter-individual differences determine the outcome of wheat bran colonization by the human gut microbiome. Environ. Microbiol. *19*, 3251–3267.

Dlugosz, A., Winckler, B., Lundin, E., Zakikhany, K., Sandström, G., Ye, W., Engstrand, L., and Lindberg, G. (2015). No difference in small bowel microbiota between patients with irritable bowel syndrome and healthy controls. Sci Rep *5*, 8508.

Dobson, A., Cotter, P.D., Ross, R.P., and Hill, C. (2012). Bacteriocin production: a probiotic trait? Appl. Environ. Microbiol. *78*, 1–6.

Donaldson, G.P., Lee, S.M., and Mazmanian, S.K. (2016). Gut biogeography of the bacterial microbiota. Nat. Rev. Microbiol. *14*, 20–32.

Dostal, A., Lacroix, C., Pham, V.T., Zimmermann, M.B., Del'homme, C., Bernalier-Donadille, A., and Chassard, C. (2014). Iron supplementation promotes gut microbiota metabolic activity but not colitis markers in human gut microbiota-associated rats. Br. J. Nutr. *111*, 2135–2145.

Dreyfus, L.A., Harville, B., Howard, D.E., Shaban, R., Beatty, D.M., and Morris, S.J. (1993). Calcium influx mediated by the *Escherichia coli* heat-stable enterotoxin B (STB). Proc. Natl. Acad. Sci. U.S.A. *90*, 3202–3206.

Dubreuil, J.D. (2012). The whole Shebang: the gastrointestinal tract, *Escherichia coli* enterotoxins and secretion. Curr Issues Mol Biol *14*, 71–82.

Dubreuil, J.D., Isaacson, R.E., and Schifferli, D.M. (2016). Animal enterotoxigenic *Escherichia coli*. EcoSal Plus *7*.

DuPont, H.L. (2009). Systematic review: the epidemiology and clinical features of travellers' diarrhoea. Alimentary Pharmacology & Therapeutics *30*, 187–196.

DuPont, H.L. (1997). Guidelines on acute infectious diarrhea in adults. The Practice Parameters Committee of the American College of Gastroenterology. Am. J. Gastroenterol. *92*, 1962–1975.

E

Edgar, R.C., Haas, B.J., Clemente, J.C., Quince, C., and Knight, R. (2011). UCHIME improves sensitivity and speed of chimera detection. Bioinformatics *27*, 2194–2200.

Edwards, B.D., Greysson-Wong, J., Somayaji, R., Waddell, B., Whelan, F.J., Storey, D.G., Rabin, H.R., Surette, M.G., and Parkins, M.D. (2017). Prevalence and Outcomes of *Achromobacter* Species Infections in Adults with Cystic Fibrosis: a North American Cohort Study. Journal of Clinical Microbiology *55*, 2074–2085.

Edwards-Ingram, L., Gitsham, P., Burton, N., Warhurst, G., Clarke, I., Hoyle, D., Oliver, S.G., and Stateva, L. (2007). Genotypic and physiological characterization of *Saccharomyces boulardii*, the probiotic strain of *Saccharomyces cerevisiae*. Appl. Environ. Microbiol. *73*, 2458–2467.

EFSA Panel on Dietetic Products, Nutrition and Allergies (NDA) (2010). Scientific Opinion on the substantiation of health claims related to live yoghurt cultures and improved lactose digestion (ID 1143, 2976) pursuant to Article 13(1) of Regulation (EC) No 1924/2006. EFSA Journal *8*.

Egger, L., Ménard, O., Delgado-Andrade, C., Alvito, P., Assunção, R., Balance, S., Barberá, R., Brodkorb, A., Cattenoz, T., Clemente, A., et al. (2016). The harmonized INFOGEST *in vitro* digestion method: From knowledge to action. Food Research International *88*, 217–225.

Eguchi, Y., Ishii, E., Hata, K., and Utsumi, R. (2011). Regulation of Acid Resistance by Connectors of Two-Component Signal Transduction Systems in *Escherichia coli*. Journal of Bacteriology *193*, 1222–1228.

Ellis, T.N., and Kuehn, M.J. (2010). Virulence and immunomodulatory roles of bacterial outer membrane vesicles. Microbiol. Mol. Biol. Rev. *74*, 81–94.

Emerson, J.B., Adams, R.I., Román, C.M.B., Brooks, B., Coil, D.A., Dahlhausen, K., Ganz, H.H., Hartmann, E.M., Hsu, T., Justice, N.B., et al. (2017). Schrödinger's microbes: Tools for distinguishing the living from the dead in microbial ecosystems. Microbiome *5*, 86.

Epand, R.F., Pollard, J.E., Wright, J.O., Savage, P.B., and Epand, R.M. (2010). Depolarization, Bacterial Membrane Composition, and the Antimicrobial Action of Ceragenins. Antimicrob Agents Chemother *54*, 3708–3713.

Estrada-Garcia, T., and Navarro-Garcia, F. (2012). Enteroaggregative *Escherichia coli* pathotype: a genetically heterogeneous emerging foodborne enteropathogen. FEMS Immunol. Med. Microbiol. *66*, 281–298.

Etienne-Mesmin, L., Livrelli, V., Privat, M., Denis, S., Cardot, J.-M., Alric, M., and Blanquet-Diot, S. (2011). Effect of a New Probiotic *Saccharomyces cerevisiae* Strain on Survival of *Escherichia coli* O157:H7 in a Dynamic Gastrointestinal Model. Appl Environ Microbiol *77*, 1127–1131.

Evans, D.G., Evans, D.J., and Tjoa, W. (1977). Hemagglutination of Human Group A Erythrocytes by Enterotoxigenic *Escherichia coli* Isolated from Adults with Diarrhea: Correlation with Colonization Factor. Infect Immun *18*, 330–337.

F

Fabich, A.J., Jones, S.A., Chowdhury, F.Z., Cernosek, A., Anderson, A., Smalley, D., McHargue, J.W., Hightower, G.A., Smith, J.T., Autieri, S.M., et al. (2008). Comparison of Carbon Nutrition for Pathogenic and Commensal *Escherichia coli* Strains in the Mouse Intestine. Infect Immun *76*, 1143–1152.

Fairbrother, P., Pinnock, H., Hanley, J., McCloughan, L., Sheikh, A., Pagliari, C., McKinstry, B., and

TELESCOT programme team (2012). Continuity, but at what cost? The impact of telemonitoring COPD on continuities of care: a qualitative study. Prim Care Respir J *21*, 322–328.

Fan, P., Li, L., Rezaei, A., Eslamfam, S., Che, D., and Ma, X. (2015). Metabolites of Dietary Protein and Peptides by Intestinal Microbes and their Impacts on Gut. Current Protein & Peptide Science *16*, 646–654.

Fehlbaum, S., Chassard, C., Haug, M.C., Fourmestraux, C., Derrien, M., and Lacroix, C. (2015). Design and Investigation of PolyFermS *In Vitro* Continuous Fermentation Models Inoculated with Immobilized Fecal Microbiota Mimicking the Elderly Colon. PLoS ONE *10*, e0142793.

Feria Gervasio, D., Tottey, W., Gaci, N., ALRIC, M., Cardot, J.-M., Peyret, P., Martin, J.-F., Pujos-Guillot, E., Sébédio, J.-L., and Brugere, J.-F. (2014). Three-stage continuous culture system with a self-generated anaerobia to study the regionalized metabolism of the human gut microbiota. Journal of Microbiological Methods *96*, 111–118.

Ferrua, M.J., Kong, F., and Singh, R.P. (2011). Computational modeling of gastric digestion and the role of food material properties. TRENDS FOOD SCI.TECHNOL. *22*, 480–491.

Fietto, J.L., Araújo, R.S., Valadão, F.N., Fietto, L.G., Brandão, R.L., Neves, M.J., Gomes, F.C., Nicoli, J.R., and Castro, I.M. (2004). Molecular and physiological comparisons between *Saccharomyces cerevisiae* and *Saccharomyces boulardii*. Canadian Journal of Microbiology *50*, 615–621.

Fijan, S. (2014). Microorganisms with Claimed Probiotic Properties: An Overview of Recent Literature. Int J Environ Res Public Health *11*, 4745–4767.

Finamore, A., Roselli, M., Imbinto, A., Seeboth, J., Oswald, I.P., and Mengheri, E. (2014). *Lactobacillus amylovorus* inhibits the TLR4 inflammatory signaling triggered by enterotoxigenic *Escherichia coli* via modulation of the negative regulators and involvement of TLR2 in intestinal Caco-2 cells and pig explants. PLoS ONE *9*, e94891.

Fleckenstein, J.M., Lindler, L.E., Elsinghorst, E.A., and Dale, J.B. (2000). Identification of a Gene within a Pathogenicity Island of Enterotoxigenic *Escherichia coli* H10407 Required for Maximal Secretion of the Heat-Labile Enterotoxin. Infect Immun *68*, 2766–2774.

Fleckenstein, J.M., Roy, K., Fischer, J.F., and Burkitt, M. (2006). Identification of a two-partner secretion locus of enterotoxigenic *Escherichia coli*. Infect. Immun. *74*, 2245–2258.

Fleckenstein, J.M., and Rasko, D.A. (2016). Overcoming Enterotoxigenic *Escherichia coli* Pathogen Diversity: Translational Molecular Approaches to Inform Vaccine Design. Methods Mol Biol *1403*, 363–383.

van der Flier, L.G., and Clevers, H. (2009). Stem cells, self-renewal, and differentiation in the intestinal epithelium. Annu. Rev. Physiol. *71*, 241–260.

Foster, J.W. (2004). *Escherichia coli* acid resistance: tales of an amateur acidophile. Nat. Rev. Microbiol. *2*, 898–907.

Fratamico, P.M., DebRoy, C., and Needleman, D.S. (2016). Editorial: Emerging Approaches for Typing, Detection, Characterization, and Traceback of *Escherichia coli*. Front Microbiol *7*.

Fröhling, A., and Schlüter, O. (2015). Flow cytometric evaluation of physico-chemical impact on Gram-positive and Gram-negative bacteria. Front Microbiol *6*.

Fukuda, S., Toh, H., Hase, K., Oshima, K., Nakanishi, Y., Yoshimura, K., Tobe, T., Clarke, J.M., Topping, D.L., Suzuki, T., et al. (2011). *Bifidobacteria* can protect from enteropathogenic infection through production of acetate. Nature *469*, 543–547.

G

Gagnon, M., Zihler, A., Chassard, C., and Lacroix, C. (2011). Ecology of Probiotics and Enteric Protection. In Probiotic Bacteria and Enteric Infections: Cytoprotection by Probiotic Bacteria, J.J. Malago, J.F.J.G. Koninkx, and R. Marinsek-Logar, eds. (Dordrecht: Springer Netherlands), pp. 65–85.

Gallier, S., and Singh, H. (2012). Behavior of almond oil bodies during *in vitro* gastric and intestinal digestion. Food Funct *3*, 547–555.

Galvao, T.F., Thees, M.F.R. e S., Pontes, R.F., Silva, M.T., and Pereira, M.G. (2013). Zinc supplementation for treating diarrhea in children: a systematic review and meta-analysis. Rev. Panam. Salud Publica *33*, 370–377.

Gayer, C.P., and Basson, M.D. (2009). The effects of mechanical forces on intestinal physiology and pathology. Cell Signal *21*, 1237–1244.

GBD Diarrhoeal Diseases Collaborators (2017). Estimates of global, regional, and national morbidity, mortality, and aetiologies of diarrhoeal diseases: a systematic analysis for the Global Burden of Disease Study 2015. Lancet Infect Dis *17*, 909–948.

Ge, S., Usack, J.G., Spirito, C.M., and Angenent, L.T. (2015). Long-Term *n* -Caproic Acid Production from Yeast-Fermentation Beer in an Anaerobic Bioreactor with Continuous Product Extraction. Environmental Science & Technology *49*, 8012–8021.

Geirnaert, A., Wang, J., Tinck, M., Steyaert, A., Van den Abbeele, P., Eeckhaut, V., Vilchez-Vargas, R., Falony, G., Laukens, D., De Vos, M., et al. (2015). Interindividual differences in response to treatment with butyrate-producing *Butyricicoccus pullicaecorum* 25-3T studied in an in vitro gut model. FEMS Microbiol. Ecol. *91*.

Gensberger, E.T., Polt, M., Konrad-Köszler, M., Kinner, P., Sessitsch, A., and Kostić, T. (2014). Evaluation of quantitative PCR combined with PMA treatment for molecular assessment of microbial water quality. Water Res. *67*, 367–376.

Geoghegan, I., Steinberg, G., and Gurr, S. (2017). The Role of the Fungal Cell Wall in the Infection of Plants. Trends in Microbiology *25*, 957–967.

Gibson, G.R., Hutkins, R., Sanders, M.E., Prescott, S.L., Reimer, R.A., Salminen, S.J., Scott, K., Stanton, C., Swanson, K.S., Cani, P.D., et al. (2017). Expert consensus document: The International Scientific Association for Probiotics and Prebiotics (ISAPP) consensus statement on the definition and scope of prebiotics. Nat Rev Gastroenterol Hepatol *14*, 491–502.

Giddings, S.L., Stevens, A.M., and Leung, D.T. (2016). Traveler's Diarrhea. Med. Clin. North Am. *100*, 317–330.

Gildemyn, S., Molitor, B., Usack, J.G., Nguyen, M., Rabaey, K., and Angenent, L.T. (2017). Upgrading syngas fermentation effluent using *Clostridium kluyveri* in a continuous fermentation. Biotechnol Biofuels *10*.

Gill, D.M., Clements, J.D., Robertson, D.C., and Finkelstein, R.A. (1981). Subunit number and arrangement in *Escherichia coli* heat-labile enterotoxin. Infect Immun *33*, 677–682.

Gill, A. (2017). The Importance of Bacterial Culture to Food Microbiology in the Age of Genomics. Front Microbiol *8*.

Girard, M., Thanner, S., Pradervand, N., Hu, D., Ollagnier, C., and Bee, G. (2018). Hydrolysable chestnut tannins for reduction of postweaning diarrhea: Efficacy on an experimental ETEC F4 model. PLoS ONE *13*, e0197878.

Gomes, T.A.T., Elias, W.P., Scaletsky, I.C.A., Guth, B.E.C., Rodrigues, J.F., Piazza, R.M.F., Ferreira, L.C.S., and Martinez, M.B. (2016). Diarrheagenic *Escherichia coli*. Braz J Microbiol *47*, 3–30.

Gonzales, L., Ali, Z.B., Nygren, E., Wang, Z., Karlsson, S., Zhu, B., Quiding-Järbrink, M., and Sjöling,

Å. (2013). Alkaline pH Is a Signal for Optimal Production and Secretion of the Heat Labile Toxin, LT in Enterotoxigenic *Escherichia Coli* (ETEC). PLoS One *8*.

Gonzales-Siles, L., and Sjöling, Å. (2016). The different ecological niches of *enterotoxigenic Escherichia coli*. Environ Microbiol *18*, 741–751.

Gorbach, S.L. (1996). Microbiology of the Gastrointestinal Tract. In Medical Microbiology, S. Baron, ed. (Galveston (TX): University of Texas Medical Branch at Galveston).

Gower, J.C. (1966). Some distance properties of latent root and vector methods used in multivariate analysis. Biometrika *53*, 325–338.

Green, E.R., and Mecsas, J. (2016). Bacterial Secretion Systems: An Overview. Microbiol Spectr *4*.

Grewal, H.M., Valvatne, H., Bhan, M.K., van Dijk, L., Gaastra, W., and Sommerfelt, H. (1997). A new putative fimbrial colonization factor, CS19, of human enterotoxigenic *Escherichia coli*. Infect Immun *65*, 507–513.

Griffiths, S.L., and Critchley, D.R. (1991). Characterisation of the binding sites for *Escherichia coli* heat-labile toxin type I in intestinal brush borders. Biochim. Biophys. Acta *1075*, 154–161.

Guarino, A., Ashkenazi, S., Gendrel, D., Lo Vecchio, A., Shamir, R., Szajewska, H., European Society for Pediatric Gastroenterology, Hepatology, and Nutrition, and European Society for Pediatric Infectious Diseases (2014). European Society for Pediatric Gastroenterology, Hepatology, and Nutrition/European Society for Pediatric Infectious Diseases evidence-based guidelines for the management of acute gastroenteritis in children in Europe: update 2014. J. Pediatr. Gastroenterol. Nutr. *59*, 132–152.

Guerra, A., Etienne-Mesmin, L., Livrelli, V., Denis, S., Blanquet-Diot, S., and Alric, M. (2012). Relevance and challenges in modeling human gastric and small intestinal digestion. Trends Biotechnol. *30*, 591–600.

Guerra, A., Denis, S., le Goff, O., Sicardi, V., François, O., Yao, A.-F., Garrait, G., Manzi, A.P., Beyssac, E., Alric, M., et al. (2016). Development and validation of a new dynamic computer-controlled model of the human stomach and small intestine. Biotechnol. Bioeng. *113*, 1325–1335.

Guerra, J.A., Romero-Herazo, Y.C., Arzuza, O., and Gómez-Duarte, O.G. (2014). Phenotypic and Genotypic Characterization of Enterotoxigenic *Escherichia coli* Clinical Isolates from Northern Colombia, South America.

Gupta, S.K., Keck, J., Ram, P.K., Crump, J.A., Miller, M.A., and Mintz, E.D. (2008). Part III. Analysis of data gaps pertaining to enterotoxigenic *Escherichia coli* infections in low and medium human development index countries, 1984-2005. Epidemiol. Infect. *136*, 721–738.

Gyles, C.L., and Fairbrother, J.M. (2008). Escherichia Coli. In Pathogenesis of Bacterial Infections in Animals, (John Wiley & Sons, Ltd), 193–223.

Gyurova, A.Y., and Zhivkov, A.M. (2009). Influence of Low Concentration Ethanol on Membrane Permeability of *E.Coli*. Biotechnology & Biotechnological Equipment *23*, 480–483.

H

Hacker, J., and Blum-Oehler, G. (2007). In appreciation of Theodor Escherich. Nature Reviews Microbiology *5*, 902.

Haines, S., Arnaud-Barbe, N., Poncet, D., Reverchon, S., Wawrzyniak, J., Nasser, W., and Renauld-Mongénie, G. (2015). IscR Regulates Synthesis of Colonization Factor Antigen I Fimbriae in Response to Iron Starvation in Enterotoxigenic *Escherichia coli*. Journal of Bacteriology *197*, 2896–2907.

Haines, S., Gautheron, S., Nasser, W., and Renauld-Mongénie, G. (2015). Identification of Novel

Components Influencing Colonization Factor Antigen I Expression in Enterotoxigenic *Escherichia coli*. PLoS ONE *10*, e0141469.

Halkjær, S.I., Christensen, A.H., Lo, B.Z.S., Browne, P.D., Günther, S., Hansen, L.H., and Petersen, A.M. (2018). Faecal microbiota transplantation alters gut microbiota in patients with irritable bowel syndrome: results from a randomised, double-blind placebo-controlled study. Gut *67*, 2107–2115.

Halvorson, H.A., Schlett, C.D., and Riddle, M.S. (2006). Postinfectious irritable bowel syndrome--a meta-analysis. Am. J. Gastroenterol. *101*, 1894–1899; quiz 1942.

Hamer, H.M., Jonkers, D., Venema, K., Vanhoutvin, S., Troost, F.J., and Brummer, R.-J. (2008). Review article: the role of butyrate on colonic function. Aliment. Pharmacol. Ther. *27*, 104–119.

Harvey, K., Esposito, D.H., Han, P., Kozarsky, P., Freedman, D.O., Plier, D.A., Sotir, M.J., and Centers for Disease Control and Prevention (CDC) (2013). Surveillance for travel-related disease--GeoSentinel Surveillance System, United States, 1997-2011. MMWR Surveill Summ *62*, 1–23.

Hatoum, R., Labrie, S., and Fliss, I. (2012). Antimicrobial and Probiotic Properties of Yeasts: From Fundamental to Novel Applications. Front Microbiol *3*.

Havenaar, R., Anneveld, B., Hanff, L.M., de Wildt, S.N., de Koning, B.A.E., Mooij, M.G., Lelieveld, J.P.A., and Minekus, M. (2013). *In vitro* gastrointestinal model (TIM) with predictive power, even for infants and children? Int J Pharm *457*, 327–332.

Hay, A.J., and Zhu, J. (2014). Microbiota Talks Cholera out of the Gut. Cell Host & Microbe *16*, 549–550.

Hayashi, H., Takahashi, R., Nishi, T., Sakamoto, M., and Benno, Y. (2005). Molecular analysis of jejunal, ileal, caecal and recto-sigmoidal human colonic microbiota using 16S rRNA gene libraries and terminal restriction fragment length polymorphism. J. Med. Microbiol. *54*, 1093–1101.

Haycocks, J.R.J., Sharma, P., Stringer, A.M., Wade, J.T., and Grainger, D.C. (2015). The molecular basis for control of ETEC enterotoxin expression in response to environment and host. PLoS Pathog. *11*, e1004605.

Hazen, T.H., Michalski, J., Luo, Q., Shetty, A.C., Daugherty, S.C., Fleckenstein, J.M., and Rasko, D.A. (2017). Comparative genomics and transcriptomics of *Escherichia coli* isolates carrying virulence factors of both enteropathogenic and enterotoxigenic *E. coli*. Scientific Reports *7*, 3513.

Hegde, A., Bhat, G.K., and Mallya, S. (2009). Effect of stress on production of heat labile enterotoxin by *Escherichia coli*. Indian Journal of Medical Microbiology *27*, 325.

Helander, A., Grewal, H.M., Gaastra, W., and Svennerholm, A.M. (1997). Detection and characterization of the coli surface antigen 6 of enterotoxigenic *Escherichia coli* strains by using monoclonal antibodies. J. Clin. Microbiol. *35*, 867–872.

Hennequin, C., Thierry, A., Richard, G.F., Lecointre, G., Nguyen, H.V., Gaillardin, C., and Dujon, B. (2001). Microsatellite typing as a new tool for identification of *Saccharomyces cerevisiae* strains. J. Clin. Microbiol. *39*, 551–559.

Herold, S., Paton, J.C., Srimanote, P., and Paton, A.W. (2009). Differential effects of short-chain fatty acids and iron on expression of iha in Shiga-toxigenic *Escherichia coli*. Microbiology *155*, 3554–3563.

Hidalgo, I.J. (1996). Cultured intestinal epithelial cell models. Pharm Biotechnol *8*, 35–50.

Hidalgo-Cantabrana, C., Sánchez, B., Milani, C., Ventura, M., Margolles, A., and Ruas-Madiedo, P. (2014). Genomic overview and biological functions of exopolysaccharide biosynthesis in *Bifidobacterium spp.* Appl. Environ. Microbiol. *80*, 9–18.

Hill, C., Guarner, F., Reid, G., Gibson, G.R., Merenstein, D.J., Pot, B., Morelli, L., Canani, R.B., Flint,

H.J., Salminen, S., et al. (2014). Expert consensus document. The International Scientific Association for Probiotics and Prebiotics consensus statement on the scope and appropriate use of the term probiotic. Nat Rev Gastroenterol Hepatol *11*, 506–514.

Hillman, E.T., Lu, H., Yao, T., and Nakatsu, C.H. (2017). Microbial Ecology along the Gastrointestinal Tract. Microbes Environ *32*, 300–313.

Hillman, K., Spencer, R.J., Murdoch, T.A., and Stewart, C.S. (1995). The effect of mixtures of *Lactobacillus spp.* on the survival of enterotoxigenic *Escherichia coli* in *in vitro* continuous culture of porcine intestinal bacteria. Lett. Appl. Microbiol. *20*, 130–133.

Hilton, null, Kolakowski, null, Singer, null, and Smith, null (1997). Efficacy of *Lactobacillus GG* as a Diarrheal Preventive in Travelers. J Travel Med *4*, 41–43.

Hodson, C., Yang, J., Hocking, D.M., Azzopardi, K., Chen, Q., Holien, J.K., Parker, M.W., Tauschek, M., and Robins-Browne, R.M. (2017). Control of Virulence Gene Expression by the Master Regulator, CfaD, in the Prototypical Enterotoxigenic *Escherichia coli* Strain, H10407. Front Microbiol *8*, 1525.

Hojsak, I., Fabiano, V., Pop, T.L., Goulet, O., Zuccotti, G.V., Çokuğraş, F.C., Pettoello-Mantovani, M., and Kolaček, S. (2018). Guidance on the use of probiotics in clinical practice in children with selected clinical conditions and in specific vulnerable groups. Acta Paediatr. *107*, 927–937.

Holmgren, J., Lindblad, M., Fredman, P., Svennerholm, L., and Myrvold, H. (1985). Comparison of receptors for cholera and *Escherichia coli* enterotoxins in human intestine. Gastroenterology *89*, 27–35.

Honda, T., Tsuji, T., Takeda, Y., and Miwatani, T. (1981). Immunological nonidentity of heat-labile enterotoxins from human and porcine enterotoxigenic *Escherichia coli*. Infect Immun *34*, 337–340.

Hooks, K.B., and O'Malley, M.A. (2017). Dysbiosis and Its Discontents. MBio *8*.

Horn, N., and Bhunia, A.K. (2018). Food-Associated Stress Primes Foodborne Pathogens for the Gastrointestinal Phase of Infection. Front Microbiol *9*.

Hornbuckle, W.E., Simpson, K.W., and Tennant, B.C. (2008). Chapter 14 - Gastrointestinal Function. In Clinical Biochemistry of Domestic Animals (Sixth Edition), J.J. Kaneko, J.W. Harvey, and M.L. Bruss, eds. (San Diego: Academic Press), pp. 413–457.

Hosseini, E., Grootaert, C., Verstraete, W., and Van de Wiele, T. (2011). Propionate as a health-promoting microbial metabolite in the human gut. Nutr. Rev. *69*, 245–258.

House, B., Kus, J.V., Prayitno, N., Mair, R., Que, L., Chingcuanco, F., Gannon, V., Cvitkovitch, D.G., and Barnett Foster, D. (2009). Acid-stress-induced changes in enterohaemorrhagic *Escherichia coli* O157 : H7 virulence. Microbiology (Reading, Engl.) *155*, 2907–2918.

Hudson, L.E., McDermott, C.D., Stewart, T.P., Hudson, W.H., Rios, D., Fasken, M.B., Corbett, A.H., and Lamb, T.J. (2016). Characterization of the Probiotic Yeast *Saccharomyces boulardii* in the Healthy Mucosal Immune System. PLoS ONE *11*, e0153351.

Hsiao, E.Y., McBride, S.W., Hsien, S., Sharon, G., Hyde, E.R., McCue, T., Codelli, J.A., Chow, J., Reisman, S.E., Petrosino, J.F., et al. (2013). Microbiota modulate behavioral and physiological abnormalities associated with neurodevelopmental disorders. Cell *155*, 1451–1463.

Huijsdens, X.W., Linskens, R.K., Mak, M., Meuwissen, S.G.M., Vandenbroucke-Grauls, C.M.J.E., and Savelkoul, P.H.M. (2002). Quantification of bacteria adherent to gastrointestinal mucosa by real-time PCR. J. Clin. Microbiol. *40*, 4423–4427.

Hunt, R.H., Camilleri, M., Crowe, S.E., El-Omar, E.M., Fox, J.G., Kuipers, E.J., Malfertheiner, P., McColl, K.E.L., Pritchard, D.M., Rugge, M., et al. (2015). The stomach in health and disease. Gut *64*, 1650–1668.

I

Ingram, L.O. (1990). Ethanol tolerance in bacteria. Crit. Rev. Biotechnol. *9*, 305–319.

Isidean, S.D., Riddle, M.S., Savarino, S.J., and Porter, C.K. (2011). A systematic review of ETEC epidemiology focusing on colonization factor and toxin expression. Vaccine *29*, 6167–6178.

J

Jalanka, J., Salonen, A., Fuentes, S., and de Vos, W.M. (2015). Microbial signatures in post-infectious irritable bowel syndrome – toward patient stratification for improved diagnostics and treatment. Gut Microbes *6*, 364–369.

Jeffery, I.B., O'Toole, P.W., Öhman, L., Claesson, M.J., Deane, J., Quigley, E.M.M., and Simrén, M. (2012). An irritable bowel syndrome subtype defined by species-specific alterations in faecal microbiota. Gut *61*, 997–1006.

Joffré, E. (2015). Genetic diversity of the heat labile (LT) and heat stable (ST) toxins of human enterotoxigenic *Escherichia coli* (ETEC): New insights into polymorphism, regulation, and gene transcription.

Joffré, E., and Sjöling, Å. (2016). The LT1 and LT2 variants of the enterotoxigenic *Escherichia coli* (ETEC) heat-labile toxin (LT) are associated with major ETEC lineages. Gut Microbes *7*, 75–81.

Johansson, M.E.V., Sjövall, H., and Hansson, G.C. (2013). The gastrointestinal mucus system in health and disease. Nat Rev Gastroenterol Hepatol *10*, 352–361.

Johnson, W.M., Lior, H., and Johnson, K.G. (1978). Heat-stable enterotoxin from *Escherichia coli*: factors involved in growth and toxin production. Infect Immun *20*, 352–359.

Johnson, A.M., Kaushik, R.S., Francis, D.H., Fleckenstein, J.M., and Hardwidge, P.R. (2009). Heat-Labile Enterotoxin Promotes *Escherichia coli* Adherence to Intestinal Epithelial Cells. J Bacteriol *191*, 178–186.

Jubelin, G., Desvaux, M., Schüller, S., Etienne-Mesmin, L., Muniesa, M., and Blanquet-Diot, S. (2018). Modulation of Enterohaemorrhagic *Escherichia coli* Survival and Virulence in the Human Gastrointestinal Tract. Microorganisms *6*, 115.

Jung, T.-H., Park, J.H., Jeon, W.-M., and Han, K.-S. (2015). Butyrate modulates bacterial adherence on LS174T human colorectal cells by stimulating mucin secretion and MAPK signaling pathway. Nutr Res Pract *9*, 343–349.

K

Kanai, T., Mikami, Y., and Hayashi, A. (2015). A breakthrough in probiotics: *Clostridium butyricum* regulates gut homeostasis and anti-inflammatory response in inflammatory bowel disease. J. Gastroenterol. *50*, 928–939.

Kane, A.V., Dinh, D.M., and Ward, H.D. (2015). Childhood Malnutrition and the Intestinal Microbiome Malnutrition and the microbiome. Pediatr Res *77*, 256–262.

Kansal, R., Rasko, D.A., Sahl, J.W., Munson, G.P., Roy, K., Luo, Q., Sheikh, A., Kuhne, K.J., and Fleckenstein, J.M. (2013). Transcriptional Modulation of Enterotoxigenic *Escherichia coli* Virulence Genes in Response to Epithelial Cell Interactions. Infect Immun *81*, 259–270.

Karimi, S., Rashidian, E., Birjandi, M., and Mahmoodnia, L. (2018). Antagonistic effect of isolated probiotic bacteria from natural sources against intestinal *Escherichia coli* pathotypes. Electron Physician *10*, 6534–6539.

Karjalainen, T.K., Evans, D.G., Evans, D.J., Graham, D.Y., and Lee, C.-H. (1991). Iron represses the expression of CFA/I fimbriae of enterotoxigenic *E. coli*. Microbial Pathogenesis *11*, 317–323.

Kennedy, D., Cronin, U.P., and Wilkinson, M.G. (2011). Responses of *Escherichia coli, Listeria monocytogenes,* and *Staphylococcus aureus* to Simulated Food Processing Treatments, Determined Using Fluorescence-Activated Cell Sorting and Plate Counting. Appl. Environ. Microbiol. *77*, 4657–4668.

Kern, M., Aschenbach, J.R., Tedin, K., Pieper, R., Loss, H., and Lodemann, U. (2017a). Characterization of Inflammasome Components in Pig Intestine and Analysis of the Influence of Probiotic *Enterococcus Faecium* during an *Escherichia Coli* Challenge. Immunol. Invest. *46*, 742–757.

Kern, M., Günzel, D., Aschenbach, J.R., Tedin, K., Bondzio, A., and Lodemann, U. (2017b). Altered Cytokine Expression and Barrier Properties after *In Vitro* Infection of Porcine Epithelial Cells with Enterotoxigenic *Escherichia coli* and Probiotic *Enterococcus faecium*. Mediators Inflamm. *2017*, 2748192.

Kerneis, S., Bernet, M.F., Coconnier, M.H., and Servin, A.L. (1994). Adhesion of human enterotoxigenic *Escherichia coli* to human mucus secreting HT-29 cell subpopulations in culture. Gut *35*, 1449–1454.

Kesty, N.C., Mason, K.M., Reedy, M., Miller, S.E., and Kuehn, M.J. (2004). Enterotoxigenic *Escherichia coli* vesicles target toxin delivery into mammalian cells. EMBO J *23*, 4538–4549.

Khafipour, E., Munyaka, P.M., Nyachoti, C.M., Krause, D.O., and Rodriguez-Lecompte, J.C. (2014). Effect of crowding stress and *Escherichia coli* K88+ challenge in nursery pigs supplemented with anti-*Escherichia coli* K88+ probiotics. J. Anim. Sci. *92*, 2017–2029.

Khalighi, A., Behdani, R., and Kouhestani, S. (2016). Probiotics: A Comprehensive Review of Their Classification, Mode of Action and Role in Human Nutrition. In Probiotics and Prebiotics in Human Nutrition and Health, V. Rao, and L.G. Rao, eds. (InTech), p.

Khan, I., Al-Awadi, F.M., and Abul, H. (1998). Colitis-Induced Changes in the Expression of the Na+/H+ Exchanger Isoform NHE-1. J Pharmacol Exp Ther *285*, 869–875.

Kitamoto, S., Nagao-Kitamoto, H., Kuffa, P., and Kamada, N. (2016). Regulation of virulence: The rise and fall of gastrointestinal pathogens. Journal of Gastroenterology *51*, 195.

Klapperstück, T., Glanz, D., Klapperstück, M., and Wohlrab, J. (2009). Methodological aspects of measuring absolute values of membrane potential in human cells by flow cytometry. Cytometry A *75*, 593–608.

Kleiveland, C.R. (2015). Co-cultivation of Caco-2 and HT-29MTX. In The Impact of Food Bioactives on Health: *In Vitro* and *Ex Vivo* Models, K. Verhoeckx, P. Cotter, I. López-Expósito, C. Kleiveland, T. Lea, A. Mackie, T. Requena, D. Swiatecka, and H. Wichers, eds. (Cham: Springer International Publishing), pp. 135–140.

Klingberg, T.D., Lesnik, U., Arneborg, N., Raspor, P., and Jespersen, L. (2008). Comparison of *Saccharomyces cerevisiae* strains of clinical and nonclinical origin by molecular typing and determination of putative virulence traits. FEMS Yeast Res *8*, 631–640.

Klingspor, S., Bondzio, A., Martens, H., Aschenbach, J.R., Bratz, K., Tedin, K., Einspanier, R., and Lodemann, U. (2015). *Enterococcus faecium* NCIMB 10415 modulates epithelial integrity, heat shock protein, and proinflammatory cytokine response in intestinal cells. Mediators Inflamm. *2015*, 304149.

Klipstein, F.A., Engert, R.F., and Houghten, R.A. (1983). Immunological properties of purified *Klebsiella pneumoniae* heat-stable enterotoxin. Infect Immun *42*, 838–841.

Klymiuk, I., Bilgilier, C., Stadlmann, A., Thannesberger, J., Kastner, M.-T., Högenauer, C., Püspök, A., Biowski-Frotz, S., Schrutka-Kölbl, C., Thallinger, G.G., et al. (2017). The Human Gastric Microbiome Is Predicated upon Infection with *Helicobacter pylori*. Front. Microbiol. *8*.

Knights, D., Ward, T.L., McKinlay, C.E., Miller, H., Gonzalez, A., McDonald, D., and Knight, R. (2014). Rethinking “enterotypes.” Cell Host Microbe *16*, 433–437.

Knutton, S., Lloyd, D.R., Candy, D.C., and McNeish, A.S. (1985). Adhesion of enterotoxigenic *Escherichia coli* to human small intestinal enterocytes. Infect Immun *48*, 824–831.

Kobayashi, H., Albarracin, L., Sato, N., Kanmani, P., Kober, A.K.M.H., Ikeda-Ohtsubo, W., Suda, Y., Nochi, T., Aso, H., Makino, S., et al. (2016). Modulation of porcine intestinal epitheliocytes immunetranscriptome response by *Lactobacillus jensenii* TL2937. Beneficial Microbes *7*, 769–782.

Kobayashi, I., Kozu, H., Wang, Z., Isoda, H., and Ichikawa, S. (2017). Development and Fundamental Characteristics of a Human Gastric Digestion Simulator for Analysis of Food Disintegration. JARQ *51*, 17–25.

Kohanski, M.A., Dwyer, D.J., Hayete, B., Lawrence, C.A., and Collins, J.J. (2007). A common mechanism of cellular death induced by bactericidal antibiotics. Cell *130*, 797–810.

Kong, F., and Singh, R.P. (2010). A human gastric simulator (HGS) to study food digestion in human stomach. J. Food Sci. *75*, E627-635.

Kong, S., Zhang, Y.H., and Zhang, W. (2018). Regulation of Intestinal Epithelial Cells Properties and Functions by Amino Acids. Biomed Res Int *2018*.

Konstantinov, S.R., Smidt, H., Akkermans, A.D.L., Casini, L., Trevisi, P., Mazzoni, M., De Filippi, S., Bosi, P., and de Vos, W.M. (2008). Feeding of *Lactobacillus sobrius* reduces *Escherichia coli* F4 levels in the gut and promotes growth of infected piglets. FEMS Microbiol. Ecol. *66*, 599–607.

Kotloff, K.L., Nataro, J.P., Blackwelder, W.C., Nasrin, D., Farag, T.H., Panchalingam, S., Wu, Y., Sow, S.O., Sur, D., Breiman, R.F., et al. (2013). Burden and aetiology of diarrhoeal disease in infants and young children in developing countries (the Global Enteric Multicenter Study, GEMS): a prospective, case-control study. Lancet *382*, 209–222.

Kotwani, A., Chaudhury, R.R., and Holloway, K. (2012). Antibiotic-prescribing practices of primary care prescribers for acute diarrhea in New Delhi, India. Value Health *15*, S116-119.

Kozich, J.J., Westcott, S.L., Baxter, N.T., Highlander, S.K., and Schloss, P.D. (2013). Development of a dual-index sequencing strategy and curation pipeline for analyzing amplicon sequence data on the MiSeq Illumina sequencing platform. Appl. Environ. Microbiol. *79*, 5112–5120.

Krezalek, M.A., DeFazio, J., Zaborina, O., Zaborin, A., and Alverdy, J.C. (2016). The shift of an intestinal “microbiome” to a “pathobiome” governs the course and outcome of sepsis following surgical injury. Shock *45*, 475–482.

Kumar, P., Luo, Q., Vickers, T.J., Sheikh, A., Lewis, W.G., and Fleckenstein, J.M. (2014). EatA, an immunogenic protective antigen of enterotoxigenic *Escherichia coli*, degrades intestinal mucin. Infect Immun *82*, 500–508.

Kumar, P., Kuhlmann, F.M., Bhullar, K., Yang, H., Vallance, B.A., Xia, L., Luo, Q., and Fleckenstein, J.M. (2016). Dynamic Interactions of a Conserved Enterotoxigenic *Escherichia coli* Adhesin with Intestinal Mucins Govern Epithelium Engagement and Toxin Delivery. Infect. Immun. *84*, 3608–3617.

Kunkel, S.L., and Robertson, D.C. (1979). Factors Affecting Release of Heat-Labile Enterotoxin by Enterotoxigenic *Escherichia coli*. Infect Immun *23*, 652–659.

L

Lääveri, T., Sterne, J., Rombo, L., and Kantele, A. (2016). Systematic review of loperamide: No proof of antibiotics being superior to loperamide in treatment of mild/moderate travellers’ diarrhoea. Travel Medicine and Infectious Disease *14*, 299–312.

Lääveri, T., Vilkman, K., Pakkanen, S.H., Kirveskari, J., and Kantele, A. (2018). A prospective study of travellers' diarrhoea: analysis of pathogen findings by destination in various (sub)tropical regions. Clin. Microbiol. Infect. *24*, 908.e9-908.e16.

Lamberti, L.M., Bourgeois, A.L., Fischer Walker, C.L., Black, R.E., and Sack, D. (2014). Estimating Diarrheal Illness and Deaths Attributable to Shigellae and Enterotoxigenic *Escherichia coli* among Older Children, Adolescents, and Adults in South Asia and Africa. PLoS Negl Trop Dis *8*.

Larsen, J.M. (2017). The immune response to *Prevotella* bacteria in chronic inflammatory disease. Immunology 151, 363–374.

Lasaro, M.A.S., Rodrigues, J.F., Mathias-Santos, C., Guth, B.E.C., Régua-Mangia, A., Piantino Ferreira, A.J., Takagi, M., Cabrera-Crespo, J., Sbrogio-Almeida, M.E., and de Souza Ferreira, L.C. (2006). Production and release of heat-labile toxin by wild-type human-derived enterotoxigenic *Escherichia coli*. FEMS Immunol. Med. Microbiol. *48*, 123–131.

Lawhon, S.D., Maurer, R., Suyemoto, M., and Altier, C. (2002). Intestinal short-chain fatty acids alter *Salmonella typhimurium* invasion gene expression and virulence through BarA/SirA. Mol. Microbiol. *46*, 1451–1464.

Leber, J.H., Crimmins, G.T., Raghavan, S., Meyer-Morse, N.P., Cox, J.S., and Portnoy, D.A. (2008). Distinct TLR- and NLR-Mediated Transcriptional Responses to an Intracellular Pathogen. PLOS Pathogens *4*, e6.

Lee, B.J., and Bak, Y.-T. (2011). Irritable Bowel Syndrome, Gut Microbiota and Probiotics. J Neurogastroenterol Motil *17*, 252–266.

Lee, C.Y., Kim, S.J., Park, B.C., and Han, J.H. (2017). Effects of dietary supplementation of bacteriophages against enterotoxigenic *Escherichia coli* (ETEC) K88 on clinical symptoms of post-weaning pigs challenged with the ETEC pathogen. J Anim Physiol Anim Nutr (Berl) *101*, 88–95.

Lee, J.S., Awji, E.G., Lee, S.J., Tassew, D.D., Park, Y.B., Park, K.S., Kim, M.K., Kim, B., and Park, S.C. (2012). Effect of *Lactobacillus plantarum* CJLP243 on the growth performance and cytokine response of weaning pigs challenged with enterotoxigenic *Escherichia coli*. J. Anim. Sci. *90*, 3709–3717.

van der Lelie, D., Taghavi, S., Henry, C., and Gilbert, J.A. (2017). The microbiome as a source of new enterprises and job creation: Considering clinical faecal and synthetic microbiome transplants and therapeutic regulation. Microb Biotechnol *10*, 4–5.

Ley, R.E., Turnbaugh, P.J., Klein, S., and Gordon, J.I. (2006). Microbial ecology: human gut microbes associated with obesity. Nature *444*, 1022–1023.

van der Lelie, D., Taghavi, S., Henry, C., and Gilbert, J.A. (2017). The microbiome as a source of new enterprises and job creation: Considering clinical faecal and synthetic microbiome transplants and therapeutic regulation. Microb Biotechnol *10*, 4–5.

Letunic, I., and Bork, P. (2016). Interactive tree of life (iTOL) v3: an online tool for the display and annotation of phylogenetic and other trees. Nucleic Acids Res. *44*, W242-245.

Levi, C.S., and Lesmes, U. (2014). Bi-compartmental elderly or adult dynamic digestion models applied to interrogate protein digestibility. Food Funct *5*, 2402–2409.

Levine, M.M., Nalin, D.R., Hoover, D.L., Bergquist, E.J., Hornick, B., and Young, C.R. (1979). Immunity to Enterotoxigenic *Escherichia coli*. Infect Immun *23*, 8.

Levitz, S.M., and Specht, C.A. (2009). Recognition of the fungal cell wall by innate immune receptors. Current Fungal Infection Reports *3*, 179–185.

Li, B., and Chen, J.-Q. (2013). Development of a sensitive and specific qPCR assay in conjunction with propidium monoazide for enhanced detection of live *Salmonella spp.* in food. BMC Microbiology *13*, 273.

Li, H., Zhang, L., Chen, L., Zhu, Q., Wang, W., and Qiao, J. (2016). *Lactobacillus acidophilus* alleviates the inflammatory response to enterotoxigenic *Escherichia coli* K88 via inhibition of the NF-κB and p38 mitogen-activated protein kinase signaling pathways in piglets. BMC Microbiology *16*, 273.

Li, X.-Q., Zhu, Y.-H., Zhang, H.-F., Yue, Y., Cai, Z.-X., Lu, Q.-P., Zhang, L., Weng, X.-G., Zhang, F.-J., Zhou, D., et al. (2012a). Risks associated with high-dose *Lactobacillus rhamnosus* in an *Escherichia coli* model of piglet diarrhoea: intestinal microbiota and immune imbalances. PLoS ONE *7*, e40666.

Li, Y., Kundu, P., Seow, S.W., Matos, D., Teixeira, C., Aronsson, L., Chin, K.C., Kärre, K., Pettersson, S., and Greicius, G. (2012b). Gut microbiota accelerate tumor growth via c-jun and STAT3 phosphorylation in APC Min/+ mice. Carcinogenesis *33*, 1231–1238.

Li, Y.-F., Poole, S., Nishio, K., Jang, K., Rasulova, F., McVeigh, A., Savarino, S.J., Xia, D., and Bullitt, E. (2009). Structure of CFA/I fimbriae from enterotoxigenic *Escherichia coli*. Proc Natl Acad Sci USA *106*, 10793–10798.

Liévin-Le Moal, V., and Servin, A.L. (2006). The front line of enteric host defense against unwelcome intrusion of harmful microorganisms: mucins, antimicrobial peptides, and microbiota. Clin. Microbiol. Rev. *19*, 315–337.

Liévin-Le Moal, V., and Servin, A.L. (2013). Pathogenesis of human enterovirulent bacteria: lessons from cultured, fully differentiated human colon cancer cell lines. Microbiol. Mol. Biol. Rev. *77*, 380–439.

Lin, L., and Zhang, J. (2017). Role of intestinal microbiota and metabolites on gut homeostasis and human diseases. BMC Immunology *18*, 2.

Linden, S.K., Sutton, P., Karlsson, N.G., Korolik, V., and McGuckin, M.A. (2008). Mucins in the mucosal barrier to infection. Mucosal Immunol *1*, 183–197.

Lindenthal, C., and Elsinghorst, E.A. (1999). Identification of a glycoprotein produced by enterotoxigenic *Escherichia coli*. Infect Immun *67*, 4084–4091.

Lodemann, U., Strahlendorf, J., Schierack, P., Klingspor, S., Aschenbach, J.R., and Martens, H. (2015). Effects of the Probiotic *Enterococcus faecium* and Pathogenic *Escherichia coli* Strains in a Pig and Human Epithelial Intestinal Cell Model. Scientifica (Cairo) *2015*, 235184.

Long, K.Z., Santos, J.I., Rosado, J.L., Lopez-Saucedo, C., Thompson-Bonilla, R., Abonce, M., DuPont, H.L., Hertzmark, E., and Estrada-Garcia, T. (2006). Impact of Vitamin A on Selected Gastrointestinal Pathogen Infections and Associated Diarrheal Episodes among Children in Mexico City, Mexico. J Infect Dis *194*, 1217–1225.

Long, K.Z., Rosado, J.L., Santos, J.I., Haas, M., Mamun, A.A., DuPont, H.L., Nanthakumar, N.N., and Estrada-Garcia, T. (2010). Associations between Mucosal Innate and Adaptive Immune Responses and Resolution of Diarrheal Pathogen Infections. Infect Immun *78*, 1221–1228.

Looft, T., Levine, U.Y., Stanton, T.B. (2013). *Cloacibacillus porcorum sp. nov.*, a mucin-degrading bacterium from the swine intestinal tract and emended description of the genus *Cloacibacillus*. Int. J. Syst. Evol. Microbiol. 63, 1960–1966.

Lothigius, A., Janzon, A., Begum, Y., Sjöling, A., Qadri, F., Svennerholm, A.-M., and Bölin, I. (2008). Enterotoxigenic *Escherichia coli* is detectable in water samples from an endemic area by real-time PCR. J. Appl. Microbiol. *104*, 1128–1136.

Louis, P., Hold, G.L., and Flint, H.J. (2014). The gut microbiota, bacterial metabolites and colorectal cancer. Nat. Rev. Microbiol. *12*, 661–672.

Love, M.I., Huber, W., and Anders, S. (2014). Moderated estimation of fold change and dispersion for RNA-seq data with DESeq2. Genome Biol. *15*, 550.

Lu, X., Fu, E., Xie, Y., and Jin, F. (2016). Electron Acceptors Induce Secretion of Enterotoxigenic

Escherichia coli Heat-Labile Enterotoxin under Anaerobic Conditions through Promotion of GspD Assembly. Infect Immun *84*, 2748–2757.

Lund, P., Tramonti, A., and De Biase, D. (2014). Coping with low pH: molecular strategies in neutralophilic bacteria. FEMS Microbiol Rev *38*, 1091–1125.

Luo, Q., Kumar, P., Vickers, T.J., Sheikh, A., Lewis, W.G., Rasko, D.A., Sistrunk, J., and Fleckenstein, J.M. (2014). Enterotoxigenic *Escherichia coli* Secretes a Highly Conserved Mucin-Degrading Metalloprotease To Effectively Engage Intestinal Epithelial Cells. Infect Immun *82*, 509–521.

Luppi, A. (2017). Swine enteric colibacillosis: diagnosis, therapy and antimicrobial resistance. Porcine Health Manag *3*, 16.

Lyte, M., Arulanandam, B., Nguyen, K., Frank, C., Erickson, A., and Francis, D. (1997). Norepinephrine induced growth and expression of virulence associated factors in enterotoxigenic and enterohemorrhagic strains of *Escherichia coli.* Adv. Exp. Med. Biol. *412*, 331–339.

M

MacDonald, E., Møller, K.E., Wester, A.L., Dahle, U.R., Hermansen, N.O., Jenum, P.A., Thoresen, L., and Vold, L. (2015). An outbreak of enterotoxigenic *Escherichia coli* (ETEC) infection in Norway, 2012: a reminder to consider uncommon pathogens in outbreaks involving imported products. Epidemiol. Infect. *143*, 486–493.

Macfarlane, S., and Macfarlane, G.T. (2003). Regulation of short-chain fatty acid production. Proc Nutr Soc *62*, 67–72.

Madec, F., Bridoux, N., Bounaix, S., Cariolet, R., Duval-Iflah, Y., Hampson, D.J., and Jestin, A. (2000). Experimental models of porcine post-weaning colibacillosis and their relationship to post-weaning diarrhoea and digestive disorders as encountered in the field. Vet. Microbiol. *72*, 295–310.

Madhavan, T.P.V. (2018). Rns regulates nonpilus adhesin EtpA in human Enterotoxigenic *E. coli* (ETEC). BioRxiv 362178.

Madhavan, T.P.V., and Sakellaris, H. (2015). Colonization factors of enterotoxigenic *Escherichia coli*. Adv. Appl. Microbiol. *90*, 155–197.

Madhavan, T.P.V., Riches, J.D., Scanlon, M.J., Ulett, G.C., and Sakellaris, H. (2016). Binding of CFA/I Pili of Enterotoxigenic *Escherichia coli* to Asialo-GM1 Is Mediated by the Minor Pilin CfaE. Infect Immun *84*, 1642–1649.

Madigan, M.T. (2012). Brock Biology of Microorganisms (Benjamin Cummings).

Maechler, M., Rousseeuw, P., Struyf, A., Hubert, M., and Hornik, K. (2016) cluster: Cluster analysis basics and extensions. r package version 2.0.4. Tech. rep.

Mainville, I., Arcand, Y., and Farnworth, E.R. (2005). A dynamic model that simulates the human upper gastrointestinal tract for the study of probiotics. Int. J. Food Microbiol. *99*, 287–296.

Mäkivuokko, H., Kettunen, H., Saarinen, M., Kamiwaki, T., Yokoyama, Y., Stowell, J., and Rautonen, N. (2007). The effect of cocoa and polydextrose on bacterial fermentation in gastrointestinal tract simulations. Biosci. Biotechnol. Biochem. *71*, 1834–1843.

Malagelada, J.R., Go, V.L., and Summerskill, W.H. (1979). Different gastric, pancreatic, and biliary responses to solid-liquid or homogenized meals. Dig. Dis. Sci. *24*, 101–110.

Malinen, E., Krogius-Kurikka, L., Lyra, A., Nikkilä, J., Jääskeläinen, A., Rinttilä, T., Vilpponen-Salmela, T., von Wright, A.J., and Palva, A. (2010). Association of symptoms with gastrointestinal microbiota in irritable bowel syndrome. World J Gastroenterol *16*, 4532–4540.

Malinen, E., Rinttilä, T., Kajander, K., Mättö, J., Kassinen, A., Krogius, L., Saarela, M., Korpela, R., and Palva, A. (2005). Analysis of the fecal microbiota of irritable bowel syndrome patients and healthy controls with real-time PCR. Am. J. Gastroenterol. *100*, 373–382.

Mann, E.R., Bernardo, D., English, N.R., Landy, J., Al-Hassi, H.O., Peake, S.T., Man, R., Elliott, T.R., Spranger, H., Lee, G.H., et al. (2016). Compartment-specific immunity in the human gut: properties and functions of dendritic cells in the colon versus the ileum. Gut *65*, 256–270.

Martin, R.M., and Bachman, M.A. (2018). Colonization, Infection, and the Accessory Genome of *Klebsiella pneumoniae*. Front Cell Infect Microbiol *8*.

Marzorati, M., Vanhoecke, B., De Ryck, T., Sadaghian Sadabad, M., Pinheiro, I., Possemiers, S., Van den Abbeele, P., Derycke, L., Bracke, M., Pieters, J., et al. (2014). The HMI™ module: a new tool to study the Host-Microbiota Interaction in the human gastrointestinal tract *in vitro*. BMC Microbiol. *14*, 133.

Masters, C.I., Shallcross, J.A., and Mackey, B.M. (1994). Effect of stress treatments on the detection of *Listeria monocytogenes* and enterotoxigenic *Escherichia coli* by the polymerase chain reaction. J. Appl. Bacteriol. *77*, 73–79.

Masuda, N., and Church, G.M. (2002). *Escherichia coli* gene expression responsive to levels of the response regulator EvgA. J. Bacteriol. *184*, 6225–6234.

McFarland, L.V. (2007). Meta-analysis of probiotics for the prevention of traveler's diarrhea. Travel Med Infect Dis *5*, 97–105.

McFarland, L.V., Evans, C.T., and Goldstein, E.J.C. (2018). Strain-Specificity and Disease-Specificity of Probiotic Efficacy: A Systematic Review and Meta-Analysis. Front Med (Lausanne) *5*, 124.

McMurdie, P.J., and Holmes, S. (2014). Waste not, want not: why rarefying microbiome data is inadmissible. PLoS Comput. Biol. *10*, e1003531.

McNabney, S.M., and Henagan, T.M. (2017). Short Chain Fatty Acids in the Colon and Peripheral Tissues: A Focus on Butyrate, Colon Cancer, Obesity and Insulin Resistance. Nutrients *9*.

Medellin-Peña, M.J., Wang, H., Johnson, R., Anand, S., and Griffiths, M.W. (2007). Probiotics Affect Virulence-Related Gene Expression in *Escherichia coli* O157:H7. Appl. Environ. Microbiol. *73*, 4259–4267.

Ménard, O., Cattenoz, T., Guillemin, H., Souchon, I., Deglaire, A., Dupont, D., and Picque, D. (2014). Validation of a new *in vitro* dynamic system to simulate infant digestion. Food Chem *145*, 1039–1045.

von Mentzer, A., Connor, T.R., Wieler, L.H., Semmler, T., Iguchi, A., Thomson, N.R., Rasko, D.A., Joffre, E., Corander, J., Pickard, D., et al. (2014). Identification of enterotoxigenic *Escherichia coli* (ETEC) clades with long-term global distribution. Nat. Genet. *46*, 1321–1326.

Mercado, E.H., Ochoa, T.J., Ecker, L., Cabello, M., Durand, D., Barletta, F., Molina, M., Gil, A.I., Huicho, L., Lanata, C.F., et al. (2011). Fecal leukocytes in children infected with diarrheagenic *Escherichia coli*. J. Clin. Microbiol. *49*, 1376–1381.

Mercuri, A., Passalacqua, A., Wickham, M.S.J., Faulks, R.M., Craig, D.Q.M., and Barker, S.A. (2011). The effect of composition and gastric conditions on the self-emulsification process of ibuprofen-loaded self-emulsifying drug delivery systems: a microscopic and dynamic gastric model study. Pharm. Res. *28*, 1540–1551.

Messerer, M., Fischer, W., and Schubert, S. (2017). Investigation of horizontal gene transfer of pathogenicity islands in *Escherichia coli* using next-generation sequencing. PLoS One *12*.

Miller, M.A., Parkman, H.P., Urbain, J.-L.C., Brown, K.L., Donahue, D.J., Knight, L.C., Maurer, A.H., and Fisher, R.S. (1997). Comparison of Scintigraphy and Lactulose Breath Hydrogen Test for Assessment of Orocecal Transit (Lactulose Accelerates Small Bowel Transit). Dig Dis Sci *42*, 10–18.

Minekus, M. (2015). The TNO Gastro-Intestinal Model (TIM). In The Impact of Food Bioactives on Health: In Vitro and Ex Vivo Models, K. Verhoeckx, P. Cotter, I. López-Expósito, C. Kleiveland, T. Lea, A. Mackie, T. Requena, D. Swiatecka, and H. Wichers, eds. (Cham: Springer International Publishing), pp. 37–46.

Minekus, M., Marteau, P., Havenaar, R., and Huis in 't Veld, J.H.H. (1995). multicompartmental dynamic computer-controlled model simulating the stomach and small intestine. Alternatives to Laboratory Animals : ATLA.

Minekus, M., Smeets-Peeters, M., Bernalier, A., Marol-Bonnin, S., Havenaar, R., Marteau, P., Alric, M., Fonty, G., and Huis in't Veld, J.H. (1999). A computer-controlled system to simulate conditions of the large intestine with peristaltic mixing, water absorption and absorption of fermentation products. Appl. Microbiol. Biotechnol. *53*, 108–114.

Mirnejad, R., Hossein, J., and Ardebilli, A. (2010). Reduction of enterotoxigenic *Escherichia coli* colonization by the oral administration of *Lactobacillus casei* as a probiotic in a murine model. Afr. J. Microbiol. Res. 5.

Mitterdorfer, G., Mayer, H.K., Kneifel, W., Viernstein, H. (2002). Clustering of *Saccharomyces boulardii* strains within the species *S. cerevisiae* using molecular typing techniques. J. Appl. Microbiol. *93*, 521–530.

Moens, F., Weckx, S., and De Vuyst, L. (2016). Bifidobacterial inulin-type fructan degradation capacity determines cross-feeding interactions between *Bifidobacteria* and *Faecalibacterium prausnitzii*. International Journal of Food Microbiology *231*, 76–85.

Mogensen, T.H. (2009). Pathogen recognition and inflammatory signaling in innate immune defenses. Clin. Microbiol. Rev. *22*, 240–273, Table of Contents.

Mokomane, M., Kasvosve, I., de Melo, E., Pernica, J.M., and Goldfarb, D.M. (2018). The global problem of childhood diarrhoeal diseases: emerging strategies in prevention and management. Ther Adv Infect Dis *5*, 29–43.

Molly, K., Woestyne, M.V., Smet, I.D., and Verstraete, W. (1994). Validation of the Simulator of the Human Intestinal Microbial Ecosystem (SHIME) Reactor Using Microorganism-associated Activities. Microbial Ecology in Health and Disease *7*, 191–200.

Monira, S., Nakamura, S., Gotoh, K., Izutsu, K., Watanabe, H., Alam, N.H., Endtz, H.P., Cravioto, A., Ali, S.I., Nakaya, T., et al. (2011). Gut Microbiota of Healthy and Malnourished Children in Bangladesh. Front Microbiol *2*.

Morabito, S. (2014). Pathogenic *Escherichia coli* (Caister Academic Press).

Moré, M.I., and Swidsinski, A. (2015). *Saccharomyces boulardii* CNCM I-745 supports regeneration of the intestinal microbiota after diarrheic dysbiosis – a review. Clin Exp Gastroenterol *8*, 237–255.

Moredo, F.A., Piñeyro, P.E., Márquez, G.C., Sanz, M., Colello, R., Etcheverría, A., Padola, N.L., Quiroga, M.A., Perfumo, C.J., Galli, L., et al. (2015). Enterotoxigenic *Escherichia coli* Subclinical Infection in Pigs: Bacteriological and Genotypic Characterization and Antimicrobial Resistance Profiles. Foodborne Pathog. Dis. *12*, 704–711.

Morrison, D.J., and Preston, T. (2016). Formation of short chain fatty acids by the gut microbiota and their impact on human metabolism. Gut Microbes *7*, 189–200.

Mortezaei, N., Singh, B., Zakrisson, J., Bullitt, E., and Andersson, M. (2015). Biomechanical and structural features of CS2 fimbriae of enterotoxigenic *Escherichia coli*. Biophys. J. *109*, 49–56.

Mouricout, M.A., and Julien, R.A. (1987). Pilus-mediated binding of bovine enterotoxigenic *Escherichia coli* to calf small intestinal mucins. Infect Immun *55*, 1216–1223.

Mudie, D.M., Murray, K., Hoad, C.L., Pritchard, S.E., Garnett, M.C., Amidon, G.L., Gowland, P.A., Spiller, R.C., Amidon, G.E., and Marciani, L. (2014). Quantification of Gastrointestinal Liquid Volumes and Distribution Following a 240 mL Dose of Water in the Fasted State. Molecular Pharmaceutics *11*, 3039–3047.

Mudrak, B., and Kuehn, M.J. (2010). Heat-Labile Enterotoxin: Beyond GM1 Binding. Toxins (Basel) *2*, 1445–1470.

Murata, K., Tomosada, Y., Villena, J., Chiba, E., Shimazu, T., Aso, H., Iwabuchi, N., Xiao, J., Saito, T., and Kitazawa, H. (2014). Bifidobacterium breve MCC-117 Induces Tolerance in Porcine Intestinal Epithelial Cells: Study of the Mechanisms Involved in the Immunoregulatory Effect. Biosci Microbiota Food Health *33*, 1–10.

N

Nair, P., Okhuysen, P.C., Jiang, Z.-D., Carlin, L.G., Belkind-Gerson, J., Flores, J., Paredes, M., and DuPont, H.L. (2014). Persistent Abdominal Symptoms in US Adults After Short-Term Stay in Mexico. J Travel Med *21*, 153–158.

Nataro, J.P., and Kaper, J.B. (1998). Diarrheagenic *Escherichia coli*. Clin. Microbiol. Rev. *11*, 142–201.

Ng, K.M., Ferreyra, J.A., Higginbottom, S.K., Lynch, J.B., Kashyap, P.C., Gopinath, S., Naidu, N., Choudhury, B., Weimer, B.C., Monack, D.M., et al. (2013). Microbiota-liberated host sugars facilitate post-antibiotic expansion of enteric pathogens. Nature *502*, 96–99.

Nicklasson, M., Sjöling, Å., Mentzer, A. von, Qadri, F., and Svennerholm, A.-M. (2012). Expression of Colonization Factor CS5 of Enterotoxigenic *Escherichia coli* (ETEC) Is Enhanced *In Vivo* and by the Bile Component Na Glycocholate Hydrate. PLOS ONE *7*, e35827.

Noel, G., Doucet, M., Nataro, J.P., Kaper, J.B., Zachos, N.C., and Pasetti, M.F. (2018). Enterotoxigenic *Escherichia coli* is phagocytosed by macrophages underlying villus-like intestinal epithelial cells: modeling *ex vivo* innate immune defenses of the human gut. Gut Microbes *9*, 382–389.

Northfield, T.C., and McColl, I. (1973). Postprandial concentrations of free and conjugated bile acids down the length of the normal human small intestine. Gut *14*, 513–518.

Novo, D., Perlmutter, N.G., Hunt, R.H., and Shapiro, H.M. (1999). Accurate flow cytometric membrane potential measurement in bacteria using diethyloxacarbocyanine and a ratiometric technique. Cytometry *35*, 55–63.

Nuccio, S.-P., and Bäumler, A.J. (2007). Evolution of the Chaperone/Usher Assembly Pathway: Fimbrial Classification Goes Greek. Microbiol. Mol. Biol. Rev. *71*, 551–575.

O

O'Donnell, M.M., Rea, M.C., O'Sullivan, Ó., Flynn, C., Jones, B., McQuaid, A., Shanahan, F., and Ross, R.P. (2016). Preparation of a standardised faecal slurry for *ex-vivo* microbiota studies which reduces inter-individual donor bias. J. Microbiol. Methods *129*, 109–116.

Oh, P.L., Martínez, I., Sun, Y., Walter, J., Peterson, D.A., and Mercer, D.F. (2012). Characterization of the Ileal Microbiota in Rejecting and Nonrejecting Recipients of Small Bowel Transplants: Microbiota Changes Associated with Intestinal Allograft Rejection. American Journal of Transplantation *12*, 753–762.

O'Hara, A.M., and Shanahan, F. (2006). The gut flora as a forgotten organ. EMBO Rep *7*, 688–693.

Oksanen, J., Blanchet, G., Friendly, M., Kindt, R., Legendre, P., McGlinn, D., Minchin, P., O'Hara, R., Simpson, G., Solymos, P., Stevens, H., Szoecs, E., and Wagner, H. (2016) Vegan: Community Ecology Package. R package version 2.4-0. https://CRAN.Rproject.org/package=vegan. Tech. rep.

Orlean, P. (2012). Architecture and biosynthesis of the *Saccharomyces cerevisiae* cell wall. Genetics *192*, 775–818.

Osmanagaoglu, O., Kiran, F., and Ataoglu, H. (2010). Evaluation of *in vitro* Probiotic Potential of *Pediococcus pentosaceus* OZF Isolated from Human Breast Milk. Probiotics Antimicrob Proteins *2*, 162–174.

Otterstedt, K., Larsson, C., Bill, R.M., Ståhlberg, A., Boles, E., Hohmann, S., and Gustafsson, L. (2004). Switching the mode of metabolism in the yeast *Saccharomyces cerevisiae*. EMBO Rep *5*, 532–537.

Otto, W., Najnigier, B., Stelmasiak, T., and Robins-Browne, R.M. (2011). Randomized control trials using a tablet formulation of hyperimmune bovine colostrum to prevent diarrhea caused by enterotoxigenic *Escherichia coli* in volunteers. Scand J Gastroenterol *46*, 862–868.

Ouwehand, A.C., ten Bruggencate, S.J.M., Schonewille, A.J., Alhoniemi, E., Forssten, S.D., and Bovee-Oudenhoven, I.M.J. (2014). *Lactobacillus acidophilus* supplementation in human subjects and their resistance to enterotoxigenic *Escherichia coli* infection. Br. J. Nutr. *111*, 465–473.

P

Pasqua, M., Michelacci, V., Di Martino, M.L., Tozzoli, R., Grossi, M., Colonna, B., Morabito, S., and Prosseda, G. (2017). The Intriguing Evolutionary Journey of Enteroinvasive *E. coli* (EIEC) toward Pathogenicity. Front Microbiol *8*.

van Passel, M.W.J., Kant, R., Palva, A., Lucas, S., Copeland, A., Lapidus, A., Glavina del Rio, T., Dalin, E., Tice, H., Bruce, D., et al. (2011). Genome Sequence of *Victivallis vadensis* ATCC BAA-548, an Anaerobic Bacterium from the Phylum Lentisphaerae, Isolated from the Human Gastrointestinal Tract. J Bacteriol *193*, 2373–2374.

Patrascu, O., Béguet-Crespel, F., Marinelli, L., Chatelier, E.L., Abraham, A.-L., Leclerc, M., Klopp, C., Terrapon, N., Henrissat, B., Blottière, H.M., et al. (2017). A fibrolytic potential in the human ileum mucosal microbiota revealed by functional metagenomic. Scientific Reports *7*, 40248.

Pearson, J.P., and Brownlee, I.A. (2010). The Interaction of Large Bowel Microflora with the Colonic Mucus Barrier. Int J Inflam *2010*.

Pettersen, V.K., Steinsland, H., and Wiker, H.G. (2018). Comparative Proteomics of Enterotoxigenic *Escherichia coli* Reveals Differences in Surface Protein Production and Similarities in Metabolism. J. Proteome Res. *17*, 325–336.

Peterson, L.W., and Artis, D. (2014). Intestinal epithelial cells: regulators of barrier function and immune homeostasis. Nat. Rev. Immunol. *14*, 141–153.

Peterson, S.N., Snesrud, E., Liu, J., Ong, A.C., Kilian, M., Schork, N.J., and Bretz, W. (2013). The Dental Plaque Microbiome in Health and Disease. PLoS One *8*.

Pfaffl, M.W., Tichopad, A., Prgomet, C., and Neuvians, T.P. (2004). Determination of stable housekeeping genes, differentially regulated target genes and sample integrity: BestKeeper – Excel-based tool using pair-wise correlations. Biotechnology Letters *26*, 509–515.

Pineton de Chambrun, G., Neut, C., Chau, A., Cazaubiel, M., Pelerin, F., Justen, P., and Desreumaux, P. (2015). A randomized clinical trial of *Saccharomyces cerevisiae* versus placebo in the irritable bowel syndrome. Dig Liver Dis *47*, 119–124.

Pop, M., Paulson, J.N., Chakraborty, S., Astrovskaya, I., Lindsay, B.R., Li, S., Bravo, H.C., Harro, C., Parkhill, J., Walker, A.W., et al. (2016). Individual-specific changes in the human gut microbiota after challenge with enterotoxigenic *Escherichia coli* and subsequent ciprofloxacin treatment. BMC Genomics *17*, 440.

Pothoulakis, C., Kelly, C.P., Joshi, M.A., Gao, N., O'Keane, C.J., Castagliuolo, I., and Lamont, J.T. (1993). *Saccharomyces boulardii* inhibits *Clostridium difficile* toxin A binding and enterotoxicity in rat ileum. Gastroenterology *104*, 1108–1115.

Pop, M., Paulson, J.N., Chakraborty, S., Astrovskaya, I., Lindsay, B.R., Li, S., Bravo, H.C., Harro, C., Parkhill, J., Walker, A.W., et al. (2016). Individual-specific changes in the human gut microbiota after challenge with enterotoxigenic *Escherichia coli* and subsequent ciprofloxacin treatment. BMC Genomics *17*, 440.

Possemiers, S., Bolca, S., Grootaert, C., Heyerick, A., Decroos, K., Dhooge, W., De Keukeleire, D., Rabot, S., Verstraete, W., and Van de Wiele, T. (2006). The Prenylflavonoid Isoxanthohumol from Hops (Humulus lupulus L.) Is Activated into the Potent Phytoestrogen 8-Prenylnaringenin *In Vitro* and in the Human Intestine. J Nutr *136*, 1862–1867.

Preidis, G.A., Hill, C., Guerrant, R.L., Ramakrishna, B.S., Tannock, G.W., and Versalovic, J. (2011). Probiotics, enteric and diarrheal diseases, and global health. Gastroenterology *140*, 8–14.

Principi, N., Cozzali, R., Farinelli, E., Brusaferro, A., and Esposito, S. (2018). Gut dysbiosis and irritable bowel syndrome: The potential role of probiotics. Journal of Infection *76*, 111–120.

Putnam, S.D., Sanders, J.W., Frenck, R.W., Monteville, M., Riddle, M.S., Rockabrand, D.M., Sharp, T.W., Frankart, C., and Tribble, D.R. (2006). Self-reported description of diarrhea among military populations in operations Iraqi Freedom and Enduring Freedom. J Travel Med *13*, 92–99.

Q

Qadri, F., Khan, A.I., Faruque, A.S.G., Begum, Y.A., Chowdhury, F., Nair, G.B., Salam, M.A., Sack, D.A., and Svennerholm, A.-M. (2005a). Enterotoxigenic *Escherichia coli* and *Vibrio cholerae* Diarrhea, Bangladesh, 2004. Emerg Infect Dis *11*, 1104–1107.

Qadri, F., Svennerholm, A.-M., Faruque, A.S.G., and Sack, R.B. (2005b). Enterotoxigenic *Escherichia coli* in developing countries: epidemiology, microbiology, clinical features, treatment, and prevention. Clin. Microbiol. Rev. *18*, 465–483.

Qadri, F., Ahmed, T., Ahmed, F., Bhuiyan, M.S., Mostofa, M.G., Cassels, F.J., Helander, A., and Svennerholm, A.-M. (2007). Mucosal and systemic immune responses in patients with diarrhea due to CS6-expressing enterotoxigenic *Escherichia coli*. Infect Immun *75*, 2269–2274.

Qiu, Y., Jiang, Z., Hu, S., Wang, L., Ma, X., and Yang, X. (2017). *Lactobacillus plantarum* Enhanced IL-22 Production in Natural Killer (NK) Cells That Protect the Integrity of Intestinal Epithelial Cell Barrier Damaged by Enterotoxigenic *Escherichia coli*. Int J Mol Sci *18*.

Quast, C., Pruesse, E., Yilmaz, P., Gerken, J., Schweer, T., Yarza, P., Peplies, J., and Glöckner, F.O. (2013). The SILVA ribosomal RNA gene database project: improved data processing and web-based tools. Nucleic Acids Res *41*, D590–D596.

Quigley, E.M.M. (2013). Gut Bacteria in Health and Disease. Gastroenterol Hepatol (NY) *9*, 560–569.

R

Rabbani, G.H., Teka, T., Saha, S.K., Zaman, B., Majid, N., Khatun, M., Wahed, M.A., and Fuchs, G.J. (2004). Green Banana and Pectin Improve Small Intestinal Permeability and Reduce Fluid Loss in Bangladeshi Children with Persistent Diarrhea. Dig Dis Sci *49*, 475–484.

Rakoff-Nahoum, S., Coyne, M.J., and Comstock, L.E. (2014). An ecological network of polysaccharide utilization among human intestinal symbionts. Curr. Biol. *24*, 40–49.

Ramette, A. (2007). Multivariate analyses in microbial ecology. FEMS Microbiol. Ecol. *62*, 142–160.

Rao, S.S.C., Kuo, B., McCallum, R.W., Chey, W.D., DiBaise, J.K., Hasler, W.L., Koch, K.L., Lackner, J.M., Miller, C., Saad, R., et al. (2009). Investigation of colonic and whole-gut transit with wireless motility capsule and radiopaque markers in constipation. Clin. Gastroenterol. Hepatol. *7*, 537–544.

Rappaport, R.S., Sagin, J.F., Pierzchala, W.A., Bonde, G., Rubin, B.A., and Tint, H. (1976). Activation of Heat-labile *Escherichia coli* enterotoxin by trypsin. J. Infect. Dis. *133 Suppl*, 41–54.

Rasheed, J.K., Guzmán-Verduzco, L.-M., and Kupersztoch, Y.M. (1990). Two precursors of the heat-stable enterotoxin of *Escherichia coli*: evidence of extracellular processing. Molecular Microbiology *4*, 265–273.

Rasko, D.A. (2017). Changes in microbiome during and after travellers' diarrhea: what we know and what we do not. J Travel Med *24*, S52–S56.

Reyneke, B., Ndlovu, T., Khan, S., and Khan, W. (2017). Comparison of EMA-, PMA- and DNase qPCR for the determination of microbial cell viability. Appl. Microbiol. Biotechnol. *101*, 7371–7383.

Rhouma, M., Fairbrother, J.M., Beaudry, F., and Letellier, A. (2017). Post weaning diarrhea in pigs: risk factors and non-colistin-based control strategies. Acta Veterinaria Scandinavica *59*, 31.

Ribet, D., and Cossart, P. (2015). How bacterial pathogens colonize their hosts and invade deeper tissues. Microbes and Infection *17*, 173–183.

Richard, H., and Foster, J.W. (2004). *Escherichia coli* glutamate- and arginine-dependent acid resistance systems increase internal pH and reverse transmembrane potential. J. Bacteriol. *186*, 6032–6041.

Riddle, M.S., and Connor, B.A. (2016). The Traveling Microbiome. Curr Infect Dis Rep *18*, 29.

Riddle, M.S., Tribble, D.R., Cachafiero, S.P., Putnam, S.D., and Hooper, T.I. (2008). Development of a travelers' diarrhea vaccine for the military: how much is an ounce of prevention really worth? Vaccine *26*, 2490–2502.

Riddle, M.S., DuPont, H.L., and Connor, B.A. (2016). ACG Clinical Guideline: Diagnosis, Treatment and Prevention of Acute Diarrheal Infections in Adults. The American Journal of Gastroenterology *111*, 602–622.

Ríos-Covián, D., Ruas-Madiedo, P., Margolles, A., Gueimonde, M., de los Reyes-Gavilán, C.G., and Salazar, N. (2016). Intestinal Short Chain Fatty Acids and their Link with Diet and Human Health. Front Microbiol *7*.

Rivera-Chávez, F., and Bäumler, A.J. (2015). The Pyromaniac Inside You: *Salmonella* Metabolism in the Host Gut. Annu. Rev. Microbiol. *69*, 31–48.

Rivière, A., Selak, M., Lantin, D., Leroy, F., and De Vuyst, L. (2016). *Bifidobacteria* and Butyrate-Producing Colon Bacteria: Importance and Strategies for Their Stimulation in the Human Gut. Front Microbiol *7*.

Roberts, C.L., Keita, Å.V., Parsons, B.N., Prorok-Hamon, M., Knight, P., Winstanley, C., O'Kennedy, N., Söderholm, J.D., Rhodes, J.M., and Campbell, B.J. (2013). Soluble plantain fibre blocks adhesion and M-cell translocation of intestinal pathogens. J Nutr Biochem *24*, 97–103.

Rocha, L.B., Ozaki, C.Y., Horton, D.S.P.Q., Menezes, C.A., Silva, A., Fernandes, I., Magnoli, F.C., Vaz, T.M.I., Guth, B.E.C., and Piazza, R.M.F. (2013). Different Assay Conditions for Detecting the Production and Release of Heat-Labile and Heat-Stable Toxins in Enterotoxigenic *Escherichia coli* Isolates. Toxins *5*, 2384–2402.

Rodea, G.E., Montiel-Infante, F.X., Cruz-Córdova, A., Saldaña-Ahuactzi, Z., Ochoa, S.A., Espinosa-Mazariego, K., Hernández-Castro, R., and Xicohtencatl-Cortes, J. (2017). Tracking Bioluminescent ETEC during *In vivo* BALB/c Mouse Colonization. Front Cell Infect Microbiol *7*.

Rodiño-Janeiro, B.K., Vicario, M., Alonso-Cotoner, C., Pascua-García, R., and Santos, J. (2018). A Review of Microbiota and Irritable Bowel Syndrome: Future in Therapies. Adv Ther *35*, 289–310.

Rolhion, N., and Chassaing, B. (2016). When pathogenic bacteria meet the intestinal microbiota. Philos. Trans. R. Soc. Lond., B, Biol. Sci. *371*.

Roselli, M., Finamore, A., Britti, M.S., Konstantinov, S.R., Smidt, H., de Vos, W.M., and Mengheri, E. (2007). The novel porcine *Lactobacillus sobrius* strain protects intestinal cells from enterotoxigenic *Escherichia coli* K88 infection and prevents membrane barrier damage. J. Nutr. *137*, 2709–2716.

Roubos-van den Hil, P.J. (2010). Bioactive components of fermented soya beans effective against diarrhoea-associated bacteria (Thesis).

Roussel, C., Cordonnier, C., Galia, W., Goff, O.L., Thévenot, J., Chalancon, S., Alric, M., Thevenot-Sergentet, D., Leriche, F., Van de Wiele, T., Blanquet-Diot, S. (2016). Increased EHEC survival and virulence gene expression indicate an enhanced pathogenicity upon simulated pediatric gastrointestinal conditions. Pediatric Research *80*, 734–743.

Roussel, C., Sivignon, A., Van de Wiele, T., and Blanquet-Diot, S. (2017). Foodborne enterotoxigenic *Escherichia coli*: from gut pathogenesis to new preventive strategies involving probiotics. Future Microbiol *12*, 73–93.

Roussel, C., Sivignon, A., de Vallée, A., Garrait, G., Denis, S., Tsilia, V., Ballet, N., Vandekerckove, P., Van de Wiele, T., Barnich, N., Blanquet-Diot, S. Anti-infectious properties of the probiotic *Saccharomyces cerevisiae* CNCM I-3856 on enterotoxigenic *E. coli* (ETEC) strain H10407. Appl. Microbiol. Biotechnol. *102*, 6175–9802.

Roussel, C., Galia, W., Leriche, F., Chalancon, S., Denis, S., Van de Wiele, T., and Blanquet-Diot, S. (2018). Comparison of conventional plating, PMA-qPCR, and flow cytometry for the determination of viable enterotoxigenic *Escherichia coli* along a gastrointestinal *in vitro* model. Appl. Microbiol. Biotechnol. *102*, 9793–9802.

Roy, K., Hamilton, D., Ostmann, M.M., and Fleckenstein, J.M. (2009). Vaccination with EtpA glycoprotein or flagellin protects against colonization with enterotoxigenic *Escherichia coli* in a murine model. Vaccine *27*, 4601–4608.

Roy, K., Hamilton, D.J., Munson, G.P., and Fleckenstein, J.M. (2011). Outer Membrane Vesicles Induce Immune Responses to Virulence Proteins and Protect against Colonization by Enterotoxigenic *Escherichia coli*. Clin Vaccine Immunol *18*, 1803–1808.

S

Sack, R.B., Gorbach, S.L., Banwell, J.G., Jacobs, B., Chatterjee, B.D., and Mitra, R.C. (1971). Enterotoxigenic *Escherichia coli* isolated from patients with severe cholera-like disease. J. Infect. Dis. *123*, 378–385.

Sahl, J.W., and Rasko, D.A. (2012). Analysis of global transcriptional profiles of enterotoxigenic *Escherichia coli* isolate E24377A. Infect Immun *80*, 1232–1242.

Said, H.M. (2012). Physiology of the Gastrointestinal Tract, Two Volume Set (Academic Press).

Salari, R., and Salari, R. (2017). Investigation of the Best *Saccharomyces cerevisiae* Growth Condition. Electron Physician *9*, 3592–3597.

Salem, W., Leitner, D.R., Zingl, F.G., Schratter, G., Prassl, R., Goessler, W., Reidl, J., and Schild, S. (2015). Antibacterial activity of silver and zinc nanoparticles against *Vibrio cholerae* and enterotoxic *Escherichia coli*. Int. J. Med. Microbiol. *305*, 85–95.

Salimian, J., Salmanian, A., Khalesi, R., Mohseni, M., and Moazzeni, S. (2010). Antibody against

recombinant heat labile enterotoxin B subunit (rLTB) could block LT binding to ganglioside M1 receptor. Iran J Microbiol *2*, 120–127.

Sánchez, J., and Holmgren, J. (2005). Virulence factors, pathogenesis and vaccine protection in cholera and ETEC diarrhea. Curr. Opin. Immunol. *17*, 388–398.

Sánchez, D., Rojas, M., Hernández, I., Radzioch, D., García, L.F., and Barrera, L.F. (2010). Role of TLR2- and TLR4-mediated signaling in *Mycobacterium tuberculosis*-induced macrophage death. Cell. Immunol. *260*, 128–136.

Sanders, J.W., Putnam, S.D., Gould, P., Kolisnyk, J., Merced, N., Barthel, V., Rozmajzl, P.J., Shaheen, H., Fouad, S., and Frenck, R.W. (2005). Diarrheal illness among deployed U.S. military personnel during Operation Bright Star 2001—Egypt. Diagnostic Microbiology and Infectious Disease *52*, 85–90.

Sarkar, A., and Mandal, S. (2016). *Bifidobacteria*—Insight into clinical outcomes and mechanisms of its probiotic action. Microbiological Research *192*, 159–171.

Sarker, S.A., Sultana, S., Reuteler, G., Moine, D., Descombes, P., Charton, F., Bourdin, G., McCallin, S., Ngom-Bru, C., Neville, T., et al. (2016). Oral Phage Therapy of Acute Bacterial Diarrhea With Two Coliphage Preparations: A Randomized Trial in Children From Bangladesh. EBioMedicine *4*, 124–137.

Sato, J.P.H., Takeuti, K.L., Andrade, M.R., Koerich, P.K.V., Tagliari, V., Bernardi, M.L., Cardoso, M.R.I., and Barcellos, D.E.S.N. (2016). Virulence profiles of enterotoxigenic *Escherichia coli* isolated from piglets with post-weaning diarrhea and classification according to fecal consistency. Pesquisa Veterinária Brasileira *36*, 253–257.

Saxena, K., Blutt, S.E., Ettayebi, K., Zeng, X.-L., Broughman, J.R., Crawford, S.E., Karandikar, U.C., Sastri, N.P., Conner, M.E., Opekun, A.R., et al. (2016). Human Intestinal Enteroids: a New Model To Study Human Rotavirus Infection, Host Restriction, and Pathophysiology. Journal of Virology *90*, 43–56.

von Schillde, M.-A., Hörmannsperger, G., Weiher, M., Alpert, C.-A., Hahne, H., Bäuerl, C., van Huynegem, K., Steidler, L., Hrncir, T., Pérez-Martínez, G., et al. (2012). Lactocepin secreted by *Lactobacillus* exerts anti-inflammatory effects by selectively degrading proinflammatory chemokines. Cell Host Microbe *11*, 387–396.

Schippa, S., and Conte, M.P. (2014). Dysbiotic events in gut microbiota: impact on human health. Nutrients *6*, 5786–5805.

Schloss, P.D., and Westcott, S.L. (2011). Assessing and improving methods used in operational taxonomic unit-based approaches for 16S rRNA gene sequence analysis. Appl. Environ. Microbiol. *77*, 3219–3226.

Schloss, P.D., Westcott, S.L., Ryabin, T., Hall, J.R., Hartmann, M., Hollister, E.B., Lesniewski, R.A., Oakley, B.B., Parks, D.H., Robinson, C.J., et al. (2009). Introducing mothur: open-source, platform-independent, community-supported software for describing and comparing microbial communities. Appl. Environ. Microbiol. *75*, 7537–7541.

Schmitz, M.L., Weber, A., Roxlau, T., Gaestel, M., and Kracht, M. (2011). Signal integration, crosstalk mechanisms and networks in the function of inflammatory cytokines. Biochimica et Biophysica Acta (BBA) - Molecular Cell Research *1813*, 2165–2175.

Schneider, S.M., Girard-Pipau, F., Filippi, J., Hébuterne, X., Moyse, D., Hinojosa, G.C., Pompei, A., and Rampal, P. (2005). Effects of *Saccharomyces boulardii* on fecal short-chain fatty acids and microflora in patients on long-term total enteral nutrition. World J Gastroenterol *11*, 6165–6169.

Schuier, M., Sies, H., Illek, B., and Fischer, H. (2005). Cocoa-related flavonoids inhibit CFTR-mediated chloride transport across T84 human colon epithelia. J. Nutr. *135*, 2320–2325.

Schultz, M., Baranchi, A., Thurston, L., Yu, Y.C., Wang, L., Chen, J., Sapsford, M., Chung, J., Binsadiq,

M., Craig, L., et al. (2011). Consumer demographics and expectations of probiotic therapy in New Zealand: results of a large telephone survey. N. Z. Med. J. *124*, 36–43.

Schulze, K. (2006). Imaging and modelling of digestion in the stomach and the duodenum. Neurogastroenterol. Motil. *18*, 172–183.Schwan, W.R., and Ding, H. (2017). Temporal Regulation of fim Genes in Uropathogenic *Escherichia coli* during Infection of the Murine Urinary Tract. J Pathog *2017*.

Schwan, W.R., Lee, J.L., Lenard, F.A., Matthews, B.T., and Beck, M.T. (2002). Osmolarity and pH growth conditions regulate fim gene transcription and type 1 pilus expression in uropathogenic *Escherichia coli*. Infect. Immun. *70*, 1391–1402.

Sears, C.L., and Kaper, J.B. (1996). Enteric bacterial toxins: mechanisms of action and linkage to intestinal secretion. Microbiol. Rev. *60*, 167–215.

Sears, K.T., Tennant, S.M., Reymann, M.K., Simon, R., Konstantopoulos, N., Blackwelder, W.C., Barry, E.M., and Pasetti, M.F. (2017). Bioactive Immune Components of Anti-Diarrheagenic Enterotoxigenic *Escherichia coli* Hyperimmune Bovine Colostrum Products. Clin. Vaccine Immunol. *24*.

Seidl, H., Gundling, F., Pfeiffer, A., Pehl, C., Schepp, W., and Schmidt, T. (2012). Comparison of small-bowel motility of the human jejunum and ileum. Neurogastroenterol. Motil. *24*, e373-380.

Sekirov, I., Russell, S.L., Antunes, L.C.M., and Finlay, B.B. (2010). Gut microbiota in health and disease. Physiol. Rev. *90*, 859–904.

Sengupta, C., Ray, S., and Chowdhury, R. (2014). Fine tuning of virulence regulatory pathways in enteric bacteria in response to varying bile and oxygen concentrations in the gastrointestinal tract. Gut Pathogens *6*, 38.

Seo, S.W., Kim, D., O'Brien, E.J., Szubin, R., and Palsson, B.O. (2015). Decoding genome-wide GadEWX-transcriptional regulatory networks reveals multifaceted cellular responses to acid stress in *Escherichia coli*. Nature Communications *6*, 7970.

Servin, A.L. (2014). Pathogenesis of human diffusely adhering *Escherichia coli* expressing Afa/Dr adhesins (Afa/Dr DAEC): current insights and future challenges. Clin. Microbiol. Rev. *27*, 823–869.

Sheikh, A., Rashu, R., Begum, Y.A., Kuhlman, F.M., Ciorba, M.A., Hultgren, S.J., Qadri, F., and Fleckenstein, J.M. (2017). Highly conserved type 1 pili promote enterotoxigenic E. coli pathogen-host interactions. PLoS Negl Trop Dis *11*.

Sherlock, O., Vejborg, R.M., and Klemm, P. (2005). The TibA Adhesin/Invasin from Enterotoxigenic *Escherichia coli* Is Self Recognizing and Induces Bacterial Aggregation and Biofilm Formation. Infect Immun *73*, 1954–1963.

Sender, R., Fuchs, S., and Milo, R. (2016). Revised Estimates for the Number of Human and Bacteria Cells in the Body. PLoS Biol. *14*, e1002533.

Shah, P., Fritz, J., Estes, M., Zenhausern, F., and Wilmes, P. (2014). HuMiX: A microfluidics-based in vitro co-culture device for investigating host-microbe molecular interactions. In 18th International Conference on Miniaturized Systems for Chemistry and Life Sciences, MicroTAS 2014, (Chemical and Biological Microsystems Society), pp. 300–302.

Sherwood, L. (2006). Physiologie humaine: A Human Perspective. De Boeck Superieur.

Shi, H., Xu, W., Luo, Y., Chen, L., Liang, Z., Zhou, X., and Huang, K. (2011). The effect of various environmental factors on the ethidium monazite and quantitative PCR method to detect viable bacteria. J. Appl. Microbiol. *111*, 1194–1204.

Shurson, G.C. (2018). Yeast and yeast derivatives in feed additives and ingredients: Sources, characteristics, animal responses, and quantification methods. Animal Feed Science and Technology *235*, 60–76.

Sieracki, M.E., Cucci, T.L., and Nicinski, J. (1999). Flow Cytometric Analysis of 5-Cyano-2,3-Ditolyl Tetrazolium Chloride Activity of Marine Bacterioplankton in Dilution Cultures. Appl Environ Microbiol *65*, 2409–2417.

Silver, N., Best, S., Jiang, J., and Thein, S.L. (2006). Selection of housekeeping genes for gene expression studies in human reticulocytes using real-time PCR. BMC Mol Biol *7*, 33.

Singh, P., Teal, T.K., Marsh, T.L., Tiedje, J.M., Mosci, R., Jernigan, K., Zell, A., Newton, D.W., Salimnia, H., Lephart, P., et al. (2015). Intestinal microbial communities associated with acute enteric infections and disease recovery. Microbiome *3*.

Sistrunk, J.R., Nickerson, K.P., Chanin, R.B., Rasko, D.A., and Faherty, C.S. (2016). Survival of the Fittest: How Bacterial Pathogens Utilize Bile To Enhance Infection. Clin Microbiol Rev *29*, 819–836.

Sivignon, A., Yan, X., Alvarez Dorta, D., Bonnet, R., Bouckaert, J., Fleury, E., Bernard, J., Gouin, S.G., Darfeuille-Michaud, A., and Barnich, N. (2015). Development of Heptylmannoside-Based Glycoconjugate Antiadhesive Compounds against Adherent-Invasive *Escherichia coli* Bacteria Associated with Crohn's Disease. MBio *6*, e01298-01215.

Sjöling, Å., Sadeghipoorjahromi, L., Novak, D., and Tobias, J. (2015). Detection of major diarrheagenic bacterial pathogens by multiplex PCR panels. Microbiological Research *172*, 34–40.

Slavin, J. (2013). Fiber and prebiotics: mechanisms and health benefits. Nutrients *5*, 1417–1435.

Sokol, H., Seksik, P., Furet, J.P., Firmesse, O., Nion-Larmurier, I., Beaugerie, L., Cosnes, J., Corthier, G., Marteau, P., and Doré, J. (2009). Low counts of *Faecalibacterium prausnitzii* in colitis microbiota. Inflamm. Bowel Dis. *15*, 1183–1189.

Sonnenburg, J.L., Xu, J., Leip, D.D., Chen, C.-H., Westover, B.P., Weatherford, J., Buhler, J.D., and Gordon, J.I. (2005). Glycan foraging *in vivo* by an intestine-adapted bacterial symbiont. Science *307*, 1955–1959.

Spiller, R., and Garsed, K. (2009). Postinfectious irritable bowel syndrome. Gastroenterology *136*, 1979–1988.

Spiller, R., Pélerin, F., Cayzeele Decherf, A., Maudet, C., Housez, B., Cazaubiel, M., and Jüsten, P. (2016). Randomized double blind placebo-controlled trial of *Saccharomyces cerevisiae* CNCM I-3856 in irritable bowel syndrome: improvement in abdominal pain and bloating in those with predominant constipation. United European Gastroenterol J *4*, 353–362.

Spindler, E.C., Hale, J.D.F., Giddings, T.H., Hancock, R.E.W., and Gill, R.T. (2011). Deciphering the Mode of Action of the Synthetic Antimicrobial Peptide Bac8c. Antimicrob Agents Chemother *55*, 1706–1716.

Sriranganathan, N., and Burger, D. (1983). Purification and Characterization of Heat-Stable Enterotoxin from Bovine Enterotoxigenic *Escherichia coli*. Infect Immun *40*, 7.

Stamatakis, A. (2014). RAxML version 8: a tool for phylogenetic analysis and post-analysis of large phylogenies. Bioinformatics *30*, 1312–1313.

Stecher, B., Berry, D., and Loy, A. (2013). Colonization resistance and microbial ecophysiology: using gnotobiotic mouse models and single-cell technology to explore the intestinal jungle. FEMS Microbiol. Rev. *37*, 793–829.

Steffen, R., Castelli, F., Dieter Nothdurft, H., Rombo, L., and Jane Zuckerman, N. (2006). Vaccination against Enterotoxigenic *Escherichia coli*, a Cause of Travelers- Diarrhea. Journal of Travel Medicine *12*, 102–107.

Stern, E.K., and Brenner, D.M. (2018). Gut Microbiota-Based Therapies for Irritable Bowel Syndrome. Clinical and Translational Gastroenterology *9*, e134.

Strugala, V., Allen, A., Dettmar, P.W., and Pearson, J.P. (2003). Colonic mucin: methods of measuring mucus thickness. Proc Nutr Soc *62*, 237–243.

Sturbelle, R.T., de Avila, L.F. da C., Roos, T.B., Borchardt, J.L., da Conceição, R. de C. dos S., Dellagostin, O.A., and Leite, F.P.L. (2015). The role of quorum sensing in *Escherichia coli* (ETEC) virulence factors. Vet. Microbiol. *180*, 245–252.

Su, C.-P., Jane, W.-N., and Wong, H. (2013). Changes of ultrastructure and stress tolerance of *Vibrio parahaemolyticus* upon entering viable but nonculturable state. Int. J. Food Microbiol. *160*, 360–366.

Su, T., Liu, R., Lee, A., Long, Y., Du, L., Lai, S., Chen, X., Wang, L., Si, J., Owyang, C., et al. (2018). Altered Intestinal Microbiota with Increased Abundance of *Prevotella* Is Associated with High Risk of Diarrhea-Predominant Irritable Bowel Syndrome. Gastroenterol Res Pract *2018*, 6961783.

Sun, Y., and Kim, S.W. (2017). Intestinal challenge with enterotoxigenic *Escherichia coli* in pigs, and nutritional intervention to prevent postweaning diarrhea. Anim Nutr *3*, 322–330.

Sun, Y., and O'Riordan, M.X.D. (2013). Regulation of Bacterial Pathogenesis by Intestinal Short-Chain Fatty Acids. Adv Appl Microbiol *85*, 93–118.

Sun, Y., Fukamachi, T., Saito, H., and Kobayashi, H. (2012). Adenosine deamination increases the survival under acidic conditions in *Escherichia coli*: Adenosine induces acid resistance. Journal of Applied Microbiology *112*, 775–781.

Sundin, O.H., Mendoza-Ladd, A., Zeng, M., Diaz-Arévalo, D., Morales, E., Fagan, B.M., Ordoñez, J., Velez, P., Antony, N., and McCallum, R.W. (2017). The human jejunum has an endogenous microbiota that differs from those in the oral cavity and colon. BMC Microbiol *17*.

Suzuki, H., Wang, Z.-Y., Yamakoshi, M., Kobayashi, M., and Nozawa, T. (2003). Probing the Transmembrane Potential of Bacterial Cells by Voltage-Sensitive Dyes. Analytical Sciences *19*, 1239–1242.

Syngai, G.G., Gopi, R., Bharali, R., Dey, S., Lakshmanan, G.M.A., and Ahmed, G. (2016). Probiotics - the versatile functional food ingredients. J Food Sci Technol *53*, 921–933.

T

Takada, T., Kurakawa, T., Tsuji, H., and Nomoto, K. (2013). *Fusicatenibacter saccharivorans* gen. nov., sp. nov., isolated from human faeces. International journal of systematic and evolutionary microbiology *63*, 3691–3696.

Takao, M., Yen, H., and Tobe, T. (2014). LeuO enhances butyrate-induced virulence expression through a positive regulatory loop in enterohaemorrhagic *Escherichia coli*. Molecular Microbiology *93*, 1302–1313.

Takashi, K., Fujita, I., and Kobari, K. (1989). Effects of short chain fatty acids on the production of heat-labile enterotoxin from enterotoxigenic *Escherichia coli*. Jpn. J. Pharmacol. *50*, 495–498.

Takeshita, K., Mizuno, S., Mikami, Y., Sujino, T., Saigusa, K., Matsuoka, K., Naganuma, M., Sato, T., Takada, T., Tsuji, H., et al. (2016). A single species of *Clostridium Subcluster XIVa* decreased in ulcerative colitis patients. Inflammatory Bowel Diseases *22*, 2802–2810.

Tamburini, S., Ballarini, A., Ferrentino, G., Moro, A., Foladori, P., Spilimbergo, S., and Jousson, O. (2013). Comparison of quantitative PCR and flow cytometry as cellular viability methods to study bacterial membrane permeabilization following supercritical CO_2 treatment. Microbiology (Reading, Engl.) *159*, 1056–1066.

Tang, X., Lee, J., and Chen, W.N. (2015). Engineering the fatty acid metabolic pathway in *Saccharomyces cerevisiae* for advanced biofuel production. Metabolic Engineering Communications *2*,

58–66.

Tauschek, M., Gorrell, R.J., Strugnell, R.A., and Robins-Browne, R.M. (2002). Identification of a protein secretory pathway for the secretion of heat-labile enterotoxin by an enterotoxigenic strain of *Escherichia coli.* Proc Natl Acad Sci U S A *99*, 7066–7071.

Taylor, D.N., Hamer, D.H., and Shlim, D.R. (2017). Medications for the prevention and treatment of travellers' diarrhea. J Travel Med *24*, S17–S22.

Tchesnokova, V., McVeigh, A.L., Kidd, B., Yakovenko, O., Thomas, W.E., Sokurenko, E.V., and Savarino, S.J. (2010). Shear-enhanced binding of intestinal colonization factor antigen I of enterotoxigenic *Escherichia coli*. Mol. Microbiol. *76*, 489–502.

Ten Bruggencate, S.J.M., Girard, S.A., Floris-Vollenbroek, E.G.M., Bhardwaj, R., and Tompkins, T.A. (2015). The effect of a multi-strain probiotic on the resistance toward *Escherichia coli* challenge in a randomized, placebo-controlled, double-blind intervention study. Eur J Clin Nutr *69*, 385–391.

Tennant, S.M., Hartland, E.L., Phumoonna, T., Lyras, D., Rood, J.I., Robins-Browne, R.M., and van Driel, I.R. (2008). Influence of Gastric Acid on Susceptibility to Infection with Ingested Bacterial Pathogens. Infect Immun *76*, 639–645.

Thévenot, J., Etienne-Mesmin, L., Denis, S., Chalancon, S., Alric, M., Livrelli, V., and Blanquet-Diot, S. (2013). Enterohemorrhagic *Escherichia coli* O157:H7 Survival in an In Vitro Model of the Human Large Intestine and Interactions with Probiotic Yeasts and Resident Microbiota. Appl Environ Microbiol *79*, 1058–1064.

Thévenot, J., Cordonnier, C., Rougeron, A., Le Goff, O., Nguyen, H.T.T., Denis, S., Alric, M., Livrelli, V., and Blanquet-Diot, S. (2015). Enterohemorrhagic *Escherichia coli* infection has donor-dependent effect on human gut microbiota and may be antagonized by probiotic yeast during interaction with Peyer's patches. Appl. Microbiol. Biotechnol. *99*, 9097–9110.

Thomas, R.J., Webber, D., Hopkins, R., Frost, A., Laws, T., Jayasekera, P.N., and Atkins, T. (2011). The Cell Membrane as a Major Site of Damage during Aerosolization of *Escherichia coli*. Appl Environ Microbiol *77*, 920–925.

Thursby, E., and Juge, N. (2017). Introduction to the human gut microbiota. Biochem J *474*, 1823–1836.

Tiago, F.C.P., Martins, F.S., Souza, E.L.S., Pimenta, P.F.P., Araujo, H.R.C., Castro, I.M., Brandão, R.L., and Nicoli, J.R. (2012). Adhesion to the yeast cell surface as a mechanism for trapping pathogenic bacteria by *Saccharomyces* probiotics. J. Med. Microbiol. *61*, 1194–1207.

Tian, Z., Liu, X., Dai, R., Xiao, Y., Wang, X., Bi, D., and Shi, D. (2016). *Enterococcus faecium* HDRsEf1 Protects the Intestinal Epithelium and Attenuates ETEC-Induced IL-8 Secretion in Enterocytes.

Timmerman, H.M., Koning, C.J.M., Mulder, L., Rombouts, F.M., and Beynen, A.C. (2004). Monostrain, multistrain and multispecies probiotics--A comparison of functionality and efficacy. Int. J. Food Microbiol. *96*, 219–233.

Toledo-Arana, A., Dussurget, O., Nikitas, G., Sesto, N., Guet-Revillet, H., Balestrino, D., Loh, E., Gripenland, J., Tiensuu, T., Vaitkevicius, K., et al. (2009). The *Listeria* transcriptional landscape from saprophytism to virulence. Nature *459*, 950–956.

Tomosada, Y., Villena, J., Murata, K., Chiba, E., Shimazu, T., Aso, H., Iwabuchi, N., Xiao, J., Saito, T., and Kitazawa, H. (2013). Immunoregulatory effect of bifidobacteria strains in porcine intestinal epithelial cells through modulation of ubiquitin-editing enzyme A20 expression. PLoS ONE *8*, e59259.

Tompkins, T.A., Mainville, I., and Arcand, Y. (2011). The impact of meals on a probiotic during transit through a model of the human upper gastrointestinal tract. Benef Microbes *2*, 295–303.

Topping, D.L., and Clifton, P.M. (2001). Short-chain fatty acids and human colonic function: roles of

resistant starch and nonstarch polysaccharides. Physiol. Rev. *81*, 1031–1064.

Torres, A.G. (2010). Pathogenic *Escherichia Coli* in Latin America (Bentham Science Publishers).

Torres, A.G. (2016). *Escherichia coli* in the Americas (Springer).

Tremaroli, V., and Bäckhed, F. (2012). Functional interactions between the gut microbiota and host metabolism. Nature *489*, 242–249.

Trevisi, P., Colombo, M., Priori, D., Fontanesi, L., Galimberti, G., Calò, G., Motta, V., Latorre, R., Fanelli, F., Mezzullo, M., et al. (2015). Comparison of three patterns of feed supplementation with live *Saccharomyces cerevisiae* yeast on postweaning diarrhea, health status, and blood metabolic profile of susceptible weaning pigs orally challenged with *Escherichia coli* F4ac. J. Anim. Sci. *93*, 2225–2233.

Trevisi, P., Latorre, R., Priori, D., Luise, D., Archetti, I., Mazzoni, M., D'Inca, R., and Bosi, P. (2017). Effect of feed supplementation with live yeast on the intestinal transcriptome profile of weaning pigs orally challenged with *Escherichia coli* F4. Animal *11*, 33–44.

Trudeau, K., Vu, K.D., Shareck, F., and Lacroix, M. (2012). Capillary Electrophoresis Separation of Protein Composition of γ-Irradiated Food Pathogens *Listeria monocytogenes* and *Staphylococcus aureus*. Plos One *7*, e32488.

Tsai, C.-C., Lin, P.-P., and Hsieh, Y.-M. (2008). Three *Lactobacillus* strains from healthy infant stool inhibit enterotoxigenic *Escherichia coli* grown *in vitro*. Anaerobe *14*, 61–67.

Tsilia, V., Kerckhof, F.-M., Rajkovic, A., Heyndrickx, M., and Van de Wiele, T. (2015). *Bacillus cereus* NVH 0500/00 Can Adhere to Mucin but Cannot Produce Enterotoxins during Gastrointestinal Simulation. Appl Environ Microbiol *82*, 289–296.

Tsuji, T., Taga, S., Honda, T., and Takeda, Y. (1982). Molecular Heterogeneity of Heat-Labile Enterotoxins from Human and Porcine Enterotoxigenic *Escherichia coli*. Infect Immun *38*, 5.

Turnbaugh, P.J., Ley, R.E., Hamady, M., Fraser-Liggett, C., Knight, R., and Gordon, J.I. (2007). The human microbiome project: exploring the microbial part of ourselves in a changing world. Nature *449*, 804–810.

Turner, S.M., Scott-Tucker, A., Cooper, L.M., and Henderson, I.R. (2006). Weapons of mass destruction: virulence factors of the global killer enterotoxigenic *Escherichia coli*. FEMS Microbiol. Lett. *263*, 10–20.

U

Urdaneta, V., and Casadesús, J. (2017). Interactions between Bacteria and Bile Salts in the Gastrointestinal and Hepatobiliary Tracts. Front Med (Lausanne) *4*, 163.

V

Vaara, M. (1992). Agents that increase the permeability of the outer membrane. Microbiol. Rev. *56*, 395–411.

Van de Wiele, T., Van den Abbeele, P., Ossieur, W., Possemiers, S., and Marzorati, M. (2015). The Simulator of the Human Intestinal Microbial Ecosystem (SHIME®). In The Impact of Food Bioactives on Health: *In Vitro* and *Ex Vivo* Models, K. Verhoeckx, P. Cotter, I. López-Expósito, C. Kleiveland, T. Lea, A. Mackie, T. Requena, D. Swiatecka, and H. Wichers, eds. (Cham: Springer International Publishing), pp. 305–317.

Van den Abbeele, P., Roos, S., Eeckhaut, V., MacKenzie, D.A., Derde, M., Verstraete, W., Marzorati, M., Possemiers, S., Vanhoecke, B., Van Immerseel, F., et al. (2012). Incorporating a mucosal environment in a dynamic gut model results in a more representative colonization by lactobacilli. Microb

Biotechnol *5*, 106–115.

Van den Abbeele, P., Belzer, C., Goossens, M., Kleerebezem, M., De Vos, W.M., Thas, O., De Weirdt, R., Kerckhof, F.-M., and Van de Wiele, T. (2013). Butyrate-producing Clostridium cluster XIVa species specifically colonize mucins in an *in vitro* gut model. ISME J *7*, 949–961.

Vandeputte, D., Kathagen, G., D'hoe, K., Vieira-Silva, S., Valles-Colomer, M., Sabino, J., Wang, J., Tito, R.Y., Commer, L.D., Darzi, Y., et al. (2017). Quantitative microbiome profiling links gut community variation to microbial load. Nature *551*, 507–511.

Vanhauteghem, D., Janssens, G.P.J., Lauwaerts, A., Sys, S., Boyen, F., Cox, E., and Meyer, E. (2013). Exposure to the Proton Scavenger Glycine under Alkaline Conditions Induces *Escherichia coli* Viability Loss. Plos One *8*, e60328.

Van Herreweghen, F., Van den Abbeele, P., De Mulder, T., De Weirdt, R., Geirnaert, A., Hernandez-Sanabria, E., Vilchez-Vargas, R., Jauregui, R., Pieper, D.H., Belzer, C., et al. (2017). *In vitro* colonisation of the distal colon by *Akkermansia muciniphila* is largely mucin and pH dependent. Benef Microbes *8*, 81–96.

Vardakou, M., Nueno, C.P., Gasson, M., Narbad, A., and Christakopoulos, P. (2007). *In vitro* three-stage continuous fermentation of wheat arabinoxylan fractions and induction of hydrolase activity by the gut microflora. Int J Biol Macromol *41*, 584–589.

Vasavid, P., Chaiwatanarat, T., Pusuwan, P., Sritara, C., Roysri, K., Namwongprom, S., Kuanrakcharoen, P., Premprabha, T., Chunlertrith, K., Thongsawat, S., et al. (2014). Normal Solid Gastric Emptying Values Measured by Scintigraphy Using Asian-style Meal: A Multicenter Study in Healthy Volunteers. J Neurogastroenterol Motil *20*, 371–378.

Vayssier-Taussat, M., Albina, E., Citti, C., Cosson, J.-F., Jacques, M.-A., Lebrun, M.-H., Le Loir, Y., Ogliastro, M., Petit, M.-A., Roumagnac, P., et al. (2014). Shifting the paradigm from pathogens to pathobiome: new concepts in the light of meta-omics. Front Cell Infect Microbiol *4*, 29.

Vedøy, O.B., Hanevik, K., Sakkestad, S.T., Sommerfelt, H., and Steinsland, H. (2018). Proliferation of enterotoxigenic *Escherichia coli* strain TW11681 in stools of experimentally infected human volunteers. Gut Pathog *10*, 46.

Venema, K., and van den Abbeele, P. (2013). Experimental models of the gut microbiome. Best Pract Res Clin Gastroenterol *27*, 115–126.

Verhelst, R., Schroyen, M., Buys, N., and Niewold, T.A. (2013). *E. coli* heat labile toxin (LT) inactivation by specific polyphenols is aggregation dependent. Vet. Microbiol. *163*, 319–324.

Villarreal, M.L.M., Padilha, M., Vieira, A.D.S., Franco, B.D.G. de M., Martinez, R.C.R., and Saad, S.M.I. (2013). Advantageous Direct Quantification of Viable Closely Related Probiotics in Petit-Suisse Cheeses under *In Vitro* Gastrointestinal Conditions by Propidium Monoazide - qPCR. PLoS One *8*.

Villmones, H.C., Haug, E.S., Ulvestad, E., Grude, N., Stenstad, T., Halland, A., and Kommedal, Ø. (2018). Species Level Description of the Human Ileal Bacterial Microbiota. Scientific Reports *8*, 4736.

W

Wachi, S., Kanmani, P., Tomosada, Y., Kobayashi, H., Yuri, T., Egusa, S., Shimazu, T., Suda, Y., Aso, H., Sugawara, M., et al. (2014). *Lactobacillus delbrueckii* TUA4408L and its extracellular polysaccharides attenuate enterotoxigenic *Escherichia coli*-induced inflammatory response in porcine intestinal epitheliocytes via Toll-like receptor-2 and 4. Mol Nutr Food Res *58*, 2080–2093.

Waldman, S.A., and Camilleri, M. (2018). Guanylate cyclase-C as a therapeutic target in gastrointestinal disorders. Gut *67*, 1543–1552.

Walker, A.W., Sanderson, J.D., Churcher, C., Parkes, G.C., Hudspith, B.N., Rayment, N., Brostoff, J., Parkhill, J., Dougan, G., and Petrovska, L. (2011). High-throughput clone library analysis of the mucosa-associated microbiota reveals dysbiosis and differences between inflamed and non-inflamed regions of the intestine in inflammatory bowel disease. BMC Microbiol. *11*, 7.

Walker, R.I., Wierzba, T.F., Mani, S., and Bourgeois, A.L. (2017). Vaccines against *Shigella* and enterotoxigenic *Escherichia coli*: A summary of the 2016 VASE Conference. Vaccine *35*, 6775–6782.

Walter, J., and Ley, R. (2011). The human gut microbiome: ecology and recent evolutionary changes. Annu. Rev. Microbiol. *65*, 411–429.

Wands, A.M., Fujita, A., McCombs, J.E., Cervin, J., Dedic, B., Rodriguez, A.C., Nischan, N., Bond, M.R., Mettlen, M., Trudgian, D.C., et al. (2015). Fucosylation and protein glycosylation create functional receptors for cholera toxin. Elife *4*, e09545.

Wang, J., Zeng, Y., Wang, S., Liu, H., Zhang, D., Zhang, W., Wang, Y., and Ji, H. (2018). Swine-Derived Probiotic *Lactobacillus plantarum* Inhibits Growth and Adhesion of Enterotoxigenic *Escherichia coli* and Mediates Host Defense. Front Microbiol *9*.

Wang, M., Ahrné, S., Jeppsson, B., and Molin, G. (2005). Comparison of bacterial diversity along the human intestinal tract by direct cloning and sequencing of 16S rRNA genes. FEMS Microbiol. Ecol. *54*, 219–231.

Wang, M., Szucs, T.D., and Steffen, R. (2008). Economic aspects of travelers' diarrhea. J Travel Med *15*, 110–118.

Wang, Q., Garrity, G.M., Tiedje, J.M., and Cole, J.R. (2007). Naive Bayesian classifier for rapid assignment of rRNA sequences into the new bacterial taxonomy. Appl. Environ. Microbiol. *73*, 5261–5267.

Wang, X., Gao, X., and Hardwidge, P.R. (2012). Heat-labile enterotoxin-induced activation of NF-κB and MAPK pathways in intestinal epithelial cells impacts enterotoxigenic *Escherichia coli* (ETEC) adherence. Cell Microbiol *14*, 1231–1241.

Wang, X., Cai, Y., Sun, Y., Knight, R., and Mai, V. (2012). Secondary structure information does not improve OTU assignment for partial 16s rRNA sequences. ISME J *6*, 1277–1280.

Weiglmeier, P.R., Rösch, P., and Berkner, H. (2010). Cure and curse: *E. coli* heat-stable enterotoxin and its receptor guanylyl cyclase C. Toxins (Basel) *2*, 2213–2229.

Wenzel, H., Kaminski, R.W., Clarkson, K.A., Maciel, M., Smith, M.A., Zhang, W., and Oaks, E.V. (2017). Improving chances for successful clinical outcomes with better preclinical models. Vaccine *35*, 6798–6802.

WHO (2006). Weekly epidemiological record. Weekly epidemiological record 8.

Wiese, M., Khakimov, B., Nielsen, S., Sørensen, H., van den Berg, F., and Nielsen, D.S. (2018). CoMiniGut-a small volume *in vitro* colon model for the screening of gut microbial fermentation processes. PeerJ *6*, e4268.

Wijemanne, P., and Moxley, R.A. (2014). Glucose Significantly Enhances Enterotoxigenic *Escherichia coli* Adherence to Intestinal Epithelial Cells through Its Effects on Heat-Labile Enterotoxin Production. PLoS One *9*.

Wilson, C.G. (2010). The transit of dosage forms through the colon. Int J Pharm *395*, 17–25.

Worsøe, J., Fynne, L., Gregersen, T., Schlageter, V., Christensen, L.A., Dahlerup, J.F., Rijkhoff, N.J., Laurberg, S., and Krogh, K. (2011). Gastric transit and small intestinal transit time and motility assessed by a magnet tracking system. BMC Gastroenterology *11*, 145.

Wu, H.-J., and Wu, E. (2012). The role of gut microbiota in immune homeostasis and autoimmunity. Gut Microbes *3*, 4–14.

Wu, Y., Zhu, C., Chen, Z., Chen, Z., Zhang, W., Ma, X., Wang, L., , X., and Jiang, Z. (2016). Protective effects of *Lactobacillus plantarum* on epithelial barrier disruption caused by enterotoxigenic *Escherichia coli* in intestinal porcine epithelial cells. Vet. Immunol. Immunopathol. *172*, 55–63.

Y

Yamanaka, H., Kobayashi, H., Takahashi, E., and Okamoto, K. (2008). MacAB Is Involved in the Secretion of Escherichia coli Heat-Stable Enterotoxin II. Journal of Bacteriology *190*, 7693–7698.

Yang, J. (2005). The H-NS protein represses transcription of the eltAB operon, which encodes heat-labile enterotoxin in enterotoxigenic *Escherichia coli*, by binding to regions downstream of the promoter. Microbiology *151*, 1199–1208.

Yang, Y., Galle, S., Le, M.H.A., Zijlstra, R.T., and Gänzle, M.G. (2015). Feed Fermentation with Reuteran- and Levan-Producing *Lactobacillus reuteri* Reduces Colonization of Weanling Pigs by Enterotoxigenic *Escherichia coli*. Appl Environ Microbiol *81*, 5743–5752.

Youmans, B.P., Ajami, N.J., Jiang, Z.-D., Campbell, F., Wadsworth, W.D., Petrosino, J.F., DuPont, H.L., and Highlander, S.K. (2015). Characterization of the human gut microbiome during travelers' diarrhea. Gut Microbes *6*, 110–119.

Z

Zachos, N.C., Kovbasnjuk, O., Foulke-Abel, J., In, J., Blutt, S.E., de Jonge, H.R., Estes, M.K., and Donowitz, M. (2016). Human Enteroids/Colonoids and Intestinal Organoids Functionally Recapitulate Normal Intestinal Physiology and Pathophysiology. J Biol Chem *291*, 3759–3766.

Zaman, S.B., Hussain, M.A., Nye, R., Mehta, V., Mamun, K.T., and Hossain, N. (2017). A Review on Antibiotic Resistance: Alarm Bells are Ringing. Cureus *9*, e1403.

Zanello, G., Berri, M., Dupont, J., Sizaret, P.-Y., D'Inca, R., Salmon, H., and Meurens, F. (2011). *Saccharomyces cerevisiae* modulates immune gene expressions and inhibits ETEC-mediated ERK1/2 and p38 signaling pathways in intestinal epithelial cells. PLoS ONE *6*, e18573.

Zeng, B., Zhao, G., Cao, X., Yang, Z., Wang, C., and Hou, L. (2013). Formation and resuscitation of viable but nonculturable *Salmonella typhi*. Biomed Res Int *2013*, 907170.

Zhang, W., and Sack, D.A. (2015). Current Progress in Developing Subunit Vaccines against Enterotoxigenic *Escherichia coli*-Associated Diarrhea. Clin. Vaccine Immunol. *22*, 983–991.

Zhang, L., Xu, Y.-Q., Liu, H.-Y., Lai, T., Ma, J.-L., Wang, J.-F., and Zhu, Y.-H. (2010). Evaluation of *Lactobacillus rhamnosus* GG using an *Escherichia coli* K88 model of piglet diarrhoea: Effects on diarrhoea incidence, faecal microflora and immune responses. Vet. Microbiol. *141*, 142–148.

Zhang, W., Zhao, M., Ruesch, L., Omot, A., and Francis, D. (2007). Prevalence of virulence genes in *Escherichia coli* strains recently isolated from young pigs with diarrhea in the US. Vet. Microbiol. *123*, 145–152.

Zhang, W., Zhu, Y.-H., Zhou, D., Wu, Q., Song, D., Dicksved, J., and Wang, J.-F. (2017). Oral Administration of a Select Mixture of *Bacillus* Probiotics Affects the Gut Microbiota and Goblet Cell Function following *Escherichia coli* Challenge in Newly Weaned Pigs of Genotype *MUC4* That Are Supposed To Be Enterotoxigenic *E. coli* F4ab/ac Receptor Negative. Applied and Environmental Microbiology *83*.

Zhao, B., and Houry, W.A. (2010). Acid stress response in enteropathogenic gammaproteobacteria: an aptitude for survival. Biochem. Cell Biol. *88*, 301–314.

Zheng, L., Kelly, C.J., and Colgan, S.P. (2015). Physiologic hypoxia and oxygen homeostasis in the healthy intestine. A Review in the Theme: Cellular Responses to Hypoxia. Am J Physiol Cell Physiol *309*, C350–C360.

Zhong, S.-S., Zhang, Z.-S., Wang, J.-D., Lai, Z.-S., Wang, Q.-Y., Pan, L.-J., and Ren, Y.-X. (2004). Competitive inhibition of adherence of enterotoxigenic Escherichia coli, *enteropathogenic Escherichia coli* and *Clostridium difficile* to intestinal epithelial cell line Lovo by purified adhesin *of Bifidobacterium adolescentis* 1027. World J. Gastroenterol. *10*, 1630–1633.

Zhou, M., Zhu, J., Yu, H., Yin, X., Sabour, P.M., Zhao, L., Chen, W., and Gong, J. (2014). Investigation into *in vitro* and *in vivo* models using intestinal epithelial IPEC-J2 cells and *Caenorhabditis elegans* for selecting probiotic candidates to control porcine enterotoxigenic *Escherichia coli*. J. Appl. Microbiol. *117*, 217–226.

Zhu, Y.-H., Li, X.-Q., Zhang, W., Zhou, D., Liu, H.-Y., and Wang, J.-F. (2014). Dose-dependent effects of *Lactobacillus rhamnosus* on serum interleukin-17 production and intestinal T-cell responses in pigs challenged with *Escherichia coli*. Appl. Environ. Microbiol. *80*, 1787–1798.

Zhu, Y., Luo, Q., Davis, S., Westra, C., Vickers, T.J., and Fleckenstein, J.M. (2018). Molecular determinants of enterotoxigenic *Escherichia coli* heat-stable toxin secretion and delivery.

Zoetendal, E.G., Rajilic-Stojanovic, M., and de Vos, W.M. (2008). High-throughput diversity and functionality analysis of the gastrointestinal tract microbiota. Gut *57*, 1605–1615.

Zoetendal, E.G., Raes, J., van den Bogert, B., Arumugam, M., Booijink, C.C.G.M., Troost, F.J., Bork, P., Wels, M., de Vos, W.M., and Kleerebezem, M. (2012). The human small intestinal microbiota is driven by rapid uptake and conversion of simple carbohydrates. ISME J *6*, 1415–1426.

Zumbrun, S.D., Melton-Celsa, A.R., Smith, M.A., Gilbreath, J.J., Merrell, D.S., and O'Brien, A.D. (2013). Dietary choice affects Shiga toxin-producing *Escherichia coli* (STEC) O157:H7 colonization and disease. Proc Natl Acad Sci USA *110*, E2126–E2133.

COPYRIGHT ATTRIBUTION

- **Fig. 1.1., Fig. 1.12., Fig. 1.13., Fig. 2.5.A, Fig. 2.1 (literature review); Fig. 1. (general discussion)**: Articles are published under a CC BY license (Creative Commons Attribution 4.0 International License). The CC BY license allows for maximum dissemination and re-use of open access materials and is preferred by many research funding bodies. Under this license users are free to share (copy, distribute and transmit) and remix (adapt) the contribution including for commercial purposes, providing they attribute the contribution in the manner specified by the author or licensor.

- **Fig. 1.2., Fig. 1.8., Fig. 1.11. (literature review)**: ASM authorizes an advanced degree candidate to republish the requested material in his/her doctoral thesis or dissertation.

- **Fig. 1.9 (literature review)**: A permission license to reprint this image was obtained from Elsevier. License number 4511910878848.

- **Fig. 1.16B and C (literature review)**: A permission license to reprint this image was obtained from Springer Nature. License number 4511921298036.

- **Fig. 2.5B (literature review)**: A permission license to reprint this image was obtained from Elsevier. License number 4511940429562.

- **Fig. 2. (general discussion)**: A permission license to reprint this image was obtained from Elsevier. License number 4526100617035.

SCIENTIFIC CURRICULUM VITAE

Personal information

Name:	Charlène Roussel
Date and place of birth:	4th of September 1990, Valence, France
Nationality:	French
Email:	Charlene.Roussel@UGent.be Charlene.roussel@uca.fr
Phone:	+33.6.33.25.39.02
Affiliation:	Clermont-Auvergne University – Faculty of Pharmacy Laboratory of Microbiology, Digestive environment and Health (UMR 454 MEDIS) France Ghent University – Faculty of Bioscience Engineering Center for Microbial Ecology and Technology (CMET, www.ugent.be) Belgium
Workplace address:	Coupure Links 653, 9000 Ghent, Belgium

Education

Oct 2015 – Present

PhD Candidate in Applied Biological Sciences
Joint PhD UMR MEDIS (France) / CMET (Belgium)
Co-supervisors: Prof. dr. ir. Stéphanie Blanquet-Diot
Prof. dr. ir. Tom Van de Wiele
Title: Enterotoxigenic *Escherichia coli* (ETEC) pathophysiology and probiotic modulation in human gastrointestinal systems

2013 – 2015

Master of Nutrition, food and health
Faculty of Pharmacy, Clermont-Ferrand (France)
Graduated with great distinction
Master thesis: Development of an infant *in vitro* gastrointestinal protocol in the TIM-1 model, for a compared study of EHEC behavior in adult and infant simulated digestion (Prof. dr. ir. Stéphanie Blanquet-Diot, Prof. dr. ir. Tom Van de Wiele)

May – August 2014

Internship at the College of Allied Health, Oklahoma City, USA
Dissertation: Nutrition education and counseling to improve health and eating habits in the Oklahoma city area (Prof. dr. ir. Allen Knehans)

2010 – 2013

Bachelor of Biology, Nutrition specialty
Faculty of Medicine, Clermont-Ferrand (France)
Graduated with great distinction

Publications

Articles on ISI Web of Science (published, A1)

↳ ROUSSEL C., GALIA W., LERICHE F., CHALANCON S., DENIS S., Van de WIELE T., BLANQUET-DIOT S. Comparison of conventional plating, PMA-qPCR, and flow cytometry for the determination of viable enterotoxigenic *Escherichia coli* along a gastrointestinal *in vitro* model. *Applied Microbiol. Biotechnol, 102, 9793-9802* (2018). https://doi.org/10.1007/s00253-018-9380-z

↳ ROUSSEL C., SIVIGNON A., DE VALLEE A., GARRAIT G., DENIS S., TSILIA V., BALLET N., VANDEKERCKOVE P., VAN DE WIELE T., BARNICH N., BLANQUET-DIOT S. Anti-infectious properties of the probiotic *Saccharomyces cerevisiae* CNCM I-3856 on enterotoxigenic *E. coli* (ETEC) strain H10407. *Applied Microbiol Biotechnol*, *102, 6175-6189* (2018). https://doi.org/10.1007/s00253-018-9053-y

↳ ROUSSEL C., SIVIGNON A., Van de WIELE T., BLANQUET-DIOT S. Review – Foodborne enterotoxigenic *Escherichia coli* : from gut pathogenesis to new preventive strategies involving probiotics. *Future Microbiology*, *12, 73-93* (2017). https://doi.org/10.2217/fmb-2016-0101

↳ ROUSSEL C., CORDONNIER C., GALIA W., LE GOFF O., THEVENOT J., CHALANCON S., THEVENOT-SERGENTER D., LERICHE F., ALRIC M., VAN DE WIELE T., LIVRELLI V., BLANQUET-DIOT S. Increased EHEC survival and virulence gene expression indicate an enhanced pathogenicity upon simulated pediatric gastrointestinal conditions. *Pediatric research, 80, 734-743* (2016). https://doi.org/10.1038/pr.2016.144

Articles in preparation

↳ ROUSSEL C., DE PAEPE K., GALIA W., DE BODT J., LERICHE F., VAN DE WIELE T., BLANQUET-DIOT S. Dynamic human gut *in vitro* models unravel the modulation of ETEC pathogenesis by abiotic factors and the human gut microbiota.

↳ ROUSSEL C., DE PAEPE K., GALIA W., DE BODT J., LERICHE F., VAN DE WIELE T., BLANQUET-DIOT S. Marry TIM-1 and M-SHIME for an in-depth understanding of the anti-infectious properties of *S. cerevisiae* CNCM I-3856 against ETEC pathogens in the human gut.

Book chapters

↳ ROUSSEL C., CORDONNIER C., VAN DE WIELE T., BLANQUET-DIOT S. Intestinal pathogenic *Escherichia coli*: survival and modulation of virulence through the human gastrointestinal tract, *Escherichia coli* (ISBN 978-953-51-5008-4), (2017). https://doi.org/10.5772/intechopen.68309

↳ ROUSSEL C., BOUDET G., CHAMOUX A. Reprendre une activité professionelle. Principaux critères à considerer pour la reprise. Evaluation de la pénibilité cardiaque au poste de travail, Coeur et travail, ou comment concilier maladie cardiaque et activité professionnelle?, (ISBN 978-2-87/671-558-5), Editions Frison-Roche, (2013).

Participation at national and international conferences

Oral presentations

MBIO- ADEBIOTECH, Paris, France, June 2018
ROUSSEL C., GALIA W., DE PAEPE K., DE BODT J., DENIS S., CHALANCON S., BALLET N., VANDEKERCKOVE P., LERICHE F., VAN DE WIELE T., BLANQUET-DIOT S. TIM & SHIME: deux modèles bio-régionalisés de l'environnement digestif humain pour une comprehension approfondie des propriétés antagonsites du probiotique *Saccharomyces cerevisiae* CNCM I-3856 vis-à-vis des ETEC.

Microbiome & Probiotic Congress, Rotterdam, Netherlands, March 2018
ROUSSEL C., GALIA W., LERICHE F., VAN DE WIELE T., BLANQUET-DIOT S. Marry TIM-1 & SHIME for an in-depth understanding of the anti-infectious properties of the probiotic *Saccharomyces cerevisiae* CNCM I-3856 against ETEC food-borne pathogen in the human gut.

Probiotic Congress, Budapest, Hungary, June 2017
ROUSSEL C., SIVIGNON A., DE VALLEE A., GARRAIT G., DENIS S., TSILIA V., BALLET N., VANDEKERCKOVE P., VAN DE WIELE T., BARNICH N., BLANQUET-DIOT S. Interest of the probiotic yeast *Saccharomyces cerevisiae* CNCM I-3856 in the control of ETEC infections : *in vitro* and *in vivo* investigation of the mechanisms of action.

Microbiologist day in Auvergne, Clermont-Ferrand, France, March 2017
ROUSSEL C., SIVIGNON A., DE VALLEE A., GARRAIT G., DENIS S., TSILIA V., BALLET N., VANDEKERCKOVE P., VAN DE WIELE T., BARNICH N., BLANQUET-DIOT S. Potentiel de *Saccharomyces cerevisiae* CNCM I-3856 dans la maîtrise des infections à *Escherichia coli* entérotoxinogènes et determination des mécanismes d'action associés.

Journée régionale des innovations thérapeutiques, Lyon, France, January 2017
ROUSSEL C., VAN DE WIELE T., BLANQUET-DIOT S. Probiotiques et innovation thérapeutique.

Poster presentations

Gordon Conference Microbial Toxins and Pathogenicity, Waterville Valley, United States, July 2018 ROUSSEL C., GALIA W., DENIS S., CHALANCON S., ALRIC M., LERICHE F., VAN DE WIELE T., BLANQUET-DIOT S. Dynamic of enterotoxigenic *E. coli* (ETEC) survival and virulence in the *in vitro* upper gastrointestinal tract.

Gordon Seminar Microbial Toxins and Pathogenicity, Waterville Valley, United States, July 2018 ROUSSEL C., GALIA W., DE PAEPE K., DE BODT J., DENIS S., CHALANCON S., ALRIC M., LERICHE F., VAN DE WIELE T., BLANQUET-DIOT S. Combination of two simulators of the human gut TIM and M-SHIME for an in-depth understanding of the behavior of enterotoxigenic *E. coli* in the digestive environment.

Beneficial Microbes, Amsterdam, Netherlands, October 2017
ROUSSEL C., GALIA W., COLETTE A., CHALANCON S., DENIS S., BALLET N., VANDEKERCKOVE P., ALRIC M., LERICHE F., VAN DE WIELE T., BLANQUET-DIOT S. Antimicrobial properties of *Saccharomyces cerevisiae* CNCM I-3856 against enterotoxigenic *E. coli* in a simulator of the human upper GI tract.

Food Microbiology Conference, Brussel, Belgium, September 2017
ROUSSEL C., GALIA W., COLETTE A., CHALANCON S., DENIS S., BALLET N., VANDEKERCKOVE P., ALRIC M., LERICHE F., VAN DE WIELE T., BLANQUET-DIOT S. *Saccharomyces cerevisiae* CNCM I-3856 alters the survival and virulence of enterotoxigenic *Escherichia coli* in a simulator of the human upper digestive tract.

↳ **Pharmabiotics, Paris, France, April 2017**
ROUSSEL C., SIVIGNON A., DE VALLEE A., GARRAIT G., DENIS S., BALLET N., VANDEKERCKOVE P., VAN DE WIELE T., BARNICH N., BLANQUET-DIOT S. Use of probiotic yeast *Saccharomyces cerevisiae* CNCM I-3856 in the control of ETEC infections : *in vitro* and *in vivo* investigation of their inhibitory effects.

↳ **Beneficial Microbes, Amsterdam, Netherlands, October 2016**
ROUSSEL C., GARRAIT G., SIVIGNON A., VAN DE WIELE T., BARNICH N., BLANQUET-DIOT S. Use of probiotic bacteria or yeast in the control of ETEC infections: *in vitro* investigation of their inhibitory potential.

↳ **Beneficial Microbes, Amsterdam, Netherlands, October 2016**
ROUSSEL C., CORDONNIER C., GALIA W., LE GOFF O., THEVENOT J., CHALANCON S., THEVENOT-SERGENTER D., LERICHE F., ALRIC M., LIVRELLI V., VAN DE WIELE T., BLANQUET-DIOT S. Use of the gastrointestinal TIM system to promote understanding of enteric pathogen behavior in the infant GIT: application to the evaluation of probiotics as an alternative strategy for infection control.

↳ **Gut Microbiology INRA-ROWETT, Clermont-Ferrand, France, June 2016**
ROUSSEL C., CORDONNIER C., GALIA W., LE GOFF O., THEVENOT J., CHALANCON S., THEVENOT-SERGENTER D., LERICHE F., ALRIC M., LIVRELLI V., VAN DE WIELE T., BLANQUET-DIOT S. Increased EHEC survival and virulence gene expression indicate an enhanced pathogenesis upon simulated infant gastrointestinal conditions.

↳ **Microbiome R&D and business collaboration forum: Europe, London, United Kingdom, April 2016** ROUSSEL C., CORDONNIER C., GALIA W., LE GOFF O., THEVENOT J., CHALANCON S., THEVENOT-SERGENTER D., LERICHE F., ALRIC M., LIVRELLI V., VAN DE WIELE T., BLANQUET-DIOT S. Use of the dynamic gastrointestinal TIM system to promote understanding of food-borne pathogen survival and virulence in the infant at-risk population.

↳ **CRNH Auvergne Scientific Day, Clermont-Ferrand, France, November 2015**
ROUSSEL C., CORDONNIER C., GALIA W., LE GOFF O., THEVENOT J., CHALANCON S., THEVENOT-SERGENTER D., LERICHE F., ALRIC M., LIVRELLI V., VAN DE WIELE T., BLANQUET-DIOT S. Comparative study of EHEC survival and virulence under adult and infant simulated digestive conditions.

↳ **VTEC Verocytotoxin-producing Escherichia coli, Boston, United States, September 2015**
CORDONNIER C., ROUSSEL C., GALIA W., LE GOFF O., THEVENOT J., CHALANCON S., THEVENOT-SERGENTER D., LERICHE F., ALRIC M., VAN DE WIELE T., LIVRELLI V., BLANQUET-DIOT S. Comparative study of EHEC survival and virulence under adult and infant simulated digestive conditions.

Teaching

↳ Teaching and supervising practical exercises for the course “Botany and vegetal science” for the students of 1st year of Medicine and 2nd year of Pharmacy (Clermont-Auvergne University, Prof. Caldefie-Chezet and Dr. Delort) (64h / year, 2015-2017).

↳ Tutor of 3 master students during their thesis (2015-2017).

APPENDIX

APPENDIX 1. ROUSSEL C., CORDONNIER C., GALIA W., LE GOFF O., THEVENOT J., CHALANCON S., THEVENOT-SERGENTER D., LERICHE F., ALRIC M., VAN DE WIELE T., LIVRELLI V., BLANQUET-DIOT S. Increased EHEC survival and virulence gene expression indicate an enhanced pathogenicity upon simulated pediatric gastrointestinal conditions. *Pediatric research, 80, 734-743* (2016) https://doi.org/10.1038/pr.2016.144

nature publishing group

Basic Science Investigation | Articles

Increased EHEC survival and virulence gene expression indicate an enhanced pathogenicity upon simulated pediatric gastrointestinal conditions

Charlène Roussel[1,2], Charlotte Cordonnier[1,3], Wessam Galia[1,4,5], Olivier Le Goff[1], Jonathan Thévenot[1,3], Sandrine Chalancon[1], Monique Alric[1], Delphine Thevenot-Sergentet[4,6], Francoise Leriche[5], Tom Van de Wiele[2], Valérie Livrelli[3,7] and Stéphanie Blanquet-Diot[1]

BACKGROUND: Enterohemorrhagic *Escherichia coli* (EHEC) are major foodborne pathogens that constitute a serious public health threat, mainly in young children. Shiga toxins (Stx) are the main virulence determinants of EHEC pathogenesis but adhesins like intimin (eae) and Long polar fimbriae (Lpf) also contribute to infection. The TNO GastroIntestinal Model (TIM) was used for a comparative study of EHEC O157:H7 survival and virulence under adult and child digestive conditions.

METHODS: Survival kinetics in the *in vitro* digestive tract were determined by plating while bacterial viability was assessed by flow cytometry analysis. Expression of *stx*, *eae*, and *lpf* genes was followed by reverse transcriptase-quantitative PCR (RT-qPCR) and Stx production was measured by ELISA (enzyme-linked immunosorbent assay).

RESULTS: Upon gastrointestinal passage, a higher amount of viable cells was found in the simulated ileal effluents of children compared to that of adults (with 34 and 6% of viable cells, respectively). Expression levels of virulence genes were up to 125-fold higher in children. Stx was detected only in child ileal effluents.

CONCLUSION: Differences in digestive physicochemical parameters may partially explain why children are more susceptible to EHEC infection than adults. Such data are essential for a full understanding of EHEC pathogenesis and would help in designing novel therapeutic approaches.

Enterohemorrhagic *Escherichia coli* (EHEC), mainly from the serotype O157:H7, are food and waterborne pathogens that constitute a serious public health concern. EHEC are responsible for hemorrhagic colitis and bloody diarrhea that can evolve toward life-threatening age-dependent complications (1). The hemolytic uremic syndrome (HUS), defined by the triad of acute renal failure, thrombocytopenia, and microangiopathic hemolytic anemia, mainly affects young children under 3 y of age (1–3) while thrombotic thrombocytopenic purpura, characterized by central nervous system damages, more commonly afflicts adults and elderly. In Europe and France, EHEC infections are the leading cause of renal failure in children. Even if Shiga toxins (Stx) are the main virulence determinants of EHEC, other factors such as intimin (eae) and adhesins (including Long polar Fimbriae (Lpf)) also contribute to human pathogenesis by mediating bacterial colonization (4,5).

Survival and virulence of EHEC strains in the human gastrointestinal (GI) tract are key factors in the infectious process (6) but they remain poorly described, mainly in children, due to a lack of relevant models. Studies in humans are obviously prohibited and results obtained in animal models are hampered by differences between animal and human digestive physiology. *In vitro* digestion methods emerge as an appropriate alternative to *in vivo* assays providing that such models can reproduce physiologically relevant conditions. Among the available systems, the dynamic multicompartmental and computer-controlled TNO gastrointestinal model (TIM) is currently the most complete simulator of the upper GI tract (7) and has been validated for microbial applications against *in vivo* data (8). Previous works in this model have assessed the survival of *E. coli* O157:H7 when ingested within a food matrix (9,10), but experiments were carried out only under adult conditions and no data are available on virulence gene expression during GI transit.

In this context, the aim of this study was to use the TIM model for a comparative analysis of *E. coli* O157:H7 survival and virulence under adults and young children (from 6 mo to 2 y)

The first two authors contributed equally to this work.
[1]EA 4678 CIDAM, Conception Ingénierie et Développement de l'Aliment et du Médicament, Université d'Auvergne, Clermont-Ferrand, France; [2]CMet, Center for Microbial Ecology and Technology, Ghent University, Ghent, Belgium; [3]M2iSH, Microbes, Intestin, Inflammation et Susceptibilité de l'Hôte UMR INSERM/Université d'Auvergne, Université d'Auvergne, Clermont-Ferrand, France; [4]UMR 5557 Ecologie Microbienne, Research Group on Bacterial Opportunistic Pathogens and Environment, CNRS, VetAgro Sup and Université de Lyon, Lyon, France; [5]Unité CALYTISS, VetAgro Sup, Lempdes, France; [6]Laboratoire d'Etude des Microorganismes Alimentaires Pathogènes, French National Reference Laboratory for Escherichia coli including Shiga Toxin-Producing E. coli, VetAgro Sup, Université de Lyon, Marcy l'Etoile, France; [7]Service de Bactériologie, CHU de Clermont-Ferrand, Clermont-Ferrand, France. Correspondence: Stéphanie Blanquet-Diot (stephanie.blanquet@udamail.fr)

Received 18 March 2016; accepted 15 May 2016; advance online publication 17 August 2016. doi:10.1038/pr.2016.144

digestive conditions, upon simulated ingestion of a glass of contaminated water.

RESULTS

Survival and Physiological State of EHEC O157:H7 in the Simulated Stomach

Whatever the simulated age group (adult or child), no significant difference was observed between the survival kinetics obtained for O157:H7 and the transit marker, showing that the growth ability of the pathogen (as assessed by numeration of cultivable cells) was not affected by gastric conditions (Figure 1a). In contrast, flow cytometry analysis of gastric effluents showed marked differences in the physiological state of bacteria between adult and child conditions (Figure 1b). At 60 min digestion, a higher percentage of viable cells was observed under child conditions compared with adult ones (59.0 vs. 21.9%), together with a lower number of damaged cells (18.0 vs. 46.2%), whereas similar initial viability profiles were observed between adult and child conditions. Our results indicate that cells that are likely to reach the small intestine would be less damaged in infants compared with adults.

Survival and Physiological State of EHEC O157:H7 in the Simulated Small Intestine

In the duodenal simulated compartment, EHEC survival was unaffected in both age conditions. In contrast, bacterial mortality was noticed halfway the jejunum- and ileum-simulated digestion time, but only under adult conditions (Figure 2a). In adults, bacterial recovery percentages after 120 min were $2.8 \pm 0.4\%$ ($n = 4$) vs. 27.5% for the transit marker ($P < 0.01$) in the jejunum and $11.4 \pm 5.5\%$ ($n = 4$) vs. 37.9% in the ileum ($P < 0.001$). At the end of digestion (240–360 min), the trend reversed with the recoveries of bacteria exceeding those of the transit marker, thus indicating bacterial outgrowth. EHEC growth was much more pronounced under simulated child conditions with differences between bacteria and transit marker being significant both in the jejunal and ileal compartments ($P < 0.05$). At 360 min during the child assays, a survival percentage of $87.3 \pm 30.7\%$ ($n = 4$) was found for O157:H7 compared with 2.2% for the marker ($P < 0.001$) in the jejunum and $441.7 \pm 341.2\%$ ($n = 4$) compared with 13.5% in the ileum ($P = 0.063$). Results based on flow cytometry analysis of ileal effluents (Figure 2b) strengthened those obtained by cultivation. The percentages of damaged cells remained constant around 15% throughout child digestions while they regularly increased during adult experiments (from 5.4% at t0 to 37.9% at 300 min). Conversely, the percentages of viable cells dramatically decreased during adult digestion (from 77.1% at t0 to 6.3% at 300 min) whereas they decreased then increased in child assays (from 77.1% at t0 to 21.9% at 180 min; and 33.9% at 360 min). This last feature is in accordance with the cell mortality followed by growth observed by cultivation, mainly under child conditions. Our results also indicate that, when entering the colon, most of bacterial cells are viable under child digestive conditions while in adults most of them have a damaged membrane.

Expression of EHEC Virulence Genes in the Simulated GI Tract

Gastric effluents of the simulated child conditions in TIM (Figure 3a) displayed significant up-regulated *stx1* and *stx2* at 10, 20, 40, and 60 min (with a fold change up to 125 for *stx1* and up to 12 for *stx2* compared with t0, $P < 0.001$). However, *stx* upregulation was not observed under simulated adult conditions, resulting in significantly higher *stx1* and *stx2* expression levels upon child gastric conditions compared with adult ones ($P < 0.01$). In the ileal effluents (Figure 3b), *stx1*, and *stx2* were up-regulated from 60 to 240 min in the child digestions, yet significant upregulation levels were only obtained at 180 min with a fivefold to sevenfold increase ($P < 0.05$). In adult ileal effluents, *stx* genes were significantly up-regulated in the same order of magnitude, but at 120 and 180 min for *stx1* ($P < 0.05$); and at 60 and 240 min for *stx2* ($P < 0.001$). *stx* expression levels were significantly higher in children compared with adults only at 60 min for *stx1* ($P < 0.01$). Results provided by enzyme-linked immunosorbent assay (Figure 4) fully support the difference obtained between adults and children with RT-qPCR. No Stx was evidenced under adult conditions while toxins were detected in the ileal effluents of children from 60 min and the amount produced regularly increased to reach 0.89 ± 0.12 ng/ml at 300 min ($n = 4$). Stx concentrations were significantly higher during child digestions compared with the adult ones from 120 min ($P < 0.05$).

In the gastric effluents from children (Figure 5a), *eae* expression was significantly ($P < 0.001$) repressed compared with the initial conditions from 10 to 60 min. On the contrary, under adult conditions, *eae* was over-expressed at 10 and 20 min ($P < 0.05$) with a fold change up to 15, resulting in significant higher expression levels in adults compared with children from 10 to 40 min ($P < 0.01$). Notably, at the end of gastric digestion (60 min), the reverse was found with *eae* mRNA levels higher in children ($P < 0.01$). In the ileal effluents (Figure 5b), *eae* mRNA expression levels tended to increase under child conditions from 180 min ($P > 0.05$), while they were significantly higher than t0 in adults at 60 and 120 min ($P < 0.001$, with up to ninefold change). At the beginning of *in vitro* digestion (until 120 min), *eae* was significantly overexpressed in adults compared with children, while the opposite trend was observed at 180 and 240 min ($P < 0.01$).

Lastly, in the gastric effluents (Figure 6a), *lpf1*, and *lpf2* were overexpressed compared with t0 under both adult and child conditions, with a fold change up to 12 for *lpf1* ($P < 0.001$, in adults and children) and up to 40 for *lpf2* ($P < 0.001$, in children). *lpf1* and *lpf2* expression levels were significantly higher in adults at 10 min ($P < 0.05$), while the reverse was observed at 40 and 60 min with significant higher levels in children ($P < 0.05$). In the ileal effluents (Figure 6b), *lpf* genes were overexpressed in both age conditions, but higher mRNA levels were found in children with a maximum fold increase of 30 and 60 at 240 min for *lpf1* and *lpf2*, respectively. *lpf* expression levels were significantly higher under child conditions compared with adult ones, but only at 180 min for *lpf1* ($P < 0.01$).

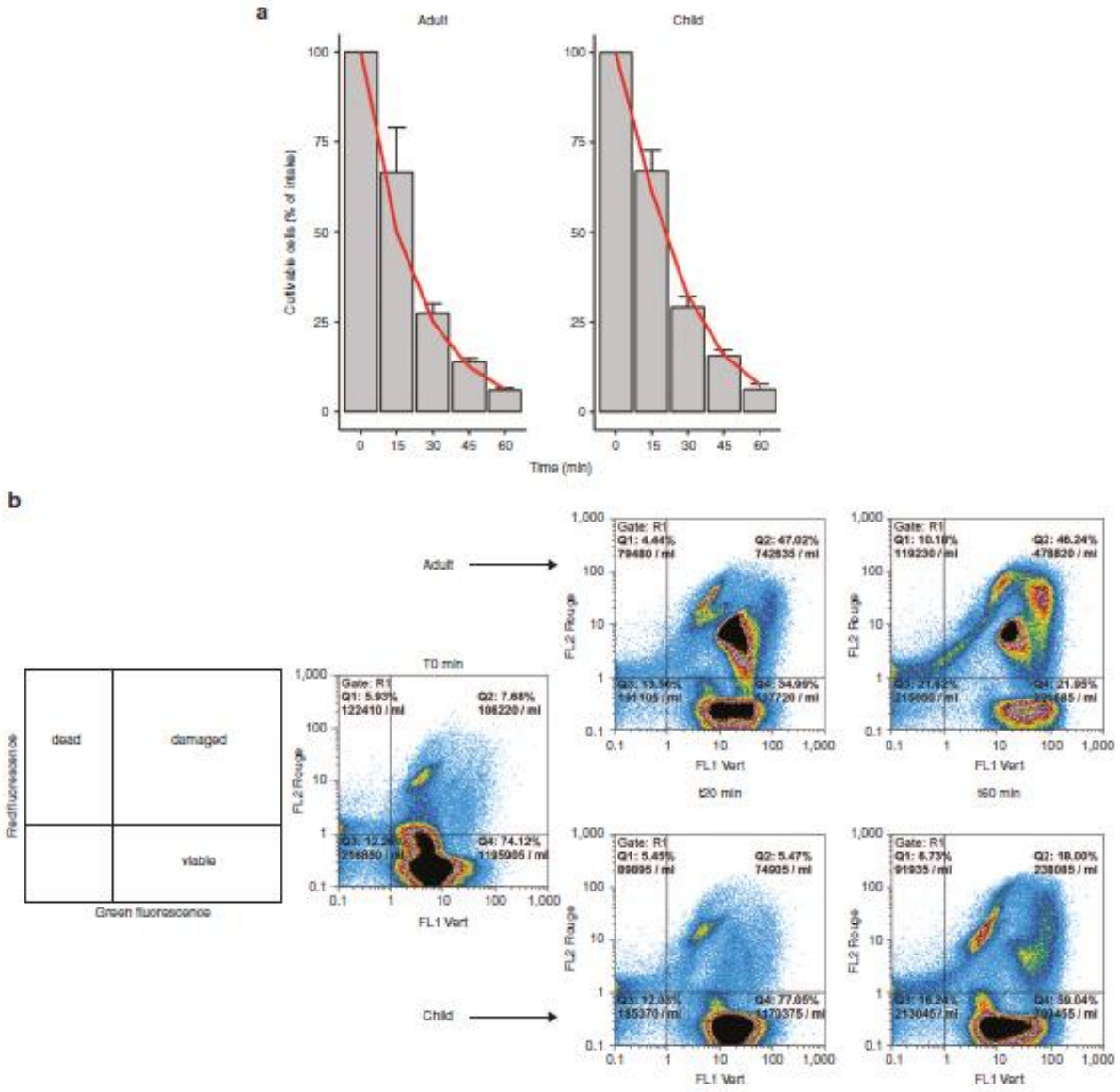

Figure 1. Survival and physiological state of EHEC O157:H7 in the TIM stomach. (**a**) The number of cultivable cells in the gastric compartment was determined by plating. Results are expressed as survival percentages ± SEM ($n = 4$) and compared with that obtained with the transit marker (red line). (**b**) Physiological state of O157:H7 was assessed by live/dead cytometry analysis. Bacteria recovered from gastric effluents were double-stained using green-fluorescent SYTO 9 (all cells) and red-fluorescent PI (bacteria with damaged membranes). TIM, TNO gastrointestinal model; EHEC, Enterohemorrhagic *Escherichia coli*.

DISCUSSION

EHEC survival and virulence in the human digestive tract are key features in bacterial pathogenesis (6). Overall, our data suggest that, in comparison with adults, a higher amount of cells, what is more less damaged, may reach the distal parts of the small intestine and the colon in children. Expression of major virulence genes, such as *stx*, is also higher under child digestive conditions.

Up to date, there was only scarce information on the behavior of EHEC strains under human simulated GI conditions (9–11). In addition, none of these studies took into account specific child conditions, despite young children forming a high-risk population for EHEC infection. The aim of this study was to assess and compare the survival and virulence of the reference strain O157:H7 EDL 933 under adult and child digestive conditions by using the well-validated dynamic and multicompartmental TIM model. An exhaustive survey of the

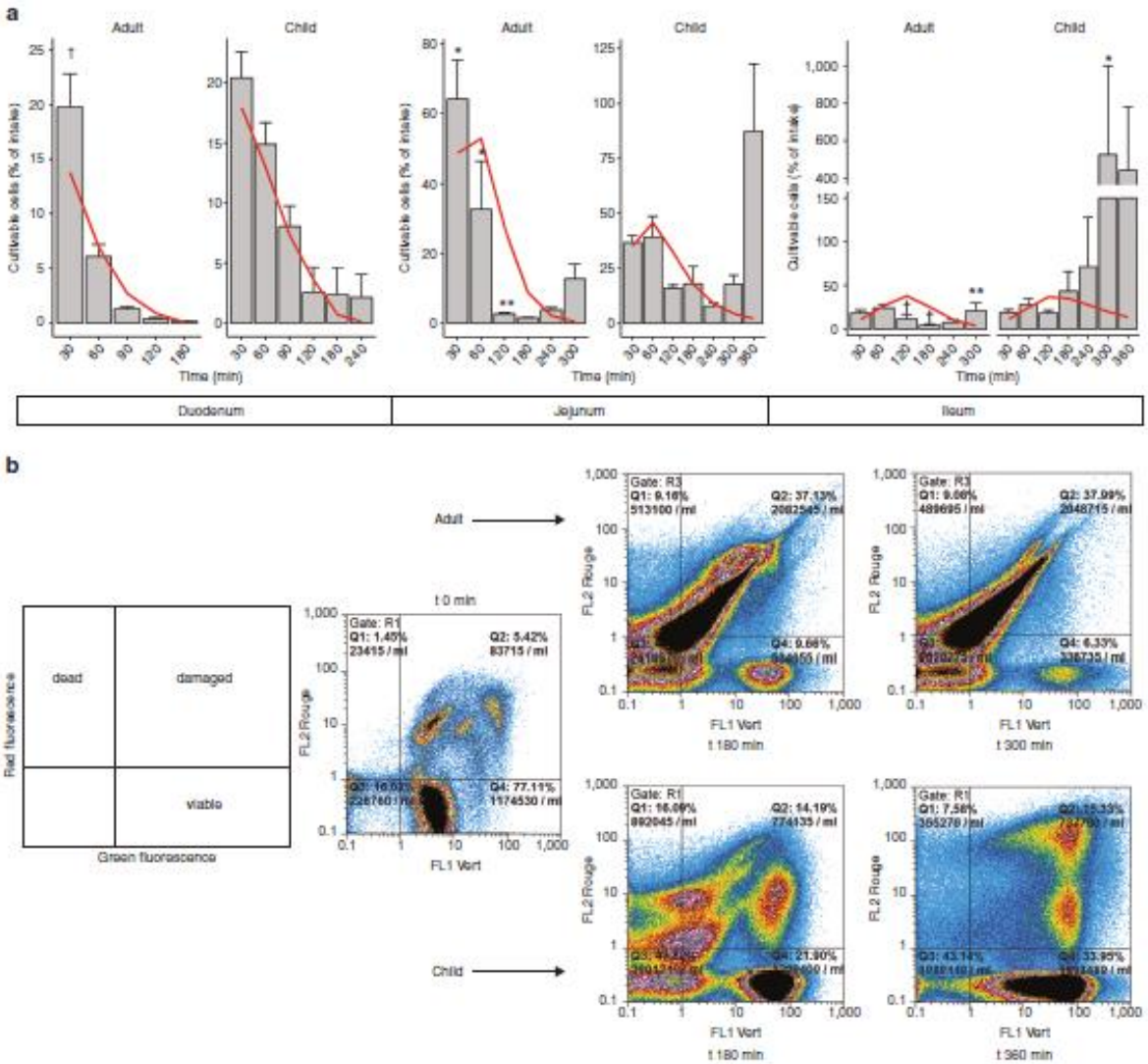

Figure 2. Survival and physiological state of EHEC O157:H7 in the TIM small intestine. (**a**) The number of cultivable cells in the small intestinal compartments was determined by plating. Results are expressed as survival percentages ± SEM ($n = 4$) and compared with that obtained with the transit marker (red line). O157:H7 significantly different from the transit marker at $P < 0.05$ (*), $P < 0.01$ (**), and $P < 0.001$ (†). (**b**) Physiological state of O157:H7 was assessed by live/dead cytometry analysis. Bacteria recovered from ileal effluents were doubled-stained using green-fluorescent SYTO 9 (all cells) and red-fluorescent PI (bacteria with damaged membranes). TIM, TNO gastrointestinal model; EHEC, Enterohemorrhagic *Escherichia coli*.

literature was made to identify the physicochemical parameters unique to the child and adult GI tract in a healthy state and subsequently implement them into the TIM program. The survey was restricted to studies involving young children aged between 6 mo and 2 y because (i) children <3 y are a high-risk population for EHEC infection and HUS (3), (ii) the newborns (under 6 mo) mostly have an exclusive milk diet and subsequently show particular digestive physiology (12), and (iii) children >2 y show a mature GI tract, with no difference compared with the adult digestion process. Contaminated water which has been involved in major EHEC outbreaks (13) was chosen as a vehicle for bacteria. A supraphysiological dose of EHEC (10^7 Colony Forming Unit (CFU)/ml compared with the infectious dose of 10–100 CFU) was used to get enough RNAs in TIM digestive samples for transcriptomic analysis.

EHEC survival kinetics were first established in the TIM model. Our results suggest that O157:H7 is less sensitive to child than adult gastric conditions. This divergence may be explained by differences in stomach pH acidification less rapid and pronounced in children (14,15), associated with gastric

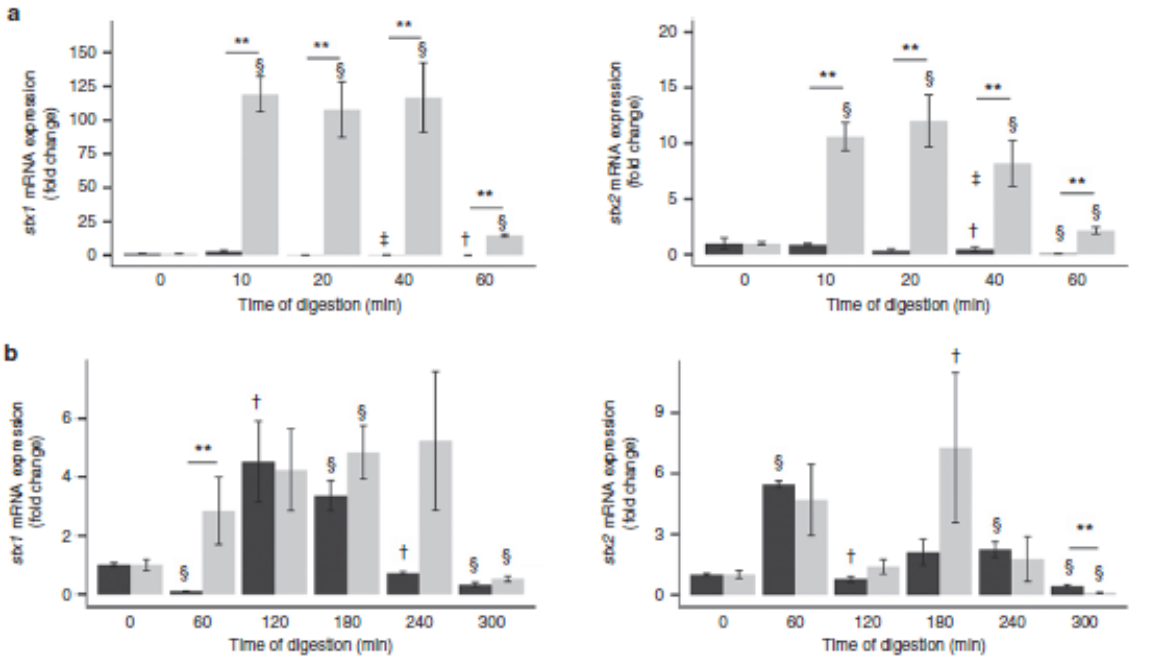

Figure 3. Expression of Shiga toxin-encoding genes in the TIM system. *stx 1/2* expression levels were measured by RT-qPCR in the gastric (**a**) and ileal (**b**) effluents of the TIM under child (in gray) and adult (in black) digestive conditions. Results are expressed as means of fold-induction ± SEM ($n = 4$). Time points statistically different from t0 at $P < 0.05$ (†), $P < 0.01$ (‡), and $P < 0.001$ (§). Child statistically different from adult at $P < 0.01$ (**).TIM, TNO gastrointestinal model; RT-qPCR, reverse transcriptase-quantitative PCR.

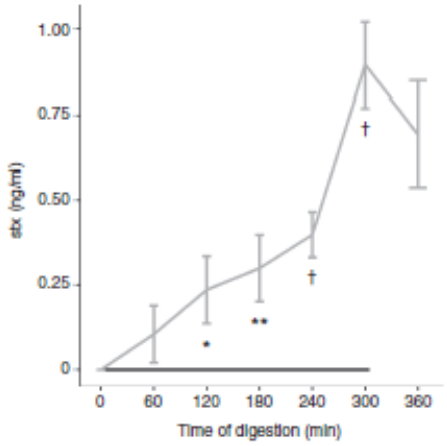

Figure 4. Shiga-toxin production in the ileal effluents of the TIM system. Stx 1/2 were measured in the ileal effluents by ELISA under child (in gray) and adult (in black) digestive conditions. Results are expressed as cumulative amounts in ng/ml ± SEM ($n = 4$). Child statistically different from adult at $P < 0.05$ (*), $P < 0.01$ (**) and $P < 0.001$ (†). TIM, TNO gastrointestinal model; ELISA, enzyme-linked immunosorbent assay.

emptying rates quite similar under both age conditions (16,17). In the small intestinal compartments, a loss of viability was noticed at the middle of digestion in the jejunum and ileum, but only during adult assays. The higher mortality observed in adults might be linked to a twofold higher concentration in bile salts and pancreatic secretions compared with children (18–24). The bactericidal effect of bile salts toward *E. coli* strains is well known and attributed to their detergent properties that may lead to the disruption of cell membrane. This phenomenon was maybe enlarged by the fact that in adults, when entering into the small intestine, bacterial cells were more damaged than under child conditions. Conversely, at the end of *in vitro* digestions, bacterial growth was noticed in the jejunum and ileum under both age conditions, but mainly in children. This growth renewal may be linked to the occurrence of less stringent conditions, such as pH values close to neutrality and lower bile salts concentrations due to their passive reabsorption (as occurs in humans). The higher growth observed during child digestions may be explained by the occurrence of less stressful conditions together with a higher small bowel transit time (25,26), as well as the "better" physiological state of bacteria when entering the small intestine. As terminal ileum and colon are assumed to be the main sites of EHEC pathogenesis (27), this finding may partly explain why young children are a high-risk population for EHEC infection.

The next step was dedicated to the assessment of O157:H7 virulence gene expression in the TIM model. Up to now, regulation of EHEC virulence genes was only investigated in oversimplified *in vitro* approaches integrating a single digestive parameter, such as acidic pH or bile, and never under child conditions. Three genes mainly involved in the virulence of EHEC strains were studied: (i) *stx* encoding Shiga

toxin, known as the main virulence trait of the pathogen and responsible for systemic complications (4), eae encoding intimin, required from intimate attachment to the host intestinal mucosa (5) and, (iii) *lpf* loci encoding Long Polar Fimbriae, adhesive factors assumed to be involved in key steps of EHEC pathogenesis, such as adhesion, translocation, and inflammation (28).

We showed for the first time that *stx* genes were upregulated during gastric and small intestinal transit in the TIM system. These results suggest that EHEC O157:H7 would be able to produce its toxins from the stomach in the upper GI tract even if Stx-mediated cytotoxicity is generally associated with distal parts of the small intestine or large intestine (29). Interestingly, we found that expression levels of *stx* genes and related toxin production were larger under child compared with adult conditions, which is in accordance with the higher sensitivity of young children to EHEC infection and HUS. The large expression levels found in the gastric compartment in children may be related to less acidic conditions, as *stx* genes were not up-regulated under adult conditions where bacteria have to cope with a higher acidity. This hypothesis was supported by additional assays in the TIM system under "modified child" gastric conditions (child gastric pH curve combined with adult transit time) where *stx* was still over-expressed (data not shown). Our results are in accordance with those obtained by Yuk and Marshall (30) and Huang *et al.* (31) who showed a decrease in Stx production in O157:H7 after acid challenge *in vitro*, but not with those of Yin *et al.* (32) who observed the opposite trend in acid treated pig ligated intestine. In the small intestine, *stx* genes were up-regulated both under adult and child conditions. It may be related to the occurrence of neutral pH, but probably not linked to bile salts which do not increase *stx* expression in LB medium (33,34). Overexpression of *stx* genes did not result in Stx detection in the ileal effluents of adults, maybe due to concentrations under the detection limit and/or degradation under low gastric pH or by proteases. It is well established that Stx synthesis requires induction of Stx prophages, caused by any stress conditions provoking the SOS response (35). In our study, surprisingly, the high percentages of damaged cells observed under adult conditions in the TIM system were not associated with any detectable toxin, while significant amounts of Stx were measured in children where most of EHEC bacteria were unspoiled. We can then hypothesize that toxin production observed during child digestions may be mostly linked to *stx1* overexpression, as it does not necessarily require prophage induction and may also occur under conditions of low iron levels (29).

As for *stx*, *eae*, and *lpf* genes were up-regulated in the gastric and small intestinal compartments of the TIM system. This implies that the expression of EHEC adhesins, such as intimin and Lpf, can be induced even if the pathogen does not come into contact with the host cells. For both adhesins, higher expression levels were found under child conditions compared with adult ones, but only at the end of gastric or GI *in vitro* digestions. It is worth noting that *eae* and *lpf* overexpression occurs in children when most of bacterial cells have reached

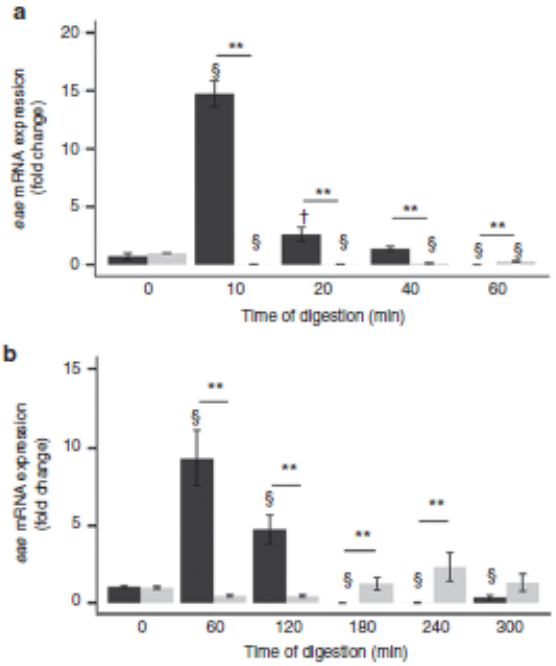

Figure 5. Expression of intimin-encoding gene in the TIM system. *eae* expression levels were measured by RT-qPCR in the gastric (**a**) and ileal (**b**) effluents of the TIM under child (in gray) and adult (in black) digestive conditions. Results are expressed as means of fold-induction ± SEM ($n = 4$). Time points statistically different from t0 at $P < 0.05$ (†) and $P < 0.001$ (§). Child statistically different from adult at $P < 0.01$ (**). TIM, TNO gastrointestinal model; RT-qPCR, reverse transcriptase-quantitative PCR.

the distal parts of the small intestine. As initial EHEC binding is assumed to occur at the follicle-associated epithelium of Peyer's Patches and villi of terminal ileum or colon (27), these results may suggest a higher ability to colonize in children. Very few studies have investigated the effect of digestive parameters on *eae* or *lpf* expression. A significant decrease in *eae* gene transcripts was observed *in vitro* when bile salts were added (33,36) and in pig intestinal loops acidified at pH 2.5 (32) while acid challenge (37) and bile salts (32,38) led to an up-regulation of *lpf* genes. Bile salts increase *lpf2* but not *lpf1* in O157:H7 (32), which may explain why *lpf2* mRNA levels were higher than *lpf1* ones in the small intestine. Current knowledge from literature does not provide any explanation from why *lpf* expression levels were higher under child conditions where a milder acidity and lower bile salt concentrations are found, nor why *eae* was mainly overexpressed in adults until 120 min digestion when the highest bile concentrations were found in the small intestinal compartments.

To conclude, our study shows that TIM model can provide meaningful insights into the comprehension of EHEC pathogenesis. Taken together, our results indicate that differences in digestive physicochemical parameters related to age conditions may partly explain the highest isolation rate of O157:H7 in the feces of children and their higher sensitivity to EHEC

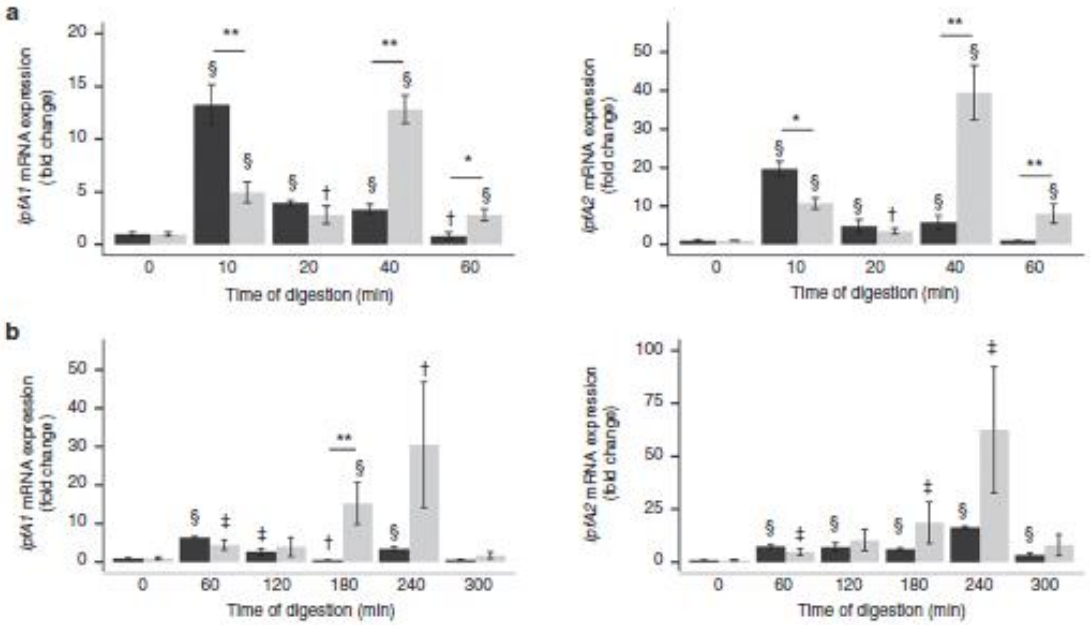

Figure 6. Expression of Long polar fimbriae-encoding genes in the TIM system. *lpf 1/2* expression levels were measured by RT-qPCR in the gastric (**a**) and ileal (**b**) effluents of the TIM under child (in gray) and adult (in black) digestive conditions. Results are expressed as means of fold-induction ± SEM ($n = 4$). Time points statistically different from t0 at $P < 0.05$ (†), $P < 0.01$ (‡) and $P < 0.001$ (§). Child statistically different from adult at $P < 0.05$ (*) and $P < 0.01$ (**). TIM, TNO gastrointestinal model; RT-qPCR, reverse transcriptase – quantitative PCR.

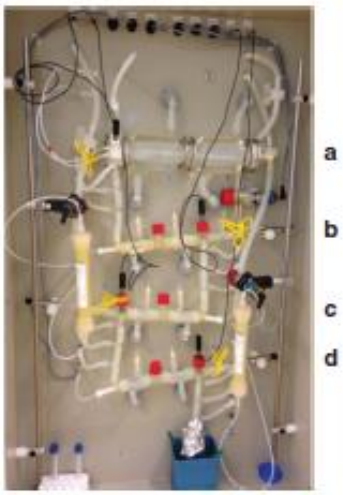

Figure 7. Gastric and small intestinal TNO gastrointestinal model (TIM). The TIM model is composed of four successive compartments simulating the human stomach (**a**) and the three parts of the small intestine, i.e., the duodenum (**b**), jejunum (**c**) and ileum (**d**).

infection and HUS (1–3). Nevertheless, other extra-digestive factors, such as immaturity of the immune system and higher expression of Stx receptor on the surface of renal cells (39) are also known to contribute to the higher susceptibility of infants to HUS. Besides, it should be noted that the results obtained in this study may be strain-specific (9). To get a more complete picture of EHEC pathogenesis, similar experiments should be carried out with other non-O157 strains that are also involved in EHEC disease. Such data are essential in the designing of novel therapeutic approaches, particularly in the young children high-risk population.

METHODS

TIM Gastrointestinal Model

The TIM model (TIM2013, TNO, Zeist, Netherlands) consists of four successive compartments simulating the human stomach, duodenum, jejunum, and ileum (Figure 7). The main parameters of digestion, such as body temperature, pH, peristaltic mixing and transport, gastric, biliary, and pancreatic secretions and passive absorption of small molecules and water, are reproduced as accurately as possible. Briefly, each compartment is composed of glass units with a flexible inner membrane. Peristaltic mixing and body temperature are achieved by pumping water at 37°C into the space between the glass jacket and the flexible wall at regular intervals. Mathematical modeling of gastric and ileal deliveries with the Elashoff power exponential equation ($f = 1-2^{-(t/t2)^{\beta}}$ where t is the time of emptying and β a coefficient describing the shape of the curve) is used for the computer control of chyme transit. Chyme transport through the TIM is regulated by the peristaltic valves that connect the successive compartments. The volume in each compartment is monitored by a pressure sensor and pH is computer-monitored and continuously controlled by adding either HCl or $NaHCO_3$. Simulated gastric, biliary and pancreatic secretions are introduced into the corresponding compartments by computer-controlled pumps. Water and products of digestion are removed from the jejunal and ileal compartments by pumping dialysis liquid through hollow fibers (SF 09L, Nipro, Zaventem, Belgium; cut-off 10 KDa).

In vitro Digestions

The TIM system was programmed to reproduce, based on *in vivo* data (16–26), the physicochemical digestive conditions observed in a healthy adult or young children (from 6 mo to 2 y) when a glass

Table 1. Set-point parameters of gastrointestinal digestions in the TIM system

Parameters of *in vitro* digestion	Adult	Child from 6 mo to 2 y old
pH	Gastric compartment (min/pH)	Gastric compartment (min/pH)
	$t = 10 \rightarrow 3.2$	$t = 10 \rightarrow 5.7$
	$t = 20 \rightarrow 2.4$	$t = 20 \rightarrow 5.3$
	$t = 40 \rightarrow 1.8$	$t = 40 \rightarrow 4.5$
	$t = 60 \rightarrow 1.6$	$t = 60 \rightarrow 3.2$
	$t = 90 \rightarrow 1.5$	$t = 90 \rightarrow 2.0$
	Duodenal compartment: 6.4	Duodenal compartment: 6.4
	Jejunal compartment: 6.9	Jejunal compartment: 6.9
	Ileal compartment: 7.2	Ileal compartment: 7.2
	Based on *in vivo* pH (14)	Based on *in vivo* pH (15)
Transit time	Stomach: $t_{1/2} = 15$ min, $\beta = 1$	Stomach: $t_{1/2} = 20$ min, $\beta = 1.2$
	Ileum: $t_{1/2} = 150$ min, $\beta = 2.4$	Ileum: $t_{1/2} = 190$ min, $\beta = 1.7$
	Based on *in vivo* transit time (16,25)	Based on *in vivo* transit time (17,26)
Digestive secretions	Gastric compartment[a]	
	130 IU/min of pepsin (18) (P7012 Sigma-Aldrich, St Quentin, France)	130 IU/min of pepsin (19) (P7012 Sigma-Aldrich)
	5 IU/min of lipase (18) (DS Amano Pharmaceutical, Aichi, Japan)	5 IU/min of lipase (19,20) (DS Amano Pharmaceutical)
	0.25 ml/min of HCl 0.3 mol/l (according to pH)	0.25 ml/min of HCl 0.1 mol/l (according to pH)
	Duodenal compartment	
	Bile salts[b] 4% during the first 30 min and then 2% (21) (B8631 and F48305 Sigma-Aldrich)	Bile salts[b] 1% (22) (B8631 and F48305 Sigma-Aldrich)
	Pancreatic juice 7% (18) (P1750 Sigma-Aldrich)	Pancreatic juice 3.5% (23) (P1750 Sigma-Aldrich)
	Trypsin 3.4 mg (24) (T4665 Sigma-Aldrich)	Trypsin 3 mg (19) (T4665 Sigma-Aldrich)
	0.25 ml/min of intestinal electrolytes solution	0.25 ml/min of intestinal electrolytes solution
	0.25 ml/min of $NaHCO_3$ 0.5 mol/l (according to pH)	0.25 ml/min of $NaHCO_3$ 0.5 mol/l (according to pH)
	Jejunal compartment	
	0.25 ml/min of $NaHCO_3$ 0.5 mol/l (according to pH)	0.25 ml/min of $NaHCO_3$ 0.5 mol/l (according to pH)
	Ileal compartment[a]	
	0.25 ml/min of $NaHCO_3$ 0.5 mol/l (according to pH)	0.25 ml/min of $NaHCO_3$ 0.5 mol/l (according to pH)
Jejunal and ileal dialysis	10 ml/min	10 ml/min
Ileal absorption	0.4 ml/min	0.4 ml/min

The table gives the main parameters of the TNO gastrointestinal model (TIM) when simulating digestive conditions of a healthy adult or child after intake of a glass of water. [a]A power exponential equation ($f = 1-2^{-(t/t_{1/2})^{\beta}}$ where f represents the fraction of meal delivered, t the time of delivery, $t_{1/2}$ the half-time of delivery, and β a coefficient describing the shape of the curve) was used for the computer control of gastric and ileal deliveries. [b]Bile is composed of porcine bile extract 1/3 and bile salts 2/3 (deoxycholate and cholate).

of water is ingested (Table 1). The bacterial suspension (200 ml) that was introduced into the TIM system consisted of mineral water experimentally contaminated with the reference strain EHEC O157:H7 EDL 933 (ATCC 43895) at a final concentration of 10^7 CFU/ml. This strain was isolated from Michigan ground beef that was linked to a multistate US outbreak in 1982 involving contaminated hamburgers, in which *E. coli* O157:H7 was first associated with human disease (40). Two types of experiments were performed: gastric digestions where the gastric compartment was solely used (total duration of 60 min) and GI digestions using the entire TIM model (total duration of 300 and 360 min for the adult and child protocol, respectively). During digestion, gastric, and ileal effluents were kept on ice and pooled on 0–10, 10–20, 20–40, and 40–60 min for gastric digestions and hour-by-hour for GI digestions. Digestions were run in quadruplicate. Samples were taken in the initial bacterial suspension (t0) and regularly collected during digestion in each digestive compartment (stomach, duodenum, jejunum, and ileum) and/or in the gastric and ileal effluents.

Bacterial Counting

Survival kinetics in each digestive compartment of the TIM model was determined by direct plating onto Luria Bertani (LB) agar (overnight incubation at 37°C). Results were expressed as percentages of initial intake and cross-compared with those obtained with a theoretical nonabsorbable transit marker provided by the TIM system and indicating a 100% survival rate for bacteria. Bacterial curves below that of the transit marker will reflect cell mortality, while curves above the transit marker will be indicative of bacterial growth.

Physiological State of Bacteria

Physiological state of bacteria was determined by a live/dead analysis with flow cytometry. Bacteria from gastric and ileal effluents were double stained (LIVE/DEAD BacLight, Molecular probes, Whaltham, MA) with the green-fluorescent DNA stain SYTO 9 labelling all bacteria and the red-fluorescent Propidium Iodide (PI) only penetrating and staining cells with damaged membranes. Adequate volumes of gastric or ileal effluents were centrifuged

Table 2. Primers used in RT-qPCR assay

Name	Sequence 5′-3′	Target	Annealing final temperature (°C)	References
VT1c	ACCCTGTAACGAAGTTTGCG	*stx1* EHEC Shiga-toxin 1	60	(41)
VT1d	ATCTCATGCGACTACTTGAC			
Stx2-F	TTGCTGTGGATATACGAGGGC	*stx2* EHEC Shiga-toxin 2	60	(42)
Stx2-R	TCCGTTGTCATGGAAACCG			
Eae-F	CCCGAATTCGGCACAAGCATAAGC	*eae* EHEC intimin	63	(32)
Eae-R	CCCGAATCCGTCTCGCCAGTATTCG			
LPF154-F	TATGGCAGGTCACCTACAGG	*lpfA2* major fimbrial subunit LpfA2	60	(32)
LPF154-R	AGGTTTCCGGGCATTGAGTC			
LPFA141-F	CATCACTATCACCACTAAAGC	*lpfA1* major fimbrial subunit LpfA1	60	(32)
LPFA141-R	ATTTACAAGGGCATTCGCTGT			
Eco1457-F	CATTGACGTTACCCGCAGAAGAAGC	*16S Enterobacteriaceae*	63	(43)
Eco1652-R	CTCTACGAGACTCAAGCTTGC			

EHEC, enterohemorrhagic *Escherichia coli*; eae, intimin; LPF, long polar fimbriae; RT-qPCR, reverse transcriptase-quantitative PCR; Stx, Shiga toxins.

(9,000×*g*, 20°C, 5 min) and bacterial pellets were suspended in phosphate buffer at pH 7.3 to get a final concentration of ~10^6 CFU/ml. Bacterial suspensions were incubated for 15 min at room temperature in the dark with SYTO 9 (5 µmol/l) and PI (30 µmol/l), according to the manufacturer's instructions. Flow cytometry analysis was performed on a CyFlow SL cytometer and data were collected with FlowMax software version 2.3 (Partec, Sainte-Geneviève-des-Bois, France). Gating on forward-angle light scatter/side-angle light scatter was used in order to differentiate bacteria from the background, then the combined red and green fluorescence dot-plots were used to distinguish among the various subpopulations. Statistical tables that show percentages of marked cells determined by each detector were used to analyze data.

Expression of Virulence Genes

Reverse transcription (RT)-PCR was used to follow the expression of *stx 1*, *stx 2*, *eae*, *lpf 1*, and *lpf 2* virulence genes in the gastric and ileal effluents of the TIM. Total RNA was extracted using TRIzol reagent (Invitrogen, Carlsbad, CA). RNAs were reversely transcribed using the PrimeScript RT Reagent Kit (TAKARA Bio, Shiga, Japan). q-PCR was performed using SYBR Green qPCR Master Mix (Agilent Technologies, Waldbronn, Germany) on a CFX96 Touch Real-Time PCR Detection System (Biorad, Hercules, CA) with the specific primers indicated in Table 2. *Enterobacteriaceae* rRNA 16S was used as housekeeping gene for quantification of mRNA expression. Fold-induction was calculated using the Ct method as follows:

$$\Delta\Delta Ct = (Ct_{\text{target gene}} - Ct_{\text{housekeeping gene}})_{\text{at time t}} - (Ct_{\text{target gene}} - Ct_{\text{housekeeping gene}})_{\text{at t0}}$$

and the final data were derived from $2^{-\Delta\Delta Ct}$.

Toxins Production

Stx1 and Stx2 produced by O157:H7 in the ileal effluents of the TIM system were dosed by enzyme-linked immunosorbent assay using the Ridascreen Verotoxin kit (R-Biopharm, Darmstadt, Germany) according to the manufacturer's instructions. Stx concentrations were determined by measuring a change in absorbance of the digestive samples using the Multiskan spectrum reader (Thermo Scientific, Waltham, MA) set at 450 nm. Supernatant from an overnight culture of EDL 933 was used to establish standard calibration curves.

Statistical Analysis

Values are given as means and SEM ($n = 4$). Significant differences in survival between treatments and time points were testing using a nonparametric analysis of repeated measures with the "f1.ld.f1" function of the R package "nparLD" in R 3.1.2 R (Development Core Team 2015). In case of a significant treatment effect, Tukey contrast effects of survival between the two treatments for each time point were calculated using the function "nparcomp" of the R package "nparcomp". In case of a significant interaction effect, a linear mixed effect model with a random intercept on experiments taking into account the repeated measures was performed and followed by function "diffsmeans" of the package "lmerTest". The kinetics of virulence genes expression was tested with the "ld.f1" function of the R package nparLD. In case of a significant time effect, pairwise comparisons with Bonferroni adjustment were performed.

Ethics Statement

Statement of study approvement by the Institutional Review Board: As this study was only performed in an *in vitro* model, no subject was enrolled and no human sample was used. Therefore, study approvement by our Institutional Review Board was not required.

Statement of subject and/or parental informed consent: As this study was only performed in an *in vitro* model, no subject was enrolled and therefore subject or parental informed consent was not required.

STATEMENT OF FINANCIAL SUPPORT

This work was supported by grants from Conseil Régional Auvergne (grant CPER T2ANSH ASTERISK, Auvergne STEC Risque) to Charlotte Cordonnier, Wessam Galia, EA CIDAM, VetAgroSup and UMR INSERM/Université d'Auvergne U1071 USC-INRA 2018 and from Lesaffre Company (Marcq-en-Bareuil, France) to Charlène Roussel.

Disclosure: The authors and Lesaffre Company declare no conflict of interest.

REFERENCES

1. Page AV, Liles WC. Enterohemorrhagic Escherichia coli infections and the hemolytic-uremic syndrome. Med Clin North Am 2013;97:681–95.
2. Keir LS. Shiga toxin associated hemolytic uremic syndrome. Hematol Oncol Clin North Am 2015;29:525–39.
3. Majowicz SE, Scallan E, Jones-Bitton A, et al. Global incidence of human Shiga toxin-producing Escherichia coli infections and deaths: a systematic review and knowledge synthesis. Foodborne Pathog Dis 2014;11:447–55.
4. Bryan A, Youngster I, McAdam AJ. Shiga toxin producing Escherichia coli. Clin Lab Med 2015;35:247–72.
5. McWilliams BD, Torres AG. Enterohemorrhagic Escherichia coli adhesins. Microbiol Spectr 2014;2.
6. Barnett Foster D. Modulation of the enterohemorrhagic E. coli virulence program through the human gastrointestinal tract. Virulence 2013;4:315–23.
7. Guerra A, Etienne-Mesmin L, Livrelli V, Denis S, Blanquet-Diot S, Alric M. Relevance and challenges in modeling human gastric and small intestinal digestion. Trends Biotechnol 2012;30:591–600.

8. Marteau P, Minekus M, Havenaar R, Huis in't Veld JH. Survival of lactic acid bacteria in a dynamic model of the stomach and small intestine: validation and the effects of bile. J Dairy Sci 1997;80:1031–7.
9. Miszczycha SD, Thévenot J, Denis S, et al. Survival of Escherichia coli O26:H11 exceeds that of Escherichia coli O157:H7 as assessed by simulated human digestion of contaminated raw milk cheeses. Int J Food Microbiol 2014;172:40–8.
10. Etienne-Mesmin L, Livrelli V, Privat M, et al. Effect of a new probiotic Saccharomyces cerevisiae strain on survival of Escherichia coli O157:H7 in a dynamic gastrointestinal model. Appl Environ Microbiol 2011;77:1127–31.
11. Tamplin ML. Inactivation of Escherichia coli O157:H7 in simulated human gastric fluid. Appl Environ Microbiol 2005;71:320–5.
12. Kaye JL. Review of paediatric gastrointestinal physiology data relevant to oral drug delivery. Int J Clin Pharm 2011;33:20–4.
13. Saxena T, Kaushik P, Krishna Mohan M. Prevalence of E. coli O157:H7 in water sources: an overview on associated diseases, outbreaks and detection methods. Diagn Microbiol Infect Dis 2015;82:249–64.
14. Koziolek M, Grimm M, Becker D, et al. Investigation of pH and temperature profiles in the GI tract of fasted human subjects using the Intellicap(®) system. J Pharm Sci 2015;104:2855–63.
15. Omari TI, Davidson GP. Multipoint measurement of intragastric pH in healthy preterm infants. Arch Dis Child Fetal Neonatal Ed 2003;88:F517–20.
16. Beckers EJ, Leiper JB, Davidson J. Comparison of aspiration and scintigraphic techniques for the measurement of gastric emptying rates of liquids in humans. Gut 1992;33:115–7.
17. Euler AR, Byrne WJ. Gastric emptying times of water in infants and children: comparison of those with and without gastroesophageal reflux. J Pediatr Gastroenterol Nutr 1983;2:595–8.
18. Kalantzi L, Goumas K, Kalioras V, Abrahamsson B, Dressman JB, Reppas C. Characterization of the human upper gastrointestinal contents under conditions simulating bioavailability/bioequivalence studies. Pharm Res 2006;23:165–76.
19. DiPalma J, Kirk CL, Hamosh M, Colon AR, Benjamin SB, Hamosh P. Lipase and pepsin activity in the gastric mucosa of infants, children, and adults. Gastroenterol 1991;101:116–21.
20. Sarles J, Moreau H, Verger R. Human gastric lipase: ontogeny and variations in children. Acta Paediatr 1992;81:511–3.
21. Vertzoni M, Archontaki H, Reppas C. Determination of intralumenal individual bile acids by HPLC with charged aerosol detection. J Lipid Res 2008;49:2690–5.
22. Challacombe DN, Edkins S, Brown GA. Duodenal bile acids in infancy. Arch Dis Child 1975;50:837–43.
23. Delachaume-Salem E, Sarles H. [Normal human pancreatic secretion in relation to age]. Biol Gastroenterol (Paris) 1970;2:135–46.
24. Whitcomb DC, Lowe ME. Human pancreatic digestive enzymes. Dig Dis Sci 2007;52:1–17.
25. Worsøe J, Fynne L, Gregersen T, et al. Gastric transit and small intestinal transit time and motility assessed by a magnet tracking system. BMC Gastroenterol 2011;11:145.
26. Oikawa-Kawamoto M, Sogo T, Yamaguchi T, et al. Safety and utility of capsule endoscopy for infants and young children. World J Gastroenterol 2013;19:8342–8.
27. Chong Y, Fitzhenry R, Heuschkel R, Torrente F, Frankel G, Phillips AD. Human intestinal tissue tropism in Escherichia coli O157: H7–initial colonization of terminal ileum and Peyer's patches and minimal colonic adhesion *ex vivo*. Microbiology 2007;153(Pt 3):794–802.
28. Farfan MJ, Cantero L, Vergara A, Vidal R, Torres AG. The long polar fimbriae of STEC O157:H7 induce expression of pro-inflammatory markers by intestinal epithelial cells. Vet Immunol Immunopathol 2013;152:126–31.
29. Schüller S. Shiga toxin interaction with human intestinal epithelium. Toxins (Basel) 2011;3:626–39.
30. Yuk HG, Marshall DL. Adaptation of Escherichia coli O157:H7 to pH alters membrane lipid composition, verotoxin secretion, and resistance to simulated gastric fluid acid. Appl Environ Microbiol 2004;70:3500–5.
31. Huang YJ, Tsai TY, Pan TM. Physiological response and protein expression under acid stress of Escherichia coli O157:H7 TWC01 isolated from Taiwan. J Agric Food Chem 2007;55:7182–91.
32. Yin X, Feng Y, Lu Y, Chambers JR, Gong J, Gyles CL. Adherence and associated virulence gene expression in acid-treated Escherichia coli O157: H7 *in vitro* and in ligated pig intestine. Microbiol 2012;158(Pt 4):1084–93.
33. Hamner S, McInnerney K, Williamson K, Franklin MJ, Ford TE. Bile salts affect expression of Escherichia coli O157:H7 genes for virulence and iron acquisition, and promote growth under iron limiting conditions. PLoS One 2013;8:e74647.
34. Kus JV, Gebremedhin A, Dang V, Tran SL, Serbanescu A, Barnett Foster D. Bile salts induce resistance to polymyxin in enterohemorrhagic Escherichia coli O157:H7. J Bacteriol 2011;193:4509–15.
35. Krüger A, Lucchesi PM. Shiga toxins and stx phages: highly diverse entities. Microbiol 2015;161(Pt 3):451–62.
36. Yin X, Zhu J, Feng Y, Chambers JR, Gong J, Gyles CL. Differential gene expression and adherence of Escherichia coli O157:H7 *in vitro* and in ligated pig intestines. PLoS One 2011;6:e17424.
37. House B, Kus JV, Prayitno N, et al. Acid-stress-induced changes in enterohaemorrhagic Escherichia coli O157: H7 virulence. Microbiology 2009;155(Pt 9):2907–18.
38. Arenas-Hernández MM, Rojas-López M, Medrano-López A, et al. Environmental regulation of the long polar fimbriae 2 of enterohemorrhagic Escherichia coli O157:H7. FEMS Microbiol Lett 2014;357:105–14.
39. Chaisri U, Nagata M, Kurazono H, et al. Localization of Shiga toxins of enterohaemorrhagic Escherichia coli in kidneys of paediatric and geriatric patients with fatal haemolytic uraemic syndrome. Microb Pathog 2001;31:59–67.
40. Riley LW, Remis RS, Helgerson SD, et al. Hemorrhagic colitis associated with a rare Escherichia coli serotype. N Engl J Med 1983;308:681–5.
41. Bonnet R, Souweine B, Gauthier G, et al. Non-O157:H7 Stx2-producing Escherichia coli strains associated with sporadic cases of hemolytic-uremic syndrome in adults. J Clin Microbiol 1998;36:1777–80.
42. Carey CM, Kostrzynska M, Ojha S, Thompson S. The effect of probiotics and organic acids on Shiga-toxin 2 gene expression in enterohemorrhagic Escherichia coli O157:H7. J Microbiol Methods 2008;73:125–32.
43. Bartosch S, Fite A, Macfarlane GT, McMurdo ME. Characterization of bacterial communities in feces from healthy elderly volunteers and hospitalized elderly patients by using real-time PCR and effects of antibiotic treatment on the fecal microbiota. Appl Environ Microbiol 2004;70:3575–81.